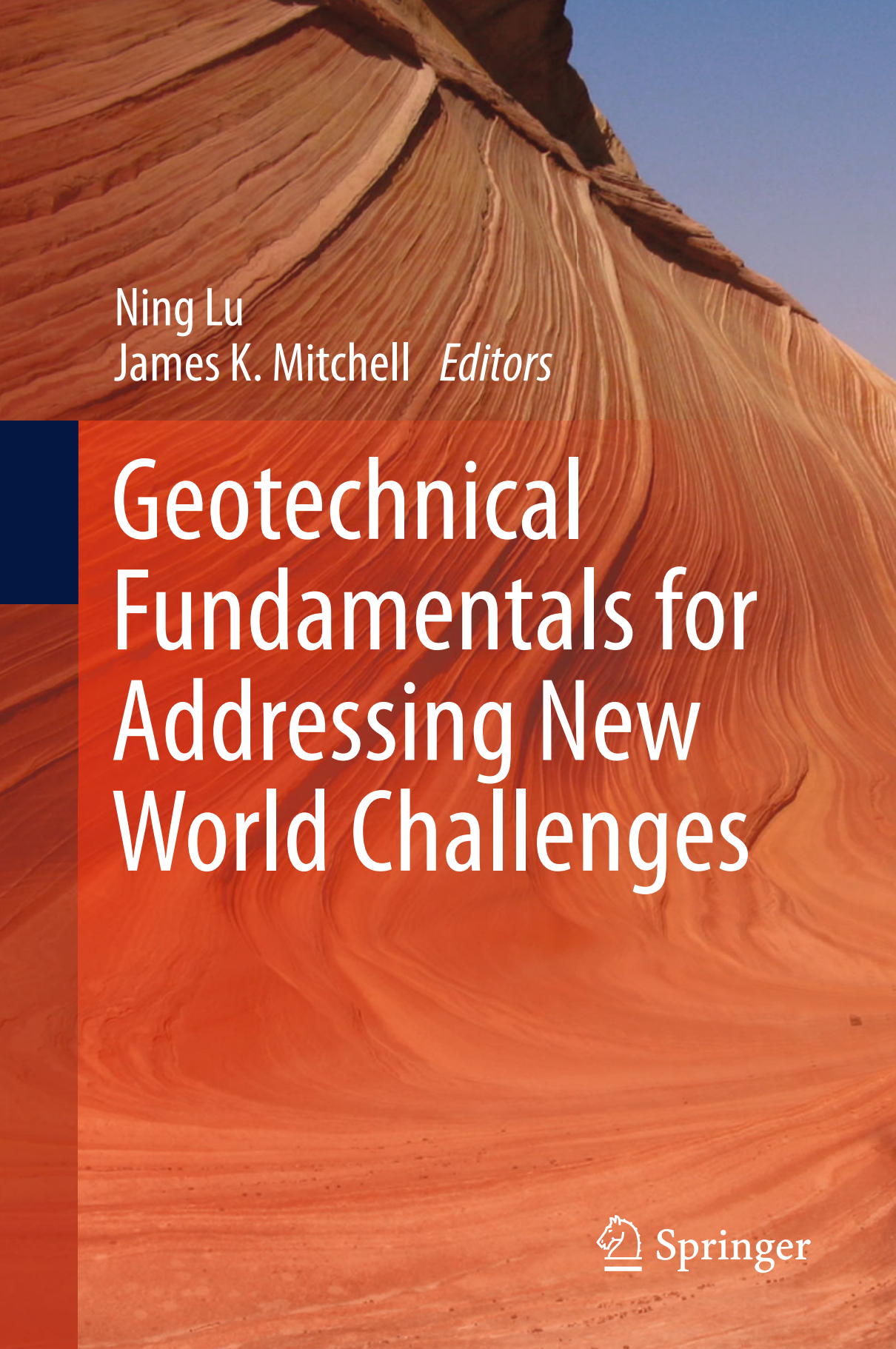
Ning Lu
James K. Mitchell Editors
Geotechnical Fundamentals for Addressing New World Challenges
Springer

Springer Series in Geomechanics and Geoengineering

Geomechanics deals with the application of the principle of mechanics to geomaterials including experimental, analytical and numerical investigations into the mechanical, physical, hydraulic and thermal properties of geomaterials as multiphase media. Geoengineering covers a wide range of engineering disciplines related to geomaterials from traditional to emerging areas.

The objective of the book series is to publish monographs, handbooks, workshop proceedings and textbooks. The book series is intended to cover both the state-of-the-art and the recent developments in geomechanics and geoengineering. Besides researchers, the series provides valuable references for engineering practitioners and graduate students.

** Now indexed by SCOPUS, EI and Springerlink **

More information about this series at http://www.springer.com/series/8069

Ning Lu · James K. Mitchell
Editors

Geotechnical Fundamentals for Addressing New World Challenges

Springer

Editors
Ning Lu
Department of Civil
and Environmental Engineering
Colorado School of Mines
Golden, CO, USA

James K. Mitchell
Department of Civil and Environmental
Engineering
Virginia Polytechnic Institute
and State University
Blacksburg, VA, USA

ISSN 1866-8755 ISSN 1866-8763 (electronic)
Springer Series in Geomechanics and Geoengineering
ISBN 978-3-030-06248-4 ISBN 978-3-030-06249-1 (eBook)
https://doi.org/10.1007/978-3-030-06249-1

Library of Congress Control Number: 2018965913

This Springer imprint is published by the registered company Springer Nature Switzerland AG
The registered company address is: Gewerbestrasse 11, 6330 Cham, Switzerland

Preface

During the latter half of the twentieth century, basic research became indispensable in advancing and improving geotechnical engineering theory and practice. Fundamental principles of physics, chemistry, biology, and thermodynamics provide the underpinning knowledge needed to address existing and emerging challenges, to advance new engineering possibilities, and to discover better solutions for problems and projects involving design, construction, and environmental management on, in, and with the earth and the many varieties of soil and rock materials and conditions that are encountered.

In 2006, a report was issued by the National Research Council of the U.S. National Academies of Sciences, Engineering, and Medicine: *Geological and Geotechnical Engineering in the New Millennium—Opportunities for Research and Technological Innovation.* This report, prepared under sponsorship of the National Science Foundation (NSF), contains a vision for the future of geotechnology for both NSF program managers and the geological and geotechnical community as a whole. A decade later in the summer of 2016, a 2.5-day workshop, entitled *Geotechnical Fundamentals in the Face of New World Challenges*, also sponsored by NSF, was held. Forty US and international researchers, representing a range of technical backgrounds, diversity, and career stages, focused on fundamental principles that underlie current and anticipated developments in geotechnical and geoenvironmental engineering. Emphasis was on recent and needed further developments in the knowledge of the fundamentals underlying specific areas of geotechnics and how the geotechnical research community can contribute to addressing the real-world challenges of today.

Among the major challenges identified at the workshop where it is believed the geotechnical community can make significant contributions are: (1) climate adaptation, (2) urban sustainability, (3) energy and material resources, and (4) global water resources. Some specific areas of geotechnics where fundamental research is greatly needed include: (1) updating and improving soil classification systems, (2) development of physics-inspired, data-driven approaches for analysis and design, (3) modeling multiscale, multiphysics problems in heterogeneous soils and rocks possessing a wide range of properties, (4) understanding unsaturated soil

behavior, and (5) upscaling property measurements and soil modification and improvement technologies from the laboratory to the field.

This book has been prepared as a post-workshop activity by the workshop participants to identify important geotechnical aspects of the major challenges, to describe several current research areas relevant to addressing these problems, and to identify future research that may yield the knowledge needed to address other projects and problems that require high-level geotechnical inputs for their solution.

Chapter 1 "The Role of Geotechnics in Addressing New World Problems" (Culligan et al.) describes four grand challenges and how fundamental geotechnical research advances can contribute to specific actions for addressing them. The remaining 10 chapters, organized sequentially and intertwined around the grand challenges, provide specific needs along the commonly referenced research themes.

Rapidly emerging new sensing and measuring technologies for geotechnics are described in Chapter 2 "Advances in Geotechnical Sensors and Monitoring" (Soga et al.). In Chapter 3 "Soil Properties: Physics Inspired, Data Driven" (Santamarina et al.), several important soil properties used in engineering practice are reviewed, and data-driven guidelines are used to develop their descriptive parameters. The powerful roles of fundamental soil physicochemical properties in characterizing geotechnical engineering properties are illuminated through several recent developments in Chapter 4 "Linking Soil Water Adsorption to Geotechnical Engineering Properties" (Lu). State-of-the-art and developing approaches to modeling multiphysics processes in soil from continuum, discrete, and multiscale perspectives are elucidated in Chapter 5 "Multiscale and Multiphysics Modeling of Soils" (Andrade and Mital). Fundamental research frontiers in geochemical processes are highlighted in Chapter 6 "Fundamental Research on Geochemical Processes for the Development of Resilient and Sustainable Geosystems" (Reddy et al.). Emerging innovative and promising technologies through applications of biological processes are provided in Chapter 7 "Bio-mediated and Bio-inspired Geotechnics" (DeJong and Kavazanjian). Many uncertainties and emerging challenges in engineering with soils under variably saturated conditions are addressed in Chapter 8 "Fundamental Challenges in Unsaturated Soil Mechanics" (Likos et al.). Critical reviews of the developments and future research opportunities in coupled fluid, heat, solute, and electrical flows in soils are provided in Chapter 9 "Research Challenges Involving Coupled Flows in Geotechnical Engineering" (Shackelford et al.). The fundamental aspects of coupled thermo-hydro-mechanical processes derived from energy, material, and water resource exploration and management are described in Chapter 10 "Emerging Thermal Issues in Geotechnical Engineering" (McCartney et al.). Some future research opportunities in deep subsurface environments are described in Chapter 11 "The Role of Rock Mechanics in the 21st Century" (Bobet et al.).

In writing the book, each chapter was spearheaded by the corresponding theme leader (lead author), with contributions from the workshop participants. For each chapter, up to 3 reviewers were identified, and they provided critical, constructive, and thorough peer reviews. These reviews were invaluable in improving the clarity and technical quality of the chapters. They are: in alphabetical order, Craig Benson, Ronaldo Borja, Malek Bouazza, Susan Burns, Jason DeJong, Andrea Dominijanni,

Matt Evans, Arvin Farid, Marte Gutierrez, Joseph Labuz, Lin Li, Qi Liu, Ning Lu, Magued Iskander, James Mitchell, Anand Puppala, Alexander Puzrin, Kristin Sample-Lord, Joseph Scalia, Greg Siemens, Zhonghao Sun, Andy Take, and Michael Tsesarsky. The workshop and some post-workshop activities were funded by NSF Award #1536733. This financial support is greatly appreciated.

Our hope is that this volume will stimulate geotechnical engineers to continuously use fundamental research as a main thrust for addressing existing and yet unknown new challenges in the twenty-first century in energy, materials, water exploration, climate adaptation, and sustainability of urban and natural environments.

Golden, USA — Ning Lu
Blacksburg, USA — James K. Mitchell
August 2018

Contents

The Role of Geotechnics in Addressing New World Problems

Patricia J. Culligan, Andrew J. Whittle and James K. Mitchell

Abstract There are many "new world", or recently emergent, global challenges whose solutions require geotechnical inputs. Included among these challenges are climate change, enhancement of urban sustainability and resilience, energy and materials resource management, and management of water resources. Fundamental advances in the understanding of soil and rock properties and behavior, coupled with advances in sensing, monitoring and modeling of geo-systems, are needed for solutions to be found or implemented satisfactorily in each of these four areas. In addition, there is need for fundamental research that can improve the subsurface characterization and monitoring of complex geo-material behavior, the handling of multi-faceted, multi-scale geotechnical and geo-environmental processes, the integration of "big-data" and data-science methods into geotechnical engineering research and practice, and the management of uncertainty and risk. In addition to advancing fundamental research in geotechnics, geotechnical engineers also need to lend expertise and leadership to the interdisciplinary research and development efforts that are essential to ensuring our sustainable future.

Keywords Geotechnics · Climate change · Urban sustainability and resilience · Energy and materials · Surface and groundwater water resources · Subsurface characterization · Multi-scale processes · Big-data · Uncertainty and risk

P. J. Culligan (✉)
Robert A.W. and Christine S., Carleton Professor of Civil Engineering, Columbia University, 626 SW Mudd Building, 500 West 120th Street, New York, NY 10027, US
e-mail: pjc2104@columbia.edu

A. J. Whittle
Edmund K. Turner Professor, Department of Civil & Environmental Engineering, MIT, 77 Massachusetts Ave, Cambridge, MA 02139, USA
e-mail: ajwhittl@mit.edu

J. K. Mitchell
Department of Civil & Environmental Engineering, University Distinguished Professor Emeritus, Virginia Tech, Patton Hall 120-D, Blacksburg, VA 24061, USA
e-mail: jkm@vt.edu

N. Lu and J. K. Mitchell (eds.), *Geotechnical Fundamentals for Addressing New World Challenges*, Springer Series in Geomechanics and Geoengineering,
https://doi.org/10.1007/978-3-030-06249-1_1

1 Introduction

There are multiple ways by which fundamental geotechnical engineering research and expertise can contribute to solving some of today's pressing problems. The focus of this Chapter is to present some "new world", or recently emergent, global challenges whose solutions require geotechnical[1] inputs. The four new world challenges that are highlighted in this chapter are climate change, enhancement of urban sustainability and resilience, energy and materials resource management, and management of water resources. By nature, these challenges are broad and complex, and thus identifying viable solutions to each will necessitate the engagement of many disciplines. Nonetheless, within each challenge area there are also clear gaps in understanding that require knowledge and advances in geotechnical fundamentals for solutions to be either found or implemented satisfactorily. The four highlighted challenges are discussed under separate headings, and examples of how fundamental geotechnical inputs might contribute to specific insights and solutions that address them are provided. Many of these inputs incorporate, or are based on, the geotechnical fundamentals described in the remaining Chapters of this book.

The challenges described in this Chapter are only a sub-set of emergent global challenges that need to be addressed as mankind advances further into the 21st century. The list of geotechnical fundamentals described under each challenge is also by no means exhaustive. Hence, the intent of this Chapter is not to present a comprehensive overview of all new world challenges and attendant geotechnical fundamental knowledge and research needs. Rather, the goal is to use examples to illustrate the important roles that geotechnical fundamentals, and thus geotechnical engineers, can play in shaping a sustainable future for our world.

2 Climate Change

We are living in what is becoming widely known as the Anthropocene Epoch [46], where human activities are generally recognized as driving the process of climate change principally through the production of greenhouse gases (GHG). The impacts of anthropogenic climate change involve significant uncertainty, not least because of unknown scenarios for future GHG emissions. For high emissions scenarios (RCP8.5[2]), global sea-level rise is projected to be about 2 m (6.6 ft) over the course of the 21st Century, while global temperature rise is projected to be about 4 °C (Fig. 1). Local sea-level and temperature rises are projected to be above or below the global levels shown in Fig. 1, depending on the region under consideration.

[1] Here, geotechnical is broadly defined to include applications involving all engineering aspects of soil and rock properties, behavior and mechanics, as well as geo-environmental engineering.

[2] Representative Concentration Pathway (RCP) 8.5 assumes CO_2—equivalent emissions continue to rise throughout the 21st Century.

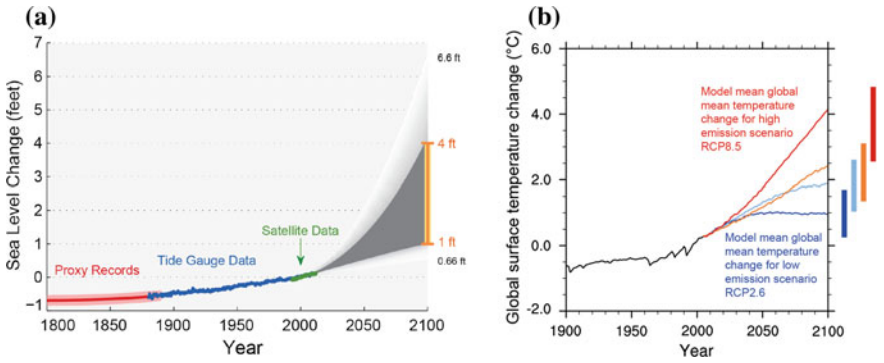

Fig. 1 **a** Past and projected changes in global sea level rise (left, USGCRP [38] predict 1–4 ft rise in mean sea level by 2100 for low and high CO_{2e} emission scenarios, respectively), and **b** Past and projected changes in global temperature rise (right, IPCC [14]—red and blue curves represent the high and low CO_{2e} emission scenarios, respectively. Figure credit: J. Willis, Jet Propulsion Laboratory. Additional info: Figure created on November 15, 2013 and derived from the Global sea level rise scenarios for the United States National Climate Assessment)

Nonetheless, despite uncertainties in the projected magnitude of climate change effects, there are several general trends that climate scientists agree upon. These include a raise in global mean sea-level; an increase in global average temperatures; changes in the patterns and amount of precipitation; a decline in snow-cover, permafrost and sea-ice; acidification of the oceans; an increase in the frequency, density and duration of extreme events (such as hurricanes, floods droughts etc.), and a change in eco-system characteristics. These effects will impact water resources, infrastructure, food supplies, eco-systems and, thus, human health and well-being. They also present a host of specific geotechnical challenges ranging from the need for new strategies to protect coastal cities against sea level rise, to dealing with the consequences of melting permafrost on Arctic infrastructure. Increased severity in extreme weather events (both floods and droughts) will also jeopardize existing dams and levees, increase slope hazards and trigger excessive erosion and scour.

The United Nations Framework Convention on Climate Change (UNFCCC) identifies two options to address climate change: mitigation of climate change by reducing GHG emissions and enhancing GHG sinks, and adaptation to the impacts of climate change [18].

2.1 Climate Mitigation: Low Carbon Economy

The United Nations (UNFCCC, Paris Agreement 2015) aims to control the long-term rise in average global temperatures by regulating the production of GHGs. The Agreement goals will only be met if industrialized nations move toward low carbon economies through investment in technologies for energy efficiency, renewable

energy resources, and methods to reduce impacts associated with current fossil fuel usage (such as carbon capture and storage). While renewable energy sources (solar, hydro, wind, geothermal) and nuclear energy are used primarily for electricity generation, fossil fuels account for most energy usage in transportation and industrial processes (notably in the production of building materials, with Portland cement being one of the largest generators of GHG worldwide). The transition to a low carbon economy will require disruptive changes in the infrastructure supporting power distribution and transportation systems. We believe that the transition to a low carbon economy will drive much future research in geotechnical engineering including:

Geothermal energy. To date geothermal energy accounts for a tiny fraction of global energy usage (less than 1%; WEC [44]) and is primarily limited to electricity generation and district heating from high-grade, hydrothermal resources (fluids with temperatures greater than 200 °C) in a small number of geographic locations (primarily in the U.S. and China). There is potential for massive growth[3] of geothermal energy through development of technologies to support Enhanced Geothermal Systems (EGS; sometimes referred to as universal heat mining) involving fracturing of hot dry rocks with circulation of a carrier fluid. Such growth would require advances in technologies for deep drilling, high-resolution geophysical and remote sensing methods for online monitoring of heat reservoirs, and simulation models for reservoir performance over different time scales that incorporate high-temperature, high-pressure (HTPT) geomechanics. Improved understanding of coupled thermal-hydrological-mechanical-chemical (THMC) process under unsaturated conditions will also be key, as will improved understanding of fluid-injection induced seismicity.

Exploitation of the subsurface environment for seasonal heat exchange or heat storage (often referred to as 'shallow geothermal' resources) via the use of ground source heat exchangers is increasing. Research in this field has taken root in the geotechnical community largely through integration of heat exchangers with foundation elements ('geothermal piles') and through potential applications of the technology to assist in district-scale heating and cooling of buildings. Inconsistent performance reported in prototype projects suggests there is a significant research challenge to improve the reliability of these systems. Additional work is also needed to understand the scale at which such systems can be adopted in dense settings without disruption to the ground's capacity to exchange heat, or to bear loads.

Current understanding, unresolved issues and needed basic research on geotechnical issues relevant to geothermal energy are summarized in several of the chapters in this book; including Chapter 6 "Fundamental Research on Geochemical Processes for the Development of Resilient and Sustainable Geosystems", which discusses geochemical processes, Chapter 8 "Fundamental Challenges in Unsaturated Soil Mechanics", which discusses unsaturated soil mechanics, Chapter 9 "Research Challenges Involving Coupled Flows in Geotechnical Engineering", which discusses coupled flow phenomena, Chapter 10 "Emerging Thermal Issues in Geotechnical Engineering", which discusses emerging thermal issues, and Chapter 11 "The Role

[3] MIT [21] estimate the potential for generating more than 100 GWe by 2050 in the US alone.

of Rock Mechanics in the 21st Century", which presents the role of rock mechanics in the 21st Century.

Wind energy. The US has been relatively slow to develop off-shore wind resources, primarily due to the distance between primary locations (i.e., those with the highest wind power density) for onshore generation and the location of major consumers, as well as the high costs of offshore wind farm installations. There are already substantial geotechnical research activities to reduce foundation costs for offshore wind turbines in Germany and the U.K.[4] Complete understanding of the dynamic soil-structure interactions is essential for both optimization of the design of structure foundations and the assurance of their long-term stability. Looking forward, the principal research needs will relate to local energy storage and power distribution infrastructures. Here, compressed air energy storage (CAES) in underground caverns is gaining attention as a means of energy storage, and geotechnical expertise is crucial to identifying feasible caverns for this approach.

Hydropower. Hydropower remains the biggest source of renewable energy in the U.S. (10% of electricity generation) and one of the most strategically important energy resources worldwide (with increased co-reliance on pumped storage systems[5]). Here, challenges in the future relate to reducing the environmental impacts of major dam projects as well as uncertainties in the output production associated with long-term changes in weather patterns. Geotechnical engineers have played a key role in the siting of major dams and the assessment of their safety. There are significant opportunities for improving methods of site characterization, long-term performance monitoring and methodologies for retrofit of existing hydropower facilities.

Carbon capture and storage. Carbon capture and storage is considered critical to reduce the atmospheric release of greenhouse gases from fossil fuels. Geological sequestration of compressed CO_2 in deep underground rock formations (typically in depleted oil and gas fields, or saline aquifers) currently represents the only viable solution for large-scale storage of greenhouse gases in the continental U.S. However, there are significant uncertainties in evaluating storage capacities and sustainable injection rates [36] and major challenges to monitoring and verifying that that the CO_2 remains trapped underground over very long-time periods (100s–1000s of years), Fig. 2. The latter challenge will require basic research on natural and enhanced mineralization processes, as well as complex fluid transport processes. Better understanding of the fundamental hydro-mechanical properties of clay and shale is also needed, including the unsaturated properties, specific surface area, cation exchange capacity, and long-term stability of these geo-materials. In addition, further research is needed on the effectiveness and durability of seals in CO_2 storage chambers.

[4]North Sea installations benefit from much shorter transmission distances to major population centers and possible power interconnects between the National Grids of countries that have substantial pumped storage capacity (such as Norway).

[5]E.g., proposed use of an abandoned mine cavity as the lower reservoir for a pumped storage project in Virginia http://www.enr.com/articles/42729-dominion-energy-eyes-2b-hydroelelctric-storage-project-in-va (September 13, 2017).

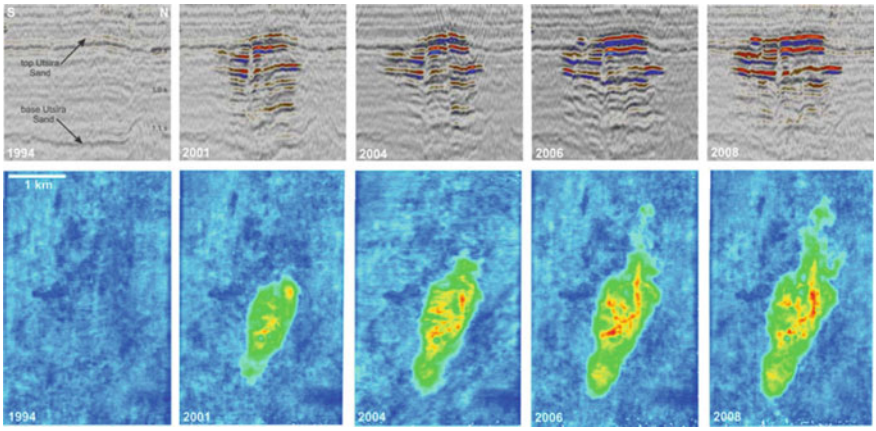

Fig. 2 Time lapse '4D' seismic images of CO_2 storage at Sleipner CCS pilot project (1994–2008) showing lateral and vertical expansion of injected CO_2 volume with time [4]

2.2 Climate Adaptation

The effects of global warming (of the atmosphere and oceans) can be seen in long-term trends in sea level rise (and associated coastal erosion), melting of glaciers and permafrost in Arctic regions, and in regional weather events including more intense tropical storms, extreme rainfall events, longer drought cycles etc.[6] Climate adaptation refers to the myriad of policies and actions that are employed to reduce the vulnerability of, and impacts on, human populations (public health and safety, water resources, and food security) and ecosystems as a result of climate change. Climate adaptation policies vary by region, by economic circumstance and by necessity. For example, while most cities in wealthy nations have detailed adaptation plans,[7] many megacities in the developing world have yet to address the issue. Some of the most dramatic effects of climate change are found in sparsely-populated Arctic regions and present the dilemma of balancing economic opportunity with protection/preservation of the environment. The geotechnical profession can contribute in several pressing areas here, including:

Adapting to Too Much Water: Geotechnical engineers have a key role in advancing new solutions for climate adaptation especially in mitigating hazards associated with flooding (coastal, surface water) and slope instability, ensuring reliable water supplies, and making infrastructure more resilient. While cities such as New Orleans have a long history in dealing with flooding (originating from the Mississippi River, monsoonal precipitation and hurricane storm surge), subsidence and coastal erosion;

[6] At the time of writing (September 2017), Texas and Louisiana have just experienced record rainfalls associated with Hurricane Harvey, and massive flood and wind damage from hurricanes Irma and Maria has occurred in Florida and across the Caribbean islands.

[7] E.g., http://www.nyc.gov/html/dep/html/about_dep/climate_resiliency.shtml.

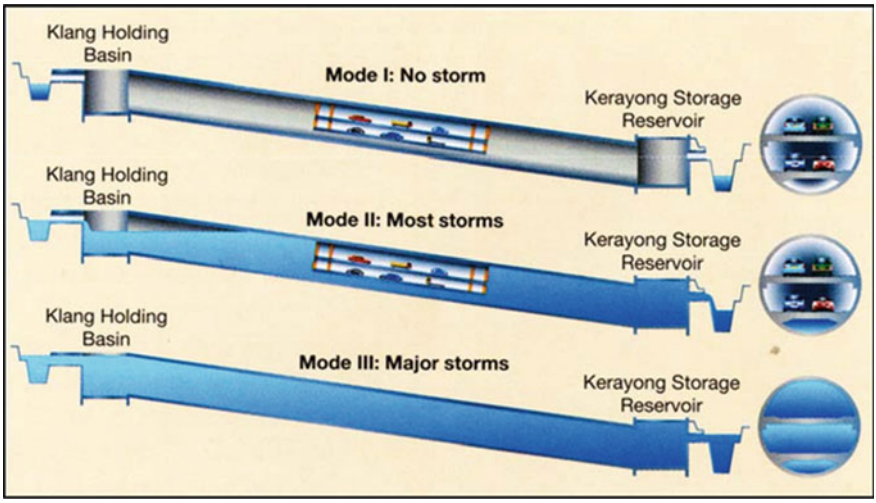

Fig. 3 Operation of stormwater management and Road Tunnel, Kuala Lumpur, Malaysia (from: http://sspsb.com.my)

others such as Miami-ranked number 1 city in the world for assets at risk due to sea level rise[8]—face long-term threats from sea level rise that have yet to be addressed and will require new technical solutions. Coastal mega-cities in the developing world lack the financial resources for major infrastructure projects and will need more cost-effective solutions.

A good example of such a solution is the multi-purpose SMART tunnel in Kuala Lumpur, which can operate as either a motorway or storm water drain, Fig. 3. Non-structural solutions such as wetland restoration are also likely to play an increasing role in coastal climate adaptation (e.g., [2]).

Adapting to Too Little Water: Prolonged droughts are potentially one of the most significant threats associated with climate change due to their impact on food and water security (as experienced already by populations in areas of desertification). There are numerous hazards associated with drought cycles especially related to soil erosion and dust (with concomitant effects on air quality and human health). Recent studies by Pu and Ginoux [28] show that climate change (changes in regional and seasonal precipitation etc.) is likely to produce increasingly dusty conditions in the Southern Great Plains of the U.S. (while reducing dust levels in the Northern Plains). There is already some geotechnical research on dust control using biopolymers (to stabilize mine/mill tailings; e.g., [6]), and there is great potential for future research to mitigate dust storms and fugitive dust arising from other sources. For example, the National Science Foundation's Engineering Research Center for Bio-mediated

[8] http://www.miamiherald.com/news/local/news-columns-blogs/andres-oppenheimer/article166217947.html.

Fig. 4 Trans-Alaska pipeline with heat exchanger to protect permafrost from melting during the summer months (from: www.en.wikipedia.org/wiki/Trans-Alaska_Pipeline_System)

and Bio-inspired Geotechnics is examining new biological approaches for fugitive dust control, among other advances—as discussed in Chapter 7 "Bio-mediated and Bio-inspired Geotechnics".

Adapting to Change in the Arctic: Arctic regions have been experiencing transformative effects of climate change for several decades. Geotechnical engineers have played a key role in solutions that enable Arctic development while protecting the environment. The construction of the Alaska oil pipeline in the 1970s successfully introduced novel heat exchangers to prevent thawing of permafrost (Fig. 4), while other technical innovations enabled the crossing of major Arctic rivers and ensured integrity of the pipeline during significant seismic events. Anticipated future changes in climate are opening up important economic opportunities, principally due to reductions in perennial sea ice that will enable new trans-Arctic shipping routes, and access to hydrocarbon and mineral reserves beneath the Arctic Ocean. Geotechnical research can contribute to environmentally responsible development. Other challenges associated with thawing of permafrost include the potential for large-scale release of greenhouse gas emissions (principally carbon dioxide and methane). This is an area of active scientific research (e.g., [35, 42]) where the geotechnical community can contribute to understanding the carbon dynamics and rates of gas emissions from melting permafrost (within diverse terrestrial, coastal and submarine sediments), and to the development of new methods to stabilize or fix organic carbon insitu. All of these advances depend on fundamental understanding of multiphase flows and hydro-mechanical soil properties which are discussed in later chapters of this book.

3 Urban Sustainability and Resilience

The United Nations World Urbanization Prospects report noted that 2009 was the year that the world's population crossed the line of being more than 50% urban—with 3.42 billion living in urban areas versus 3.41 billion in rural areas. Indeed, Ban Ki-moon, then Secretary-General of the UN, stated that we are now living in "the urban century". As the world's population expands, urbanization trends are only expected to intensify, with the bulk of projected growth occurring in the less developed regions of Asia, Africa and China. Meeting the global challenge of urbanization is key to the future health and well-being of most of the world's population. Geotechnical engineering research can contribute to emerging interdisciplinary research in urban sustainability and resilience in several key areas, including:

Underground infrastructure mapping, maintenance and development. Most essential urban infrastructure services (potable water, wastewater, energy and communications, etc.) are located below ground (in networks of pipes and conduits) along with many vital transportation facilities (transit networks etc.), Fig. 5. Under-investment in maintenance has left a legacy of aging underground infrastructures in many cities worldwide, while underground space is increasingly seen as a panacea for future urban development (from high-speed rail[9] in London, to re-use of underground space for the Lowline proposed space in New York City, to a necessity in space-constrained states such as Singapore[10]). Given the high costs and complexity of re-using underground space, cities such as Helsinki and Singapore have developed long-term master-plans for underground space and utilization.

The restoration and improvement of buried infrastructure is part of a larger global challenge related to the overall restoration and improvement of urban infrastructure, and Geotechnical Engineers have much to contribute in this area. For example, several issues related to underground construction, geology and geotechnical risk are discussed, and important areas of needed research are noted in Section 2 of Chapter 11 "The Role of Rock Mechanics in the 21st Century".

In cities, underground mapping is urgently needed to improve the management of existing subsurface infrastructure and the planning of future underground construction. Although temporal and spatial data on underground conditions exist in most developed cities, including information on subsurface stratigraphy, depth to groundwater, location of underground infrastructure, services, openings, foundations, etc., city-wide underground maps remain largely unavailable. This is because existing data are housed in multiple, dispersed sets that have yet to be merged, analyzed and visualized. By combining new data analytics approached with traditional expertise, the geotechnical community can lead in merging available data with other information to create geo-data banks, subsurface BIM (Building Information Modeling) systems and comprehensive urban underground maps. Advances in technologies for mapping the location and condition of buried infrastructure (within the congested

[9] http://www.crossrail.co.uk.

[10] http://www.straitstimes.com/singapore/experts-warn-of-hefty-price-tag-for-singapores-underground-ambitions.

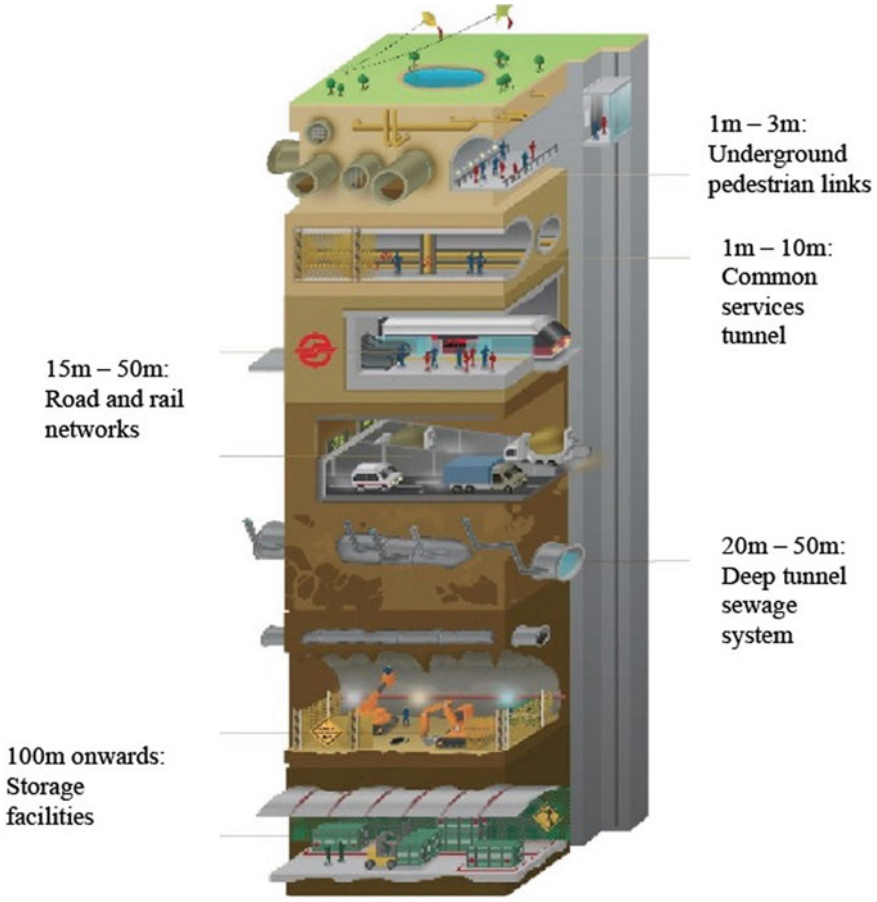

Fig. 5 Vertical planning of underground space in Singapore (modified from: www.citi.io/2017/10/09/the-secret-underground-world-of-singapore/)

urban environment) can help accelerate the development and utility of such new tools. For example, when combined with advances in sensing technologies (from embedded sensors to ubiquitous platforms such as smart phones, as described in Chapter 2 "Advances in Geotechnical Sensors and Monitoring"), these tools can lead to new advance-warning systems for mitigating disruptions to underground services, reducing maintenance costs and, more importantly, saving lives. For example, Whittle et al. [43] have developed a wireless sensor network for real-time monitoring and detection of underground bursts and leaks in water distribution networks.

Stormwater management. Because of imperviousness (e.g. land surface coverage by buildings, pavements, parking lots, etc.), a typical city block generates over five times as much stormwater runoff as a woodland area of the same size [9]. This runoff contains pollutants including oils, heavy metals, particulates and nutrients,

that are harmful to human health and the environment. In urban areas not served by stormwater systems, overland flow discharges this polluted runoff directly into local water bodies. In areas served by storm-drains the runoff will be collected in an underground pipe network, however, the network also often discharges directly into a local water body. In older cities, including New York, San-Francisco and Seattle, among many others, stormwater is directed into the same pipe network that collects the city's sewage.

In so-called "dry-weather" flows, the combined stormwater and sewage are sent to wastewater facilities for treatment prior to discharge. During wet-weather flows, however, these older single-pipe systems do not have the capacity to deal with modern day volumes. As a result, combined stormwater and sewage, often containing harmful levels of human pathogens and other toxic waste, is discharged untreated. Overall, urban stormwater runoff is estimated to be responsible for impairing more than a third of the water bodies in the U.S. [24], and very many more globally.

Inadequate infrastructure for stormwater management is also blamed for catastrophic flooding events during extreme wet-weather flow, such as the devastating flood Houston suffered as a result of Hurricane Harvey [31]. Tackling this problem requires the development of comprehensive, urban hydrologic models that can improve our basic understanding of stormwater transport during wet weather. Geotechnical engineers can contribute by advancing urban groundwater modeling and monitoring approaches. In addition, research into new underground construction techniques that could enable subterranean infrastructure for stormwater capture and conveyance is needed. Furthermore, current trends toward the use of urban green infrastructure for stormwater management can be supported by research into new engineered soils for water and pollutant capture. Of special interest are engineered soils that can sequester nutrients, especially nitrate, while supporting vegetative health. Enhanced understanding of the long-term behavior of existing engineered soils is also needed to understand the long-term sustainability of urban green infrastructure.

Mega-Scale Land Reclamation. As the World continues to urbanize, existing cities are seeking to expand their current footprints, and the rapid construction of new cities is underway in many parts of the globe. As has been historically the case (e.g., Boston), land-reclamation, the process of creating new land from estuaries, oceans, rivers or lakes, is often a prominent part of urban expansion or growth. In China, the coastal city of Longkou recently created seven new islands, with a total land area of about 35 km^2, which are expected to house 200,000 people by 2020.[11] Singapore has added 720 km^2 through land reclamation since 1965 (25% of its total land area), and the United Arab Emirates has expanded its coastline from about 70 km to approximately 1000 km via land reclamation activities. A significant challenge here, is the sustainable, and ecologically sound, sourcing of the fill needed to create new land. Another challenge is ground improvement of reclaimed land, which is often needed prior to land usage to prevent excessive consolidation and long-term secondary settlement, and assure seismic safety. In both situations,

[11] Wade Shepard, City Metric, August 25th, 2015.

geotechnical engineers can contribute by advancing the re-use of waste materials with novel chemical and or biological stabilization (currently demonstrated at scales up to 800 m^3; [41]) that meet the needs of mega-scale land reclamation projects. In addition, new processes and techniques for large scale ground improvement are needed, as well as better understanding of how land-reclamation impacts existing systems, including the stability of natural coastlines.

Coastal cities and sea-level rise. Over seventy percent of the world's metropolises with a population greater than 5 million are located on or near the coast.[12] Global sea-level rise is projected to dramatically increase the damage of flooding due to storm surges in many of these cities, as well as others. Interdisciplinary research on adaptation and mitigation strategies to deal with the potential effects of coastal city flooding is urgently needed if these cities are to avoid devastating impacts, including cascading failures of critical infrastructure systems. Geotechnical engineers need to be actively engaged in finding solutions to achieve the appropriate balance between the design of robust flood defense systems and strategies to improve the resilience of critical infrastructures. Figure 6 illustrates the novel flap-gate solution found for Venice), Italy.

Natural hazard resilience for cities. In addition to sea-level rise, cities can also be vulnerable to a multitude of other hazards including earthquakes, mudslides, tsunamis, tornados, etc. As above, this is another area where interdisciplinary research is needed, and where geotechnical engineers can play a leadership role. For example, geotechnical expertise in earthquake engineering can feed into research that informs new designs for buildings and infrastructures that are resilient to multiple hazards (e.g., earthquakes and windstorms, flooding and slope instability[13]). Geotechnical engineers can also collaborate with colleagues on examining natural hazards and their spatial and temporal relationships to each other, as well as to secondary hazards (e.g., the triggering of a landslide by an earthquake). Advances that enable the creation of probabilistic event trees summarizing potential hazard scenarios for specific locations are needed [25]. Geotechnical expertise can also contribute to advances in risk and performance-based design and risk communication approaches.

4 Management of Energy and Material Resources

Current projections [37], Fig. 7, estimate that global energy demand is likely to grow by more than 30% over the next 25 years (much of this growth is in non-OECD countries, notably India and China). The U.S. Energy Information Administration (EIA) expects this demand be met by large growth in renewable energy resources (especially solar and wind) and natural gas (especially in the U.S. and China), with smaller increases in oil and nuclear power generation. Nonetheless, the optimal

[12] United Nations Department of Economic and Social Affairs, 2012. *World Urbanization Prospects The 2011 Revision*, New York.

[13] Exemplified by typhoon Morakot (2009 https://en.wikipedia.org/wiki/Typhoon_Morakot).

(a) Venetian Lagoon (55km^2 with average water depth 1m)

(b) Concept of flapping gate

(c) Field demonstration

Fig. 6 Novel design of buoyant flap gates for protecting Venice against frequent storm surge events and preserving unique lagoonal environment (MOSE project). In calm weather the gates fill with water and sit on the seabed. During high tide conditions the water is expelled by compressed air, and the gates surface to provide the necessary flood protection (from: www.mosevenezia.eu/mose/). **Ministero delle Infrastrutture e dei Trasporti—Provveditorato Interregionale per le Opere Pubbliche del Vento—Trentino Alto Adige—Friuli Venezia Giulia gia Magistrato alle Acque di Venezia**

management of conventional ad unconventional oil and gas supplies, as well as nuclear energy, continues to be of importance. It should be noted that the current EIA projections do not consider impacts of large-scale disruptions in energy use within the transport sector (where large-scale electrification is likely to occur over the next 25 years).

With technological advances and a growing need to source energy from more diverse environments, new challenges are continually arising. At the same time, increased attention to the sustainable use of natural and constructed resources, especially those that incorporate significant embodied energy, is also opening new areas of inquiry. Geotechnical engineering inputs can contribute to meeting the challenges associated with the management of energy and material resources in several key areas, including:

Natural gas. Hydraulic fracturing (HF; 'fracking') has revolutionized the extraction of natural gas from tight formations (shales) and has reshaped the energy landscape of the U.S. over the last 10–20 years. While many consider natural gas an intermediate step in the migration to a low carbon economy (e.g., as a replacement

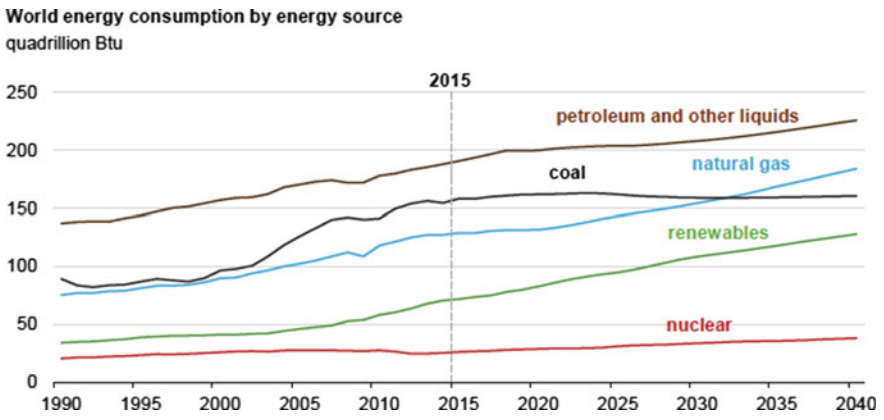

Fig. 7 Current baseline projections on world energy consumption by energy source [37]

for coal in power generation) it presents an important set of research challenges of special interest to geotechnical engineers. There are significant risks associated with induced seismicity caused by disposal of large volumes of fracking wastewater that remain poorly understood, while substantial advances are needed to better understand and control fracturing of gas shales in order to reduce energy and water consumption and potential groundwater contamination associated with this technology.

Gas Hydrates. Gas hydrate is an ice-like crystalline phase of methane (clathrate) that occurs naturally (from underlying biogenic sources) within voids in marine continental shelf sediments within a gas hydrate stability zone (GHSZ) that typically ranges up to 300–500 m below the mudline worldwide. Other stable locations for gas hydrates are within and beneath permafrost zones (depending on the combinations of temperature and pressure). Current estimates suggest that up to 1.5×1017 m^3 of methane is stored in gas hydrates worldwide (99% in the marine sediments). Extraction of natural gas from gas hydrates is a major challenge due to: (i) the low saturation levels of gas hydrates within the pore space; (ii) the difficulty in accurately detecting the presence of gas hydrates using current geophysical methods; and (iii) the need for new technology that can reliably control dissociation of gas hydrates in production wells. Advances in multiphase geomechanics are fundamental in addressing the latter problem (e.g., [10]). Recent reports[14] suggest successful performance of hydrate pilot wells in the Nankai Trough (offshore Japan), and this may lead to the first commercial use of gas hydrates as a source of natural gas.

Uncontrolled dissociation of gas hydrate can generate hazards such as submarine slope instability, while reformation of hydrates is a major problem for clogging of submarine gas pipelines. While these hazards are well known, there is a continuing need for better detection and modeling of gas hydrates within the marine environment to reduce risks in exploration and production.

[14] http://www.reuters.com/article/japan-methane-hydrate/japan-reports-successful-gas-output-test-from-methane-hydrate-idUSL4N1IA35A.

Offshore Energy Resources. The development of offshore oil and gas resources has generated some of the most significant challenges for foundation engineering over the last 30 years, associated with oil production in deepwater environments (e.g., [29]). There are large proven (commercially viable) oil reserves located in extreme environments, including ultra-deepwater conditions (>1500 m), and areas with unusual geological hazards (e.g., high seismicity, tsunamis), as well as large potential reserves in previously unexplored areas of the Arctic Ocean. Exploitation of these resources requires massive capital investments and present challenges and opportunities for new technologies (such as subsea completions, safety of deepwater pipelines etc.) that will rely heavily upon geotechnical expertise.

Offshore oil developments also impose very high environmental risks, as witnessed by the massive oil spill from the Macondo well [20] and its impacts on the Gulf Coast region. Geotechnical engineers can contribute in reducing these risks at all stages in the lifecycle of oil production—from the use of advanced geocomposite materials to improve wellbore integrity during drilling and production, to the sealing of abandoned wells (an emerging environmental problem in the Gulf of Mexico), to advances in remote sensing of leakage from wellbores, to innovative methods for rapid well closure following a blowout event.

Nuclear Energy: According to the Nuclear Energy Institute (NEI), as of April 2017 thirty countries are operating a total of about 450 nuclear reactors for energy generation worldwide, with a combined capacity of close to 400,000 MW.[15] Although some countries have put nuclear energy programs on hold after the 2011 Fukushima disaster, other counties remain interested in the use of nuclear power and 60 new nuclear plants are currently under-construction around the globe. A primary challenge with nuclear energy remains the disposition of spent fuel. In the U.S., the Nuclear Waste Policy Act (NWPA) restricts consideration of geological repositories for high-level nuclear waste to Yucca Mountain, Nevada. Nonetheless, there has been increasing interest in examining alternative disposal options, including a geographically distributed repository system that would involve deep (~5 km) borehole disposal in crystalline basement rocks.[16] Successful realization of this alternative would require accurate site characterization of potential disposal sites, including the thermal, chemical and mechanical characteristics of the host rock system. Fundamental understanding of the in situ stresses and the chemical and fluid flow regimes generated by decaying heat from the emplaced waste will also be necessary for successful borehole design, as will the design of effective seals for the waste disposal zone that have high radionuclide sorption capacity, are self healing and durable. There are many opportunities for fundamental geotechnical research to contribute to evaluating the feasibility of this alternative disposal option.

Mineral Resources. Mining for critical and non-critical minerals is only likely to escalate as demand for resources increases on a global scale. Locating viable mineral resources will require better integration of expertise in geology, mineral economics

[15] https://www.nei.org/Knowledge-Center/Nuclear-Statistics/World-Statistics/World-Nuclear-Generation-and-Capacity.

[16] http://prod.sandia.gov/techlib/access-control.cgi/2009/094401.pdf.

and geotechnical engineering. As mining extends into deeper, and potentially more hazardous, environments, understanding of rock overstress conditions will become more important, as will the use of automation and advanced sensing and warning systems to improve mine safety. As the quality of available ore deposits decreases, there is also a growing trend toward the extraction of ore from historic mining operations. Bioleaching of existing mine tailings represents one promising avenue for extracting metals from mining wastes [12]. Progress in this area will require research advances at the intersection of geotechnics, microbiology and chemistry.

Sustainable Development. The concept of sustainable development is most succinctly defined as 'development that meets the needs of the present without compromising the ability of future generations to meet their own needs' [3]. In practice, this implies the need to balance the use of resources with economic, environmental and social equity considerations in the planning and design of projects. These issues should be of utmost importance to geotechnical engineers who are involved in the construction of major infrastructure projects that involve large energy costs, the massive use of natural resources (including space) and have significant (and long-lasting) impacts on the landscape. There are major opportunities for geotechnical engineers to contribute to goals of sustainable development through the recycling and re-use of waste materials and ground improvement, brownfield development projects (including re-use and retrofit of foundations), and creative uses and management of underground space.

The last 10 years have seen the emergence of tools for appraising and comparing the sustainability of projects through a series of indicator metrics (e.g., GeoSpeAR; [13]). There has also been a great deal of work on more quantitative tools that develop sustainability indices through the application of methods of Life Cycle Assessment (LCA—covering resource usage and environmental impacts over the lifecycle of a project) with classic Cost-Benefit Analyses (CBA—that addresses social and economic dimensions). LCA methods rely on indices such as embodied energy[17] to evaluate resource efficiency, and carbon or ecological footprint[18] to characterize environmental impacts, as described and illustrated by Shillaber et al. [33, 34]. Although the principles and framework of LCA have been formalized by the International Organization for Standardization [15], the U.S. has been slow to apply these methods in construction projects. The geotechnical community should play a much bigger role in this process, which has great potential to spur innovation in design and construction methods.

[17]Embodied energy of a material is defined as the sum total of all the energy required to produce that material.

[18]Ecological footprint of a project is the area of productive land required for executing different activities and for assimilating the emissions from such activities. Carbon footprint is an accounting tool that calculates the total emissions from different activities that lead to global climate change.

5 Management of Water Resources

According to the World Bank, if we continue with current water management practices against the backdrop of a growing world population, we will be facing a 40% shortfall between forecasted demand of water and available supplies by 2030.[19] This is against a setting of changing climate, which will increase the risks of flooding in some areas of the world, while inducing periods of drought in others. There is thus an urgency to improve water security via better management of our groundwater and surface resources.

5.1 Groundwater Resources

Groundwater is a vital global resource. In developing countries, and also for many communities in developed countries, groundwater is often the only viable source of drinking water [11]. Moreover, a majority of the world's irrigation needs are provided by groundwater [27]. In addition, there are many parts of the globe where groundwater supports industries key to the local economy. Despite recognition of the significance of groundwater to human, as well as ecological, well-being, many groundwater resources are being depleted at rates faster than natural recharge, and groundwater contamination, via industrial, agricultural and waste disposal practices, continues to be a serious problem. According to recent estimates, roughly one-third of the world's largest 37 aquifers are currently under stress [30], and factors such as climate variability, climate change and population growth are only projected to make matters worse. Geotechnical engineering research can contribute to better management of the world's groundwater resources in several areas, including:

Reversal of groundwater depletion. The United States Geological Survey (USGS) defines groundwater depletion as "long-term water level declines caused by sustained groundwater pumping". According to a 2013 report [17], groundwater depletion rates in the US are rapidly accelerating, with 25% of the total groundwater depletion since 1900 estimated to have occurred within the first decade of the 21st century, Fig. 8. Managed aquifer recharge, subsurface water banking and smart irrigation systems are all approaches that might help reverse groundwater depletion rates. However, to be effective, they require improved mapping of current aquifer resources and better understanding of aquifer recharge and storage capacities. Fundamental research in subsurface mapping technologies, including remote sensing and in situ monitoring methods, can contribute in this area. In addition, better understanding of the multi-scale impacts of large-scale aquifer recharge can be supported by advances in coupled deformation and flow modeling. Wireless sensor network technologies have enabled the next generation of real-time monitoring and control systems (the Internet of Things, IoT) that are now impacting geotechnical engineering practice. For example,

[19] http://www.worldbank.org/en/topic/waterresourcesmanagement.

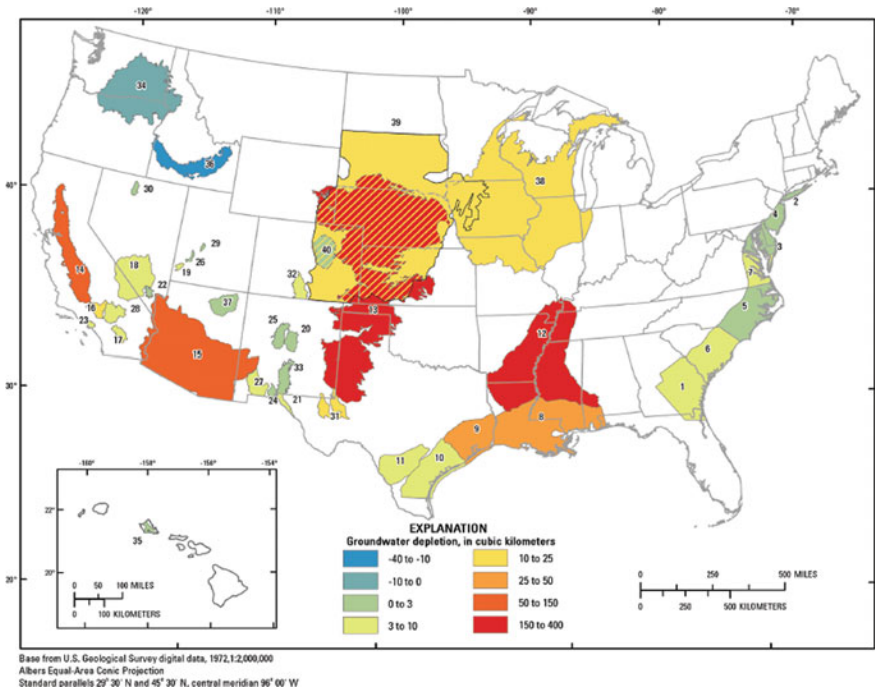

Fig. 8 Cumulative groundwater depletion 1900–2008 in 40 major aquifer systems in the US [17]

the Opti Platform,[20] has the potential to enable remote monitoring and smart, active control of crop irrigation systems at aquifer-basin scales.

Long-Term containment of contaminants and buried waste. There remain many instances where the extent of groundwater contamination or the hazard of buried waste is too great to make aquifer restoration technically or economically feasible with today's knowledge. Examples include operational units at the U.S. Department of Energy (DOE) legacy waste sites, such the Hanford 300 area—where 650,000 m^3 of groundwater are believed to be impacted by uranium contamination [45]. To prevent further degradation of groundwater resources, strategies for the safe, long-term containment of contamination and buried waste are required. Research on geochemical processes (Chapter 6 "Fundamental Research on Geochemical Processes for the Development of Resilient and Sustainable Geosystems") and coupled flow processes (Chapter 9 "Research Challenges Involving Coupled Flows in Geotechnical Engineering") can be helpful in improving the strategies and technologies for safe long-term containment of wastes and contaminants.

[20]Opti is an internet of things approach to manage distributed stormwater infrastructure—see: https://optirtc.com/products. It is part of an emerging suite of geoenvironmental approaches to "smart" water management.

Fundamental research that improves site characterization and the long-term monitoring of contaminant fate and transport can also support long-term containment of contaminants and buried waste, as can advances in the design and performance evaluation of new barrier systems, such as capillary barriers. Geotechnical engineers can also contribute, alongside others, to the development of publically acceptable approaches for the risk-based management of long-lived, in situ contamination and waste. Research needs in this area include probabilistic risk assessment tools that combine human and ecological risk, as well as the incorporation of multiple stressors, such as climate and land-use change, into risk assessment tools. In addition, geotechnical engineers can work alongside others on research to improve risk communication.

Pathogens in drinking water. The presence of fecal bacteria in groundwater remains a primary cause of diarrheal disease, an illness that impacts nearly 1.7 billion people per year and remains the second leading cause of death in children under five (World Health Organization, fact sheet No 330, 2013).[21] Access to safe drinking water is a key to preventing diarrheal disease. For the multitude of communities that rely on untreated groundwater as their potable water source, this requires strategies that stop fecal bacteria entering drinking water wells, as well as methods to detect bacteria at harmful levels once contamination is present.

Bacteria are micron-sized particles, often classified as colloidal particles, whose subsurface fate and transport are controlled by physical, chemical and biological interactions between the particles and the solid phase of the aquifer material itself. Despite almost half a century of research, robust models for predicting bacteria fate and transport remain elusive, with model predictions often grossly under-estimating the extent of fecal contamination detected at field sites [32]. As a result, the placement and management of groundwater wells in many communities is not protective of human health. Here, fundamental research is needed to improve understanding of the bio-geo-chemical processes mediating subsurface colloidal particle transport, from micrometer to kilometer scales. New, multi-scale modeling approaches for predicting colloidal particle transport are also needed, in addition to low-cost, in situ monitoring techniques for detecting fecal bacteria.

Emerging organic contaminants. Organic micro-pollutants are a class of emerging contaminants that can have adverse human and/or ecological health effects, and which have been widely detected in aquifers in the U.S., Europe and elsewhere. Organic micro-pollutants include nanomaterials, pesticides, pharmaceuticals, personal care products, caffeine and nicotine, among others. Unless specifically removed by waste water treatment processes, these synthetic contaminants can end up in receiving waters, including groundwater, that are a direct or indirect source of drinking water [23].

In a review of Emerging Organic Contaminants (EOCs) published by Lapworth et al. [19], the authors note that EOCs are likely to have long residence times (decades or more), and that future regulation of EOCs demands a better understanding of their spatial extend and behavior in both the vadose zone and groundwater. Here,

[21] http://www.who.int/en/news-room/fact-sheets/detail/diarrhoeal-disease.

geotechnical engineers can contribute to fundamental research that improves the detection, monitoring, modeling and remediation of EOCs in the subsurface.

5.2 Surface Water Resources

Surface water resources include water in rivers, streams, creeks, lakes and reservoirs. In the U.S. the primary use of surface water withdrawals is thermoelectric[22] followed by irrigation and then public water supply.[23] Management of surface water resources, both in the U.S. and elsewhere, frequently involves systems of dams and levees. These systems are not only integral to water management on the supply side, they are also often integral to flood management, as well as many energy supply systems. The vast majority of dams in the world are earth embankments: In the U.S. most of these are more than 50 years old, with close to 70% being managed by private owners. The U.S. portfolio of levees remains largely unknown, with estimates indicating up to 48,500 km of levees, which exceeds the circumference of the world. Only 10 U.S. states even keep a list of levees within their borders, and most states have no comprehensive levee safety program.[24] Given the tens of millions of people in the U.S. alone who live behind levees, and the likely increasing reliance on dam and levee systems to off-set water scarcity and manage flooding and sea-level rise under climate change, dam and levee safety and management is becoming a pressing challenge. Geotechnical research can contribute to several areas that fall under this specific topic, including performance under partly saturated soil conditions (Chapter 8 "Fundamental Challenges in Unsaturated Soil Mechanics"), something currently not considered in analysis and design methodologies for major levee systems.

Remote Inspection: Techniques for evaluating the conditions of dams, and most especially levees, that can enable remote inspection and monitoring are urgently needed to better understand the portfolio and conditions of these assets —now and into the future, Fig. 9. High-resolution image capture techniques, via satellite technology, unmanned aircraft and/or drones, coupled with advanced image processing offers promise in this area. As data banks of remote, and on-the-ground, inspection outcomes grow, statistical and machine learning techniques might also aid the prediction of conditions and settings that are more or less hazardous, enabling inspections to be prioritized. Collaborations between the geotechnical community, the remote sensing community and data-scientists could lead to significant advances under this topic area.

Evaluating Risk Under a Changing Climate: Climate change impacts are expected to lead to wetter conditions in some areas of the globe and dryer conditions in

[22] Water for thermoelectric power is used in generating electricity with steam-driven turbine generators.

[23] https://water.usgs.gov/edu/wusw.html.

[24] https://www.nap.edu/read/13393/chapter/5#59.

Fig. 9 A broken levee under repair in the Sacramento River delta (from [39]). California has more than 21,000 km of levees to protect dryland from floods

others. In addition, increased intensity of rainfall during precipitation events is also projected over many regions. These changes in hydrology are going to impact the conditions under which earthen dams and levees have to operate, so understanding when changing conditions lead to increased hazards is important for the protection of lives and property. Collaborations between climate scientists and geotechnical engineers, which can help introduce the non-stationarity of environmental conditions into geotechnical risk assessments, are needed to create climate-based hazards maps for dams and levees. Such maps can be used to help develop and prioritize adaption and mitigation strategies for assets and populations at risk.

Enhancing stability: Cost-effective methods for stabilizing, or extending the lifetime of, dams and levees are needed. The development of new physical, chemical and/or biological methods for enhancing earthen dam and levee stability can contribute to addressing this challenge. Here, collaborations between the geotechnical and material science community might yield innovative, new approaches. In addition, there is a need to develop new, and reliable, methods for injecting and mixing additives into large volumes of earthen materials. This will require improved understanding of complex fluid and soil behavior in porous systems at multiple scales and at varying degrees of saturation, as well as methods for monitoring the effectiveness of injection and mixing processes.

6 Over-Arching Challenges

The field of geotechnical engineering is defined by a set of common underlying challenges (after [26]), some of which were called-out in the preceding sections: (1) the incomplete or inadequate state of knowledge regarding subsurface conditions; (2) the resulting uncertainty in design and associated construction risks; (3) the increasing availability and need for better management of data; (4) the limited ability to predict engineering properties/behavior of complex geomaterials at the macroscale based on knowledge of their structure.[25] These challenges require long-term sustained research if major advances are to be achieved. The following paragraphs offer some perspectives for potential research in subsurface characterization, multiscale modeling of geomaterials, geotechnics and big-data, and handling of uncertainties and risk in design and construction.

Subsurface Characterization. Subsurface characterization is critical for all aspects of geotechnical engineering from site characterization, flow and transport processes, condition assessment, identification of subsurface resources and monitoring applications. As a result, geotechnical practice uses a wide range of invasive (drilling and sampling), non-invasive (geophysical and remote sensing)[26] and structural health monitoring techniques. Recent advances in geophysical imaging methods and remote sensing tools (notably in Interferometric Synthetic Aperture Radar [InSAR], Light Detection and Ranging [LIDAR] and Ground Penetrating Radar [GPR][27]), have addressed some of these topics and are useful for ground surface characterization as well. For example, InSAR enables high resolution mapping of ground displacements; i.e., 1 cm over large surface areas [10–100 km^2], while LIDAR is widely used to map landslide hazards. Similarly, new paradigms in wireless sensor networks and low-cost, low-power sensors have greatly increased the spatial and time resolution for structural health monitoring. However, there remain major challenges

[25] I.e., Interparticle forces and fabric (particle orientation and distribution).

[26] Often used in combination (e.g., seismic cone penetrometers).

[27] InSAR mainly uses spaceborne antennae, while LIDAR and GPR can be measured from airborne or ground stations.

in mapping subsurface stratigraphy, rock mass fracture systems and other geological features at scales that are important for geotechnical projects (such as urban tunneling) and geo-environmental projects (such as buried waste management). Advances in invasive techniques such as directional drilling also offer many intriguing opportunities to expand the capabilities of subsurface investigation. Sampling remains a critical component of site characterization that is essential for characterizing engineering properties. There have been few advances in technology in this field (with the noted exception of pressure coring used in offshore engineering) and new innovations are urgently required. Emerging sensor technologies are discussed in Chapter 2 "Advances in Geotechnical Sensors and Monitoring" of this book.

Engineering Properties of Geomaterials. Major advances in understanding the behavior of idealized granular materials (with particles of mm scale) have been achieved through combinations of experimental measurements (notably microCT scanning technology), numerical simulations (notably using Discrete Element Methods, after [7]) and multi-scale analyses that bridge between micro- and macro-scales (using hierarchical or concurrent modeling approaches). However, there remain major challenges in understanding the behavior of geomaterials with clay-sized particles. This is due, in large part, to the complex surface properties of these (sub-micron sized) particles and resulting surface/interfacial forces, as discussed in Chapter 3 "Soil Properties: Physics Inspired, Data Driven" and Chapter 4 "Linking Soil Water Adsorption to Geotechnical Engineering Properties". Advances in micro- and nano-scale imaging and testing capabilities (e.g., confocal microscopy, cryo-SEM, nano-indentation, Atomic Force microscopy) and molecular simulations methods (with specific force fields for clays; e.g., [8]) provide the basis for major advances in understanding the fundamentals of clay behavior. Further advances in characterizing properties for a broader range of geomaterials will require additional research relating to the 'geotechnical cycle' [5] including processes of diagenesis (lithification of sediments through compaction, precipitation of mineral cements and phase transformations), mineralization of organic matter, and formation of residual soil from weathering processes. Better understanding of the properties and characteristics of so-called "soft rocks" is also needed [16].

Geotechnics and Big-Data. As with many fields of research and practice, the role of "big-data" in geotechnical engineering is taking on increasing importance, although few results of geotechnical "big data" studies have been reported to date. The agglomeration of existing geotechnical data sets into common data bases offers enormous promise to improve understanding of the state of the subsurface, as well as the behavior of geo-materials under wide-ranging conditions. Data science methods can be used to agglomerate data sets, while new observation, sensing and monitoring techniques can be used to expand data bases and fill in data-gaps. Common data bases will also afford the geotechnical community with common platforms for model development, testing and validation. The application of advanced statistical analyses and machine learning techniques can also aid with development of new predictive methods that are based on a combination of statistically meaningful patterns in large data sets and fundamental geotechnical understanding.

Uncertainty and Risk. Geotechnical engineers are used to handling physical uncertainties associated with variability of natural geological materials (aleatoric) and with epistemic sources associated with incomplete measurements or model limitations [1]. Indeed, scales of physical variability in natural geological materials range from the micro-scale (e.g., particle and pore characteristics) to mega-scale features associated with geomorphological processes. The scales of variability are increasingly considered in geotechnical design, notably through random field representations [40] and Monte Carlo simulations. Micro-scale variability is also central to multi-scale modeling of material behavior and transport processes, while mega-scale variability has to date been principally linked to understanding rock mass behavior. There are many opportunities for further research to incorporate physical variability in geotechnical analyses. Chapter 5 "Multiscale and Multiphysics Modeling of Soils" addresses the multiscale and multiphysics modeling of geological materials, with an emphasis on soils.

Methods of probabilistic risk assessment are now well established within the geotechnical field, especially for seismic hazards. Other hazards (from landslides to flood events etc.) are closely linked to the consequences of climate change. The underlying assumptions of stationarity in the magnitude-frequency relationships for these events are clearly no longer valid [22] and hence, new non-stationary probabilistic models will need to be developed to enable more rational planning and design to mitigate these risks.

7 Conclusions

Several areas where geotechnical research can contribute to solving some of the pressing challenges of today have been highlighted: These include climate change, urban sustainability and resilience, the management of energy and material resources, and water resource management. Each of the following chapters in this book deals with topics that are relevant to the role of geotechnics in addressing key aspects of these four, global challenges. Over-arching themes that were also highlighted included the need for fundamental research to address issues associated with subsurface characterization and monitoring of complex geo-material behavior, multi-faceted, multi-scale processes, "big-data" and the management of uncertainty and risk. In addition, the need for geotechnical engineers to lend expertise and leadership to interdisciplinary research and development efforts aimed at protecting natural resources, infrastructure and human life in the face of stressors, such as climate change, rapid urbanization, global energy demands, resource depletion and water scarcity, was under-scored. The authors believe that the future of geotechnical engineering will require research advances within the field itself, as well as advances at the intersection of geotechnical engineering and a myriad of other disciplines, including those within the natural, social and computational sciences.

Acknowledgements This Book Chapter evolved from contributions made to a workshop entitled "Geotechnical Fundamentals in the Face of New World Challenges", held at the National Science Foundation, Arlington, Virginia, July 17th–19th, 2016. Funding for the workshop was provided by the National Science Foundation grant CMMI-1536733. Any opinions, findings, and conclusions expressed in this paper are those of the authors and do not necessarily reflect the views of any supporting institution. The authors would like to thank Dr. Ning Lu for his constructive review comments and feedback on the contents of this Book Chapter.

References

1. Baecher, G.B., Christian, J.T.: Reliability and Statistics in Geotechnical Engineering. Wiley (2003)
2. Birnal, P., Rashid, H. (Eds.): Climatic Hazards in Coastal Bangladesh. Elsevier Inc. (2016)
3. Brundtland Commision.: Our common future. UN Commission on World Environment and Development, p. 383. Oxford University Press (1987)
4. Chadwick R.A., Eiken, O.: Offshore CO_2 storage: sleipner natural gas field beneath the North Sea (Chap. 10). In: Gluyas, J., Mathias, S. (Eds.) Geological Storage of Carbon Dioxide (CO_2)—Geoscience, Technologies, Environmental Aspects and Legal Frameworks, pp. 227–250. Woodhead Publishing Ltd (2013). ISBN 978-0-85709-427-8
5. Chandler, R.J.: Clay sediments in depositional basins: the geotechnical cycle. Q. J. Eng. Geol. Hydrol. **33**, 7–39 (2000)
6. Chen, R., Zhang, L., Budhu, M.: Biopolymer stabilization of mine tailings. ASCE J. Geotech. Geoenvironmental Eng. 1802–1807 (2013). https://doi.org/10.1061/(asce)gt.1943-5606.0000902
7. Cundall, P.A., Strack, O.: The development of constitutive laws for soil using the distinct element method. Int. J. Numer. Anal. Meth. Geomech. **1**, 289–317 (1979)
8. Cygan, R.T., Liang, J.J., Kalinichev, A.G.: Molecular models of hydroxide, oxyhydroxide, and clay phases and the development of a general force field. J. Phy. Chem. B **108**, 1255–1266 (2004)
9. EPA.: Protecting water quality from urban runoff, United States Environmental Protection Agency, nonpoint source control branch report, EPA 841-F-03-003 (2013)
10. Falser, S., Uchida, S., Palmer, A.C., Soga, K., Tan, T.S.: Increased gas production from hydrates by combining depressurization with heating of the wellbore. Energy Fuels **26**, 2667–6529 (2012)
11. Feighery, J., Mailloux, B.J., Ferguson, A S., Ahmed, K.M., van Geen, A., Culligan, P.J.: Transport of E. coli in aquifer sediments of Bangladesh: implications for widespread microbial contamination of groundwater. Water Resour. Res. **49**(7), 3897–3911 (2013). http://doi.org/10.1002/wrcr.20289
12. Falagan, C., Grail, B.M., Johnson, D.B.: New approaches for extracting and recovering metals from mine tailings. Miner. Eng. **106**, 71–78 (2017)
13. Holt, D.G.A, Jefferson, I., Braithwaite, P.A., Chapman, D.N.: Embedding sustainability into geotechnics. Part A: Methodology. In: Proceeding of the Institution of Civil Engineers, vol. 163 no. 3, pp. 127–135 (2009)
14. IPCC.: Climate Change 2013: The physical science basis contribution of working group I to the fifth assessment report of the intergovernmental panel on climate change. In: Stocker, T.F., Qin, D., Plattner, D., Tignor, M., Allen, S.K., Boschung, J., Nauels, A., Xia, Y., Bex, V. and Midgley, P.M. (Eds.). Cambridge University Press, Cambridge, United Kingdom and New York, NY, USA (2013)
15. ISO.: International Organization for Standardization 1s0 14040:2006 (en): Environmental Management—Life Cycle Assessment—Principles and Framework (2016). www.iso.org/obp/ui/#iso:std:iso:14040:ed-2:v1:en

16. Kanji, M.A.: Critical issues in soft rocks. J. Rock Mech. Geotech. Eng. **6**(3), 186–195 (2014)
17. Konikow, L.F.: Groundwater depletion in the United States (1900–2008). USGS Sci. Inv. Rep. **2013–5079**, 75p (2013)
18. Klein, et al.: Integrating mitigation and adaptation into climate and development policy: three research questions. Environ. Sci. Policy **8**(6), 579–588 (2005)
19. Lapworth, D.J., Baran, N., Stuart, M.E., Ward, R.S.: Emerging organic contaminants in groundwater: a review of sources, fate and occurrence. Environ. Pollut. **163**, 287–303 (2012). https://doi.org/10.1016/j.envpol.2011.12.034
20. McNutt, M.K., Chu, S.M., Lubchenco, J., Hunter, T., Dreyfus, G., Murawski, S.A., Kennedy, D.M.: Applications of science and engineering to quantify nd control the deepwater horizon oil spill. PNAS **109**(50), 20222–20228 (2012)
21. MIT.: The future of geothermal energy: impact of enhanced geothermal systems (EGS) on the United States in the 21st century. Report prepared for Idaho National Laboratory, (2006). ISBN: 0615134386
22. Milly, P.C.D., Betancourt, J., Falkenmark, M., Hirsch, R.M., Kunzewicz, Z.W., Lettenmaier, D.P., Stouffer, R.J.: Stationarity is dead. Whither water management? Science. **319**, 573–574 (2008)
23. Murray, K.E., Thomas, S.M., Bodour, A.A.: Prioritizing research for trace pollutants and emerging contaminants in the freshwater environment. Environ. Pollut. **158**(12), 3462–3471 (2010). http://doi.org/10.1016/j.envpol.2010.08.009
24. National Academies Press.: Urban Stormwater Management in the United States, pp. 610. National Academies Press (2009)
25. Neri, A., Aspinall, W.P., Cioni, R., Bertagnini, A., Baxter, P.J., Zuccaro, G., Woo, G.: Developing an event tree for probabilistic hazard and risk assessment at Vesuvius. J. Volcanol. Geoth. Res. **178**(3), 397–415 (2008). https://doi.org/10.1016/j.jvolgeores.2008.05.014
26. NRC: Geological and geotechnical engineering in the new millennium: opportunities for research and technological innovation. In: Committee on Geological and Geotechnical Engineering, National Research Council, p. 222 (2006). ISBN: 0-309-65331-2
27. Ojha, R., Ramadas, M., Govindaraju, R.S.: Current and future challenges in groundwater. I: modeling and management of resources. J. Hydrol. Eng. 131023192005004 (2013). http://doi.org/10.1061/(ASCE)HE.1943-5584.0000928
28. Pu, B., Ginoux, P.: Projection of American dustiness in the late 21st century due to climate change. Sci. Rep. **7**, 5553 (2017). https://doi.org/10.1038/s41598-017-05431-9
29. Randolph, M.F., Gourvenec, S.: Offshore Geotechnical Engineering, pp. 347. Spon Press, NY (2011)
30. Richey, A.S., Thomas, B.F., Lo, M.-H., Reager, J.T., Famiglietti, J.S., Voss, K., Rodell, M.: Quantifying renewable groundwater stress with GRACE. Water Resour. Res., n/a–n/a. (2015) http://doi.org/10.1002/2015WR017349
31. Schaper, D.: 3 reasons Houston was a "sitting duck" for harvey flooding, NPR WNYC Radio (2017). http://www.npr.org/2017/08/31/547575113/three-reasons-houston-was-a-sitting-duck-for-harvey-flooding. Accessed 14 Oct 2017
32. Schijven, J.F., Hassanizadeh, S.M.: Removal of viruses by soil passage: overview of modeling, processes, and parameters. Crit. Rev. Environ. Sci. Technol. **30**(1), 49–127 (2000). https://doi.org/10.1080/10643380091184174
33. Shillaber, C.M., Mitchell, J.K., Dove, J.E.: Energy and carbon assessment of ground improvement works. I: Definitions and Background. J. Geotech. Geoenvironmental Eng. (2015a). https://ascelibrary.org/doi/10.1061/%28ASCE%29GT.1943-5606.0001410
34. Shillaber, C.M., Mitchell, J.K., Dove, J.E.: Energy and carbon assessment of ground improvement works II: working model and example. J. Geotech. Geoenvironmental Eng. (2015b). https://ascelibrary.org/doi/10.1061/%28ASCE%29GT.1943-5606.0001411
35. Schuur, E.A.G., McGuire, A.D., Schadel, C., Grosse, G., Harden, J.W., Hayes, D.J., Hugelius, G., Koven, C.D., Kuhry, P., Lawrence, D.M., et al.: Climate change and the permeafrost carbon feedback. Nature **520**(7546), 171–179 (2015)

36. Szulczewski, M.L., MacMinn, C.W., Herzog, H.J., Juanes, R.: Lifetime of carbon capture and storage as climate-change mitigation technology. PNAS **109**(14), 5185–5189 (2012)
37. US Energy Information Administration (US EIA).: International Energy Outlook (2017). www.eia.gov/pressroom/presentations/mead_91417.pdf, www.eia.gov
38. USGCRP Melillo, J.M., Richmond, T.C., Yohe, G.W., (Eds.): Climate Change Impacts in the United States: The Third National Climate Assessment. U.S. Global Change Research Program (2014)
39. Vahedifard, F., AghaKouchak, A., Robinson, J. D.: Drought threatens California's levees. Science **329**(6250), 799 (2015)
40. Vanmarcke, E.: Random fields: Analysis and Synthesis, 2nd edn. World Scientific Publishing Company Pte. Ltd., Singapore (2010)
41. Van Paassen, L.A., Ghose, R., van der Linden, T.J.M., van der Star, W.R.L., van Loosdrecht, M.C.M.: Quantifying biomediated ground improvement by ureolysis: large-scale biogrout experiment. ASCE J. Geotech. Geoenvironmental Eng. **136**, 1721–1728 (2010)
42. Vonk, J.E., Sánchez-García, L., van Dongen, B.E., Alling, V., Kosmach, D., Charkin, A., Semiletov, I.P., Dudarev, O.V., Shakhova, N., Roos, P., Eglington, T.I., Andersson, A., Gustafsson, Ö.: Activation of old carbon by erosion of coastal and subsea permafrost in Arctic Siberia. Nature **489**, 137–140 (2012)
43. Whittle A.J., Allen, M., Preis, A., Iqbal, M.: Sensor networks for monitoring and control of water distribution systems. In: Proceeding of the 6th International Conference on Structural Health Monitoring of Intelligent Infrastructure, Hong Kong, 13p (2013). http://www.ishmii.org/wp-content/uploads/2015/04/K07.pdf
44. World Energy Council.: World Energy Resources, Geothermal (2016). www.worldenergy.org/wp-content/uploads/2017/03/WEResources_Geothermal_2016.pdf
45. Zachara, J.M., Long, P.E., Bargar, J., Davis, J.A., Fox, P., Fredrickson, J.K., Yabusaki, S.B.: Persistence of uranium groundwater plumes: contrasting mechanisms at two DOE sites in the groundwater-river interaction zone. J. Contam. Hydrol. **147**, 45–72 (2013)
46. Zalasiewicz, J., Williams, M., Steffen, W., Crutzen,P.: The new world of the anthropocene. Environ. Sci. Technol. **44**(7), 2228–2231 (2010)

Advances in Geotechnical Sensors and Monitoring

Kenichi Soga, Amr Ewais, James Fern and Jinho Park

Abstract The recent advances in sensor and communication technologies are making significant impacts on the monitoring methods used for geotechnical engineering. This chapter introduces several emerging technologies that have shown to provide new types of dataset that were not available a decade ago. Technologies such as computed tomography scanning, environmental scanning electron microscope, microfluidics, particle image velocimetry and transparent soils are now used to observe the behavior of geomaterials under various changes in the surrounding environment at the laboratory scale. Computer vision technologies, distributed fiber optic sensing, LiDAR, wireless sensor network and satellite images produce data of high resolution and large spatial coverage at relatively low cost at the field scale. They can be used for life-time performance monitoring of geotechnical structures. The new dataset obtained from these new emerging technologies can be the catalysts to transform the geotechnical engineering methods used for risk assessment, design, construction and maintenance to a higher level.

Keywords Monitoring · Sensors · Communications · Emerging technologies

1 Introduction

Observing the behavior of geomaterials under changes in the surrounding environment (hydro-mechanical, chemical, thermal and more recently biological) has been one of the core activities of geotechnical engineering. There are two motivations why geotechnical engineers wish to monitor geotechnical-related processes.

Type I 'mechanism' monitoring: This activity is to monitor the behavior of geomaterials at different scales (from the particle scale to the field scale) so that new design and construction methodologies can be developed. This type of monitoring is often conducted in the laboratory (particle-scale characterization, element testing,

K. Soga (✉) · A. Ewais · J. Fern · J. Park
University of California, Berkeley, USA
e-mail: soga@berkeley.edu

N. Lu and J. K. Mitchell (eds.), *Geotechnical Fundamentals for Addressing New World Challenges*, Springer Series in Geomechanics and Geoengineering,
https://doi.org/10.1007/978-3-030-06249-1_2

and physical/centrifuge testing) and sometimes in the field (i.e., heavily instrumented sites). The ultimate goal is to make a step change in geotechnical engineering practice for improved safety, better economy and minimal damage to the environment.

The recent advances in microscopic imaging techniques (e.g., computer tomography scanning, particle image velocimetry) and testing methods (e.g., microfluidics, transparent soils) have enabled geotechnical engineers to observe the micro-particle scale behavior of a particle assembly of different solid minerals with various components (fluids, chemicals, biological organisms in various phases) inside the pores. This chapter introduces some notable achievements made in observing the microscopic behavior of geomaterials.

Type II 'performance' monitoring: This activity is to observe the actual performance of an operational geotechnical structure so that the risk of various uncertainties inherent to the site can be reduced. This type of monitoring involves monitoring during construction (e.g., the observational method) and ideally during its lifetime for better maintenance and improved safety against hazards (such as earthquakes, flooding). The ultimate goals are to extend the asset life and to reduce the management cost of the geotechnical structures that are monitored.

Although Type I mechanism monitoring has been the dominant one so far in geotechnical engineering, there is increasing interest and demand for Type II performance monitoring. This is driven by the societal demand for a better economy to manage aging geotechnical structures and improved safety of such structures against natural hazards and human-induced disasters. Sensing technologies are now becoming more affordable than before for large scale field implementation.

A list of conventional soil characterization and monitoring technologies currently used in geotechnical engineering is given in Table 1. Further details of these conventional technologies can be found in [10, 11, 21, 32]. The recent advances in sensor and communication technologies are making significant impacts on the monitoring methods used for geotechnical engineering. Table 1 also presents a selection of emerging technologies that may change the way soil characterization and monitoring are conducted in the future. Some are suitable for Type I mechanism monitoring, but others have potentials to be used for Type II performance monitoring. Emerging technologies that can potentially fulfill the latter role (e.g., satellite imaging, distributed fiber optic sensing, LiDAR and computer vision techniques) are introduced in this Chapter.

A detailed review of the emerging technologies listed in Table 1 is beyond the scope of this Chapter. For more information, readers are encouraged to check publications dedicated to sensors and monitoring such as [73, 93, 114].

Table 1 Soil characterization and monitoring technologies for geotechnical engineering

Parameters	Established technologies	Emerging technologies
Density	• Nuclear gauge • Ground penetration radar • Xray imaging	• Micro-Xray computed tomography scanning
Porosity	• Electrical resistivity (+tomography) • Nuclear magnetic resonance (NMR) • Mercury intrusion porosimetry	• Micro-Xray computed tomography scanning
Water content	• Nuclear gauge • Time domain reflectometry (TDR)	• Magnetic resonance imaging (MRI) • Frequency-dependent permittivity measurement
Soil fabric	• Scanning electron microscope (SEM) • 3D sectioning and reconstruction	• Micro-Xray computed tomography scanning • Transparent soil testing
Movement and displacements	• Linear variable differential transformer (LVDT) • Vibrating wire and foil strain gages • Extensometer and convergence gages • Inclinometer and tilt sensors • Crack meter • Electro-level sensors • (Robotic) Total station • Acoustic emission sensing	• Particle image velocimetry (PIV) or Digital image correlation (DIC) • Fiber Bragg grating (FBG) sensing • Distributed Fiber Optic Sensing • Shape accelerometer arrays • Differential Global Positioning System • Interferometric synthetic-aperture radar (InSAR) • Light Detection and Ranging (LIDAR) • Computer vision coupled with structure for motion (SfM) • MEMS-based systems
Stress/load	• Load/stress cell	• Tactile pressure sensor
Small strain stiffness	• Bender elements • Multichannel analysis of surface waves (MASW) • Spectral-Analysis-of-Surface-Waves (SASW)	• Fiber optic based distributed acoustic sensing (DAS) • Ambient noise tomography
Water pressure	• Piezometers • Pore pressure transducers	• Suction probes
Temperature	• Thermo-couples	• Fiber optic based distributed temperature sensing (DTS) • Thermal integrity testing
Acceleration	• Accelerometer • Geophones	• Fiber optic based distributed acoustic sensing (DAS)
Soil-Water interaction	• Sampling and chemical analysis	• Environmental scanning electron microscope (ESEM) • Microfluidics

2 Sensing and Monitoring at the Laboratory Scale

2.1 Computed Tomography (CT) Scanning

The earlier work of studying the behavior of grains in granular assemblies utilized radiography equipment used for medical application, but image-based techniques such as radiographic computed tomography (CT) scanning are now available to perform detailed microscopic-scale studies of granular assemblies (e.g., [111]). A work on CT scanning of specimens in triaxial compression tests was presented by Desrues et al. [19], who showed that the void ratio in shear bands reached a unique value locally. Although this work was pioneering, CT scans at that time could not distinguish individual grains or small granular assemblies. Using the latest CT technologies, it is now possible to track the kinematics of individual grains (e.g., [7]), grain orientation (e.g., [20, 33]), and the number of inter-granular contacts (e.g., [26]).

High resolution CT scans and imaging (e.g., Micro-Xray CT scanning) are used to conduct 3D studies of individual grains. Karatza et al. [41] studied the behavior of individual grains crushed inside shear bands. Druckrey et al. [22] improved the image processing of synchrotron micro-computed tomography (SMT) scans to monitor the evolution of strain localization at the particle scale. Zhao et al. [122] carried out CT scans to study the breakage of an individual grain and were able to track the formation of fragments, as shown in Fig. 1.

CT scanning has also been used to explore the deformation and failures patterns of soils in different states. For example, Higo et al. [34, 35] observed the failure patterns of Toyoura sand specimens compressed in triaxial compression in dry, saturated and unsaturated states and showed that partial saturation favored the development of shear bands. Bruchon et al. [14] monitored the changes in homogeneity of an unsaturated sand specimen during imbibition. Viggiani et al. [111] visualized the progression of freezing inside a kaolin specimen (Fig. 2). Sato and Ikeda [87] monitored the pore fluid diffusion phenomena in porous media by tracking the movement of solid grains. Matsumura et al. [58] used X-ray tomography imaging of natural gravel specimens to create synthetic gravel-size resin specimens using 3D printer (Fig. 3). Triaxial

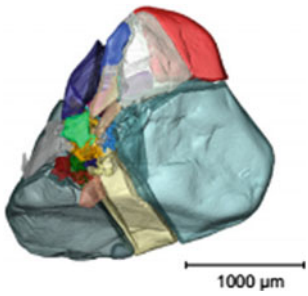

Fig. 1 3D CT-scan of a crushed grain [122]

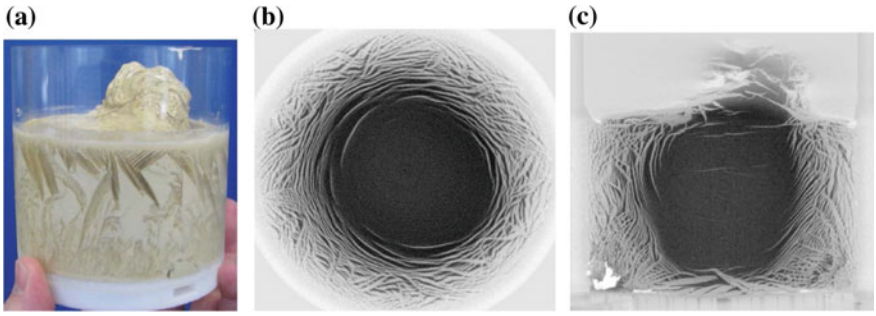

Fig. 2 CT scan of frozen kaolin: **a** photograph of specimen, **b** horizontal cross section and **c** vertical cross section [111]

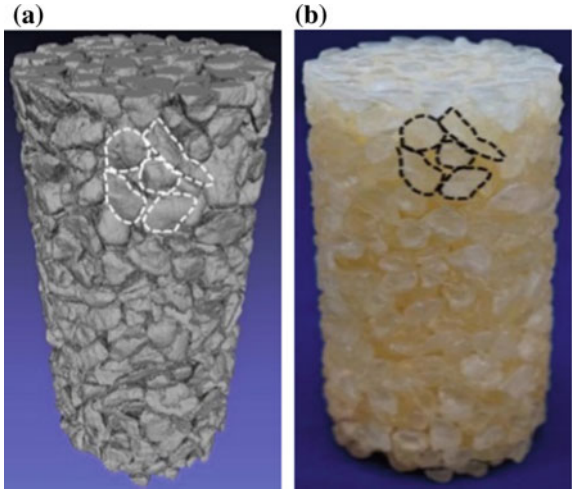

Fig. 3 3D image of **a** original unbonded gravel specimen and **b** synthetic specimen using 3D printing technology [58]

compression tests were performed on original gravel specimens and the synthetic specimens, and the results were compared.

Although the accuracy and resolution of CT scans have significantly improved in the past years, the scanned volume is still small to observe the particle scale behavior of soils. Tests have to be paused to scan the specimen and creep may occur during this period, which in turn affects the data interpretation. Further advances in the CT technology are expected to overcome these issues.

2.2 *Environmental Scanning Electron Microscope and Microfluidics*

Scanning electron microscope (SEM) is used in geotechnical engineering to investigate soil structure in its dry state. The environmental scanning electron microscope (ESEM) is an imaging technique that permits the visualization of soil grains and their structure in the presence of water [83]. Lourenco et al. [55] obtained ESEM images at inter-granular contact in which the meniscus is visible (Fig. 4). They showed that not all the pore water was at inter-granular contact, but some water droplets were located in grain dips. Romero et al. [84] used ESEM to investigate the different scales of porosity and the form of menisci in the voids. Manca et al. [59] used ESEM to study the distribution of macro and micro-pores in sandy soils, giving insight into the inhomogeneity.

Microfluidic technology enables manipulation of small amounts of fluid using channels of tens to hundreds of micrometers [119]. The channels are built into a small device, called a microfluidic chip. Microfluidics has revolutionized fundamental and applied research to investigate and observe small-scale physical, chemical, and biological processes in the fields of chemical, biological, medical and environmental engineering (e.g., [53, 107]). Soft lithography technology, which utilizes the advances in microanalytical methods and microelectronic circuits, creates microfluidic chips based on patterned elastomeric polymers [117].

Wang et al. [115] fabricated a microfluidic chip that replicated key features of the porous matrix of sandy soil as shown in Fig. 5a, b. The surface properties such as wetting properties (hydrophobic and hydrophilic) and charges (positive and negative) can be varied using different surface treatment technologies. Wang et al. [115] used this microfluidic chip to observe the particle scale behavior of microbial-induced calcite precipitation process. The observation of nucleation and crystal growth inside the porous medium was made to find the mechanisms responsible for the development and spatial distribution of calcite at the particle scale, as well as by estimating possible reasons for the formation of different types, sizes, and amount of calcite (Fig. 5c, d).

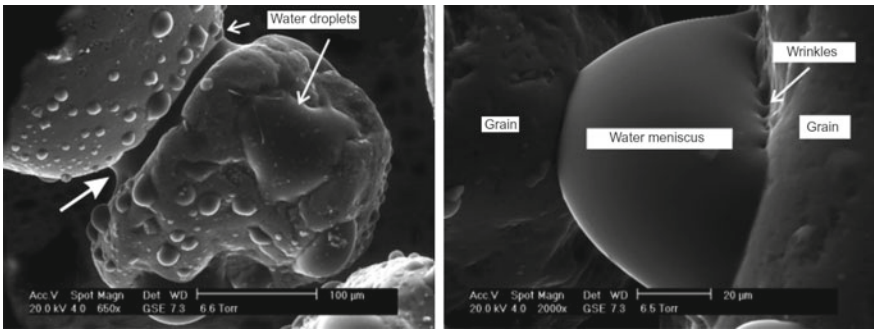

Fig. 4 ESEM image of water meniscus/droplets on soil [55]

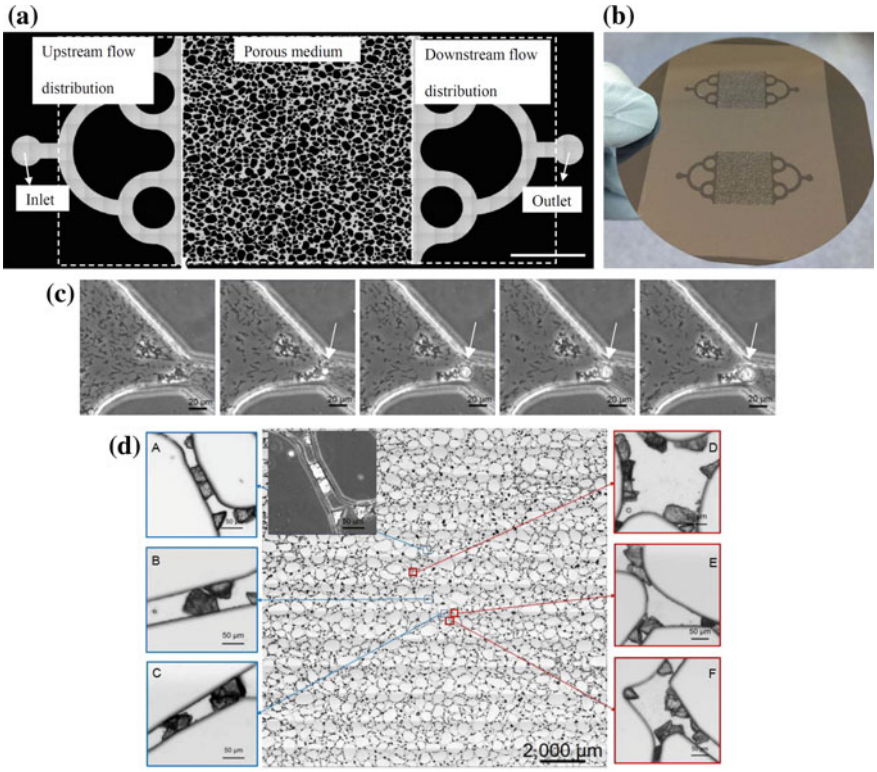

Fig. 5 **a** Microfluidic pattern, **b** Manufactured microfluidic chip, **c** movement of bacterial and calcite precipitation process at a pore throat, **d** calcite particles in pore space

2.3 Particle Image Velocimetry or Digital Image Correlation

The recent advances in photogrammetry-based movement tracking techniques, including particle image velocimetry (PIV) (as part of digital image correlation (DIC)—see Sect. 3.2), offer new sensing opportunities for laboratory scale measurement of soil deformation. PIV was originally developed for fluid mechanics [3]. It consists of taking a series of photographs in sequence and calculating the velocity field by comparing them. PIV was made popular in geotechnical engineering by White et al. [118] thanks to the falling prices and increasing image quality of digital cameras.

PIV is an alternative to radiography, which is difficult to carry out in large physical model tests. Teng et al. [104] used two sets of cameras to obtain large and small scale measurements and demonstrated the usefulness of the technology for centrifuge testing of a foundation footing with images of 'macro' failure mechanism and 'micro' scale deformation. Tran et al. [106] developed new image processing technologies to increase the accuracy of the measurements and demonstrated its performance by

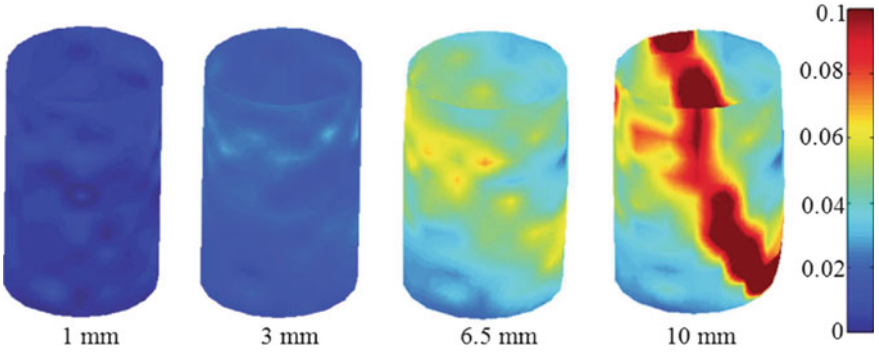

Fig. 6 Contour plot of vertical strains of an unsaturated sample of soil in which a shear band has developed [49]

measuring the surface roughness of the kaolin samples. There are also attempts to use PIV to measure the local deformation of unsaturated soil specimen in triaxial test (i.e., [49, 86]). Figure 6 shows the contour plots of vertical strain inside an unsaturated sample, showing the development of a localized shear band.

Some technical difficulties exist with the currently available PIV algorithms for dealing with rotation and large deformation of the material. Pinyol and Alvarado [77] developed a new algorithm dedicated to large deformation granular flows, whereas Stanier et al. [96] improved the algorithm for rotating and deforming objects. Other issues ranging from camera noise to image analyses have been discussed by Take [100].

PIV is restricted to measurements at the 'observable' boundary of the model, where photos can be taken. It is therefore only possible to apply this technique to planar models, which can be the top surface of the model or a cross-section obtained by truncating the model with a transparent panel. Take [100] pointed out that it was possible to obtain a 3D PIV image by using two cameras. However, the third dimension is only obtained by interpolation of the boundary measurement without any direct measurement of the movements within the soil. Some researchers have overcome this issue by using transparent soil (see next Section) and creating a 2D cross-section with a laser [52, 67]. De Cataldo et al. [18] used fluorescent markers and tracked the movements in three dimensions (see Fig. 7).

2.4 Transparent Soils

Transparent soil is a mixture of solid particles and saturating fluids that have the same refractive index [36, 37, 39]. Solid particles that can be used as transparent soils are shown in Fig. 8. The saturating fluids are either oil-based or water-based mixed with mineral oils and/or organic chemicals. Kong et al. [47] studied 19 mixtures of

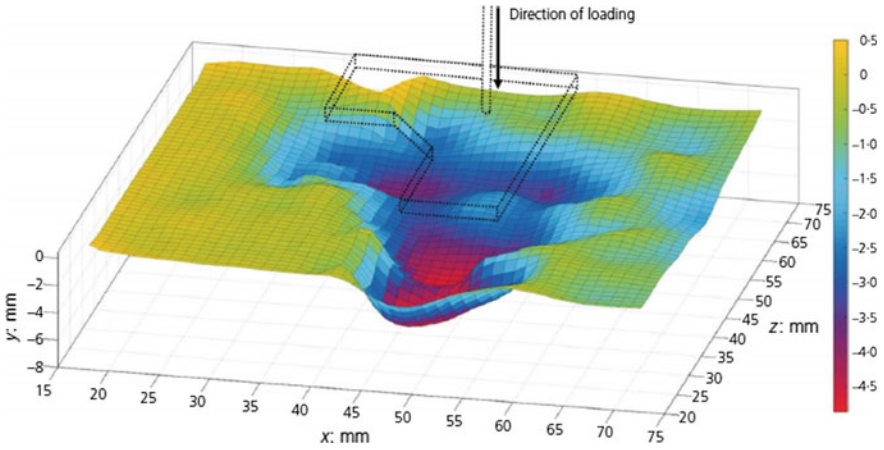

Fig. 7 Three dimensional surface deformation obtained from PIV with fluorescent markers [18]

saturating fluids for transparent soils. Some fluids are hazardous and may degrade materials in contact such as latex membranes used in triaxial tests [24, 123]. It may have a higher viscosity than that of natural pore fluid, and the refractive index may change with temperature. Careful selection of materials for a given aim of the research is necessary.

Iskander and Liu [38] proposed that the movement of soil particles within the transparent soil could be done using laser light sheets to slice the soil and adapting PIV, as shown in Fig. 9. Transparent soil allows the visualization of internal movements within the soil mass. Transparent soils have been used for different geotechnical, geoenvironmental and geoenergy applications. These include (i) soil deformations underneath footings [38], (ii) unsaturated soil [74], (iii) quicksand [27] (iv) grout injection in soils [28], (v) geogrid soil reinforcement (Fig. 10., [12, 24, 25]), (vi) soil-pile interaction [46], and (vii) soil-projectile interaction [69]. See also transparent soil wiki (wp.nyu.edu/ts).

2.5 Pressure Sensors

Although there have been notable advances in movement measurements (strain, displacement, velocity, and acceleration) in the past decade, measurement of forces, stresses and pressure remains to be challenging, and there are ongoing developments. For example, Talesnick [101] developed the null soil pressure system to remove the compliance of the soil pressure sensor.

Tactile pressure sensor (Fig. 11) is used in physical model experiments to measure a profile of pressure over a certain area rather than a conventional load cell, which provides measurement at a given point in space [72]. Palmer et al. [71] reviewed

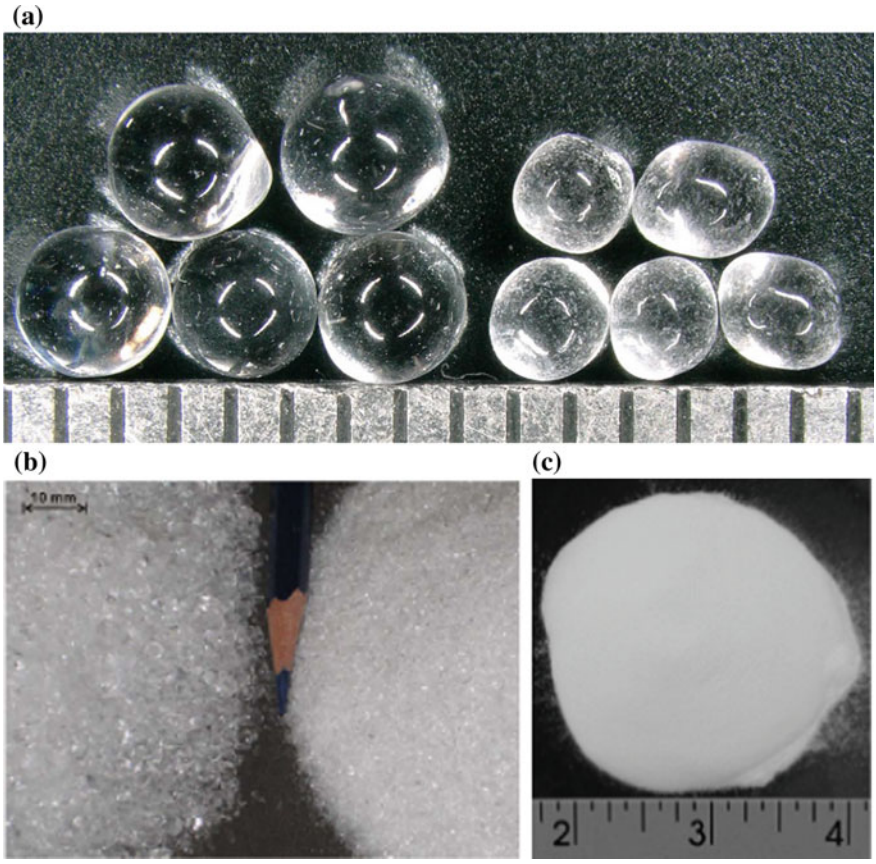

Fig. 8 Photos of different types of transparent soil solid particles: **a** spherical fuse quartz particle for transparent sand (1 mm division) [45], **b** crushed fused quartz particles for transparent sand [24] and **c** Laponite for transparent clay [17]

the use of tactile pressure sensors for soil-structure interaction studies. El Ganainy et al. [23] and Muszynski et al. [66] used tactile pressure sensors to measure earth pressures in centrifuge tests and showed that these sensors could be effectively used, even though the data requires some processing to take into account the interaction between the sensor and the soil.

Investigating the mechanics of unsaturated soils has been one of the hot topics of geotechnical engineering research in the past decade. Compared to the measurement of positive pore pressures, measurement of soil suction is proven to be difficult, especially in the field. Although matric suction can be accurately measured and controlled in the laboratory (Fig. 12), reliable field measurements are still challenging [56]. Rahardjo and Leong [79], Tarantino et al. [103] and Toll et al. [109] reviewed various techniques for measuring suction.

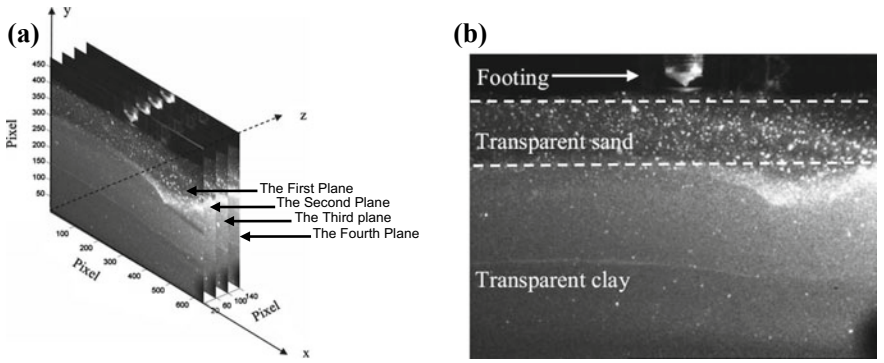

Fig. 9 **a** Visualization inside a transparent soil model at different vertical planes using laser light sheets, **b** tracking the particle level movement of transparent soils by a footing along the second plane [36]

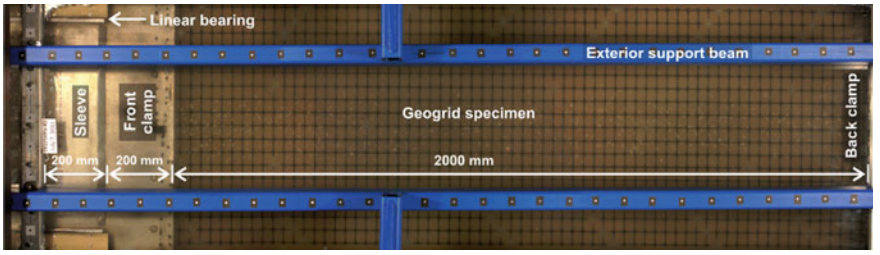

Fig. 10 Image of a geogrid embedded in transparent soil in a large pullout box apparatus. Note that the geogrid can only be seen because the soil is transparent [12]

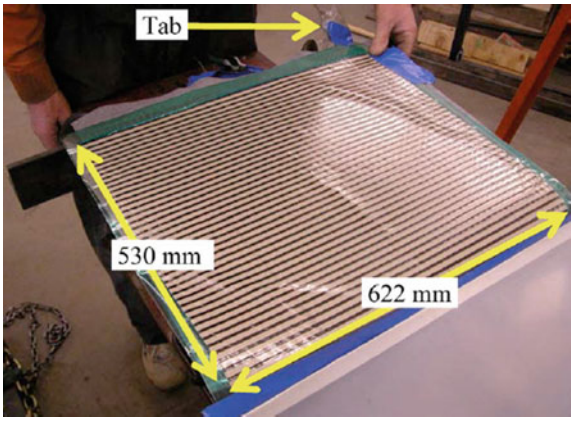

Fig. 11 A tactile pressure sensor [71]

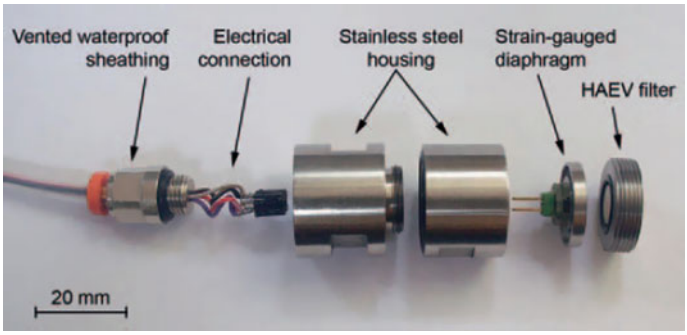

Fig. 12 A high-capacity tensiometer [108]

3 Sensing and Monitoring at the Site Scale

3.1 Fiber Optic Sensing—Point and Distributed Sensors

By using the light scattering feature of optic fiber, different types of fiber optic sensors have been invented in the past three decades to measure strain, temperature, vibration, and humidity. The development of fiber optic sensor goes in two directions: point sensor and distributed sensor.

Fiber Bragg grating (FBG) sensor is a well-established fiber optic-based point sensor. It provides highly accurate measurement of strain or temperature through the refractive index grating on the fiber core. FBGs are fabricated by photolithography using a grating mask-covered UV light, as shown in Fig. 13a. The distance between each grating is selected by a wavelength of the light that is designed to be reflected. When the temperature or strain changes in the fiber, the spacing of the grating changes. This in turn changes the wavelength of light that is scattered. By measuring the wavelength, the temperature or strain at that point can be deduced. Normally the resolution is less than 1 $\mu\varepsilon$. The multiple points on a single fiber can be achieved by distributing different wavelength ranges at different points. At present, FBG sensor is a popular point sensor because of its wide application in many disciplines [29].

Distributed Fiber Optic Sensing (DFOS) is one of the emerging technologies for monitoring geotechnical structures at the site scale (e.g., [42, 91, 92]). When a light wave travels through an optical fiber, it interacts with the constituent atoms and molecules, and the light is forced to deviate from a straight trajectory due to their non-uniformity. This deviation creates back scattering that brings a very small portion of the beam to go back to the source. When a fiber experiences a strain or temperature change, there is density fluctuation, which in turn changes the characteristics of the back scattered beam. DFOS technologies use these changes in the recovered beam to quantify strain, temperature or vibration occurring along the standard optical fiber cable. By attaching an optical fiber cable to a geotechnical structure or embedding it

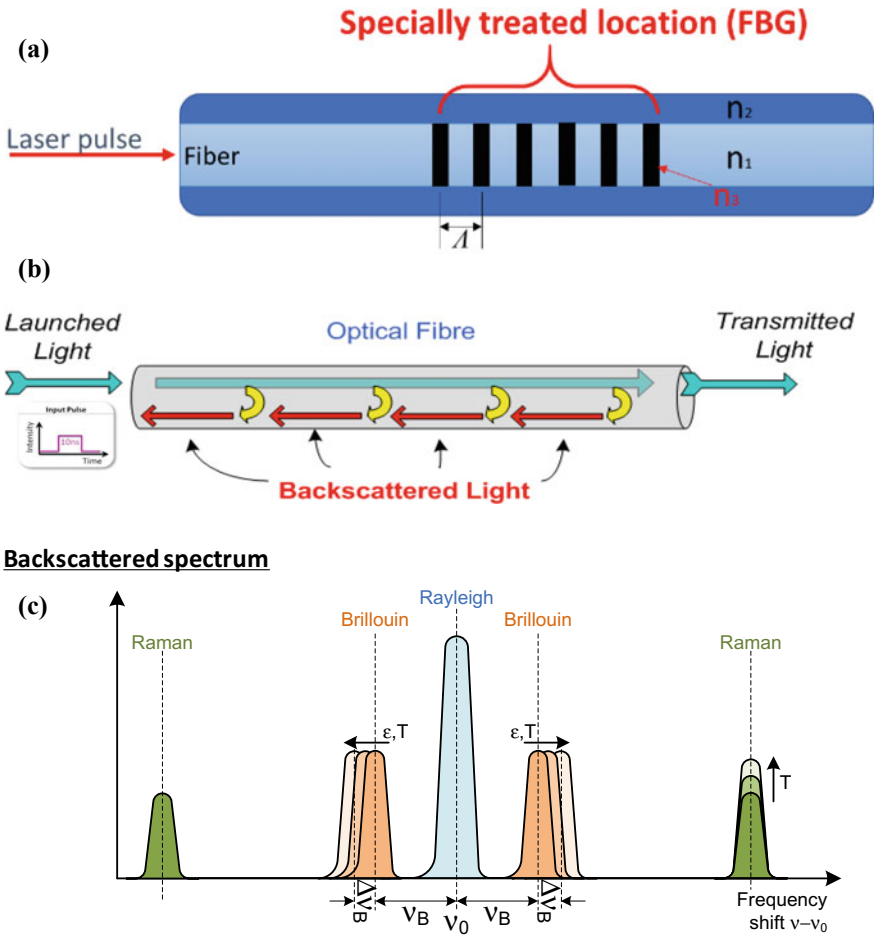

Fig. 13 **a** Fiber Bragg grating, **b** Backscattered lights from different locations of fiber and (c) three scattering modes

inside a structure or soil, it is possible to monitor the changes of ambient parameters of the monitored object.

When light is launched from one end of the fiber, backscattered lights are generated at every point of the fiber as shown in Fig. 13b. A backscattered light coming back earlier in time is the one close to the original launching point. The location of each backscattered light can be evaluated by the recorded flight time and the speed of light. For each backscattered light coming back from a given location along the fiber, a frequency profile is plotted as shown in Fig. 13c and this is used to evaluate the strain/temperature/vibration at every location along the fiber. A DFOS analyzer measures physical quantities (such as temperature, strain, and vibration) of the fiber continuously (e.g., 5 cm reading interval) along its length for long distance (e.g., a

few to tens of kilometers) due to its low-loss characteristic. Typical resolutions are 10–30 με for strain and 0.1–1 °C for temperature [92].

Figure 13c shows the frequency bands of three types of scattering (Rayleigh, Brillouin, and Raman), in relation to the frequency of input light. Different types of analyzer detect different scattering signals differently. Rayleigh scattering based Distributed Acoustic Sensing (DAS) system detects ambient vibrations for seismic surveying. Raman scattering is used to measure the temperature profile along a fiber optic cable, whereas Brillouin scattering is used to measure the strain and temperature profiles. Distributed temperature sensing system (DTS) is a Raman scattering based system, which can be used for power cable and transmission line monitoring, fire detection, leakage detection at dikes, dams, and sewers. It is widely used in downhole temperature monitoring of oil and gas wells. Brillouin scattering based techniques such as time domain techniques called 'Brillouin optical time-domain reflectometery (BOTDR)' and 'Brillouin optical time domain analysis (BOTDA)' are used for distributed strain measurement.

The main advantage of DFOS is its high sensitivity over large distances (a few to tens of kilometers) and the ability to interface with a wide range of measurands in a distributed manner (data samples of every 2 cm to 1 m). The system provides thousands of strain gauges, thermo-couples, or accelerometers along a single fiber optic cable, which results in a low-cost monitoring solution considering the density of the data obtained. As the loading patterns on geotechnical structures such as retaining walls, underground structures, tunnels, and pipelines are often a distributed load, the distributed nature of movement measurement is attractive in geotechnical engineering. Moreover, the deterioration rate of the glass optical fiber material is slow. Hence it is considered to be an ideal measurement method for long-term monitoring by embedding it into structures. Figure 14 shows photos of fiber optic cable installation in different geotechnical structures.

Mohamad et al. [63] used DFOS to examine the performance of an old masonry tunnel during the construction of a new tunnel beneath it in London. Fiber optic cables were attached along the intrados of the tunnel lining, recording the relative strains of tunnel deformation and detecting localized strain such as cracking in the masonry tunnel (Fig. 15). Flexural behavior along the longitudinal section of the tunnel was examined by measuring strain along the springlines and crown. Pelecanos et al. [76] used DFOS to provide a continuous strain profile within a test pile, offering more confidence in determining the shaft friction profiles along the pile at different pile loads. The dataset was used to estimate the shaft friction development curves with the applied load or vertical displacement (i.e., load-transfer relationship) (Fig. 16). The continuous strain measurements provided the condition assessment of the entire pile, and hence any localized regions of weakness, shaft area inhomogeneity, or strain concentration could potentially be detected. Rui et al. [85] used the DFOS technology to measure the changes in concrete curing temperature profile inside a pile. The dataset was used to infer concrete cover thickness through modeling of heat transfer processes from the concrete to the adjacent ground. The shape of the pile was estimated from the thermal data as shown in Fig. 17.

Fig. 14 Installation of optical fiber cables for monitoring distributed strains in pile, tunnel and diaphragm wall

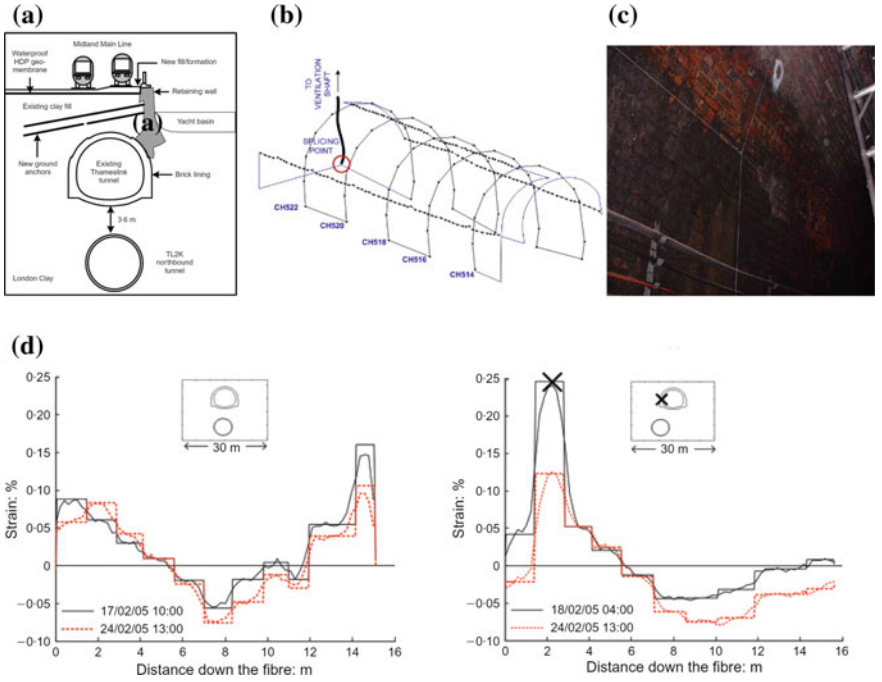

Fig. 15 DFOS monitoring of an old tunnel affected by a new tunnel construction underneath. **a** Geometry, **b** Cable attachment diagram, **c** FO cable installation, **d** strain development around the old tunnel [63]

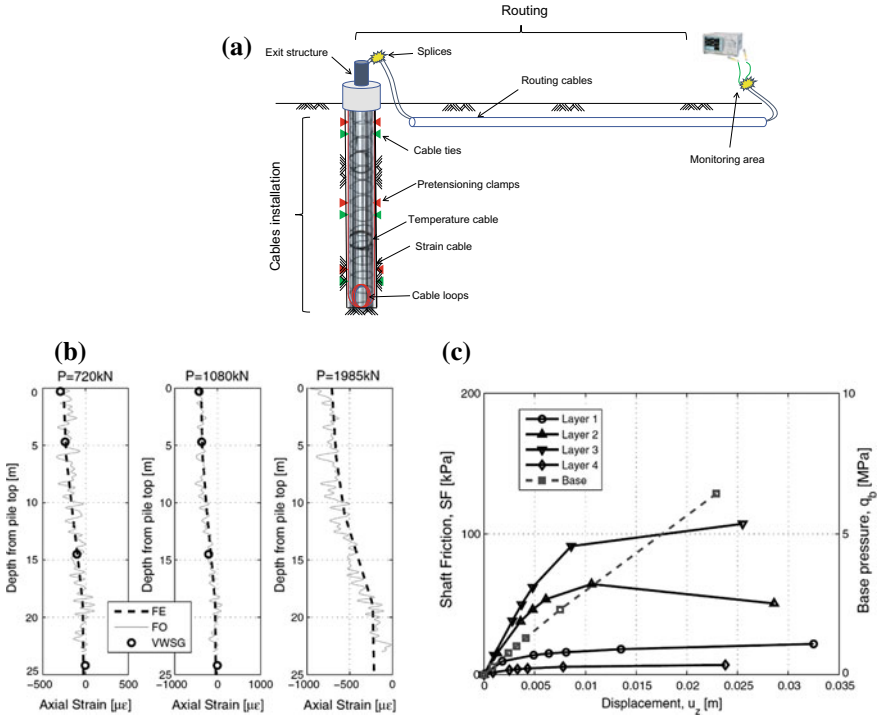

Fig. 16 DFOS monitoring of a test pile **a** Geometry, **b** Strain profiles at different loads, **c** evaluated shaft friction and displacement curves [76]

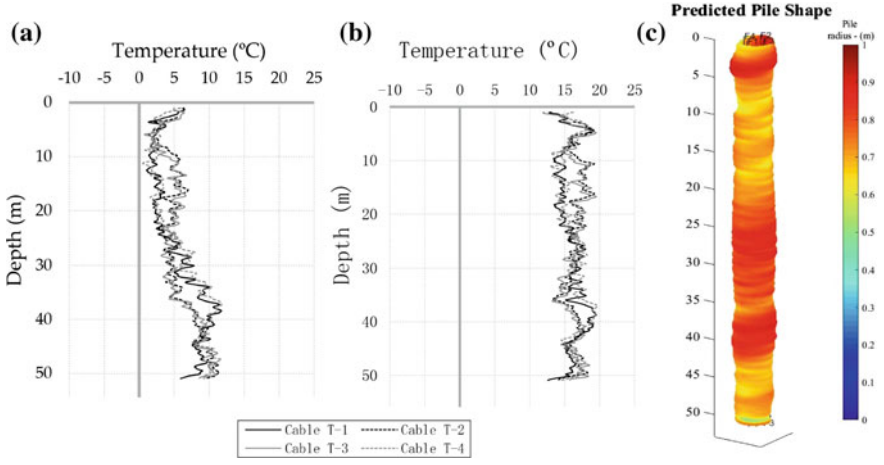

Fig. 17 DFOS monitoring of a cast-in-place pile during hydration **a** distributed temperature profile rising during hydration, **b** peak temperature profile and **c** estimated pile shape [85]

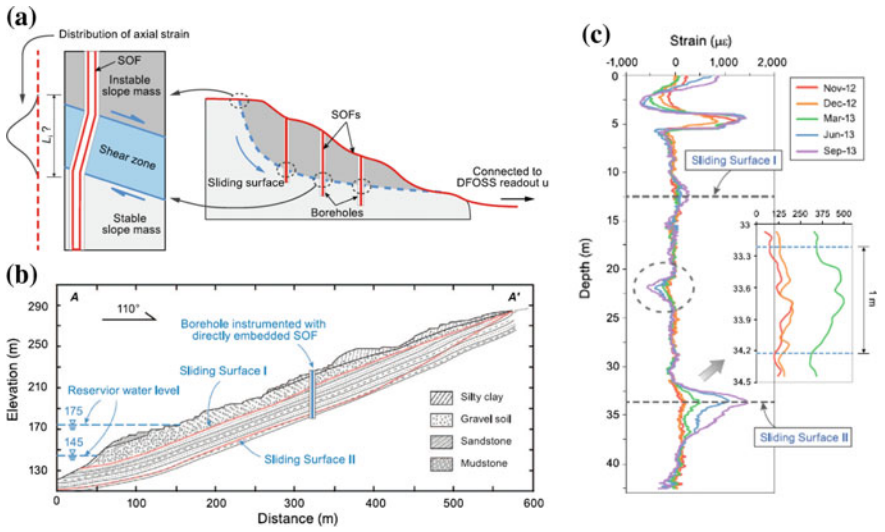

Fig. 18 DFOS monitoring of slope movements **a** detection of sliding shear zone, **b** DFOS instrumented slope of the Majiagou landslide, **c** Distributed strain profiles over a 1 year period, showing the locations of sliding surfaces [121]

The DFOS technology can also be used to monitor landslides. Zhang et al. [121] show its usage for identifying sliding direction, shear zone width and the magnitude of shear displacement as shown in Fig. 18. They used this technology for monitoring the movement of Majiagou landslide in Three Gorges Reservoir region, China. The distributed strain measurements captured two sliding surfaces of this landslide: (i) at the contact between surface deposits and bedrock and (ii) the main sliding surface occurring within the bedrock. The monitoring results show that the landslide responded more to the fluctuation of the reservoir water level than to rainfall.

Other examples of DFOS technology applications on geotechnical structures include (i) pipeline monitoring [50, 62, 68, 113], (ii) ground movements [40, 95, 120, 121], (iv) performance monitoring of soil retaining wall [64, 88–90], (vi) tunnel movement monitoring [1, 16, 30, 31, 44, 63, 65], and (vii) pile performance monitoring [13, 43, 75, 76].

Further details of this technology can be found in [42, 91, 92].

3.2 Digital Image Correlation (DIC), Structure from Motion (SfM) and Change Detection

Recent advances in digital image quality have reached to the stage of renewing existing surveying techniques. The use of DIC (or PIV) does not need to be limited to laboratory environments (see Sect. 2.4). It has been implemented in the field for

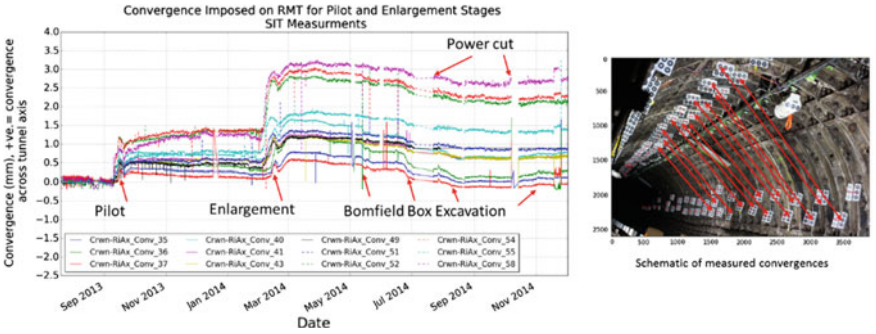

Fig. 19 Convergence monitoring of an existing tunnel affected by other nearby underground construction in London [5]

structural health monitoring of infrastructure assets. Challenges in the field become more rigorous than in the laboratory when considering the real-world illumination conditions. Lighting is non-homogeneous due to the varying usage of flashlights, and shadows and darkness are observed in local areas.

The most common application of DIC has been on bridge monitoring with deployment over a short period and for applications that need high levels of frequency of images, such as vibration monitoring (e.g., [60]). Alhaddad et al. [6] show the use of DIC for monitoring a distortion of an old tunnel subjected to a new tunnel construction nearby (see Fig. 19). The displacement resolution is shown to be better than 0.012 mm for convergence and 0.008 mm for the radius of curvature (ROC) measurement.

3D point cloud-based image mosaicing and model reconstruction are accomplished based on multiple overlap 2D images with various camera position using the technique called Structure from Motion (SfM) (Fig. 20a). A 3D model construction algorithm typically starts with the SIFT matching algorithm to extract features and their associated descriptor vectors for each image [54] (Fig. 20b). The object appearing in the image can then be constructed as a three-dimensional one using surveying technique. Figure 20(c) and (d) shows 3D point cloud models of tunnels and rock slopes made from their images.

3D point clouds were created to measure ground movements after a landslide in a residential suburb in the City of North Salt Lake, Utah in August 2014 [80]. After the landslide occurred, an unmanned aerial vehicle (UAV) was used to capture 700 photographs of the landslide from the air at two different times (8 months apart). Figure 21a, b show the 3D point cloud models of the two acquisition times, and Fig. 21c gives the displacement vector amplitudes by comparing the two point cloud datasets (see Sect. 3.3 for the challenges to achieve this). The largest computed displacements (2–3 m) occurred at the edges of the main scarp, and these areas represent zones of sloughing that occurred between the acquisition of the two sets of images.

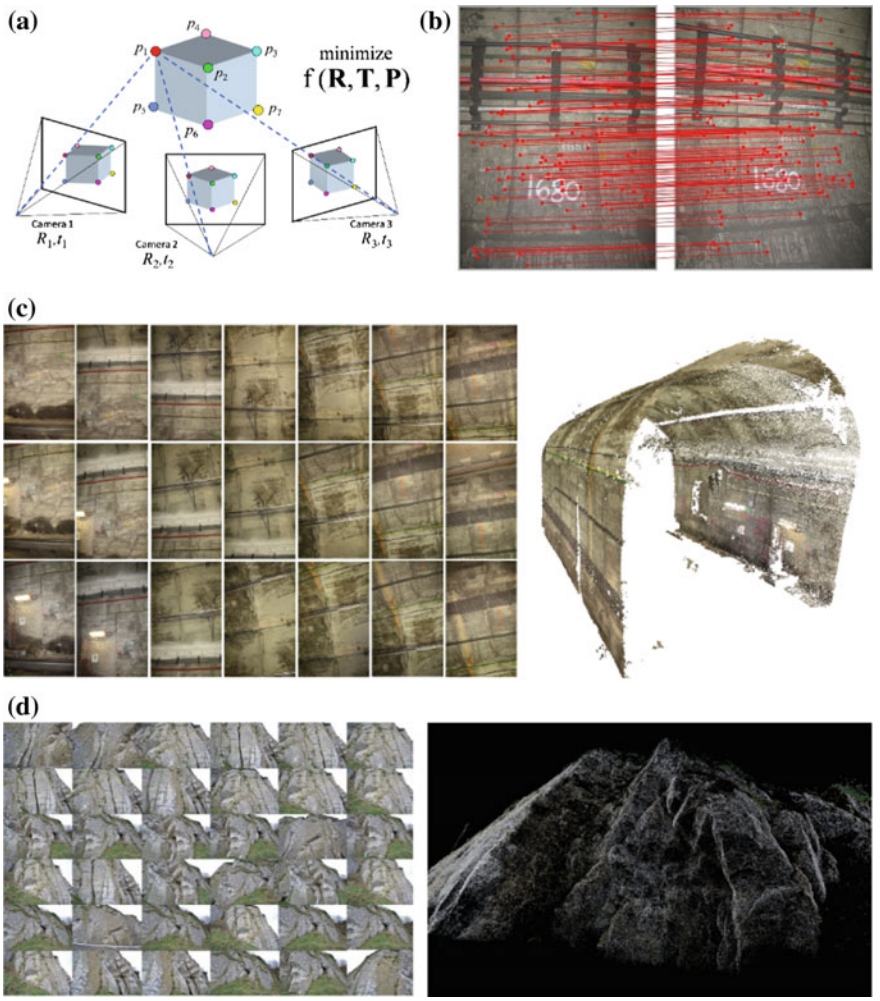

Fig. 20 **a** Structure-from-Motion (SfM) concept to create a 3D model, **b** SIFT matching algorithm to identify the same points in two images, **c** 3D construction of a Barcelona Metro tunnel [15] and **d** 3D construction of a rock slope in Northern Ireland [98]

Visual inspection is one of the maintenance works of civil engineering structures to detect abnormalities such as cracks. Comparing the two images can be difficult because the camera positions are different. However, if these images are linked to the three-dimensional model, it is possible to digitally transform the two images as if they were taken from the same location. Stent et al. [99] proposed a tunnel change detection system for detecting, localizing, clustering and ranking visual changes on tunnel surfaces (Fig. 22a). A 3D model of a tunnel in London is created using a series of images taken from the inside (Fig. 22b). A 3D point cloud of a tunnel was

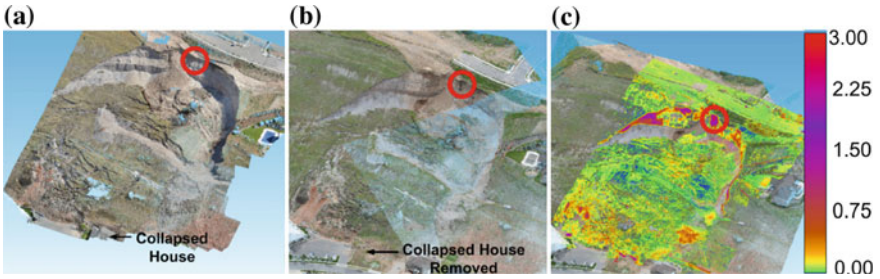

Fig. 21 A SfM 3D model of a landslide in the city of North Salt Lake in Utah **a** Soon after the slide in August 2014, **b** 9 months later in May 2015, **c** Displacement magnitude contours (in meters) by comparing the two 3D models [80]

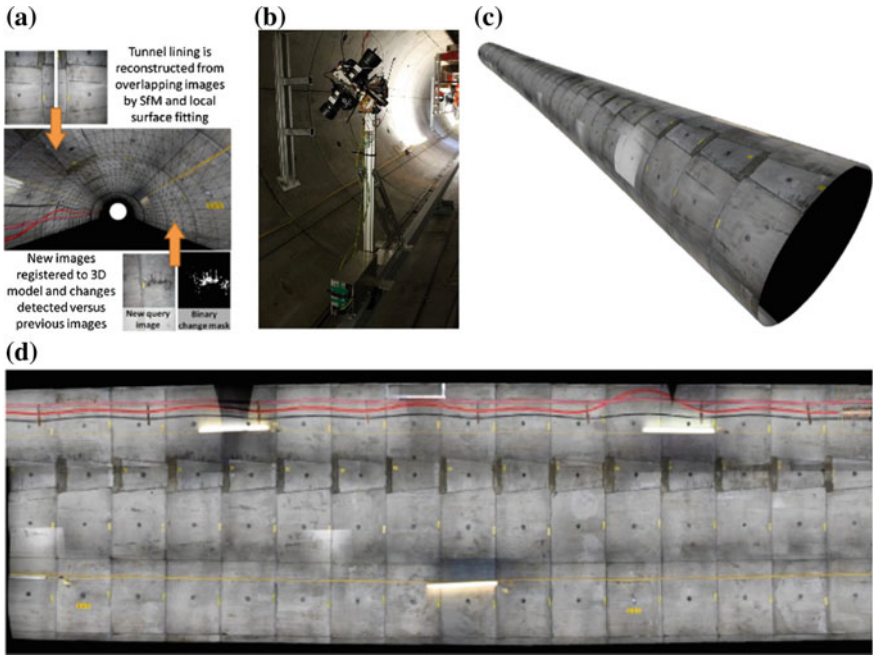

Fig. 22 A 3D model of a new tunnel in London with images are mosaiced to the model **a** Acquisition process, **b** camera robot, **c** 3D view and **d** a 2D unwrapped view. (after [99])

created from uncalibrated images using SfM, and then a cylindrical proxy is fitted onto the point cloud (Fig. 22c). By this operation, all the images are associated with their point cloud coordinates (Fig. 22d).

Once images are linked with their coordinates, those that are taken from a different camera at different times can be geometrically transformed as if they were taken from the camera positions where other images from other times are taken. Figure 23a shows images that contain changes from older transformed images of Fig. 23b. They

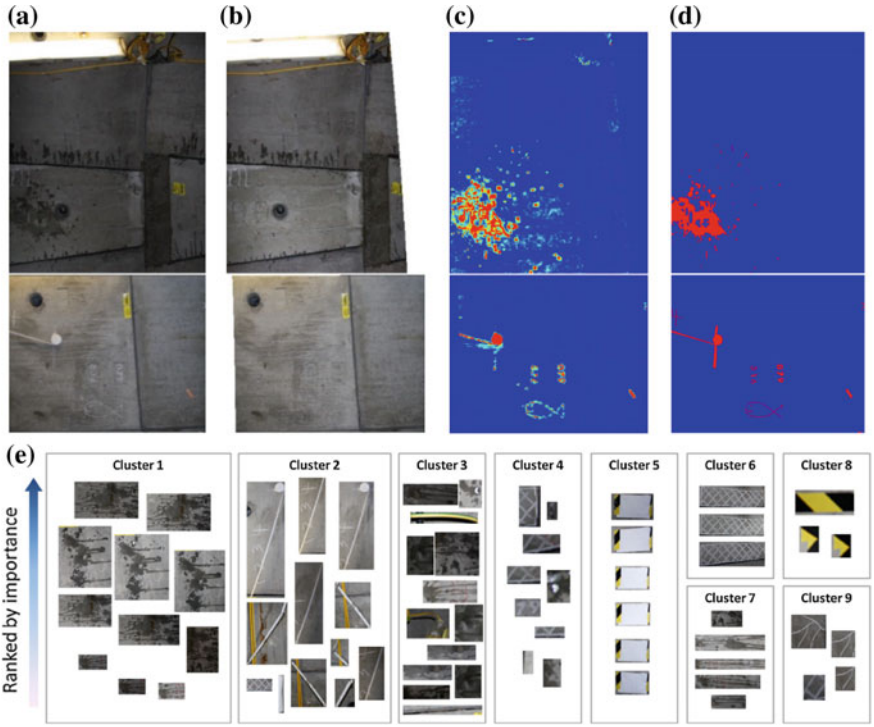

Fig. 23 **a** New images, **b** older images that are geometrically transformed, **c** outcomes of the change detection algorithm proposed by Stent et al. [99], **d** ground truth, and **e** results of unsupervised clustering and ranking, where changes of similar features were extracted [99]

are now localized accurately within the model, and changes are detected versus the reference images of Fig. 23a and model geometry. Stent et al. [99] further formulated the problem of detecting changes probabilistically and evaluated the use of different feature maps and a novel geometric before achieving invariance to noise and nuisance sources such as parallax and lighting changes (Fig. 23c, d). The use of unsupervised clustering and ranking method were also proposed to efficiently present detected changes and to further improve the inspection efficiency (Fig. 23e).

3.3 LiDAR

The light detection and raging (LiDAR) is a remote sensing technique that measures distance with pulsed laser light and collects the measurement points to build a 3D point cloud model of the scanned object. Terrestrial laser scanners are geomatic devices equipped with a laser beam and precise servomotors. They collect 3D point data and can carry out similar surveying operations to total stations. Figure 24 shows

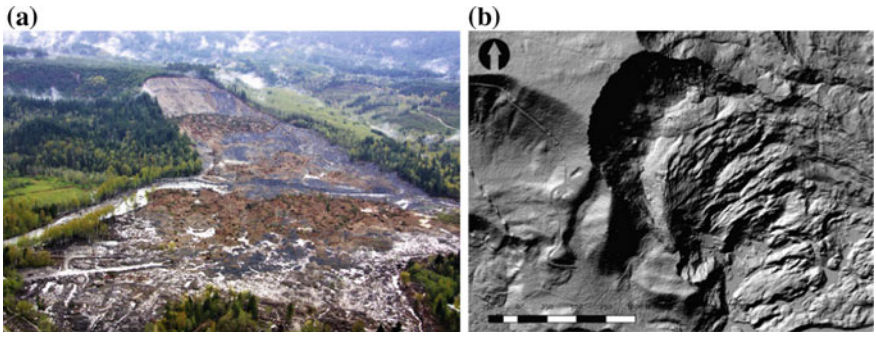

Fig. 24 **a** Aerial photo (by courtesy of Snohomish County Sheriff) and **b** LiDAR image of the 2014 Oso Landslide [78]

a LiDAR image of the 2014 Oso Landslide in which the surface topography can be seen in the absence of any vegetation. In the recent years, there have been attempts to carry out LiDAR measurements from unmanned aerial vehicles (UAV).

Aryal et al. [8] discuss the use of LiDAR and point clouds for deformation tracking using PIV for the slow-moving Cleveland Corral landslide in California. Using this dataset, Aryal et al. [9] evaluated a 3-D ground displacement field to estimate the slip depth and slip magnitude of the slide, as shown in Fig. 25. The estimated slip surface depth matches in situ observations from shear rods installed in the slide within the ± 0.45 m for investigating the landslide geometry and slip behavior.

Comparing different point clouds taken at different times is challenging. Registering clouds to the same coordinate system accurately is critical, as slight errors in registration may render further comparisons unreliable. Robust surveying registration techniques are needed, and the survey grid coordinates of optical targets (which are recognized by laser scans) need to be used for a resection-based registration and georeferencing.

Computing displacement fields from feature-less clouds is another challenge. Currently, the existing approaches to comparing point clouds can be grouped under two approaches. The first approach computes distances between clouds. Existing methods include the determination of the closest point-to-point distance between two point clouds. Lague et al. [48] proposed a method called Multiscale Model to Model Cloud Comparison (M3C2), where local plane fits to the cloud reduce measurement noise errors and allow determination of the distance between clouds in predefined directions. The second approach is the computation of displacement vectors by identifying corresponding sections of two point clouds. These methods determine the rigid body roto-translation matrix of the displaced object between two scans. The piecewise alignment method (PAM) by Teza et al. [105] uses the Iterative Closest Point algorithm to compute this matrix. In this method, the distances between the corresponding object in two clouds are minimized with an optimization algorithm, starting with an initial guess based on the closest distance between clouds.

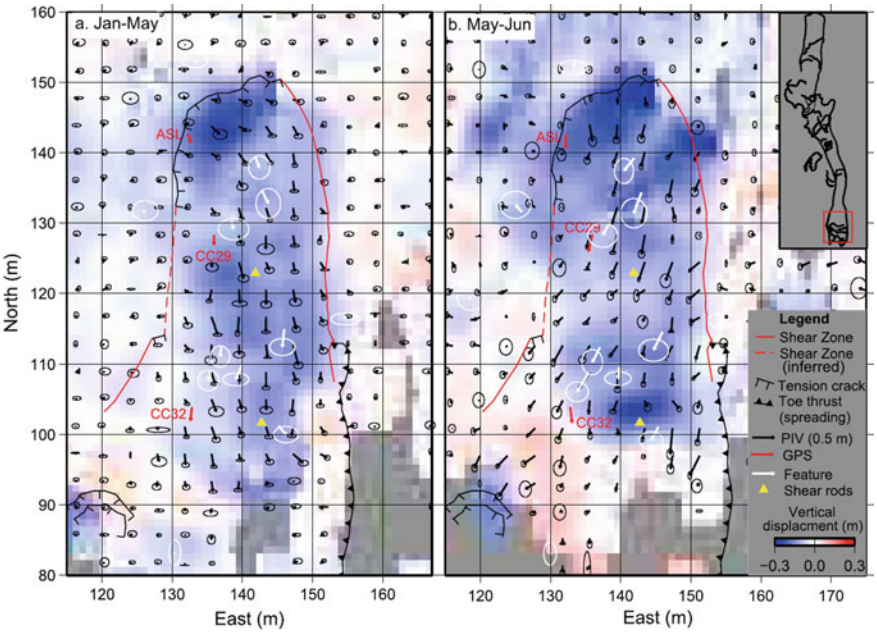

Fig. 25 Three dimensional displacement fields of the Cleveland Corral Landslide evaluated from LiDAR data taken at different times [9]

Acikgoz et al. [1, 2] conducted movement monitoring of a masonry structure before, during and after piling using a commercial laser scanner, as shown in Fig. 26a. Piles were constructed inside historic brick barrel vault of a stration. To ensure safe operation of the tracks above, movements of the vaults were regularly monitored by total stations. Figure 26b shows a comparison of vertical deformations estimated from total stations and cloud comparison techniques M3C2 and PAM. Typical displacement resolution was about a few mm. The M3C2 method resulted in vertical movement estimates of high accuracy but low precision, whereas the PAM described movements in three dimensions but with decreased accuracy. Using these data, the two hinge-response mechanism of the vault was revealed. The rich distributed data enable the calibration of the 2D mechanism and the finite element models, elucidating the contribution of arch stiffness, arch and backfill interaction, potential lateral movements and inter-ring sliding to the response.

3.4 Wireless Sensor Network

For monitoring large-scale infrastructure, introducing a wired monitoring system takes a great deal of time and cost. On the other hand, wireless sensor network (WSN)

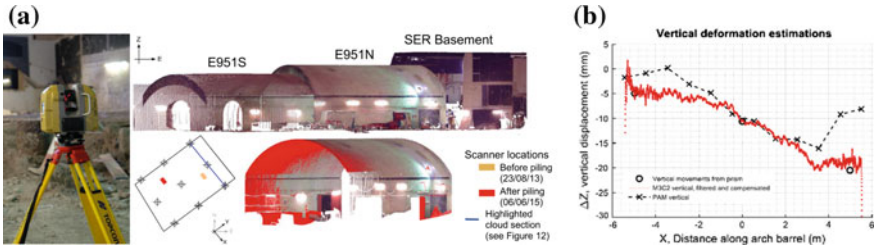

Fig. 26 **a** A laser scanner in operation, a colorized point cloud and cleaned point clouds from laser scan surveys before and after piling, **b** Comparison of vertical deformations estimated from total stations and cloud comparison techniques M3C2 and PAM [1]

is an attractive technology because cable installation is not necessary. By combining it with high precision and low-cost sensors, it enables large scale monitoring which was not possible in the past. The advantages of WSN to monitor the behavior of civil infrastructure are as follows. (i) multiple numbers and types of sensors can be deployed without installing cables, (ii) sensing in areas difficult to connect is possible, (iii) since it is possible to obtain a wide range of data in real time, decision making can be made quickly, and (iv) each node is self-sustainable with its internal battery over long period of time without battery change. An advanced WSN system contains mesh network capability and hence any node can behave as a sensor node as well as a relay node. This gives the maximum flexibility to non-radio professionals to deploy the system with the minimum efforts (time and cost).

Figure 27 shows the evolution of typical WSN systems developed in the past decade for geotechnical applications. The key features are ultra-low power, small size, and artificial intelligence. The performance of WSN hardware and software has dramatically improved in recent years, not only in data collection and abnormal signal detection but also in data compression processing, data analysis and network processing. Data communication is optimized, and power consumption is suppressed. With low power high-performance CPUs, it is now possible to perform data processing at the sensing level, which in turn saves energy by sending only the necessary data.

WSNs have been already recognized as a low-cost and resource-efficient alternative to these wired technologies for deployments in structures (e.g., [82]), enabling numerous monitoring opportunities that would hardly even be thought of a decade ago. Uchimura et al. [110] developed a WSN monitoring method for the early warning of rainfall-induced landslides (Fig. 28). Tilting angles in the surface layer of the slope were mainly monitored using a Micro Electro Mechanical Systems (MEMS) tilt sensor. Coupled with a volumetric water content sensor, they developed an optional arrangement of tilt sensors that gave distinct behaviors in the tilting angles in the pre-failure stage. Based on several field sites in Japan and China, they proposed that a precaution would be issued at a tilting rate of 0.011 per hour and a warning would issued at a tilting rate of 0.11 per hour.

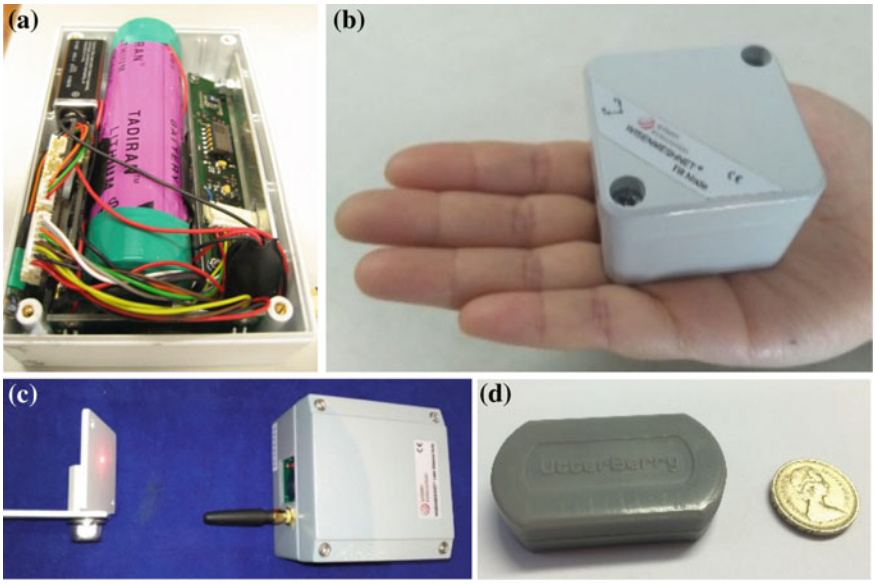

Fig. 27 **a** Original WSN system developed at the University of Cambridge in 2009, **b** tilt mote (Wisen innovation), **c** laser distance mote (Wisen innovation) and **d** displacement/acceleration mote (Utterberry)

If WSNs are to be used pervasively on civil infrastructure, they need to be deployed by site engineers; they must be straightforward to install. Radio connectivity is not automatically guaranteed, and neither is the security of the resulting installation. Data interpretation and presentation offer their challenges [97]. One must carefully consider the trade-off between fast network set-up, network stability and resistance to routing attacks on one hand, versus system availability on the other.

When using the 2.4 GHz ISM frequency band, standard WSN technology establishes an upper limit of 250 kbps, which is much lower than the achievable transmission bit rates of wired alternatives. Also, the size of information units exchanged among nodes is 127-bytes long, out of which around 80 to 102 bytes are available for actual useful information (e.g., measurement data). More recently, sub-1 GHz transceivers that utilize a low-power band frequency of 315 MHz (North America), 426 MHz (Japan) and 433 MHz (Europe, Asia, Africa, South America and Australia) have been introduced into the monitoring market (e.g., LoraWSN). This narrowband application provides the optimum tradeoff between range and transmission time for ranges over 10 km and data rates of 1.2 kbps. Narrowband systems are characterized by excellent link budgets because narrow receiver filters remove most of the noise. These practical limits might not be a problem in low-rate data collection applications where only a few bytes of sensor data are delivered at the sink on an hourly or daily basis.

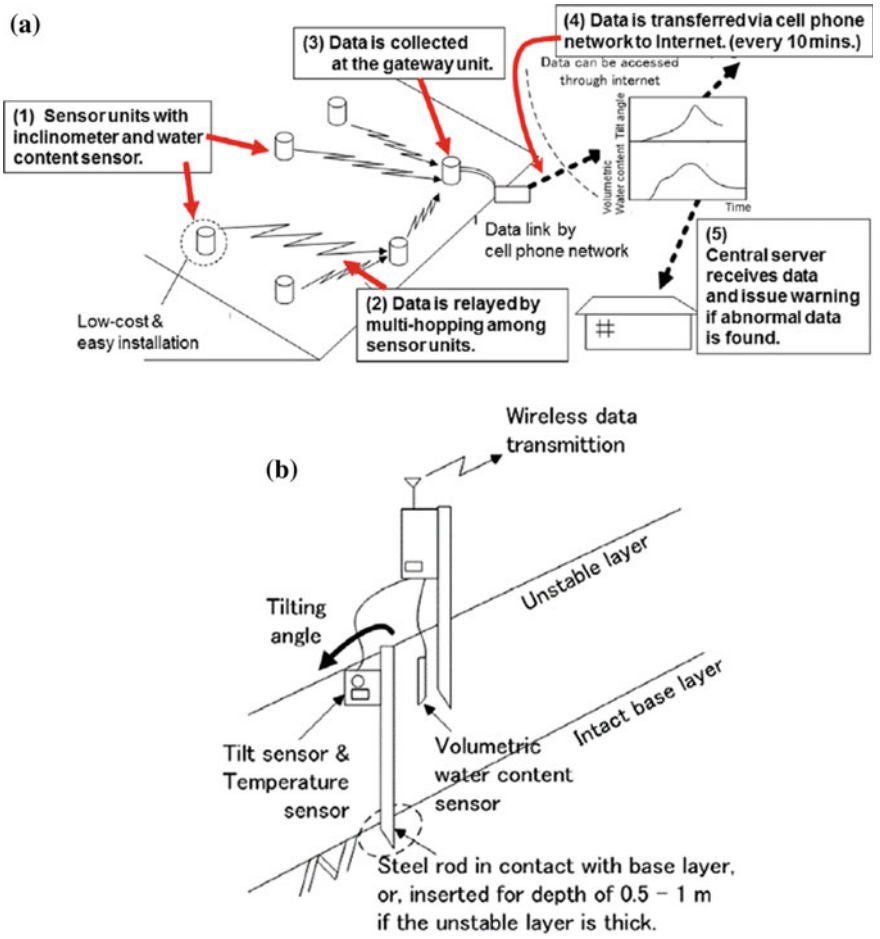

Fig. 28 WSN system to monitor slope movements **a** System overview and **b** tilt sensors [110]

Applications involving high data rate sampling, such as vibration monitoring, where millions of data points can be observed every day, still pose a big challenge to the system designer as for how to transmit such amount of data while accomplishing the monitoring system requirements, e.g., regarding battery lifetime. A solution to this concern is exploited by data compression and/or data reduction techniques along with the embedded processing capabilities. Also the future is expected to permit vastly denser networks (such as 5G protocols) and higher throughput than what has been achieved today.

One of the recent research interests in WSN is the application for underground communication (B(uried)-WSN). Buried systems are much more challenging to deploy in the field because of the significant attenuation of electromagnetic (EM) waves in soils. Several studies have addressed radio propagation in below-ground

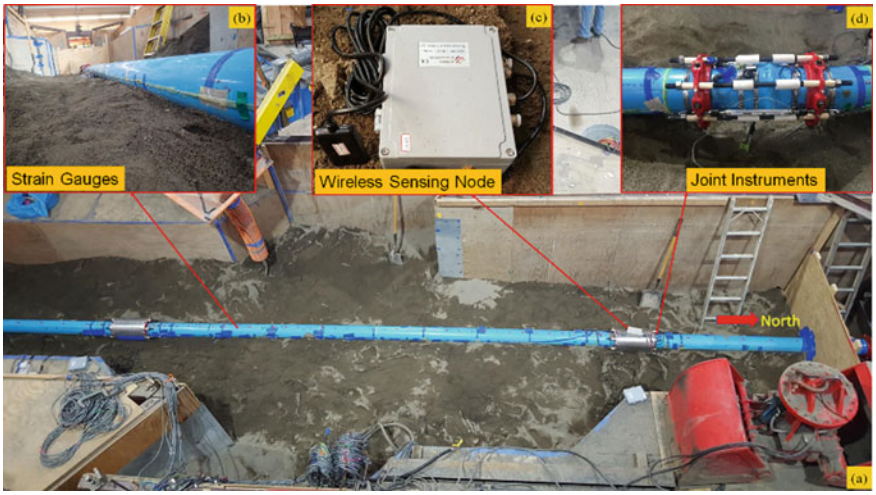

Fig. 29 B(uried)-WSN system tested to detect water leakage from pipeline joint breakage in a fault movement induced pipeline rupture experiment conducted at Cornell University [51]

conditions. Akyildiz et al. [4] conducted a review of the methods for predicting path losses in underground link applications, and Vuran and Silva [112] reported the parameters critical to B-WSN, such as burial depth, reflection, refraction, and multipath fading effects on EM waves. Lin et al. [51] recently tested their newly developed B-WSN system for monitoring pipeline joint leakage (Fig. 29).

Another alternative for buried WSN is to use the magnetic induction technique, which can penetrate much deeper underground. Sun et al. [94] proposed a magnetic induction (MI)-based WSN system called MISE-PIPE for underground pipeline monitoring, whereas Tan et al. [102] examined MI underground communication and evaluate its performance in a small-scale testbed by measuring essential characteristics, such as path loss, bandwidth, and packet error rate (PER).

Further details on WSN application to civil engineering monitoring can be found in [82].

4 Sensing and Monitoring at the District Scale

4.1 Satellite Images

Satellites take images of the earth. For example, WorldView-3 satellite captures (i) panchromatic data of 450–800 nm wavelengths at 0.30 m resolution, (ii) multispectral data (spectral bands of 50–60 nm wide between 400 and 1000 nm wavelengths at 1.25 m resolution and (iii) shortwave infrared data of 1000–2500 nm wavelengths

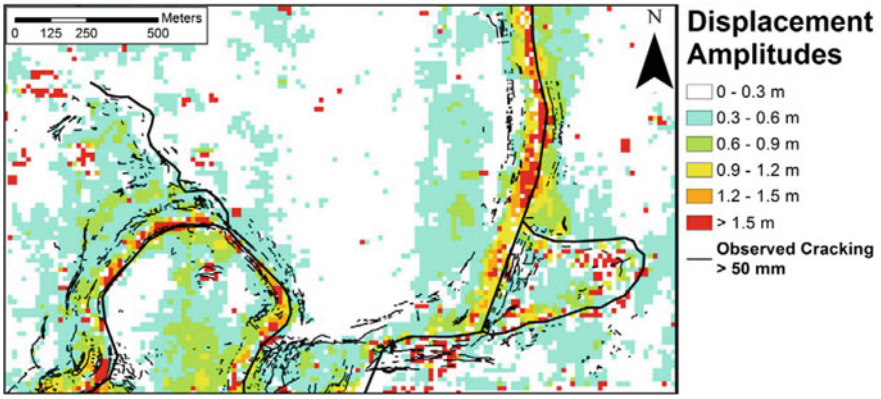

Fig. 30 Horizontal displacement amplitudes from optical image correlation from Satellite images taken before and after the Christchurch earthquake. The field mapped ground cracking is also shown [81]

at 4 m resolution. Passive sensors are mounted on the satellite to capture the solar radiation reflected from the earth surface. This is in contrast to an active sensor capture system, which sends an energy wave to the earth surface and records the reflected wave (see Sect. 4.2).

Rathje et al. [81] present a lateral displacement map of Christchurch, New Zealand by comparing satellite images taken before and after the 2010–2011 Canterbury Earthquake Sequence, as shown in Fig. 30. Using techniques similar to PIV and DIC, the displacements were estimated to be less than 20 m intervals. Horizontal displacements as small as 0.2–0.3 m were measured. Cracks (larger than 50 mm wide) identified in the field run parallel to the waterways and the locations coincide to the area of large lateral displacements.

4.2 InSAR

Synthetic aperture radar (SAR) can produce high-resolution radar images of earth's surface and can typically cover a surface area of between 2500 and 10,000 km^2, by mounting the system on a satellite. Since SAR uses the microwave band in the broad radio spectrum, it has a day-and-night imaging capability, and ability to penetrate through rain/water clouds.

The potential information in the phase of SAR complex images has led to a technology called interferometric SAR (InSAR) [57]. The cross-track InSAR (CT-InSAR) is used for producing topographic maps, and measurements of crust movement caused by earthquakes and volcanic activity, and those of glacier movement. PS-InSAR (Permanent Scatterer InSAR), InSAR CTM (Coherent Target Monitoring), and CPT (Coherent Pixel Technique) use the temporal phase changes of semi-

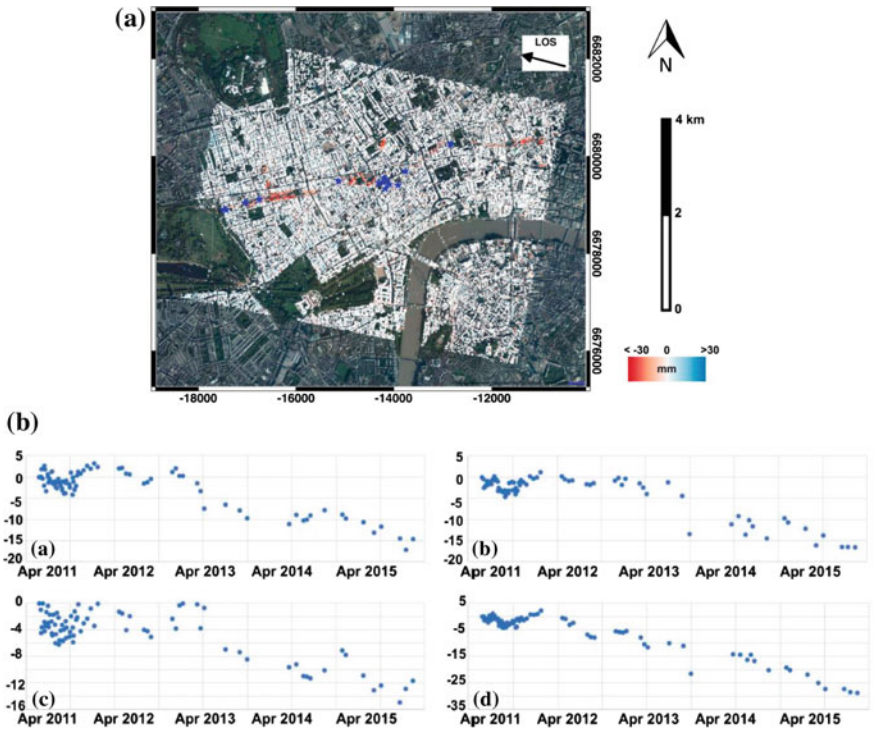

Fig. 31 **a** Cumulative displacement map along the Crossrail tunnel construction alignment in London from Apr 2011 to Dec 2015. Negative value is subsidence. **b** Settlement-time curves at four locations along the alignment [61]

permanent scatterers that consistently give rise to strong backscatter, and the measurement accuracy is of the order of several millimeters per year [70].

Satellite-based multi-temporal interferometric synthetic aperture radar (MT-InSAR) is a monitoring technique capable of extracting cumulative surface displacement measurements with millimeter accuracy (e.g., [116]). Milillo et al. [61] conducted InSAR time-series analysis of 72 images acquired from April 2011 to December 2015 to produce time-series of cumulative deformation over the city of London, where the Crossrail twin tunnels were excavated starting in 2012. Figure 31a shows that ground settlements in the order of 30 mm are observed along the route of the tunnel. The time-dependent settlements at selected four locations along the tunnel are plotted in Fig. 31b. A dense set of ground-based measurements from InSAR data was used to analyze the performance of 14 buildings affected by the tunnel construction at the millimeter level.

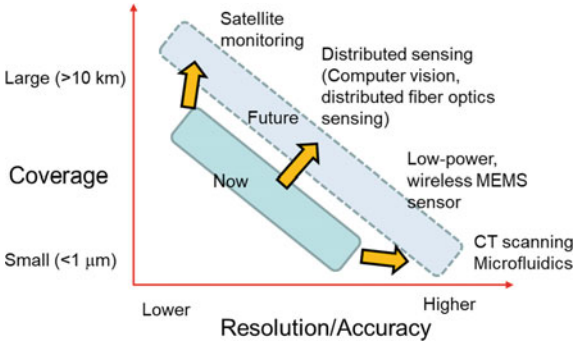

Fig. 32 Geotechnical sensor and monitoring with larger coverage and higher resolution and accuracy

5 Conclusions

In general, the smaller the scale of measurement is, the higher the measurement resolution and accuracy become, as shown by the general relationship given in Fig. 32. The technologies presented in this Chapter are pushing this relationship toward the right-top direction; that is, larger coverage and higher resolution.

As illustrated by the several case studies and examples presented in this chapter, the new dataset obtained from the new sensor and monitoring technologies can be used to improve geotechnical engineers' understanding of soil behavior and soil-structure interactions. Technologies such as CT scanning, microfluidics, pressure sensors and transparent soils can be used for Type I mechanism monitoring. These technologies can measure the bio-chemo-thermo-hydro-mechanical processes occurring at the particle scale. Type II Performance monitoring requires cost-effective sensor technologies such as computer vision, distributed fiber optic sensing, WSNs, LiDAR and satellite image analysis. For example, DFOS technology records strain and temperature every 5 cm along a fiber optic cable of a few kilometer length. LiDAR and computer vision technologies create three-dimensional model and movements of the scanned object at the resolution similar to the conventional robotic total station but with dense dataset. The rich and large data set (i.e., large coverage with high resolution) obtained from these technologies can give new insights into the mechanisms of ground deformation and soil-structure interaction at the site scale.

To accelerate the adaptation of new sensor and monitoring technologies in geotechnical engineering practice, it may be necessary to update the current geotechnical engineering methods (e.g., assessing the stability of a slope, evaluating shaft and end bearing characteristics of a pile, and estimating the bending and axial forces in tunnel lining) so that they can accommodate this new dataset directly. This can be achieved by making all stages of sensing monitoring and data analysis processes more tightly coupled as shown in Fig. 33. By doing so, the confidence in delivering new technologies could be developed, and the value of sensing becomes more evident to the stakeholders. With better data in hand, the ultimate goal is to make a step

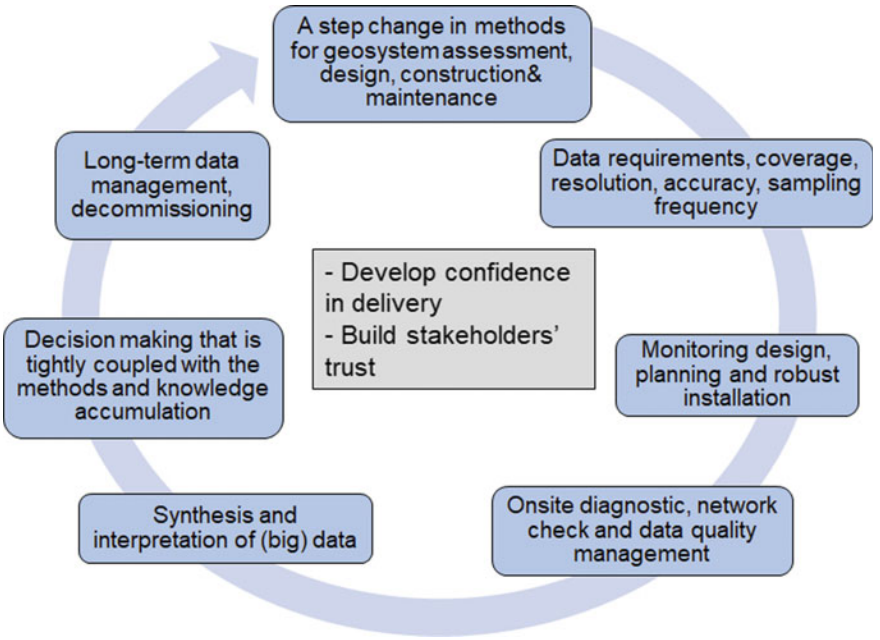

Fig. 33 A cycle of new sensor and monitoring technology adaptation for geotechnical engineering

change in the way geotechnical engineering is conducted for improved safety, more reliability, and better economy.

Acknowledgements The first author likes to acknowledge the Cambridge Centre of Smart Infrastructure and Construction, the University of Cambridge and the UK Engineering and Physical Sciences Research Council for their support on several sensor technologies presented in this chapter.

References

1. Acikgoz, S., Pelecanos, L., Giardina, G., Aitken, J., Soga, K.: Distributed sensing of a masonry vault during nearby piling. Struct. Control Health Monit. **24**(3), e1872 (2017)
2. Acikgoz, S., Soga, K., Woodhams, J.: Evaluation of the response of a vaulted masonry structure to differential settlements using point cloud data and limit analyses. Constr. Build. Mater. **150**, 916–931 (2017)
3. Adrian, R.J.: Particle-image techniques for experimental fluid mechanics. Annu. Rev. Fluid Mech. **23**, 261–304 (1991)
4. Akyildiz, I.F., Sun, Z., Vuran, M.C.: Signal propagation techniques for wireless underground communication networks.". Phys. Commun. **2**(3), 167–183 (2009)
5. Alhaddad, M.: Pers. Commun. (2018)
6. Alhaddad, M., Wilcock, M., Gue, C.Y., Elshafie, M.Z.B.E, Soga, K., Mair, R.J., Devriendt, M., Wright, P.: Imposed longitudinal settlement on a cast-iron tunnel from the excavation of

a new tunnel beneath. In: Proceedings of the 9th International Symposium on Geotechnical Aspects of Underground Construction in Soft Grounds (IS-São Paulo 2017), p. 343 (2017)
7. Andò, E., S.A. Hall, G. Viggiani, J. Desrues., P. Bésuelle.: Grain-scale experimental investigation of localised deformation in sand: a discrete particle tracking approach. Acta Geotechnica **7**(1), 1–13 (2012)
8. Aryal, A., Brooks, B.A., Reid, M.E., Bawden, G.W., Pawlak. G.R.: Displacement fields from point cloud data: application of particle imaging velocimetry to landslide geodesy. J. Geophy. Res. Earth Surf. **117**(1), 1–15 (2012)
9. Aryal, A., Brooks, B.A., Reid, M.E.: Landslide subsurface slip geometry inferred from 3-D surface displacement fields. Geophys. Res. Lett. **42**, 1411–1417 (2015)
10. ASCE Task Committee on Instrumentation and Monitoring Dam Performance.: Guidelines for instrumentation and measurements for monitoring dam performance. Am. Soc. Civil Eng. 715 pp (2000)
11. Bassett, R.: A guide to field instrumentation in geotechnics: principles, installation and reading. CRC Press, 232 pp (2012)
12. Bathurst, R.J., Ezzein, F.M.: Geogrid and soil displacement observations during pullout using a transparent granular soil. Geotech. Test. J. **38**(5), 673–685 (2015)
13. Bourne-Webb, P.J., Amatya, B., Soga, K., Amis, T., Davidson, C., Payne, P.: Energy pile test at Lambeth College, London: geotechnical and thermodynamic aspects of pile response to heat cycles. Géotechnique **59**(3), 237–248 (2009)
14. Bruchon, J.-F., Pereira, J.M., Vandamme, M., Delage, P., Bornert, M., Lenoir, N.: X-ray microtomography characterisation of the changes in statistical homogeneity of an unsaturated sand during imbibition. Géotechnique Lett. **3**, 84–88 (2013)
15. Chaiyasarn, K.: Pers. Commun. (2011)
16. Cheung, L.L.K., Soga, K., Bennett, P.J., Kobayashi, Y., Amatya, B., Wright, P.: Optical fibre strain measurement for tunnel lining monitoring. Proc. Inst. Civil Eng. Geotech. Eng. **163**(3), 119–130 (2010)
17. Chini, C.M., Wallace, J.F., Rutherford, C.J., Peschel, J.M.: Shearing failure visualization via particle tracking in soft clay using a transparent soil. Geotech. Test. J. **38**(5), 708–724 (2015)
18. De Cataldo, D., Chen, K., Airey, D.: Three-dimensional deformations in transparent soil using fluorescent markers. Int. J. Phys. Model. Geotech. **17**(2), 1–13 (2017)
19. Desrues, J., Chambon, R., Mokni, M., Mazerolle, F.: Void ratio evolution inside shear bands in triaxial sand specimens studied by computed tomography. Géotechnique **46**(3), 529–546 (1996)
20. Desrues, J., Andò. E.: Strain localisation in granular media. Comptes Rendus Physique **16**(1), 26–36 (2015)
21. Dunnicliff, J.: Geotechnical instrumentation for monitoring field performance. Wiley-Interscience, 577 pp (1988)
22. Druckrey, A.M., Alshibli, K.A., Al-Raoush, R.I.: Discrete particle translation gradient concept to expose strain localisation in sheared granular materials using 3D experimental kinematic measurements. Géotechnique **68**(2), 162–170 (2018)
23. El Ganainy, H., Tessari, A., Abdoun, T., Sasanakul, I.: Tactile pressure sensors in centrifuge testing. Geotech. Test. J. **37**(1), 151–163 (2014)
24. Ezzein, F.M., Bathurst. R.J.: A transparent sand for geotechnical laboratory modeling. Geotech. Test. J. **34**(6), 590–601 (2011)
25. Ferreira, J.A.Z., Zornberg, J.G.: A transparent pullout testing device for 3D evaluation of soil–geogrid interaction. Geotech. Test. J. **38**(5), 686–707 (2015)
26. Fonseca, J., O'Sullivan, C., Coop, M.R., Lee, P.D.: Quantifying the evolution of soil fabric during shearing using scalar parameters. Géotechnique **63**(10), 818–829 (2013)
27. Gao, B., Sui. W.: Experimental modeling of quicksand with transparent soil through an orifice. Geotech. Test. J. **40**(5), 798–809 (2017)
28. Gao, Y., Sui, W., Liu, J.: Visualization of chemical grout permeation in transparent soil. Geotech. Test. J. **38**(5), 774–786 (2015)

29. Glisic, B., Inaudi, D.: Fibre optic methods for structural health monitoring. Wiley-Interscience, 276 pp (2007)
30. Gue, C.Y., Wilcock, M., Alhaddad, M.M., Elshafie, M.Z.B.E., Soga, K., Mair, R.J.: The monitoring of an existing cast iron tunnel with distributed fibre optic sensing (DFOS). J. Civil Struct. Health Monit. **5**(5), 573–586 (2015)
31. Gue, C.Y., Wilcock, M.J., Alhaddad, M.M., Elshafie, M., Soga, K., Mair, R.J.: Tunnelling close beneath an existing tunnel in clay–perpendicular undercrossing. Géotechnique **67**(9), 795–807 (2017)
32. Hanna, T.H.: Field instrumentation in geotechnical engineering. Trans Tech Publication, 843 pp (1985)
33. Hasan, A., Alshibli, K.: Three dimensional fabric evolution of sheared sand. Granular Matter **14**(4), 469–482 (2012)
34. Higo, Y., Oka, F., Kimoto, S., Sanagawa, T., Matsushima, Y.: Study of strain localization and microstructural changes in partially saturated sand during triaxial tests using microfocus X-ray CT. Soils Found. **51**(1), 95–111 (2011)
35. Higo, Y., Oka, F., Sato, T., Matsushima, Y., Kimoto, S.: Investigation of localized deformation in partially saturated sand under triaxial compression using microfocus X-ray CT with digital image correlation. Soils Found. **53**(2), 181–198 (2013)
36. Iskander, M.: Modeling with transparent soils—visualizing soil structure interaction and multi phase flow, non-intrusively. Springer, 331 pp (2010)
37. Iskander, M., Bless, S., Omidvar, M.: Rapid penetration into granular Media. Visualizing the Fundamental Physics of Rapid Earth Penetration, Elsevier, 458 pp (2015)
38. Iskander, M., Liu, J.: Spatial deformation measurement using transparent soil. Geotech. Test. J. **33**(4), 314–321 (2010)
39. Iskander, M., Bathurst, R. J., Omidvar. M.: Past, present, and future of transparent soils. Geotech. Test. J. **38**(5), 557–573 (2015)
40. Janmonta, K. Uchimura, T. Amatya, B.L., Soga, K. Bennett, P.J., Lung, R., Robertson, I.: Fibre optics monitoring of clay cuttings and embankments along London's ring motorway, Geo-Congress 2008, Characterization, Monitoring and Modeling of Geotechnical, ASCE Geotechnical Special Publication No. 179, pp. 509–516 (2008)
41. Karatza, Z., Andò, E., Papanicolopulos, S.A., Ooi, J.Y., Viggiani. G.: Evolution of deformation and breakage in sand studied using X-ray tomography. Géotechnique, **68**(2), 107–117 (2018)
42. Kechavarzi, C., Soga, K., de Battista, N, Pelecanos, L., Elshafie, M., Mair, R.J.: Distributed Optical Fibre Sensing for Monitoring Geotechnical Infrastructure—A Practical Guide. ICE Publishing, 192 pp (2016)
43. Klar, A., Bennett, P.J., Soga, K., Mair, R.J., Tester, P., Fernie, R., St John, H., Torp-Peterson, G.: The importance of distributed strain measurement for pile foundations. Proc. ICE—Geotech. Eng. **159**(GE3), 135–144 (2006)
44. Klar, A., Linker, R.: Feasibility study of automated detection of tunnel excavation by Brillouin optical time domain reflectometry. Tunn. Undergr. Space Technol. **25**(5), 575–586 (2010)
45. Kobayashi, T.: Pers. Commun. (2018)
46. Kong, G.Q., Cao, Z.H., Zhou, H., Sun, X.J.: Analysis of piles under oblique pullout load using transparent-soil models. Geotech. Test. J. **38**(5), 725–738 (2015)
47. Kong, G. Q., Li, H., Hu, Y.X., Yu, Y.X., Xu. W.B.: New suitable pore fluid to manufacture transparent soil. Geotech. Test. J. **40**(4), 658–672 (2017)
48. Lague, D., Brodu, N., Leroux, J.: Accurate 3D comparison of complex topography with terrestrial laser scanner: application to the Rangitikei canyon (N-Z). ISPRS J. Photogrammetry Remote Sens. **82**, 10–26 (2013)
49. Li, L., Zhang, Z., Chen, G., Lytton, R.: Measuring unsaturated soil deformations during triaxial testing using a photogrammetry-based method. Can. Geotech. J. **53**(3), 472–489 (2016)
50. Lim, K., Wong, L., Chiu, W.K., Kodikara, J.: Distributed fiber optic sensors for monitoring pressure and stiffness changes in out-of-round pipes. Struct. Control Health Monit. **23**(2), 303–314 (2016)

51. Lin, T., Wu, Y., Soga, K., Wham, B.P. Pariya-Ekkasut, C., Berger, B., O'Rourke, T.D.: Buried wireless sensor networks for monitoring pipeline joint leakage caused by large ground movements. J. Pipeline Syst. Eng. Pract. (2018). (Under review)
52. Liu, J., Iskander, M.G.: Modelling capacity of transparent soil. Can. Geotech. J. **47**(4), 451–460 (2010)
53. Long, Z., Nugent, E., Javer, A., Cicuta, P., Sclavi, B., Cosentino Lagomarsino, M., Dorfman, K.D.: Microfluidic chemostat for measuring single cell dynamics in bacteria. Lab Chip **13**(5), 947–954 (2013)
54. Lowe, D. G.: Object recognition from local scale-invariant features. In: Proceeding of the 7th IEEE International Conference on Computer Vision, New York, vol. 2, pp. 1150–1157 (1999)
55. Lourenco, S., Gallipoli, D., Augarde, C., Toll, D.G., Charles Fisher, P., Congreve, A.: Formation and evolution of water menisci at contacts in unsaturated granular media. Géotechnique **62**(3), 193–199 (2012)
56. Lourenço, S., Gallipoli, D., Toll, D.G., Augarde, C.E., Evans, F.D., Medero, G.M.: Calibrations of a high-suction tensiometer. Géotechnique **58**(8), 659–668 (2008)
57. Massonnet, D., Souyris, J.C.: SAR interferometry: towards the ultimate ranging accuracy. In: Imaging with Synthetic Aperture Radar; CRC Press, pp. 177–228 (2008)
58. Matsumura, S., Kobayashi, T., Mizutani, T., Bathurst, R.: Manufacture of bonded granular soil using X-ray CT Scanning and 3D printing. Geotech. Test. J. **40**(6), 1000–1010 (2017)
59. Manca, D., Ferrari, A., Laloui, L.: Fabric evolution and the related swelling behaviour of a sand/bentonite mixture upon hydro-chemo-mechanical loadings. Géotechnique **66**(1), 41–57 (2016)
60. McCormick, N.J., Lord, J.D.: Practical in situ applications of DIC for large structures. Appl. Mech. Mater. **24–25**, 161–166 (2010)
61. Milillo, P., Giardina, G., DeJong, M.J., Perissin, D., Milillo, G.: Multi-temporal InSAR structural damage assessment: the London Crossrail case study. Remote Sensing **10**(2), 287 (2018)
62. Minardo, A., Bernini, R., Zeni, L.: Vectorial dislocation monitoring of pipelines by use of Brillouin-based fiber-optics sensors. Smart Mater. Struct. **17**(1), 015006 (2008)
63. Mohamad, H., Bennett, P.J., Soga, K., Mair, R.J., Bowers, K.: Behaviour of an old masonry tunnel due to tunnelling induced ground settlement. Géotechnique **60**(12), 927–938 (2010)
64. Mohamad, H., Soga, K., Pellow, A.: Performance Monitoring of a secant piled wall using distributed fibre optic strain sensing. J. Geotech. Geoenviron. Eng. **137**(12), 1236–1243 (2011)
65. Mohamad, H., Soga, K., Bennett, P.J., Mair, R.J., Lim, C.S.: Monitoring twin tunnel interaction using distributed optical fiber strain measurements. J. Geotech. Geoenviron. Eng. **138**(8), 957–967 (2011)
66. Muszynski, M.R., Olson, S.M., Hashash, Y.M.A., Phillips, C.: Earth pressure measurements using tactile pressure sensors in a saturated sand during static and dynamic centrifuge testing. Geotech. Test. J. **39**(3), 371–390 (2016)
67. Ni, Q., Hird, C.C., Guymer, I.: Physical modelling of pile penetration in clay using transparent soil and particle image velocimetry. Géotechnique **60**(2), 121–132 (2010)
68. Ni, P., Moore, I.D., Take, W.A.: Distributed fibre optic sensing of strains on buried full-scale PVC pipelines crossing a normal fault. Géotechnique **68**(1), 1–17 (2018)
69. Omidvar, M., Doreau Malioche, J., Chen, Z., Iskander, M., Bless, S.: Visualizing kinematics of dynamic penetration in granular media using transparent soils. Geotech. Test. J. **38**(5), 656–672 (2015)
70. Ouchi, K.: Recent trend and advance of synthetic aperture radar with selected topics. Remote Sens. **5**(2), 716–807 (2013)
71. Palmer, M.C., O'Rourke, T.D., Olson, N.A., Abdoun, T., Ha, D., O'Rourke, M.J.: Tactile pressure sensors for soil-structure interaction assessment. J. Geotech. Geoenviron. Eng. **135**(11), 1638–1645 (2009)
72. Paikowsky, S., Hajduk, E.: Calibration and use of grid-based tactile pressure sensors in granular material. Geotech. Test. J. **20**(2), 218–241 (1997)
73. Pamukcu, S., Cheng, L.: Underground Sensing. Academic Press, 522 pp (2018)

74. Peters, S.B., Siemens, G., Take. W.A.: Characterization of transparent soil for unsaturated applications. Geotech. Test. J. **34**(5), 445–456 (2011)
75. Pelecanos, L., Soga, K., Chunge, M.P.M., Ouyang, Y., Kwan, V., Kechavarzi, C., Nicholson, D.: Distributed fibre-optic monitoring of an Osterberg-cell pile test in London. Geotechnique Lett. **7**(2), 152–160 (2017)
76. Pelecanos, L., Soga, K., Elshafie, M., Nicholas, d. B., Kechavarzi, C., Gue, C. Y., Ouyang, Y., Seo, H.: Distributed fibre optic sensing of axially loaded bored piles. J. Geotech. Geoenviron. Eng. **144**(3), 04017122 (2018)
77. Pinyol, N.M., Alvarado, M.: Novel analysis for large strains based on particle image velocimetry. Can. Geotech. J. **54**(7), 933–944 (2017)
78. Pyles, M.R., Rogers, J.D., Bray, J.D., Skaugset, A., Storesund, R., Schlieder, G.: Expert opinion report, Superior Court of Washington for King County. Case No. 14-2-18401-8 SEA, June 30 (2016)
79. Rahardjo, H., Leong, E. C.: Suction measurements. In: Unsaturated Soils 2006, pp. 81–104. American Society of Civil Engineers (2006)
80. Rathje, E.M., Franke, K.: Remote sensing for geotechnical earthquake reconnaissance. Soil Dyn. Earthquake Eng. **91**, 304–316 (2016)
81. Rathje, E.M., Secara, S.S., Martin, J.G., van Ballegooy, S., Russell, J.: Liquefaction-induced horizontal displacements from the Canterbury earthquake sequence in New Zealand measured from remote sensing techniques. Earthquake Spectra **33**(4), 1475–1494 (2017)
82. Rodenas-Herráiz, D., Soga, K., Fidler, P., de Battista, N.: Wireless Sensor Networks for Civil Infrastructure Monitoring—A Best Practice Guide. ICE Publishing, 208 pp (2016)
83. Romero, E., Simms, P.H.: Microstructure investigation in unsaturated soils: a review with special attention to contribution of mercury intrusion porosimetry and environmental scanning electron microscopy. Geotech. Geol. Eng. **26**(6), 705–727 (2008)
84. Romero, E., Della Vecchia, G., Jommi, C.: An insight into the water retention properties of compacted clayey soils. Géotechnique **61**(4), 313–328 (2011)
85. Rui, Y., Kechavarzi, C., O'Leary, F., Barker, C., Nicholson, D., Soga, K.: Integrity testing of pile cover using distributed fibre optic sensing. Sensors **17**, 2949 (2017)
86. Salazar, S.E., Barnes, A., Coffman, R.A.: Development of an internal camera-based volume determination system for triaxial testing. Geotech. Test. J. **38**(4), 549–555 (2015)
87. Sato, A., Ikeda, K.: Visualization of diffusion phenomena in porous media by means of X-ray computed tomography (CT) scanning. Can. Geotech. J. **52**(10), 1448–1456 (2015)
88. Schwamb, T., Soga, K., Mair, R.J., Elshafie, M.Z., Sutherden, R., Boquet, C., Greenwood, J.: Fibre optic monitoring of a deep circular excavation. Proc. ICE Geotech. Eng. **167**(2), 144–154 (2014)
89. Schwamb, T., Soga, K.: Numerical modelling of a deep circular excavation at Abbey Mills in London. Géotechnique **65**(7), 604–619 (2015)
90. Schwamb, T., Elshafie, M., Soga, K., Mair, R.J.: Considerations for monitoring of deep circular excavations. Proc. Inst. Civil Eng. Geotech. Eng. **169**(6), 477–493 (2016)
91. Soga, K., Kwan, V., Pelecanos, L., Rui, Y., Schwamb, T., Seo, H., Wilcock, M.: The role of distributed sensing in understanding the engineering performance of geotechnical structures. In: Geotechnical engineering for Infrastructure and Development, XVI ECSMGE. ICE Publishing, pp. 13–48 (2015)
92. Soga, K., Luo, L.: Distributed fiber optics sensors for civil engineering infrastructure sensing. J. Struct. Integrity Maintenance **3**(1), 1–21 (2018)
93. Soga, K., Schooling, J.: Infrastructure sensing. Interface Focus, Royal Soc. Publishing **6**(4), 20160023 (2016)
94. Sun, Z., Wang, P., Vuran, M.C., Al-Rodhaan, M.A., Al-Dhelaan, A.M., Akyildiz, I.F.: MISE-PIPE: magnetic induction-based wireless sensor networks for underground pipeline monitoring. Ad Hoc Netw. **9**(3), 218–227 (2011)
95. Suo, W., Lu, Y., Shi, B., Zhu, H., Wei, G., Jiang, H.: Development and application of a fixed-point fiber-optic sensing cable for ground fissure monitoring. J. Civil Struct. Health Monit. **6**(4), 715–724 (2016)

96. Stanier, S.A., Blaber, J., Take, W.A., White, D.J.: Improved image-based deformation measurement for geotechnical applications. Can. Geotech. J. **53**(5), 727–739 (2016)
97. Stajano, F., Hoult, N., Wassell, I., Bennett, P., Middleton, C., Soga, K.: Smart bridges, smart tunnels: transforming wireless sensor networks from research prototypes into robust engineering infrastructure. Ad Hoc Netw. **8**(8), 872–888 (2010)
98. Stent, S.: Pers. Commun. (2014)
99. Stent, S., Gherardi, R., Stenger, B., Soga, K., Cipolla, R.: Visual change detection on tunnel linings. Mach. Vis. Appl. **27**(3), 319–330 (2016)
100. Take, W.A.: Thirty-sixth canadian geotechnical colloquium: advances in visualization of geotechnical processes through digital image correlation. Can. Geotech. J. **52**(9), 1199–1220 (2015)
101. Talesnick, M.: Measuring soil pressure within a soil mass. Can. Geotech. J. **50**, 716–722 (2013)
102. Tan, X., Sun, Z., Akyildiz, I.F.: Wireless underground sensor networks: MI-based communication systems for underground applications. IEEE Antennas Propag. Mag. **57**(4), 74–87 (2015)
103. Tarantino, A., Ridley, A.M., Toll, D.G.: Field measurement of suction, water content, and water permeability. Geotech. Geol. Eng. **26**(6), 751–782 (2008)
104. Teng, Y., Stanier, S.A., Gourvenec, S.M.: Synchronised multi-scale image analysis of soil deformations. Int. J. Phys. Model. Geotech. **17**(1), 53–71 (2017)
105. Teza, G., Galgaro, A., Zaltron, N., Genevois, R.: Terrestrial laser scanner to detect landslide displacement fields: a new approach. Int. J. Remote Sens. **28**(16), 3425–3446 (2007)
106. Tran, T.V., Tucker-Kulesza, S.E., Bernhardt-Barry, M.L: Determining surface roughness in erosion testing using digital photogrammetry. Geotech. Test. J. **40**(6), 917–927 (2017)
107. Tohidi, B., Anderson, R., Clennell, M.B., Burgass, R.W., Biderkab, A.B.: Visual observation of gas-hydrate formation and dissociation in synthetic porous media by means of glass micromodels. Geology **29**(9), 867–870 (2002)
108. Toll, D.G., Lourenco, S.D.N., Mendes, J., Gallipoli, D., Evans, F.D., Augarde, C.E., Cui. Y.J. et al.: Soil suction monitoring for landslides and slopes. Q. J. Eng. Geol. Hydrogeol. **44**(1), 23–33 (2011)
109. Toll, D.G., Lourenço, S.D.N., Mendes, J.: Advances in suction measurements using high suction tensiometers. Eng. Geol. **165**(24), 29–37 (2013)
110. Uchimura, T., Towhata, I., Wang, L., Nishie, S., Yamaguchi, H., Seko, I., Qiao, J.: Precaution and early warning of surface failure of slopes using tilt sensors. Soils Found. **55**(5), 1086–1099 (2015)
111. Viggiani, G., Andò, E., Takano, D., Santamarina, J.C.: Laboratory X-ray tomography: a valuable experimental tool for revealing processes in soils. Geotech. Test. J. **38**(1), 61–71 (2015)
112. Vuran, M. C., Silva, A. R.: Communication through soil in wireless underground sensor networks–theory and practice. In: Sensor Networks, pp 309–347 (2010)
113. Vorster, T.E.B., Soga, K., Mair, R.J., Bennett, P.J., Klar, A., Choy, C.K.: The use of fibre optic sensors to monitor pipeline behaviour. ASCE Geocongr. **2006**, 1–6 (2006)
114. Wang, M.L, Lynch, J.P., Sohn, H.: Sensor Technologies for Civil Infrastructures: Applications in Structural Health Monitoring, Woodhead Publishing Ltd. 728 pp (2014)
115. Wang, Y., Soga, K., DeJong, J., Kabla, A.: A microfluidic chip and its use in charterising the particle-scale behaviour of Microbial-Induced Carbonate Precipitation (MICP), Géotechnique, arXiv:1804.02946 (2018)
116. Wasowski, J., Bovenga, F.: Investigating landslides and unstable slopes with satellite multi temporal interferometry: current issues and future perspectives. Eng. Geol. **174**, 103–138 (2014)
117. Weibel, D.B., Diluzio, W.R., Whitesides, G.M.: Microfabrication meets microbiology. Nat. Rev. Microbiol. **5**(3), 209–218 (2007)
118. White, D.J., Take, W.A., Bolton, M.D.: Soil deformation measurement using particle image velocimetry (PIV) and photogrammetry. Géotechnique **53**(7), 619–631 (2003)
119. Whitesides, G.M.: The origins and the future of microfluidics. Nature **442**, 368–373 (2006)

120. Wu, J., Jiang, H., Su, J., Shi, B., Jiang, Y., Gu, K.: Application of distributed fiber optic sensing technique in land subsidence monitoring. J. Civil Struct. Health Monit. **5**(5), 587–597 (2015)
121. Zhang, C.C., Zhu, H.H., Liu, S.P., Shi, B., Zhang, D.: A kinematic method for calculating shear displacements of landslides using distributed fiber optic strain measurements. Eng. Geol. **234**(21), 83–96 (2018)
122. Zhao, B., Wang, J., Coop, M.R., Viggiani, G., Jiang, M.: An investigation of single sand particle fracture using X-ray micro-tomography. Géotechnique **65**(8), 625–641 (2015)
123. Zhao, H., Ge, L., Luna, R.: Low viscosity pore fluid to manufacture transparent soil. Geotech. Test. J. **33**(6), 463–468 (2010)

Soil Properties: Physics Inspired, Data Driven

J. Carlos Santamarina, Junghee Park, Marco Terzariol, Alejandro Cardona, Gloria M. Castro, Wonjun Cha, Adrian Garcia, Farizal Hakiki, Chuangxin Lyu, Marisol Salva, Yuanjie Shen, Zhonghao Sun and Song-Hun Chong

Abstract Research and engineering projects during the last century have advanced the understanding of soil behavior and contributed extensive datasets. Nevertheless, the granular nature of soils challenges the accurate prediction of soil properties. In this context, a physics-inspired and data-driven approach helps us anticipate the soil response. The granular nature of soils defines their inherent properties (e.g., non-linear, non-elastic, porous, pervious) and their effective stress-dependent stiffness, frictional strength and dilation upon shear. The revised soil classification builds on the physical understanding of soils (e.g., packing characteristics and the effect of pore fluid chemistry on fines) and the extensive data accumulated in the field. Asymptotically correct compression models adequately fit experimental data and avoid numerical difficulties. Constant volume friction reflects particle shape and it is strongly dependent on stress path. Repetitive loading leads to characteristic asymptotic conditions (terminal density, and either ratcheting or shakedown). Data and physical analyses suggest a power relationship between void ratio and hydraulic conductivity. The pore-scale origin of suction is interfacial tension and contact angle. P-wave velocity is a good indicator of loss of saturation and S-wave velocity measures the skeletal shear stiffness. Permittivity, electrical conductivity and thermal conductivity are sensitive to water content. Finally, ubiquitous sensors, information technology and cellular communication support the development of effective laboratory characterization techniques and allow us to access large databases. These are transformative changes in geotechnical engineering.

Keywords Soil classification · Repetitive loading · Constitutive model · Geophysics · Stiffness · Strength · Conductivity · Permeability

J. C. Santamarina (✉) · J. Park · M. Terzariol · A. Cardona · G. M. Castro · W. Cha · A. Garcia · F. Hakiki · C. Lyu · M. Salva · Y. Shen · Z. Sun
King Abdullah University of Science and Technology (KAUST), Thuwal, Saudi Arabia
e-mail: carlos.santamarina@kaust.edu.sa

S.-H. Chong
Sunchon National University, Sunchon, South Korea

N. Lu and J. K. Mitchell (eds.), *Geotechnical Fundamentals for Addressing New World Challenges*, Springer Series in Geomechanics and Geoengineering,
https://doi.org/10.1007/978-3-030-06249-1_3

1 Introduction: Soils Are Particulate Materials

The particulate nature of soils was recognized in the early stages of soil mechanics. However, the analysis of soils masses as equivalent continua has prevailed in most cases. Quoting Terzaghi (Note: The statement can be generalized to all granular materials, from fine grained soils to fractured rocks) [52]:

> … Coulomb … purposely ignored the fact that sand consists of individual grains, and … dealt with the sand as if it were a homogenous mass with certain mechanical properties. Coulomb's idea proved very useful as a working hypothesis … but it developed into an obstacle against further progress as soon as its hypothetical character came to be forgotten by Coulomb's successors. The way out of the difficulty lies in dropping the old fundamental principles and starting again from the elementary fact that the sand consists of individual grains.

In fact, the particulate nature of soils allows us to anticipate inherent characteristics and behaviors, as summarized in Table 1.

The rest of this chapter explores a selection of soil properties frequently used in engineering practice. In each case, we identify the underlying physical processes and provide physics-inspired yet data-driven guidelines to estimate these parameters. The chapter starts with the classical problem of soils classification. References throughout the manuscript point to classical studies and prior publications from our group where additional references are extensively cited.

2 Revised Soil Classification System RSCS

Soil classification systems have been developed to assist engineers by grouping soils into similar response categories. There are several limitations to the current systems: (1) they use fixed boundaries despite the broad range of fines plasticity, (2) they underestimate fines-dominant soil behavior even when the fines fraction is significantly lower than $F_F = 50\%$, (3) they do not consider the effect of particle shape, (4) and they disregard the critical role of pore-fluid chemistry on fines response. These observations together with large amounts of laboratory and field data accumulated during the last decades support the development of the revised soil classification system RSCS summarized herein. The overall classification is based on a soil-specific triangular texture chart that is developed using volumetric-gravimetric analyses adjusted with soil property data (Note: a user-friendly RSCS application built in an Excel-sheet is available on the authors' website: egel.kaust.edu.sa). Additional analyses follow for fines-dominant soils.

Table 1 Soils are particulate geo-materials

Soils are inherently *non-linear* (Hertz and electrical contacts), *non-elastic* (Mindlin contact), *porous* and *pervious* (i.e., porosity between grains is interconnected)
Particle-level characteristics and processes integrate to yield the macroscale response • Size determines the balance between particle-level forces (capillary and electrical forces gain relevance when particles are smaller than 10–50 μm in size) • Well graded soils can attain higher packing density • Shape reflects formation history and it affects grain packing, anisotropy, stiffness, strength and permeability—among others • Spatial arrangement depends on electrical forces in fine-grained sediments (pore fluid pH and ionic concentration), and by grain shape and relative grain size in coarse-grained soils • Porosity varies widely and it is stress-dependent in [unstructured] fine grained soils, but it varies in a narrow range and is mostly defined at the time of packing in coarse grained soils
The particulate skeleton (frictional) coexists with the pore fluids (viscous) • They are very different from each other; the key is to anticipate their distinct responses to imposed boundary changes • The skeleton and the fluid interact; this gives rise to coupled fluid pressure, effective stress, volumetric strains and shear response • Mixed fluids add capillary effects onto the particulate skeleton • Generalization: hydro-chemo-bio-thermo-mechanical processes are coupled in soils
The mechanical behavior of the particulate skeleton is effective stress-dependent: • Related phenomena includes stiffness (Hertz), frictional strength (Coulomb), and dilation upon shear (Taylor) • Frictional strength limits the maximum stress anisotropy a soil can experience • Other properties may depend on effective stress as well (e.g., the thermal conductivity of dry soils)
Particle-level deformation mechanisms change with strain level • Small-strain deformation takes place at constant-fabric and grain deformations concentrate at inter-particle contacts; in this strain regime, volume change, pore pressure generation and frictional losses are minimal • Large-strain deformation involves fabric changes (the role of contact-level grain deformation vanishes) • The threshold strain between the two regimes is higher for finer soils and at higher confinement
Soils are not inert, and often change within the time scale of engineering projects Corollary: natural soils may behave differently than freshly remolded clay or recently packed sand

Note details and implications for educational strategies in [45]

2.1 Overall Classification

Volumetric-gravimetric analyses define the threshold for gravel F_G, sand F_S, and fines F_F fractions (Table 2). The low and high threshold fraction ($F_F|^L$ and $F_F|^H$ in Fig. 1) divide soils into three categories: coarse-dominant, transitional, and fines-dominant mixtures. The threshold fractions can be estimated from attainable packing densities in sands and gravels (a function of their coefficient of uniformity and particle shape), and characteristic compaction values for the fine fraction (a function of its plasticity). The soil fraction that forms the load-carrying skeleton is responsible for mechanical

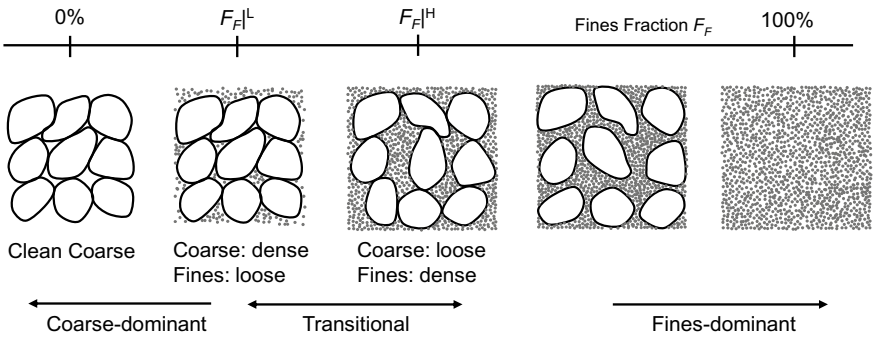

Fig. 1 Threshold fractions. Coarse, transitional, and fines-dominant mixtures after [37]

properties, while the soil fraction that controls the pore size determines the hydraulic conductivity.

Experimental data indicate that coarse grains in a fines-matrix affect the mechanical properties even beyond e^{max} (Fig. 1—sketches d and e). This observation leads to the use of data-adjusted soil classification boundaries. The physics-inspired and data-driven approach renders the 13 "notable mixtures" that define the classification boundaries (specified in Table 2).

The soil-specific RSCS triangular chart encompasses 10 soil groups. The RSCS uses a dual nomenclature to recognize the mechanical and the flow-controlling fractions; for example, a S(F) indicates that the soil will exhibit sand-controlled mechanical properties yet fines-controlled hydraulic conductivity.

2.2 Fines Classification

The classification requires further analysis when fines are responsible for either the mechanical and/or the flow response of a soil [i.e. including either F or (F)]. In particular, the new fines classification system identifies the type of fines in terms of their plasticity and sensitivity to pore-fluid chemistry. It is also based on physics (i.e., specific surface and electrical forces), and data-adjusted to benefit from the accumulated lab data and field experiences over the last decades (Note: details in [23, 24]).

The method is based on three liquid limits using the fines fraction passing sieve #200, i.e., threshold for relevant electrical and capillary forces (Note: we recommend the fall cone method for repeatability [21]). We selected three common fluids readily available at geotechnical laboratories: (1) deionized water DW, (2) brine prepared as a 2 M NaCl solution, and (3) kerosene. Deionized water hinders the formation of face-to-face aggregation, the 2 M NaCl solution collapses the double layer, and the low-polarity kerosene probes the effect of Van der Waals forces.

Table 2 Revised soil classification system RSCS

Revised soil classification system RSCS				Packing void ratio		
				Gravel	Sand	Fines
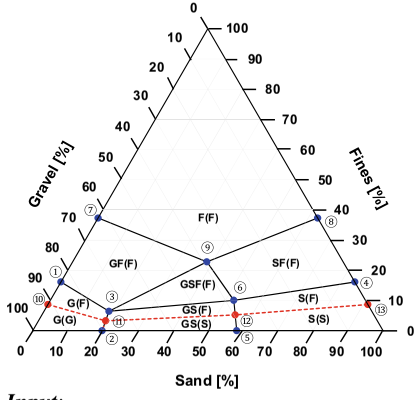	(a) Mechanical properties	G-control	①	e_G^{min}	–	$e_F\|^{10\,kPa}$
			②	e_G^{min}	e_S^{max}	–
			③	e_G^{min}	e_S^{max}	$e_F\|^{10\,kPa}$
		S-control	④	–	e_S^{min}	$e_F\|^{10\,kPa}$
			⑤	$2.5e_G^{max}$	e_S^{min}	–
			⑥	$2.5e_G^{max}$	e_S^{min}	$e_F\|^{10\,kPa}$
		F-control	⑦	$1.3e_G^{max}$	–	$e_F\|^{1MPa}$
			⑧	–	$1.3e_S^{max}$	$e_F\|^{1MPa}$
			⑨	$2.5e_G^{max}$	$1.3e_S^{max}$	$e_F\|^{1MPa}$
	(b) Fluid flow	F-control	⑩	e_G^{min}	–	$\lambda e_F\|^{LL}$
			⑪	e_G^{min}	e_S^{max}	$\lambda e_F\|^{LL}$
			⑫	$2.5e_G^{max}$	e_S^{min}	$\lambda e_F\|^{LL}$
			⑬	–	e_S^{min}	$\lambda e_F\|^{LL}$

Input:
Gravel *G* (> 4.75 mm) F_G e_G^{max} and e_G^{min} or R & C_u
Sand S (0.075 ~ 4.75 mm) F_S e_S^{max} and e_S^{min} or R & C_u
Fines F (< 0.075 mm) F_F $e_F|^{10\,kPa}$, $e_F|^{1MPa}$, and $e_F|^{LL}$

(continued)

Table 2 (continued)

Revised soil classification system RSCS				Packing void ratio
Compute Threshold fractions: $F_G = M_G/M_T$, $F_S = M_S/M_T$, $F_F = M_F/M_T$ $F_G = \left(1 + \frac{e_G}{1+e_S} + \frac{e_S}{1+e_F}\frac{e_G}{1+e_S}\right)^{-1}$ $F_S = \left(\frac{1+e_S}{e_G} + 1 + \frac{e_S}{1+e_F}\right)^{-1}$ $F_F = \left(\frac{1+e_S}{e_G}\frac{1+e_F}{e_S} + \frac{1+e_F}{e_S} + 1\right)^{-1}$ Support information and Correlations: Fines: Fluid flow $e_F\vert^{flow} = 0.05LL\log(LL-25)$ Fines: Load carrying $e_F\vert^{10\,kPa} = 0.026LL + 0.07$ $e_F\vert^{1\,MPa} = 0.011LL + 0.21$ Gravel and sand: $e_C^{max} = 0.032 + \frac{0.154}{R} + \frac{0.522}{C_u}$, $e_C^{min} = -0.012 + \frac{0.082}{R} + \frac{0.371}{C_u}$				
Soil classification boundaries: Mechanical control (blue points) and fluid flow control (red points). Soil properties used for this chart: angular and uniform gravel $e_G^{max} = 0.81$ and $e_G^{min} = 0.45$; angular and uniform sand $e_S^{max} = 0.81$ and $e_S^{min} = 0.45$; fines resemble kaolinite with liquid limit $LL = 50$, $e_F\vert^{10\,kPa} = 1.33$, $e_F\vert^{1\,MPa} = 0.76$, $e_F\vert^{LL} = 1.32$, and $\lambda = 2.8$. Note: flow-controlling fine fractions are $F_F = 3.3\%$ at point ⑪ and $F_F = 5.2\%$ at point ⑫. Refer to [3] for the case of well-graded sand and gravel				

Note Details in [36–38]

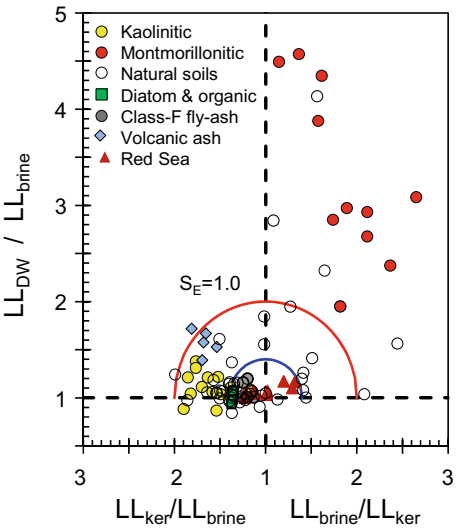

Fig. 2 Sediment response to changes in fluid conductivity and permittivity; circular boundaries correspond to electrical sensitivities S_E = 1.0 and 0.4—Corrected ratios. Updated after [24]

The three liquid limits combine into two ratios that reflect the sensitivity of fines to the pore fluid electrical conductivity and permittivity [Eqs. (1) and (2)—they take into account the specific gravity of kerosene and precipitated salts].

$$\left.\frac{LL_{\text{ker}}}{LL_{brine}}\right|_{corr} = \frac{LL_{\text{ker}}}{LL_{brine}} \frac{1 - c_{brine}\frac{LL_{brine}}{100}}{G_{\text{ker}}} \tag{1}$$

$$\left.\frac{LL_{DW}}{LL_{brine}}\right|_{corr} = \frac{LL_{DW}}{LL_{brine}}\left(1 - c_{brine}\frac{LL_{brine}}{100}\right) \tag{2}$$

The corrected ratios define the electrical sensitivity S_E as the distance between measured values and the absolutely "non-sensitive" soil response point at $LL_{DW}/LL_{brine} = 1$ and $LL_{ker}/LL_{brine} = 1$ [Fig. 2 and Eqs. (3) and (4)]:

$$S_E^{(left)} = \sqrt{\left(\frac{LL_{\text{ker}}}{LL_{brine}} - 1\right)^2 + \left(\frac{LL_{DW}}{LL_{brine}} - 1\right)^2} \quad (left : LL_{\text{ker}}/LL_{\text{brine}} > 1) \tag{3}$$

$$S_E^{(right)} = \sqrt{\left(\frac{LL_{brine}}{LL_{\text{ker}}} - 1\right)^2 + \left(\frac{LL_{DW}}{LL_{brine}} - 1\right)^2} \quad (right : LL_{\text{ker}}/LL_{\text{brine}} < 1) \tag{4}$$

Figure 3 presents the fines classification chart in view of plasticity and electrical sensitivity. There are 12 fines groups in the chart as a function of their plasticity (first letter: N, L, I, or H) and electrical sensitivity (second letter: L, I, or H). Data for well-known clays, diatoms, silts, and fly ash are superimposed on the fines classification chart (Fig. 3). The boundary for LL = 30 represents the maximum water content when pore water begins to bleed out from loosely-packed non-plastic silts or

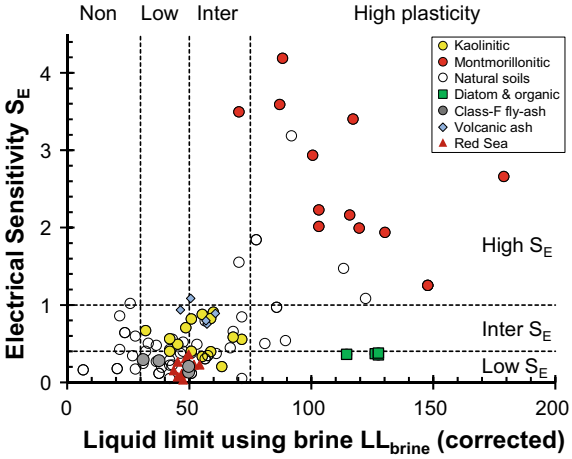

Fig. 3 Fines classification chart. Report a two-letter nomenclature; the first one corresponding to plasticity (N, L, I or H), and a second letter corresponding to electrical sensitivity (L, I or H). Updated after [23, 24]

sands; the zone between LL = 30 and LL = 50 involves the intermediate plasticity fines; and the boundary for LL = 75 separates kaolinite and illite from smectites. In terms of electrical sensitivity, the soil group below $S_E < 0.4$ includes non-plastic diatomaceous, silty and sandy soils, the fines group between $0.4 < S_E < 1.0$ involves intermediate sensitivity such as kaolinites, while the fines above $S_E > 1.0$ capture highly electrically-sensitive fines such as montmorillonite.

3 Load-Deformation Response

Soils are granular materials; therefore, their load-deformation response is inherently non-linear and non-elastic, the stiffness of the soil skeleton increases with effective confinement, and both cementation and stress history can have a major influence on stiffness and volume changes.

Deformation mechanisms depend on strain level and particle size. Soils deform at constant-fabric during small-strain deformation, the drained Poisson's ratio is $\nu < 0.2$, energy losses are minimal, and there is no accumulation of deformation or pore pressure during repetitive loading. At large strains, soil deformation involves fabric changes, and soils may either contract or dilate under drained shear (Note: drained loading implies that the rate of loading is slower than the rate of pore water dissipation).

3.1 Small-Strain Stiffness

The constant-fabric small-strain shear stiffness G_{max} reflects the deformation of adsorbed layers in fine-grained soils (<10 μm), and contact deformation in coarse-grained soils (>100 μm). Guided by contact mechanics, stiffness-stress data are readily fitted with a power function of the effective stress (inspired in Hertzian contact theory).

$$G_{\max} = A\left(\frac{\sigma_1' + \sigma_3'}{2\,\text{kPa}}\right)^{\Omega} \tag{5}$$

where A [kPa] and Ω are related to physical and geometrical particle-level soil characteristics. Typically, Ω ranges from 1/3 (elastic contacts) and 1/2 for cone-to-plane contacts, and >1 for electrical interaction. Section 7 provides additional information for parameter estimation based on shear wave propagation data.

3.2 Compressibility (Isotropic and Zero-Lateral Strain)

The compression of loosely-packed small grains resembles the compression of a gas. Boyle-Mariotte's law ignores the size of molecules, and concludes that pressure and volume are inversely related. Later, van der Waals corrected this expression to take into consideration the size of molecules and rewrote Boyle's equation in terms of the "contractible volume", i.e., the volume of voids. This expression is as a power relationship between void ratio and effective stress.

The clay type and the chemical environment during formation/deposition determine the initial fabric and associated void ratio at low stress $e_{1\,kPa}$, which is strongly related to the clay specific surface, hence the liquid limit: $e_{1\,kPa} \approx LL/30$. The compression index C_c is positively correlated to the initial void ratio $e_{1\,kPa} \approx 0.48 + 3.4C_c$. Natural clayey sediments retain higher void ratios than remolded sediments at the same effective stress [7, 14, 20]. Differences between natural and remolded sediments highlight the role of diagenesis and fabric memory in natural sediments; clearly, remolding destructures the natural soil.

On the other hand, the compressibility of non-plastic coarse-grained soils depends on their initial packing density. As the stress level increases, particle crushing becomes the prevailing deformation mechanism, and sand specimens with different initial void ratios tend to converge towards a unique compression line [40]. Mineralogy, grain size, grading and shape affect particle crushing.

The classical $e - \log(\sigma')$ compressibility model [53] is not asymptotically correct since it predicts infinite low stress void ratio e_L as $\sigma' \to 0$, and negative void ratio at high stress e_H as $\sigma' \to \infty$. Table 3 identifies alternative models, including a power law (anticipated for gasses). These models fit the full stress range and avoid numerical discontinuities (Note: clayey sediments can reach lower void ratio e_H than sands at high stress, e.g., shales compared to sandstones).

Table 3 Asymptotically correct compression models—Wide stress range applications

Modified Terzaghi	$e = e_c - C_c \log\left(\frac{1\,kPa}{\sigma' + \sigma'_L} + \frac{1\,kPa}{\sigma'_H}\right)^{-1}$
Power	$e = e_H + (e_L - e_H)\left(\frac{\sigma' + \sigma'_c}{\sigma'_c}\right)^{-\beta}$
Exponential	$e = e_H + (e_L - e_H) \cdot \exp^{-\left(\frac{\sigma'}{\sigma_c}\right)^{\beta}}$
Hyperbolic	$e = e_L - (e_L - e_H)\frac{1}{1+\left(\frac{\sigma_c'}{\sigma'}\right)^{\beta}}$

Note See 1-D compression data fitted with the four different models in [14]

3.3 Deviatoric Loading

The soil secant shear stiffness G_{sec} degrades from the maximum shear stiffness G_{max} as the shear strain γ increases and the soil approaches the ultimate shear strength τ_{ult} (hyperbolic equation—generalized: Ramberg-Osgood).

$$G_{\text{sec}} = \frac{G_{\max}}{1 + \gamma \frac{G_{\max}}{\tau_{ult}}} \tag{6}$$

3.4 Shear Strength: Friction

Soils are granular materials; thus their strength is frictional and effective stress dependent (Table 1). The maximum stress anisotropy soils can attain reflects the Coulomb failure strength: $(\sigma'_1/\sigma'_3)_{\max} = \tan^2(45 + \phi/2)$.

Under monotonic shear loading, soils reach a terminal state known as the critical state where shear progresses at constant volume. Critical state implies statistical equilibrium between local dilation (to overcome rotational frustration among particles with high coordination) and local contraction (chain buckling where particles have low coordination). It follows from this observation that (For a comprehensive review of soil friction see [48]):

(a) Particle shape controls the balance between rotation and contact slippage, thus the constant volume friction angle for uniform sands is roundness *R*-dependent $\phi_{CV} = 42 - 17R$ (Fig. 4a) [11].
(b) Critical states depend on convergent-versus-divergent granular flow, i.e., stress-path dependent. In particular, the friction angle in axial extension AE is larger than in axial compression AC, and typically $\phi_{AC} \leq \phi_{AE} \leq 1.5\phi_{AC}$ (Fig. 4b) [28, 29, 32, 54]

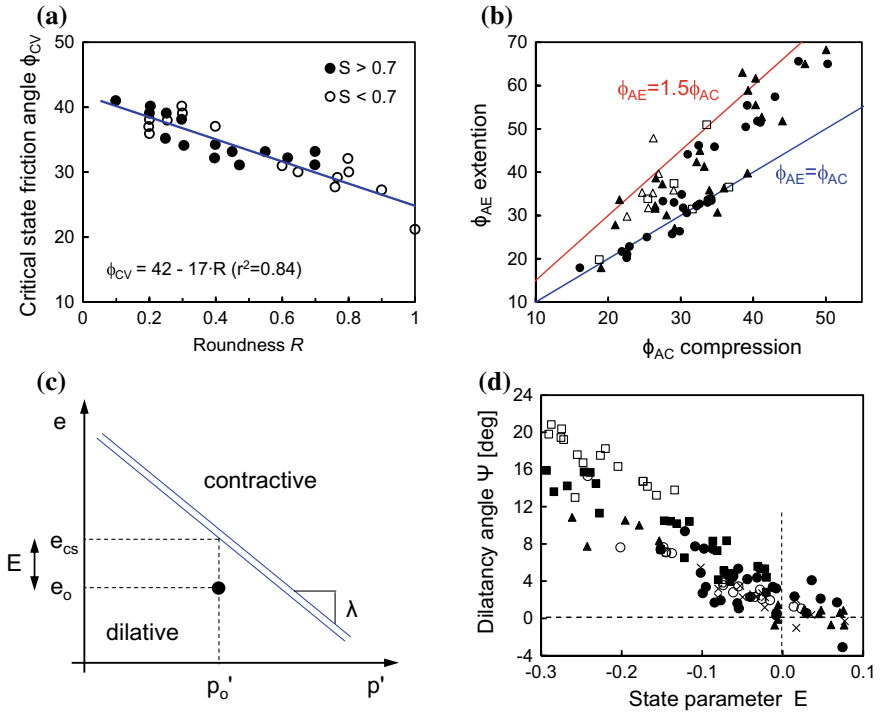

Fig. 4 Shear strength: Friction. **a** Critical state friction angle and particle shape [11], **b** stress path dependency [28, 29, 32, 54], **c** and **d** state parameter E and dilatancy angle. Combined from [2, 5]

(c) Dilation requires additional work against the confining stress and adds to the shear resistance. The angle of dilation Ψ is a function of the distance E between the initial void ratio and the void ratio at critical state, known as the state parameter $E = e_0 - e_{cs}$ (Figs. 4c, d) [2].

(d) The peak friction angle adds the dilative resistance to the constant volume shear strength, $\phi_p = \phi_{CV} + 0.8\Psi$ [5].

Shear localization implies positive feedback: the incremental work decreases as shear continues; eventually, less work is required to shear a soil after shear localization. Then, we can expect shear localization in a wide range of soil conditions including: dilative-drained shear (shear localization averts work of dilation against the confining stresses), dilative-undrained if cavitation takes place, contractive undrained if locally undrained, shear of soils made of eccentric particles with low residual strength, cemented soils due to the progressive breakage of cementation, unsaturated soils due to meniscus failure, non-homogeneous specimen in drained and undrained shear, non-uniform grain crushing or void collapse.

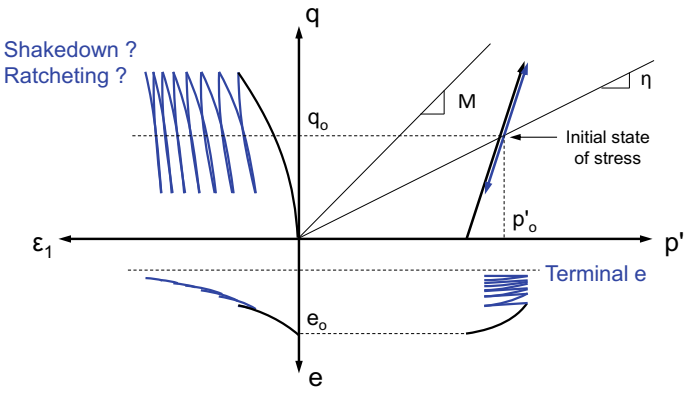

Fig. 5 Behavior of a granular material subjected to drained cyclic triaxial loading [39]

4 Repetitive Loading

Geotechnical systems impose a wide range of static and repetitive loads on soils. Common repetitive loads include:

(a) Mechanical cycles: traffic loads (cars, trucks, railroads, and cranes), wind loads on turbines and buildings, and lock operation for water navigation
(b) Wet-dry cycles: daily and seasonal moisture changes, water table fluctuations and associated changes in effective stress
(c) Pore-fluid chemistry cycles: such as tides, rain, and industrial operations; they alter the balance between interparticle electrical forces, and affect the fabric, permeability and void ratio
(d) Temperature cycles: temperature changes are associated with daily and seasonal thermal cycles (including thermal piles) and industrial activities (e.g., foundation of LNG tanks, buried cables). Thermal oscillations trigger consolidation, swelling, pore water pressure changes and creep. Phase transformations—such as freeze-thaw—exacerbate the consequences of thermal cycles.

Soils subjected to repetitive mechanical or environmental cyclic loads experience volumetric and shear strain accumulation when cyclic strains are larger than the elastic threshold strain (Fig. 5).

The accumulation of plastic shear strain can lead to either

(a) shakedown: plastic shear strain accumulation stops after a certain number of cycles and the soil reaches a stable deformation state; or
(b) ratcheting: shear strain accumulates indefinitely (typically under high-stress obliquity) [1].

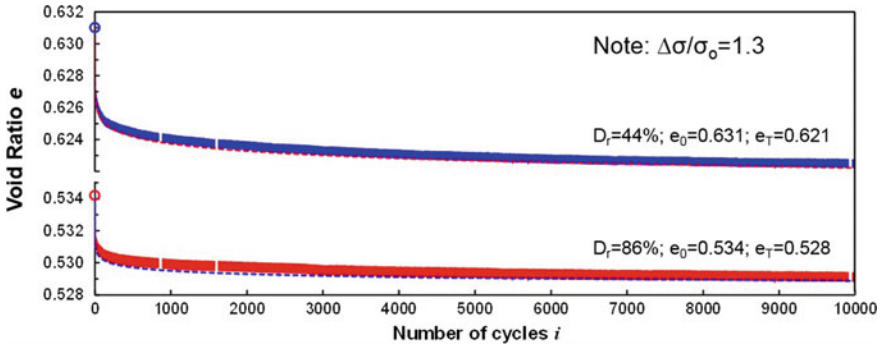

Fig. 6 Evolution of void ratio under repetitive K_0-loading condition [35]

Table 4 Plastic strain accumulation models

Type	Strain accumulation	For volume	For shear
Exponential	$\varepsilon_i^{acc} = \varepsilon_1 + b\{1 - \exp[-c(i-1)]\} + d(i-1)$	$b = \varepsilon_\infty - \varepsilon_1$, $d = 0$	Shakedown $d = 0$ Ratcheting $d > 0$
Polynomial	$\varepsilon_i^{acc} = \varepsilon_1 + b(1 - i^c) + d(i-1)$	$b = \varepsilon_\infty - \varepsilon_1$, $d = 0$	Shakedown $d = 0$ Ratcheting $d > 0$
Power	$\varepsilon_i^{acc} = \varepsilon_1 + b(i^c - 1) + d(i-1)$	Requires shutoff	Shakedown required shutoff Ratcheting $d > 0$

Source See [13] for a discussion of model parameters in these accumulation models

On the other hand, the accumulation of *volumetric strain* is inherently limited by diminishing porosity, and the asymptotic state is herein referred to as "terminal void ratio" or "terminal density" [34].

The terminal void ratio e_T for k_0-loading is a function of the initial void ratio e_0 and the cyclic stress amplitude relative to the static load $\Delta\sigma/\sigma_0$. As long as the deformation mechanism remains the same, the void ratio versus the number of cycles trend can be fitted as (Fig. 6):

$$\frac{e_i - e_T}{e_0 - e_T} = \frac{1}{\alpha + \left(\frac{i}{\beta}\right)^m} \tag{7}$$

Table 4 presents various plastic strain accumulation models for both shear and volumetric strain accumulation. These models can accommodate ratcheting, shakedown, and asymptotic terminal density.

5 Hydraulic Conductivity

The theoretical Hagen-Poiseuille analysis considers the driving pressure difference and the resisting viscous drag to compute the flow rate through a cylindrical tube as a function of the tube diameter and the gradient in total energy. The Kozeny-Carman model considers a soil as a set of parallel tubes, assumes Hagen-Poiseuille flow in the tubes [8] and provides an estimate of the hydraulic conductivity of soils as a function of the specific surface area S_s and the void ratio e (Fig. 7).

Published hydraulic conductivity data spans more than 12 orders of magnitude [10, 16, 30]. Trends follow a power-law relationship with void ratio (Fig. 7). Data points collapse onto a single trend (±1 order of magnitude) when plotted against the estimated mean pore size computed from both the void ratio e and specific surface S_s of the soil as $d_{pore} = 2e/(S_s \rho_m)$. This result confirms the robustness of the Kozeny-Carman model (see data in [42]).

The parallel and series configurations are the upper and lower bounds for the hydraulic conductivity in spatially varying media (see other bounds in [22]):

Physics-based: Kozeny-Carman

$$k_h = \frac{C_f g}{\mu_f \rho_m^2} S_s^{-2} \frac{e^3}{1+e}$$

μ_f: kinematic viscosity
ρ_m: mineral density
S_s: specific surface [m^2/g]

C_f: pore topology const. (≈ 0.2)
g: gravity

Data-based

$$k_h = k_o \left(\frac{e}{e_o}\right)^{\beta}$$

e_o: reference void ratio (e_o=1)
k_o: conductivity at e_o

$$\log\left(\frac{k_o}{cm/s}\right) = -5 - 2\log\left(\frac{S_s}{m^2/g}\right)$$

β : soil dependent (2<β<6)
β = 3 ± 1 for coarse-grained to β = 5 ± 1 for fine-grained soils

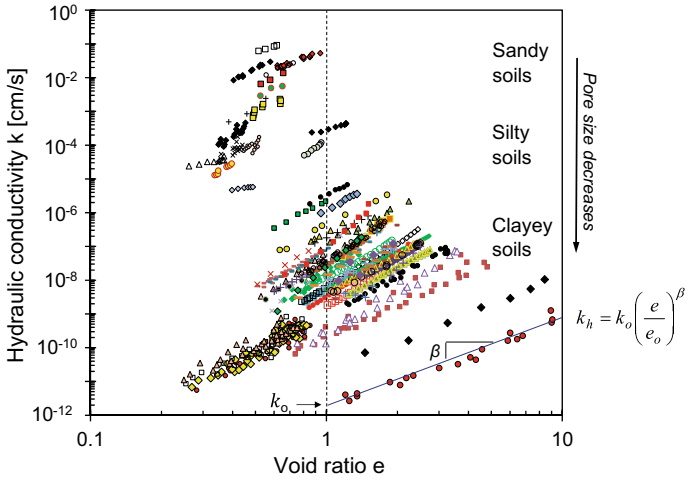

Fig. 7 Hydraulic conductivity. Fundamental concepts and data trends (after [42])

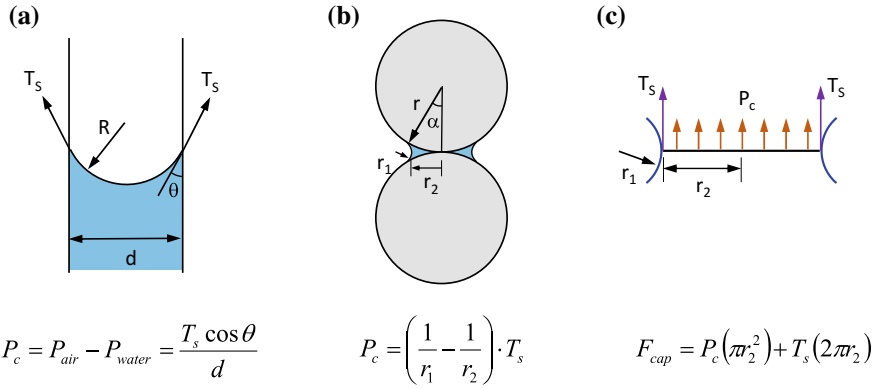

Fig. 8 Capillary pressure and contact forces—Laplace-Young equation

$$\frac{\Sigma w_i}{\Sigma \frac{w_i}{k_i}} \leq k \leq \frac{\Sigma w_i k_i}{\Sigma w_i} \tag{8}$$

If the hydraulic conductivity is anisotropic (i.e., a tensor), it cannot be estimated from the void ratio and specific surface alone (scalars). Changes in pore fluid chemistry affect the hydraulic conductivity of fine-grained soils. Pressure gradients imply gradients in effective stress, hence variations in void ratio and hydraulic conductivity; therefore, all measurements for hydraulic conductivity are integral measurements across the specimen and require proper interpretation.

6 Unsaturated Soils

Water in soils experiences negative pressures during drying (Refer to Chapter 4 "Linking Soil Water Adsorption to Geotechnical Engineering Properties" and Chapter 8 "Fundamental Challenges in Unsaturated Soil Mechanics"). The pressure difference between air and water is the capillary pressure or matric suction. At the pore scale, capillarity results from the water–air interfacial tension and the contact angle the air-water interface forms with the mineral surface, as predicted by the Laplace equation (Fig. 8a, b). Furthermore, it follows from Laplace's equation that the capillary pressure required to force a non-wetting fluid to invade a pore increases as the pore size decreases. In later stages of drying, water forms rings around particle contacts (Fig. 8b). The smaller the menisci radii, the higher the capillary pressure.

Suction is transferred onto the soil skeleton and capillary-induced interparticle forces emerge (Fig. 8c [12]). At the macro-scale this resembles an additional component to the effective stresses [3]. However, this simple mathematical trick must be carefully analyzed: capillary-induced interparticle forces are internally generated while effective stress are externally imposed. Furthermore, the spatial variability of

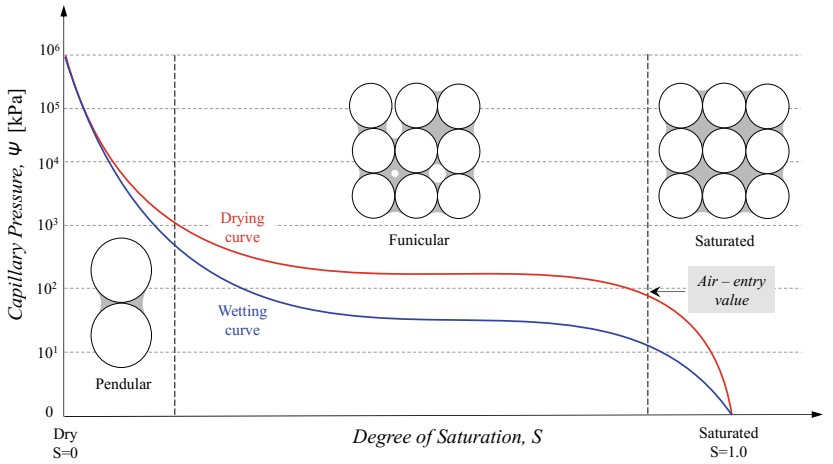

$P_c(S_e) = P_0(S_e^{-1/m} - 1)^{1/n}$	P_0: air entry pressure m and n: parameters	van Genuchten [55]
$P_c(S_e) = P_d \cdot S_e^{-1/\lambda}$	S_e: effective saturation P_d (Pa): air entry pressure λ: pore size distribution index	Brooks & Corey [6]
Brooks-Corey parameters from grain size distribution		
$P_d = 285766 \cdot f^{0.79} M_d^{-0.96}$ $\lambda = 1.512 \cdot [\exp(0.3f) - 1]$	f: grain size distribution index M_d: median grain size (mm)	Bloemen [4] Rawls et al. [41]

Fig. 9 Capillary pressure-saturation curve, also known as the soil water characteristic curve. Common fitting equations for capillary pressure-saturation curve

residual water creates a non-uniform distribution of forces. Note that the capillary pressure increases but the affected area decreases during drying.

The macroscale soil-water characteristic curve (or pressure-saturation curve) relates capillary pressure to degree of saturation. The pressure-saturation curve reflects the pore size distribution, pore connectivity and spatial correlation [31]. The pressure-saturation curve is used to predict the evolution of relative permeability, deformation, shear strength and other unsaturated soil parameters [19]. Several mathematical equations have been proposed to represent the capillary pressure-saturation curve; parameters can be estimated from particle-size distribution (For example, see Fig. 9).

Table 5 Longitudinal P-wave velocity: Sequential computation of constrained modulus and mass density

$V_P = \sqrt{\frac{M_{soil}}{\rho_{soil}}} = \sqrt{\frac{B_{soil}+4/3G_{sk}}{\rho_{soil}}}$		Water $V_P = 1482$ m/s Air $V_P = 343$ m/s
Skeleton	$B_{sk} = \frac{2(1+\nu)}{3(1-2\nu)} G_{sk}$	G_{sk} from $G_{sk} = V_S^2 \rho$
Soil (fluid + skeleton)	$B_{soil} = B_{sus} + B_{sk}$	$\rho_{soil} = \rho_{sus} = (1-n)\rho_g + n\rho_{fl}$
Suspension (fluid + particles)	$B_{sus} = \left(\frac{1-n}{B_g} + \frac{n}{B_{fl}}\right)^{-1}$	$\rho_{sus} = (1-n)\rho_g + n\rho_{fl}$ $n =$ porosity
Fluid mixture	$B_{fl} = \left(\frac{S_r}{B_w} + \frac{1-S_r}{B_a}\right)^{-1}$	$\rho_{fl} = (1-S_r)\rho_a + S_r\rho_w$ $\rho_{fl} = S_r\rho_w$ if a $\equiv$ air

Note Details in [46]. The formula for V_P assumes $B_{sk}/B_g \approx 0$ and applies to low frequencies. $B_w = 2.18$GPa for water. $B_g = 142$ kPa for air at 1 atm. S_r = degree of saturation

7 Geophysical Properties

7.1 Elastic Waves

Long wavelength and small-strain mechanical perturbations traverse soils as elastic waves across an equivalent continuum; in other words, this is a constant-fabric phenomenon and the wave does not "see" the grains. Longitudinal particle motion in P-waves, and transverse particle motion in S-waves are the two possible propagation modes in a boundless, homogeneous, isotropic, linear-elastic, single-phase continuum. In fact, the relaxation of any of these assumptions leads to other propagation modes [46].

The P-wave velocity V_P is a function of soil density ρ_{soil} and the constrained modulus M_{soil}. Table 5 summarizes the sequential computation of M_{soil} from the shear stiffness of the skeleton G_{sk} and the bulk stiffness of the components B_{soil} and B_{fl}. Given the low bulk modulus of air, the P-wave velocity is a reliable indicator of lack of liquid saturation. On the other hand, given the high bulk modulus of water B_w compared to the bulk modulus of the skeleton B_{sk}, the P-wave velocity is not sensitive to the skeleton stiffness in saturated soils under low effective stress.

The S-wave velocity V_s measures the skeleton shear stiffness G_{sk}, which is determined by the effective stress, cementation and suction. A Hertzian-inspired power equation adequately fits experimental data (Fig. 10), where the α-factor is the shear wave velocity at a mean stress $\sigma'_{mean} = 1$ kPa (on the polarization plane), and the β-exponent captures the sensitivity of the skeletal stiffness to stress changes. Both α and β are related to the soil compressibility, i.e., the nature of contact interaction, coordination number, grain angularity, cementation, and diagenesis (Fig. 10).

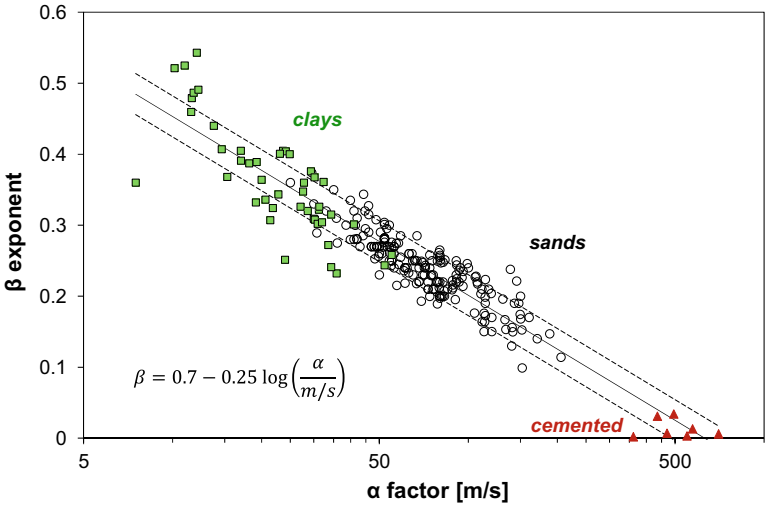

saturated or dry	$V_S = \sqrt{\frac{G_{sk}}{\rho}} = \alpha\left(\frac{\sigma'_{mean}}{1kPa}\right)^{\beta}$ $\beta = 0.7 - 0.25 \log\left(\frac{\alpha}{m/s}\right)$
unsaturated soils	$V_S \approx V_{S\,(for\ S_r=1.0)}\left[1 + \frac{suction \cdot S_r}{0.75\sigma'_v}\right]^{\beta}$

Fig. 10 Shear S-wave velocity. Details in [9, 47]

7.2 *Electromagnetic Waves*

Maxwell's equations describe the propagation of electromagnetic waves through soils, whereby the electrical and magnetic fields oscillate transversely to each other and to the direction of wave propagation.

The electromagnetic properties of soils are: (1) the electrical conductivity σ_{el}, (2) the permittivity $\kappa = \varepsilon^*/\varepsilon_0 = \kappa' - j\kappa''$, and (3) the magnetic permeability $\mu^*/\mu_0 = \mu'_r - j\mu''_r$. Permittivity and permeability are frequency-dependent, complex quantities. The three electromagnetic properties combine to determine the wave velocity V and the skin depth S_d (i.e., the penetration distance where a plane wave amplitude decays by $1/e$—Note: $S_d = 1/\alpha$ where α is the attenuation coefficient):

$$V = c_0 \frac{1}{\sqrt{\frac{1}{2}\left[\sqrt{\kappa^2 + \left(\frac{\sigma_{el}}{\varepsilon_0 \omega}\right)^2} + \kappa\right]}} \tag{9}$$

Table 6 (a) Electrical conductivity (b) Permittivity [43, 46, 49]

(a) Electrical Conductivity 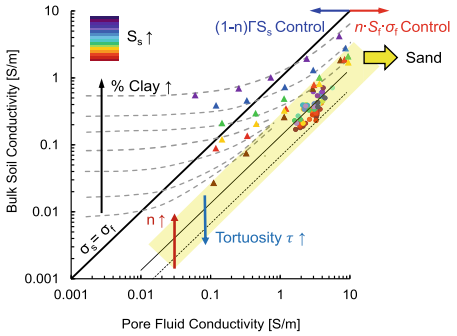	*Typical values* Organic fluid ~10^{-11} S/m Dry soil ~10^{-8} to ~10^{-4} S/m De-ionized water 5.5 × 10^{-8} S/m Distilled water ~0.5–3 × 10^{-6} S/m Freshwater ~1.5–5 × 10^{-4} S/m Sea water ~5 S/m *Soils* Archie's equation $\sigma = a \cdot \sigma_f \cdot S^c(n)^m$ σ_f: fluid conductivity S: degree of saturation a, c, m: fitting coefficients (m: 1-to-2.4; c: ~ 4-to-5) See surface conduction in [27]
(b) Permittivity 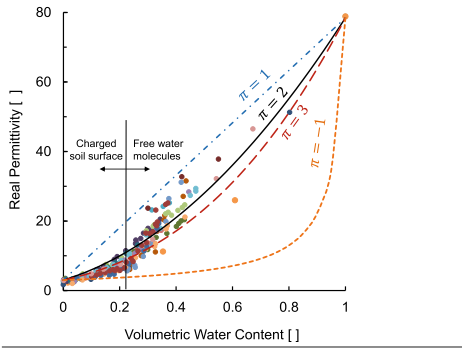	*Typical values* Air 1 Organic fluid ~2–6 Quartz 4.2–5 Calcite 7.6–8.8 Sea water ~65–70 De-ionized water 78.5 *Soils* $(\kappa')^{1/\pi} = (1-n)\,(\kappa_m')^{1/\pi} + nS_f(\kappa_f')^{1/\pi}$ linear, π = 1 complex refractive index model, CRIM, π = 2 cube, π = 3 inverse, π = −1

$$S_d = \frac{c_0}{\omega} \frac{1}{\sqrt{\frac{1}{2}\left[\sqrt{\kappa^2 + \left(\frac{\sigma_{el}}{\varepsilon_0 \omega}\right)^2} - \kappa\right]}} \tag{10}$$

where the velocity in free space is $c_0 = 3 \times 10^8$ m/s. High electrical conductivity reduces the skin depth.

The DC electrical conductivity of soils measures the movement of hydrated ions (in the pore fluid and in double layers). Therefore, the electrical conductivity of dry soils is very small ~10^{-8} to ~10^{-4} [S/m], but it increases as precipitated salts and mineral surfaces hydrate; clearly, high ionic concentration in the pore water and high specific surface clays contribute to conductivity (Table 6a).

Conversely, non-conductive organic fluids, coarse grained sediments, and frozen soils will exhibit low electrical conductivity. The soil electrical conductivity σ_{el}^{soil} allows us to estimate the porosity n of a saturated soil S = 1 if the electrical conductivity of the pore fluid σ_{el}^{fl} is known; as a first-order estimate, $n \approx \sigma_{el}^{soil}/\sigma_{el}^{fl}$.

Permittivity measures the polarization of charges within the medium in the presence of an external electric field. The prevalent polarization mechanisms in soils are the orientational polarization of free water, the displacement of diffuse counter-ion clouds relative to particles, and spatial polarization at interfaces. Analogous to conductivity, permittivity data allows us to estimate the volumetric water content in a soil (first order estimate: $\theta_w = nS_f$) or the porosity if soils are water saturated $S_f = 1$ (Table 6b). The soil permittivity increases with volumetric water content; conversely, it decreases in soils with high specific surface and in frozen soils due to the hindered polarizability of water molecules.

Most soil components are either dia- or paramagnetic. However, ferromagnetic impurities are not uncommon, particularly in many mine tailings and most fly ash accumulations. Ferromagnetism affects electromagnetic measurements in the laboratory and in the field.

7.3 Thermal Properties

Conduction controls heat transport in soils in the absence of seepage (Note: consider convection when the mean grain size $D_{50} \geq 6$ mm). Conduction paths in soils include: the solid, pore fluid, solid-to-solid contacts, interstitial liquid film and the solid-to-fluid or fluid-to-solid pathways [18, 55–57]. The thermal resistance at contacts depends on (1) the effective particle-to-particle contact area due to roughness, asperities and the acting normal force, (2) the thermal conductivity of interstitial fluids, and (3) the often negligible scattering of phonons at the material boundary [33]. Then, the thermal conductivity of a soil increases with dry mass density (increased coordination number), effective stress (reduced contact resistance), grain size (fewer contacts per volume), quartz content (high conductivity mineral), water content (interstitial water and conduction through pores) and ice content (higher conductivity than water). Data-driven empirical equations for dry [25] and water-saturated [17] soils follow:

$$\text{Dry soils}: \quad k_{T,dry} = \frac{0.135\rho_{dry} + 64.7}{\rho_g - 0.947\rho_{dry}} \tag{11}$$

$$\text{Wet soils}: \quad k_{T,wet} = k_{T,dry} + (1 - e^{-8.9S_r})(k_{T,sat} - k_{T,dry}) \tag{12}$$

The specific heat c_p is the gravimetric average of the specific heat of all components. As inferred from values in Table 7: (1) the presence of saturating liquids has a marked effect on the specific heat of soils, and (2) either water-to-steam or water-to-ice transformations rapidly decrease the specific heat capacity of a soil over a narrow temperature range.

Thermally induced volumetric strains in soils are often irreversible due to fabric changes, grain fractures, and chemical alterations (usually at high temperatures). Water saturated soils experience large volumetric thermal expansion during heating

Table 7 Typical thermal properties of selected materials

Material		Latent heat (kJ/kg)	Specific heat ($Jkg^{-1}K^{-1}$)	Thermal conduct. ($Wm^{-1}K^{-1}$)	Vol. thermal expansion coefficient (10^{-6} K^{-1})
Quartz			750	12 ∥–6.8 ⊥	45
Feldspars			630	1.56	10.3–22.4
Limestone			900	1.3	24
Sand	dry		800	0.15–0.33	
	Sat.		2200	2–4	
Water		334	4200	0.6	200 (at 293 K)*
Ice (0 °C)		334	2040	2.2	51 (at 273 K)**
Steam		2257	1990	0.028	
Air			1000	0.024	

Note *water-to-steam: > 1000 expansion. **water-to-ice: 1.09 expansion
Sources [15, 26, 44, 50]

under undrained conditions; the situation is aggravated if steam forms (Refer to Table 7 and to Chapter 10 "Emerging Thermal Issues in Geotechnical Engineering").

8 Closing Thoughts: New Developments and Pending Challenges

The ongoing revolution in sensors, information technology and cellular communication opens doors to new possibilities in our field. This section anticipates two key developments: the "ITsoil" database and probing tool, and "Lab-on-a-Bench" technology designed to measure critical parameters. Lab-on-a-Bench combines with ITsoil to provide users a set of self-consistent multi-physics soil parameters for a given soil specimen. Details follow.

8.1 ITsoil: Soil Properties Database and Probing Tool

Our community has characterized a large number of soils around the world since the beginning of modern soil mechanics a century ago. We have been compiling published data into a multi-dimensional database (see part of the dataset in Fig. 11). The probing tool built into ITsoil assumes that soils with similar properties will exhibit similar responses. Then, the user can input available information about a given soil (e.g., index properties and soil properties) and the tool returns a self-consistent set of thermo-chemo-hydro-mechanical properties. This is particularly relevant with the

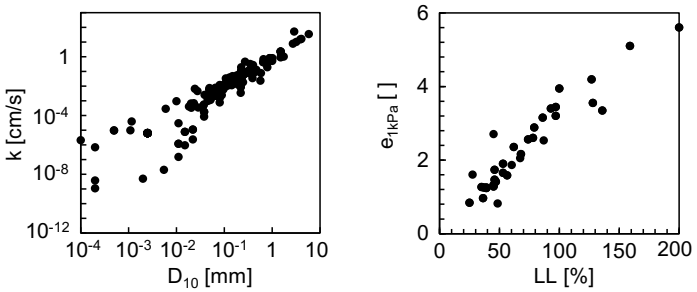

Fig. 11 ITsoil: Examples of available two-dimensional data

ongoing increased use of numerical methods and coupled process simulators (Refer to Chapter 9 "Research Challenges Involving Coupled Flows in Geotechnical Engineering" and Chapter 10 "Emerging Thermal Issues in Geotechnical Engineering").

At present, the database has limited multi-dimensional data for each soil, and the probing tool uses interval constraint propagation for decision making. Other algorithms such as Bayesian updating (with physics-inspired priors), multi-variate normal distribution and various forms of machine learning do not offer advantages at this stage, but will be implemented as the database increases in size and dimensionality. ITsoil will be available through cell-apps accessible from any location in the world.

8.2 Lab-on-a-Bench Technology

Cutting-edge sensors and sensing concepts allow for the development of compact tools for multi-physics soil characterization, herein referred to as "Lab-on-a-Bench". This set of devices maximizes the information that gained about a soil in order to anticipate its properties. Our starting set includes:

For coarse grained sediments	For fine grained sediments
• Grain size dist. (optical and sieves) • Particle shape (optical) • Packing γ_{max} and γ_{min} (shear and compaction)	• Silts: size distribution (light absorption) • Clays: specific surface (colorimetry) • Liquid limit (fall cone) • Ionic strength (probe) • pH

Effectively deployed and complementary in situ tests will gather in situ density, shear stiffness (shear waves), and shear strength (instrumented penetrometer).

8.3 Pending Challenges

Geotechnical engineering is well positioned to address new problems related to some of the great challenges society faces today, such as in the energy sector (infrastructure, resource recovery, water-energy nexus, energy waste geo-storage, energy geo-storage, and decommissioning). Associated technical needs include:

- Recalibration of engineering procedures to incorporate new testing methods and soil classification schemes (e.g., RSCS).
- Understanding of complex mixed-fluids (often three phases), differences between 'gas invasion' and 'gas nucleation', and long-term effects in mixed-fluid conditions.
- Test protocols, numerical simulators and design procedures to take into consideration shear localization, repetitive loads of all kinds, spatial variability, and inherently coupled hydro-chemo-bio-thermo-mechanical processes.
- Further understanding of soil behavior under high-stress, high-temperature, reactive fluid flow in bio-chemically active environments, and soil response in very long time scales.
- Enhanced multi-physics in situ characterization.

Acknowledgements Support for the preparation of this manuscript was provided by the KAUST Endowment at King Abdullah University of Science and Technology. G. E. Abelskamp edited the manuscript. S. Burns and J. DeJong reviewed the manuscript and provided insightful comments.

References

1. Alonso-Marroquin, F., Herrmann, H.J.F.: Ratcheting of granular materials. Phys. Rev. Lett. **92**, 054301 (2004)
2. Been, K., Jefferies, M.G.: A state parameter for sands. Géotechnique **35**, 99–112 (1985)
3. Bishop, A.W., Blight, G.E.: Some aspects of effective stress in saturated and partly saturated soils. Geotechnique **13**, 177–197 (1963)
4. Bloemen, G.W.: Calculation of capillary conductivity and capillary rise from grain size distribution. Instituut voor Cultuurtechniek en Waterhuishouding (1977)
5. Bolton, M.D.: The strength and dilatancy of sands. Geotechnique **36**, 65–78 (1986)
6. Brooks, R., Corey, T.: HYDRAU uc properties of porous media. Hydrology Papers, Colorado State University (1964)
7. Burland, J.B.: On the compressibility and shear strength of natural clays. Géotechnique **40**, 329–378 (1990)
8. Carman, P.C.: Fluid flow through granular beds. Trans. Am. Inst. Chem. Eng. **15**, 150–167 (1937)
9. Cha, M., Santamarina, J.C., Kim, H.S., Cho, G.C.: Small-strain stiffness, shear-wave velocity, and soil compressibility. J. Geotech. Geoenviron. Eng. **140**, 06014011 (2014)
10. Chapuis, R.P.: Predicting the saturated hydraulic conductivity of soils: a review. Bull. Eng. Geol. Env. **71**, 401–434 (2012)
11. Cho, G.C., Dodds, J., Santamarina, J.C.: Particle shape effects on packing density, stiffness and strength: natural and crushed sands. J. Geotech. Geoenviron. Eng. **132**, 591–602 (2006)

12. Cho, G.C., Santamarina, J.C.: Unsaturated particulate materials—particle-level studies. J. Geotech. Geoenviron. Eng. **127**, 84–96 (2001)
13. Chong, S.H., Santamarina, J.C.: Sands subjected to repetitive vertical loading under zero lateral strain: accumulation models, terminal densities, and settlement. Can. Geotech. J. **53**, 2039–2046 (2016)
14. Chong, S.H., Santamarina, J.C.: Soil compressibility models for a wide stress range. J. Geotech. Geoenviron. Eng. **142**, 06016003 (2016)
15. Cortes, D.D., Martin, A.I., Yun, T.S., Francisca, F.M., Santamarina, J.C., Ruppel, C.: Thermal conductivity of hydrate-bearing sediments. J. Geophys. Res. Solid Earth **114** (2009)
16. Dunn, R.J., Mitchell, J.K.: Fluid conductivity testing of fine-grained soils. J. Geotech. Eg. **110**, 1648–1665 (1984)
17. Ewen, J., Thomas, H.R.: The thermal probe—a new method and its use on an unsaturated sand. Geotechnique **37**, 91–105 (1987)
18. Farouki, O.T.: Thermal properties of soils (No. CRREL-MONO-81-1). Cold Regions Research and Engineering Lab Hanover NH (1981)
19. Fredlund, D.G.: The 1999 RM Hardy Lecture: the implementation of unsaturated soil mechanics into geotechnical engineering. Can. Geotech. J. **37**, 963–986 (2000)
20. Hong, Z.S., Zeng, L.L., Cui, Y.J., Cai, Y.Q., Lin, C.: Compression behavior of natural and reconstituted clays. Géotechnique **62**, 291–301 (2012)
21. BSI (British Standards Institution): Code of Practice for Site Investigations. BS 5930, London (1999)
22. Jang, J., Narsilio, G.A., Santamarina, J.C.: Hydraulic conductivity in spatially varying media a pore-scale investigation. Geophys. J. Int. **184**, 1167–1179 (2011)
23. Jang, J., Santamarina, J.C.: Fines classification based on sensitivity to pore-fluid chemistry. J. Geotechn. Geoenviron. Eng. **142**, 06015018 (2016)
24. Jang, J., Santamarina, J.C.: Closure to "Fines classification based on sensitivity to pore-fluid chemistry" by Junbong Jang and J. Carlos Santamarina. J. Geotech. and Geoenviron. Eng. **143**, 07017013 (2017)
25. Johansen, T.A.: Thermal conductivity of soils. US Army Corps of Engineers, Trondheim, Hanover, New Hampshire (1975)
26. Keyes, F.G., Vines, R.G.: The thermal conductivity of steam. Int. J. Heat Mass Transf. **7**, 33–40 (1964)
27. Klein, K.A., Santamarina, J.C.: Electrical conductivity in soils: underlying phenomena. J. Environ. Eng. Geophys. **8**, 263–273 (2003)
28. Ladd, C.C.: Stress-deformation and strength characteristics, state of the art report. In: Proceedings of 9th International Conference on Soil Mechanics, Foundation Engineering, vol. 4, pp. 421–494 (1977)
29. Lade, P.V.: Assessment of test data for selection of 3-D failure criterion for sand. Int. J. Numer. Anal. Meth. Geomech. **30**, 307–333 (2006)
30. Libardi, P., Reichardt, K., Nielsen, D., Biggar, J.: Simple field methods for estimating soil hydraulic conductivity. Soil Sci. Soc. Am. J. **44**, 3–7 (1980)
31. Lu, N., Likos, W.J.: Unsaturated Soil Mechanics. Wiley (2004)
32. Mayne, P.W., Holtz, R.D.: Effect of principal stress rotation on clay strength. In: Proceedings of 11th ICSMFE, vol. 2, pp. 579–582, San Francisco (1985)
33. Mikić, B.B.: Thermal contact conductance; theoretical considerations. Int. J. Heat Mass Transf. **17**, 205–214 (1974)
34. Narsilio, N.A., Santamarina, J.C.: Terminal densities. Géotechnique **58**, 669–674 (2008)
35. Park, J., Santamarina, J.C.: Sand response to large numbers of cycles under zero-lateral strain condition: evolution of void ratio and small strain stiffness. Géotechnique (2018). https://doi.org/10.1680/jgeot.17.p.124
36. Park, J., Castro, G.M., Santamarina, J.C.: Closure to "Revised soil classification system for coarse-fine mixtures". J. Geotech. Geoenviron. Eng. **144**, 07018019 (2018)
37. Park, J., Santamarina, J.C.: Revised soil classification system for coarse-fine mixtures. J. Geotech. Geoenviron. Eng. **143**, 04017039 (2017)

38. Park, J., Santamarina, J.C.: Revised soil classification system RSCS. In: Proceedings of the 19th International Conference on Soil Mechanics and Geotechnical Engineering, Seoul, pp. 1081–1084 (2017b)
39. Pasten, C., Shin, H., Santamarina, J.C.: Long-term foundation response to repetitive loading. J. Geotech. Geoenviron. Eng. **140**, 04013036 (2014)
40. Pestana, J.M., Whittle, A.J.: Compression model for cohesionless soils. Géotechnique **45**, 611–631 (1995)
41. Rawls, W.J., Gish, T.J., Brakensiek, D.L.: Estimating soil water retention from soil physical properties and characteristics. Adv. Soil Sci. **16**, 213–234 (1991)
42. Ren, X.W., Santamarina, J.C.: The hydraulic conductivity of sediments: a pore size perspective. Eng. Geol. **233**, 48–54 (2018)
43. Revil, A., Coperey, A., Shao, Z., Florsch, N., Fabricius, I.L., Deng, Y., Delsman, J., Pauw, P., Karaoulis, M., de Louw, P.G.B., van Baaren, E.S.: Complex conductivity of soils. Water Resour. Res. **53**, 1–27 (2017)
44. Robertson, E.C.: Thermal properties of rocks (No. 88-441). US Geological Survey (1988)
45. Santamarina, J.C.: [What] to teach or not to teach—that is the question. Geotech. Res. **2**(4), 135–138 (2016)
46. Santamarina, J.C., Klein, K., Fam, M.: Soils and waves: particulate materials behavior, characterization and process monitoring. Wiley, Chichester, U.K. (2001)
47. Santamarina, J.C., Park, J.: Geophysical properties of soils. Aust. Geomech. J. **51**, 183–194 (2016)
48. Santamarina, J.C., Shin, H.: Friction in Granular Media. Meso-scale Shear Physics in Earthquake and Landslide Mechanics, pp. 157–188. CRC Press, London (2009)
49. Shevnin, V., Mousatov, A., Ryjov, A., Delgado-Rodriquez, O.: Estimation of clay content in soil based on resistivity modelling and laboratory measurements. Geophys. Prospect. **55**, 265–275 (2007)
50. Skinner, B.J.: Section 6: thermal expansion. Geol. Soc. Am. **97**, 75–96 (1966)
51. Sverdrup, H.U., Johnson, M.W., Fleming, R.H.: The Oceans: their physics, chemistry, and general biology. Prentice-Hall, New York (1942)
52. Terzaghi, K.: Old earth-pressure theories and new test results. Eng. News-Record **85**, 632–637 (1920)
53. Terzaghi, K., Peck, R.B.: Soil Mechanics in Engineering Practice. Wiley (1948)
54. Vaid, Y.P., Sivathayalan, S.: Static and cyclic liquefaction potential of Fraser Delta sand in simple shear and triaxial tests. Can. Geotech. J. **33**, 281–289 (1996)
55. Van Genuchten, M.T.: A closed-form equation for predicting the hydraulic conductivity of unsaturated soils. Soil Sci. Soc. Am. J. **44**, 892–898 (1980)
56. Yagi, S., Kunii, D.: Studies on effective thermal conductivities in packed beds. An Official Publication of the Am. Inst. Chem. Eng. J. **3**, 373–381 (1957)
57. Yun, T.S., Santamarina, J.C.: Fundamental study of thermal conduction in dry soils. Granular Matter **10**, 197–207 (2008)

Linking Soil Water Adsorption to Geotechnical Engineering Properties

Ning Lu

Abstract Geotechnical engineering properties such as elastic modulus, small-strain shear modulus, and thermal conductivity are governed by soil fundamental properties such as specific surface area, cation exchange capacity, suction stress, and matric potential. The linkages between geotechnical properties and soil fundamental properties can be established through the use of soil water retention mechanisms of capillarity and adsorption. This chapter highlights some of the advances in establishing such linkages in the past decade. Future research challenges, opportunities, and potential pathways are also provided.

Keywords Inter-atomic forces · Free energy of soil water · Specific surface area · Cation exchange capacity · Capillary water retention · Adsorption water retention · Suction stress · Soil water density · Elastic modulus · Small-strain shear modulus · Thermal conductivity

1 Introduction

The relationship between inter-atomic forces and geotechnical engineering properties of earth materials is not always clear, even though the former plays the governing role in the latter and can be considered scientifically as the "root" for geotechnical engineering properties and material properties at any scale between them. This is, in part, due to the lack of establishment of firm relationships, and consequently a proper appreciation by the geotechnical engineering community. However, an appreciation of such relationships can be envisioned and used as a promising guiding principle for geotechnical engineering research.

N. Lu (✉)
Colorado School of Mines, Golden, CO, USA
e-mail: ninglu@mines.edu

N. Lu and J. K. Mitchell (eds.), *Geotechnical Fundamentals for Addressing New World Challenges*, Springer Series in Geomechanics and Geoengineering,
https://doi.org/10.1007/978-3-030-06249-1_4

We can ask ourselves a few questions to illustrate the linkage between properties at inter-atomic (nano) and engineering (macro) scales. What is the relationship between the Hamaker constant, an inter-atomic attractive force property, and small-strain shear modulus, a governing property for shear wave propagation in soil? The answer for most people is likely blurred, if not in doubt that there is any. Let's repose the question into the following questions.

(1) Is seismic wave propagation in soil governed by small-strain shear modulus?
(2) Is small-strain shear modulus governed by inter-particle stress?
(3) Is inter-particle stress governed by inter-atomic forces like van der Waals forces?

The answer to the first question is YES and has been firmly established at least a century ago. The answer to the second is YES and has been fully illustrated in the past several decades.

The answer to the third question is YES, and is firmly established in modern interfacial science starting in the middle of the last century. Van der Waals forces among atoms, molecules, and particles are universally characterized by the Hamaker constant and the distances among atoms, molecules, and particles.

The geotechnical engineering community began to be aware of the importance of inter-atomic forces in soil behavior in the late 1950s. The use of electrical double-layer theory to explain osmotic swelling in saturated clayey soil (e.g., [12]) is an example. The change in soil water potential due to inter-atomic forces is also used as a part of total water potential and a way to unify macroscopic pore water pressure and excess inter-particle pore pressure (e.g., [13, 81]).

Compaction is a widely-used engineering practice traditionally for improving mechanical properties of clayey soil. For a soil, why there exists an optimum water content for a maximum dry soil density has been a research subject for a long time. Bishop's effective stress theory has been used to theorize the phenomenon under unsaturated and negative pore water pressure conditions [90, 91]. Since the nineties of the last century, compacted clay liners have been used for various waste containments [8–10]. Compaction theory has been used to delineate unique hydraulic conductivity behavior and utilized as a way to improve barrier function of clay liners [25]. These works demonstrated that inter-particle stress, pore water pressure, pore geometries, and pore fluid chemistry fundamentally control saturated hydraulic conductivity.

Small-strain shear modulus has been used to understand earthquake-induced shear wave propagation in soil (e.g., [19, 101]) and liquefaction resistance (e.g., [3]). In the past two decades, the linkage between the small-strain shear modulus and inter-particle stress is clearly demonstrated and firmly established [23]. Suction stress, a unified inter-particle stress by capillarity and adsorption including implicitly van der Waals forces and electric double layer forces, has been demonstrated in recent years to govern the variation of small-strain shear modulus of soil under variably saturated conditions [30]. Therefore, even without yet explicitly and firmly establishing the direct relationship between the small-strain shear modulus and the Hamaker constant, such a relationship is likely to be established in the near future.

The promise of any relationship between fundamental properties and engineering properties is that it is scientifically sound and should provide more general and revealing information than any empirical relation, as it directly links the "cause" and "result" under more general conditions or environment.

1.1 Soil Physicochemical Properties

Soil physicochemical properties are material properties influenced by inter-atomic and inter-particle forces. The adjective "physicochemical" indicates that they attain to inter-atomic or intermolecular forces responsible for both physical and chemical bonding such as covalent, ionic, and van der Waals. To date, these bonds are known to be the main inter-atomic and particle forces existing in soils filled with water, air and solute. Soil physicochemical properties are either the intrinsic constitutive characteristics or the consequence of the physics laws governing the interactions among soil constituents at inter-atomic and inter-particle scales. The reviews of the advancements in understanding of and quantification of soil physicochemical properties covered in this chapter are: soil water retention curve (SWRC) (Sect. 4.1), specific surface area (SSA) (Sect. 4.2), cation exchange capacity (CEC) (Sect. 4.3), suction stress characteristic curve (SSCC) (Sect. 4.4), and soil water density (SWD) (Sect. 4.5). These properties, through application of scientific principles, can be directly related to geotechnical engineering properties such as Young's modulus (Sect. 5.3), small-strain shear modulus (Sect. 5.2), compressibility, swelling potential, drained cohesion, thermal conductivity function (TCF), and plasticity as indicated by Atterberg limits (Sect. 5.1). By reviewing the recent advances in linking soil physicochemical properties and geotechnical engineering properties, it could facilitate identifying new areas of research that can lead to improved understanding of soil properties and behavior, better designs, and new technologies for dealing with soils and rocks on, in, and with the earth.

1.2 Geotechnical Engineering Properties

Geotechnical engineering problems, from the classical ones to new challenges such as those identified in Chapter 1 "The Role of Geotechnics in Addressing New World Problems" of this book, can be divided into three broad categories according to their relations to the above-mentioned fundamental soil properties: strength, deformation, and flows. Thus, geotechnical engineering properties can be broadly defined as material properties needed to directly describe these three categories of problems. Strength of soil, compressive, shear and tensile, depends on inter-atomic and inter-particle forces, and external loading. In the case of a soil under fully saturated condition, the cohesive inter-atomic and inter-particle forces are considered herein as a material constant and captured by the material property termed cohesion. In the

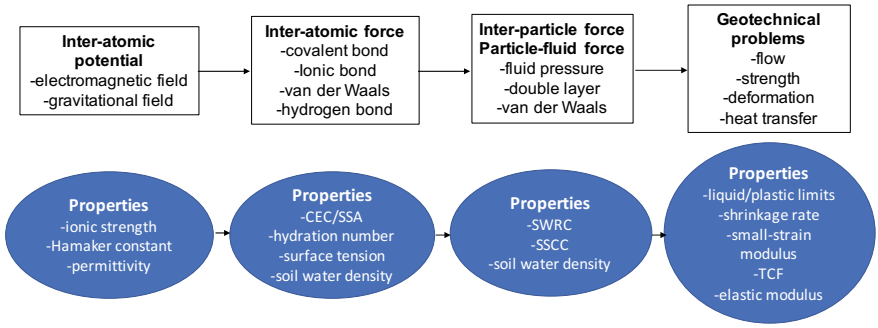

Fig. 1 Illustration of the linkages of atomic scale forces to engineering scale properties. The fundamental phenomena in soil (upper diagrams) form the foundation to define the soil properties (lower diagrams)

case of a soil under unsaturated conditions, inter-particle forces, including physicochemical and capillary, are material variables meaning that they depend on soil constituents, pore size distribution, and inter-atomic forces among soil, water, and air. In recent years, such dependency has been fully established by the concept of the SSCC, as illustrated in Sect. 4.4. In general, the relationships between soil physicochemical properties and geotechnical engineering properties, in the order from micro (left) to macro scale (right), are illustrated in Fig. 1.

Compressibility of soil is a geotechnical engineering property used for characterizing the volume change of soil and ultimate deformation under external loading or gravitational force (e.g., [77, 99, 103]). Compression can be caused by suction stress under no change in external loading but environmental change in term of water content or matric potential (e.g., [1, 38]). Some recent study, as summarized in Sect. 5.1, indicates that it can be directly related to some fundamental physicochemical properties of suction stress, SSA, and CEC. It can also be linked to geotechnical index property of Atterberg limits.

Deformation of a soil or other porous materials is a direct consequence of two quantities: modulus and stress (e.g., [36, 55, 56, 87, 96]). Under saturated conditions, modulus is often considered as effective stress-dependent. However, under unsaturated conditions, as illustrated later, moduli, both small-strain (Sect. 5.2) and finite-strain (Sect. 5.3), are highly functions of soil water content, in addition to effective stress, including suction stress. It is also shown that such variation can be scaled by using fundamental inter-particle forces originating from capillary and adsorption (Sect. 5.4).

Flows in soil could be multiple coupled or uncoupled physical processes: fluid flow, solute transport, electric current, and heat transfer (e.g., [74, 79, 89, 97, 111]). Coupled flows are exclusively dealt with in Chapter 9 "Research Challenges Involving Coupled Flows in Geotechnical Engineering". Heat flow or heat transfer in the

shallow subsurface generally involve multi-phase heat conduction. The challenges of heat transfer problems are described in Chapter 10 "Emerging Thermal Issues in Geotechnical Engineering". Because thermal conductivity, like many other geotechnical engineering properties, is dependent on inter-atomic and inter-particle forces, soil's constituents, pore-size distribution, and interfacial properties, it can be intrinsically related to the soil water retention curve, as shown in Sect. 5.5.

2 Physics Laws Beyond Traditional Soil Mechanics

Classical soil mechanics evolved without full consideration of physicochemical and thermal influences on properties and behavior. In effect, the solid particles were assumed to be physicochemically stable and inert. However, adequately describing and quantifying real soil behavior require that several aspects of the physics, chemistry and thermodynamics of soil–water systems be considered. Some of them are discussed in this section.

2.1 Mineral Structures and Bonding Forces

Four common soil minerals, namely: quartz, kaolinite, illite, and montmorillonite (smectite) are used for illustrating bonding forces. The main bonding forces among atoms in clay minerals are covalent, ionic, and van der Waals in the order of strong to weak. Some ionic bonding forces could be larger than covalent bonding forces. Covalent bonds among oxygen and silicon (bonding energy on the order of −500 kJ/mol) are the strongest of all, as is the case in quartz (Fig. 2a). So even though quartz hydrates on the surface, the water does not affect the internal crystal structure. Covalent bonds also exist in tetrahedron sheets and octahedron sheets in kaolinite, illite and montmorillonite (Fig. 2b, d), providing the basic crystal structures of these minerals remain intact during interactions with water and other dissolved materials. Coulomb forces also strongly interact among charged atoms. These forces generally decay slowly, so the influenced distance is much greater than for a single atom. Van der Waals attractive forces exist between octahedral and tetrahedral sheets. Together, these forces provide stable crystal structure of minerals. These forces, in terms of the potential energy (in kJ) between the charge sites (atoms), can be written as (e.g., [7, 48]):

$$\Phi = -A_{ij}e^{-B_{ij}r_{ij}} + C_{ij}e^{-D_{ij}r_{ij}} + \frac{q_i q_j}{r_{ij}} \tag{1}$$

where A_{ij} is Hamaker constant, B_{ij} is material constant, C_{ij}, is Born constant, and D_{ij} is material constant, all describing the interactions between a particular pair of atoms i and j, q_{i} and q_{j} are the effective charges (in Coulombs) of an atom, and r_{ij} is the

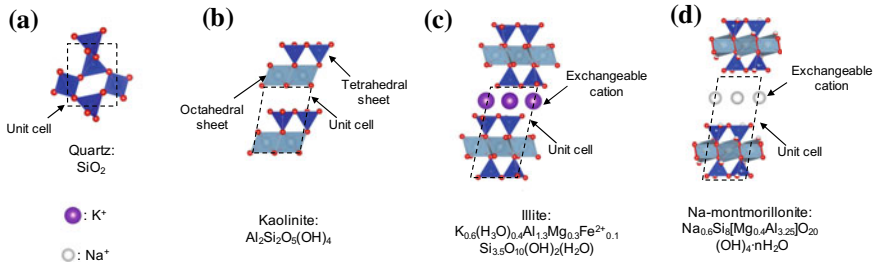

Fig. 2 Chemical structures of unit cells for typical soil minerals: **a** quartz (sand), **b** kaolinite (non-swelling clay), **c** illite (slightly swelling clay), and **d** montmorillonite (highly swelling clay)

inter-atomic separation distance. The first term represents the attractive London force (van der Waals), the second term the short-distance repulsions and the third term the Coulomb force (repulsive or attractive). If converting these interaction energies into unit cells of soil minerals, they are on the order of thousands to tens of thousands of kJ/mol (e.g., [46]).

Ionic bonds also play an important role in retaining mineral structure stability and chemical compositions, but with strengths much less than covalent bonding forces in common soils. Due to the isomorphous substitution of lower valence Mg for Al in octahedral sheets and lower valence Al for Si in tetrahedral sheets when clay minerals are formed, cations are attracted to the nearby oxygen atoms. These cations are called exchangeable cations, as one cation type can exchange positions with another cation type through physical interaction with cations in soil water. These cations, reside both in the inter-lamella and near the particle surface, and are dominated by ionic bonds with negatively charged sites in clay mineral sheets, leading to exchanges between in situ cations and the surrounding cations in pore fluid. The capacity of a mineral to exchange in situ cations with other types of cation through physical interaction under the most favorable conditions can be defined as the cation exchange capacity (CEC). CEC is the positive charge that that is needed to counter-balances the total negative charge on mineral surface, which could exist on particle surface and crystalline interlayers. The in situ cations can also re-orientate surrounding water molecules permanently through ionic bond between in situ cation and oxygen ion of water, leading to cation hydration (~−250 to −1500 kJ/mol interaction energy) (e.g., [75, 94]).

Cation hydration has several effects on soil behavior. Cations near the particle surface create a diffused double layer. Cations in the inter-lamella can overcome the van der Waals force, which is on the order of negative thousands of kJ/mol in magnitude between the mineral sheets dominated by covalent bond, leading to crystalline swelling. Cation hydration can cause swelling behavior, pore water pressure increase, and pronounced structure change in hydrated water, leading to significant water density increase, up to 1.6 (e.g., [112]).

2.2 Surface Adsorption Law

The relationship between the mass fraction of adsorbate on the particle surface with respect to adsorbent and thermodynamic conditions of the environment is commonly described through isotherms or under constant temperature conditions. According to Freundlich [41]:

$$w = k(RH)^{1/m} \tag{2}$$

where w is the gravimetric adsorbate (water) content, RH is the relative humidity of ambient environment in gas phase, k and m are the Freundlich adsorption coefficients corresponding to the adsorption capacity and the adsorption strength, respectively. It will be shown that this law is applicable for clayey soil-water interaction at low water potential range (−tens of kJ/mol) when adsorptive force is dominating.

The first scientifically based adsorption equation was the Langmuir equation [57], with several strict assumptions, including energetically homogeneous surfaces and only one full layer of adsorbate. Brunauer et al. [20] developed an equation (BET model) to account for multilayers of surface adsorption:

$$\frac{RH}{w(1-RH)} = \left(\frac{c-1}{c}\right)\frac{RH}{w_m} + \frac{1}{w_m c} \tag{3}$$

where w_m is the gravimetric adsorbate content at a full monolayer coverage and c is the BET coefficient representing the enthalpy of sorption at the full monolayer coverage. Note that Eq. (3) can be plotted as a linear function if the left-hand side is considered as the dependent variable, and RH as the independent variable, with a slope of $(c-1)/(cw_\mathrm{m})$ and intercept of $1/(cw_\mathrm{m})$, as described in Sect. 4.2 and illustrated in Fig. 8b. This equation has been extensively used for deducing the soil specific surface area (SSA) from clay-water adsorption isotherms. The assumption of an energetically homogeneous surface is not valid for some clay minerals, leading to a characteristic non-linear behavior for Eq. (3) (e.g., Fig. 8b). However, as summarized in Sect. 4.2 this non-linear feature can be utilized to distinguish between cation hydration and surface hydration. The relative magnitudes of hydration and other energy lowering mechanisms in soil water are illustrated in Fig. 3. Matric suction, defined here as the free energy per unit volume of soil water (i.e., $\mathrm{J/m^3} = \mathrm{N{\cdot}m/m^3} = \mathrm{Pa}$) below the ambient pore air pressure (Pa), is also shown in Fig. 3 for reference.

2.3 Osmotic Law

By dissolving solutes or most salts, some liquid water molecules are in hydrated (ordered) state, further lowering water potential down to −6.6 kJ/mol (e.g., [64]), depending on solute concentration. At the equilibrium state, the amount of water

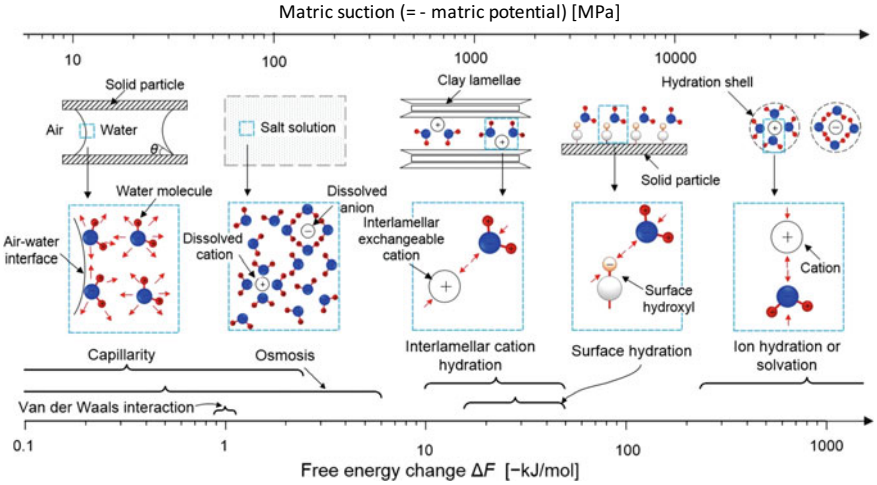

Fig. 3 Free energy lowering mechanisms associated with physicochemical interactions in soil, water, air, and solute system (after [112]). Pure water at room temperature is used as the reference state, i.e., free energy is 0 kJ/mol

potential lowering is equal to the pressure ψ_0 developed in the solution and can be described by van't Hoff's law for low solute concentration, typically, less than mass per volume concentration C of 0.02.

$$\psi_o = -CRT \tag{4}$$

where R is the universal gas constant (8.134 J/mol K), and T is temperature (K).

More rigorous equations based on chemical potential have been established for higher concentration. For example, the so-called "virial" expansion (e.g., [98]) with higher order concentration power terms can be used in lieu of van't Hoff's equation for any concentration C:

$$\psi_o = -CRT\left(1 + B_2C^2 + B_3C^3 + \cdots\right) \tag{5}$$

where $B_2, B_3, \ldots$ are virial coefficients. It is important to recognize that as a corollary of lowering water potential by osmosis, fluid pressure in the same amount by Eq. (4) or (5) at the intermolecular scale is increased, which is called osmotic pressure. The order of magnitude of osmosis in lowering the water potential is illustrated in Fig. 3.

2.4 Interfacial Equilibrium: Kelvin's Equation and Young-Laplace Equation

If liquid and vapor water, and other gas co-exist, thermodynamic second law dictates that an energy equilibrium between the two phases should be reached ultimately. The equilibrium condition can be described in terms of a few experimentally measurable quantities: vapor pressure in gas, inter-atomic force in liquid, pore air pressure, pore water (liquid) pressure, liquid-air interfacial tension, and the curvature of the liquid-gas interface. Two types of equilibrium conditions are often assumed as the starting point for many theoretical formulations and experimental characterizations: total water potential and matric potential. Kelvin's equation governs both types and the Young-Laplace equation dictates the second.

In soil, matric potential originates from two distinct physical mechanisms or interactions: adsorption between solid and liquid and capillarity among solid, liquid, and gas. As illustrated in Fig. 3, adsorption occurs at much lower free energy level than capillarity, so that the ambient suction is smaller than the maximum suction of a soil (see Sect. 4.1 Soil water retention curve), adsorptive water is always present whereas capillary water only exists when the ambient suction is smaller than the soil's cavitation pressure. In the presence of adsorption water and capillary water, matric potential can be captured by the Young-Laplace equation linking pore air pressure u_a, pore water pressure u_w, liquid-air interfacial tension T_s, contact angle β between liquid and soil, and the radius of the liquid-gas interface r (see Fig. 4 for illustration):

$$\psi_m = u_a - u_a = -2T_s \cos\beta / r \tag{6}$$

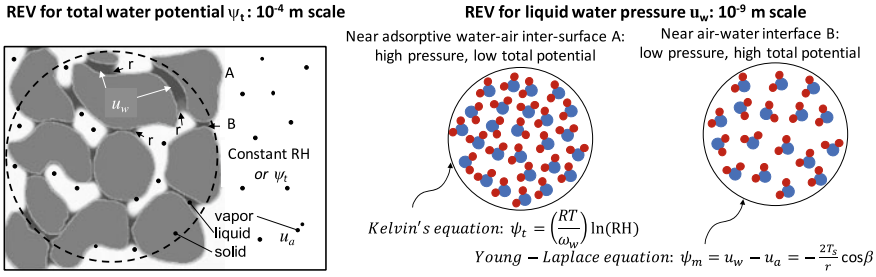

Fig. 4 Soil-water-air system under constant chemical potential equilibrium (from constant potential or relative humidity (grand conical) Monte Carlo simulation result). Kelvin's equation is for total water potential and works for both interfaces A and B whereas the Y-L equation is for matric potential and is limited to interface B

Following the above equation, when the interface curvature becomes zero (a flat interface), the pore air pressure is equal to pore water pressure. In soil pore, due to the hydrophilic nature of soil particle surfaces, the curvature is greater than zero, implying that pore water pressure is lower than pore air pressure.

Dissolved salts or other chemicals in soil water further lower the water potential as expressed in Eq. (4). The energy equilibrium conditions between soil liquid water and ambient vapor lead to, in the absence of the gravitational effect, the decomposition of the total water potential into two parts: matric potential and osmotic potential, i.e.:

$$\psi_t = \psi_m + \psi_o \tag{7}$$

Kelvin's law describes the energy (total water potential) equilibrium statement in terms of vapor pressure u_{v}, inter-atomic force in liquid (saturated vapor pressure $u_{\mathrm{v\text{-}sat}}$, and relative humidity RH (see Fig. 4 for illustration):

$$\psi_{\mathrm{t}} = \frac{\mu}{\omega_{\mathrm{w}}} = \frac{RT}{\omega_{\mathrm{w}}} \ln \frac{u_{\mathrm{v}}}{u_{\mathrm{v\ -\ sat}}} = \frac{RT}{\omega_{\mathrm{w}}} \ln(RH) \tag{8}$$

where ψ_{t} is the total water potential or free energy of soil water with respect to free water in pressure units, μ is the chemical potential of soil water in J/mol, ω_{w} is the molar volume of the liquid (18 g/mol), and RH is the relative humidity. Considering Kelvin's equation (8), and the total water potential Eq. (7) in soil free of salt, the vapor pressure is less than its saturated vapor pressure, or the relative humidity is less than unity. This implies that the water potential equilibrium between pure liquid and vapor can be reached for the relative humidity below 100% and is likely the case in soil.

An important implication of Kelvin's equation, and Young-Laplace equation to thermodynamic equilibrium in soil is that the equilibrium relative humidity is always less than 100% or vapor density is always lower than the saturated vapor pressure at the prevailing temperature. Therefore, whenever capillary water is present, for soil-water-air energy equilibrium, not only the pressure difference between the pore air and water needs to satisfy Young-Laplace equation (6), but also the vapor pressure in pore air needs to satisfy Kelvin's equation (8).

2.5 Cavitation and Condensation

Any matter could be in the form of solid, liquid, and gas, depending on thermodynamic conditions, i.e., temperature and pressure. For example, in liquid water, when the inter-atomic pressure reaches the tensile strength of liquid water, cavitation or spontaneous expansion of volume from liquid to vapor occurs. The tensile strength of liquid water depends on temperature and is equal to saturated vapor pressure that can be described by the Tetens [104] equation:

$$u_{v-sat} = 0.611 \exp\left(17.27\frac{T - 273.2}{T - 36}\right) \tag{9}$$

At the room temperature of 25 °C, it is 3.167 kPa. Condensation is the opposite, i.e., when the vapor pressure falls below the tensile strength or saturated vapor pressure, vapor collapses into liquid. It is important to recognize that the pressure described by Eq. (9) is the absolute value with respect to vacuum (zero pressure), not with respect to the ambient atmospheric pressure. Thus, for liquid exposed to ambient atmospheric pressure of 101.3 kPa, cavitation will occur when water pressure reaches −98.133 kPa (i.e., 101.3 − 3.167 = 98.133) with respect to the ambient atmospheric pressure (gauge pressure) if metastable state is ignored. To avoid cavitation of liquid water in laboratory unsaturated soil testing operations, a technique called "axis translation" [45] is widely used to elevate air pressure so the pore water pressure and water pressure in the chamber and pipeline are above the cavitation pressure. One implication is whether such technique is physically equivalent to what happens in field conditions. At the moment, this subject is being debated regarding the technique's theoretical basis and experimental limitations (e.g., [42, 88, 105]).

Cavitation is an endothermic process whereas condensation is an exothermic process: cavitation absorbs heat from the environment to expand inter-atomic distance; condensation releases heat to reach a lower energy state. The heat exchange during evaporation or condensation is called specific latent heat, and for water it is 334 J/g, which is 80 times the heat needed to change 1 g of liquid water by 1 degree. The latent heat transfer process is important for many emerging thermal issues in geotechnical engineering, such as those covered in Chapter 1 "The Role of Geotechnics in Addressing New World Problems" and Chapter 10 "Emerging Thermal Issues in Geotechnical Engineering".

2.6 *Heat Conduction: Fourier's Law*

Heat transfer in porous materials is through two distinct physical mechanisms: conduction and convection. Conduction is a result of thermal vibration of molecules in soil, whereas convection is a result of heat carried by fluid displacement. Macroscopically, the magnitude or rate of heat transfer q_t [$\mathrm{Wm^{-2}}$] by conduction is proportional to the negative gradient of temperature ΔT [$\mathrm{Km^{-1}}$] and is quantified by Fourier's law:

$$q_t = -\lambda \nabla T \tag{10}$$

The proportionality coefficient λ is the thermal conductivity [$\mathrm{Wm^{-1}K^{-1}}$]. The negative sign comes from the consequence of the thermal dynamic second law; energy transmits from higher energy state to lower state, which is opposite to the temperature gradient. Thermal conductivity in soil under unsaturated conditions mainly depends on soil water content. The dependence of thermal conductivity on soil water

content, specifically thermal conductivity increases as soil water content increases, has been recognized in the past in soil physics (e.g., [27, 49]) and geotechnical engineering (e.g., [16, 37, 80]). More recent work summarized in Sect. 5.5 shows that thermal conductivity can be fundamentally and explicitly related to soil-water retention mechanisms of adsorption and capillarity.

3 Physics Principles

Linkages between soil physicochemical properties and geotechnical engineering properties can be established through applications of scientific principles such as phase change, mass conservation, and thermodynamic energy equilibrium. Several essentials of these principles pertinent to geotechnical engineering properties are briefly described below.

3.1 Phase Change Principle

Changes in the liquid and gas phases in a soil occur as a result of changes in thermodynamic conditions. The direction of phase change is dictated by the thermodynamic second law: matter or energy moves from a high-energy place to a low-energy place. If the gas phase of water has higher free energy than the liquid phase, condensation occurs (or vice versa, evaporation occurs). When the chemical potential at each point within the system is equal, an equilibrium state is reached, as illustrated in Fig. 4.

3.2 Principle for Defining Representative Elementary Volume (REV)

The representative elementary volume (REV) or unit cell is the smallest volume over which a variable such as matric suction or pore water pressure, or a property such as elastic modulus or thermal conductivity can be defined. For example, the REV size for total water potential and matric suction in fine sand is ~10^{-4} m, but the REV size for pore water pressure is ~10^{-9} m, 5 orders of magnitude in difference, as illustrated in Fig. 4. At a scale greater than the REV of a variable, spatial and temporal variation of the variable needs be described mathematically under continuum mechanics. So for a REV of fine sand under energy equilibrium principle, a unique matric suction can be defined. On the other hand , pore water pressure can vary greatly within a

REV of fine sand, as illustrated in Fig. 4b, c, even though the total energy in a REV of pore water remains a constant value equal to the prevailing matric suction. Due to the physicochemical forces of adsorption, pressure near the particle surface is higher than that near the air-water interface. As such, pore water near the air-water interface is more likely to cavitate than that near the particle surface. Because the disparity between these two REV scales, matric suction cannot be used as a state variable for pore water cavitation or condensation in soil, but pore water pressure can.

3.3 Free Energy of Soil Water

Chemical potential of soil water, or total potential of soil water, unifies all transferable energies or free energy with different physical and chemical mechanisms and can be used as a criterion for energy equilibrium state. The physical and chemical mechanisms, in terms of free energies in the order of low to high, occurring in soil water are: salt solvation, particle and inter-lamella surface hydration, exchangeable cation hydration, van der Waals forces in film water, salvation, capillarity, and Earth's gravity. Each of these physicochemical mechanisms can be captured by the laws described in the previous sections. The combined energy reduction by all of these mechanisms (except gravity), is lumped into the term called matric potential. As a result, matric potential could be as low as −1.6 GPa (e.g., [63], also see hydration range in Fig. 3 at dry state in some soils).

The chemical potential of soil liquid water is called the total water potential and is widely defined as the superposition of three components; matric potential ψ_{m}, osmotic potential ψ_{o}, and gravitational potential ψ_{g}:

$$\psi_t = \psi_m + \psi_o + \psi_g \tag{11}$$

The superposition principle shown above implies that at the representative elementary volume (REV) scale for many engineering scale problems such as water flow, strength, and soil displacement, the spatial distribution or variation of each of the individual components at the sub-REV or micro-scale can be ignored. However, for some problems such as cavitation, and swelling pressure, the pressure and stress distribution vary locally from point to point at the particle or pore-scale, and a homogenization approach like Eq. (11) at the REV scale is not useful. Another potential omission of Eq. (11) is that there may exist some coupling between osmotic potential and matric potential (e.g., [47]). For example, in clay barrier materials for waste containment, salt concentration could greatly affect double layer interaction, leading to different soil fabric and matric potential, and membrane efficiency, as described

in Chapter 9 "Research Challenges Involving Coupled Flows in Geotechnical Engineering" on coupled flows. Better understanding of these two implications and their quantitative effects on fundamental properties of pore water pressure, water density, and suction and geotechnical properties is a challenge remaining to be answered.

3.4 Local Thermodynamic Equilibrium Principle

Under the principle of local thermodynamic equilibrium within the same phase material, the superposition principle can be applied within a unit volume of liquid or gas for individual gases or physical mechanisms. For air with total pressure u_a that consists of mixture of O_2, N_2, CO_2, with partial pressures of u_{O2}, u_{N2}, u_{CO2}, and volumes of V_{O2}, V_{N2}, V_{CO2}, …, the application of the superposition principle on ideal gases can lead to Dalton's partial pressure law (e.g., [64]):

$$u_a = u_{O_2} + u_{N_2} + u_{CO_2} \cdots = u_a \left(\frac{V_{O_2}}{V_a} + \frac{V_{N_2}}{V_a} + \frac{V_{CO_2}}{V_a} + \cdots \right) \tag{12}$$

For soil water, the total (chemical) potential of soil water defined by Eq. (10) is established at the air-water-soil REV for engineering scale problems like water flow, soil strength, and soil displacement, thus allowing it to vary spatially and temporally outside the particular REV or point. Furthermore, within the REV, matric potentials, according to the origin of mechanisms, can be conceptually divided into 5 spatially-varying components [60]: van der Waals film water hydration $\psi_{\mathrm{vdw}}(x)$, electrical double layer $\psi_{\mathrm{ele}}(x)$, hydration $\psi_{\mathrm{hyd}}(x)$, local pore pressure $\psi_{\mathrm{pre}}(x)$, and local osmotic pressure $\psi_{\mathrm{osm}}(x)$. Here x is the statistical distance from the particle surfaces, which is defined as $x = w/(SSA\ \rho_{\mathrm{w}}^{\mathrm{ave}})$, where w is the gravimetric water content, SSA is the specific surface area, and $\rho_{\mathrm{w}}^{\mathrm{ave}}$ is the average soil water density. Therefore, the total potential of soil water (Eq. (11)) becomes:

$$\psi_{\mathrm{t}}(w) = \psi_{\mathrm{vdW}}(x) + \psi_{\mathrm{ele}}(x) + \psi_{\mathrm{hyd}}(x) + \psi_{\mathrm{pre}}(x) + \psi_{\mathrm{osm}}(x) + \psi_{\mathrm{o}} + \psi_{\mathrm{g}} \tag{13}$$

This conceptualization is consistent with the local thermodynamic equilibrium principle, which states that the total potential of soil water within the REV should be the same, but each individual component can vary spatially within the REV. For example, in a clay-air-water-electrolyte system, matric potential [the first 5 terms on the right-hand side of Eq. (13)] in an equilibrium state is the same throughout the entire system, but the electrical potential varies exponentially with the distance x from the particle surfaces. Similarly, van der Waals potential , hydration potential,

local pore water pressure, and local osmotic pressure vary spatially. Recognizing such spatial variations in water potential components is important for characterizing soil properties such as cavitation pressure, super-cooling, swelling pressure, and soil water density.

3.5 Adsorption Water Content Versus Capillary Water Content

Because soil-water interactions have different physiochemical mechanisms, their roles in engineering scales processes such as flow, strength, and suction stress are different. The importance of individual physicochemical mechanisms in soil macroscopic behavior can be studied by understanding the variation of individual water content components. The application of the local thermodynamic equilibrium principle can lead to the decomposition of total water content into two physically-based components: adsorption volumetric water content θ_a and capillary volumetric water content θ_c. They co-exist under the same matric potential ψ_m, i.e.:

$$\theta(\psi_m) = \theta_a(\psi_m) + \theta_c(\psi_m) \tag{14}$$

For clean sand, the adsorption volumetric water content is practically zero, but for montmorillonite, the adsorption volumetric water content could be 25% (e.g., [63]). The above principle allows us to develop new SWRC theories, as illustrated in recent theoretical developments summarized Sect. 4.1 below.

4 Soil Physicochemical Properties

Recent developments in characterizing several soil physicochemical properties important to some current and emerging challenges described in Chapter 1 "The Role of Geotechnics in Addressing New World Problems" are provided in this section. They are: soil water retention curve (SWRC) aka soil water characteristic curve, specific surface area (SSA), cation exchange capacity (CEC), suction stress characteristic curve (SSCC), and soil water density (SWD). The table below summarizes the answers to three basic questions on these 5 properties: what are they? why are they important to geotechnical engineering problems? and how do they relate to the grand challenges outlined in Chapter 1 "The Role of Geotechnics in Addressing New World Problems" and detailed throughout the other chapters?

What is it?	Why is it important?	Relevance to challenges in Chapter 1 "The Role of Geotechnics in Addressing New World Problems"
4.1 Soil water retention curve (SWRC)		
Characteristic relationship between soil water content and matric suction or relative humidity	Indications of shrink-swell behavior on wetting and drying; strength-deformation behavior; hysteresis behavior; water adsorption characteristics; water mass balance and flow	Climate change: carbon storage and capture, desertification, extreme precipitation event, storm water management Management of Energy and Resources: nuclear energy Management of water resources: reversal of groundwater depletion, evaluating risk under a changing climate, long-term waste containment, emerging organic contaminants, remote inspection, enhancing ground stability
4.2 Specific surface area (SSA)		
Total surface area of solid particles per unit weight (or volume) of dry soil; strongly dependent on soil gradation and mineralogy	Indications of soil gradation and mineralogy; higher the specific surface area the more plastic the soil, the lower the hydraulic conductivity, the higher the shrink-swell potential, the greater the potential for water and chemical adsorption	Climate change: carbon storage and capture Management of energy and materials resources: gas hydrates, nuclear energy Management of water resources: long-term waste containment, pathogens in drinking water, emerging organic contaminants, enhancing stability
4.3 Cation exchange capacity (CEC)		
Clay minerals carry a net negative electrical charge owing to isomorphous substitution in their crystal structures. This negativity is balanced by cations; e.g., N+, K+, Ca++. Mg++, heavy metals, pollutants; CEC is a quantitative measure of this electronegativity	Indications of the ability of the soil to attract and hold different cations; shrink-swell behavior; adsorption sites can be used to bond stabilizers, pollutants	Climate change: carbon storage and capture Management of energy and materials resources: nuclear energy Management of water resources: long-term waste containment, pathogens in drinking water, emerging organic contaminants, enhancing stability

(continued)

(continued)

What is it?	Why is it important?	Relevance to challenges in Chapter 1 "The Role of Geotechnics in Addressing New World Problems"
4.4 Suction stress characteristic curve (SSCC)		
Relationship between soil suction and degree of saturation. Suction stress has two components: capillary stress within the pore water and adsorption stresses to particle surfaces and to adsorbed cations	Unification of effective stress using one relationship for both saturated and unsaturated conditions: $\sigma' = (\sigma - u_a) - \sigma^s$ where σ^s is the suction stress that will equal pore water pressure u when soil is saturated but varies characteristically as soil de-saturates; u_a is the pore air pressure for saturation <100%	Climate change: extreme precipitation event Management of energy and materials resources: natural gas, gas hydrates Management of water resources: reversal of groundwater depletion, enhancing stability
4.5 Soil water density (SWD)		
Mass per unit volume of soil water. It may vary from point to point within the water in a soil pore. It can be further defined in two ways: average (global) or differential (local). The local water density depends on the water structure at that point	Indications of thermodynamic state of soil water and its physical properties such as strength, compressibility, thermal conductivity, and wave travel velocity. The thermodynamic state at any point is influenced by adsorptive forces from nearby mineral surfaces and dissolved cations and anions and the structure of free pore water. Potential surrogate to define soil physical properties such as pore water pressure and super-freezing point	Management of water resources: remote inspection Overarching challenges: engineering properties of geomaterials

4.1 Soil Water Retention Curve

Soil water retention curve (SWRC) describes the energy equilibrium state of soil water with soil. The energy state refers to the so-called "matric suction," whose compositions or physical mechanisms are described in Sects. 2.1 and 3.5. Most SWRC models were not based on explicit consideration of physicochemical mechanisms. Instead, they were established based on the shape or geometry of SWRC for different soils (e.g., [18, 39, 107]). Some of the parameters in these models can be clearly physically interpreted, such as air-entry values and pore-size distribution, others such as residual water content are less clear in physical interpretations. Fur-

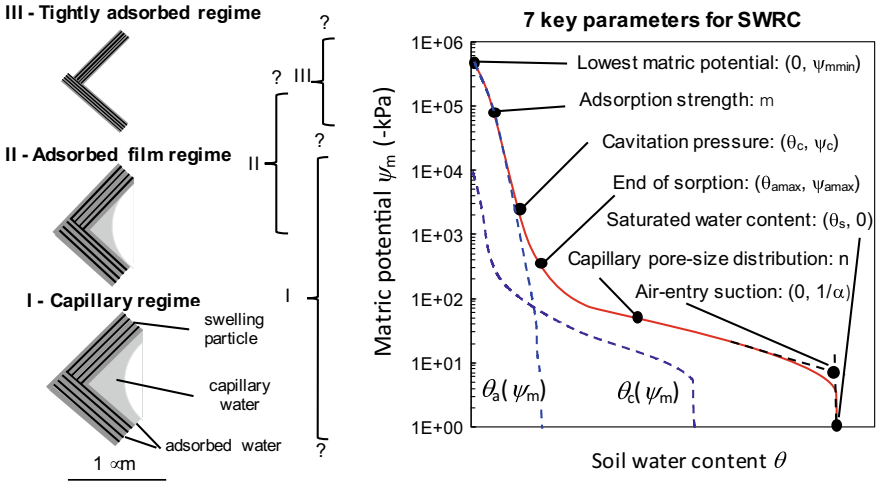

Fig. 5 Conceptual model for SWR characteristic states and key parameters (after [63])

thermore, parameters with clear physical interpretations are mostly related to SWR in the capillary regime. These SWRC models have proven to be effective and accurate in modeling SWR behavior in the capillary regime or when matric suction is less than a few thousands of kPa. They are generally not suitable for SWR behavior in high matric suction or low matric potential where adsorption rather than capillarity becomes dominating.

Several issues related to SWRC remain highly debatable, as cast in the following questions:

(1) Can matric suction be defined as the difference between pore air pressure and pore water pressure?
(2) What is the cavitation pressure for soil water?
(3) Is soil matric suction higher than several tens of MPa important for engineering problems?
(4) What is the highest soil matric suction?
(5) What is the physical mechanism for SWR hysteresis in the high matric suction regime?

The answers to these questions not only are important for how we define SWR properties, but also bear implications to how we measure SWR properties.

Recently, a systematic effort has been made to answer the above questions and some major advances are summarized here. Regarding the first question, in recent years, Revil and Lu [93] show that at any state of matric suction, soil water can be physically and quantitatively decomposed into two components: adsorption and capillarity under the local thermodynamic equilibrium principle described in Sect. 3.4. To answer the first four questions, a complete SWR conceptual model was proposed by Lu and Khorshidi [65] and Lu [63], as illustrated in Fig. 5.

Because the SWR has the two distinguishable physical mechanisms of capillarity and adsorption, the two soil water contents follow different physical laws. Capillarity requires the existence of curved air-water interface and can be described by the Young-Laplace equation (6), whereas adsorption does not require a curved air-water interface and can be described by Kelvin's equation (8) or adsorption laws (2) or (3). Therefore, under the capillary regime, pore water pressure can be defined and quantified by the Young-Laplace equation and the common way of defining matric suction as the difference between pore air and pore water pressure is appropriate. However, when adsorption is dominant or is the sole mechanism for SWR in the high matric suction regime, the pore water pressure varies from location to location. As such, the common definition of matric suction is not physically meaningful. A more general way is to define matric suction as the negative of matric potential, which could be defined in Eq. (13). This definition does not require the validity of capillary pore pressure, but specifies the physical origin and energy level of soil water, as described in Eq. (13).

Adsorbed water can only co-exist with a soil matrix, and the chemical structure of adsorbed water should differ significantly from that of capillary water. Consequently, adsorbed water may not cavitate like capillary water. Capillary water, on the other hand, likely retains bulk water structure for its existence under high matric potential or low maric suction. Therefore, capillary water is subject to cavitation when pore water pressure is equal to saturated vapor pressure. Because of the co-existence of capillary water and adsorption water and the pressure increase in adsorptive water, cavitation can occur under much lower matric potential than in pure liquid water. Cavitation pressure is an intrinsic property for a soil, thus it varies with soils and may provide a mechanism for transitional SWR process between capillary water and adsorptive water regimes [88, 105]. As illustrated in Fig. 5, because the adsorptive SWR mechanism depends on soil mineralogy, an intrinsic matric potential or highest soil suction exists for each soil. Therefore, expressing SWRC equations with an infinite suction (e.g., [107] or a universal value (e.g., [39]) is physically incorrect.

Revil and Lu [93] developed the first SWRC model explicitly incorporating adsorption and capillarity using the adsorption laws of Freundlich (Eq. (2)) for adsorptive water and van Genuchten's [107] SWR model for capillary water. Lu [63] further developed a generalized SWRC model by (1) a new adsorptive water $\theta_a(\psi_m)$ equation capable of defining the lowest matric potential and by (2) a new cavitation model capable of defining probabilistic process of cavitation transition between capillary water $\theta_c(\psi_m)$ and adsorption water $\theta_a(\psi_m)$:

$$\theta_a(\psi_m) = \theta_{a\,\max}\left\{1 - \left[\exp\left(-\frac{\psi_{m\,\min} + \psi_m}{\psi_m}\right)\right]^m\right\} \tag{15a}$$

$$\theta_c(\psi_m) = \frac{1}{2}\left[1 - erf\left(-\sqrt{2}\frac{\psi_m + \psi_c}{\psi_c}\right)\right][\theta_s - \theta_a(\psi_m)]\left[1 + (\alpha\psi)^n\right]^{(1/n-1)} \tag{15b}$$

where ψ_c is the cavitation pressure, $\psi_{m\min}$ is the lowest matric potential, $\theta_{a\max}$ is the maximum adsorptive water content, θ_s is the porosity, m is the fitting parameter

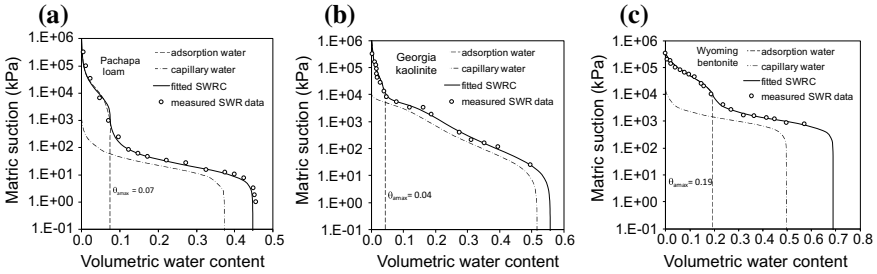

Fig. 6 Fitted SWRCs for: **a** silty soil, **b** non-swelling clay, and **c** swelling clay (after [63]). Volumetric water content is defined the ratio of the volume of water to the total volume of soil

for adsorption strength, n is a fitting parameter for pore size distribution, and a is the fitting parameter related to the air-entry matric potential. Equations (14)–(15) completely define the generalized SWRC.

As illustrated and defined in Fig. 5, seven physically meaningful parameters are used to define the generalized SWRC model. Using a widely-ranged SWR dataset, it is shown that the generalized SWRC model is not only able to distinguish soil water content between adsorption and capillarity, but also is statistically better than the other models that have been proposed (van Genuchten's [107] model and Fredlund and Xing's model [39], and Revil and Lu's [93] model). The performance of the generalized SWRC model for silty soil (Fig. 6a), non-swelling clay (Fig. 6b), and swelling clay (Fig. 6c) is illustrated.

Two theoretical and experimental challenges remain regarding SWRC modeling: understanding of soil water cavitation and soil water retention in the high suction regime. From a thermodynamic viewpoint, cavitation of liquid water is controlled by local pressure and temperature. However, matric suction, in general, is not indicative of pore water pressure at the inter-atomic scale, because pore water pressure in soil is controlled not only by capillarity, but also by adsorption. As such, the magnitude of pore water pressure at a specific point is determined by mineral and gradation characteristics of soil and the water content. Quantitative theories or experimental methods to measure pore water pressure distribution within a representative elementary volume for matric suction remain largely unexplored. Another frontier of research is in SWRC behavior at high suction. With a few exceptions, such as the filter paper methods and the latest isotherm measurement techniques by VSA [58], nearly all existing techniques for measuring or controlling matric potential are limited for matric potential values >-100 MPa. However, as illustrated in Fig. 5, adsorptive water retention is the dominant mode for matric potential <-100 MPa. For clayey soils shown in Fig. 6, adsorptive water content is significant and can be as high as 20% in volumetric water content for swelling clays. These studies also indicate that each soil has a unique minimum matric potential or maximum suction, as theoretically predicted by Eq. (18) in Sect. 4.3. The maximum suction varies between 0.5 GPa and 1.6 GPa [51]. Thus, quantitative experimental techniques, particularly for continuous measurements or control potential, are needed.

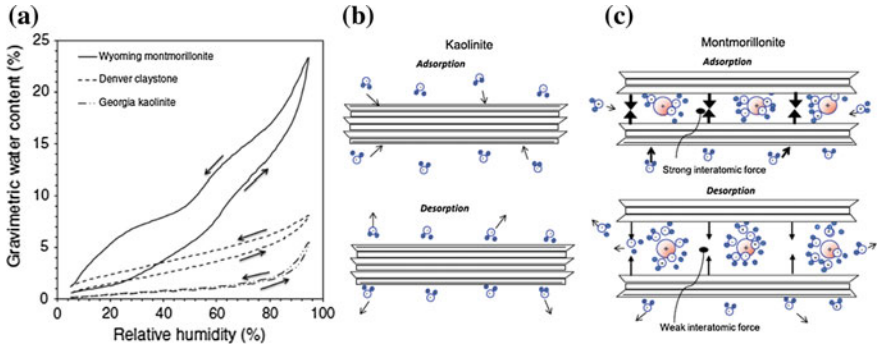

Fig. 7 Experimental data showing hysteresis of SWRC under low matric potential for kaolinite, illite, and montmorillonite (**a**), conceptual illustration of hysteresis mechanism in adsorption water retention regime in non-swelling clay (**b**), and in swelling clay (**c**) (after [65])

Another frontier in understanding SWR behavior is the mechanism for SWR hysteresis. Until recently, hydraulic hysteresis has been attributed to two physical mechanisms: contact angle and ink-bottle (e.g., [64]). The contact angle here refers to the angle between liquid-solid interface and liquid-air interface, and the ink-bottle refers to the shape of soil pore that mimics an inverted ink bottle. Both mechanisms are established based on the existence of capillary water in soil pores, which may not be applicable for explaining SWR behavior under low matric potential where adsorption is the dominating SWR mechanism. Figure 7 shows the SWR data for three different clays: kaolinite, illite, and montmorillonite. The hydraulic hysteresis is relatively small in kaolinite, moderate in illite, and strong in montmorillonite. Because capillary water is unlikely to exist when the relative humidity is less than 80% or the matric potential <-30 MPa, the commonly used contact angle and ink-bottle mechanisms cannot explain why hysteresis exists and what controls its magnitude.

Lu and Khorshidi [65] proposed a conceptual model to explain the hysteresis in clay based on the interplay between exchangeable cation hydration and van der Waals forces between inter-layer crystalline sheets [terms expressed in Eq. (1)], as conceptually illustrated in Fig. 7b, c. In non-swelling clay (Fig. 7b), adsorption and desorption occur on soil particle surfaces leading to small hysteresis. In contrast, in swelling clay (Fig. 7c), adsorption and desorption can also occur on interlayer sheets where exchangeable cations reside, thus water molecules are subject to additional strong resistance of inter-sheet van der Waals forces during adsorption but weaker (larger separation in interlayer sheets) assistance of van der Waals forces during desorption. This hysteresis mechanism may open a new window to address several important questions regarding expansive clay behavior: What is the interplay between exchangeable cation hydration and crystalline van der Waals forces? what is the free energy or swelling potential involved in clay swelling? How does swelling potential depend on the hysteresis and relate to swelling pressure? Answers to these questions

would provide insight to better define geotechnical properties and quantify expansive clay behavior.

4.2 Specific Surface Area

The surface of soil is where solid and water as well as other chemicals interact, providing physical linkages between atomic-scale forces and physicochemical properties. Soil specific surface area (SSA) is defined as the solid surface area per unit solid mass. However, the solid surface is a concept vaguely defined, as it could be on the particle surface, between inter-sheets, or around exchangeable cations. Therefore, SSA is sorbent (soil solid) or/and sorbate (water or other materials) dependent (e.g., [95]). Different sorbates (e.g., water and ethylene glycol) have different affinity with the same sorbent (e.g., montmorillonite) or accessibility to adsorb onto solid surface.

Currently, the standard methods to measure SSA are to use one of three polar materials [methylene blue, ethylene glycol, and ethylene glycol monoethyl ether (EGME)] as sorbate or probing material. Once the equilibrium between soil and sorbate is reached at monolayer coverage, the SSA for sorbate i is calculated as follows (e.g., [5]):

$$SSA_i = \frac{m_{i,j}}{M_i} \times N \times A_i \tag{16}$$

where $m_{i,j}$ is the mass of sorbate i per unit mass of sorbent j at monolayer coverage, M_i is the molecular mass of the sorbate (g/mol), N is Avogadro's number (6.023×10^{23} per mol), and A is the surface area (m^2) covered by one sorbate molecule (e.g., [5]).

Water has been used as a sorbate to calculate SSA (e.g., [4, 5, 84]). The advantages of using water as a probe are: it is directly related to water contents that are most relevant to many real problems and SWRC or isotherm data. Using non-water polar materials in standard methods, on the other hand, may cause underestimation due to inaccessibility of large molecules to areas around exchangeable cations in inter-sheets in expansive clay [65]. In general, the water-based methods yield comparable results to the standard methods but with some considerable differences in uncertainties associated with: determination of the monolayer coverage point (relative humidity), and the validity of the BET equation as the adsorption law in soil. Fixing a relative humidity (e.g., [5, 84]) is not physically consistent as different exchangeable cations will have different monolayer coverage point. The BET equation is also not strictly applicable for soil as surfaces are non-homogeneous among particle surface, inter-sheet surface, and exchangeable cations.

To overcome these uncertainties, a universally applicable procedure [52] has been developed to identify monolayer or bilayer point along SWRC or isotherms. Two criteria were developed and concurrently used: specific moisture capacity (derivative

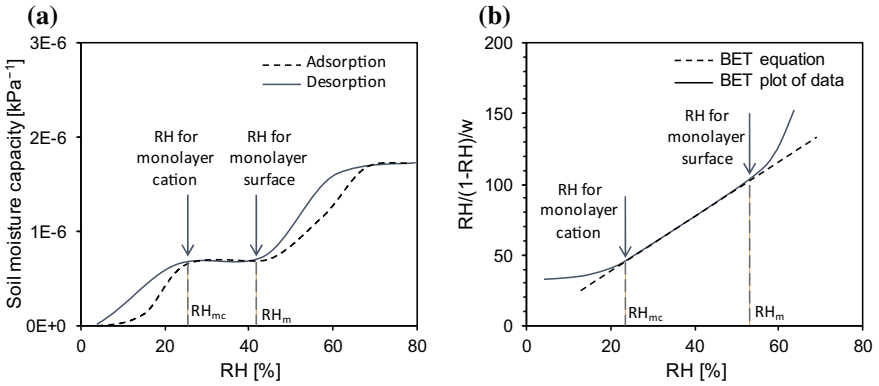

Fig. 8 Illustration of the determination of monolayer cation relative humidity RH_{mc}, surface coverage relative humidity RH_m by: **a** the specific moisture capacity method (suitable for swelling clay), and **b** BET plot method (suitable for non-swelling clay)

of water content with respect to soil matric suction) and the BET plot. For soil with significant CEC, cross points between the wetting and drying specific moisture capacity curves provide points for monolayer cation and surface coverage and bilayer surface coverage, and each of them can be used to infer SSA (Fig. 8a). For soil with small, or insignificant CEC, the BET plot (Fig. 8b), which differs from the traditional BET equation method can be used to identify points for both monolayer cation and monolayer surface coverage.

Comparisons of this new water-based method with the other water-based methods and the EGME method for various soils over a wide range of SSA indicate that the new method is reliable and more accurate. Some challenges remain in distinguishing types of surface area: particle surface, inter-particle contact surface, and crystalline inter-sheet surface. Each type of surface may have a distinct role in hydrologic and mechanical behavior. For example, particle surface is directly related to film flow phenomenon, which may not be governed by Darcy's law. All traditional methods for SSA do not distinguish SSA among different surface types. Therefore, further theories and experimental techniques are needed to quantify types of specific surface area.

4.3 Cation Exchange Capacity

Recent studies show that the CEC of a soil can be inferred directly from the soil's SWRC data by several ways. As illustrated in Fig. 8 and described in Sect. 4.2, the monolayer cation hydration point or water content m_{mc} can be estimated by either SMC or BET plot method for all soils with exchangeable cations. Because the first layer cation hydration (i.e., Na^+, K^+, Ca^{++}, and Mg^{++}) is dominating by ionic bond,

a soil's CEC is considered as a function of types of cation i with valence V_i, and hydration number I_i through the following equation [53]:

$$w_{mc} = \omega_w \sum_i I_i CEC_i / V_i \tag{17}$$

The above equation has been experimentally validated using the SWR data for different mono-ionic bentonite and kaolinite-Sodium bentonite mixtures. The monolayer water content measured from the SMC/BET plot method follows the same trend with that from the right-hand side of Eq. (17), indicating that Eq. (17) can be used to infer CEC of soil.

Because surface hydration and cation hydration are dominant for RH <30% and each of them has their own distinct ranges of RH for monolayer coverage, a theoretical SWRC for RH <30% can be developed. A theoretical SWRC for cation hydration was developed by Khorshidi and Lu [51] for all types of exchangeable cations where matric potential ψ_m is considered as a function of CEC, valence V_i, hydration radius r_i, and water content w:

$$\psi_m = -\frac{3\times 10^{-10} V_i CEC}{r_i^2 (4 V_i w + 9.3 CEC)} \tag{18}$$

To validate the above equation, various types of soils from silty non-swelling clay, to swelling clay were used and their CECs were qualified by the SWR data using the above equation and an independent Ammonium acetate method (ASTM D7503). Excellent agreement (correlation coefficient of 0.99) was obtained for the RH range of 4–30% (corresponding to matric potential range of −443 to −166 MPa), indicating the validation of Eq. (18) and its usefulness to quantify CEC directly from SWR data. Khorshidi and Lu [50] also found that the full coverage of monolayer cation hydration for common cations in soils like Ca^{++}, Na^{++}, Mg^{++}, K^{+}, and Li^{+} occurs between RH = 5–26%. The RH value for full monolayer cation coverage is dependent on cation type, but independent of soil mineral type, i.e., kaolinite or montmorillonite. However, because soil mineral type determines CEC, the water content for full monolayer cation coverage depends on both soil type and cation species, as predicted by Eq. (18). Therefore, for the same soil with different exchangeable cations, the SWRC could be very different, depending on cation species.

As a corollary of Eq. (17), the superposition principle is applied [50] to quantify exchangeable cations with unknown types of cations and their quantities. For 26 different soils and mixtures, the comparisons between the identified and quantified exchangeable cation and those by an independent method were found to be excellent [50], demonstrating that Eq. (17) can be used to identify types of exchangeable cations and their quantities for all types of soils. Because some overlap exists between surface and cation hydration in free energy ranges, differentiating surface areas between cation hydration and surface hydration is challenging. Separating between the specific surface area of cation hydration and the specific surface area of surface hydration

has implications to better understanding the roles of each of these two surfaces in swelling behavior, suction stress, and modulus variations.

4.4 Suction Stress Characteristic Curve

Effective stress is the state of stress in soil that determines its resistance to volume change, shear deformation, and shear failure. It is described as the stress on soil skeleton [102]. For unsaturated soil, Bishop [11] proposed a form of effective stress σ':

$$\sigma' = (\sigma - u_a) - [-\chi(u_a - u_w)] \tag{19}$$

where σ is the total stress, and χ is a parameter suggested by Bishop to be a function of degree of saturation. Parameter χ is constrained between 0 when soil is completely dry and 1 when soil is fully saturated. The form of interparticle stress expressed in the bracket in the Bishop's effective stress Eq. (19) accounts for only capillarity and dictates a zero interparticle stress expressed in the second term on the right-hand side of Eq. (19) when soil is completely dry. This contradicts the finite interparticle stresses in fine-grained soils like silty and clayey soils where adsorptive forces are important.

In 2006, Lu and Likos [73] conceptualized a suction stress characteristic curve (SSCC) to unify effective stress under both saturated and unsaturated conditions, i.e.:

$$\sigma' = (\sigma - u_a) - \sigma^s \tag{20}$$

where σ^s is the suction stress that will equal the pore water pressure when a soil is saturated, but varies characteristically as soil de-saturates. Suction stress can be further divided into two components dependent on two-distinguishable physical water retention mechanisms:

$$\sigma^s(\psi_m) = \sigma_a^s(\psi_m) + \sigma_c^s(\psi_m) \tag{21}$$

where $\sigma_a^s(\psi_m)$ is the suction stress caused by adsorptive water, and $\sigma_c^s(\psi_m)$ is the suction stress caused by capillary water. Lu and Likos [73] synthesized all the existing shear strength data available and demonstrated that the SSCC-based effective stress Eq. (20) is valid. Under the SSCC based effective stress, shear strength, under both saturated and unsaturated conditions, can be predicted by the same failure criterion, such as Mohr-Coulomb, so there is no need to use different failure criteria for soil under unsaturated conditions. Under capillary mechanism, suction stress has an intrinsic relationship with SWRC, as illustrated in Fig. 9a. Matric suction is the free energy of soil water per unit volume of soil water, whereas suction stress is the free energy of soil water per unit volume of effective soil void (shaded area). Con-

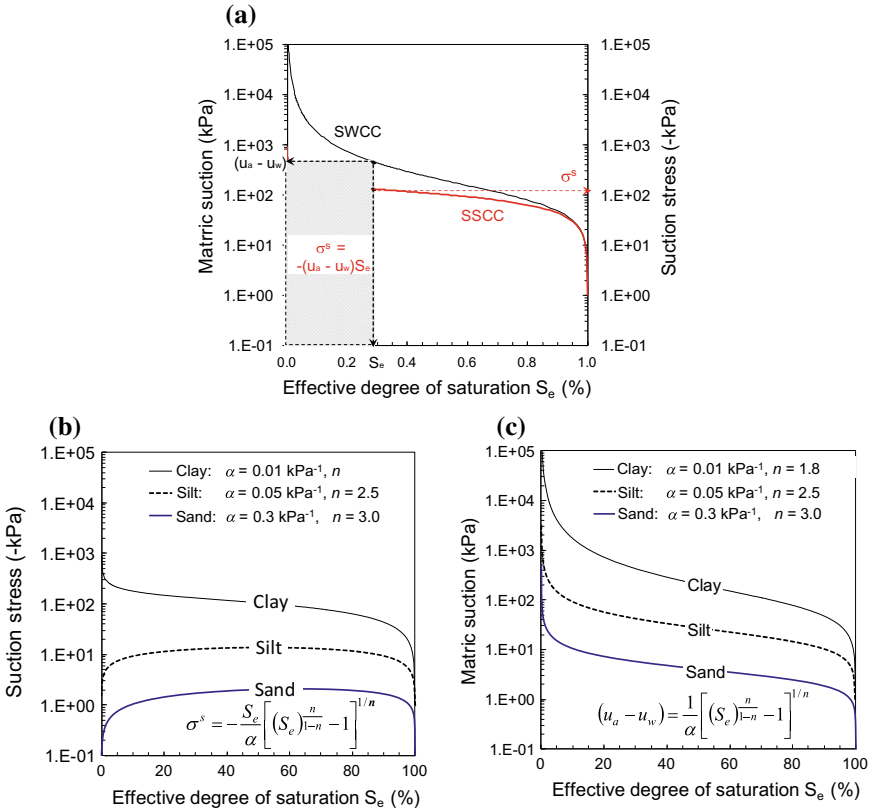

Fig. 9 Illustration of the intrinsic relationship between SSCC and SWRC: **a** physical linkage between SSCC and SWRC, **b** SSCC (Lu et al.'s [71] model), and **c** SWRC (van Genuchten's model) for three typical soils

sequently, SSCC due to capillary water can be directly calculated from the SWRC as $\sigma^s = -S_e\,(u_a - u_w)$.

Lu et al. [71] further demonstrated theoretically and experimentally that a closed form equation for the SSCC can be established for all types of soils (Fig. 9b):

$$\sigma^s = -S_e(u_a - u_w) = -\frac{S - S_r}{(1 - S_r)\alpha}\left[\left(\frac{S - S_r}{1 - S_r}\right)^{\frac{n}{1-n}} - 1\right]^{1/n} = -\frac{S_e}{\alpha}\left[(S_e)^{\frac{n}{1-n}} - 1\right]^{1/n} \tag{22}$$

where S is the degree of saturation, S_r is a fitting parameter commonly called residual saturation, S_e is the equivalent degree of saturation and is equal to $(S - S_r)/(1 - S_r)$, α is a fitting parameter related to the inverse of air-entry pressure, and n is

a fitting parameter related to pore size distribution. The closed form Eq. (22) for SSCC completely utilizes the identical parameters defined in van Genuchten's SWRC equation shown in Fig. 9c.

The intrinsic relationships between SWRC and SSCC are further validated [67, 68] by a deformation-based method along with the shear strength and SWR data. Challenges remain in developing theoretical formulas for suction stress due to adsorption. The major obstacles are lack of experimental techniques to reliably quantify suction stress at very low matric potential, i.e., $\psi < -50$ MPa. From a theoretical viewpoint, suction stress at very low matric potential would provide an important physical constraint for the lower bound. Nevertheless, practical implications of suction stress at very low matric potential are unknown and remain to be explored.

In 2008, Lu [72] illustrated that matric suction, though has stress unit per se, is not a stress variable, though matric suction can be used as a variable to describe stress through other functions. In nearly all two-stress state variable theories, matric suction has been widely used as a stress variable parallel to other stress variables such as the total stress. Considering matric suction as a stress variable would unlikely lead to a unified treatment of shear strength and deformation under the Terzaghi's effective stress principle for soil under variably saturated conditions. The practical corollary is that theories based on the two-stress state variables would unavoidably lead to functional parameters that do not have a clear physical basis.

Recently, the traditional definition of matric suction being the difference between pore air and pore water pressures is challenged [65]. This definition is only valid when pore water pressure can be calculated by the Young-Laplace equation (6). Because soil-water retention by two distinct physical mechanisms; capillarity in pores and hydration on the particle and inter-sheet surface, and around exchangeable cations, soil water structure or densities are very different (see Sect. 4.5). Under capillary mechanism where there exists curved air-liquid interface, and the traditional pore water pressure can be calculated by the Young-Laplace equation (6). On the other hand, under surface or cation hydration there is no need for the curved air-liquid interface. Water is tightly bonded for the first few layers, water density varies significantly, so the traditional pore pressure concept is not appropriate or measurable or controllable by traditional methods such as tensiometer or axis translation techniques. Instead, Kelvin's equation (8) should be used to define and calculate the total suction and matric suction. A general matric suction definition, being the negative of matric potential defined in Eq. (11), will provide a unified way to describe soil water potential.

Several important questions regarding the unified effective stress remain. While interparticle physicochemical forces have been recognized as the deficiency in Bishop's effective stress Eq. (20) and are used in the suction stress-based effective stress framework shown in Eq. (22), theories on suction stress due to these physicochemical forces are incomplete. Currently, suction stress due to adsorptive water is treated roughly in Eq. (22) as the contribution due to the residual water content. Though widely used in many SWRC models, the concept of residual water content is physically blurred and thus empirical. The explicit functional relationship between matric potential and adsorptive water content should be and has been recently used

in lieu of the residual water content [63, 93]. Such relationship should provide a physical basis to further develop better suction stress functions for adsorptive water content appeared in Eq. (21).

4.5 Soil Water Density

Density of a material reflects its thermodynamic state and impacts its physical properties such as strength, compressibility, thermal conductivity, and wave travel velocity. Soil water density can be remarkably different than free liquid water density due to adsorption that causes water structure change (e.g., [2, 76, 79]). To date, however, there is no unanimously accepted experimental approach to measure soil water density or a physical model to describe soil water density as a function of water content. Better understanding the causes for changes in soil water density may light pathways to utilizing soil water density as a powerful surrogate to define soil physical properties. The major obstacles can be summarized in three areas: the limitations or flaws in the existing measurement techniques, how to interpret soil water density as a function of soil water content, and ambiguous physical mechanisms responsible for soil water density variation [112].

Commonly used experimental techniques for determining soil water density are X-ray diffraction (e.g., [83, 85]), specific gravity bottle (e.g., [59, 86]), and swelling test [109]. Each of these techniques provides a quantitative way to determine soil water density, but each has flaws or inherent limitations [112]. Commonly used theoretical techniques are molecular dynamics and molecule simulation (Monte Carlo). While these methods have a rigorous thermodynamic basis, they are limited by simulation time, size, and ideal conditions [112]. Specifically, molecular dynamics can only simulate real time up to on the order of pico-seconds, Monte Carlo simulation requires an unknown number of iterations for convergent results, and the simulation domain for both methods is primarily constrained at the unit cell of mono mineral crystals.

Soil water density is generally defined as the ratio of soil water mass (M_w) to volume of soil water (V_w), and can be further refined in two ways: average (global) $\rho_\mathrm{w}^\mathrm{ave}$ or differential (local) $\rho_\mathrm{w}^\mathrm{inc}$:

$$\rho_w^{ave}(w) = \frac{M_w(w)}{V_w(w)} = \frac{w}{V_w(w)} M_s \tag{23}$$

$$\rho_w^{inc}(w) = \frac{\Delta M_w(w)}{\Delta V_w(w)} = \frac{\Delta w}{\Delta V_w(w)} M_s \tag{24}$$

where gravimetric water content w and solid mass M_s are commonly introduced as a reference state.

Both experimental and theoretical studies in the past demonstrate that in swelling soil under low matric potential environment, soil water density can be as high as

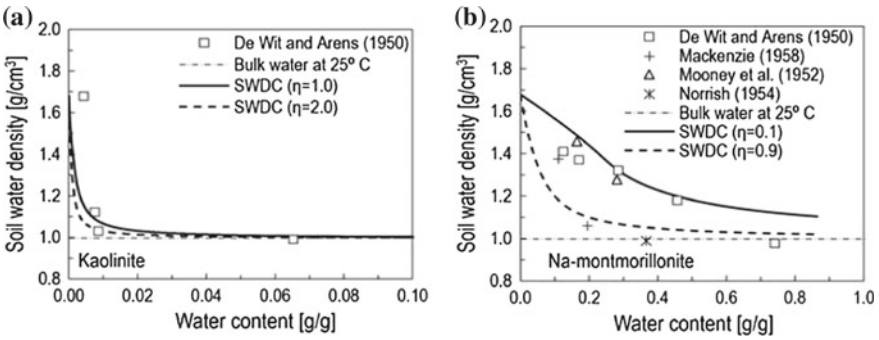

Fig. 10 Comparisons of predicted soil water density curves with experimental data for **a** kaolinite and **b** Na-montmorillonite (from [112])

1.68 g/cm^3 [28], whereas in some clayey soil under high matric potential, soil water density could be as low as 0.74 g/cm^3 [14].

A conceptual model unifying the above abnormal soil water density has been recently proposed and theorized in a soil water density model [112]. Herein two mechanisms are responsible for soil water potential and therefore density variations: capillarity and adsorption. Both lower the matric potential but in fundamentally different ways. As described in Sect. 4.1, capillarity lowers pore water pressure, thus creating tensile stress among water molecules and enlarged liquid volume. This leads to soil water density lowering. However, soil water density is subject to a lower bound due to cavitation. Two types of adsorption mechanisms exist in soil: surface and inter-sheet hydration, and cation hydration. Both adsorption mechanisms lower matric potential but have different impacts on soil water density. Since water molecules are tightly bound around the particle surface or cations, inter-atomic forces or local pressure would increase. Under ionic and van der Waals forces, the water structure could be altered significantly in comparison with capillary water. This leads to a significant increase in local pressure and soil water density. Because clayey soil could have very high SSA, the adsorption water content could be dominating under low matric potential. This leads to soil water density much higher than that in free or capillary water. A new soil water density function integrating both adsorption and capillary mechanisms is proposed [112]:

$$\rho_w^{inc} = (\rho_{\max} - \rho_{w0})\left[\exp\left(\frac{\psi_m - \psi_{m\,\min}}{\psi_m}\right)\right]^{\eta} + \rho_{w0} \tag{25}$$

where $\rho_{\max}$ is the maximum soil water density, ρ_{w0} is the bulk soil water density, $\psi_{m\min}$ is the lowest matric potential, and η denotes the exponential decay rate. Utilizing the generalized SWRC model [63], the new soil water density function model (Eq. (25)) can reproduce the experimental trends in kaolinite and montmorillonite, as illustrated in Fig. 10.

The experimental data for montmorillonite shown in Fig. 10b were obtained by different investigators under different water content. Thus, at a given water content, the differences among different measurements could result from the different total water contents. For example, at a water content around 0.2, which is equivalent to about two layers of adsorbed water, or 6 nm from the particle or interlayer surface, soil water density data fluctuates between 1.35 to 1.45, because the experimental data points were obtained at different water contents.

Several fundamental issues with both theoretical and practical implications remain unresolved. The density, structure, and energy state of the water is recognized to be different at a given distance from the particle surface in the case of a saturated soil than in an unsaturated soil at a low water content [76, 79, 82]. This implies that the pore water pressure and consequently soil water density (local) at a fixed point depend on saturation or water content. Whether this is true, and the practical significance are unclear.

In principle, as defined in Eq. (13), matric potential, which governs the equilibrium state, has origins in capillarity and adsorption. Near the particle surface, adsorptive matric potential is caused by van der Waals forces, surface cation hydration, hydrogen bonds, and the electrical double layer, which lower the energy of soil water, leading to potentially significant compressive pressure near particle surfaces. At the far field where the air-water interface is located, matric potential could be controlled by either capillarity (Eq. (6)) or adsorption (Eq. (8)), depending on water content. Fundamental research on pore water pressure distribution within a representative elementary volume of matric potential under variably unsaturated conditions is needed.

Currently, there is no reliable technique for measuring soil water density in either average or incremental form. Data on soil water density would provide a physical basis for developing theoretical models describing the soil water density function. Soil water density function can be used as a surrogate to better define matric potential, SSA, specific gravity of soil, and to quantify swelling behavior in clay.

5 Geotechnical Engineering Properties

Recent developments in characterizing four geotechnical properties important to current and emerging challenges described in Chapter 1 "The Role of Geotechnics in Addressing New World Problems" are provided in this section: soil shrinkage curve (SSC), small-strain shear modulus G_{max}, Young's or finite-strain modulus E, and thermal conductivity function. The table below summarizes three basic questions on these four properties: what are they? why are they important to geotechnical engineering problems? and how do they relate to the grand challenges as well as specific emerging problems outlined in Chapter 1 "The Role of Geotechnics in Addressing New World Problems".

What is it?	Why is it important?	Relevance to challenges in Chapter 1 "The Role of Geotechnics in Addressing New World Problems"
5.1 soil shrinkage curve		
Soil shrinkage curve is the characteristic relationship between volumetric reduction (void ratio) and soil moisture content (moisture ratio equal to volume of soil water to volume of solid) under drying and zero total stress conditions	Provides linkages between CEC/SSA and Atterberg limits, and between CEC/SSA and soil deformation (swelling/shrinkage) properties	Management of energy and materials resources: nuclear energy Management of water resources: remote inspection, evaluating risk under a changing climate
5.2 small strain shear modulus		
G_{max} is ratio between a small shear stress and the accompanying shear deformation; i.e., a deformation so small that it does not cause any permanent deformation following stress removal (elastic behavior). Once the shear strain γ exceeds some small value γ_{ref} the shear modulus degrades progressively to smaller values with further deformation	Determines the velocity at which shear waves travel through the ground. Important parameter in soil dynamics problems and geotechnical earthquake engineering	Urban sustainability and resilience: natural hazard resilience for cities Overarching challenges: engineering properties of geomaterials
5.3 Young's modulus function		
E is ratio between applied stress and deformation in the same direction (usually compressive or tensile); a constant if within the range of linear elasticity, degrades for higher stress levels because of disruption of soil structure	Used for computation of deformations and displacements of earth and earth-structure systems	Urban sustainability and resilience: natural hazard resilience for cities Management of Water resources: reversal of groundwater depletion Overarching challenges: engineering properties of geomaterials
5.4 Thermal conductivity function		
The constant of proportionality that relates rate of heat flow by conduction through a material to the thermal gradient across the material (Fourier's Law)	Essential parameter for solution of any steady state or transient problems involving heat flows, freezing, thawing, or temperature changes in the ground	Climate change: thermal energy (climate change) Overarching challenges: engineering properties of geomaterials

5.1 Soil Shrinkage Curve

The soil shrinkage curve is the characteristic relationship between volumetric reduction (as indicated by decrease in void ratio) and moisture ratio during drying under zero applied total stress conditions. Moisture ratio equals to the ratio of volume of soil water and volume of solid. It has been studied for at least over one hundred years for silty and clayey soils. Historically, remolded soil has been assumed to have three volumetric behavior regimes (Fig. 11a): normal shrinkage where soil is saturated and volume change is due entirely to water content reduction, residual shrinkage where soil becomes de-saturated with a large amount of water evaporation and the water content reduction is greater than the volume reduction, zero shrinkage where there is no or little volume reduction as soil dries. This conceptual model has been widely accepted to the extent that few of the documented relationships contain data for moisture ratios less than about 0.1.

Recently, Lu and Dong [62] proposed a SWR-based shrinkage curve model as illustrated in Fig. 11b. Particle Image Velocimeter (PIV) has been used to quantify the soil shrinkage curve. Consistently for clayey soils, Lu and Dong [62] found that shrinkage rate (slope of void ratio vs. moisture ratio illustrated in Fig. 11b) of soil is not zero as soil approaches dry; instead, it is a constant characteristically related to SSA, CEC, and the maximum adsorption water content. This implies that the relationships among any of the three soil physicochemical properties SSA, CEC, and the maximum adsorption water content are by a constant. Further research on broad soil is needed to assess the generality of this discovery.

In light of the new discovery and the conceptual model depicted in Fig. 11b, Chen and Lu [22] developed a generalized equation for the soil shrinkage curve. In this

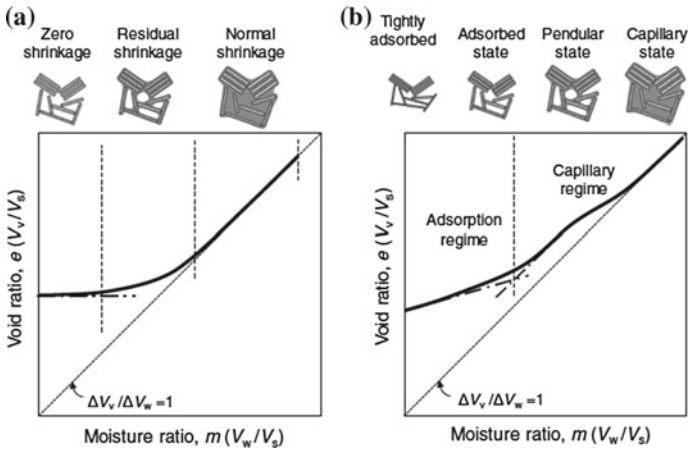

Fig. 11 Illustration of soil shrinkage characteristic curve: **a** traditional interpretation, and **b** interpretation based on adsorption and capillary soil water retention (from [62])

equation, the soil shrinkage rate turns to zero when soil does not have significant CEC, whereas the shrinkage rate could be non-zero and as high as 0.4 for montmorillonite.

One interesting finding is that the maximum adsorption water content of SWR of a soil is not equal to the maximum adsorption water content of SSC, but is highly correlated. The ratio between these two maximum adsorption water contents was found to be persistently ~2.45 for different types of soils. This has an important implication on one long-standing question: is there a one-to-one relation between SSA/CEC and Atterberg limits? Strong correlation has been found, but no unique relationship has been established. In light of the unique relationship between SSA/CEC and soil shrinkage rate, Lu and Dong [62] offered the following explanations. Atterberg limits tests are fundamentally mechanical tests; the plastic limit making radial cracks perpendicular to soil thread is a tensile failure test under unsaturated static conditions, whereas the liquid limit shaking a grooved soil specimen is a shear failure test under saturated dynamic conditions. As such, the determining factor for each of these two tests is soil strength under different water content. Suction stress provides exactly such strengths; one in tensile and the other in shear resistance. Following such logic, strengths of soil are fundamentally governed by inter-particle stress, i.e., suction stress. Suction stress originates from two types of inter-particle stresses: capillary and adsorption. Adsorption-induced suction stress is governed at more fundamental inter-atomic scale by physicochemical forces through SSA/CEC. Capillary induced suction stress is governed at more fundamental pore scale by capillary forces of surface tension and negative pore water pressure. Adsorption-induced suction stress is independent of pore size distribution and controls the suction stress in clayey soil, leading to the observed strong correlation between SSA/CEC and shrinkage rate [62].

Capillary induced suction stress is greatly controlled by molding and pore pore-size distribution, leading to different suction stress for different soils with the same pore-size distribution or the same soil with different pore-size distributions. This causes the non-unique relationship between SSA/CEC and Atterberg limits. Stiffness, in terms of compressibility defined as the slope between the void ratio and logarithm of negative suction stress under shrinkage test conditions, is governed by both suction stress and pore-size distribution, therefore should have a stronger correlation to Atterberg limits, as demonstrated experimentally in (Fig. 12).

Future research should examine the generality of the non-zero shrinkage rate assumption as well as the shrinkage rate variation in low moisture ratios. Some experimental data [70, 108] indicate that the shrinkage rate can abruptly become negative as kaolinite soil approaches to dry state, leading to volume expansion. Possible physical explanations are vanishing capillarity [108] and the last adsorbed layer on particle surface. Because the resolution limit in controlling moisture ratio and measuring void ratio in the current shrinkage curve measurement techniques, the nature of the abrupt reverse in volume change remains unknown.

Future research should also focus on linking soil shrinkage behavior and Atterberg limits, which will provide pathways to ultimately develop a fundamentally sound, robust, and practical method to classify and characterize clayey soil.

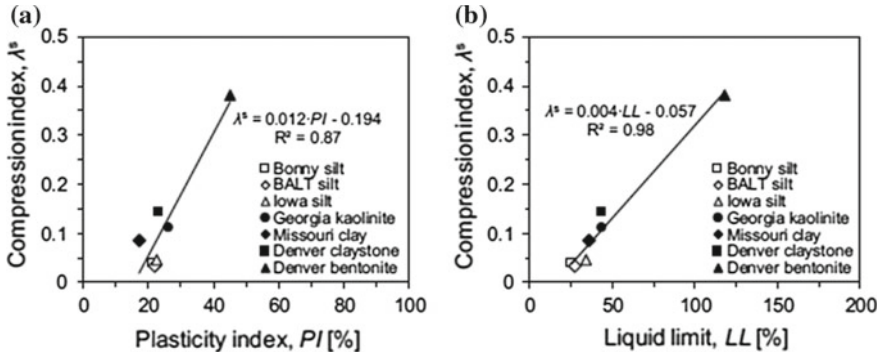

Fig. 12 Experimental data illustrating the relationship between compressibility and Atterberg limits. Compressibility of remolded soil is defined as the slope of the void ratio vs logarithm of negative suction stress (from [29])

5.2 Small Strain Shear Modulus

Small-strain shear modulus $G_{\max}$ is a governing parameter for shear wave propagation in porous materials; the travel velocity is proportional to the square root of $G_{\max}$ and depends on soil type, void ratio e and effective stress σ'. $G_{\max}$ can be described by a power law proposed by Hardin and Richart [43] as follows:

$$G_{\max} = A \cdot F(e)\left(\sigma'\right)^{\gamma_1} \tag{26}$$

where A and γ_1 are fitting parameters, and F is empirical function of void ratio e. By explicitly considering the role of suction stress in material's stiffness, some recent works on generalizing the above law to variably-saturated conditions will be reviewed here. The relationship between finite strain modulus and small-strain modulus can be also established (Sect. 5.4).

In continuum mechanics, there are two geotechnical properties governing wave propagation in soil: small-strain shear modulus and damping factor. Typical stress wave problems in earthen structures are due to dynamic loading by machine, structure and vehicle vibration, and seismic wave propagation. Small-strain shear modulus or $G_{\max}$ as it is commonly called, varies greatly in different soils. Even in the same soil it can vary from a few MPa at the complete saturated state to a few GPa at the complete dry state. Stress conditions, both inter-particle and external, have shown to greatly affect $G_{\max}$ variation in granular soil [23]. Recent studies also indicate that $G_{\max}$ is subject to wetting and drying hysteresis.

The variation of $G_{\max}$ is most pronounced in soil with clay content. Several questions arise: why does $G_{\max}$ vary so much from dry to saturated? Why are there two rapid changes in $G_{\max}$ (shown in Fig. 13a), one at high water content and the other at relatively low water content? Why is hysteresis pronounced at high water content whereas there is little at low water content? Employing the SSCC-based

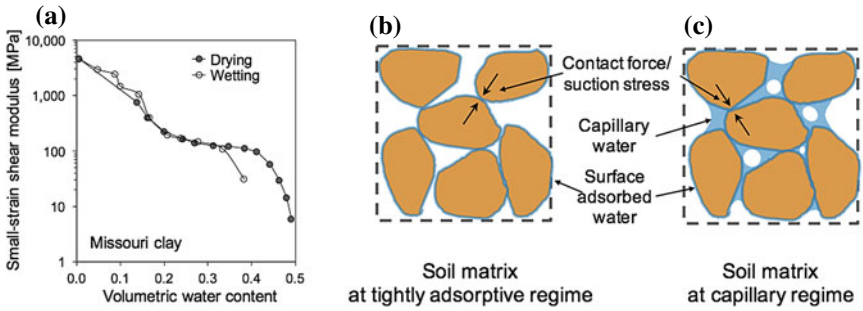

Fig. 13 Small-strain shear modulus behavior: **a** as a function of volumetric water content (from [31]), and **b**, **c** conceptual mechanism of contributions of capillary and adsorption water to small-strain shear modulus: adsorption-induced suction stress, capillary-induced suction stress (after [30])

effective stress principle, Dong and Lu [30] proposed a conceptual model illustrated in Fig. 13b, c. Herein suction stress controls the large variation in $G_{\max}$. The two rapid changes coincide with de-saturated state at high water content and onset of adsorption (θ_{amax}) state; thus capillary-induced suction stress is responsible for the first stage of rapid change, and adsorption-induced suction stress for the second rapid change. By the same token, capillary-induced suction stress causes some significant irreversible pore size change, whereas adsorption-induced causes little. The small suction stress hysteresis in adsorption water retention regime and large suction stress in capillary water retention regime are experimentally confirmed in several studies [32].

Hardin and Richart's Eq. (26) is extended with the above conception by Dong and Lu [31], where a simple constant scalar is found between $G_{\max}$ and capillary-induced suction stress:

$$G\max = -\frac{\sigma_c^s}{4.3 \times 10^{-3} \times (\alpha u_{atm})^{-1.33}} \tag{27}$$

Experimental validation of Eq. (27) for 12 different soils is shown in Fig. 14. The high correlation between the measured and calculated by Eq. (27) validates the conception that suction stress or effective stress controls the small-strain shear modulus. Some considerable discrepancies exist between the measured and predicted data, probably since Eq. (27) only establishes a linkage to one SWR parameter related to air-entry pressure and ignores pore size distribution, and most importantly, characteristic SWR parameters related to adsorption.

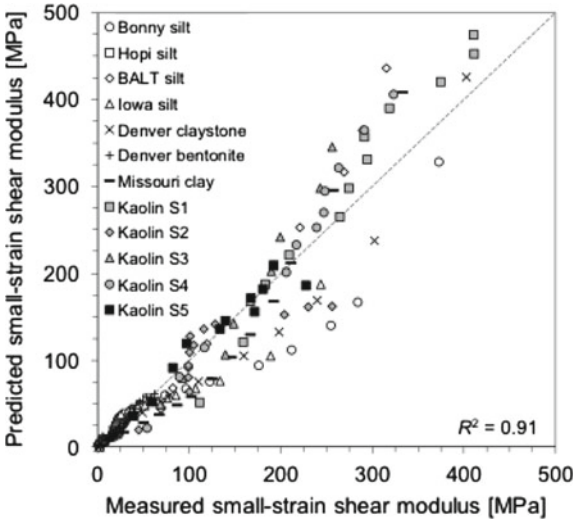

Fig. 14 Comparison of measured small-strain shear modulus G_{max} and G_{max} calculated by Eq. (27) for 12 soils from dry to saturated (data from [31])

5.3 Young's Modulus Function

Elastic modulus can vary up to 50 times between dry and saturated states and it is fundamentally controlled by inter-particles stresses through soil water content. A power law was established [68]:

$$\mathrm{E}_e = \frac{E - E_d}{E_w - E_d} = \left(\frac{\theta - \theta_d}{\theta_w - \theta_d}\right)^p = \Theta^p \tag{28}$$

where $\mathrm{E_e}$ is the normalized elastic modulus with respect to the difference between the elastic modulus at dry state E_d and at wet state E_w, E is the elastic modulus, θ is volumetric water content, θ_w and θ_d is respectively volumetric water content at certain wet and dry states, Θ is the normalized water content, and p is empirical fitting parameter. By explicitly considering the hardening due to capillary and adsorption, a new equation can be established to better represent the dependence of elastic modulus on soil water content.

Young's modulus is widely used for many problems in geotechnical engineering such as estimating instantaneous settlement of earthen structures after constructions. For soil under saturated or dry conditions, Young's modulus is often considered constant. However, Young's modulus can increase up to 50 times from fully saturated to completely dry state under a constant total stress condition. Can we establish simple, practical yet fundamentally sound laws to describe such variation for all soils?

Based on the experimental data of 16 different soils from sandy to silty, to clayey soil, Lu and Kaya [68] proposed a one-parameter power Eq. (28). This equation is practical, as the only parameter p can be experimentally determined by measuring the

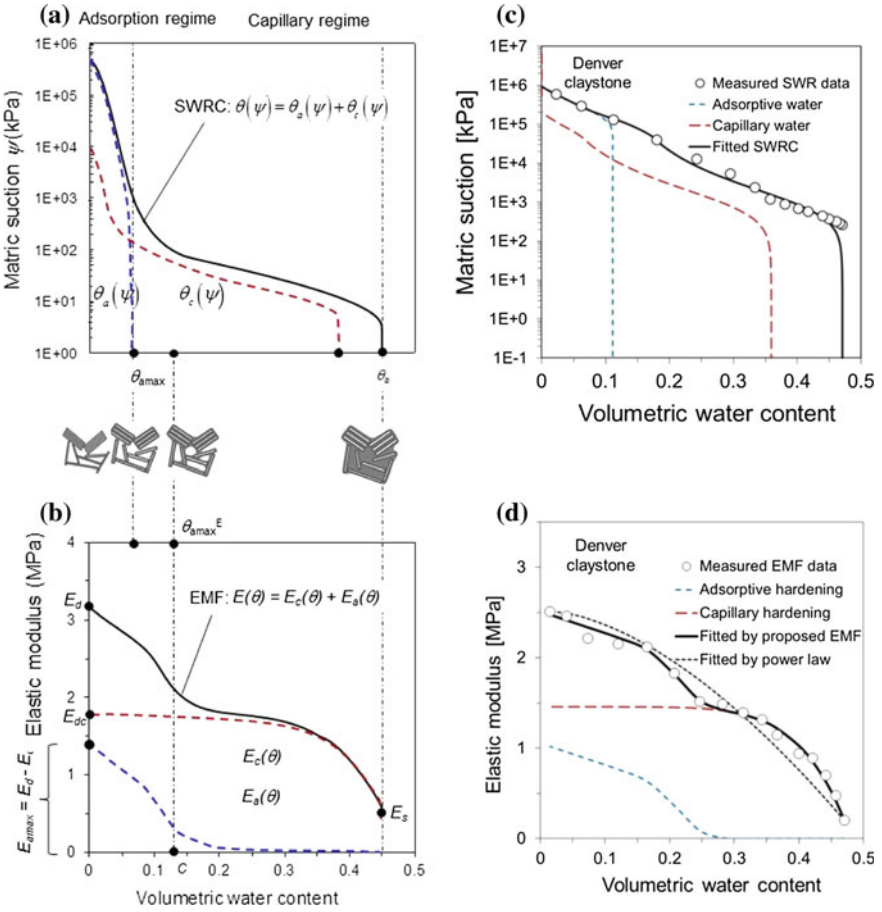

Fig. 15 Illustration of soil water retention mechanisms and elastic modulus function (EMF) behavior: **a** SWR mechanisms of capillary and adsorption, **b** elastic modulus hardening by capillary and adsorption, **c** SWR for Denver bentonite, and **d** elastic modulus hardening for Denver bentonite (from [61])

modulus at two water contents of certain dry and wet states. Further analysis on the correlation between the fitting parameter *m* and the SWRC parameters shown in Lu's [63] SWRC model indicates that there is a positive correlation between parameter *m* and SSA, though not very strong. By recognizing that capillary water and adsorption water play distinguishable roles in suction stress thereby in modulus, a quantitative model [61] conceptually illustrated in Fig. 15a, b is established.

Experimental validation for 9 different types of soil indicated that the new elastic modulus function model can well represent hardening of various soils and differentiate effects due to capillarity and adsorption, as illustrated in Fig. 15c, d. One pattern

is observed: the maximum adsorption water content for SWR (Fig. 15c) is ~half of the maximum adsorption water content for elastic modulus function (Fig. 15d), which is consistent with soil shrinkage curve behavior described in 5.1.

5.4 *Scaling Between Small-Strain and Finite-Strain Shear Moduli*

Many shear stress-strain relationships exhibit the maximum shear modulus $G_{\max}$ at strain near zero, or maximum tangent modulus as illustrated in Fig. 16a, and decreasing monotonically as strain increases. This behavior is called modulus degradation. Shear modulus G is defined as the slope of the shear stress-strain curve, so the modulus degradation behavior can be illustrated through the normalized shear modulus $G/G_{\max}$ vs. shear strain (Fig. 16b). Strains in the range of 10^{-4}–10^{-3} are called small strains and are characteristic of shear waves in soil.

The relationship between the small-strain and finite-strain shear modulus for soil under saturated conditions can be expressed in the following form [26, 33]:

$$G = \frac{G_{\max}}{1 + \left(\gamma/\gamma_{ref}\right)^{M}} \tag{29}$$

where γ is shear strain, and γ_{ref} is reference strain defined in Fig. 16a, and m is a fitting parameter describing the curvature of the shear stress-strain curve. When $M = 1$, it reduces to the Hardin and Drnevich's [44] equation.

For soil under variably saturated conditions, Hardin and Richart's [43] law (26) and Darandeli's [26] Eq. (29) can be used as a basis. Considering the roles of capillary water and adsorption water, therefore their induced suction stress in both small-strain

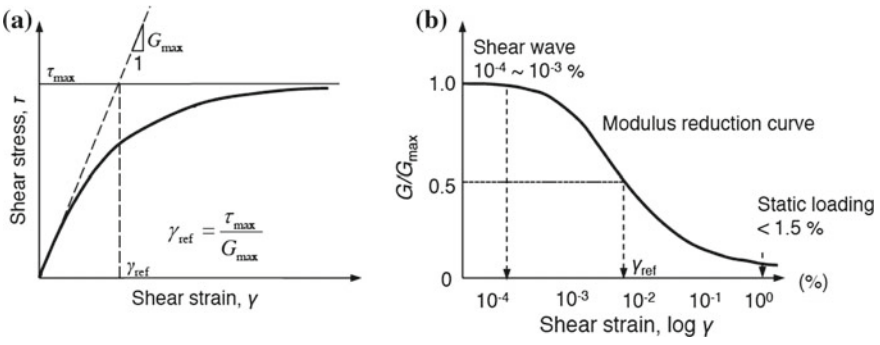

Fig. 16 Typical shear stress-strain relationship (**a**), and shear modulus degradation with increased strain magnitude (**b**) for modulus degradation soils (after [33])

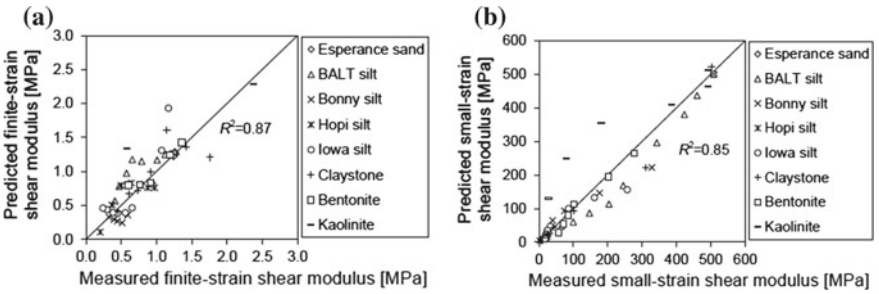

Fig. 17 Experimental validation of scaling between finite- and small-strain shear modulus by Eq. (28) for various soils (from [29])

and finite strain (described in Sects. 5.2 and 5.3), Dong et al. [29] developed the following equation for scaling:

$$G = \frac{G_{\max}}{1 + \left(\gamma / \alpha\sigma' \gamma_{ref}\right)^M}, \quad M = \frac{1}{4} \ln \theta_{a\max} + 2.34, \quad \gamma_{ref} = \frac{\theta_{a\max}}{10} \theta^{-3n+6.9} \tag{30}$$

Predictions made by Eq. (30) for various soils are shown in Fig. 17. While Eq. (30) can catch the inter-relationship between the small- and finite-strain shear modulus, considerable deviations exist. This can be attributed to several factors that require further research: lack of data in frequency/strain domain, and role of damping factor on modulus under different strain, frequency and water content conditions.

5.5 *Thermal Conductivity Function*

Heat transfer in soil is an important phenomenon in many current engineering problems, including: groundwater resource exploration (Chapter 1 "The Role of Geotechnics in Addressing New World Problems"), radioactive waste disposal (e.g., [114]), ground-source heat pumps [92], energy foundation systems (e.g., [15, 17]), heat storage in soils [78], geological carbon dioxide sequestration (e.g., [35]), and recovery of unconventional hydrocarbon resources (e.g., [24]).

Like Darcy's law, Fourier's law (10) holds for soil under both saturated and unsaturated conditions. However, the material property, i.e., thermal conductivity can vary with both temperature and water content (e.g., [37, 80]). In general, heat transfer in variably saturated porous media can be carried out by heat conduction, liquid or/and air convection, and evaporation and condensation in pores. Heat conduction occurs principally through solid grain networks, in situ liquid fluid, and in situ air. Critical reviews on heat conduction in soil [34] indicate that although many models have been developed, most of the efforts are on mathematical models that idealize soil pore networks such as series or parallel models or combination of them. Models

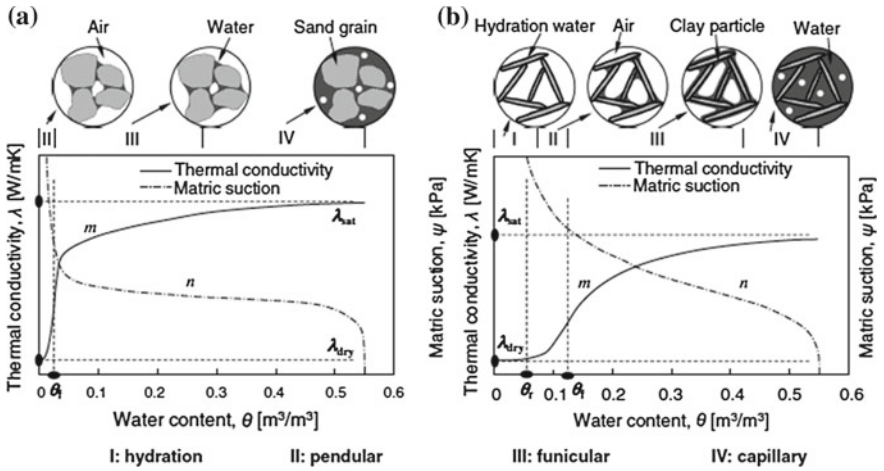

Fig. 18 A conceptual model illustrating the roles of adsorption and capillary water retention mechanism thermal conductivity in variably saturated soil (from [34, 66]). Parameter m is defined as the pore fluid network connectivity parameter for thermal conductivity

based on these idealized, though mathematically complex, generally poorly predict thermal conductivity under variably saturated conditions [34]. Some models explicitly considered soil water content variations, but do not consider soil water retention mechanisms. These models tend to perform better than idealized mathematical models, particularly in high matric potential or high water content conditions or for sandy soil. They generally are poor in predicting thermal conductivity for silty and clayey soil or under low matric potential or low water content conditions [34].

Considering the roles of capillary and adsorption water in heat transfer, Dong et al. [34] developed a conceptual model for heat conduction in variably saturated soil as shown in Fig. 18. A thermal conductivity model explicitly considering SWR behavior is developed (see definition of the physical parameters in Fig. 18) [66]:

$$\frac{\lambda - \lambda_d}{\lambda_s - \lambda_d} = 1 - \left[1 + \left(\frac{\theta}{\theta_f}\right)^m\right]^{1/m-1} \tag{31}$$

Using thermal conductivity data of 27 soils from the literature, Lu and Dong [66] showed that Eq. (31) can accurately describe the characteristic behavior of thermal conductivity function under both capillary and adsorption regimes and Eq. (31) is statistically further more accurate than other popular models. Predictions made by Eq. (31) for these various soils are shown in Fig. 19.

All the experiments reported in Fig. 19 were conducted under room temperature conditions. Previous studies indicate that thermal conductivity is also a function of temperature, particularly when the temperature is high and soil is under unsaturated conditions (e.g., [21, 100]). At high temperature, thermal conductivity function behaves non-monotonically. As water content increases, thermal conductivity will

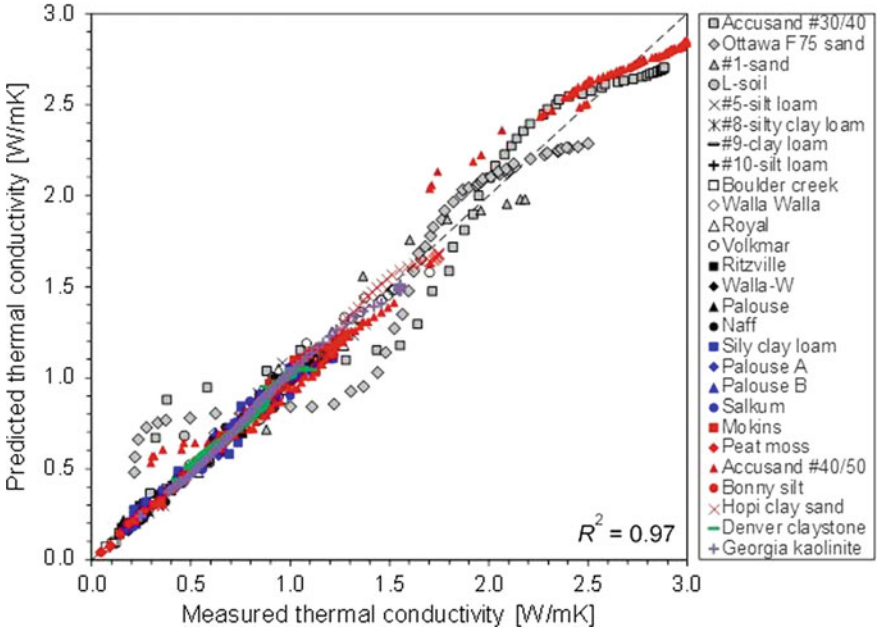

Fig. 19 Comparisons of the thermal conductivity between the measured and predicted by equation (data for the 27 soils are from [34, 66])

first increase, reach some peak values, then reduce (e.g., [21]). Such behavior is associated with the latent heat transfer due to evaporation and condensation (Sect. 2.5) and is particularly important for many emerging energy-related geotechnical engineering problems as illustrated in Chapter 10 "Emerging Thermal Issues in Geotechnical Engineering".

6 Concluding Remarks

Research opportunities open when one seeks the underpinning scientific basis for challenging geotechnical problems such as those illustrated in Chapter 1 "The Role of Geotechnics in Addressing New World Problems". In return, many effective solutions for those scientific and engineering problems can be found. Within our profession, historically, we often focused on working in different aspects of geotechnical problems such as theoretical formulation, modeling geosystem, computation method and algorithm development, experiment technique, and field characterization. A common goal for all of these aspects is seeking better solutions for engineering problems. Fundamental research starting from physics and chemistry of soil at inter-atomic scale, established firmly by the geotechnical discipline in the second half of the last century,

has been the engine providing the most promising pathways for better engineering solutions, and will be so in the future. Discovering new laws, or modifying the existing ones, is often necessary, and is an indispensable part, if not all, of better engineering solutions. It is important to recognize that the powerful solutions for practical problems, no matter the paths, always have their scientific roots. The paths between the root and problems are multiples, if not infinite. Furthermore, on the way to finding solutions for engineering problems, many surprises and new discoveries may be encountered.

One of the important shifts in the scientific basis of unsaturated soil research in recent years is recognition and use of the adsorption mechanism as the starting point instead of the capillary mechanism. Most theories regarding soil water retention, hydraulic conductivity, and effective stress or stress state in variably saturated conditions in the past half century are based on capillary mechanism. This is incomplete and a major overlook. Because adsorption takes place at much lower matric potential than capillary water, whenever capillary water is present in soil, adsorption water is always present. As such, theories based on capillary mechanism are not adequate as adsorption mechanism is fundamentally important for fine-grained soils in their hydrological and mechanical behavior. The importance of adsorption mechanism, which is rooted from inter-atomic forces, for hydraulic and mechanical behavior of silty and clayey soil is illustrated in this chapter. Many earthen infrastructures such as levees, embankments, shallow foundations, reinforced earth walls, energy foundations, and engineered and natural slopes are in variably saturated environment. Theories capable of quantifying stress and property changes in these infrastructures under variably saturated conditions that are rooted in fundamental physics laws and principles can provide promising solutions for many challenges encountered in geotechnical engineering.

Acknowledgements I am grateful for numerous critical and insightful comments by James K. Mitchell and Craig H. Benson on various versions of the chapter. However, all errors and bias are mine.

References

1. Alonso, E.E., Gens, A., Josa, A.: A constitutive model for partially saturated soils. Géotechnique **40**(3), 405–430 (1990)
2. Anderson, D.M., Low, P.F.: Density of water adsorbed on Wyoming bentonite. Nature **180**(4596), 1194 (1957)
3. Andrus, R.D., Stokoe II, K.H.: Liquefaction resistance of soils from shear-wave velocity. J. Geotech. Geoenviron. Eng. **126**(11), 1015–1025 (2000)
4. Akin, I.D., Likos, W.J.: Specific area of clay using water vapor and EGME sorption methods. Geotech. Test. J. **39**(2), 291–300 (2014)
5. Akin, I.D., Likos, W.J.: Single-point and multi-point water sorption methods for specific surface area of clay. Geotech. Test. J. **36**(7), 1016–1027 (2016)
6. American Society for Testing Materials, Designation D7503-10: Standard test method for measuring the exchange complex and cation exchange capacity of inorganic fine-grained soils. ASTM (2010)

7. Bathija, A.P., Liang, H., Lu, N., Prasad, M., Batzle, M.L.: Stressed swelling soils. Geophysics **74**(4), A47–A52 (2009). https://doi.org/10.1190/1.3131385
8. Benson, C.H., Daniel, D.E.: Influence of clods on the hydraulic conductivity of compacted clay. J. Geotech. Eng. **116**(8), 1231–1248 (1990)
9. Benson, C.H., Zhai, H., Wang, X.Z.: Estimating hydraulic conductivity of compacted clay liners. J. Geotech. Eng. **120**(2), 366–387 (1994)
10. Benson, C.H., Daniel, D.E., Boutwell, G.P.: Field performance of compacted clay liners. J. Geotech. Geoenviron. Eng. **125**(5), 390–403 (1999)
11. Bishop, A.W.: The principle of effective stress. Teknisk Ukeblad I Samarbeide Med Teknikk **106**(39), 859–863 (1959)
12. Bolt, G.H.: Physico-chemical analysis of the compressibility of pure clays. Geotechnique **6**(2), 86–93 (1956)
13. Bolt, G.H., Miller, R.D.: Calculation of total and component potentials for water in soils. Trans. Am. Geophys. Union **39**(5), 917–928 (1958)
14. Bradley, W.F.: Density of water sorbed on montmorillonite. Nature **183**(4675), 1614–1615 (1959)
15. Brandl, H.: Energy foundations and other thermo-active ground structures. Géotechnique **56**(2), 81–122 (2006)
16. Brandon, T.L., Mitchell, J.K.: Factors influencing thermal resistivity of sands. J. Geotech. Eng. **115**(12), 1683–1698 (1989)
17. Brettmann, T., Amis, T.: Thermal conductivity evaluation of a pile group using geothermal energy piles. In: Geo-Frontiers 2011, pp. 499–508. ASCE, Reston, VA (2011)
18. Brooks, R.H., Corey, A.T.: Hydraulic Properties of Porous Media. Colorado State University, Hydrology Paper No. 3 (1964)
19. Brignoli, E.G., Gotti, M., Stokoe, K.H.: Measurement of shear waves in laboratory specimens by means of piezoelectric transducers. Geotech. Test. J. **19**(4), 384–397 (1996)
20. Brunauer, S., Emmett, P. H., Teller, E.: Adsorption of gases in multimolecular layers. J. Am. Chem. Soc. **60**(2):309–319 (1938). ISSN 0002-7863. https://doi.org/10.1021/ja01269a023
21. Cass, A., Campbell, G.S., Jones, T.L.: Enhancement of thermal water vapor diffusion in soil. J. Soil Sci. Soc. Am. **48**(1), 25–32 (1984)
22. Chen, P., Lu, N.: Generalized equation for soil shrinkage curve. J. Geotech. Geoenviron. Eng. **144**(8), 04018046 (2018)
23. Cho, G.C., Santamarina, J.C.: Unsaturated particulate materials-particle-level studies. J. Geotech. Geoenviron. Eng. **127**(1), 84–96 (2001). https://doi.org/10.1061/(asce)1090-0241(2001)127:1(84)
24. Cortes, D.D., Martin, A.I., Yun, T.S., Francisca, F.M., Santamarina, J.C., Ruppel, C.: Thermal conductivity of hydrate-bearing sediments. J. Geophys. Res. **114**(B11), B11103 (2009)
25. Daniel, D.E., Benson, C.H.: Water content-density criteria for compacted soil liners. J. Geotech. Eng. **116**(12), 1811–1830 (1990)
26. Darendeli, M. B.: Development of a New Family of Normalized Modulus Reduction and Material Damping Curves. Ph.D. Thesis, University of Texas at Austin (2001)
27. De Vries, D. A.: Thermal properties of soils. Phys. Plant Environ. (1963)
28. De Wit, C. T., Arens, P. L.: Moisture content and density of some clay minerals and some remarks on the hydration pattern of clay. In: Transactions of the International Congress of Soil Science, pp. 59–62, 12 edn. Amsterdam (1950)
29. Dong, Y., Lu, N.: Measurement of suction-stress characteristic curve under drying and wetting conditions. Geotech. Test. J. **40**(1), 107–121 (2017). https://doi.org/10.1520/gtj20160058
30. Dong, Y., Lu, N.: Correlation between small-strain shear modulus and suction stress in capillary regime under zero total stress conditions. J. Geotech. Geoenviron. Eng. (2016a). https://doi.org/10.1061/(asce)gt.1943-5606.0001531
31. Dong, Y., Lu, N.: Dependencies of shear wave velocity and shear modulus of soil on saturation. J. Eng. Mech. (2016b). https://doi.org/10.1061/(asce)em.1943-7889.0001147
32. Dong, Y., Lu, N., McCartney, J.S.: Unified model for small-strain shear modulus of variably saturated soil. J. Geotech. Geoenviron. Eng. (2016). https://doi.org/10.1061/(asce)gt.1943-5606.0001506

33. Dong, Y., Lu, N., McCartney, J.S.: Scaling shear modulus from small to finite strain for unsaturated soils. J. Geotech. Geoenviron. Eng. (2018). https://doi.org/10.1061/(asce)gt.1943-5606.0001819
34. Dong, Y., McCartney, J.S., Lu, N.: Critical review of thermal conductivity models for unsaturated soils. Geotech. Geol. Eng. **33**(2), 207–221 (2015)
35. Ebigbo, A.: Thermal Effects of Carbon Dioxide Sequestration in the Subsurface. Doctoral dissertation, Institut für Wasserbau, Universität at Stuttgart, Stuttgart, Germany (2005)
36. Edil, T. B.: Influence of Fabric and Soil-water Potential on Stress-strain Response of Clay. Ph.D. dissertation, Northwestern University, Evanston, IL (1973)
37. Farouki, O. T.: Physical properties of granular materials with reference to thermal resistivity. In: Proceedings of 45th Annual Meeting of the Committee of Physico- Chemical Phenomena in Soils, pp. 25–44 (1966)
38. Fredlund, D.G., Rahardjo, H.: Soil Mechanics for Unsaturated Soils. Wiley (1993)
39. Fredlund, D.G., Xing, A.: Equations for the soil-water characteristic curve. Can. Geotech. J. **31**, 521–532 (1994)
40. Freeze, R.A., Cherry, J.A.: Groundwater, 604 p. Prentice-Hill, Inc. (1979)
41. Freundlich, H.: Kapillarchemie, eine Darstellung der Chemie der Kolloide und verwandter Gebiete. Akademische Verlagsgesellschaft (1922)
42. Frydman, S., Baker, R.: Theoretical soil-water characteristic curves based on adsorption, cavitation, and a double porosity model. Int. J. Geomech. 250–257 (2009). https://doi.org/10.1061/(asce)1532-3641(2009)9:6(250)
43. Hardin, B. O., Richart, F. E.: Elastic wave velocities in granular soils. J. Soil Mech. Found. Div. 33–65 (1963)
44. Hardin, B.O., Drnevich, V.P.: Shear modulus and damping in soils: design equations and curves. J. Soil Mech. Found. Div. **98**, 667–692 (1972)
45. Hilf, J.W.: An Investigation of Pore Water Pressure in Compacted Cohesive Soils. Technical Memorandum No. 654, United States Department of the Interior, Bureau of Reclamation, Design and Construction Division, Denver, CO (1956)
46. Israelachvili, J. N.: Intermolecular and Surface Forces. Academic Press (2011)
47. Iwata, S., Tabuchi, T., Warkentin, B.P.: Soil-water Interactions. Mechanisms and Applications. Marcel Dekker, Inc. (1995)
48. Katti, D.R., Schmidt, S.R., Ghosh, P., Katti, K.S.: Modeling the response of pyrophyllite interlayer to applied stress using steered molecular dynamics. Clays Clay Miner. **53**(2), 171–178 (2005)
49. Kersten, M. S.: Thermal properties of soils (1949)
50. Khorshidi, M., Lu, N.: Quantification of exchangeable cations using soil water retention curve. J. Geotech. Geoenviron. Eng. (2017a). https://doi.org/10.1061/(asce)gt.1943-5606.0001732
51. Khorshidi, M., Lu, N.: Determination of cation exchange capacity from soil water retention curve. J. Eng. Mech. (2017b). https://doi.org/10.1061/(asce)em.1943-7889.0001220
52. Khorshidi, M., Lu, N., Khorshidi, A.: Intrinsic relationship between matric potential and cation hydration. Vadose Zone J. (2016). https://doi.org/10.2136/vzj2016.02.0001
53. Khorshidi, M., Lu, N.: Intrinsic relation between soil water retention and cation exchange capacity. J. Geotech. Geoenviron. Eng. (2016). https://doi.org/10.1061/(asce)gt.1943-5606.0001633
54. Khorshidi, M., Lu, N., Akin, I.D., Likos, W.J.: Intrinsic relationship between specific surface area and soil water retention. J. Geotech. Geoenviron. Eng. (2016). https://doi.org/10.1061/(asce)gt.1943-5606.0001572
55. Khosravi, A., McCartney, J.S.: Resonant column test for unsaturated soils with suction-saturation control. ASTM Geotech. Test. J. **36**(6), 730–739 (2011)
56. Khoury, N. N., Zaman, M. M.: Correlation between resilient modulus, moisture variation, soil suction for subgrade soils. In: Transportation Research Record 1874, Transportation Research Board, Washington, DC (2004)
57. Langmuir, I.: The adsorption of gases on plane surfaces of glass, mica and platinum. J. Am. Chem. Soc. **40**(9), 1361–1403 (1918)

58. Likos, W.J., Lu, N., Wenzel, W.: Performance of a dynamic dew point method for moisture isotherms of clays. Geotech. Test. J. **34**(4), 373–382 (2011)
59. Low, P.F., Anderson, D.M.: The partial specific volume of water in bentonite suspensions. Soil Sci. Soc. Am. J. **22**(1), 22–24 (1958)
60. Lu, N., Zhang, C.: Soil sorptive potential: concept, theory, and verification. J. Geotech. Geoenviron. Eng. (under review)
61. Lu, N.: Generalized elastic modulus equation for unsaturated soil. In: Proceeding of The Second Pan-American Conference on Unsaturated Soils, ASCE (2017)
62. Lu, N., Dong, Y.: Correlation between soil-shrinkage curve and water-retention characteristics. *Journal of Geotechnical and Geoenvironmental Engineering*, https://doi.org/10.1061/(asce)gt.1943-5606.0001741 (2017)
63. Lu, N.: Generalized soil water retention equation for adsorption and capillarity. J. Geotech. Geoenviron. Eng. (2016). https://doi.org/10.1061/(asce)gt.1943-5606.0001524
64. Lu, N., Likos, W.J.: *Unsaturated Soil Mechanics*, John Wiley and Sons, Inc. (2004)
65. Lu, N., Khorshidi, M.: Mechanisms for soil-water retention and hysteresis at high suction range. J. Geotech. Geoenviron. Eng. **141**(8), 04015032 (2015)
66. Lu, N., Dong, Y.: Closed-form equation for thermal conductivity of unsaturated soils at room temperature. J. Geotech. Geoenviron. Eng. **141**(6), 04015016 (2015)
67. Lu, N., Kaya, M., Godt, J.W.: Interrelations among the soil-water retention, hydraulic conductivity function, and suction stress characteristic curves. J. Geotech. Geoenviron. Eng. (2014) https://doi.org/10.1061/(asce)gt.1943-5606.0001085
68. Lu, N., Kaya, M.: Power law for elastic moduli of unsaturated soil. J. Geotech. Geoenviron. Eng. **140**(1), 46–56 (2014)
69. Lu, N., Godt, J.W.: Hillslope Hydrology and Stability, Cambridge University Press (2013)
70. Lu, N., Kaya, M.: A drying cake method for measuring suction stress characteristic curve, soil-water retention, and hydraulic conductivity function. Geotech. Test. J. **36**, 1–19 (2013). https://doi.org/10.1520/GTJ20120097
71. Lu, N., Godt, J., Wu, D.: A closed-form equation for effective stress in variably saturated soil. Water Res. Res. **46** (2010). https://doi.org/10.1029/2009wr008646
72. Lu, N.: Is matric suction a stress variable? J. Geotech. Geoenviron. Eng. **134**(7), 899–905 (2008)
73. Lu, N., Likos, W.J.: Suction stress characteristic curve for unsaturated soil. J. Geotech. Geoenviron. Eng. **132**(2), 131–142 (2006)
74. Malusis, M.A., Shackelford, C.D.: Chemico-osmotic efficiency of a geosynthetic clay liner. J. Geotech. Geoenviron. Eng. **128**(2), 97–106 (2002)
75. Marcus, Y.: Thermodynamics of solvation of ions. Part 5.—Gibbs free energy of hydration at 298.15 K. J. Chem. Soc., Faraday Trans., (Intergovernmental Panel on Climate Change, ed.), Cambridge University Press, Cambridge, 87(18), 2995–2999 (1991)
76. Martin, R.T.: Adsorbed water on clay: a review. Clays Clay Miner. **9**(1), 28–70 (1960)
77. Mayne, P.W.: Cam-clay predictions of undrained strength. J. Geotech. Eng. Div. ASCE **106**(11), 1219–1242 (1980)
78. McCartney, J.S., Ge, S., Reed, A., Lu, N., Smits, K.: Soil-borehole thermal energy storage systems for district heating. In: European Geothermal Congress 2013, European Geothermal Energy Council, Brussels, Belgium (2013)
79. Mitchell, J.K., Soga, K.: Fundamentals of Soil Behavior, 3rd edn. Wiley (2005)
80. Mitchell, J.K., Kao, T.C.: Measurement of soil thermal resistivity. J. Geotech. Eng. ASCE **104**(5), 1307–1320 (1978)
81. Mitchell, J.K.: Components of pore water pressure and their engineering significance. In: Proceeding of the Ninth National Clay Conference, pp. 162–184, Clays and Clay Minerals (1962)
82. Mitchell, J.K.: Fabric, structure, and property relationships. Fundam. Soil Behav. 222–252 (1976)
83. Mooney, R.W., Keenan, A.G., Wood, L.A.: Adsorption of water vapor by montmorillonite. II. Effect of exchangeable ions and lattice swelling as measured by X-ray diffraction. J. Am. Chem. Soc. **74**(6), 1371–1374 (1952)

84. Newman, A.C.D.: The specific surface of soils determined by water sorption. J. Soil Sci. **34**(1), 23–32 (1983)
85. Norrish, K.: The swelling of montmorillonite. Discuss. Faraday Soc. **18**, 120–134 (1954)
86. Richards, S., Bouazza, A.: Determination of particle density using water and gas pycnometry. Geotechnique **57**(4), 403–406 (2007)
87. Ng, C.W.W., Xu, J., Yung, S.Y.: Effects of imbibition-drainage and stress ratio on anisotropic stiffness of an unsaturated soil at very small strains. Can. Geotech. J. **46**(9), 1062–1076 (2009)
88. Or, D., Tuller, M.: Cavitation during desaturation of porous media under tension. Water Resour. Res. **38**, 1061 (2002). https://doi.org/10.1029/2001WR000282
89. Olsen, H.W., Yearsley, E.N., Nelson, K.R.: Chemico-osmosis Versus Diffusion-Osmosis. Transportation Research Record 1288, pp. 15–22. Transportation Research Board, Washington, D.C. (1990)
90. Olson, R.E.: Effective stress theory of soil compaction. J. Soil Mech. Found. Div. **89**(2), 27–46 (1963)
91. Olson, R.E., Langfelder, L.J.: Pore water pressures in unsaturated soils. J. Soil Mech. Found. Div. **97**(SM1) (1965)
92. Preene, M., Powrie, W.: Ground energy system: from analysis to geotechnical design. Géotechnique **59**(3), 261–271 (2009)
93. Revil, A., Lu, N.: Unified water isotherms for clayey porous media. Water Resour. Res. **49**, 1–15 (2013). https://doi.org/10.1002/wrcr.20426
94. Salles, F., Bildstein, O., Douillard, J.-M., Jullien, M., Van Damme, H.: Determination of the driving force for the hydration of the swelling clays from computation of the hydration energy of the interlayer cations and the clay layer. J. Phys. Chem. C **111**(35), 13170–13176 (2007)
95. Santamarina, J.C., Klein, K.A., Wang, Y.H., Prencke, E.: Specific surface: determination and relevance. Can. Geotech. J. **39**(1), 233–241 (2002)
96. Sawangsuriya, A., Edil, T.B., Bosscher, P.J.: Modulus-suction-moisture relationship for compacted soils in postcompaction state. J. Geotech. Geoenvironmental Eng. **135**(10), 1390–1403 (2009)
97. Shackelford, C.D., Daniel, D.E.: Diffusion in saturated soil: I. Background. J. Geotech. Eng. **117**(3), 467–484 (1991)
98. Shaw, D.J.: Introduction to Colloid and Surface Chemistry. Butterworth Heinemann, London (1992)
99. Skempton, A.W.: Notes on the compressibility of clays. Q. J. Geol. Soc. Lond. **100**(2), 119–135 (1944)
100. Smits, K.M., Sakaki, T., Howington, S.E., Peters, J.F., Illangasekare, T.H.: Temperature dependence of thermal properties of sands across a wide range of temperatures (30–70 °C). Vadose Zone J. **12**(1), 1–13 (2013)
101. Stokoe, K.H., Woods, R.D.: In situ shear wave velocity by cross-hole method. J. Soil Mech. Found. Div. **98**(sm5) (1972)
102. Terzaghi, K.: Theoretical Soil Mechanics. Wiley, New York (1943)
103. Terzaghi, K., Peck, R.B.: Soil Mechanics in Engineering Practice, 2nd edn. Wiley, New York (1967)
104. Tetens, O.: Über einige meteorologische Begriffe. Z. Geophys. **6**, 207–309 (1930)
105. Toker, N.K., Germaine, J.T., Culligan, P.J.: Comment on cavitation during desaturation of porous media under tension. Water Resour. Res. **39** (2003). https://doi.org/10.1029/2002wr001834
106. Tunega, D., Gerzabek, M.H., Lischka, H.: Ab initio molecular dynamics study of a monomolecular water layer on octahedral and tetrahedral kaolinite surfaces. J. Phys. Chem. B **108**(19), 5930–5936 (2004)
107. Van Genuchten, M.T.: A closed-form equation for predicting the hydraulic conductivity of unsaturated soils 1. Soil Sci. Soc. Am. J. **44**(5), 892–898 (1980)
108. Vesga, L. F. Direct tensile-shear test (DTS) on unsaturated kaolinite clay. Geotech. Testing J. **32**(5), 397–409 (2009)

109. Villar, M.V., Lloret, A.: Influence of dry density and water content on the swelling of a compacted bentonite. Appl. Clay Sci. **39**(1–2), 38–49 (2008)
110. Wang, J., Kalinichev, A.G., Kirkpatrick, R.J.: Effects of substrate structure and composition on the structure, dynamics, and energetics of water at mineral surfaces: A molecular dynamics modeling study. Geochim. Cosmochim. Acta **70**(3), 562–582 (2006)
111. Yeung, A.T., Mitchell, J.K.: Coupled fluid, electrical and chemical flows in soil. Geotechnique **43**(1), 121–134 (1993)
112. Zhang, C., Lu, N.: What is the soil water density? Critical reviews with a unified model. Rev. Geophys. (2018) https://doi.org/10.1029/2018rg000597
113. Zhang, C., Dong, Y., Liu, Z.: Lowest matric potential in quartz: metadynamics evidence. Geophys. Res. Lett. 1–8, 1706–1713 (2017)
114. Zhang, Y.Q., Lu, N., Ross, B.: Convective instability of moist gas in a porous medium. Int. J. Heat Mass. Transf. **37**(1), 129–138 (1994)

Multiscale and Multiphysics Modeling of Soils

José E. Andrade and Utkarsh Mital

Abstract This chapter addresses the multiscale and multiphysics modeling of soils explicitly. The presentation revolves around three main paradigms: continuum, discrete, and multiscale. The advantages and disadvantages of each of the paradigms are discussed and their particular developments are addressed. We show that continuum models are the backbone of current analysis at the engineering scale and furnish an appropriate framework to implement multiphysics couplings including thermal, hydraulic, mechanical, and chemical (THMC) effects. On the other side of the spectrum, discrete models have emerged and they are capable of capturing explicitly the discrete nature of granular soils. Progress has been made to make discrete models accurate. More recent developments include multiscale methods connecting continuum and discrete approaches. Multiscale methods show much promise and have been able to reproduce material behavior in the laboratory. We anticipate that future applications will demand more multi-scale and analysis of geologic materials.

Keywords Continuum mechanics · Discrete element method · Multiscale modeling · Multiphysics

1 Introduction

As described in Chapter 1 "The Role of Geotechnics in Addressing New World Problems" and throughout this book, geotechnical engineering in the 21st century faces a number of challenges that will require effective and sustained leadership. Climate change, urban sustainability and resilience, energy and materials management, and water management are pressing challenges that will necessitate advanced and accurate modeling techniques. While previous methods in geotechnical engineering have relied on experience and the observational method, these new challenges will require a more sophisticated and rigorous approach that explicitly acknowledges the

J. E. Andrade (✉) · U. Mital
California Institute of Technology, Pasadena, CA, USA
e-mail: jandrade@caltech.edu

N. Lu and J. K. Mitchell (eds.), *Geotechnical Fundamentals for Addressing New World Challenges*, Springer Series in Geomechanics and Geoengineering,
https://doi.org/10.1007/978-3-030-06249-1_5

multiscale and multiphysics nature of soils and, in doing so, can help fill the gap in our understanding to make transformative advances.

While it has been known that soils are multiscale and multiphysical in nature, only recently have observations, experiments, and simulations been able to begin to cope with this notion directly. Multiphysics have been more actively pursued, with pioneering work on hydro-mechanical coupling dating back to the theory of consolidation by Terzaghi [1]. Other physics have now been accounted for–there exists a thermo, hydro, mechanical, and chemical (THMC) framework. Pivotal also have been continuum mechanics theories that have provided the governing laws that have served as the underpinnings of the continuum framework, including the THMC framework. To close the system, constitutive theories have been developed, mostly around the theory of plasticity and predicated upon the macroscopic observations of drained soil behavior provided by triaxial compression tests (monotonic and cyclic).

The multiscale modeling of soils has been less developed until fairly recently. While it has been known that grain-scale mechanics control the behavior of the material at the macroscopic scale and soil classification systems attempt to link grain scale information, such as shape, size and distribution, there has been little direct connection between grain and continuum scale. At best, some of the continuum theories have been "micromechanically-inspired". For example, the idea of dilatancy pioneered by Reynolds has roots in grain-scale mechanics but quickly dilutes to a direct macroscopic property that is modeled using phenomenological arguments. X-ray tomography and the introduction of the discrete element method [2] have made possible the direct observation and modeling of granular materials. With these developments, efforts have started to try and connect the continuum and traditional approach, with more discrete and emergent descriptions.

The objective of this chapter is to summarize the state of the art in the multiphysics and multiscale modeling of soils. In particular, we focus on the modeling techniques, with only minor attention placed on the experimental techniques. We describe the continuum framework, which is still the most widely used approach to simulate soils. Then, the discrete approach is described, mostly from the point of view of the discrete element method and its variants. Finally, we describe recent developments in multiscale techniques. We have chosen a relatively narrow approach for compactness of presentation and also reflecting the authors' implicit biases. However, we believe this chapter provides an important starting point in the discussion of multiscale and multiphysical nature of soils, which is likely to become an incredibly important aspect of soil mechanics in the near future.

2 Continuum Scale Modeling

The continuum scale refers to a scale whose dimensions are large compared to those of individual soil grains. Owing to computational limitations, continuum analysis is the preferred mode of analysis for typical geotechnical systems such as foundations, retaining structures, slopes, and excavations. In its most basic form, continuum anal-

ysis focuses on the mechanical behavior and seeks to relate kinematical quantities such as displacement and velocity to stresses. However, many geotechnical problems are inherently multiphysical in nature. This necessitates a framework that allows the mechanics of geotechnical systems to be coupled with hydro, thermal, chemical, and biological processes.

The continuum framework involves formulating equations that fall under two broad categories—balance laws and constitutive models. Balance laws refer to universal physical laws such as conservation of mass, momentum, and energy. Constitutive equations describe material behavior. Together, these equations are solved to model static and dynamic behavior of mechanical systems. These equations can be modified to incorporate coupled hydro, thermal, chemical, or biological processes, depending on the problem at hand (e.g., liquefaction modeling, ground freezing, radioactive waste disposal). In addition, the mechanical behavior is usually constrained by boundary conditions and kinematic restraints.

The most common manifestation of multiphysics in continuum modeling of geotechnical systems involves hydro-mechanical coupling. Geotechnical systems are primarily composed of soil which at the continuum scale, is a porous material composed of solid particles and void spaces. The void spaces are filled with pore fluid which can be either liquids or gases, implying that soil is an inherently multiphase material. Hydro-mechanical coupling accounts for the deformation of both solid and fluid phases.

2.1 Governing Equations

Balance of linear momentum. Under conditions of static equilibrium, the total stress in soil satisfies the following equation:

$$\nabla \cdot \boldsymbol{\sigma} = \mathbf{0} \tag{1}$$

where ∇ is the divergence operator, $\boldsymbol{\sigma}$ is the (total) stress tensor, and $\mathbf{0}$ is the zero vector. The equilibrium equation can be easily extended to incorporate effects of body forces (e.g., gravity) and dynamic loading (e.g., earthquakes) [3].

Balance of mass. Using mixture theory [4, 5], the balance of mass equation can be expressed as:

$$\nabla \cdot \boldsymbol{v} = -\nabla \cdot \boldsymbol{q} \tag{2}$$

where $\boldsymbol{v}$ is the instantaneous velocity of the solid phase, and $\boldsymbol{q}$ is the Darcian velocity of pore water. This relationship assumes that soil is fully saturated where all the void spaces are filled with water. It also assumes that both solid and water phases are incompressible. For a detailed derivation and the more general case of a partially

saturated soil with compressible phases, the interested reader may refer to work by Borja [4].

Effective stress. The total stress $\boldsymbol{\sigma}$ in soil is shared between the solid and fluid phases. In soil mechanics, it is usual to denote the stress carried by the solid phase (or the soil skeleton) as the 'effective stress'. The stress carried by the fluid phase is assumed to be isotropic on account of fluids (usually water) having negligible shear resistance. The effective stress equation can be expressed as:

$$\boldsymbol{\sigma}' = \boldsymbol{\sigma} - p\boldsymbol{I} \tag{3}$$

where $\boldsymbol{\sigma}'$ is the effective stress carried by the solid phase, p is the isotropic pore water pressure, and $\boldsymbol{I}$ is the identity tensor. The effective stress equation is considered to be one of the most important equations in soil mechanics [1]. The above expression assumes that the soil is fully saturated with water. For partially saturated soils and for pore fluid with shear resistance, the effective stress equation may be modified using coefficients proposed by Skempton [6].

Constitutive models. The coupling of pore water pressure with the deformation of the soil skeleton implies that material behavior corresponding to both fluid flow and soil deformation needs to be incorporated. The evolution of effective stress is modeled using an elasto-plastic constitutive model:

$$\dot{\boldsymbol{\sigma}}' = \mathbb{C}^{\text{ep}} : \dot{\boldsymbol{\epsilon}} \tag{4}$$

where $\dot{\boldsymbol{\sigma}}'$ is the increment in effective stress, $\dot{\boldsymbol{\epsilon}}$ is the increment in strain, and $\mathbb{C}^{ep}$ is a constitutive tangent operator relating increment in strain to increment in effective stress. Note that the constitutive model is in terms of the effective stress, not the total stress. Determination of $\mathbb{C}^{ep}$ has been and continues to be an area of extensive research—falling under the realm of continuum plasticity—and will be reviewed a little more in the next sub-section.

Pore water pressure is typically modeled using Darcy's law:

$$\boldsymbol{q} = -\frac{\kappa}{\mu}\nabla p \tag{5}$$

where $\boldsymbol{q}$ is the flux or Darcian velocity of pore water (units of velocity, e.g., m/s), κ is the medium's permeability (units of area, e.g., m^2), μ is the dynamic viscosity of the pore fluid (e.g., Pa · s), and ∇p is the gradient in pressure. Note that Eq. (5) ignores the elevation head. Also note that κ is related to hydraulic conductivity K (units of velocity, e.g., m/s) as $\kappa = K\mu/\rho g$, where ρ is the density of the fluid (e.g., kg/m^3), and g is the acceleration due to gravity (units of acceleration, e.g., m/s^2). The true seepage velocity $\boldsymbol{v_w}$ of the pore water can be obtained by dividing the flux with porosity η (i.e., $\boldsymbol{v_w} = \boldsymbol{q}/\eta$). The linear relationship between flux and pressure gradient as proposed by Darcy's law assumes slow, viscous flow with a Reynolds number

(where the representative length scale is the average grain diameter) in the range of 1–10 [7], and is typically applicable to groundwater flows. Non-linear corrections to Darcy's law have been proposed for fluid flow that deviates from the aforementioned conditions [8–10]. For applications involving dynamic excitation, additional pore pressure models can be found in the literature [11, 12].

2.2 *Continuum Plasticity Models*

Continuum plasticity revolves around determining an appropriate constitutive model for the incremental stress-strain relationship of the type shown in Eq. 4. Any constitutive model must satisfy the First and Second Laws of Thermodynamics since all real materials obey these laws. These are fundamental laws of energy conservation and dissipation. Modeling continuum soil behavior is a challenging undertaking on account of the array of complexity displayed by soils. For instance, soils are multiphase, granular, highly heterogeneous, anisotropic materials exhibiting non-linear, history-dependent, pressure-dependent, irreversible, dilatant, and rate-dependent behavior [3]. Figure 1 shows a three-dimensional view of a pressure-dependent yield surface modeled by Andrade and Borja [13]. Therefore, it comes as no surprise that continuum plasticity modeling of soils has gained a lot of attention over the past few decades.

Early efforts at modeling assumed soil as an elastic-perfectly plastic material to analyze geotechnical stability problems involving earth pressures and retaining walls. The Mohr-Coulomb [14] and Drucker-Prager [15] models were two of the most popular models under this framework and are widely used by the geotechnical community even to this day on account of their simplicity. However, soils are not elastic-perfectly plastic materials, and the aforementioned models often show discrepancies

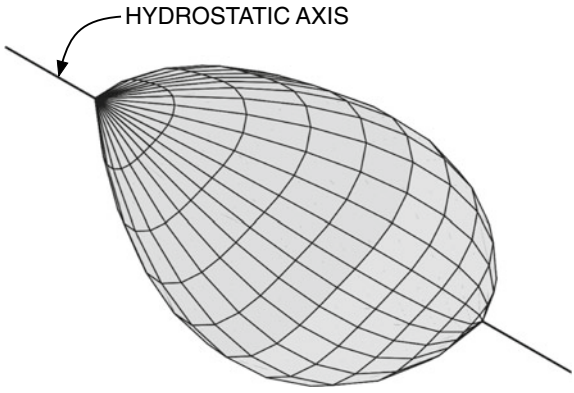

Fig. 1 Three-dimensional view of a pressure-dependent yield surface [13]

with observed experimental behavior. As a result, more complex soil models came into existence that utilized concepts of isotropic work-hardening and stress history dependence, resulting in the development of the critical state soil mechanics framework [16, 17] which was first implemented in the Cambridge models—Cam clay and modified Cam clay [18, 19]. Further experimental observations led to the development of the so-called state parameter [20] that built on the critical state framework. These ideas are encapsulated in several Cambridge-type models [13, 21, 22].

A number of important developments took place in parallel with the development of the aforementioned critical state framework. For instance, advances were made in modeling elastic or small-strain nonlinear behavior of soils. This was driven by the fact that the assumption of small-strain linearity overestimated strains and displacements in geotechnical problems [3]. Notable small-strain nonlinear models include the hyperbolic model [23], the Ramberg-Osgood model [24], and the logarithmic model [25].

Plasticity models such as the ones described previously typically require specification of (i) yield function (when the material exhibits plastic behavior), (ii) plastic potential (how the plastic strains develop as a function of stresses after yielding), and (iii) hardening law (how the yield function evolves after yielding) [26]. Alternate approaches to modeling soil plasticity also exist, chief among which include theories of hypoplasticity [27–32] and hyperplasticity [33–40]. A key aspect of these theories is that they do not specify a prior yield criterion [41], but rather it is an outcome of the model formulation. Hyperplasticity, in particular, utilizes a framework which builds the constitutive equations from the ground up using the first and second laws of thermodynamics. Houlsby [35] has shown that it is possible to derive the critical state models using the framework of hyperplasticity.

Eventually, it was realized that although the aforementioned plasticity models were capable of modeling monotonic loading paths, a gap existed when it came to modeling the cyclic response of soils. This motivated another wave of model development where more advanced concepts such as kinematic hardening, multisurface plasticity and bounding surface plasticity were explored [42–46]. The current wave of continuum model development is centered on incorporating the effect of microstructure or ‘fabric’ on continuum soil behavior [45, 47, 48], facilitated in part by the advent of discrete element method (DEM).

Continuum plasticity models, have been used to great effect to model slopes, retaining walls, foundations, and excavations [15, 49–54]. A number of recent studies have extended the continuum framework to incorporate hydro-mechanical coupling (the equations for which were presented earlier). Such studies have had some success in modeling failure mechanisms where pore pressure plays an important role, such as localized shear banding as well as liquefaction behavior of soils [1355–60].

2.3 Double Porosity

An important distinction must be when it comes to continuum modeling of soil aggregates. Soil aggregates refer to clumps of soil particles that adhere to each other more strongly than to neighboring particles. The pore size distribution in such materials has two dominant values of porosity, one corresponding to inter-aggregate pores (macropores) and the other corresponding to intra-aggregate pores (micropores). Therefore, such materials exhibit a 'double porosity'. Fluid flow can take place through both the larger macropores and the smaller micropores, and fluids may also exchange between the two types of pores. It has been observed that under mechanical loading, the volume and structure of macropores gets affected disproportionately [61]. This implies that the constitutive framework for modeling soil aggregates must capture two different compressibility responses [62–64]. Such features have implications for how the effective stress evolves under hydro-mechanical loading conditions in soil aggregates [65–69].

2.4 Extensions to Incorporate Multiphysics in Continuum Soil Modeling

A number of circumstances exist where an accurate description of soil mechanics makes it necessary to couple behavior of fluid-saturated soils with heat flow, commonly referred to as thermo-hydro-mechanical (THM) coupling. For instance, temperature effects become important to model problems such as extraction of oil or geothermal energy, pavement subjected to heating-cooling cycles, radioactive waste disposal, and artificial ground freezing. THM models simultaneously solve for deformation of soil skeleton, pore water pressure, and temperature [70–75].

In addition, there are a number of situations where in addition to temperature, geochemistry also becomes important, necessitating a framework for coupled thermal, hydrodynamic, mechanical, and chemical processes, commonly referred to as coupled THMC models. Examples include radioactive waste disposal, extraction of oil and gas, CO_2 sequestration, and backfilling coal mines [76–80].

Another important development in modeling soil behavior and accompanying geotechnical applications centers on incorporating biological processes. This approach considers soil as a living ecosystem and explores innovative and sustainable solutions to geotechnical problems [81]. This topic is explored in detail in the Chapter 7 "Bio-mediated and Bio-inspired Geotechnics" of this book.

2.5 Common Tools and Codes for Continuum Soil Modeling

The governing equations, along with the accompanying boundary conditions, need to be solved in order to model soil deformation (and other coupled parameters as the case may be). Unless the equations and model geometry are simple, analytical solutions are generally not available to solve the equations. The solution involves resorting to a numerical approach, where the equations are solved approximately.

By far the most popular numerical scheme in soil mechanics is the Finite Element Method (FEM), on account of its ability to model irregular geometries and deal with multiphysics. For modeling fracture mechanics in porous media, a popular scheme is the "Extended" Finite Element Method or XFEM [82]. The Finite Difference Method (FDM) has also gained popularity over the years, especially for simple geometries since it is more efficient in terms of computer memory and is simpler to implement. These factors sometime make FDM the preferred method for large-scale simulations on supercomputers. Compared to FEM, it can more easily deal with non-linear problems and unstable boundary value problems [3].

Both FEM and FDM require discretizing the problem domain into a mesh, which inherently makes it difficult for such methods to deal with large deformations and post-failure modeling. For such problems, mesh-free or meshless methods are gaining popularity. Some common meshless methods are Smoothed Particle Hydrodynamics (SPH), and Material Point Method (MPM).

A number of open-source and commercial codes exist where numerical models have been implemented by researchers. For hydro-mechanical problems, PLAXIS [83], FLAC [84], OpenSees [85], and ABAQUS [86] are used widely. For THM and THMC models, some available codes with the requisite capability are OpenGeoSys [87], CODE-BRIGHT [88, 89], TOUGH-FLAC [78], FADES-CORE [77, 90], and COMSOL Multiphysics [91].

3 Discrete Scale Modeling

As discussed in the previous section, continuum models fare well in analyzing field-scale problems. However, there exist many scenarios where continuum models have trouble in capturing soil behavior. For instance, there have issues modeling the strain localization phenomenon where strain is localized in regions so small that granular structure cannot be safely ignored (e.g. localized failure in landslides, gouge zone, orifice flow). Furthermore, there is evidence that suggests that the method of soil deposition affects the continuum properties of soil [92–94]. The method of soil deposition influences how individual soil grains are arranged together, and traditional continuum models, due their inherent nature of ignoring the effect of individual grains, are unable to take grain arrangement (sometimes referred to as 'fabric') into account. These models often have to be recalibrated if the original calibration was based on an experiment with a different method of deposition. Such examples point

to a need to model the relationship between grain-scale behavior and the overall material response.

The discrete element method, or DEM [2] is a particle-scale model that aims to model what continuum models cannot, namely how interactions at the scale of individual grains collectively affect the behavior of entire soil assemblies. The advantage of DEM lies in its ability to conduct "virtual" experiments [95] where kinematic and force data of individual particles can be obtained—providing key insight into the micro-mechanics of a granular assembly.

The following discussion provides a brief overview of DEM, along with some examples of how this technique has been useful. The insight provided by DEM into the micro-mechanics of soil behavior has also led to recent advances in continuum modeling [96].

3.1 Basic Equations of DEM

The discrete element method models contact forces and displacements on individual grains in a stressed granular assembly. These quantities are obtained through a series of calculations that trace the movements of individual grains for each time step. The movements are a result of disturbances propagating from the boundaries of the assembly. For instance, consider the following two particles in contact (Fig. 2).

The particles are assumed to be rigid but may have an 'overlap'. This overlap models the deformations between the particles. This type of contact model is very prevalent in geomechanics and is sometimes referred to as the 'soft-sphere' approach [95]. Modeling the contact as a linear spring (Hooke's law), the increment in contact force is:

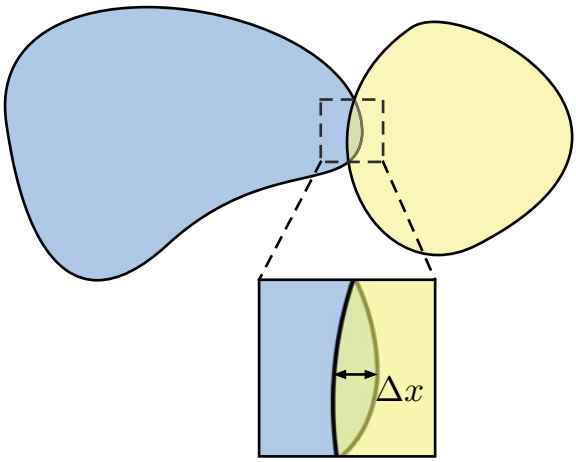

Fig. 2 Two particles in contact. The overlap Δx has been exaggerated for clarity

$$\Delta F = k\,\Delta x \tag{6}$$

where Δx is the overlap, k is the contact stiffness and ΔF is the increment in contact force. The accelerations can be modeled using Newton's second law:

$$a_i = \Delta F / m_i \tag{7}$$

where the subscript i refers to particle i, a is the acceleration, and m is the mass of the particle. These accelerations can be integrated to obtain particle velocities, which can be used to update particle displacements at the next time step. This cycle is then repeated over and over again. Forces corresponding to the displacements are found using Hooke's law (or any other force-displacement law), and the forces in turn are used to obtain displacements using Newton's second law. This formulation can be easily extended to consider a general case of an assembly with many particles, and can be further extended to include damping and shear force. The original work by Cundall and Strack [2] may be referred to for details.

A key assumption in the DEM formulation is that during a single time step, disturbances from a particle cannot propagate further than its immediate neighbors. Hence, DEM analyses with explicit time-stepping schemes require that the chosen time steps be small enough so that the above assumption holds true. Tu and Andrade [97] present a good treatment on the subject. An alternative DEM approach involves using contact dynamics [98–101] which is an implicit time-stepping scheme using a slightly different contact formulation than the one presented above. Two key advantages of the contact dynamics approach are that it enables modeling stiffer particles and allows selection of larger time steps. More details can be found in Lim et al. [101].

3.2 *Sample Progresses Made with Simple DEM Models of Discs and Spheres*

It may be of interest to know that although the seminal paper on DEM was published in 1979 [2], the use of DEM in research picked up only in the late 1990s [95, 102]. The most common particle geometries used in DEM are discs (in 2D) and spheres (in 3D). This is on account of computational complexity surrounding contact detection. In the case of discs and spheres, the distance between two particles can be determined by the distance between their respective centroids. This distance can be compared with the summation of the respective radii, which can be used to determine if the two particles are in contact. Even with such simple particle geometries, DEM simulations have been used to great effect in modeling different problem types and have given useful insights into micro-mechanics of granular behavior. While an exhaustive review is insurmountable, we give a few examples. Although DEM has found applications in

a number of different fields, we will limit our discussion to applications relevant to soil mechanics.

Perhaps some of the earliest research developments using DEM could be attributed to Rothenburg and Bathurst [103], who proposed a stress-force-fabric relationship for idealized planar granular assemblies. The relationship relates average stress in the assembly to statistical averages of contact fabric and contact forces. Further insight into granular behavior was obtained by Iwashita and Oda [104], who introduced a modification to DEM to take into account rolling resistance. This modification helped them model shear bands in numerical assemblies, in a manner similar to those of natural granular soils. Radjai et al. [105] simulated a two-dimensional dense packing of rigid spheres and showed that under biaxial loading, the granular force network follows a 'bimodal' character—the strong force chains are supported by weak lateral forces. Estrada et al. [106] further studied the bimodal character and observed a dependence on rolling resistance in assemblies subjected to simple shear.

Simple DEM models have also been used to investigate the phenomenon of force-chain buckling in granular assemblies [107, 108]. Such models have also provided key insights into micro-mechanics of diffuse instabilities and liquefaction failure in granular assemblies, as well as dilatancy and critical state [109–113]. Furthermore, DEM has also enabled modeling a numerical version of the bender element test, which helps model dynamic properties (e.g. shear wave velocity) of granular assemblies [114, 115]. Key insights have also been obtained in rheology of granular media [116]. Further examples on the application of simple DEM models to simulate different geomechanical systems can be obtained in the review paper written by O'Sullivan [95].

3.3 Extensions to Incorporate Shape

In the previous section, we provided a number of examples of how DEM models using idealized shapes of discs and spheres have proven useful. Although such models provide useful qualitative insight, it has been observed in literature that characterization of particle shape is important when it comes to reproducing quantitative bulk behavior of granular assemblies [117–119]. Such observations have spurred the development of a number of DEM variants to capture particle shape (Fig. 3). Chief among these efforts have involved the use of ellipsoids [120–122], use of clumps or clusters of spherical particles [123–126], polyhedra [127, 128], non-uniform rational basis splines or NURBS [100, 101, 129], and level sets [119, 130, 131].

Among the aforementioned approaches, the simplest DEM variant involves use of ellipsoids. However, ellipsoids have the drawback of being inherently convex, and still fall short of approximating particle shape. Clumping and polyhedral approach can approximate the general shape and volume of particles (commonly denoted as "sphericity"). However, these approaches fall short when it comes to capturing particle "roundness". Roundness is a measure of particle curvature at the local scale and has been shown to affect particle behavior [117, 119]. Clumping methods tend

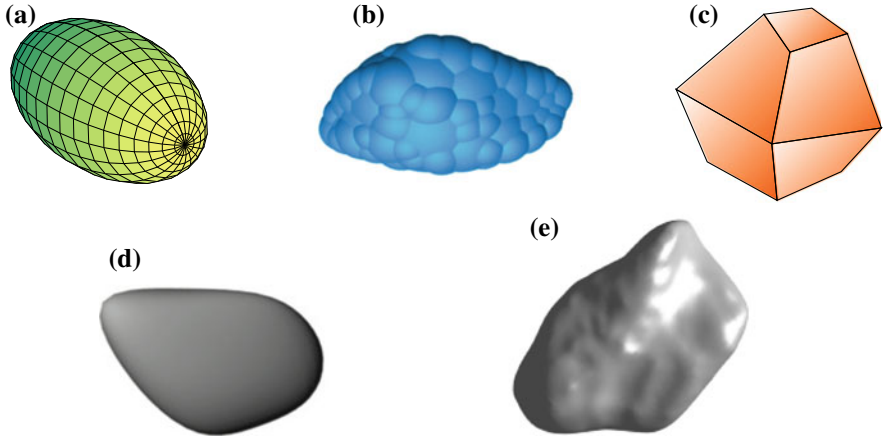

Fig. 3 DEM variants to capture shape. **a** Ellipsoids, **b** Clumps [126]—reproduced under CC BY 4.0 (https://creativecommons.org/licenses/by/4.0/), **c** Polyhedra, **d** NURBS [132], **e** Level sets

to underestimate the roundness, while polyhedral methods tend to overestimate the roundness. NURBS-based DEM has the ability to accurately capture the particle shape, both in terms of sphericity and roundness. However, contact detection in NURBS is computationally time-expensive, restricting its use to only being able to simulate about one thousand particles [129].

The most promising approach to capture particle shape seems to be the level set discrete element method (LS-DEM), which is able to circumvent all the issues faced by the aforementioned DEM variants. In addition to being able to faithfully capture shape [119], LS-DEM has also been able to quantitatively capture stress-strain and volume-strain behavior in triaxial experiments [130]. In fact, the most recent iteration of LS-DEM has succeeded in comparing model to experiment at an unprecedented level of quantitative agreement, involving a one-to-one model where every particle in the actual experiment has a digital twin. The model simulated an array of over 53,000 particles and was able to capture the mechanics of the experiment across scales ranging from macroscopic behavior to local behavior to particle behavior [131]. Significantly, the model was able to replicate the experimentally obtained shear band and predict its orientation, inclination, and thickness.

3.4 Multiphysics Coupling with DEM

All discussions pertaining to DEM up to this point assumed that the particles are infinitely rigid and do not undergo fragmentation. Understanding the mechanics of particle breakage is of great importance in geomechanics (with applications in civil engineering, earthquake mechanics, and mining). For instance, in earthquake

mechanics, nearly all the shear displacement of a fault is accommodated within the fault gouge—a zone of a few centimeters thickness containing highly crushed granular material [133]. This has led to several techniques to simulate the physics of granular fracture. A popular approach involves modeling individual particles as clumps or clusters that can be split on achievement of a maximum inter-particle force [134]. Another approach involves replacing a single particle with 'spawning' children when a stress-based criterion is met [135].

The discussions in the previous sections also assumed that we are analyzing dry assemblies under isothermal conditions with no chemical interactions. However, as discussed in the section on continuum modeling, scenarios exist where it is necessary to couple mechanics of dry assemblies with fluid flow, heat flow, and chemistry.

From a geomechanics perspective, coupling of fluid flow with DEM has obtained a lot of attention. O'Sullivan [136] provides a good review on the topic. The easiest boundary value problem to incorporate effect of pore fluid involves modeling a saturated soil subjected to completely undrained conditions. By assuming that the bulk modulus of the pore fluid is large relative to the bulk modulus of the soil skeleton, the soil assembly can be assumed to be deforming under the constraint of constant-volume. This allows the effect of fluid to be considered without explicitly modeling the fluid. This approach has been used to model soil behavior in laboratory tests such as the undrained triaxial test [113, 137]. An approach to explicitly consider the effect of the pore fluid involves the use of Darcy's equation. This approach allows simulation of large boundary value problems involving fluid flow [138], but its implementation is quite complex [136]. Another approach involves solving the averaged Navier-Stokes equations to determine the motion of pore fluid in the soil assembly [139–141]. The Navier-Stokes equations are solved on a coarse grid superimposed on the soil assembly to give fluid velocities and pressures. These values are used to calculate the net force on a particle, which is used by the DEM algorithm to update particle positions and velocities. This information is in turn passed to the fluid model and the cycle continues. This coarse grid approach is suitable to solve large boundary value problems. There also exist alternative modeling schemes where the fluid flow is discretized on the scale smaller than those of soil particles. The most popular schemes involve the use of Lattice-Boltzmann method [142–144] and smoothed particle hydrodynamics or SPH [145, 146]. These sub-particle discretization approaches are suitable for fundamental research.

Examples also exist of cases where DEM has been coupled with heat flow. Within the context of geomechanics, however, work is more limited. Examples of thermal coupling can be found in the work of Vargas and McCarthy [147], Feng et al. [148], and Zhao et al. [149]. Oñate and Rojek [150] used a combined DEM-FEM approach to model geomechanics problems involving substantial thermal effects, such as a tool cutting through a rock.

Coupling of chemistry with DEM has been employed to model physico-chemical interactions in cohesive clays [151, 152]. More recently, Jiang et al. [153] used DEM to model micro-mechanics of chemical weathering in rocks. Coupling of biological processes was undertaken by Chen et al. [154] where DEM was used to simulate behavior of mine tailings stabilized with a biopolymer.

It is worth mentioning that DEM is largely used to model behavior of coarse cohesionless geomaterials such as rocks and sands. Fine-grained particles such as clays have a tendency to aggregate and disperse owing to the molecular scale of their interactions, and are not amenable to accurate characterization using DEM. A promising approach to model clay particles at the discrete scale involves the use of molecular dynamics [155–158, 174].

3.5 Role of Imaging

With the advent of high-resolution X-ray imaging capabilities, it has become possible to visualize the soil microstructure as well as grain-scale kinematics in great detail. Such data is crucial when it comes to validating the aforementioned DEM models which can in turn inspire the next generation of continuum models, as well as facilitate development of multiscale modeling schemes (as described in the next section).

A variety of techniques exist to conduct high-resolution imaging. Some examples include X-ray computed tomography [159–161], X-ray micro-tomography [162, 160, 163–167], and focused ion beam/scanning electron microscopy [164, 168, 169]. It must be noted that high-resolution imaging typically has a limited field of view [170], which restricts its applicability to small sample sizes. To obtain high-resolution images for large samples, a new technique of imaging called "Multiscale Imaging" has emerged which employs statistical methods to enhance the field of view [170–177]. Multiscale imaging employs statistics to generate representative realizations of the microstructure.

In cases where it is of interest of track fluid flow through geomaterials (e.g. hydraulic fracture), neutron imaging can be deployed. X-ray imaging cannot capture fluid flow since it is only sensitive to dense materials. Neutrons, on the other hand, can detect hydrogen atoms which enables neutron radiography to track fluid flow [178–181].

3.6 Some State-of-the-Art Codes for DEM

A number of open-source and commercial codes exist to simulate DEM. Some open-source options are LMGC90 [182], ESyS Particle [183], Oval [184], Mercury-DPM [185], YADE [186], and LIGGGHTS [187]. Commercial options involve PFC by Itasca [188], Chute Maven, EDEM, ELFEN, PASSAGE®, Bulk Flow Analyst™, and Rocky®.

4 Multiscale Modeling

As described previously, continuum methods are quite versatile and possess the ability of capturing some of the main features of soil behavior. In particular, the finite element method, equipped with elastoplastic models, has become a standard of practice and has been used to solve boundary-value problems at the engineering scale. However, continuum methods present several shortcomings, perhaps the most significant one has to do with constitutive models having numerous parameters (10–15 in many cases) without having a clear physical meaning or processes for calibration. This has made calibration/prediction exercises using continuum models difficult. At a more fundamental level, continuum methods have difficulty coping with discontinuities and failures such as shear bands, which are a classic mode of failure in geomaterials. For instance, the thickness and location of shear bands predicted by continuum models is often dependent on the scheme of discretization [189–191]. On the other hand, discrete methods such as the discrete element method (DEM) have been predicated on the premise that soils are discrete in nature and that their complex behavior emerges from relatively simple interactions at the grain scale. While this is true in principle, in practice DEM has struggled to have the level of accuracy boasted by continuum methods, for example, in capturing triaxial compression tests. This has been attributed to classic DEM's simplistic rendering of particle shape. Although progress has been made in capturing shape more faithfully (as described in the previous section), such modeling efforts tend to be the exception, not the norm. At the same time, DEM is more computationally demanding than its continuum counterparts (e.g., FEM) and hence can only resolve problems in the order of millions of particles at the time of this writing, even after exploiting parallel computation. The appeal of DEM is its simplicity and natural way of capturing granular soil behavior from its fundamental scale. Hence, a new line of research has emerged with the idea of combining continuum methods (e.g., FEM) with DEM. These multiscale approaches can be broadly divided into concurrent, semi-concurrent and hierarchical approaches [192].

4.1 Concurrent Approaches

Concurrent approaches deal with replacing portions of the continuum domain with DEM. Hence, the domain is discretized concurrently using FEM and DEM, typically deploying DEM in areas of the domain where interesting physics are happening—for example, where shear bands are occurring. Perhaps the most salient example of concurrent approaches in granular materials has been developed by Regueiro at CU Boulder [193], who used this approach to model interfacial mechanics between granular materials and deformable solid bodies. Another example involves concurrent coupling between FDM and DEM [194] to model dynamic problems. Concurrent methods offer the great advantage of deploying DEM into areas where obtaining a

solution with FEM would be difficult or impossible. The disadvantage of concurrent methods is that they necessitate significant treatment of the boundary between FEM and DEM and also need special instructions for how to grow or move the portion of the domain allocated to DEM.

4.2 Semi-concurrent Approaches

Semi-concurrent multiscale approaches (sometimes referred to as hierarchical in the literature) do not replace portions of the continuum domain with DEM. On the contrary, the entire domain continues to be resolved using continuum techniques such as FEM but resorting to DEM to enhance the constitutive description of the material, typically at the material point or Gauss integration point. Hence, semi-concurrent approaches partially or completely bypass the material subroutine and replace it with a DEM calculation. The approach is called semi-concurrent in the sense that both scales are active, with FEM typically passing an incremental deformation down to a DEM unit cell and, in return, the DEM unit cell passing back a corresponding incremental stress. Therefore, semi-concurrent approaches enjoy an exchange of information between scales, which is essential in granular materials since they are stress/deformation path-dependent. Within the semi-concurrent approach, there are at least two philosophical methods. The first one can be labeled as the "purist" approach which has also been called the FEM $\times$ DEM approach where DEM serves as a direct material subroutine to the FEM calculation. So, at every Gauss point of the FEM calculation and at every time step, a DEM calculation is performed given an incremental strain obtained from the FEM calculation. The outcome of the DEM calculation is a corresponding incremental stress. This FEM $\times$ DEM [195–203] approach has the advantage that it completely bypasses constitutive models and obtains the entire stress response directly from the microstructure. A recent scheme even deployed MPM instead of FEM to model granular pile collapse [204]. However, the main disadvantages of the approach are that (i) convergence of these methods can be difficult due to their inability to compute consistent tangents that would guarantee smooth convergence in FEM, and (ii) the computation of the incremental stress at the DEM level is a "black box" where an incremental strain is given as input and an incremental stress is obtained as output—because no other information is extracted, not much else is learned about the material as a function of deformation.

The second flavor of semi-concurrent methods exploits the existence of very robust computational techniques for plasticity models. The idea is to replace the evolution of internal plastic variables, such as dilatancy and internal friction, and compute them directly using DEM. Hence, similar to FEM $\times$ DEM an incremental strain is passed to the DEM unit cell and an incremental response is obtained and used to update the plastic internal variables [205, 206]. This approach has the advantage that it exploits all of the computational plasticity toolkit and gives insight into the physical evolution of fundamental properties of granular materials. It has the disadvantage of its continuous dependence on plasticity models, despite deploying simple ones such

as Drucker-Prager that only need two physically-sound plastic internal variables: friction and dilatancy.

4.3 Hierarchical Methods

Along the line of the latter flavor of semi-concurrent approaches exploiting computational plasticity, there is a special class of hierarchical methods that focus on upscaling continuum plasticity parameters based on grain-scale calculations. Hence, in these hierarchical methods, there is no iteration or passing of information from the continuum scale into the grain scale and then sending information back to the continuum scale. Instead, a one-way evolution of plastic internal variables, for example, dilatancy, is obtained using grain scale simulations that may or may not correspond to strain histories experienced at different Gauss points in the continuum calculation. One limitation of these hierarchical methods is that the evolution calculated using grain-scale simulations may not reflect the strain path experienced in the continuum domain and hence produce inaccurate results. Hence, care must be taken to probe the grain scale with strain paths that are broadly compatible with those seen in the continuum calculation.

For example, Fig. 4 shows results obtained using a hierarchical approach to simulate shear bands in a sample of dense sand that was also imaged using X-ray computed tomography [129]. The grain scale simulation was performed with boundary conditions similar to those in simple shear, which has a strain history similar to that observed in shear banding. As can be seen from these results, the hierarchical calculation is able to realistically capture the response of the experiment: the macroscopic stress-strain curve, as well as the main pattern and value of strain around the shear band. These are remarkable results since they open the door to an immense opportunity afforded by multiscale techniques: they can marry the best features of each of the current methods. They can exploit the reliability and scalability of FEM while at the same time exploit the accuracy of DEM to render a superior computational approach that can have accurate results comparable to the most advanced experiments. It is expected that the next two decades will see an explosion of multiscale approaches fueled by increased computational power, more faithful grain-scale computational approaches, and more powerful imaging and probing experimental techniques that can connect the macro and microscopic processes in granular matter.

5 Conclusions

We have explicitly addressed the multiphysical and multiscale modeling of soils and have done a narrow but representative survey of the methods currently available. We showed that there are three common approaches: continuum, discrete and multiscale. Continuum mechanics is by far the most widely utilized since it has been around

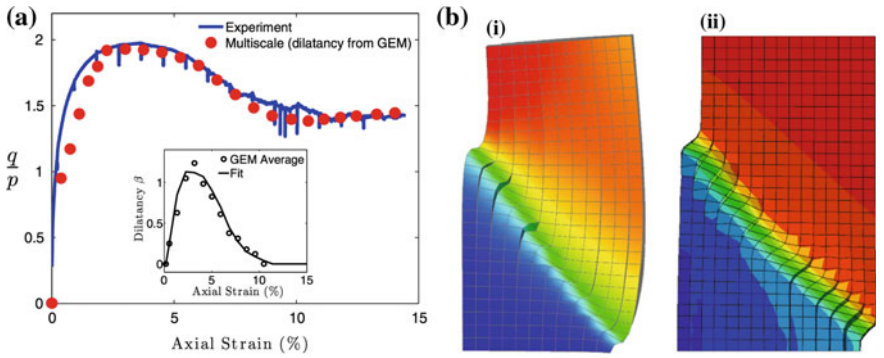

Fig. 4 Results using a hierarchical approach to simulate shear bands in a sample of dense sand that was also imaged using X-ray CT [129]. **a** Global response from multiscale computation using evolution information from GEM (inset). **b** Comparison between (i) the deformed configuration of a finite element model and (ii) the deformed shape obtained from digital image correlation (both at 12% axial strain)

much longer. Around continuum mechanics, THMC methods have been developed to explicitly cope with the multiphysical aspects of soils. Also, plasticity theories have been a central player in furnishing constitutive models that can relate deformations and stresses—key concepts in continuum theories. On the other hand, discrete methods have been introduced since the late seventies and have endeavored to explicitly represent soil behavior from the grain scale. New methods can even represent arbitrary shape and have been shown to capture macroscopic responses of soils, just like constitutive models can. To cope with the higher computational efforts associated with discrete models, multiscale techniques have been proposed to bridge the scale gap between discrete methods and continuum methods. The development of multiscale methods has been fairly successful despite the fact that these techniques are just in their infancy. Higher computational power, advanced experimental tools and, above all, grand challenges facing humanity, will push the boundaries of what is possible and will test our knowledge of the fundamentals of soil mechanics. The future looks multiphysical and multiscale.

References

1. Terzaghi, K., Peck, R.B., Mesri, G.: Soil Mechanics in Engineering Practice, 3rd edn. Wiley (1996)
2. Cundall, P.A., Strack, O.D.L.: A discrete numerical model for granular assemblies. Géotechnique **29**(1), 47–65 (1979)
3. Puzrin, A.M.: Constitutive modelling in geomechanics: introduction. Springer Science & Business Media (2012)
4. Borja, R.I.: Cam-Clay plasticity. part V: a mathematical framework for three-phase deformation and strain localization analyses of partially saturated porous media. Comput. Meth. Appl.

Mech. Eng. **193**(48–51), 5301–5338 (2004). https://doi.org/10.1016/j.cma.2003.12.067
5. Voyiadjis, G.Z., Song, C.R.: The coupled theory of mixtures in geo-mechanics with applications. Springer, Berlin, New York (2006)
6. Skempton, A.W.: The pore-pressure coefficients a and b. Géotechnique **4**(4), 143–147 (1954)
7. Bear, J.: Dynamics of fluids in porous media. Dover, New York (1988)
8. Forchheimer, P.H.: Wasserbewegung durch boden. Zeitz Ver Duetch Ing **45**, 1782–1788 (1901)
9. Firdaouss, M., Guermond, J-L., Le QuéRé, P.: Nonlinear corrections to Darcy's law at low reynolds numbers. J. Fluid Mech. **343**, 331–350. (1997). https://doi.org/10.1017/S0022112097005843
10. Adler, P.M., Malevich, A.E., Mityushev, V.V.: Nonlinear correction to Darcys law for channels with wavy walls. Acta Mech. **224**(8), 1823–1848 (2013). https://doi.org/10.1007/s00707-013-0840-3
11. Martin, G.R., Seed, H.B., Finn, W.D.L.: Fundamentals of liquefaction under cyclic loading. J. Geotech. Eng. Div. **101** (1975)
12. Byrne, P.M.: A cyclic shear-volume coupling and pore pressure model for sand. In: International Conferences on Recent Advances in Geotechnical Earthquake Engineering & Soil Dynamics (1991)
13. Andrade, J.E., Borja, R.I.: Capturing strain localization in dense sands with random density. Int. J. Numer. Meth. Eng. **67**(11), 1531–1564 (2006). https://doi.org/10.1002/nme.1673
14. Coulomb, C.A.: Essai sur une application des règles de maximis et minimis à quelques problèmes de statique relatifs à l'architecture. Mem. Div. Sav. Acad. **7**, 343–382 (1773)
15. Drucker, D.C., Prager, W.: Soil mechanics and plastic analysis or limit design. Q. Appl. Math. **10**(2), 157–165 (1952)
16. Roscoe, K.H., Schofield, A.N., Wroth, C.P.: On the yielding of soils. Géotechnique **8**(1), 22–53 (1958). https://doi.org/10.1680/geot.1958.8.1.22
17. Parry, R.H.G.: Strength and deformation of clay. Ph. D. Thesis, University of London (1956)
18. Roscoe, K.H., Schofield, A.N.: Mechanical behavior of an idealized 'wet' clay. In: Proceedings of the 3rd European Conference on Soil Mechanism, Wiesbaden, vol. 1, pp. 47–54 (1963)
19. Roscoe, K., Burland, J.B.: On the generalised stress-strain behaviour of wet clay. Eng. Plast. 535–609 (1968)
20. Been, K., Jefferies, M.G.: A state parameter for sands. Géotechnique **35**(2), 99–112 (1985)
21. Jefferies, M.G.: Nor-sand: a simple critical state model for sand. Géotechnique **43**(1), 91–103 (1993)
22. Yu, H.S.: CASM: A unified state parameter model for clay and sand. Int. J. Numer. Anal. Meth. Geomech. **22**(8), 621–653 (1998). https://doi.org/10.1002/(SICI)1096-9853
23. Kondner, R.L.: Hyperbolic stress-strain response: cohesive soils. J. Soil Mech. Found. Div. **89**(1), 115–144 (1963)
24. Ramberg, W., Osgood, W.R.: Description of stress-strain curves by three parameters. National Advisory Committee for aeronautics Technical Note (1943)
25. Puzrin, A.M., Burland, J.B.: A logarithmic stress–strain function for rocks and soils. Géotechnique ue **46**(1), 157–164 (1996). https://doi.org/10.1680/geot.1996.46.1.157
26. Wood, D.M.: Soil behaviour and critical state soil mechanics. Cambridge university press, Cambridge, New York (1990)
27. Kolymbas, D.: A rate-dependent constitutive equation for soils. Mech. Res. Commun. **4**(6), 367–372 (1977). https://doi.org/10.1016/0093-6413(77)90056-8
28. Darve, F., Labanieh, S.: Incremental constitutive law for sands and clays: simulations of monotonic and cyclic tests. Int. J. Numer. Anal. Meth. Geomech. **6**(2), 243–275 (1982). https://doi.org/10.1002/nag.1610060209
29. Kolymbas, D.: An outline of hypoplasticity. Arch. Appl. Mech. **61**(3), 143–151 (1991)
30. Desrues, J., Chambon, R.: A new rate type constitutive model for geomaterials: Cloe. In: Modern Approaches to Plasticity, pp. 309–324. Elsevier (1993)
31. Gudehus, G.: A comprehensive constitutive equation for granular materials. Soils Found. **36**(1), 1–12 (1996). https://doi.org/10.3208/sandf.36.1

32. Kolymbas, D.: Constitutive modelling of granular materials. Springer, Berlin, Heidelberg (2013)
33. Ziegler, H.: An introduction to thermomechanics. North-Holland Publishing Company (1977)
34. Ziegler, H., Wehrli, C.: The derivation of constitutive relations from the free energy and the dissipation function. In: Advances in applied mechanics, pp. 183–238. Elsevier (1987)
35. Houlsby, G.T.: Study of plasticity theories and their applicability to soils. Ph.D. thesis, University of Cambridge (1981)
36. Houlsby, G.T.: A derivation of the small-strain incremental theory of plasticity from thermomechanics. In: Deformation and failure of granular materials. IUTAM symposium, Delft, pp. 109–118. Balkema (1982)
37. Collins, I.F., Houlsby, G.T.: Application of thermomechanical principles to the modelling of geotechnical materials. In: Proceedings of the Royal Society of London A: Mathematical, Physical and Engineering Sciences, vol. 453, pp. 1975–2001. The Royal Society (1997). https://doi.org/10.1098/rspa.1997.0107
38. Houlsby, G.T., Puzrin, A.M.: A thermomechanical framework for constitutive models for rate-independent dissipative materials. Int. J. Plast **16**(9), 1017–1047 (2000). https://doi.org/10.1016/S0749-6419(99)00073-X
39. Houlsby, G.T., Puzrin, A.M.: Principles of hyperplasticity: an approach to plasticity theory based on thermodynamic principles. Springer-Verlag, London Limited (2006)
40. Collins, I.F., Kelly, P.A.: A thermomechanical analysis of a family of soil models. Géotechnique **52**(7), 507–518 (2002). https://doi.org/10.1680/geot.2002.52.7.507
41. Yu, H-S.: Plasticity and geotechnics. Springer-Verlag, New York (2006)
42. Mrŏz, Z., Norris, V.A., Zienkiewicz, O.C.: An anisotropic hardening model for soils and its application to cyclic loading. Int. J. Numer. Anal. Meth. Geomech. **2**(3), 203–221 (1978). https://doi.org/10.1002/nag.1610020303
43. Prevost, J.H.: Plasticity theory for soil stress-strain behavior. J. Eng. Mech. Div. **104**(5), 1177–1194 (1978)
44. Dafalias, Y.F., Herrmann, L.R.: Bounding surface plasticity. ii: Application to isotropic cohesive soils. J. Eng. Mech. **112**(12), 1263–1291 (1986)
45. Dafalias, Y.F., Manzari, M.T.: Simple plasticity sand model accounting for fabric change effects. J. Eng. Mech. **130**(6), 622–634 (2004)
46. Elgamal, A., Yang, Z., Parra, E.: Computational modeling of cyclic mobility and post-liquefaction site response. Soil Dyn. Earthquake Eng. **22**(4), 259–271 (2002). https://doi.org/10.1016/S0267-7261(02)00022-2
47. Li, X.S., Dafalias, Y.F.: Anisotropic critical state theory: role of fabric. J. Eng. Mech. **138**(3), 263–275 (2012). https://doi.org/10.1061/(ASCE)EM.1943-7889.0000324
48. Dafalias, Y.F., Taiebat, M.: Sanisand-z: zero elastic range sand plasticity model. Géotechnique **66**(12), 999–1013 (2016). https://doi.org/10.1680/jgeot.15.P.271
49. Prevost, J.H.: A simple plasticity theory for frictional cohesionless soils. Int. J. Soil Dyn. Earthquake Eng. **4**(1), 9–17 (1985). https://doi.org/10.1016/0261-7277(85)90030-0
50. Borja, R.I.: Cam-clay plasticity, part II: implicit integration of constitutive equation based on a nonlinear elastic stress predictor. Comput. Meth. Appl. Mech. Eng. **88**(2), 225–240 (1991)
51. Manzari, M.T., Nour, M.A.: Significance of soil dilatancy in slope stability analysis. J. Geotech. Geoenviron. Eng. **126**(1), 75–80 (2000)
52. Swan, C.C., Seo, Y-K.: Limit state analysis of earthen slopes using dual continuum/fem approaches. Int. J. Numer. Anal. Meth. Geomech. **23**(12), 1359–1371 (1999)
53. Mroueh, H., Shahrour, I.: A full 3-D finite element analysis of tunneling–adjacent structures interaction. Comput. Geotech. **30**(3), 245–253 (2003). https://doi.org/10.1016/S0266-352X(02)00047-2
54. Lee, J.S, Pande, G.N.: Analysis of stone-column reinforced foundations. Int. J. Numer. Anal. Meth. Geomech. **22**(12), 1001–1020 (1998)
55. Oka, F., Yashima, A., Shibata, T., Kato, M., Uzuoka, R.: FEM-FDM coupled liquefaction analysis of a porous soil using an elasto-plastic model. Appl. Sci. Res. **52**(3), 209–245 (1994). https://doi.org/10.1007/BF00853951

56. Gallipoli, D., Wheeler, S.J, Karstunen, M.: Modelling the variation of degree of saturation in a deformable unsaturated soil. Géotechnique **53**(1), 105–112 (2003). https://doi.org/10.1007/BF00853951
57. Taiebat, M., Shahir, H., Pak, A.: Study of pore pressure variation during liquefaction using two constitutive models for sand. Soil Dyn. Earthquake Eng. **27**(1), 60–72 (2007). https://doi.org/10.1016/j.soildyn.2006.03.004
58. Andrade, J.E., Borja, R.I.: Modeling deformation banding in dense and loose fluid-saturated sands. Finite Elem. Anal. Des. **43**(5), 361–383 (2007). https://doi.org/10.1016/j.finel.2006.11.012
59. Mohammadnejad, T., Andrade, J.E.: Flow liquefaction instability prediction using finite elements. Acta Geotech. **10**(1), 83–100 (2015). https://doi.org/10.1007/s11440-014-0342-z
60. Mital, U., Mohammadnejad, T., Andrade, J.E.: Flow liquefaction instability as a mechanism for lower end of liquefaction charts. J. Geotech. Geoenviron. Eng. **143**(9), 04017065 (2017). https://doi.org/10.1061/(ASCE)GT.1943-5606.0001752
61. Koliji, A., Lehmann, P., Vulliet, L., Laloui, L., Carminati, A., Vontobel, P., Hassanein, R.: Assessment of structural evolution of aggregated soil using neutron tomography. Water Resour. Res. **44**(5) (2008). https://doi.org/10.1029/2007WR006297
62. Anagnostopoulos, A.G., Kalteziotis, N., Tsiambaos, G.K., Kavvadas, M.: Geotechnical properties of the Corinth Canal marls. Geotech. Geol. Eng. **9**(1), 1–26 (1991). https://doi.org/10.1007/BF00880981
63. Koliji, A., Vulliet, L., Laloui, L.: Structural characterization of unsaturated aggregated soil. Can. Geotech. J. **47**(3), 297–311 (2010). https://doi.org/10.1139/T09-089
64. Koliji, A., Laloui, L., Vulliet, L.: Constitutive modeling of unsaturated aggregated soils. Int. J. Numer. Anal. Meth. Geomech. **34**(17), 1846–1876 (2010). https://doi.org/10.1002/nag.888
65. Khalili, N., Valliappan, S.: Unified theory of flow and deformation in double porous media. Eur. J. Mech. A. Solids **15**(2), 321–336 (1996)
66. Callari, C., Federico, F.: Fem validation of a double porosity elastic model for consolidation of structurally complex clayey soils. Int. J. Numer. Anal. Meth. Geomech. **24**(4), 367–402 (2000)
67. Pao, W.K.S., Lewis, R.W.: Three-dimensional finite element simulation of three-phase flow in a deforming fissured reservoir. Comput. Methods Appl. Mech. Eng. **191**(23–24), 2631–2659 (2002). https://doi.org/10.1016/S0045-7825(01)00420-0
68. Khalili, N., Witt, R., Laloui, L., Vulliet, L., Koliji, A.: Effective stress in double porous media with two immiscible fluids. Geophys. Res. Lett. **32**(15) (2005). https://doi.org/10.1029/2005GL023766
69. Borja, R.I., Choo, J.: Cam-clay plasticity, part VIII: a constitutive framework for porous materials with evolving internal structure. Comput. Methods Appl. Mech. Eng. **309**, 653–679 (2016). https://doi.org/10.1016/j.cma.2016.06.016
70. Gawin, D., Schrefler, B., Galindo, M.: Thermo-hydro-mechanical analysis of partially saturated porous materials. Eng. Comput. **13**(7), 113–143 (1996). https://doi.org/10.1108/02644409610151584
71. Gatmiri, B., Delage, P.: A formulation of fully coupled thermal–hydraulic–mechanical behaviour of saturated porous media: Numerical approach. Int. J. Numer. Anal. Meth. Geomech. **21**(3), 199–225 (1997)
72. Wu, W., Li, X., Charlier, R., Collin, F.: A thermo-hydro-mechanical constitutive model and its numerical modelling for unsaturated soils. Comput. Geotech. **31**(2), 155–167 (2004). https://doi.org/10.1016/j.compgeo.2004.02.004
73. Gens, A., Nishimura, S., Jardine, R., Olivella, S.: Thm-coupled finite element analysis of frozen soil: formulation and application. Géotechnique **59**(3), 159–171 (2009). https://doi.org/10.1680/geot.2009.59.3.159
74. Zhou, M.M., Meschke, G.: A three-phase thermo-hydro-mechanical finite element model for freezing soils. Int. J. Numer. Anal. Meth. Geomech. **37**(18), 3173–3193 (2013). https://doi.org/10.1002/nag.2184

75. Sánchez, M., Gens, A., Villar, M.V., Olivella, S.: Fully coupled thermo-hydro-mechanical double-porosity formulation for unsaturated soils. Int. J. Geomech. **16**(6), D4016,015 (2016). https://doi.org/10.1061/(ASCE)GM.1943-5622.0000728
76. Lanru, J., Xiating, F.: Numerical modeling for coupled thermo-hydro-mechanical and chemical processes (THMC) of geological media: International and Chinese experiences. Chin. J. Rock Mechan. Eng. **22**, 1704–1715 (2003)
77. Zheng, L., Samper, J., Montenegro, L., Fernandez, A.M.: A coupled THMC model of a heating and hydration laboratory experiment in unsaturated compacted FEBEX bentonite. J. Hydrol. **386**(1–4), 80–94 (2010). https://doi.org/10.1016/j.jhydrol.2010.03.009
78. Rutqvist, J., Zheng, L., Chen, F., Liu, H.H., Birkholzer, J.: Modeling of coupled thermo-hydro- mechanical processes with links to geochemistry associated with bentonite-backfilled repository tunnels in clay formations. Rock Mech. Rock Eng. **47**(1), 167–186 (2014). https://doi.org/10.1007/s00603-013-0375-x
79. Zhang, R., Winterfeld, P.H., Yin, X., Xiong, Y., Wu, Y.S.: Sequentially coupled THMC model for CO_2 geological sequestration into a 2-D heterogeneous saline aquifer. J. Nat. Gas Sci. Eng. **27**, 579–615 (2015). https://doi.org/10.1016/j.jngse.2015.09.013
80. Wu, D., Deng, T., Zhao, R.: A coupled THMC modeling application of cemented coal gangue-fly ash backfills. Constr. Build. Mater. **158**, 326–336 (2018). https://doi.org/10.1016/j.conbuildmat.2017.10.009
81. DeJong J.T., Soga K., Kavazanjian E., et al.: Biogeochemical processes and geotechnical applications: progress, opportunities and challenges. Géotechnique -London **63**, 287 (2013)
82. Belytschko, T., Black, T.: Elastic crack growth in finite elements with minimal remeshing. Int. J. Numer. Meth. Eng. **45**(5), 601–620 (1999)
83. Brinkgreve, R.B.J., Kumarswamy, S., Swolfs, W.M.: Plaxis 3D Reference Manual Anniversary Edition Version 1. Plaxis Bv, Delft (2015)
84. Itasca, F.: 3D Version 4.0 Users Manual. Minneap Itasca (2009)
85. Mazzoni, S., Mckenna, F., Scott, M.H., Fenves, G.L.: The open system for earthquake engineering simulation (OPENSEES) user command-language manual (2006)
86. Corporation, D.S.S.: Abaqus, ver6.14 Documentation 651 (2014)
87. Kolditz, O., Bauer, S., Bilke, L., Bottcher, N., Delfs, J.O., Fischer, T., Gorke, U.J., Kalbacher, T., Kosakowski, G., McDermott, C., et al.: Opengeosys: an open-source initiative for numerical simulation of thermo-hydro-mechanical/chemical (THM/C) processes in porous media. Environ. Earth Sci. **67**(2), 589–599 (2012). https://doi.org/10.1007/s12665-012-1546-x
88. UPC CODE-BRIGHT, U.: 3-D program for thermo-hydro-mechanical analysis in geological media. USER'S GUIDE (2002)
89. Guimaraes, L.D.N., Gens, A., Olivella, S.: Coupled thermo-hydro-mechanical and chemical analysis of expansive clay subjected to heating and hydration. Transp. Porous Media **66**(3), 341–372 (2007)
90. Zheng, L., Samper, J.: A coupled THMC model of FEBEX mock-up test. Phys. Chem. Earth, Parts A/B/C **33**, S486–S498 (2008)
91. Hamamatsu, P.T.: COMSOL, inc, COMSOL multiphysics reference manual, version 5.3 (2008)
92. Ladd, R.S.: Specimen preparation and liquefaction of sands. J. Geotech. Geoenviron. Eng. **100**:1180–1184 (1974)
93. Ladd, R.S.: Specimen preparation and cyclic stability of sands. J. Geotech. Geoenviron. Eng. **103**:535–547 (1977)
94. Mulilis, J.P., Arulanandan, K., Mitchell, J.K., Chan, C.K., Seed, H.B.: Effects of sample preparation on sand liquefaction. J. Geotech. Eng. Div. **103**(2), 91–108 (1977)
95. O'Sullivan, C.: Particle-based discrete element modeling: geomechanics perspective. Int. J. Geomech. **11**(6), 449–464 (2011). https://doi.org/10.1061/(ASCE)GM.1943-5622.0000024
96. Gao, Z., Zhao, J., Li, X.S., Dafalias, Y.F.: A critical state sand plasticity model accounting for fabric evolution. Int. J. Numer. Anal. Meth. Geomech. **38**(4), 370–390 (2014)
97. Tu, X., Andrade, J.E.: Criteria for static equilibrium in particulate mechanics computations. Int. J. Numer. Meth. Eng. **75**(13), 1581–1606 (2008)

98. Moreau, J.J.: Evolution problem associated with a moving convex set in a Hilbert space. J. Differ. Equ. **26**(3), 347–374 (1977)
99. Radjai, F., Richefeu, V.: Contact dynamics as a nonsmooth discrete element method. Mech. Mater. **41**(6), 715–728 (2009)
100. Lim, K-W., Krabbenhoft, K., Andrade, J.E.: On the contact treatment of non-convex particles in the granular element method. Comput. Part. Mech. **1**(3), 257–275 (2014)
101. Lim, K-W., Krabbenhoft, K., Andrade, J.E.: A contact dynamics approach to the granular element method. Comput. Methods Appl. Mech. Eng. **268**, 557–573 (2014)
102. Zhu, H.P., Zhou, Z.Y., Yang, R.Y., Yu, A.B.: Discrete particle simulation of particulate systems: theoretical developments. Chem. Eng. Sci. **62**(13), 3378–3396 (2007)
103. Rothenburg, L., Bathurst, R.J.: Analytical study of induced anisotropy in idealized granular materials. Géotechnique **39**(4), 601–614 (1989)
104. Iwashita, K., Oda, M.: Rolling resistance at contacts in simulation of shear band development by dem. J. Eng. Mech. **124**(3), 285–292 (1998)
105. Radjai, F., Wolf, D.E., Jean, M., Moreau, J.J.: Bimodal character of stress transmission in granular packings. Phys. Rev. Lett. **80**(1), 61 (1998)
106. Estrada, N., Taboada, A., Radjai, F.: Shear strength and force transmission in granular media with rolling resistance. Phys. Rev. E **78**(2), 021301 (2008)
107. Tordesillas, A.: Force chain buckling, unjamming transitions and shear banding in dense granular assemblies. Phil. Mag. **87**(32), 4987–5016 (2007)
108. Tordesillas, A., Muthuswamy, M.: On the modeling of confined buckling of force chains. J. Mech. Phys. Solids **57**(4), 706–727 (2009)
109. Darve, F., Servant, G., Laouafa, F., Khoa, H.D.V.: Failure in geomaterials: continuous and discrete analyses. Comput. Methods Appl. Mech. Eng. **193**(27–29), 3057–3085 (2004)
110. Nicot, F., Sibille, L., Donze, F., Darve, F.: From microscopic to macroscopic second-order work in granular assemblies. Mech. Mater. **39**(7), 664–684 (2007)
111. Sitharam, T.G., Vinod, J.S., Ravishankar, B.V.: Post-liquefaction undrained monotonic behavior of sands: experiments and dem simulations. Géotechnique **59**(9), 739–749 (2009)
112. Mesarovic, S.D., Padbidri, J.M., Muhunthan, B.: Micromechanics of dilatancy and critical state in granular matter. Géotechnique Lett. **2**(2), 61–66 (2012)
113. Mital, U., Andrade, J.E.: Mechanics of origin of flow liquefaction instability under proportional strain triaxial compression. Acta Geotech. **11**(5), 1015–1025 (2016). https://doi.org/10.1007/s11440-015-0430-8
114. O'Donovan, J., O'Sullivan, C., Marketos, G.: Two-dimensional discrete element modelling of bender element tests on an idealised granular material. Granular Matter **14**(6), 733–747 (2012). https://doi.org/10.1007/s10035-012-0373-9
115. O'Donovan, J., O'Sullivan, C., Marketos, G., Wood, D.: Analysis of bender element test interpretation using the discrete element method. Granular Matter **17**(2), 197–216 (2015). https://doi.org/10.1007/s10035-015-0552-6
116. Hurley, R.C., Andrade, J.E.: Friction in inertial granular flows: competition between dilation and grain-scale dissipation rates. Granular Matter **17**(3), 287–295 (2015)
117. Cho, G-C., Dodds, J., Santamarina, J.C.: Particle shape effects on packing density, stiffness, and strength: natural and crushed sands. J. Geotech. Geoenvironmental Eng. **132**(5), 591–602 (2006)
118. Andrade, J.E., Lim, K.W., Avila, C.F., Vlahinic, I.: Granular element method for computational particle mechanics. Comput. Meth. Appl. Mech. Eng. **241**, 262–274 (2012)
119. Jerves, A.X., Kawamoto, R.Y., Andrade, J.E.: Effects of grain morphology on critical state: a computational analysis. Acta Geotech. **11**(3), 493–503 (2016). https://doi.org/10.1007/s11440-015-0422-8
120. Rothenburg, L., Bathurst, R.J.: Numerical simulation of idealized granular assemblies with plane elliptical particles. Comput. Geotech. **11**(4), 315–329 (1991)
121. Lin, X., Ng, T-T.: A three-dimensional discrete element model using arrays of ellipsoids. Géotechnique **47**(2), 319–329 (1997)

122. Yan, B., Regueiro, R., Sture, S.: Three-dimensional ellipsoidal discrete element modeling of granular materials and its coupling with finite element facets. Eng. Comput. **27**(4), 519–550 (2010). https://doi.org/10.1108/02644401011044603
123. Favier, J.F., Abbaspour-Fard, M.H., Kremmer, M.: Modeling non-spherical particles using multisphere discrete elements. J. Eng. Mech. **127**(10), 971–977 (2001)
124. McDowell, G.R., Harireche, O.: Discrete element modelling of soil particle fracture. Géotechnique **52**(2), 131–135 (2002)
125. Garcia, X., Latham, J-P., Xiang, J., Harrison, J.P.: A clustered overlapping sphere algorithm to represent real particles in discrete element modelling. Géotechnique **59**(9), 779–784 (2009). https://doi.org/10.1680/geot.8.T.037
126. Li, H., McDowell, G.R.: Discrete element modelling of under sleeper pads using a box test. Granular Matter **20**(2), 26 (2018). https://doi.org/10.1007/s10035-018-0795-0
127. Hart, R., Cundall, P.A., Lemos, J.: Formulation of a three-dimensional distinct element model part II: mechanical calculations for motion and interaction of a system composed of many polyhedral blocks. In: International Journal of Rock Mechanics and Mining Sciences & Geomechanics Abstracts, vol. 25, pp. 117–125. Elsevier (1988)
128. Nezami, E.G., Hashash, Y.M.A., Zhao, D., Ghaboussi, J.: A fast contact detection algorithm for 3-d discrete element method. Comput. Geotech. **31**(7), 575–587 (2004). https://doi.org/10.1016/j.compgeo.2004.08.002
129. Lim, K., Kawamoto, R., Andò, E., Viggiani, G., Andrade, J.E.: Multiscale characterization and modeling of granular materials through a computational mechanics avatar: a case study with experiment. Acta Geotech. **11**(2), 243–253 (2016). https://doi.org/10.1007/s11440-015-0405-9
130. Kawamoto, R., Andò, E., Viggiani, G., Andrade, J.E.: Level set discrete element method for three- dimensional computations with triaxial case study. J. Mech. Phys. Solids **91**, 1–13 (2016). https://doi.org/10.1016/j.jmps.2016.02.021
131. Kawamoto, R., Andò, E., Viggiani, G., Andrade, J.E.: All you need is shape: Predicting shear banding in sand with LS-DEM. J. Mech. Phys. Solids **111**, 375–392 (2018). https://doi.org/10.1016/j.jmps.2017.10.003
132. Lim, K-W., Andrade, J.E.: Granular element method for three-dimensional discrete element calculations. Int. J. Numer. Anal. Meth. Geomech. **38**(2), 167–188 (2013)
133. Billi, A.: Grain size distribution and thickness of breccia and gouge zones from thin (<1 m) strike-slip fault cores in limestone. J. Struct. Geol. **27**(10), 1823–1837 (2005)
134. Cheng, Y.P., Nakata, Y., Bolton, M.D.: Discrete element simulation of crushable soil. Géotechnique **53**(7), 633–641 (2003)
135. McDowell, G.R., de Bono, J.P.: On the micro mechanics of one-dimensional normal compression. Géotechnique **63**(11), 895–908 (2013)
136. O'Sullivan, C.: Particulate discrete element modelling: a geomechanics perspective. Taylor & Francis, London, New York (2011)
137. Guo, N., Zhao, J.: The signature of shear-induced anisotropy in granular media. Comput. Geotech. **47**, 1–15 (2013)
138. Calvetti, F., Nova, R.: Micromechanical approach to slope stability analysis. In: Darve F, Vardoulakis I (eds), Degradations and Instabilities in Geomaterials, pp. 235–254. Springer (2004)
139. Zeghal, M., El Shamy, U.: A continuum-discrete hydromechanical analysis of granular deposit liquefaction. Int. J. Numer. Anal. Meth. Geomech. **28**(14), 1361–1383 (2004)
140. El Shamy, U., Aydin, F.: Multiscale modeling of flood-induced piping in river levees. J. Geotech. Geoenviron. Eng. **134**(9), 1385–1398 (2008)
141. Jeyisanker, K., Gunaratne, M.: Analysis of water seepage in a pavement system using the particulate approach. Comput. Geotech. **36**(4), 641–654 (2009)
142. Cook, B.K., Noble, D.R., Williams, J.R.: A direct simulation method for particle-fluid systems. Eng. Comput. **21**(2/3/4), 151–168 (2004)
143. Galindo-Torres, S.A.: A coupled discrete element lattice boltzmann method for the simulation of fluid—solid interaction with particles of general shapes. Comput. Methods Appl. Mech. Eng. **265**, 107–119 (2013)

144. Feng, Y.T., Han, K., Owen, D.R.J.: Coupled lattice boltzmann method and discrete element modelling of particle transport in turbulent fluid flows: Computational issues. Int. J. Numer. Meth. Eng. **72**(9), 1111–1134 (2007)
145. Cleary, P.W., Prakash, M.: Discrete-element modelling and smoothed particle hydrodynamics: potential in the environmental sciences. Philos. Trans.-Royal Soc. Lond. Ser. A Math. Phy. Eng. Sci. **362**, 2003–2030 (2004)
146. Komoróczi, A., Abe, S., Urai, J.L.: Meshless numerical modeling of brittle–viscous deformation: first results on boudinage and hydrofracturing using a coupling of discrete element method (DEM) and smoothed particle hydrodynamics (SPH). Comput. Geosci. **17**(2), 373–390 (2013). https://doi.org/10.1007/s10596-012-9335-x
147. Vargas, W.L., McCarthy, J.J.: Thermal expansion effects and heat conduction in granular materials. Phys. Rev. E **76**(4), 041,301 (2007). https://doi.org/10.1103/PhysRevE.76.041301
148. Feng, Y.T., Han, K., Li, C.F., Owen, D.R.J.: Discrete thermal element modelling of heat conduction in particle systems: Basic formulations. J. Comput. Phys. **227**(10), 5072–5089 (2008). https://doi.org/10.1016/j.jcp.2008.01.031
149. Zhao, S., Evans, T.M., Zhou, X., Zhou, S.: Discrete element method investigation on thermally-induced shakedown of granular materials. Granular Matter **19**(1), 11 (2017). https://doi.org/10.1007/s10035-016-0690-5
150. Oñate, E., Rojek, J.: Combination of discrete element and finite element methods for dynamic analysis of geomechanics problems. Comput. Methods Appl. Mech. Eng. **193**(27–29), 3087–3128 (2004). https://doi.org/10.1016/j.cma.2003.12.056
151. Anandarajah, A.: Discrete-element method for simulating behavior of cohesive soil. J. Geotech. Eng. **120**(9), 1593–1613 (1994)
152. Yao, M., Anandarajah, A.: Three-dimensional discrete element method of analysis of clays. J. Eng. Mech. **129**(6), 585–596 (2003)
153. Jiang, M., Liao, Z., Zhang, N., Jianfud, S.: Discrete element analysis of chemical weathering on rock. Eur. J. Environ. Civil Eng. **19**(sup1), s15–s28 (2015). https://doi.org/10.1080/19648189.2015.1064617
154. Chen, R., Ding, X., Zhang, L., Xie, Y., Lai, H.: Discrete element simulation of mine tailings stabilized with biopolymer. Environ. Earth Sci. **76**(22), 772 (2017). https://doi.org/10.1007/s12665-017-7118-3
155. Teppen, B.J., Rasmussen, K., Bertsch, P.M., Miller, D.M., Schafer, L.: Molecular dynamics modeling of clay minerals. 1. gibbsite, kaolinite, pyrophyllite, and beidellite. J. Phys. Chem. B **101**(9), 1579–1587 (1997). https://doi.org/10.1021/jp961577z
156. Ebrahimi, D., Pellenq, R.J-M., Whittle, A.J.: Nanoscale elastic properties of montmorillonite upon water adsorption. Langmuir **28**(49), 16855–16863 (2012). https://doi.org/10.1021/la302997g
157. Ebrahimi, D., Whittle, A.J., Pellenq, R.J-M.: Mesoscale properties of clay aggregates from potential of mean force representation of interactions between nanoplatelets. J. Chem. Phys. **140**(15), 154309 (2014). https://doi.org/10.1063/1.4870932
158. Ebrahimi, D., Pellenq, R.J-M., Whittle, A.J.: Mesoscale simulation of clay aggregate formation and mechanical properties. Granular Matter **18**, 49 (2016). https://doi.org/10.1007/s10035-016-0655-8
159. Lenoir, N., Bornert, M., Desrues, J., Besuelle, P., Viggiani, G.: Volumetric digital image correlation applied to X-ray microtomography images from triaxial compression tests on argillaceous rock. Strain **43**(3), 193–205 (2007). https://doi.org/10.1111/j.1475-1305.2007.00348.x
160. Josh, M., Esteban, L., Delle Piane, C., Sarout, J., Dewhurst, D., Clennell, M.: Laboratory characterization of shale properties. J. Petrol. Sci. Eng. **88**, 107–124 (2012). https://doi.org/10.1016/j.petrol.2012.01.023
161. Alikarami, R., Andò, E., Gkiousas-Kapnisis, M., Torabi, A., Viggiani, G.: Strain localisation and grain breakage in sand under shearing at high mean stress: insights from in situ X-ray tomography. Acta Geotech. **10**(1), 15–30 (2015). https://doi.org/10.1007/s11440-014-0364-6

162. Arns, C.H., Bauget, F., Limaye, A., Sakellariou, A., Senden, T., Sheppard, A., Sok, R.M., Pinczewski, V., Bakke, S., Berge, L.I., et al.: Pore scale characterization of carbonates using X-ray microtomography. SPE Journal **10**(04), 475–484 (2005). https://doi.org/10.2118/90368-PA
163. Wildenschild, D., Sheppard, A.P.: X-ray imaging and analysis techniques for quantifying pore-scale structure and processes in subsurface porous medium systems. Adv. Water Resour. **51**, 217–246 (2013). https://doi.org/10.1016/j.advwatres.2012.07.018
164. Hemes, S., Desbois, G., Urai, J.L., Schroppel, B., Schwarz, J.O.: Multi-scale characterization of porosity in boom clay (hades-level, mol, Belgium) using a combination of x-ray μ-ct, 2d bib-sem and fib-sem tomography. Microporous Mesoporous Mater. **208**, 1–20 (2015). https://doi.org/10.1016/j.micromeso.2015.01.022
165. Tatone, B.S.A., Grasselli, G.: Characterization of the effect of normal load on the discontinuity morphology in direct shear specimens using X-ray micro-CT. Acta Geotech. **10**(1), 31–54 (2015). https://doi.org/10.1007/s11440-014-0320-5
166. Druckrey, A.M., Alshibli, K.A.: 3d finite element modeling of sand particle fracture based on in situ X-ray synchrotron imaging. Int. J. Numer. Anal. Meth. Geomech. **40**(1), 105–116 (2016). https://doi.org/10.1002/nag.2396
167. Zhou, B., Wang, J.: Generation of a realistic 3d sand assembly using x-ray micro-computed tomography and spherical harmonic-based principal component analysis. Int. J. Numer. Anal. Meth. Geomech. **41**(1), 93–109 (2017). https://doi.org/10.1002/nag.2548
168. Curtis, M.E., Sondergeld, C.H., Ambrose, R.J., Rai, C.S.: Microstructural investigation of gas shales in two and three dimensions using nanometer-scale resolution imaging microstructure of gas shales. AAPG Bull. **96**(4), 665–677 (2012). https://doi.org/10.1306/08151110188
169. Bennett, K.C., Berla, L.A., Nix, W.D., Borja, R.I.: Instrumented nanoindentation and 3d mechanistic modeling of a shale at multiple scales. Acta Geotech. **10**(1), 1–14 (2015). https://doi.org/10.1007/s11440-014-0363-7
170. Semnani, S.J., Borja, R.I.: Quantifying the heterogeneity of shale through statistical combination of imaging across scales. Acta Geotech. **12**(6), 1193–1205 (2017). https://doi.org/10.1007/s11440-017-0576-7
171. Efros, A.A., Freeman, W.T.: Image quilting for texture synthesis and transfer. In: Proceedings of the 28th Annual Conference on Computer Graphics and Interactive Techniques, pp. 341–346. ACM (2001)
172. Strebelle, S.: Conditional simulation of complex geological structures using multiple-point statistics. Math. Geol. **34**(1), 1–21 (2002). https://doi.org/10.1023/A:1014009426274
173. Okabe, H., Blunt, M.J.: Pore space reconstruction using multiple-point statistics. J. Petrol. Sci. Eng. **46**(1–2), 121–137 (2005). https://doi.org/10.1016/j.petrol.2004.08.002
174. Hu, L.Y., Chugunova, T.: Multiple-point geostatistics for modeling subsurface heterogeneity: A comprehensive review. Water Resour. Res. 44(11) (2008). https://doi.org/10.1029/2008WR006993
175. Zhang, T., Lu, D., Li, D.: Porous media reconstruction using a cross-section image and multiple- point geostatistics. In: Advanced Computer Control, 2009. ICACC'09. International Conference on, pp. 24–29. IEEE (2009)
176. Mariethoz, G., Renard, P., Straubhaar, J.: The direct sampling method to perform multiple-point geostatistical simulations. Water Resour. Res. **46**(11) (2010). https://doi.org/10.1029/2008WR007621
177. Zhang, T., Du, Y., Huang, T., Li, X.: Reconstruction of porous media using multiple-point statistics with data conditioning. Stoch. Env. Res. Risk Assess. **29**, 727–738 (2015). https://doi.org/10.1007/s00477-014-0947-7
178. Hassanein, R., Meyer, H.O., Carminati, A., Estermann, M., Lehmann, E., Vontobel, P.: Investigation of water imbibition in porous stone by thermal neutron radiography. J. Phys. D Appl. Phys. **39**(19), 4284 (2006). https://doi.org/10.1088/0022-3727/39/19/023
179. Kim, F.H., Penumadu, D., Gregor, J., Kardjilov, N., Manke, I.: High-resolution neutron and x-ray imaging of granular materials. J. Geotech. Geoenviron. Eng. **139**(5), 715–723 (2013). https://doi.org/10.1061/(ASCE)GT.1943-5606.0000809

180. Perfect, E., Cheng, C-L., Kang, M., Bilheux, H., Lamanna, J., Gragg, M., Wright, D.: Neutron imaging of hydrogen-rich fluids in geomaterials and engineered porous media: a review. Earth-Sci. Rev. **129**, 120–135 (2014)
181. Kim, F.H., Penumadu, D., Kardjilov, N., Manke, I.: High-resolution X-ray and neutron computed to- mography of partially saturated granular materials subjected to projectile penetration. Int. J. Impact Eng. **89**, 72–82 (2016). https://doi.org/10.1016/j.ijimpeng.2015.11.008
182. Dubois, F., Jean, M., Renouf, M., et al.: LMGC90 10e colloque national en calcul des structures. p Clé USB (2011)
183. Weatherley, D., Boros, V., Hancock, W.: Esys-particle tutorial and users guide version 2.1. Earth Systems Science Computational Centre, The University of Queensland (2011)
184. Kuhn, M.R.: Smooth convex three-dimensional particle for the discrete-element method. J. Eng. Mech. **129**(5), 539–547 (2003)
185. Thornton, A.R., Krijgsman, D., Fransen, R.H.A., Briones, S.G., Tunuguntla, D.R., te Voortwis, A., Luding, S., Bokhove, O., Weinhart, T.: Mercury-DPM: fast particle simulations in complex geometries. EnginSoft Newslett Simul. Based Eng. Sci. **10**(1), 48–53 (2013)
186. Kozicki, J., Donzé, F.V.: Yade-open dem: an open-source software using a discrete element method to simulate granular material. Eng. Comput. **26**(7), 786–805 (2009)
187. Kloss, C., Goniva, C.: Liggghts–open source discrete element simulations of granular materials based on lammps. In: Supplemental Proceedings. John Wiley & Sons, Inc., Hoboken, NJ, USA, **2**, 781–788 (2011)
188. Itasca, C.: Pfc (particle flow code in 2 and 3 dimensions), version 5.0 [User's manual]. Minneapolis (2014)
189. Ortiz, M., Leroy, Y., Needleman, A.: A finite element method for localized failure analysis. Comput. Methods Appl. Mech. Eng. **61**(2), 189–214 (1987). https://doi.org/10.1016/0045-7825(87)90004-1
190. Belytschko, T., Fish, J., Engelmann, B.E.: A finite element with embedded localization zones. Comput. Meth. Appl. Mech. Eng. **70**(1), 59–89 (1988). https://doi.org/10.1016/0045-7825(88)90180-6
191. Lin, J., Wu, W., Borja, R.I.: Micropolar hypoplasticity for persistent shear band in heterogeneous granular materials. Comput. Methods Appl. Mech. Eng. **289**, 24–43 (2015). https://doi.org/10.1016/j.cma.2015.02.005
192. Xu, M., Gracie, R., Belytschko, T.: Concurrent coupling of atomistic and continuum models. Multiscale Methods: Bridging the Scales in Science and Engineering, pp. 93–133 (2010)
193. Regueiro, R.A., Yan, B.: Concurrent multiscale computational modeling for dense dry granular materials interfacing deformable solid bodies. In: Wan R, Alsaleh, M., Labuz, J. (eds.), Bifurcations, Instabilities and Degradations in Geomaterials, pp. 251–273. Springer (2011)
194. Li, M., Yu, H., Wang, J., Xia, X., Chen, J.: A multiscale coupling approach between discrete element method and finite difference method for dynamic analysis. Int. J. Numer. Meth. Eng. **102**(1), 1–21 (2015). https://doi.org/10.1002/nme.4771
195. Nguyen, T.K., Combe, G., Caillerie, D., Desrues, J.: FEM $\times$ DEM modelling of cohesive granular materials: numerical homogenization and multi-scale simulations. Acta Geophys. **62**(5), 1109–1126 (2014). https://doi.org/10.2478/s11600-014-0228-3
196. Guo, N., Zhao, J.: A coupled fem/dem approach for hierarchical multiscale modelling of granular media. Int. J. Numer. Meth. Eng. **99**(11), 789–818 (2014). https://doi.org/10.1002/nme.4702
197. Guo, N., Zhao, J.: 3D multiscale modeling of strain localization in granular media. Comput. Geotech. **80**, 360–372 (2016). https://doi.org/10.1016/j.compgeo.2016.01.020
198. Guo, N., Zhao, J.: Multiscale insights into classical geomechanics problems. Int. J. Numer. Anal. Meth. Geomech. **40**(3), 367–390 (2016). https://doi.org/10.1002/nag.2406
199. Liu, Y., Sun, W., Yuan, Z., Fish, J.: A nonlocal multiscale discrete-continuum model for predicting mechanical behavior of granular materials. Int. J. Numer. Meth. Eng. **106**(2), 129–160 (2016). https://doi.org/10.1002/nme.5139
200. Cheng, H., Yamamoto, H., Guo, N., Huang, H.: A simple multiscale model for granular soils with geosynthetic inclusion. In: Li, X., Feng, Y., Mustoe, G. (eds.), International Conference on Discrete Element Methods, pp. 445–453. Springer (2017)

201. Zhao, J.: Hierarchical multiscale modeling of strain localization in granular materials: A condensed overview and perspectives. In: Papamichos, E., Papanastasiou, P., Pas-ternak, E., Dyskin, A. (eds.), International Workshop on Bifurcation and Degradation in Geomaterials, pp. 349–359. Springer (2017)
202. Wu, H., Guo, N., Zhao, J.: Multiscale modeling and analysis of compaction bands in high-porosity sandstones. Acta Geotech. **13**(3), 575–599 (2017). https://doi.org/10.1007/s11440-017-0560-2
203. Argilaga, A., Desrues, J., Pont, S.D., Combe, G., Caillerie, D.: FEM × DEM multiscale modeling: model performance enhancement from newton strategy to element loop parallelization. Int. J. Numer. Meth. Eng. **114**(1), 47–65 (2018)
204. Liu, C., Sun, Q., Yang, Y.: Multi-scale modelling of granular pile collapse by using material point method and discrete element method. Procedia Eng. **175**, 29–35 (2017). https://doi.org/10.1016/j.proeng.2017.01.009
205. Andrade, J.E., Tu, X.: Multiscale framework for behavior prediction in granular media. Mech. Mater. **41**(6), 652–669 (2009). https://doi.org/10.1016/j.mechmat.2008.12.005
206. Tu, X., Andrade, J.E., Chen, Q.: Return mapping for non-smooth and multiscale elastoplasticity. Comput. Methods Appl. Mech. Eng. **198**(30–32), 2286–2296 (2009). https://doi.org/10.1016/j.cma.2009.02.014

Fundamental Research on Geochemical Processes for the Development of Resilient and Sustainable Geosystems

Krishna R. Reddy, Gretchen L. Bohnhoff, Angelica M. Palomino and Marika C. Santagata

Abstract Fundamental understanding and control of geochemical processes in soils/rock and groundwater are vital for rational design of new and innovative resilient and sustainable geosystems. Geochemical processes such as adsorption-desorption, ion-exchange, oxidation-reduction, precipitation-dissolution, complexation, acid-base reactions, volatilization, and biodegradation processes are generally interrelated and are highly dependent on the soil/rock and pore-water characteristics such as mineralogy, oxides/carbonate content, organic carbon content, pH, solution chemistry, temperature, among others. Moreover, the geochemical processes in engineered systems can be transient and reversible, drastically impacting the performance of geosystems under different anthropogenic and natural perturbations that could occur over their design life. Non-invasive, less energy-intensive, and less resource intensive strategies and technologies are increasingly being sought for rehabilitation and/or development of sustainable geosystems. Harnessing natural biological processes has been emphasized recently toward sustainable geoengineering such as bio-cementation, bioremediation, phytoremediation, among others. However, an in-depth understanding of the fundamental dynamic geochemical processes in all such cases has been lacking, and the current research should embrace and encourage such fundamental research.

K. R. Reddy (✉)
Department of Civil & Materials Engineering, University of Illinois at Chicago, 842 West Taylor Street, 60607 Chicago, IL, USA
e-mail: kreddy@uic.edu

G. L. Bohnhoff
Department of Civil & Environmental Engineering, University of Wisconsin-Platteville, 53818 Platteville, WI, USA
e-mail: bohnhoffg@uwplatt.edu

A. M. Palomino
Department of Civil & Environmental Engineering, University of Tennessee, Knoxville, USA
e-mail: apalomin@utk.edu

M. C. Santagata
Lyles School of Civil Engineering, Purdue University, West Lafayette, IN, USA
e-mail: mks@ecn.purdue.edu

N. Lu and J. K. Mitchell (eds.), *Geotechnical Fundamentals for Addressing New World Challenges*, Springer Series in Geomechanics and Geoengineering,
https://doi.org/10.1007/978-3-030-06249-1_6

Keywords Geochemistry · Resiliency · Sustainability · Geotechnical and geoenvironmental engineering · Waste containment · Bioreactor landfills · Biocovers · Geoenvironmental remediation · Tunable materials · Clay-water dispersions

1 Introduction

Global greenhouse gas emissions (GHG) and population growth are some of the major problems the world is facing today. With the rapidly increasing population comes the relentless use of resources for energy and other purposes. These global challenges come with their associated consequences namely sea-level rise, extreme weather patterns, natural hazards, increased generation of wastes, environmental pollution, depletion of natural resources, and loss of biodiversity to name a few. These problems are often worsened by the civil engineering (construction and infrastructure) industry because of the significant use of earth and natural resources. Even while civil engineers contribute to the release of GHG emissions, they have the great potential to play a critical role in reducing these emissions and waste generation by incorporating innovative yet sustainable technologies in the civil engineering projects, particularly in geotechnical and geoenvironmental projects, which often deals with earth and its environment. It is important to recognize that in order to build stable, resilient and sustainable infrastructure, it is imperative to seek interdisciplinary/multidisciplinary solutions, or smart solutions.

In recent years, such smart solutions are aimed at addressing the abovementioned global issues by developing climate-adaptive systems, adaptable or tunable materials; green chemistry and bioengineered systems, improved waste-containment systems, and innovative monitoring tools; effective and efficient use of renewable or alternate energy sources, recycling and beneficial use of waste materials. There is a major impetus to develop innovative, resilient and sustainable geosystems. However, there are several practical and research challenges associated with realizing these technologies in geotechnical and geoenvironmental applications. The fundamental basis to develop these technologies for geotechnical and geoenvironmental applications requires a thorough understanding of the geochemistry associated with the soils and their interaction with other materials (e.g., any chemical amendments, polymers, and waste materials with beneficial characteristics).

Geochemistry is the study of chemical composition and chemical reactions within soils, rocks, groundwater, as well as their interaction with other waste materials such as fly ash, scrap tires, foundry sand, slag, biochar, etc. used in combination with or in lieu of soils. In addition, understanding the geochemistry is essential to create engineered soils and geosystems that can possess targeted properties and can perform as intended in the real-world geotechnical and geoenvironmental applications. Geochemical processes can be quite complex because many reactions (sorption/desorption, acid/base reactions, precipitation/dissolution, complexation, volatilization, biodegradation, etc.) may occur within and between the constituents

of three phases of the earth's surface and subsurface (solids, liquid, and gas). These processes may be transient, in nonequilibrium, and are dependent on the environmental conditions such as moisture content, ionic strength, pH, temperature, etc [57]. The geotechnical properties of the soils (such as the shear strength) and the geoenvironmental aspects of the subsurface (such as transport and fate of the contaminants) are also dictated by the underlying geochemistry within these materials. Understanding the geochemistry allows us to engineer adaptable geo-materials and geo-systems to give them the desired properties and functions (e.g., high soil strength for structural support, effective contaminant containment/remediation). More importantly, the role of geochemistry is of utmost importance for the development of sustainable and resilient materials and geosystems to address the grand challenges of the 21st century (e.g., waste/pollution control, natural resource depletion, urban sprawl and new infrastructure demand, climate change and resiliency, etc.).

The geochemical processes in engineered systems are influenced by several geochemical factors and the changes in these controlling factors induced by different anthropogenic and natural perturbations can drastically impact the performance of geosystems over the design life of the system. Harnessing natural biological processes has been emphasized recently toward sustainable geoengineering. However, an in-depth understanding of the dynamic geochemical processes in all such cases has been lacking, and the future research agendas should embrace and encourage such fundamental research. This chapter addresses the importance of geochemistry and its interplay in the development of sustainable and resilient geosystems. In addition, some of the ongoing studies involving the geochemical aspects are briefly described, and the importance of studying the geochemistry in those systems is highlighted.

2 Geochemistry in Sustainable and Resilient Geosystems

2.1 Tunable/Adaptable Materials

It is often not likely for the soils at a site to possess the desired engineering properties needed for the execution of a geotechnical project. Thus, soil minerals, oxides/hydroxides, and organic content of the soils can greatly influence the geochemistry and, consequently, the engineering properties and behavior of the soils. For example, it is well-known that the fabric of fine-grained clay-based soils is influenced by the surrounding pore-fluid chemistry (pH, type and concentration of ions). Further, the resulting fabric impacts the engineering properties (shear strength, deformability, hydraulic conductivity) of the soil. The extent to which the soil fabric can be manipulated depends on the geochemistry of the system. The recent advances in the synthesis of tunable clay-polymer composites is an example of such effort. Clay dispersions are also being created using surfactants, polymers, colloids, and biomaterials that possess "large response function" in that they can have targeted

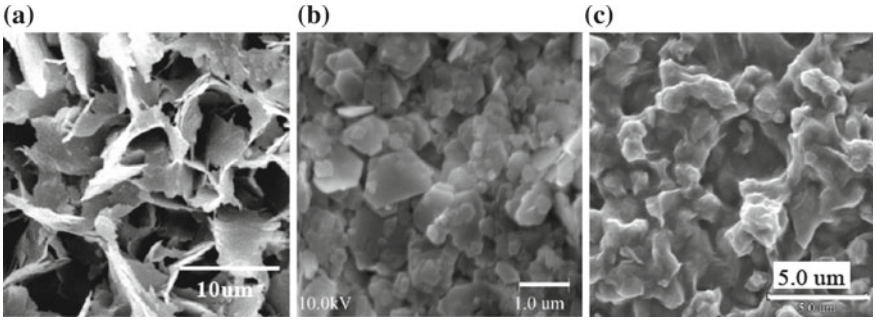

Fig. 1 Examples of mineral grains with contrasting characteristics: **a** illite [38]; **b** kaolinite, and **c** bentonite

Table 1 Properties of Clay Minerals Commonly Used in Fine-Grained Soil Research

Mineral	Theoretical formula[a]	Specific surface area[a] (m^2/g)	CEC[a] (meq/100 g)	CEC pH dependence[b]	pH_{PZNPC}
Illite	$(K,H_2O)_2(Si)_8(Al, Mg, Fe)_{4,6}O_{20}(OH)_4$	65–100	10–40	low	3.5[c]
Kaolinite	$(OH)_8Si_4Al_4O_{11}$	10–20	3–15	high	≤2–4.66[b]
Montmorillonite	$(OH)_4Si_8Al_4O_{20}$ H_2O	700–840	80–150	low	≤2–3[b]

[a][33], [b][35], [c][25], PZNPC-point of zero net proton charge

structure and behavior through manipulation of geochemical parameters. A brief overview on the research pertaining to these topics is illustrated below.

For fine-grained soils composed of clay minerals, predicting a soil's response is further complicated by changing environmental conditions as well as variation in soil mineral composition. In other words, the mineral surface geochemistry of the particles plays a critical role in the overall material properties, and thus, influences the material's response to applied chemical or mechanical forces. Control of soil properties is possible by controlling the inter-particle and interlayer spacings. In addition, the ability to modify these spacings at will aids in creating engineered adaptable materials. Figure 1 and Table 1 show examples of clay minerals and their contrasting characteristics and the macro-scale properties.

Some of the experimental findings on the amendment of Polyacrylamide (PAM), a pH responsive polymer, with the clay minerals (e.g., kaolinite, montmorillonite) as micro and macro-composites indicated that the interlayer spacing varies as a function of pH (Fig. 2). Furthermore, the polymer amendment could be used to vary the engineering properties (e.g., swell index) as required by altering the pH, thus, controlling the behavior of clay as required (see Fig. 3).

As shown in Fig. 3, the potential for responsive clay-polymer composites for use as a "smart" engineering material stems from the ability to manipulate meso-scale soil

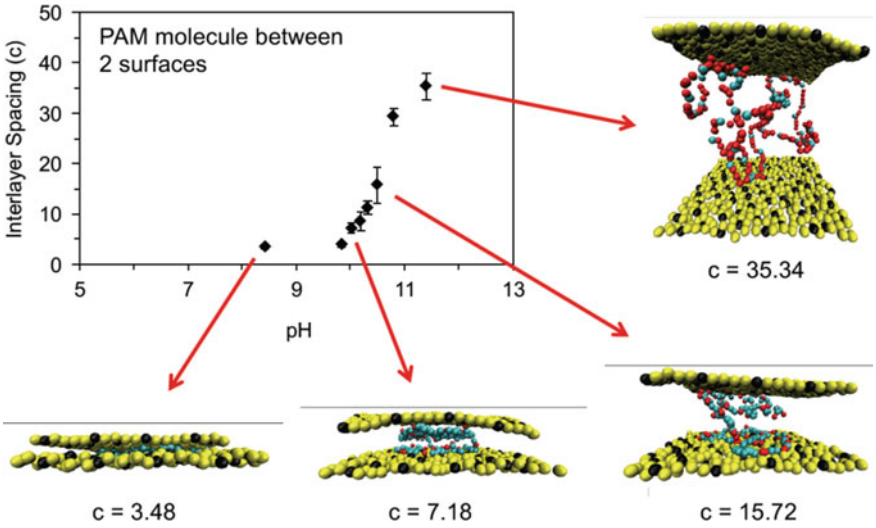

Fig. 2 Interlayer spacing (in nm) of clay particles as a function of pH [23]

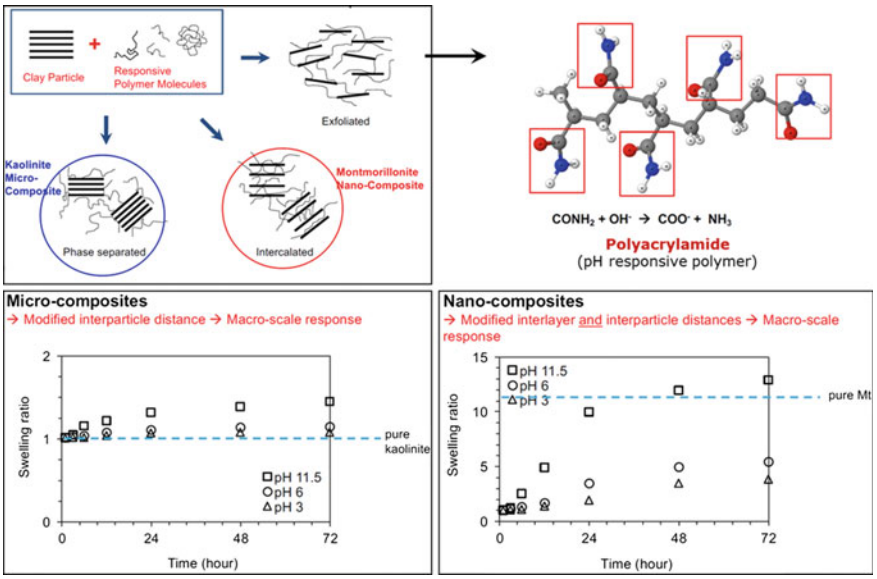

Fig. 3 Variation in swell index with pH of the polymer-amended mineral composites (after [21, 22])

properties simply by altering the chemistry of the pore fluid or some other environmental trigger. In the case of clay-PAM composites, recent studies have demonstrated controlled changes in fabric of kaolin-PAM composites with various pH and ionic concentration conditions [16]. This particle-level fabric was then shown to influence meso-scale behavior of the composite, namely the consolidation behavior [3] and undrained shear strength [17].

2.2 Clay-Water Dispersions

The clay-water dispersions, which fall within the broad class of materials referred as soft matter, have significance in several contexts within and outside the geotechnical field. The dependence of structure and rheology of clay dispersions on geochemical parameters and on polymeric additions provides the opportunity to control the properties of these complex colloid-water systems to achieve a desired response at the macro-scale. Due to their low strength and stiffness, investigation of the mechanical response of these materials must rely on techniques outside those of traditional geotechnical engineering. Specifically, rheological tests allow probing the mechanical response under a broad range of conditions and characterizing the visco-elastic properties of these materials.

It has been pointed out that one of the most interesting properties of soft matter is the fact that diverse very complex structures with unique properties can arise depending on the conditions and can evolve as a result of even subtle changes in chemistry, flow, thermal, electric or magnetic field. This is certainly the case also for clay-water dispersions, and the foundation for our ability to control their response and for their potential use in a number of applications. Within the geotechnical field, the study of these geomaterials is relevant in a range of contexts, including the behavior of dredged sediments, of surficial coastal and underwater deposits, and of tailings generated from various mining operations; the performance of drilling fluids used in reservoir exploration and trenchless technologies; grouts for soil treatment; and slurries used for cutoff walls and ground support.

The structure and properties of clay dispersions depend on molecular and colloidal interactions, which occur at the nano-scale, and which are affected by a variety of factors including the type of clay mineral(s) present, solid concentration and pore- fluid chemistry, in particular pH and type and concentration of the ions present in solution. This dependence is illustrated in the qualitative illustration of a phase diagram shown in Fig. 4 for a purified Wyoming Na-montmorillonite (see also [1, 58]).

The diagram (Fig. 4) illustrates how, for a given clay mineral and given ions in solution, the structure of the dispersion changes depending on the solid concentration and ionic strength. Specifically, the diagram distinguishes between sol, gel, glass structure and a region in which the formation of flocs leads to phase separation. Associated with the change in structure is a modification in the mechanical response.

The dependence of structure and rheology of clay dispersions on geochemical parameters provides the opportunity to control the properties of these complex

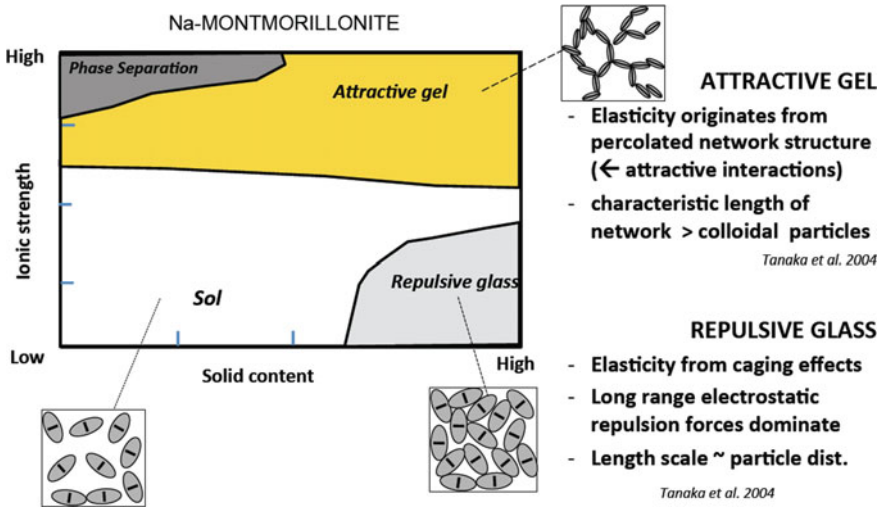

Fig. 4 Structure of clay-water dispersions

colloid-water systems to achieve a target rheological response at the macro-scale. Depending on the application and circumstance, a different structure/response may be targeted. Polymers offer additional means to modify the properties and functionality of clay-water systems, further expanding the application and significance of these materials. In some industrial applications (e.g., in paper coating), liquidity at high solids concentrations is typically desirable. This is the case also in the case of grouts, where injectability in the porous medium to be treated is often the primary concern. In the case of trenchless technology fluids, the clay dispersion may be engineered to achieve one or more of the following objectives: maximize the lubrication properties, enable the fluid to carry spoil and to seal the formation, or improve the ability of the fluid to tolerate changes in environmental condition (e.g., water salinity). Finally, when engineering tailings, the goal is generally to accelerate the separation of water and solids.

Depending on type and concentration and nature of the solvent, the presence of the polymer may produce flocculation through either bridging of particles by the polymer molecule or charge neutralization, as the polymer is adsorbed on particle surfaces of opposite charge. At higher polymer concentrations, stabilization may occur through a steric hindrance effect. The use of "additives" allows, in some cases, the ability to "tune" the response as a function of time (e.g., see use of sodium pyrophosphate to control the time-dependent rheology of bentonite presented in [50] and laponite dispersions as discussed in more detail below) and, environmental conditions.

The mechanical properties of clay dispersions fall significantly below those measured even on soils, classified as extremely soft from a traditional geotechnical engineering perspective (e.g., shear modulus, G in the Pa to kPa range). As a result, with the exception of wave-propagation measurements, traditional geomechanics

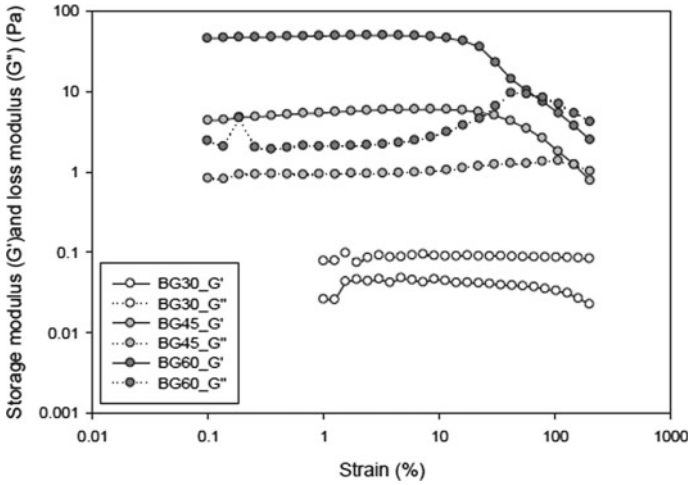

Fig. 5 Amplitude sweep results on bentonite-based drilling fluids (modified from [18])

experimental methods are, in general, not suited for the investigation of clay-water dispersions. Instead, rheometrical techniques, extensively used to date to study soft materials in other fields, represent an effective way of characterizing these geo-materials. Of particular interest are oscillatory tests (also termed dynamic tests), through which, it is possible to probe the visco-elastic response of a material. The tests involve the application of shear strain (or stress) oscillations while measuring the resulting shear stress (or strain). The storage (G') and loss (G'') moduli, which represent the elastic and viscous components of the response, are derived from these measurements.

The results of amplitude sweep tests (oscillatory tests in which the amplitude of the applied oscillation is gradually increased) conducted on bentonite dispersions of different concentrations shown in Fig. 5 illustrate the different response of a material in the sol state (3% dispersion in which $G'' > G'$ at rest, and over the entire strain range examined), and in the gel state (4.5 and 6% dispersions in which $G' \gg G''$ at rest). In the second case, the response is observed to be predominantly elastic ($G' \gg G''$) over a very large shear-strain range, with the solid-liquid transition occurring at a shear strain greater than 50% (cross-over strain where $G' = G''$). Clear patterns are identified between the measured values of the rheological parameters (G', G'', stress and strain at the cross-over point) and the characteristics (concentration and salinity) of the dispersion, allowing inferences on the architecture of the dispersion and the inter-particle interactions, which control the response (see also [10]). Oscillatory tests can also be used to probe the response as a function of frequency and time. This latter test type is especially useful to monitor state changes and structuring processes, while frequency sweeps can provide further insights into the internal architecture of these clay-water systems.

Two examples are discussed below to illustrate practical applications of the concepts outlined above. The first example pertains to dispersions of laponite, a synthetic clay with characteristics similar to natural hectorite, which can be modified through the addition of sodium pyro-phosphate decahydrate (e.g., [34]) to control the development of the rheological behavior over time. In the geotechnical field, dispersions of laponite are being considered for improving the liquefaction resistance of granular deposits (e.g., [36, 37]). Through the use of sodium pyro-phosphate decahydrate ($Na_4P_2O_7 \cdot 10H_2O$), referred to in the following as SPP, the rheology of high-laponite dispersions can be carefully "tuned" to deliver high concentrations of clay in the sand pore space, and to achieve the desired time-dependent rheological properties.

An illustration of this is provided in Fig. 6. Figure 6a shows flow curves for a 6.5% laponite dispersion with 5% SPP (by mass of the clay) obtained 15 min, 1 h, 2 h, 4 h after preparation of the dispersion, and highlights the Newtonian response with viscosity of less than 10 times that of water up to 2 h. Note that without SPP, for this clay concentration, the dispersion would gel instantaneously. With time the rheology of the dispersion shows a dramatic evolution, as shown in Fig. 6b, which presents the variation of the phase angle, δ ($tan\ \delta = G''/G'$) measured through oscillatory tests in the linear viscoelastic region. Over the three-week testing period, δ transitions from a value of 90° corresponding to a completely "liquid-like" response ($G'' \gg G'$, consistent with the Newtonian behavior observed in Fig. 6a) to values close to 0 ($G' \gg G''$, solid-like behavior corresponding to the formation of a gel). Measurements of the storage (elastic) modulus, G' after the liquid to solid transition ($\delta = 45°$ at ~ 10 h), show a continuous improvement in the mechanical response (Fig. 6c). Also, included in the figures are data for a second dispersion with 9% laponite and 7% SPP (curves with red solid circles). While with this material there is an improvement in the long term mechanical properties (Fig. 6c), the data show that this occurs at the expense of a rapid increase in the short-term viscosity (which at 15 min is ~ to the value measured on the first dispersion after 2 h—see Fig. 6a), and an earlier sol to gel transition (Fig. 6b). Overall, the data shown illustrate that design of materials for this application requires careful consideration of both short-term and long-term flow and visco-elastic properties.

Tailings are another class of clay-dispersions that have significant interest from a geotechnical perspective. This second example pertains to mature fine tailings (MFTs) generated from the processing of oil sands in the Athabasca region in Canada. MFTs are soft gel-like materials, formed by ~70% water and 30% fine clays, along with residual hydrocarbons and hydrocarbon diluents (e.g., naphtha) added to improve bitumen extraction and, in some cases, the presence of a gas phase deriving from bacterial activity in the MFT ponds. While small, the ultrafine fraction formed by sub-micron (20–300 nm) particles dispersed during extraction plays a critical role in governing the colloidal properties and thus the management of the MFTs. The slow consolidation rate of these materials has led to a growing inventory of tailing ponds, estimated, in 2011 [20] at over 800 million cubic meters. Management of MFTs represents a significant engineering and environmental challenge, a prime example of the significance of understanding and characterizing the behavior of this class of geomaterials.

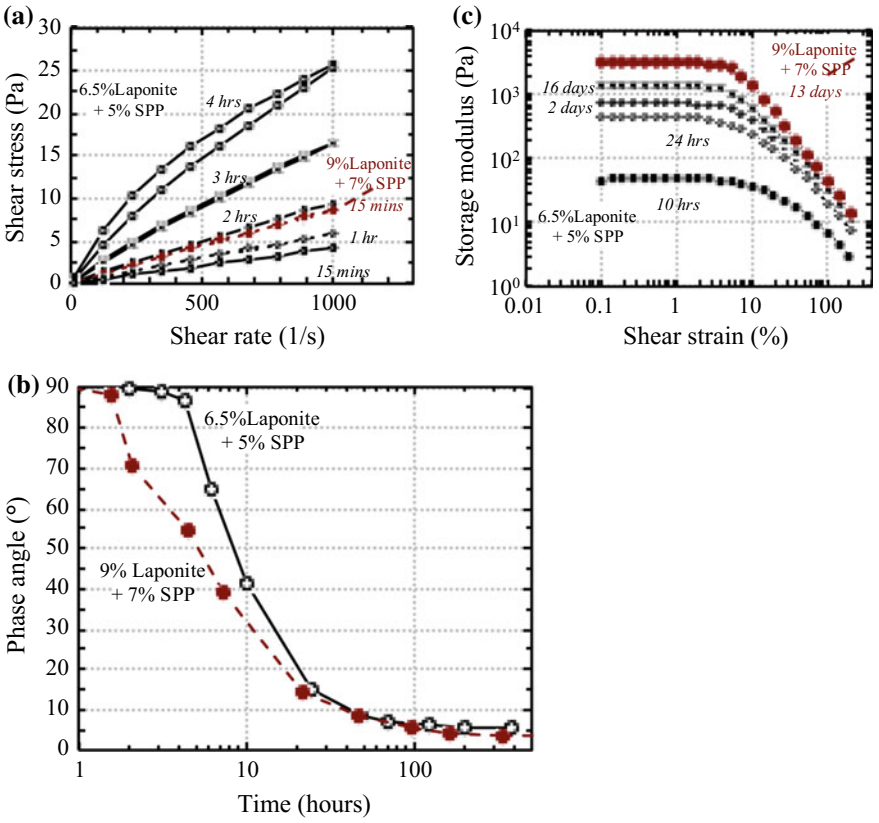

Fig. 6 Behavior of laponite dispersions modified with SPP: **a** early age viscosity; **b** sol to gel transition; and **c** increase in storage modulus of gel with time

High molecular-weight anionic polymers represent to date the most effective approach to dewatering MFTs (e.g., [11, 59]). The active sites on these polymers interact with the clay particles, binding them together, resulting in the elimination of water previously held between the particles. Rheological tests on polymer-treated and untreated MFTs (see Fig. 7) reveal that the treatment results in a modification of the "architecture" of the clay particle arrangement, which is reflected in a ten-fold increase of the cross-over strain from ~30% to over 400%. From a geotechnical perspective, the resulting geomaterial can be considered extremely sensitive, with the stiffness degrading with increased disturbance and ultimately falling below that of the untreated material at similar clay-water ratio (CWR) (Note: clay-water ratio rather than solid-water ratio or water content has been shown to provide better correlations with material behavior for this class of materials). The treatment is greatly dependent on the characteristics of the MFT, in particular the amount and the nature of organics, highlighting the critical importance of understanding the geochemistry

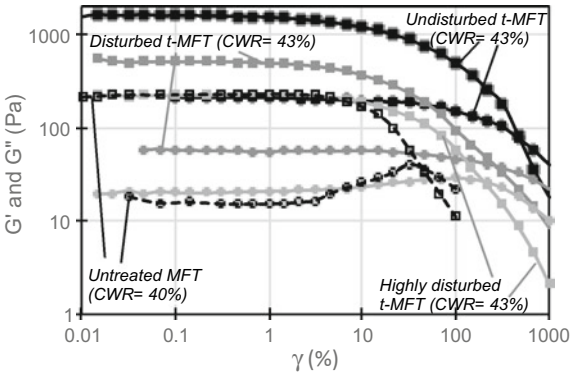

Fig. 7 G′ and G″ of untreated and polymer treated MFT showing effects of treatment and disturbance (CWR = clay-water ratio; t-MFT = polymer-treated MFT)

of these materials. Moreover, the effectiveness of the treatment is very sensitive to small changes in polymer dosage and mixing conditions, and laboratory experiments show that over mixing by as little as a few seconds negates the formation of the desired microstructure. This is obviously an enormous challenge, for a process that is intended to be implemented at a very large scale.

Polymer addition affects not only particle-particle interactions (evident also from the different degree of thixotropy observed in small-strain oscillatory tests conducted to monitor structure build-up following a disturbance stage on treated and untreated materials), but also the interactions between mineral phase and organics, as demonstrated by surface chemistry analyses, which indicate that polymeric flocculation results in some redistribution of bitumen [19]. In light of the above, there appear to be great opportunities in: applying existing knowledge from the field of soft matter to the investigation of clay-water dispersions encountered in geotechnical settings; leveraging our ability to control the structure and rheology of clay-water systems to devise new solutions to problems facing the geotechnical profession; and utilizing clays and clay minerals in new applications.

2.3 Waste Containment

Sodium bentonites (Na-bentonites) are commonly used in barriers or components of barriers in hydraulic-containment applications because of the high swell potential and correspondingly low permeability, k, to water and dilute aqueous solutions. In addition, Na-bentonite can exhibit substantial semipermeable membrane behavior for dilute concentrations of simple salts (e.g., [27, 29]). Membrane behavior and low k are beneficial in hydraulic containment applications; low k results in limited advective contaminant transport whereas, membrane behavior results in hyperfiltration, chemico-osmosis, and reduced diffusion of aqueous-phase chemicals (e.g., [55]). Examples of bentonite-based barriers include geosynthetic clay liners (GCLs), highly compacted bentonite for radioactive-waste storage, compacted soil-bentonite

mixtures for compacted clay liners and soil-bentonite backfills used in vertical cutoff walls [13–15].

However, Na-bentonite is thermodynamically unstable in most naturally occurring pore waters in earthen materials and most leachates where multivalent cations are predominant [48, 52]. These environments promote the exchange of multivalent cations for monovalent cations leading to a reduction in the osmotic swelling, an increase in the k, and a destruction in the membrane performance of the Na-bentonite. Therefore, this exchange potentially results in an increase in the advective and diffusive chemical mass flux and a decrease in hyperfiltration and chemico-osmotic counter flow [24, 28, 30].

The incompatibility of Na-bentonite with chemicals in solution has led to great interest in creating chemically modified bentonites, or CMBs (e.g., bentonites amended with organic modifiers, such as polymers) that may be more compatible with the surrounding environment. There is potential for CMBs to offer greater chemical resistance and more sustainable performance [4]. These CMBs include dense-prehydrated bentonite used in GCLs (DPH-GCL), multi-swellable bentonite (MSB), and polymer-modified bentonite such as bentonite polymer composite (BPC or BPN), Hyper-clay (HC), and many commercially available forms or contaminant-resistant clays (CRC) or polymer-treated bentonite (PTB).

To create DPH-GCLs, bentonite is prehydrated with dilute solutions of sodium carboxylmethyl cellulose (Na-CMC), and then the hydrated bentonite is densified [26]. The MSB is a sodium-rich montmorillonite modified with propylene carbonate [31]. Formation of BPN, also referred to as a bentonite polymer alloy (BPA) and bentonite polymer composite (BPC), occurs through polymerization of an organic monomer in a bentonite slurry (see [5]). HYPER-clay (HC) is another polymerized bentonite that is modified with 2% or more by dry weight of the Na-CMC anionic polymer [12].

There is a growing body of knowledge regarding the k of CMBs to various permeant liquids (refer to [7] and Fig. 8). For example, recent studies have shown that CMBs maintain lower k than Na-bentonite even after exposure to "aggressive" permeant solutions (500 mM $CaCl_2$) where k was $<10^{-11}$ m/s for the BPC versus 4.5×10^{-7} m/s for the Na-bentonite [53]. In addition, for the different types of CMBs considered in Fig. 8, some data indicate low k ($<10^{-10}$ m/s) despite low swell index (SI < 20 mL/2 g), indicating that the correlation between SI and k of CMBs can be complicated by the chemistry of the CMB.

For example, Scalia [51] reported that the SI of BPN correlated with the k for concentrations up to 50 mM $CaCl_2$. However, at concentrations greater than 50 mM $CaCl_2$, the k was decoupled from swell, such that the BPC maintained a low k ($<3 \times 10^{-11}$ m/s) even with a low SI (<8 mL/2 g). Bohnhoff and Shackelford [7] reported that 82% of the 96 reported k values for the CMBs permeated with a variety of liquids were lower than 10^{-9} m/s, suggesting a generally improved performance relative to what typically has been reported for Na-bentonites permeated with similar liquids. However, in some cases, the CMBs provide results that are similar or poorer compared to traditional Na-bentonite.

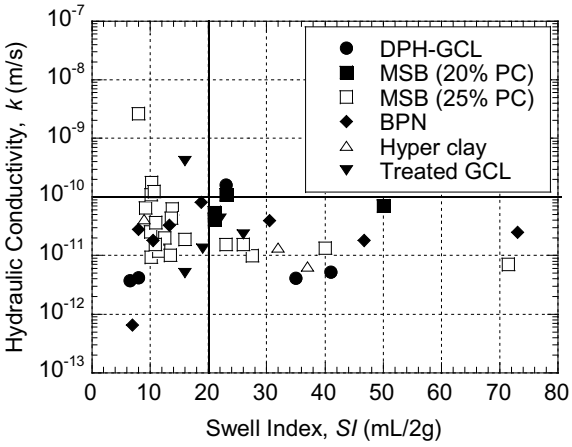

Fig. 8 Hydraulic conductivity versus swell index for various chemically modified bentonites (from [7])

At k values $<10^{-9}$ m/s diffusion has been shown to be a significant transport mechanism contributing to total contaminant flux. In fact, diffusion becomes the dominant transport mechanism around $k < 5 \times 10^{-10}$ m/s [54], which is in the range of many CMBs that have been investigated. Bohnhoff and Shackelford [7] reported that 70 of the 96 k values (72%) summarized for CMBs were $\leq 10^{-10}$ m/s. Therefore, based on the k data alone, conclusions regarding the superior performance of CMBs relative to Na-bentonites cannot be developed with certainty. The total contaminant flux is comprised both of advective flux and diffusive flux. Therefore, evaluating the performance of clay barrier systems based on advective properties alone is unconservative when diffusion is a significant or dominant transport mechanism (i.e., when $k < 10^{-9}$ m/s). In order to achieve effective containment of contaminants, low k is necessary but not a sufficient condition to ensure containment [54]. Therefore, an understanding of the diffusive properties of CMBs is essential to confirm the enhanced performance of CMBs. Limited information on the diffusive properties of CMBs is available, and the test methods for determining diffusion properties (e.g., through-diffusion testing) are time consuming and require relatively expensive equipment (>$10,000).

Figure 9 presents effective diffusion coefficients for a nonreactive tracer, Cl^-, for a polymerized bentonite (BPC) and a traditional Na-bentonite GCL. Values of the effective diffusion coefficient for Cl^-, D^*_{Cl}, for the BPC evaluated by Bohnhoff and Shackelford [6] were similar to those reported previously for the traditional Na-bentonite, as would be expected for a conservative tracer. However, results of the effective diffusion coefficients for K+ (D^*_K, not included) were lower for the BPC than the Na-bentonite likely because steady-state diffusion had not been achieved (even with test durations of 105 days or more) due to cation exchange with Na^+. Thus, additional experimentally measured values of diffusive transport properties of CMBs are necessary. Innovative methods to determine diffusive properties, such as those described by Sample-Lord and Shackelford [49] and Sample-Lord [48], should be

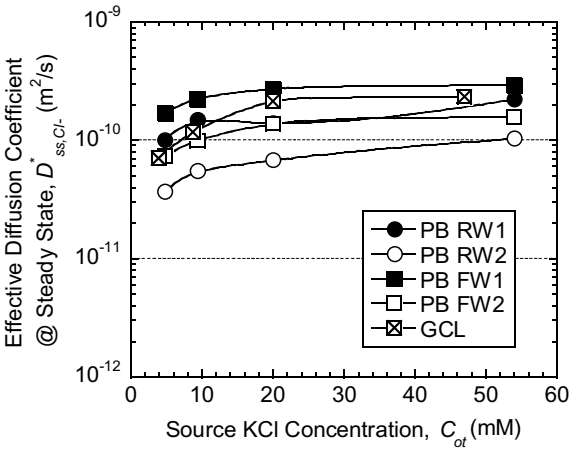

Fig. 9 Comparison of the effective diffusion coefficients at steady state for polymerized bentonite (PB) versus a geosynthetic clay liner (GCL) reported by Malusis and Shackelford [28] as a function of source KCl concentration [RW = rigid-wall test; FW = flexible-wall test] (from [6]. Reproduced with permission of The Clay Minerals Society, publisher of Clays and Clay Minerals)

investigated. In addition, correlations of diffusion coefficients with index properties such as SI and fluid loss should be considered.

The k and compatibility results for many of the CMBs are promising. However, the improved performance of the CMBs may be limited to the extent that such improved performance may decrease with increasingly chemically aggressive permeant liquids. It is essential to perform site-specific compatibility tests with contaminated liquids at the sites for practical applications. The experimentally measured values of diffusive and advective transport properties of CMBs are necessary in order to determine the expected contaminant flux attributed to each transport mechanism (advective and diffusive) in clay barrier systems. These values are necessary in order to accurately compare the performance of clay barrier systems containing Na-bentonite and CMB and make predictions regarding potential contaminant flux into the environment with modelling techniques.

2.4 Waste Management

Landfills are the most common waste management option in the U.S. and many other parts of the world. Conventional landfills are designed according to the regulatory requirements to effectively contain the municipal solid waste (MSW). The bottom liner system and the top cover system essentially isolate the waste from the surrounding environment. In addition, their components limit the moisture infiltration and the generation of excess leachate thus maintaining very dry conditions within the waste mass. The absence of adequate moisture within the waste hinders the microbial activity and lowers the rate of biochemical reactions associated with the anaerobic degradation of waste. This leads to several problems, including low gas generation and settlement rates, prolonged waste stabilization time, need for leachate treatment

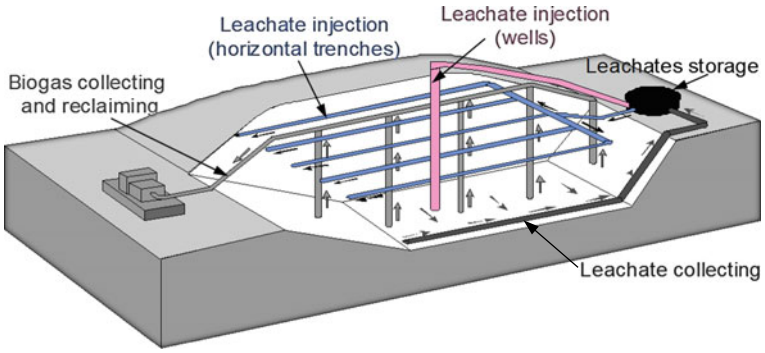

Fig. 10 Bioreactor landfill and its major operations

and disposal, increased post-closure monitoring, and increased methane (CH_4) and carbon dioxide (CO_2) emissions over the prolonged monitoring period.

In this regard, bioreactor landfills are being considered a promising technology for sustainable management of waste. Bioreactor landfills essentially involve recirculation of the collected leachate from the bottom of the landfill back into the waste mass. A schematic of the bioreactor landfill and the fundamental operations involved are shown in Fig. 10.

The leachate and other permitted liquids are injected into the waste mass under pressurized conditions through various leachate injection systems. The enhanced moisture levels by the introduction of leachate promote rapid degradation of waste thus leading to early waste stabilization. In addition, it offers several other benefits such as high gas generation and settlement rates, low leachate treatment and disposal costs, and landfill space reclamation among many others.

The concept of bioreactor landfills is appealing however, the design of such landfills for safe and effective operations is challenging due to many reasons [42]. The MSW in landfills is highly heterogeneous and anisotropic, which makes the uniform injection and distribution of leachate across the entire landfill highly uncertain. One of the major reasons that make the landfill system highly complex to understand is the biodegradation of waste. The conversion of biodegradable solids to gas influences the engineering properties of the waste and thereby the mechanical response (e.g., settlement) and hydraulic flow of leachate within the waste. In order to design a stable and effective bioreactor landfill, it is imperative to understand the fundamental system processes during the course of landfill construction and operation. More importantly, the biodegradation of the waste involves various biochemical reactions, mediated by the microbial activity, which are sensitive to various parameters (moisture, pH, temperature). A schematic of a simplified anaerobic digestion process as presented by McDougall [32] is shown in Fig. 11.

Several researchers have performed experimental investigations to delineate the possible biodegradation mechanisms in MSW [42]. Furthermore, many researchers have also formulated mathematical models to simulate these biochemical reactions

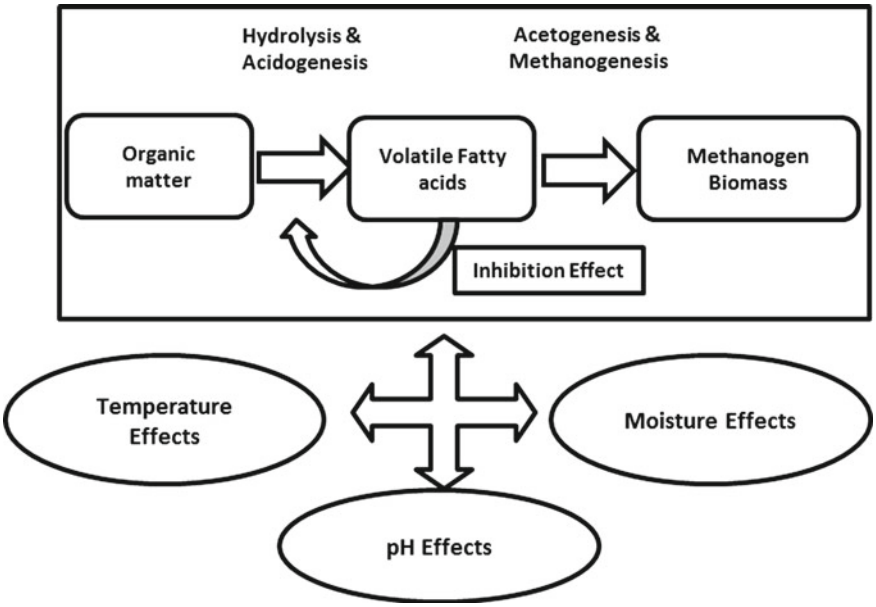

Fig. 11 Two-stage anaerobic biodegradation process [30]

and incorporating its influence on the hydraulic and mechanical behavior of MSW [43]. However, most of these models simplify the physical processes thus losing the reality. The ones, which do involve simulating the coupled interactions between different processes, do not holistically assess the influence of these processes on the overall performance (landfill stability and integrity of landfill components) of the bioreactor landfill [44, 45]. MSW is a geo-material, and understanding its behavior is crucial in understanding the landfill system itself. The sustainable management of waste through bioreactor landfills can only be realized if the bio-geochemical reactions within the waste can be manipulated as required. The control over these reactions is possible only by detailed experimental investigation of the biochemical behavior and trying to simulate it mathematically to understand its long-term impacts on the other processes within the landfill.

2.5 Mitigation of Landfill Gas Emissions

MSW in landfills undergoes anaerobic decomposition and generates CH_4 and CO_2 gases predominantly. The gas extraction wells installed at the landfills can capture most of the gases generated and use it for several purposes (e.g. thermal energy, electricity). However, there is always some portion of these gases that escapes the influence of the extraction wells and gets released into the atmosphere through the

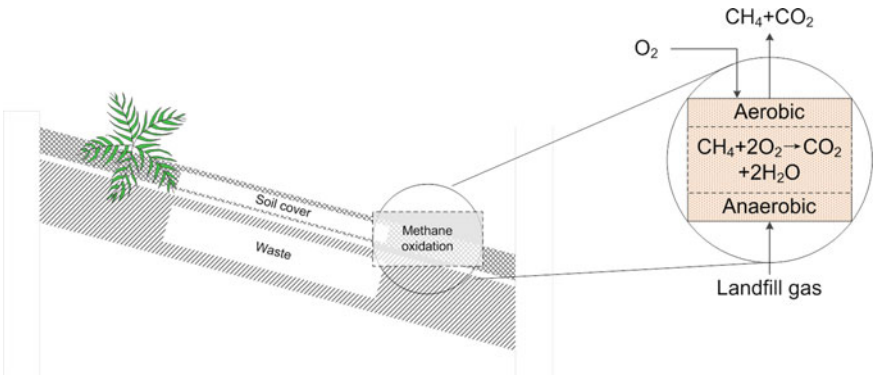

Fig. 12 Microbial oxidation of methane in biochar-amended soil cover system

landfill covers. In the U.S., these emissions from landfills are one of the largest sources of greenhouse gas emissions into the atmosphere. The cover soil in the landfill covers naturally consists of microbes called as methanotrophs, which can feed on the CH_4 passing to the cover and oxidize it to CO_2 thus mitigating some of the CH_4 emissions into the atmosphere. However, the microbial oxidation in cover soil is limited due to the lack of favorable conditions for the microbial activity.

In recent years, biocovers, which involve addition of organic matter to the cover soil in order to enhance microbial activity, have gained more prominence. The addition of organic matter enhances the microbial oxidation of CH_4 thus alleviating the CH_4 emissions. However, the organic matter such as compost, sewage sludge, and biosolids may undergo anaerobic degradation in the cover soil emitting CH_4, thus, exacerbating the emissions. In this regard, biochar, a solid byproduct derived out of gasification or pyrolysis of biomass, has shown great promise. The addition of biochar as an amendment to the soil promotes microbial growth and activity due to its unique characteristics such as high internal porosity and specific surface (see Fig. 12).

Biochar is a stable form of carbon, and it neither undergoes any degradation nor creates any odor. Several recent investigations on the biochar-amended soils for landfill cover systems have shown its effectiveness in mitigating the CH_4 emissions [60–63]. The addition of biochar into the cover soil induces beneficial physical and chemical characteristics into the soil. However, one of the most critical aspects in the biochar-amended soil cover system is to maintain the physical and more importantly the chemical environment within the soil cover that favors the microbial growth and activity. The availability of O_2 for the microbes, gas fluxes out of the waste mass into the soil cover, retention time for the chemical reactions to occur, adequate moisture content, pH and temperature play a crucial role in the geochemical processes that take place within the cover system. Thus, investigation of the abovementioned geochemical factors on the microbial activity and the biogeochemical interactions in the soil cover is of utmost importance for optimal CH_4 oxidation.

2.6 Geoenvironmental Remediation

The geoenvironmental remediation involves active or passive treatment of contaminated air, water, and soil to protect the human health and the environment. The nature of the problem addressed in geoenvironmental remediation is diverse and requires multidisciplinary solutions. Several technologies for the remediation of contaminated soils have been developed over the past three decades. These methods include soil vapor extraction, soil washing, chemical oxidation, thermal desorption, and bioremediation, but they are often limited to a particular type of contaminant [56]. Most of the traditional remediation technologies are highly energy intensive, indirectly leading to more problems. In recent years, biological-based technologies or bioengineered systems have gained wide attention due to their passive yet effective performance in remediation of contaminated sites. In the case of contaminated sites with mixed contamination, few technologies have proven to be efficient. However, they too have major limitations, and their application for large field sites can be very expensive [39]. In this context, phytoremediation has the potential to be a benign, cost effective alternative for the treatment of contaminated sites with mixed contamination [8, 9].

Phytoremediation is the use of plants to degrade (phytodegradation), extract (phytoextraction) from, and contain or immobilize (phytostabilization) contaminants within soil [56]. This green and sustainable remedial option can be adopted to remediate soils with a mixture of organic and inorganic contaminants that can be removed by the plants through different mechanisms [41]. Some mechanisms target certain types of contaminants over others, e.g., several organic compounds (e.g., tetrachloroethylene (PCE) and trichloroethylene (TCE)) can be completely degraded by the plant, while inorganic contaminants tend to be sequestered or accumulated within the plant.

Figure 13 shows the comparison of three areas at the same contaminated site. The difference in the chemical properties of the soil underlying those areas dictates the survival of plants. The effectiveness of the phytoremediation at a contaminated site highly depends on the physical and chemical properties of the soil. The growth and survival of the plant species used for phytoremediation are dictated by the conditions that prevail at the site. The ability to remain resilient to adverse chemical conditions (e.g., unfavorable pH) depends on the adaptability of the plants' growth to changing environmental conditions. In addition, the contaminant mobility, microbial activity, and availability of the nutrients also limits the contaminant uptake in plants.

The addition of organic matter to the soil was found to enhance the remediation of contaminated areas while increasing the chances of growth and survival of the plants [2, 40, 46, 47]. The geochemistry within the roots of the plants and the soil can immobilize, uptake, or degrade the contaminants, but the concentration levels and the speciation of the contaminants significantly impact the contaminant reduction. The fundamental issues that need to be addressed for an effective phytoremediation are selection of potential plant species understanding the effect of different soil conditions, contaminant type, and contaminant concentrations on growth and survival of plants. Furthermore, identifying suitable soil amendments for enhanced contam-

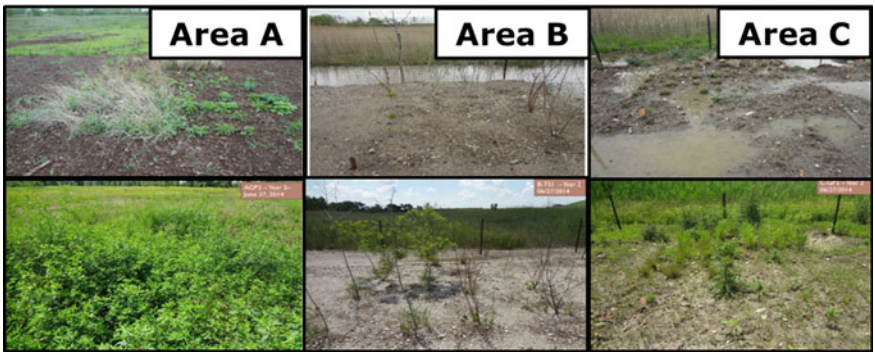

Fig. 13 Effect of varying physical and chemical conditions of soil in three areas at the same site on the growth and survival of plant species used in phytoremediation

inant uptake and bioaugmentation of microbial degradation of contaminants is most desirable.

Similar to phytoremediation, bioremediation is another treatment technology, which relies on the biological processes for contaminant reduction through biodegradation. The microbial activity involved in the bioremediation is sensitive to the contaminant concentrations in the media (e.g., soil, groundwater). For example, in Fig. 14, it is observed that in the presence of appropriate biostimulation, the concentration of Cr^{6+} could be reduced to acceptable levels. However, it does not degrade other contaminants such as TCE that may co-exist. The addition of suitable microbes (bioaugmentation), into the system at a later stage, degraded the TCE concentrations. This emphasizes the fact that the right biogeochemical conditions such as the right nutrients and microbial inoculum are essential for addressing diverse contaminants in an environmental medium.

3 Concluding Remarks

Geochemistry plays a vital role in sustainable geoengineering with development of tunable/smart materials and processes for infrastructure and environmental protection applications. For example, the use of waste materials such as fly ash, foundry sand, slag, and biochar in combination with soils or in lieu of soils has often been thought as a sustainable engineering practice. However, the environmentally benign use of these materials requires geochemical assessment of potential leachability of them for any undesirable constituents. Geochemical assessment is also needed to understand their long-term enhanced performance in geotechnical or

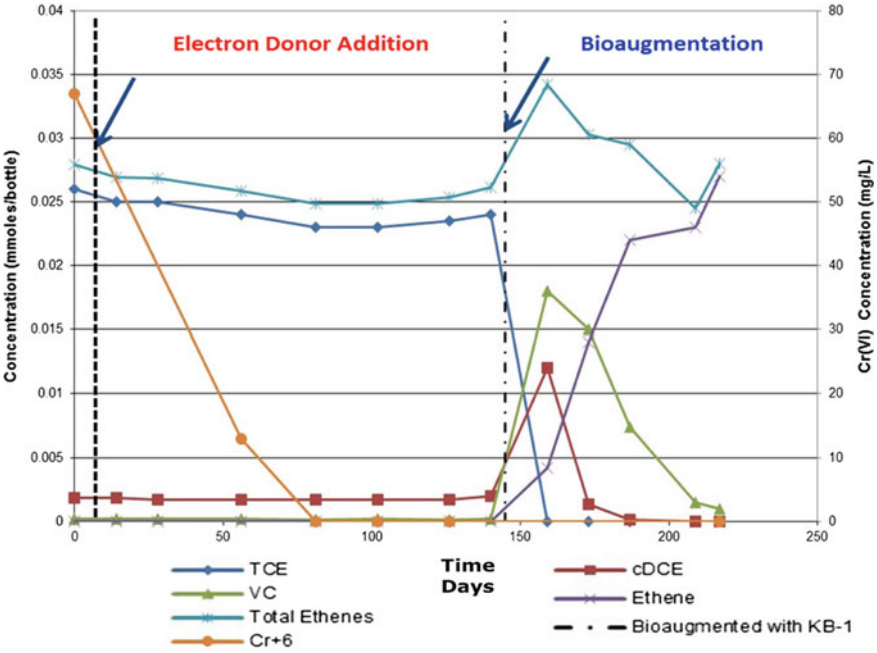

Fig. 14 Bioremediation with biostimulation and bioaugmentation (*Source* Jeff Roberts, SiREM)

geoenvironmental applications. Life cycle assessment and life cycle cost analysis will help match the most sustainable materials and systems to different geotechnical/geoenvironmental problems. Long-term performance and resiliency to the changing extreme environmental conditions (extreme dry or wet, extreme low or high pH, etc.) are also critical to evaluate. Bioengineered materials and systems are considered sustainable (e.g., biocovers for landfills and bioremediation of polluted soils), but biological processes are highly sensitive to the geochemistry (for example microbes may be intolerant to anticipated pH conditions), and therefore the understanding of the geochemical interactions in the subsurface will be critical for the performance of the biological processes.

All the aforementioned technologies and the ongoing research are focused on developing geosystems by leveraging on the biogeochemistry within the system. In most of the engineered geosystems, there is a limited importance given to the long-term impacts that these technologies pose. Several tools exist to quantify and holistically assess the environmental, economic and social impacts of an engineered geosystem considering its intended application. A thorough evaluation of the engineered materials toward environmental safety is essential because the production and use of such materials while addressing one issue should not create or lead to another problem.

Acknowledgements This chapter is developed based on the deliberations in the Geochemistry session at the workshop entitled "Geotechnical Fundamentals in the Face of New World Challenges" held at the National Science Foundation, Arlington, Virginia, July 17–19, 2016. The authors are grateful for the support of National Science Foundation for funding the workshop. The authors are also thankful to Ning Lu and Girish Kumar for their encouragement and assistance in preparing this chapter.

References

1. Abend, S., Lagaly, G.: Sol–gel transitions of sodium montmorillonite dispersions. Appl. Clay Sci. **16**(3), 201–227 (2000)
2. Amaya-Santos, G., Reddy, K.R.: Phytoremediation of heavy metals and PAHs in alkaline slag fill at wet meadow site. J. Hazard. Toxic Radioactive Waste **21**(4) (2017)
3. Bishop, M.D., Kim, S., Palomino, A.M., Lee, J.-S.: Deformation of "Tunable" clay-polymer composites. Appl. Clay Sci. **101**, 265–271 (2014)
4. Bohnhoff, G.L., Shackelford, C.D., Malusis, M., Scalia, J., Benson, C., Edil, T., Di Emidio, G., Katsumi, T., Mazzieri, F.: Novel benonites for containment barrier applications. In: Delage,P., Desrues, J., Frank, R., Puech, A., Schlosser, F. (eds.) 18th International Conference on Soil Mechanics and Geotechnical Engineering—Challenges and Innovations in Geotechnics, vol. 4, pp. 2997–3000. Presses des Ponts, Paris (2013)
5. Bohnhoff, G.L., Shackelford, C.D.: Improving membrane performance via bentonite polymer nanocomposites. Appl. Clay Sci. **86**, 83–98 (2013)
6. Bohnhoff, G.L., Shackelford, C.D.: Salt diffusion through a polymerized bentonite membrane. Clay and Clay Minerals **63**(3), 145–162 (2015)
7. Bohnhoff, G. L., Shackelford, C. D.: Hydraulic conductivity of modified clays for containment barriers. In: 7th International Congress on Environmental Geotechnics, pp. 440–447. ISSMGE, Engineers Australia (2014)
8. Cameselle, C., Chirakkara, R.A., Reddy, K.R.: Electrokinetic-enhanced phytoremediation of soils: status and Opportunities. Chemosphere **93**(4), 626–636 (2013)
9. Chirakkara, R.A., Cameselle, C., Reddy, K.R.: Assessing the applicability of phytoremediation of soils with mixed organic and heavy metal contaminants. Rev. Environ. Sci. Bio/Technol. **15**(2), 299–326 (2016)
10. Coussot, P.: Rheophysics of pastes: a review of microscopic modelling approaches. Soft Matter **3**, 528–540 (2007)
11. Demoz, A., Mikula, R.J.: Role of mixing energy in the flocculation of mature fine tailings. J. Environ. Eng. **138**(1), 129–136 (2011)
12. Di Emidio, G., Mazzieri, F., Verastegui-Flores, R.-D., Van Impe, W., Bezuijen, A.: Polymer-treated bentonite clay for chemical-resistant geosynthetic clay liners. Geosynthetics Int. **22**(1), 1–13 (2015)
13. Estornell, P., Daniel, D.E.: Hydraulic conductivity of 3 geosynthetic clay liners. J. Geotech. Eng. **118**, 1592–1606 (1992)
14. Evans, J.: Hydraulic conductivity of vertical cutoff walls. In: Daniel, D.E., Trautwein, S. (eds.) Hydraulic Conductivity and Waste Contaminant Transport in Soil, pp. 79–94. ASTM, West Conshohocken, Pennsylvania (1994)
15. Gates, W.P., Bouazza, A., Churchman, G.J.: Bentonite clay keeps pollutants at bay. Elements **5**(2), 105–110 (2009)
16. Halder, B.K., Palomino, A.M., Hicks, J.: Influence of Polyacrylamide Conformation on the Fabric of a "Tunable" Kaolin-Polymer Composite. https://doi.org/10.1139/cgj-2017-0200 (2018) (In press)
17. Halder, B.K.: Meso-Scale Behavior Characterization of "Tunable" Clay-Polymer Composites, Ph.D. dissertation, University of Tennessee, Knoxville (2017)

18. Huang, P.T.: Rheological Properties and Lubrication Performance of Clay-based Drilling Fluids for Trenchless Technologies, Ph.D. thesis, Lyles School of Civil Engineering, Purdue University, West Lafayette, IN (2013)
19. Johnston. C., Sasar, M., Santagata, M., Bobet. A., Duan, L., Kaminsky, H.A.: Polymer-MFT interactions: from surface chemistry to rheology. In: Sego, D., Wilson, G.W., Beier, N.A. (eds.) Proceedings 5th International Oil Sands Tailings Conference, pp. 201–213. Lake Louise, Canada, 4– December 2016
20. Kasperski, K.L., Mikula, R.J.: Waste streams of mined oil sands: characteristics and remediation. Elements **7**(6), 387–392 (2011)
21. Kim, S., Moyotyka, M.A., Palomino, A.M., Podraza, N.J.: Conformational effects of adsorbed polymer on the swelling behavior of engineered clay minerals. Clays Clay Miner. **60**(4), 363–373 (2012)
22. Kim, S., Palomino, A.M.: Factors Influencing the Synthesis of tunable clay-polymer nanocomposites using bentonite and polyacrylamide. Appl. Clay Sci. **51**, 491–498 (2011)
23. Kim, S., Palomino, A.M., Colina, C.M.: Responsive polymer conformation and resulting permeability of clay-polymer nanocomposites. Mol. Simul. **38**(8–9), 723–734 (2012)
24. Kolstad, D., Benson, C., Edil, T.: Hydraulic conductivity and swell of nonprehydrated GCLs permeated with multi-species inorganic solutions. J. Geotech. Geoenviron. Eng. 1236–1249 (2004)
25. Lan, Y., Deng, B., Kim, C., Thornton, E.C.: Influence of soil minerals on chromium (VI) reduction by sulfide under anoxic conditions. Geochem. Trans. **8**(4) (2007). http://www.geochemicaltransactions.com/content/8/1/4
26. Malusis, M.A., Daniyarov, A.S.: Membrane efficiency of a Dense, Prehydrated GCL. In: 7th International Congress on Environmental Geotechnics, pp. 1166–1173. ISSMGE, Engineers Australia (2014)
27. Malusis, M., Shackelford, C.: Chemico-osmotic efficiency of a geosynthetic clay liner. J. Geotech. Geoenviron. Eng. **128**, 97–106 (2002)
28. Malusis, M., Shackelford, C.: Coupling effects during steady-state solute diffusion through a semipermeable clay membrane. Environ. Sci. Technol. **36**, 1312–1319 (2002)
29. Malusis, M., Shackelford, C., Olsen, H.: A laboratory apparatus to measure chemico-osmotic efficiency coefficients for clay soils. Geotech. Test. J. **24**, 229–242 (2001)
30. Manassero, M., Dominijanni, A.: Modelling the osmosis effect on solute migration through porous media. Geotechnique **53**, 481–492 (2003)
31. Mazzieri, F., Di Emidio, G., Van Impe, P.O.: Diffusion of calcium chloride in a modified bentonite: impact on osmotic efficiency and hydraulic conductivity. Clays Clay Miner. **58**(3), 351–363 (2010)
32. McDougall, J.: A hydro-bio-mechanical model for settlement and other behaviour in landfilled waste. Comput. Geotech. **34**(4), 229–246 (2007)
33. Mitchell, J.K., Soga, K.: Fundamentals of Soil Behavior, 3rd edn. Hoboken, NJ (2005)
34. Mongondry, P., Nicolai, T., Tassin, J.F.: Influence of pyrophosphate or polyethylene oxide on the aggregation and gelation of aqueous laponite dispersions. J. Colloid Interface Sci. **275**(1), 191–196 (2004)
35. Langmuir, D.: Aqueous environmental geochemistry. Ground Water **35**(5), 919–920 (1997)
36. Ochoa-Cornejo, F., Bobet. A., Johnston. C., Santagata, M., Sinfield, J.: Liquefaction 50 years after Anchorage 1964—how nanoparticles could prevent it. In: 10th U.S. National Conference on Earthquake Engineering—Frontiers of Earthquake Engineering (EERI), Anchorage, 21–25 July 2014
37. Ochoa-Cornejo, F., Bobet. A., Johnston. C., Santagata, M., Sinfield, J.: Cyclic behavior and pore pressure generation in sand with laponite, a super-plastic nano-particle. Soil Dyn. Earthquake Eng. (2016) (In press)
38. Images of Clay: Platy Illite from the Rotliegend of Northern Germany. A joint initiative of the Clay Minerals Society and The Clay Minerals Group. http://www.minersoc.org/pages/gallery/claypix/illite/hems24_4.html. Accessed July 16 2009

39. Reddy, K.R.: Technical challenges to in-situ remediation of polluted sites. Geotech. Geol. Eng. J. **28**(3), 211–221 (2010)
40. Reddy, K.R., Amaya-Santos, G.: Effects of variable site conditions on phytoremediation of mixed contaminants: field-scale investigation at Big Marsh site. J. Environ. Eng. **143**(9), 04017057 (2017)
41. Reddy, K.R., Chirakkara, R.A.: Green and sustainable remedial strategy for contaminated site: case study. Geotech. Geol. Eng. J. **31**(6), 1653–1661 (2013)
42. Reddy, K.R., Kumar, G., Giri, R.K.: Modeling coupled processes in municipal solid waste landfills: an overview with key engineering challenges. Int. J. Geosynthetics Ground Eng. **3**(1), 6 (2017a)
43. Reddy, K.R., Kumar, G., Giri, R.K.: Influence of dynamic coupled hydro-bio-mechanical processes on response of municipal solid waste and liner system in bioreactor landfills. Waste Manag. **63**, 143–160 (2017b)
44. Reddy, K.R., Kumar, G., Giri, R.K.: System effects on bioreactor landfill performance based on coupled hydro-bio-mechanical modeling. J. Hazard. Toxic Radioact. Waste **22**(1), 04017024 (2017c)
45. Reddy, K.R., Kumar, G., Giri, R.K., Basha, B.M.: Reliability assessment of bioreactor landfills using Monte Carlo simulation and coupled hydro-bio-mechanical model. Waste Manag. **72**, 329–338 (2018)
46. Reddy, K.R., Amaya-Santos, G., Yargicoglu, E., Cooper, D.E., Negri, M.C.: Phytoremediation of PAHs and heavy metals at slag disposal site: three-year field investigation. Int. J. Geotech. Eng. 1–16 (2017d)
47. Reddy, K.R., Amaya-Santos, G., Copper, D.: Field-scale phytoremediation of mixed contaminants in upland area at Big Marsh site, Chicago, USA. Ind. Geotech. J. 1–16 (2017e)
48. Sample-Lord, K.: Membrane Behavior and Diffusion in Unsaturated Sodium Bentonite. Ph.D. Dissertation, Colorado State University, Fort Collins, CO (2015)
49. Sample-Lord, K., Shackelford, C.: Dialysis method to control exchangeable cations and remove excess salts from bentonite. Geotech. Test. J. **39**(2), 1–11 (2016). https://doi.org/10.1520/GTJ20150065
50. Santagata, M., Clarke, J.P., Bobet, A., Drnevich, V.P., El Mohtar, C.S., Huang, P.T., Johnston, C.T.: Rheology of concentrated bentonite dispersions treated with sodium pyrophosphate for application in mitigating earthquake-induced liquefaction. Appl. Clay Sci. **99**, 24–34 (2014)
51. Scalia, J.: Bentonite-polymer composites for containment applications, Ph.D. dissertation, University of Wisconsin, Madison, Madison, WI, USA (2012)
52. Scalia, J., Benson, C.H.: Effect of permeant water on the hydraulic conductivity of exhumed geosynthetic clay liners. Geotech. Test. J. **33**(1), 1–11 (2010)
53. Scalia, J., Benson, C.H., Bohnhoff, G.L., Edil, T.B., Shackelford, C.D.: Long-term hydraulic conductivity of a bentonite polymer nanocomposites permeated with aggressive inorganic solutions. J. Geotech. Geoenviron. Eng. **140**(3), 04013025 (2014)
54. Shackelford, C.D.: The ISSMGE Kerry Rowe Lecture: The role of diffusion in environmental geotechnics. Can. Geotech. J. **51**(11), 1219–1242 (2014)
55. Shackelford, C.: Membrane behavior in engineered bentonite-based containment barriers: State of the art. In: Manassero, M., Dominijanni, A., Foti, S., Musso, G. (eds.) Coupled Phenomena in Environmental Geotechnics, pp. 45–60. CRC Press/Balkema, Taylor & Francis Group, London (2013)
56. Sharma, H.D., Reddy, K.R.: Geoenvironmental engineering: site remediation, waste containment, emerging waste management technologies. Wiley, Hoboken, New Jersey (2004)
57. Sposito, G.: The Chemistry of Soils. Oxford University Press, New York (1989)
58. Tanaka, H., Meunier, J., Bonn, D.: Nonergodic states of charged colloidal suspensions: repulsive and attractive glasses and gels. Phys. Rev. **69**(3), 03140 (2004)
59. Wang, X.T., Feng, X., Xu, Z., Masliyah, J.H.: Polymer aids for settling and filtration of oil sands tailings. Can. J. Chem. Eng. **88**(3), 403–410 (2010)
60. Yargicoglu, E., Sadasivam, B.Y., Reddy, K.R., Spokas, K.: Physical and chemical characterization of waste wood derived biochars. Waste Manag. **36**(2), 256–268 (2015)

61. Yargicoglu, E.Y., Reddy, K.R.: Microbial abundance and activity in biochar-amended landfill cover soils: Evidences from large-scale column and field experiments. J. Environ. Eng. **143**(9), 04017058 (2017)
62. Yargicoglu, E.Y., Reddy, K.R.: Effects of biochar and wood pellets amendments added to landfill cover soil on microbial methane oxidation: A laboratory column study. J. Environ. Manage. **193**, 19–31 (2017)
63. Yargicoglu, E.Y., Reddy, K.R.: Biochar-amended soil cover for microbial methane oxidation: Effect of biochar amendment ratio and cover profile. J. Geotech. Geoenviron. Eng., ASCE **144**(3), 04017123 (2018)

Bio-mediated and Bio-inspired Geotechnics

Jason T. DeJong and Edward Kavazanjian

Abstract Bio-mediated geotechnics, wherein biogeochemical processes are employed to directly modify the engineering properties of soil, and bio-inspired geotechnics, wherein natural biological systems provide inspiration for the development of novel geotechnical solutions, provide two complimentary opportunities for geotechnical engineering innovation. The field of bio-mediated geotechnics has been developing for more than one decade while the field of bio-inspired geotechnics is just now emerging. Both domains require geotechnical engineers to reconsider the importance and role of biology and biological systems in geotechnical engineering. This chapter provides the context and general principles for these emerging fields followed by specific examples of both fields. The importance of sustainability and how these fields can contribute to sustainable development is discussed. The chapter concludes by briefly addressing some of the steps required for biogeotechnics to become a recognized sub-discipline within the domain of geotechnical engineering.

Keywords Bio-mediated geotechnics · Bio-inspired geotechnics · Biogeotechnical engineering · Biocementation · Calcite precipitation

1 Introduction

Engineers have, by necessity, always simplified the complexity of soils. For decades, soil properties and behavior were attributed to gravimetric forces and the presence of water. In the second half of the 20th century, work by Mitchell and others revealed that chemical processes are at work in all soils and form the scientific basis for clay

J. T. DeJong (✉)
Civil and Environmental Engineering, University of California, One Shields Ave, Davis, CA 95616, USA
e-mail: jdejong@ucdavis.edu

E. Kavazanjian
Geotechnical Engineering, Arizona State University, MS 3005, Tempe, CA 85287-3005, USA
e-mail: edkavy@asu.edu

N. Lu and J. K. Mitchell (eds.), *Geotechnical Fundamentals for Addressing New World Challenges*, Springer Series in Geomechanics and Geoengineering,
https://doi.org/10.1007/978-3-030-06249-1_7

behavior (e.g. [50]). As understanding of the role of chemistry in soils developed, the profession advanced and began harnessing chemical processes to manipulate engineering properties (e.g. lime stabilization and electrokinetics; e.g. [35, 71]).

A new frontier with respect to soil properties and behavior for the geotechnical profession is the recognition that the soil itself is a living ecosystem [19]. The bacterial count in near surface soils with significant organic content often exceeds 10^9 bacteria per 1 cm^3 [49, 53, 70]. More than 10^6 bacteria are also present in a cubic centimeter of poorly graded quarry sand typically used as backfill or roadway subgrade materials. Bacterial activity occurs in a variety of ways that can result in modification of groundwater conditions and soil properties. The "inert" backfill materials used in construction are not actually inert, but instead living ecosystems.

The living nature of soil can involve biological and chemical changes that challenge our traditional understanding of time-dependent mechanical and hydraulic properties in soils. Such changes can improve or degrade soil properties from the as-constructed condition over the service life of a geotechnical system. Often, the net effect of detrimental changes is not sufficient to compromise the conservatism embedded in the design, but they are present nonetheless. In other cases, such as reductions in hydraulic conductivity and increases in liquefaction resistance, it may be beneficial to acknowledge, understand, and account for time-dependent biogeochemical effects.

Over the past 15 years, geotechnical researchers have formed interdisciplinary teams with microbiologists and geochemists in an effort to merge their knowledge and identify bio-mediated processes that may be accelerated in time or relocated in space to induce changes in soil that result in significant improvements in engineering soil properties or geosystem performance [15, 18–20, 29, 32, 33, 38, 60]. More recently, a parallel effort using bio-inspiration has been explored wherein natural biological processes, organisms, and systems are studied; the forms, behaviors and principles abstracted; and the abstracted concepts are applied to develop innovative solutions to geotechnical problems that realize improvement of soil properties and system performance [16, 24]. Together, these two approaches to biologically based design comprise the emerging field of biogeotechnical engineering. In essence, the bio-mediated approach directly uses biological systems and processes, while the bio-inspired approach extracts forms, behaviors, and principles from nature to inspire new engineered solutions [16]. Bio-mediated and bio-inspired geotechnics are both relatively young fields and require significant additional work to realize their full potential for addressing geotechnical challenges, but research results to date are promising.

This chapter provides a broad overview of these two complimentary emerging fields, outlines the general approach taken in each area, provides examples of select accomplishments, and closes with thoughts on the path forward.

2 General Principle

The conceptual underpinning of both bio-mediated and bio-inspired approaches for geotechnical innovation stem from a perspective that over millennia the environmental constraints (stressors) in nature have resulted in the development and selection (optimization) of specific biological processes that provide a competitive survival advantage in the given ecosystem [20, 49]. Environmental constraints typically include energy, nutrients, water, and physical space, and environmental stressors include structural, temperature, and pressure loading conditions. These multiple constraints and stressors produce systems that often serve multiple simultaneous functions. Importantly, biological systems are often selected or optimized for a specific environment, which often may not be directly transferrable to a system of geotechnical interest in a different environment. Thus, abstraction processes that shed context specific details are often important for bio-inspired design [25].

The development of bio-mediated geotechnical solutions to date has focused on the identification, control, and application of bio-geochemical processes to induce changes to soil conditions that can be permanent under particular long-term conditions [18, 20]. Geotechnical applications of bio-mediated processes can range from simply mobilizing (e.g., accelerating) an existing process, using a bio-mediated process to accelerate an abiotic chemical reaction, or using a biological process to control application variables such as the location and rate of where a process occurs. For example, and as discussed further below, biogeochemical processes can be used to precipitate calcium carbonate at the contacts of soil particles which results in improvement of engineering properties including strength, stiffness, hydraulic conductivity, and dilatancy among others [1, 9, 10, 17, 21, 22, 43, 51, 59, 63–66, 69]. Following calcium carbonate precipitation, the long-term stability is largely dictated by groundwater environmental conditions; under favorable conditions the service life may far exceed engineering requirements (typically 30–50 years) while under adverse conditions the improvement may degrade faster than the structure it is supporting. Other environments and other biogeochemical processes, on the other hand, may be easily reversible and have a shorter service life, lending their application to limited, short term, construction time periods.

The development of bio-inspired geotechnical solutions has underpinning in the field of bio-inspired engineering design, for which research methodologies have been developed only in the past couple of decades [6]. And even in the past few years, the practice of biologically inspired design has been described as having little systemization [25]. The bio-inspiration innovation process can be cast in a problem-based or solution-based framework [25]. The former stems from identification of a specific engineering problem and then searching the biological space for inspiration of a new solution. The latter stems from idea inspiration through scientific biological study and then identification of engineering problems that would benefit. Both methods include the critical components of problem identification, generalization of required performance, biological system understanding, bio-inspired idea abstraction, and application towards solution development [25]. Application of this methodology,

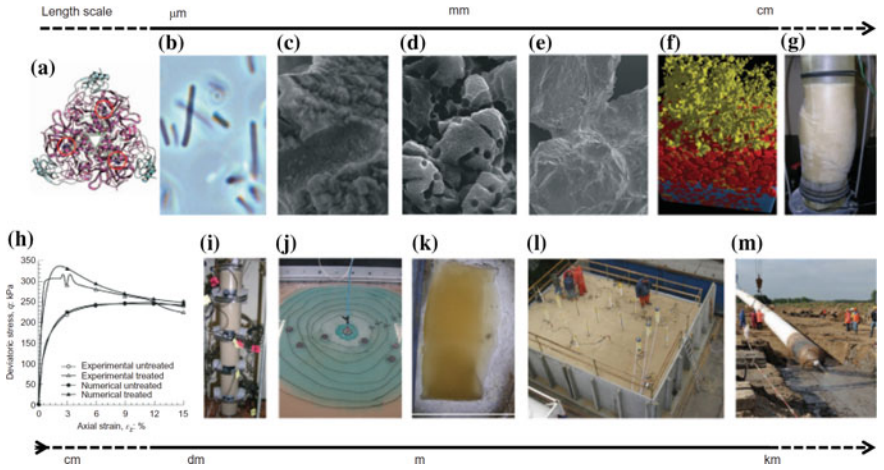

Fig. 1 Overview of upscaling of MICP: **a** urease enzyme structure housed within microbes [5]; **b** *Porosarcina pasteuri* microbe (image supplied by DeJong); **c** bacterial impression within precipitated calcite [44]; **d** structure of precipitated calcite [14]; **e** MICP-cemented sand grains [8]; **f** CT scan of MICP-cemented sand (image supplied by DeJong); **g** MICP-cemented triaxial specimen [52]; **h** modelling of MICP triaxial compression test [28]; **i** 1D column tests [42]; **j** radial flow treatments [56]; **k** MICP impermeable skin for retention basin [62]; **l** MICP treatment of 100 m^3 sand [21, 64]; **m** field trial (used with permission from ICE)

regardless of its inception as a problem-based or solution-based approach, requires engineers, life scientists, and earth scientists to work collaboratively to leverage their complimentary expertise, as none of these disciplinary experts typically have the knowledge base, creativity, and entrepreneurship individually for realization of a successful outcome [7].

The development of new biogeotechnical solutions often initially requires high-risk, small-scope stages of inquiry and, for ideas that demonstrate potential, systematic upscaling from nm-scale (e.g. enzymes, bacteria) to m-scale field applications (e.g. liquefaction mitigation). Stages of this work for calcite precipitation is exemplified in the following Fig. 1 [19].

3 Bio-mediated Engineering Solutions

Understanding the role of biology is critical for developing bio-mediated solutions as biological processes directly influence the rate, timing, and location of the geochemical reaction network(s) that induce changes to the soil structure [18, 19]. In some cases, a biological process creates a permanent inorganic precipitate that could also be produced solely using chemistry in a beaker on the laboratory bench. However, by mediating this process with biology, the reaction can be controlled and enabled

such that they occur within a soil mass at a targeted location. In other cases, the stability of an organic polymer that forms around bacteria is directly coupled to continued bacterial growth; when the bacteria die, the change in engineering properties induced by the biopolymer may be reversed. Yet in other cases, a biological process may generate small gas bubbles in the pore space resulting in desaturation of the soil, and the longevity of soil desaturation may be a function of the dissolution rate of the gas into solution.

Microbially mediated calcite precipitation (MICP), an inorganic mineral precipitation technique, is the process that has received the greatest research focus to date in the geotechnical community due to its promise as a ground improvement technique (summarized in [20]). Recent research, illustrated in Fig. 2, in which sand in 2-m-diameter tanks was treated to induce microbially mediated calcite precipitation demonstrated that it is possible to solidify loose uncemented sand (relative density, $D_r = 40\%$, initial shear wave velocity, $V_s = 120$ m/s) into a weak sandstone-like material ($V_s = 970$ m/s) over a period of 10 days, while controlling the spatial distribution of improvement [26]. The improvement level can be monitored in real time by measuring shear wave velocity and with cone penetration testing [27]. While the bacteria that facilitated this process were cultured externally and then introduced to the tank in Fig. 2 (i.e. bio-augmentation was used), this process can be equally effective through bio-stimulation [28], wherein bacteria already present in the sand (native bacteria) are first stimulated with nutrients to increase their population and activity, and then used to mediate the calcite cementation process.

This mineral precipitation process can also be induced chemically using an agriculturally-derived isolated urease enzyme (the same enzyme that the bacteria use in this process) [36]. Figure 3 shows a "donut" of stabilized soil created by radially infusing a 19 L container of sand with an enzyme-based cementation solution through perforations in a 76.2 mm diameter plastic pipe [37]. Calcite precipitation in the void space, cladding the soil particles, and particularly at particle-particle contacts increases soil stiffness, strength, and liquefaction triggering resistance, and decreases hydraulic conductivity. The resulting potential applications are wide ranging and include liquefaction mitigation beneath existing structures, stabilization of low volume roadways, control of groundwater flow, and contaminant immobilization, among others [20].

Another microbially mediated process, biogas-induced desaturation, also shows promise as a liquefaction mitigation mechanism [54]. Over the past decade, abiotic desaturation has been identified as a potential mitigation measure for earthquake-induced soil liquefaction. Laboratory testing has shown that biogenic gas, and in particular biogenic nitrogen gas due to its low solubility in water, can rapidly desaturate sandy soil [54]. Figure 4 presents the results of a benchtop column experiment in which native bacteria were stimulated to produce nitrogen gas. Both compression wave (p-wave) velocity measurements and the volume of gas expelled from the specimen indicated that the degree of saturation of the initially saturated sand decreased to 94% saturation in less than 48 h. Abiotic testing using the same soil indicated that decreasing the degree of saturation to 94% increased the cyclic stress ratio required to induce liquefaction by more than 40%.

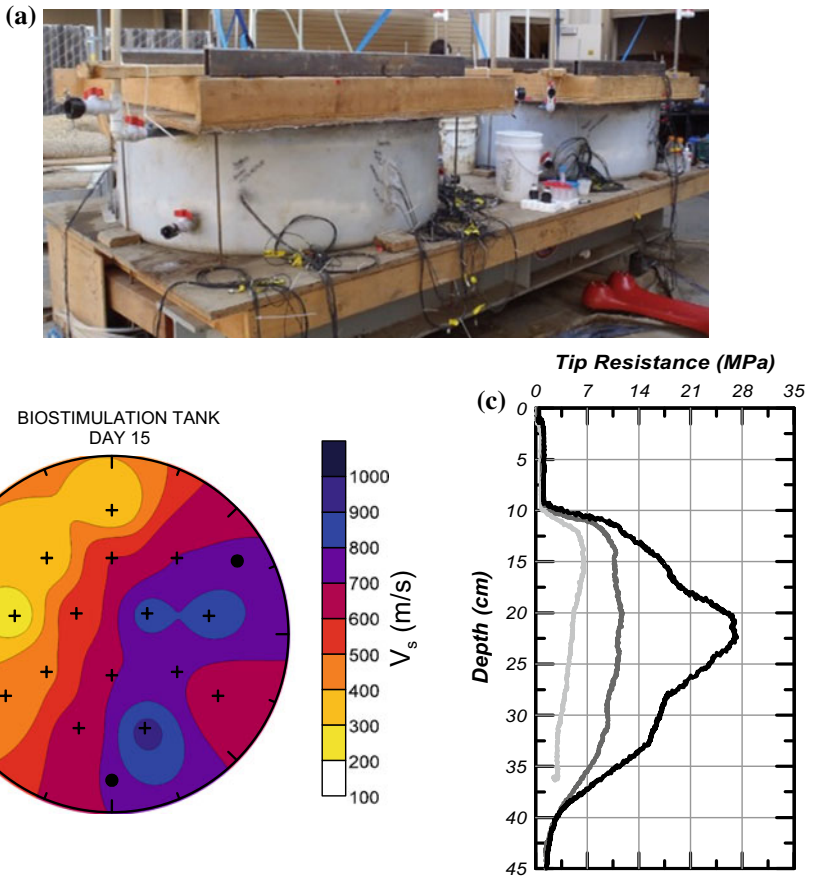

Fig. 2 Biocementation treatment in 2 m diameter tanks **a** setup, **b** shear wave velocity mapping, **c** CPT penetration increase with MICP cementation level (courtesy of Jason T. DeJong)

Fig. 3 "Donut" of stabilized soil created by enzyme-induced cementation in a 19-L bucket by radial infusion through a 76.2 mm-diameter perforated plastic pipe (courtesy of Edward Kavazanjian Jr.)

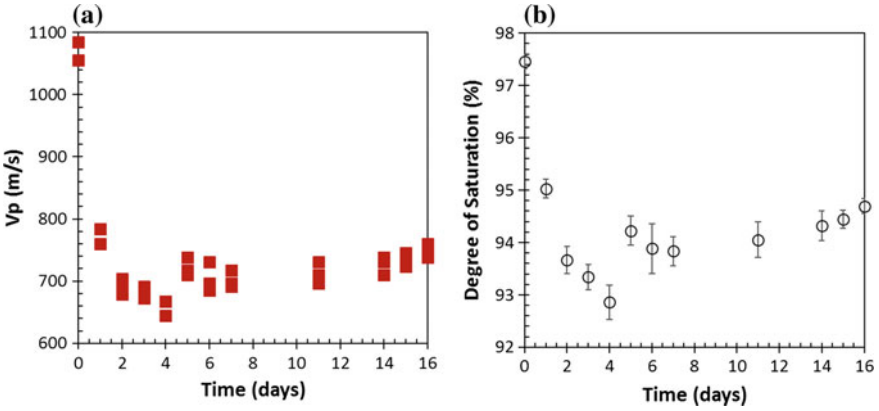

Fig. 4 Microbially induced desaturation in a 50.8 mm-diameter column as indicated by **a** compressional- (P-) wave velocity measurements and **b** volume of expelled water (courtesy of Edward Kavazanjian Jr.)

The growth of biofilms, films generated by bacterial communities that secrete a gel-like substance known as EPS (extra-cellular poly saccharide, [12]), has been shown to coat coarse-grained soil particles and plug voids for short-term modification of soil properties [2, 23, 31, 57, 61]. The generation of EPS within sands can effectively reduce hydraulic conductivity by more than 100 times over a period of about two weeks [55], as illustrated in Fig. 5. Recent column experiments have demonstrated that this process can also be achieved by stimulating native bacterial populations. Once reduced, the hydraulic conductivity reduction can remain stable for more than 60 days, after which it degrades, as illustrated in Fig. 5. If desired, retreatment can sustain or recover the full reduction in hydraulic conductivity. Alternatively, the biofilm could be allowed to degrade, and the hydraulic conductivity can attenuate back to its natural condition. This type of short-term reduction may be useful for dewatering excavation projects, for example, since only temporary hydraulic conductivity reduction is needed.

4 Bio-inspired Engineering Solutions

Comparison of the performance efficiency of biological systems with analogous geotechnical systems, albeit sometimes at different length scales, can highlight the inefficiencies of current geotechnical processes and designs. For example, ant excavation processes are 100–1000 times more energy efficient than current tunnel boring machines, root systems are 10 times more energy efficient than current ground reinforcement/foundation systems, and moles advance through soils with amazing efficiency. While geotechnical engineers may not be able to employ such activities directly for infrastructure scale applications, the forms, behaviors, principles, and

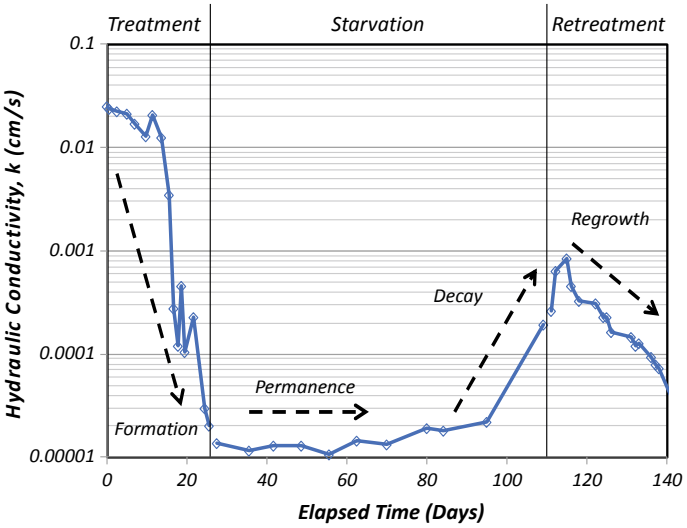

Fig. 5 Biofilms formation, permanence, decay, and regrowth stages during treatment of clean sand in a laboratory column experiment (courtesy of Jason T. DeJong)

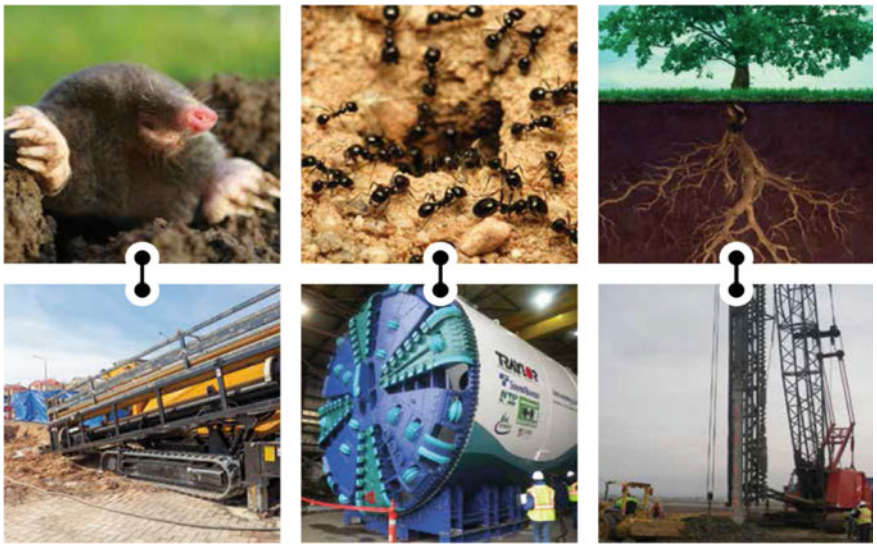

Fig. 6 Biological analogs to our geotechnical systems (used with permission from ASCE)

processes they employ, many of which have been refined over millennia for their respective environments, can inspire new geotechnical solutions [67, 68]. Figure 6 illustrates a few of the numerous analogs between current geotechnical processes and biological systems.

A majority of geotechnical ground improvement, slope stabilization, foundation and anchorage systems, and underground construction solutions, as well as their associated construction processes, are either mechanically based or use Portland cement or other energy intensive produced materials. These current technologies are largely direct-cost and/or brute force driven; optimization has largely been in the form of incremental improvements. The goal of bio-inspired geotechnical solutions is to reconsider the performance requirements for a geotechnical system and identify new solutions that leverage, to the extent appropriate, efficiencies optimized in the biological analogs. Biological analogs for excavation, reinforcement, penetration, erosion control, densification, and other geotechnical functions can often be readily identified [16, 24].

One example of where a bio-inspired approach may have significant potential is in pile foundations and soil retention systems [16, 24]. Nearly all deep foundation and soil reinforcement systems employ linear, constant cross-sectional elements to transfer the structural load to the surrounding soil. The biological analog, the tree root system, is 10 times more efficient with respect to capacity normalized to system mass and highly spatially non-linear [48]. Insight from the root anchorage literature about root allocation strategies and influences [11] paired with direct study of root anchorage performance continues to reveal more about the topological and morphological aspects of root systems that are most important for their structural (anchorage) function. The knowledge gained from this type of study enables exploration of the potential performance increase that is possible with a root-inspired foundation or reinforcement element. This bio-inspired design process is exemplified in Fig. 7.

Another bio-inspired engineering solution being explored to improve soil-structure interaction and load transfer is based on the anisotropic surface properties of the ventral scales of snakes. The skin along the underbody of snakes is comprised of flexible scales that collectively form a highly anisotropic surface [4, 47]. Snake motility is highly efficient and enabled by this frictional anisotropy; shearing in the cranial direction (towards the head) produces higher interface friction than in the caudal direction (towards the tail) [41, 46]. Further, the ventral scales differ between snakes, and are primarily correlated with the surface properties and sizes of the materials they move over in their habitat (e.g. trees, sand, rock). The envi-

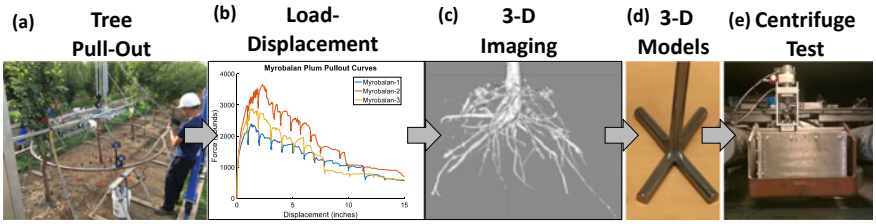

Fig. 7 Process of bio-inspired design from tree roots to inspired engineering solution. **a** Field tree pull-out tests, **b** load-displacement performance, **c** 3-D image reconstruction and analysis, **d** 3-D printed foundation models, and **e** centrifuge testing of 3-D models (courtesy of Jason T. DeJong)

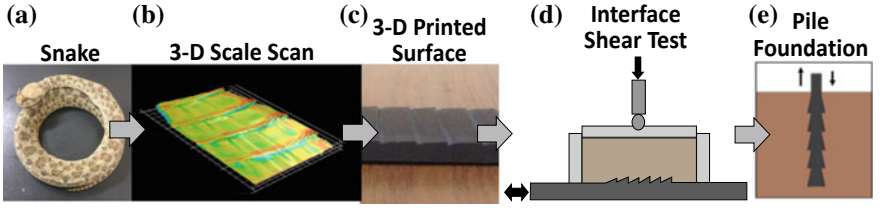

Fig. 8 Process of bio-inspired design from snake skin to inspired engineering solution. **a** Preserved snake specimens, **b** 3D scan of snake skin, **c** 3D printed snakeskin-inspired surfaces, **d** interface shear testing, and **e** centrifuge pile load testing of snakeskin-inspired piles (courtesy of Alejandro Martinez)

sioned end use is improved anisotropic soil-structure interface behavior that would improve performance and/or installation of piles, pipelines, and geomembranes [45]. The bio-inspired design process is outlined in Fig. 8.

5 Sustainability in Geotechnical Engineering Innovation

The responsibility of the civil engineer is to provide essential services to society and the built environment, both to individuals and the community at large. Safety is the highest priority in accomplishing this task. In a capitalistic marketplace, a second priority is cost. The desired services are to be provided safely using the most economical solutions. These two criteria (safety and cost) have driven, and continue to drive, final design selections. This approach, in combination with an assumption of nearly unlimited materials (e.g., cement) and energy (e.g., fuel) resources has led to the development of material- and energy-intensive geotechnical solutions and construction operations.

It is now widely recognized that there are serious environmental and societal costs to these approaches [3, 30] Conventional, brute force construction activities are exacerbating climate change, ozone depletion, deforestation, desertification, and soil erosion as well as land, water, and air pollution [40]. Moreover, the materials and resources that are used are finite. In time, these business as usual (BAU) technologies and methods must change.

The change, or rebalancing of the factors driving decision making must include environmental sustainability in addition to the existing criteria of safety and cost. The impacts of a given technology can be evaluated using life cycle assessment (LCA) and quantified in terms of environmental metrics like energy consumption, global warming potential, photochemical oxidation (i.e., smog formation) potential, or terrestrial acidification potential, among many others [39]. A comparative LCA can be used to quantify the impacts that geotechnical systems have and provide a basis for quantitative comparison between alternate solutions [34]. Preliminary work in this area has shown that the global warming potential between different ground

improvement methods can differ by a factor of 10 or greater [58], and between different earth retaining systems can differ by more than 3 times [13].

The criteria of safety must not be compromised, but the cost calculations can include a solution's sustainability cost in addition to capital costs. The challenge, of course, is that capital costs are measured in real dollars out of the investor's wallet, while the sustainability costs are realized in damages or equivalent dollars that society will experience, often to be realized in future time.

6 Closure

Collectively, the development of bio-mediated and bio-inspired geotechnical solutions, or biogeotechnical engineering, constitutes a rapidly growing emphasis in geotechnical engineering on nature-compatible and nature-inspired design and construction. This field lies at the confluence of geotechnical engineering and microbiology, geochemistry, zoology, and plant science, mobilizing biological processes to directly influence geotechnical systems. In the coming decades biogeotechnical engineering is expected to become part of mainstream geotechnical engineering due to improvements in performance efficiency, sustainability, and cost-effectiveness that may be realized. Figure 9 illustrates a vision for the biogeotechnical future along a transportation corridor [19].

The development of biogeotechnical solutions forces a paradigm shift in which geotechnical engineers must recognize and consider soil as a living ecosystem and not as a sterile, non-reactive, stable material. This will require training, or re-training, geotechnical engineers to be informed and engaged as biogeotechnical engineers [19].

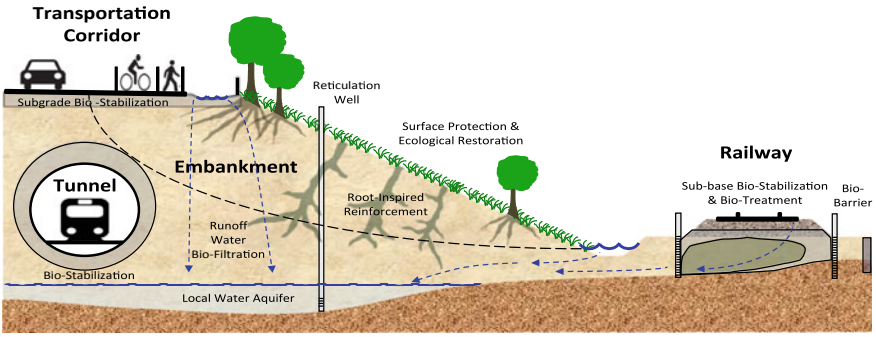

Fig. 9 Vision of bio-mediated and bio-inspired solutions along a travel corridor (used with permission from ASCE)

Acknowledgements The thoughts and ideas within this article have been informed and inspired by many individuals, but particularly by members of the NSF ERC Center for Bio-mediated and Bio-inspired Geotechnics, the Soil Interactions Laboratory at UC Davis, the Biogeotechnical Research Group at ASU, and collaborators who participated in the NSF-funded BioSoils workshops of 2007 and 2011. This material presented herein is in part based upon work supported in part by the National Science Foundation (NSF) under NSF CA No. EEC-1449501. Any opinions, findings and conclusions or recommendations expressed in this material are those of the author(s) and do not necessarily reflect those of the NSF.

References

1. Al Qabany, A., Soga, K.: Effect of chemical treatment used in MICP on engineering properties of cemented soils. Geotechnique **63**(4), 331–339 (2013). https://doi.org/10.1680/geot.SIP13.P.022
2. Allison, L.E.: Effect of microorganisms on permeability of soil under prolonged submergence. Soil Sci. **63**(6), 439–450 (1947)
3. Basu, D., Misra, A., Puppala, A.J.: Sustainability and geotechnical engineering: perspectives and review. Can. Geotech. J. **52**(1), 96–113 (2014)
4. Baum, M.J., Kovalev, A.E., Michels, J., Gorb, S.N.: Anisotropic friction of the ventral scales in the snake lampropeltis getula californiae. Tribol. Lett. **54**(2), 139–150 (2014)
5. Benini, S., Rypniewski, W.R., Wilson, K.S., Miletti, S., Ciurli, S., Mangani, S.: A new proposal for urease mechanism based on the crystal structures of the native and inhibited enzyme from bacillus pasteurii: why urea hydrolysis costs two nickels. Structure **7**(2), 205–216 (1999)
6. Benyus, J.M.: Biomimicry: innovation inspired by nature. William Morrow & Company, New York, NY. ISBN 978-0-688-16099-9 (1997)
7. Benyus, J.M.: Foreword: curating natures patent database. In': Goel, A.K., McAdams, D.A., Stone, R.B. (eds.) Biologically Inspired Design-Computational Methods and Tools, vii–xi (2014)
8. Chou, C.W., Aydilek, A., Seagren, E., Maugel, T.: Bacterially-induced calcite precipitation via ureolysis (2008)
9. Chou, C.W., Seagren, E.A., Aydilek, A.H., Lai, M.: Bio-calcification of sand through ureolysis. J. Geotech. Geoenviron. Eng. **137**(12), 1179–1189 (2011)
10. Chu, J., Ivanov, V., He, J., Naeimi, M., Li, B., Stabnikov, V.: Development of microbial geotechnology in Singapore. In: Geo-Frontiers 2011: Advances in Geotechnical Engineering, pp. 4070–4078 (2011)
11. Coutts, M., Nielsen, C., Nicoll, B.: The development of symmetry, rigidity and anchorage in the structural root system of conifers. Plant Soil **217**(1–2), 1–15 (1999)
12. Cunningham, A.B., Characklis, W.G., Abedeen, F., Crawford, D.: Influence of biofilm accumulation on porous media hydrodynamics. Environ. Sci. Technol. **25**(7), 1305–1311 (1991)
13. Damians, I.P., Bathurst, R.J., Adroguer, E.G., Josa, A., Lloret, A.: Environmental assessment of earth retaining wall structures. Environ. Geotech. **4**(6), 415–431 (2016)
14. Day, J.L., Ramakrishnan, V., Bang, S.S.: Microbiologically induced sealant for concrete crack remediation. In: Processing of 16th Engineering Mechanics Conference, pp. 1–8. Seattle, America (2003)
15. DeJong, J., Mortensen, B., Martinez, B.: Bio-soils interdisciplinary science and engineering initiative. In: Final Report on Workshop, 84 pp. National Science Foundation, Arlingon, VA, USA (2007)
16. DeJong, J. T., Burrall, M., Wilson, D. W., Frost, J. D.: A Bio-inspired perspective for geotechnical engineering innovation. In: Geotechnical Frontiers: Geotechnical Materials, Modeling, and Testing, pp. 862–870 (2017)

17. DeJong, J.T., Fritzges, M.B., Nusslein, K.: Microbial induced cementation to control sand response to undrained shear. ASCE J. Geotech. Geoenviron. Eng. **132**(11), 1381–1392 (2006)
18. DeJong, J.T., Mortensen, M.B., Martinez, B.C., Nelson, D.C.: Bio-mediated soil improvement. Ecol. Eng. **36**(2), 197–210 (2010)
19. DeJong, J.T., Soga, K., Banwart, S.A., Whalley, W.R., Ginn, T., Nelson, D.C., Mortensen, B.M., Martinez, B.C., Barkouki, T.: Soil engineering in vivo: harnessing natural bio-geochemical systems for sustainable, multi-functional engineering solutions. J. R. Soc. Interface **8**(54), 1–15 (2011)
20. DeJong, J.T., Soga, K.S., Kavazanjian, E., Burns, S., van Paassen, L., Al Qabany, A., Aydilek, A., Bang, S.S., Burbank, M., Caslake, L., Chen, C.Y., Cheng, X., Chu, J., Ciurli, S., Fauriel, S., Filet, A.E., Hamdan, N., Hata, T., Inagaki, Y., Jefferis, S., Kuo, M., Laloui, L., Larrahondo, J., Manning, D.A.C., Martinez, B., Montoya, B.M., Nelson, D.C., Palomino, A., Renforth, P., Santamarina, J.C., Seagren, E.A., Tanyu, B., Tsesarsky, M., Weaver, T.: Bio-geochemical processes and geotechnical applications: progress, opportunities and challenges. Geotechnique **63**(4), 287–301 (2013)
21. Esnault-Filet, A., Gadret, J.P., Loygue, M., Borel, S.: Biocalcis and its application for the consolidation of sands. In: Johnsen, L.F., Bruce, D.A., Byle, M.J. (eds.) Grouting and deep mixing, Geotechnical Special Publication 288, vol. 2, pp. 1767–1780. ASCE, Reston, VA, USA (2012)
22. Fauriel, S.: Bio-chemo-hydro-mechanical modeling of soils in the framework of microbial induced calcite precipitation. Ph.D. thesis, Ecole Polytechnique Federale de Lausanne, Switzerland (2012)
23. Frankenberger, W.T., Troeh, F.R., Dumenil, L.C.: Bacterial effects on hydraulic conductivity of soils. Soil Sci. Soc. Am. J. **43**(2), 333–338 (1979)
24. Frost, J.D., Martinez, A., Mallett, S.D., Roozbahani, M.M., DeJong, J.T.: Intersection of modern soil mechanics with ants and roots. In: Geotechnical Frontiers 2017: Geotechnical Materials, Modeling, and Testing, pp. 862–870 (2017)
25. Goel, A.K., Vattam, S., Wiltgen, B., Helms, M.: Information-processing theories of biologically inspired design. In: Biologically Inspired Design, pp. 127–152. Springer (2014)
26. Gomez, M.G., Anderson, C.M., Graddy, C.M., DeJong, J.T., Nelson, D.C., Ginn, T.R.: Large-scale comparison of bio-augmentation and biostimulation approaches for biocementation of sands. J. Geotech. Geoenviron. Eng. **143**(5), 04016124 (2017)
27. Gomez, M.G., DeJong, J., Anderson, C.M.: Effect of biocementation on geophysical and cone penetration measurements in sands. Can. Geotech. J., in press (2018)
28. Graddy, C.M., Gomez, M.G., Kline, L.M., Morrill, S.R., DeJong, J.T., Nelson, D.C.: Diversity of *Sporosarcina*-like bacterial strains obtained from meter-scale augmented and stimulated biocementation experiments. Environ. Sci. Technol. **52**(7), 3997–4005 (2018)
29. Hata, T., Tsukamoto, M., Inagaki, Y., Mori, H., Kuwano, R., Gourc, J.: Evaluation of multiple soil improvement techniques based on microbial functions. In: Geo-Frontiers 2011: Advances in Geotechnical Engineering, ASCE Geotechnical Special Publication 211, pp. 3945–3955, Dallas, TX (2011)
30. Horvath, A.: Construction materials and the environment. Annu. Rev. Environ. Resour. **29**, 181–204 (2004)
31. Hoskins, B.C., Fevang, L., Majors, P.D., Sharma, M.M., Georgiou, G.: Selective imaging of biofilms in porous media by NMR relaxation. J. Magn. Reson. **139**(1), 67–73 (1999)
32. Ivanov, V.: Microbial geotechniques. Environmental microbiology for engineers. CRC Press, Boca Raton, FL, USA. pp. 279–286 (2010)
33. Ivanov, V., Chu, J.: Applications of microorganisms to geotechnical engineering for bioclogging and biocementation of soil in situ. Rev. Environ. Sci. Bio/Technol. **7**(2), 139–153 (2008)
34. ISO (International Organization for Standardization): ISO 14044:2006: Environmental management—life cycle assessment—requirements and guidelines. ISO, Geneva, Switzerland (2006)
35. Karol, R.H.: Chemical grouting and soil stabilization, p. 558. Marcel Dekker, New York, NY, USA (2003)

36. Kavazanjian, E., Hamdan, N.: Enzyme induced carbonate precipitation (EICP) columns for ground improvement. In: International Foundation Congress and Equipment Exposition (IFCEE 2015), pp. 2252–2261. ASCE Geotechnical Special Publication. https://doi.org/10.1061/9780784479087.209 (2015)
37. Kavazanjian, Jr. E., Almajed, A., Hamdan, N.: Bio-inspired soil improvement using EICP soil columns and soil nails. In: Proceedings of Grouting 2017, ASCE. https://doi.org/10.1061/9780784480793.002 (2017)
38. Kavazanjian, E. Jr., Karatas, I.: Microbiological improvement of the physical properties of soil. In: Proceedings of the 6th International Conference on Case Histories in Geotechincal Engineering, Rolla, MO (CD-ROM) (2008)
39. Kendall, A., Raymond, A.J., Tipton, J., DeJong, J.T.: Review of life-cycle-based environmental assessments of geotechnical systems. In: Engineering Sustainability, vol. 171, pp. 57–67. Thomas Telford Ltd. (2017)
40. Kibert, C.J.: Sustainable construction: green building design and delivery, 4th edn. Wiley, New Jersey (2016)
41. Martinez, A., Palumbo, S.: Anisotropic shear behavior of soil-structure interfaces: bio-inspiration from snake skin. In: In Proceedings for International Foundations Congress and Equipment Expo, pp. 94–104, Orlando, FL (2018)
42. Martinez, B.: Experimental and numerical upscaling of MICP for soil improvement. Doctoral dissertation, University of California, Davis, CA, USA (2012)
43. Martinez, B., DeJong, J., Ginn, T., Montoya, B., Barkouki, T., Hunt, C., Tanyu, B., Major, D.: Experimental optimization of microbial-induced carbonate precipitation for soil improvement. J. Geotech. Geoenviron. Eng. **139**(4), 587–598 (2013)
44. Martinez, B.C., DeJong, J.T.: Bio-mediated soil improvement: load transfer mechanisms at the micro-and macro-scales. In: Advances in Ground Improvement: Research to Practice in the United States and China, pp. 242–251 (2009)
45. Martınez, A.J., O'Hara, K.: Monotonic and cyclic centrifuge testing of snake skin-inspired piles. Submitted for publication in 2019 GeoCongress. Philadelphia, PA (2019)
46. Martinez, A., Palumbo, S.: Anisotropic load transfer mechanisms at bio-inspired soil-structure interfaces. Submitted for possible publication in J. Geotechn. Geoenviron. Eng. (2019)
47. Marvi, H., Hu, D.L.: Friction enhancement in concertina locomotion of snakes. J. R. Soc. Interface **9**, 3067–3080 (2012)
48. Mickovski, S.B., Bengough, A.G., Bransby, M.F., Davies, M.C.R., Hallett, P.D., Sonnenberg, R.: Material stiffness, branching pattern and soil matric potential affect the pull out resistance of model root systems. Eur. J. Sci. **58**, 1471–1481 (2007)
49. Mitchell, J.K., Santamarina, J.C.: Biological considerations in geotechnical engineering. J. Geotech. Geoenviron. Eng. **131**(10), 1222–1233 (2005)
50. Mitchell, J.K.: Fundamentals of Soil Behavior. Wiley, New York, NY, USA (1975)
51. Montoya, B., DeJong, J.: Stress-strain behavior of sands cemented by microbially induced calcite precipitation. J. Geotech. Geoenviron. Eng. **141**(6), 04015019 (2015)
52. Mortensen, B.M., Haber, M., DeJong, J.T., Caslake, L.F., Nelson, D.C.: Effects of environmental factors on microbial induced calcite precipitation. J. Appl. Microbiol. **111**(2), 338–349 (2011)
53. Nature Reviews Editorial: Microbiology by numbers. Nat. Rev. Microbiol. **9**, 628 (2011). https://doi.org/10.1038/nrmicro2644
54. O'Donnell, S.T., Rittmann, B.E., Kavazanjian Jr.: Liquefaction mitigation via microbial denitrification as a two-stage process. Stage I: desaturation. J. Geotech. Geoenviron. Eng. **143**(12), 04017094. https://doi.org/10.1061/(asce)gt.1943-5606.0001818, December (2017)
55. Proto, C., DeJong, J., Nelson, D.: Bio-mediated permeability reduction of saturated sands. J. Geotech. Geoenviron. Eng. **142**(12), 04016073 (2016)
56. Qabany Al, A.: Microbial carbonate precipitation in soils. Doctoral dissertation, University of Cambridge, UK (2011)
57. Raiders, R., McInerney, M., Revus, D., Torbati, H., Knapp, R., Jenneman, G.: Selectivity and depth of microbial plugging in Berea sandstone cores. J. Ind. Microbiol. **1**(3), 195–203 (1986)

58. Raymond, A.J., Pinkse, M.A., Kendall, A., DeJong, J.T.: Life-cycle assessment of ground improvement alternatives for the Treasure Island, California, redevelopment. In: Geotechnical Frontiers 2017, pp. 345–354, Orlando, FL (2017)
59. Rusu, C., Cheng, X.H., Li, M.: Biological clogging in Tangshan sand columns under salt water intrusion by *Sporosarcina pasteurii*. Adv. Mater. Res. **250**, 2040–2046 (2011)
60. Seagren, E.A., Aydilek, A.H.: Biomediated geomechanical processes. In: Mitchell, R., Gu, J.-D. (eds.) Environmental Micro-biology, 2nd edn, pp. 319–348. Wiley, Hoboken, NJ, USA (2010)
61. Sharp, R.R., Stoodley, P., Adgie, M., Gerlach, R., Cunningham, A.: Visualization and characterization of dynamic patterns of flow, growth and activity of biofilms growing in porous media. Water Sci. Technol. **52**(7), 85–90 (2005)
62. Stabnikov, V., Naeimi, M., Ivanov, V., Chu, J.: Formation of water-impermeable crust on sand surface using biocement. Cem. Concr. Res. **41**(11), 1143–1149 (2011)
63. Tagliaferri, F., Waller, J., Ando, E., Hall, S.A., Viggiani, G., Bésuelle, P., DeJong, J.T.: Observing strain localisation processes in bio-cemented sand using x-ray imaging. Granular Matter **13**(3), 247–250 (2011)
64. Van Paassen, L.: Bio-mediated ground improvement: from laboratory experiment to pilot applications. In: Geo-Frontiers 2011: Advances in Geotechnical Engineering, ASCE Geotechnical Special Publication 211, pp. 4099–4108, Dallas, TX (2011)
65. Van Paassen, L.A., Ghose, R., van der Linden, T.J., van der Star, W.R., van Loosdrecht, M.C.: Quantifying biomediated ground improvement by ureolysis: large-scale biogrout experiment. J. Geotech. Geoenviron. Eng. **136**(12), 1721–1728 (2010)
66. Van Paassen, L., Harkes, M., Van Zwieten, G., Van der Zon, W., Van der Star, W., Van Loosdrecht, M.: Scale up of biogrout: a biological ground reinforcement method. In: Proceedings of the 17th international conference on soil mechanics and geotechnical engineering, pp. 2328–2333. Lansdale IOS Press (2009)
67. Vogel, S.: Cat's Paws and Catapults: Mechanical Worlds of Nature and People. W. W. Norton & Company Inc, New York, NY (1998)
68. Wacey, D., Kilburn, M.R., Saunders, M., Cliff, J., Brasier, M.D.: Microfossils of sulfur metabolizing cells in 3.4 billion-year-old rocks of Western Australia. Nature Geosci. **4**(10), 698–702 (2011)
69. Whiffin, V.S., van Paassen, L.A., Harkes, M.P.: Microbial carbonate precipitation as a soil improvement technique. Geomicrobiol. J. **24**(5), 417–423 (2007)
70. Whitman, W.B., Coleman, D.C., Wiebe, W.J.: Prokaryotes: the unseen majority. Proc. Natl. Acad. Sci. **95**(12), 6578–6583 (1998)
71. Xanthakos, P.P., Abramson, L.W., Bruce, D.A.: Ground Control and Improvement. Wiley, New York, NY (1994)

Fundamental Challenges in Unsaturated Soil Mechanics

William J. Likos, Xiaoyu Song, Ming Xiao, Amy Cerato and Ning Lu

Abstract Fundamental challenges in unsaturated soil mechanics have been identified in four major areas: quantifying internal stress state, developing a new paradigm for soil classification, developing new computational and theoretical constructs for unsaturated soil behavior, and tackling emerging problems in geotechnical engineering practice from the perspective of unsaturated soil mechanics. This chapter addresses each of these needs by critically reviewing some of the history in each area and summarizing recent research advances as current understanding of unsaturated soil behavior continues to evolve.

Keywords Unsaturated soil · Suction · Expansive soil · Effective stress · Molecular dynamics · Multiscale

W. J. Likos (✉)
University of Wisconsin-Madison, Madison, WI, USA
e-mail: likos@wisc.edu

X. Song
University of Florida, Gainesville, FL, USA

M. Xiao
Pennsylvania State University, University Park, PA, USA

A. Cerato
University of Oklahoma, Norman, OK, USA

N. Lu
Colorado School of Mines, Golden, CO, USA

N. Lu and J. K. Mitchell (eds.), *Geotechnical Fundamentals for Addressing New World Challenges*, Springer Series in Geomechanics and Geoengineering,
https://doi.org/10.1007/978-3-030-06249-1_8

1 Introduction

Fundamental challenges in unsaturated soil mechanics have been identified in four major areas driven by four major needs. These include the need to resolve a generally applicable and practically implementable way to quantify internal stress state in unsaturated soils, the need to develop a new paradigm for soil classification on the basis of fundamental soil properties rather than index properties that only indirectly capture soil behavior, the need to support limited experimental evidence for unsaturated soil behavior by developing new computational and theoretical constructs, and the need to tackle emerging problems in geotechnical engineering practice from the perspective of unsaturated soil mechanics.

Many of the fundamental research challenges in unsaturated soil mechanics identified here also have significant overlap with other theme areas described in this volume. Among others, these include bio-mediated geo-processes, which are often near-surface problems that depend on phenomena occurring at air-water interfaces (e.g., evaporation, solid/gas solubility), thermal energy and foundations, which often involve heat transport and storage in partially saturated soils, multiphysics and mechanics, where upscaling from particle or pore scale phenomena to larger scales remains a major challenge, and coupled phenomena, where unsaturated soils are ubiquitous (e.g., precipitation-induced slope failure, waste storage and containment, energy geotechnics, contaminant transport). Overlap between the research challenges in unsaturated soils and the challenges described throughout this volume reflects the importance and relevance of unsaturated soil mechanics. Broad impact may be achieved when advances in the many challenges involving unsaturated soils are made.

2 Internal Stress State

One of the historical challenges required to establish a robust predictive framework for the mechanical behavior of unsaturated soil has been to resolve a generally applicable and practically implementable way to quantify internal stress state. By internal stress state, we refer to a notion similar to Terzaghi's effective stress for saturated soils, but which also includes local interparticle forces that arise under both saturated and unsaturated conditions. Terzaghi's effective stress describes forces that propagate through the soil skeleton and is quantified or controlled in experiments with macroscopic stresses applied at the boundary level (total stress and pore water pressure) [128]. Internal stress state, on the other hand, includes these skeletal forces, as well as local forces that concentrate at or near particle contacts. Such forces arise from physicochemical or cementation effects, and uniquely in unsaturated soils from the effects of capillarity. Passive particle-particle contact forces must develop to counterbalance the active skeletal and local forces, which leads to an internal stress state that depends on soil fabric and magnitude of the internal forces [99]. It is this internal stress

state that governs mechanical soil behavior such as shear strength, tensile strength, stiffness, and volume change. Changes in stress state that result from changes in either the boundary stress (e.g., from external loading) or from changes in the internal stress (e.g., from wetting or drying) have a consequent effect on unsaturated soil behavior. A framework for quantifying internal stress state and its evolution with saturation, pore water potential, and wetting-drying or loading-unloading history is thus essential to effectively and fully capture mechanical behavior of unsaturated soils.

2.1 Effective Stress in Unsaturated Soil

Karl Terzaghi's effective stress (σ') is the cornerstone of modern soil mechanics. Mathematically, Terzaghi's effective stress is defined as the difference between total stress (σ) and pore water pressure (u_w):

$$\sigma' = \sigma - u_w \tag{1}$$

and has been widely used for characterizing strength and deformation (consolidation) behavior for soil under saturated conditions. It is not suitable, however, for soil under unsaturated conditions. This is because pore water pressure, or by extension matric suction (quantified as the difference between pore air pressure and pore water pressure, $(u_a - u_w)$, is fundamentally not a stress variable [99].

Until recently, two mutually exclusive approaches have been used to quantify stress state for unsaturated soils: Bishop's effective stress approach [14] and Fredlund and Morgenstern's independent stress state variable approach [49]. In Bishop's effective stress approach, the skeleton stress includes two independent components: net normal stress $(\sigma - u_a)$ and net pore pressure, or matric suction $(u_a - u_w)$. The latter is weighted by a coefficient χ such that:

$$\sigma' = (\sigma - u_a) - [-\chi (u_a - u_w)] \tag{2}$$

The parameter χ has been suggested to be a function of degree of saturation (S) constrained between 0 when soil is dry and 1 when soil is saturated ($0 \leq \chi(S) \leq 1$). Determining the form of $\chi(S)$, however, has historically been a challenge because when soil approaches a dry state, χ is presumably close to zero, but matric suction could be very high (likely on the order of 1 GPa), thus producing unrealistically large values for the product $\chi(u_a - u_w)$. For other erroneous reasons, and not necessarily all due to the form of Eq. (2), Bishop's effective stress had been questioned since the late 1960s [99].

A different paradigm spearheaded by Fredlund and Morgenstern [49] became popular in the 1980s and 1990s. Here two independent stress state variables, net normal stress $(\sigma - u_a)$ and matric suction $(u_a - u_w)$, were used to construct theories

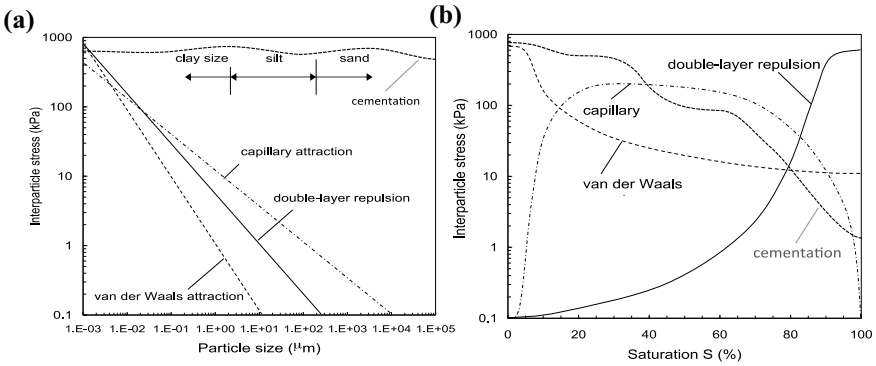

Fig. 1 Suction stress components and dependence on **a** soil type and **b** saturation (after [98])

for shear strength (e.g., [50]) and volumetric strain (e.g., [5]). These theories and others based on two independent stress state variables have encountered practical and theoretical problems that have precluded a unified and effective framework for describing soil strength and deformation. Lu and Likos [99] clarified that matric suction, although it has units of stress per se, is fundamentally not a stress variable. Considering matric suction as a stress quantity in such theories for strength and deformation is thus physically incorrect.

By around the turn of this century, experimental data for various soil types became available to demonstrate that Bishop's effective stress can be effective for predicting shear strength for matric suction less than about 1500 kPa [66, 67]. At higher suction and corresponding lower water content, however, some data indicate that Bishop's effective stress may not be valid, most notably for fine-grained soils. Starting in the early 2000s, Lu and associates launched a series of studies to clarify what had been missing or incorrect in Bishop's effective stress and the independent stress state variable approaches. Lu and Likos [99] concluded that Bishop's effective stress only considers the contribution of pore fluid pressure (u_a and u_w) and inherently overlooks the contribution of inter-particle physicochemical forces, namely those associated with van der Waals and electrical double layer forces. An interparticle stress intended to capture both fluid pressure and physicochemical stresses, referred to as suction stress (σ^s) was coined, along with the suction stress characteristic curve (SSCC) to capture how suction stress depends on pore water potential (ψ) or saturation [i.e., $\sigma^s(\psi)$ or $\sigma^s(S)$].

Components of suction stress and their variation with soil type and saturation are illustrated semi-quantitatively in Fig. 1. The suction stress concept unifies effective stress under both saturated and unsaturated conditions and is in the same form as Terzaghi's effective stress, which has practical significance because it is readily implementable within the classical saturated soil mechanics framework. Effective stress according to the suction stress construct is [99]:

$$\sigma' = (\sigma - u_a) - \sigma^s \tag{3}$$

where σ^s recovers to pore water pressure when a soil is saturated but varies characteristically according to the SSCC as saturation changes.

Lu and Likos [99] synthesized existing shear strength data at the time and demonstrated that the SSCC based effective stress Eq. (3) is valid for predicting shear strength. Shear strength under both saturated and unsaturated conditions can be predicted using historically established failure criteria (e.g., Mohr-Coulomb), so there is no need to construct different failure criteria or create additional material parameters for unsaturated conditions. Further advances have included developing a closed form equation for the SSCC [93], establishing a link between the SSCC and the soil water retention curve (SWRC) [95], and establishing a link between the SSCC and deformation behavior [94]. Each of these developments is described in Chapter 4 "Linking Soil Water Adsorption to Geotechnical Engineering Properties".

2.2 Hydration-Capillary Transition

Adsorption and retention of soil pore water occur primarily by two mechanisms: (i) short-ranged physicochemical mechanisms, which include surface hydration on mineral surfaces at low water content, hydration of exchangeable cations, and osmotic interlayer swelling for expandable clay minerals; and (ii) capillary condensation in larger pores at higher water content. Factors controlling water adsorption and retention in the hydration regime are associated primarily with properties of soil mineral surfaces, including mineralogy, specific surface area (SSA or S_a), cation exchange capacity (CEC), and exchangeable cation type. Factors controlling water adsorption and retention in the capillary regime, on the other hand, are associated primarily with pore and particle fabric features, including pore size, pore size distribution, and pore connectivity. Differentiation between these two retention regimes and pore water within them has been suggested using a number of qualitative descriptors, including "hygroscopic water" versus "free water," "bound water" versus "capillary water," "microscopic" versus "macroscopic" water, and "tightly adsorbed, adsorbed, and capillary" water.

Transition between a water retention regime dominated by surface hydration at low moisture content and a water retention regime dominated by capillary mechanisms at higher water content corresponds to a transition in mechanical soil behavior. For coarse-grained soils such as sand, where surface hydration is minor due to its low surface area, the capillary-hydration transition is relatively unimportant in terms of mechanical behavior. For fine-grained soils such as clay, on the other hand, where surface hydration is a major mechanism for water retention over a wide range, the capillary-hydration transition and the implications to mechanical behavior are more significant, but less clear [2].

Both Bishop's effective stress and the independent stress state variable approach implicitly assume the validity of pore pressure concept because matric suction has

been defined as the difference between the air and water pressure ($u_a - u_w$). In light of the physics of soil water retention, capillary water retention requires a pressure difference between the pore air and pore water, whereas water retention by short-ranged adsorption does not [96]. Adsorption energy can thus only be defined in terms of matric potential and not in terms of a pressure. Pore water pressure is a special case only when capillary water exists, which is the case in fine-grained soils at relatively high water content or in coarse-grained soils over a wide range of saturation.

A new paradigm to define stress state variables in unsaturated soil is needed. This first requires developing SWRC models capable of distinguishing between adsorption water and capillary water. Unified formulations for water retention in porous media, for example, have been proposed to independently capture adsorbed water and capillary water (e.g., [11, 75, 89, 115, 121, 150]). Revil and Lu [121] and Lu [90] explicitly differentiated hydration and capillary water by employing local thermodynamic equilibrium principles. Such models provide a physical basis for developing more general SSCC models that may be applicable for capturing effective stress over a wide range of saturation. Ultimately, suction stress could be divided into two components to differentiate a component due to adsorption (σ_a^s) and a component due to capillarity (σ_c^s):

$$\sigma^s(\psi) = \sigma_a^s(\psi) + \sigma_c^s(\psi) \tag{4}$$

but there is currently no closed-form model for suction stress due to adsorption.

While knowledge of suction stress attributable to adsorption is in its infancy, insight can be gained from experimental evidence and theoretical considerations (e.g., [3, 92, 94, 96]). As shown in Fig. 1, for example, suction stress due to capillarity is zero at either the dry or saturated state, and reaches a maximum at some intermediate saturation [96]. SSCCs for sandy soils deduced from shear and tensile strength test results have been shown to follow this general trend because capillary water retention dominates over essentially the complete range of saturation. Because matric potential due to capillarity can be quantified in terms of fluid pressure, the SSCC proposed by Lu and Likos [99] as the product of ($u_w - u_a$) and effective degree of saturation (S_e) has become an effective representation for sandy soils. In contrast, because suction stress due to physicochemical stresses could be very high at the dry state and non-zero at the saturated state, most notably for fine-gained soils, its magnitude could be very high (several hundreds of kPa), and its variation with saturation could be quite different. Experimental evidence indicates that suction stress could be on the order of several hundreds of kPa for dry bentonite [42] and is non-monotonic over a wide range of saturation for kaolinite [2]. Because physicochemical stresses also depend on the soil fabric (structure and particle contacts) and the mineral and pore fluid chemical characteristics, suction stress cannot be fully defined by matric potential and saturation alone. Resolving this challenge remains an active area of ongoing research.

3 Fundamentals-Based Soil Classification

Current soil classification frameworks based on grain size and plasticity only indirectly reflect fundamental material properties that govern soil behavior. A new paradigm for soil classification is viewed as central to solving current global societal and environmental challenges, including energy and resource needs, infrastructure development, environmental protection and enhancement, and protection and recovery from natural disasters [22]. There is a need for the geotechnical engineering community to approach these grand challenges from the perspective of fundamentals, rather than historical geotechnical engineering approaches reliant on empirical observation. Unsaturated soil mechanics has an important place in moving the state of practice toward this direction because the mineral-water interactions that occur at low water content are a direct reflection of fundamental mineral and surface characteristics with which soils may be more effectively classified.

Fine-grained soil behavior is dominated by interaction forces occurring at the interface between mineral surfaces and water. Soil compositional properties that influence these interactions, most notably specific surface area (SSA or S_a) and cation exchange capacity (CEC), are being increasingly recognized as valuable measures for characterizing fine-grained soils. Numerous studies have shown that SSA and CEC can be related to more general aspects of fine-grained soil behavior [26, 27], including Atterberg limits [34, 47, 109], dispersion and frost heave [9, 113, 123], swelling potential [1, 32, 40, 89, 108, 117, 125], and compressibility [26].

SSA quantifies surface area per unit mass (m^2/g) and can be differentiated into total surface area, external surface area, and, for expansive clays and diatomaceous soils, internal surface area. CEC, which is expressed in milliequivalents per 100 g of dry clay (meq/100 g or meq/g), is a measure of exchangeable mineral charge, where larger values reflect a greater layer charge and surface activity. A related property, surface charge density, is defined as CEC divided by SSA. Together SSA and CEC characterize the fundamental surface properties of soil minerals and play a critical role in governing interactions between mineral surfaces and molecules that approach the surface (e.g., [60, 111, 143]).

Robust consideration of fundamental mineral and surface properties has been lacking in all previous soil classification frameworks. Recent efforts, however, demonstrate a shift toward more fundamental approaches for soil classification. Lin and Cerato [84], for example, recognized the importance of SSA, CEC, mineralogy, microstructure, mineral-water-ion interactions, permittivity, electrical conductivity, and suction. As noted in Chapter 4 "Linking Soil Water Adsorption to Geotechnical Engineering Properties" of this volume, Jang and Santamarina [61] explicitly recognized the lack of consideration of pore-fluid chemistry and proposed an approach for fines classification based on liquid limits obtained with electrically contrasting pore fluids. Methods have been established for determining water vapor sorption isotherms of clays [79], and to link sorption isotherms to SSA [2, 3, 68] and CEC [96]. Direct linkages among SSA, CEC, Atterberg limits, and volume change have

been established [42, 90, 91]. These types of studies provide a basis for implementation in new soil classification frameworks.

3.1 Microstructural Clay Parameters

Expansive soil—that is, clayey soil that experiences volumetric swelling or shrinkage with adsorption or desorption of water—covers one-fourth of the United States, and is distributed worldwide in semi-arid or arid regions in China, Brazil, and the Middle East. Expansive soil poses potential damage to foundations for structures, bridges, and roads and can induce landslides along transportation corridors. On the other hand, expansive soil can be beneficial when used as low hydraulic conductivity lining material for canals or irrigation ducts, as engineered clay barrier material for nuclear waste repositories, or to retard the movement of gas and liquid phase contaminants at disposal sites such as landfills.

Understanding the microstructure of expansive soils is of vital importance in physical interpretation and mechanical modeling of expansive soil behavior at the macro-scale [124]. Currently, design engineers cannot reliably predict how an expansive soil will behave at the macroscale in terms of volume change and shear strength because the controlling mechanisms are complex and governed by surface physicochemical forces rather than mechanical forces. Volume change of expansive clay in response to water sorption (or desorption) includes two mechanisms. The first, crystalline swelling, is controlled by interlayer forces that cause hydration of crystalline surfaces [71, 76, 78, 110, 114, 163]. Crystalline swelling is confined to the first several water layers, depending on the particle composition and the aqueous chemistry in the external surface of the tetrahedral sheet [163]. Crystalline swelling thus describes the water holding capacity of clays at very low water contents (i.e., crystalline swelling takes place as a result from the hydration process upon first exposure to water or water vapor). The second mechanism, double-layer swelling [71, 163] or osmotic swelling [80, 105], originates from the chemical gradient between the phyllosilicate interlayer surface and the external environment (i.e., water in macropores). Volume change is manifest by expansion (or contraction) of the diffuse layer and is governed by interplay between surface forces such as capillary forces, Coulombian electrostatic attraction, van der Waals forces, and double layer repulsion [6–8, 105].

An innovative approach to characterize expansive soils and quantitatively predict volume change and swell pressure behavior lies in understanding surface phenomena for individual clay platelets or aggregates within the soil matrix and the interaction of contacting particles under the influence of various surface forces. It is the surface area and mineral composition of the soil solid phase, and the available cations of the external pore fluid that largely determine the nature and behavior of expansive soil, including its internal geometry and porosity, its mineralogy and geochemical composition, its interaction with fluids and solutes, and its mechanical behavior such as compressibility and strength.

Identification and quantification of surface forces, however, can be extremely challenging. SSA (S_a) and CEC are inherent soil properties that depend only on composition, pore fluid chemistry, and time, and therefore are fundamental in describing fine-grained soil behavior. Similarly, surface conductance (λ_{ddl}) can be estimated as the product of surface charge density and cation mobility [128] in the following form [84]:

$$\lambda_{ddl} = \frac{\sum u_i P_i \cdot CEC}{S_a} \tag{5}$$

where u_i is cation mobility and P_i is the percentage of each exchangeable cation (in quantity) in the exchange complex. Cation mobility determines the drift velocity of electrons mobilized under an applied electrical field. In addition to these four properties, there are at least seven other microscale properties that reflect soil composition, structure, and pore fluid chemistry. These include mineralogy, structure, elemental composition, diffuse double layer thickness (t), real relative permittivity (κ'), effective electrical conductivity (σ), and suction. Among these, diffuse double layer thickness, real relative permittivity, effective electrical conductivity, and suction are anticipated to govern the macroscopic behavior of expansive soil.

3.2 Sorption-Based Clay Characterization

Swelling potential of expansive soils is most commonly classified by correlation to routinely measured index and soil compositional properties, usually including Atterberg limits, clay content, and activity. Well-established techniques in this "plasticity-based" family include, for example, those proposed by Holtz and Gibbs [58], Seed et al. [130], and Chen [29]. Suction-based methodologies have also been proposed, including those by Johnson [63], McKeen and Nielson [102], and McKeen [101]. McKeen's methodology [101], for example, relies on determining a parameter referred to as the total suction – water content index to quantify the slope of the SWRC in the high suction range. Soils with a relatively flat SWRC adsorb a greater amount of water for a given change in suction than those exhibiting a relatively steep SWRC, and are thus classified as having higher swelling potential.

In many respects, suction-based expansive soil characterization methodologies are an advancement over plasticity-based methodologies by acknowledging that the source of volume change and swelling pressure is the energy released by adsorbing water from a high-energy state (free water condition) to a low energy state (adsorbed condition). Some of this energy translates to heat, some translates to work done as volume change, and some translates to work done as swelling pressure. The distribution between work done as volume change and work done as swelling pressure is governed by environmental factors such as particle fabric, density, confining conditions, pore fluid chemistry, and initial moisture conditions [130]. Despite the fundamental link between suction behavior and swelling behavior, however, practical difficulties with

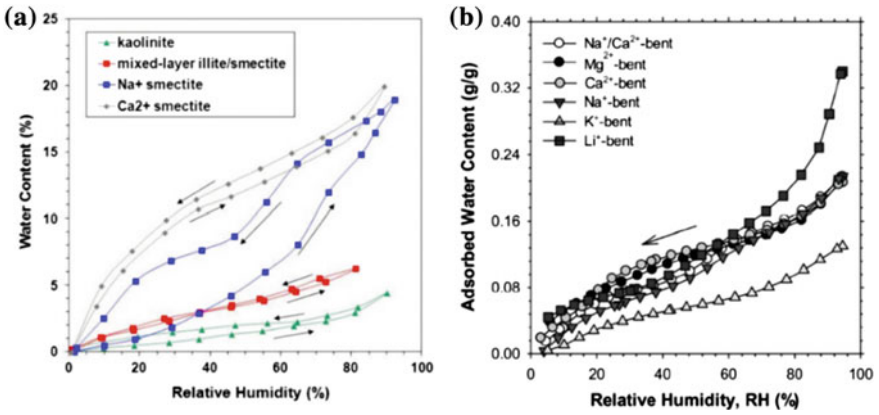

Fig. 2 Water vapor sorption isotherms illustrating the effects of **a** mineralogy [79] and **b** exchange cations [2]

measuring suction in practice have generally limited confidence in and accessibility to suction-based methodologies. Current suction-based methods require difficult and time consuming measurements, such that plasticity-based methods remain the norm [73].

When a hydrophilic material is placed in an atmosphere containing water vapor, water condenses on its surface under physical and chemical bonding mechanisms that decrease the energy of the adsorbed water. A water vapor sorption isotherm quantifies the relation between relative humidity (RH) of that atmosphere and equilibrium moisture content of the material along an adsorption and/or desorption path at some temperature. RH is a measure of water vapor pressure in the headspace of the atmosphere, and thus also quantifies the potential of the adsorbed water. Because RH and total soil suction are related by Kelvin's equation (e.g., [143]), a water vapor sorption isotherm is equivalent to an SWRC in the high suction range. A sorption isotherm, therefore, is a direct measure of how physical and chemical interactions between water and a mineral surface result in water retention, and thus is an indirect measure of fundamental compositional and surface properties (mineralogy, SSA, CEC).

Sorption isotherms for clays have been studied using a variety of experimental and computational approaches [25, 37, 78, 79, 81, 82, 102, 107, 151]. Figure 2a, for example, shows adsorption/desorption isotherms for samples of kaolinite, illite-smectite, Na^+-smectite, and Ca^{2+}-smectite obtained along wetting and drying paths using the mixed-flow apparatus of Likos and Lu [79]. Figure 2b shows isotherms obtained along sorption paths for bentonite exchanged to produce several homoionic forms (Mg, Ca, Na, K, Li) and a mixed Na/Ca form [2]. Together these results illustrate the influences of mineralogy and exchange cation on the shape, slope, and hysteresis of sorption isotherms for typical clays.

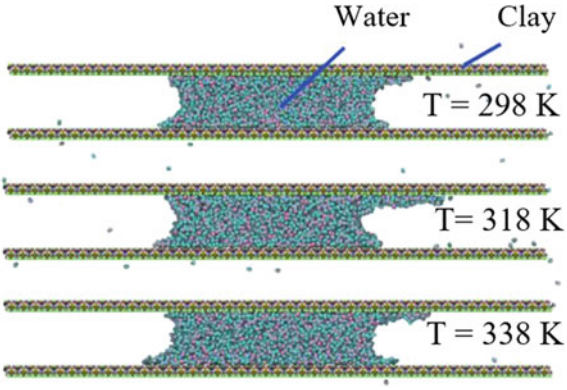

Fig. 3 Molecular dynamics simulation of clay-water system at different temperatures [142]

Sorption in the range of an isotherm (RH <~90%) is governed by several competing soil-water interaction mechanisms, most notably including hydrogen bonding between water and oxygens or hydroxyls comprising the mineral surfaces, dipole polarization effects arising from surface charge, van der Waals forces, and hydration of exchangeable cations residing at or near mineral surfaces [60, 96, 104, 111]. Adsorbed water resides in the form of thin films on the mineral surfaces and as "bunches" of water grouped about mineral charge sites and cations. As evident in Fig. 2b, cation type has a significant influence, where in general clays with smaller or higher valance cations adsorb more water than clays with larger or lower valence cations, a direct reflection of the differences in cation hydration energy [65, 152].

For expansive clay minerals, water is also adsorbed in the mineral interlayer space in a step-wise fashion associated with successive adsorption of discrete water layers (crystalline swelling) as evidenced by the wavy shape of the isotherm for the Na^+-smectite in Fig. 3a [76, 80, 114]. As RH increases to beyond about 80% to 90%, adsorbed films on the particle surfaces are generally thick enough to extend beyond the influence of short-ranged hydration mechanisms. At this point, coarse-grained and non-expansive soils enter a regime dominated by capillary water retention such that continued adsorption becomes a function of pore fabric, and thus is sensitive to compaction or disturbance. Depending on the type of the predominant exchange cation (for Na^+-smectite) and pore fluid chemistry, expansive soils enter a regime dominated by osmotic swelling driven by a gradient in osmotic potential between the solute-rich interlayer water and free water in the larger pores. A sorption isotherm might thus be used as a signature to differentiate water adsorption by crystalline, capillary, and osmotic swelling and potentially exploited for expansive soil classification. This remains an active area of research.

4 Computational Frameworks for Unsaturated Soil

Physical measurements of unsaturated soil behavior remain challenging, which limits the availability of quality experimental data by which emerging theoretical and empirical constructs for unsaturated soil behavior may be validated. Historical measurement techniques preclude comprehensive observations over a wide range of suction or soil type. Advances in computational experiments or modeling thus play an increasingly important role in obtaining better fundamental understanding of unsaturated soil properties and processes, including mineral-water interactions, pore fluid retention, soil fabric, strength, and coupled deformation and fluid flow in multiphase porous media. Several of these computational frameworks are described herein.

4.1 Strain Localization

Strain localization is a ubiquitous failure mode of geomaterials. In a localized deformation zone, geomaterials involve intense shear deformation that usually serves as a precursor of failure [15, 16, 140]. For this reason, numerous theoretical, experimental and computational research efforts have been conducted to study the inception of localized deformation and its triggering mechanism in geomaterials under dry or fluid saturated conditions [10, 15, 48, 126, 154]. Rudnicki and Rice [126] first derived a mathematical condition for the onset of shear banding in pressure-sensitive geomaterials. Recently, this mathematical criterion has been extended to study the drained [15, 133, 136] and transient bifurcation conditions at finite strain [134] for unsaturated soils. Results demonstrate that spatial variations of density and fluid saturation have a major influence on the inception of localized deformation. Researchers have also investigated the bifurcation of unsaturated geomaterials at the material point level via constitutive modeling under both isothermal and non-isothermal conditions [116, 129, 140].

While theoretical and experimental methods provide insight into localized deformation in multiphase geomaterials, computational modeling is a useful approach to study the onset and triggering mechanisms for localized deformation [23, 45, 74, 133]. For example, Callari et al. [23] studied localized deformation in unsaturated porous media via the finite element enhanced by strong discontinuities method in an effort to resolve the pathological mesh sensitivity issue with the finite element method [41]. A two-scale model was formulated to study fluid flow in an unsaturated and progressively fracturing porous medium [120]. Lazari et al. [74] formulated a non-local constitutive model to simulate localized deformation in unsaturated soil under non-isothermal conditions. However, few of these numerical formulations considered spatially varying material properties such as density and fluid saturation and the associated impacts on inception of localized deformation. Recent numerical investigations via a mesoscale finite element method have demonstrated that material heterogeneities, such as density and degree of saturation, have a first-order role in trig-

gering strain localization in unsaturated porous media [18, 19, 133, 134, 137–139]. However, such studies have been based on a numerical framework that assumes a passive pore air pressure and thus cannot capture the active role of gas movement and its impact on progressive failures such as slope failures [103]. Recently, Song et al. [141] formulated a three-phase numerical model for unsaturated soils via the stabilized mixed finite element method in which pore air pressure is considered explicitly. Numerical simulations demonstrate that a three-phase model with active pore air pressure is physically more appropriate to numerically simulate the inception of strain localization in unsaturated soils.

4.2 Molecular Dynamics

Clays and related phases present a particularly daunting set of challenges for the experimentalist and computational chemist. For this reason, molecular computer simulations have become helpful in providing an atomic perspective on the structure and behavior of clay minerals [39]. Molecular dynamics (MD) is a technique for computing the equilibrium and transport properties of a classical many-body system [4]. MD modeling is a useful tool for investigating the physical and chemical properties of materials at atomic scales. In MD, the positions, velocities, and accelerations of atoms in a molecular system are computed by numerically solving the equations of Newton's second law of motion. External force can be directly applied to selected atoms. Energy of the molecular system is expressed using suitable empirical potential energy functions or force fields.

Successful application of any computational molecular modeling technique requires the use of interatomic potentials (force fields) that effectively and accurately account for the interactions of all atoms in the system. In the geomechanics community, two force fields for clays, CHARMm [21] and CLAYFF [39], have been commonly applied. In the CHARMm force field, the total potential energy is expressed as the sum of the bounded energy and the non-bounded energy. The CLAYFF force field for clay minerals is a versatile force field built around the flexible version of the simple point charge (SPC) water model [12] to represent water, hydroxyl, and oxygen-oxygen interactions.

Ebrahimi et al. [44] used MD with the CLAYFF force field to simulate isothermal isobaric water adsorption of interlayer Wyoming Na-montmorillonite. In this work, nanoscale elastic properties of the clay-interlayer water systems were calculated from the potential energy of the model system at 0 K as a function of water uptake. Carrier et al. [24] investigated the elastic properties of swelling clay particles at finite temperature upon hydration via MD and found that the elastic properties of montmorillonite cannot be extrapolated from computation at 0 K. Teich-McGoldrick et al. [147] adopted the CLAYFF force field to determine the pressure and temperature dependence of the elastic properties of muscovite. Recently, Weinan [159] and Song et al. [142] studied the impact of temperature on capillary force between clay platelet particles via full-scale MD modeling (Fig. 3). These and other studies demonstrate

that MD simulation is a useful numerical technique for studying unsaturated soils at the atomistic scale and should continue to play a significant role in formulating an atomic-informed multiscale modeling technique.

4.3 Monte Carlo Simulations

While MD provides atomic-scale behavior of soil water interaction, it is limited to the nanometer scale. Many physical processes such as soil-water retention, evaporation, condensation, and heat transfer occur at the mesoscale or pore scale. Monte Carlo simulations provide excellent tools to upscale behavior at pore scale while retaining the physics at inter-atomic scales. For example, if capillary water distribution and air-water interface configuration in unsaturated soil are of interest, mesoscale Monte Carlo simulation (also called Coarse-Grained Monte Carlo or CG-MC) can be used to develop the soil-water retention curve resulting from the atomic scale interacting energies among air (vapor), liquid, and soil (solid) at the energy equilibrium state.

Similar to the Lattice Boltzmann method [30], the CG-MCS conceptualizes multiple individual molecules into effective groups that reside on lattice sites [69, 100]. However, these lattice site groups contain information only about which phase is most prevalent at that location [100, 164]. These lattice sites interact with neighboring sites through free-energetic interactions, and thus are capable of naturally capturing interfacial behavior. Just as molecular Monte Carlo simulation is an efficient alternative to MD, the CGMC is an efficient alternative to the Lattice Boltzmann method for coarse-grained simulations of local equilibrium phase distribution [164].

Figure 4 shows the results of a three-phase simulation of capillarity in Ottawa sand. The microXCT (micro X-ray computed tomography) technique was first used to obtain images of unsaturated Ottawa sand at different water saturations (Fig. 4a–d). The images of soil particles and pore water retained were used as the geometric domain for the CG-MCS. The results of the CG-MCS is shown in Fig. 4e–h under different matric potential conditions (also called grand canonical). Visual comparisons between the microXCT images and the CG-MCS are excellent in the occurrences and distribution of capillary water and pore air. The simulated results can be used to compute the soil-water retention curve and compared with the experimental results from the conventional Tempe cell method (Fig. 4i), and to calculate the specific surface areas and compared with that directly computed from the microXCT images (Fig. 4j). Excellent comparisons are obtained, indicating the validity of the CG-MCS methodology.

4.4 Multiscale Modeling

Multiphase porous media (e.g., unsaturated clay and sand) play a major role in geotechnical and geoenvironmental engineering (e.g., slope stability, embankment

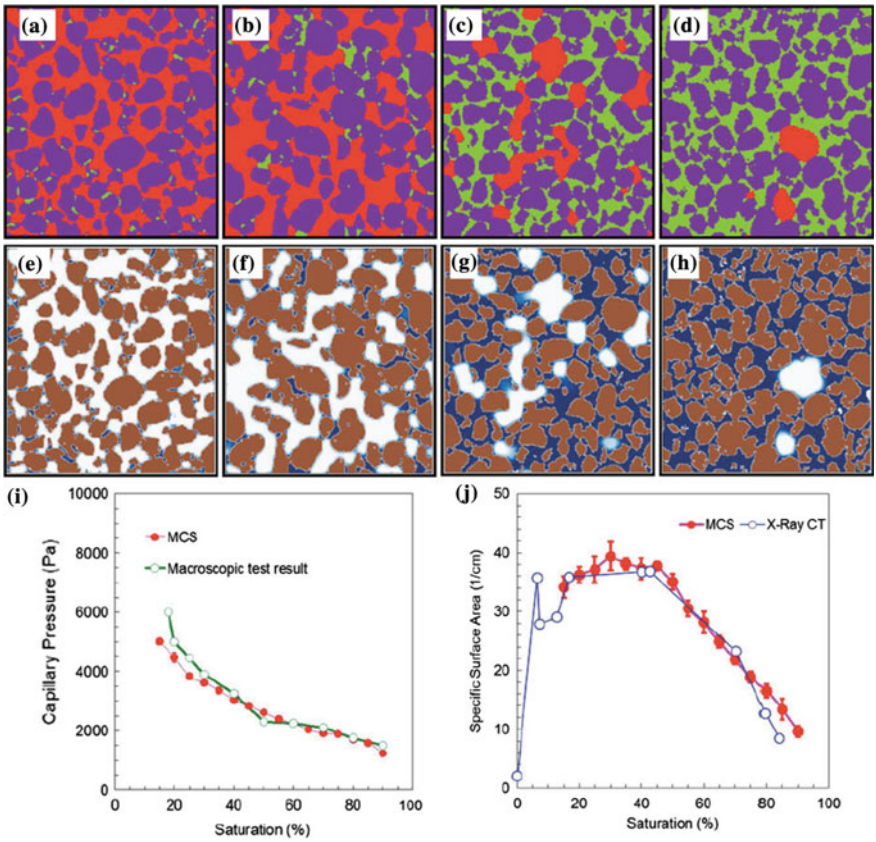

Fig. 4 Coarse-Grained Monte Carlo simulation of capillarity and soil-water retention curve of Ottawa sand: **a–d** microXCT images with saturations of 15, 25, 75, and 90% (solid as purple, gas as red, and water as green), **e–h** simulation results with the same saturations to **a–d** (solid as brown, gas as white, and water as blue), **i** comparison of soil-water retention curve between the experimental and simulated results, and **j** comparison of specific surface area between the experimental and simulated results [164]

erosion, and sinkholes) [50, 98]. However, current knowledge of fundamental mechanisms of the instability of multiphase porous media under environmental loads (e.g., humidity and temperature) is limited. Computational experiments are playing an increasingly important role in obtaining a better understanding of such failures, as well as more general coupled deformation and fluid flow phenomena in multiphase porous media. Concurrent and hierarchal multiscale computational modeling methodologies have been developed to study the instability of single phase materials (e.g., metal or dry granular materials) [88]. However, it is still challenging to formulate high-fidelity multiscale computational frameworks for modeling multiphase porous media, such as unsaturated soils. This deficiency is rooted in the limited knowledge of the physics (e.g., the interfaces among soil particles, water, and air for

unsaturated soils) of multiphase porous media at different length scales (e.g., nano, particle, and continuum scales) and the linkages between scales [159]. In particular, four challenges for multiscale modeling of unsaturated soils are: (1) understanding the physical models at different scales; (2) understanding how models of different complexity are related to each other; (3) understanding how models of different complexity can be coupled together smoothly, without creating artifacts; and (4) understanding how to formulate models at intermediate levels of complexity, (mesoscale models) [159]. To tackle these challenges, thermodynamic consistent average theory (TCAT) [53] can be used to upscale the physical properties of unsaturated soils at the pore scale [77] to the continuum scale and to formulate a thermodynamically-consistent multiscale model from the pore scale to the continuum scale for modeling unsaturated soils.

5 Emerging Problems in Unsaturated Soil Mechanics

5.1 Unsteady (Finger) Flow

Multiphase flow in porous media is a significant research topic in soil physics, agronomy, chemical engineering, petroleum engineering, environmental engineering, water resources, and geotechnical engineering. The last several decades have shown a tremendous increase in the number of theoretical and experimental studies on unstable (finger) flow in porous media (e.g., [46, 55, 59, 112, 157]). The fingering phenomenon was first described as viscous fingering in petroleum engineering (e.g., [33, 54, 59, 127, 146]). Since the late 1960s, unstable flow has been widely reported and described as gravity fingering in soils and fractured rocks during infiltration and redistribution by gravity. Unstable flow is distinct from other forms of preferential flows in that unstable flow occurs in both heterogeneous and homogeneous porous media.

Figure 5 shows an experimental observation of finger flow for water in uniform sand. This phenomenon is affected by capillarity, gravity, and pore structure and can be further complicated if there are varying characteristics of the liquid phase, such as non-aqueous phase liquids (NAPL). This research topic has implications for water resources and liquid contaminant management because fingering can move water and chemicals far below the expected root zone of wetting and can increase the possibility of groundwater contamination.

5.2 Multiphase Transport and Transfer in Rocks

In hydraulic fracturing for oil or natural gas extraction, multiphase flow interactions among gas, pore water, and fracking fluids with sand suspensions in dynamically

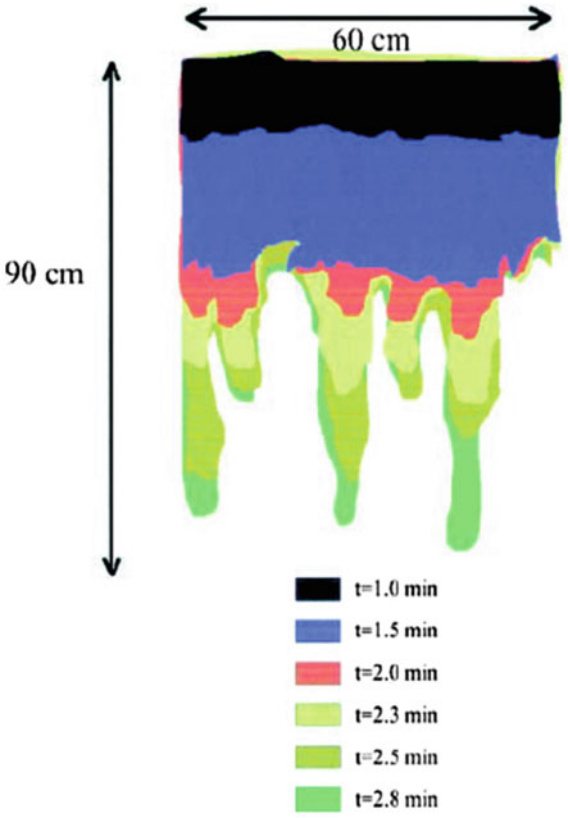

Fig. 5 Unstable (finger) flow occurring in homogeneous sand in flow redistribution experiments by Wang et al. [158]. The illustrated region is a subset of 1.0 m wide, 1.0 m deep, 1 cm thick slab chamber [64]

varying rock fractures under high pore pressure and stress may have significant scientific, engineering, and economic values. As illustrated in Fig. 6, gas transport through tight shales is a multi-mechanistic flow process including both Darcy and non-Darcy flows [35, 38, 62]. Assuming that only the Darcy's flow regime dominates, gas transport in porous rocks can be described by the one-dimensional mass balance equation [157]:

$$\varphi \frac{\partial \rho}{\partial t} + (1-\varphi)\frac{\partial q}{\partial t} = \frac{1}{r^m}\frac{\partial}{\partial r}\left(r^m \frac{\rho k}{\mu}\frac{\partial p}{\partial r}\right) \tag{6}$$

where t is time; ρ is gas density; q is adsorbate density per unit sample volume; φ is porosity of rock sample; p is pressure; k is Darcy permeability; μ is gas viscosity; r is pore radius, and $m = 0$, 1, and 2 represents slab, cylindrical, and spherical shapes, respectively. If one assumes that gas transport is dominated by gas diffusion through micropores and governed by Fick's law, Eq. (6) becomes [157]:

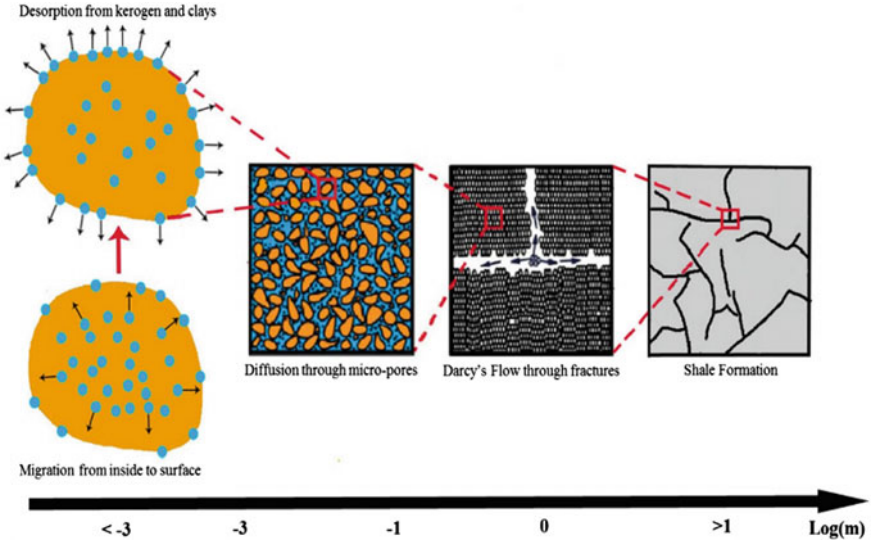

Fig. 6 Migration process of gas in shale formation (Image courtesy: Prof. Shimin Liu, Pennsylvania State University)

$$\varphi\frac{\partial\rho}{\partial t}+(1-\varphi)\frac{\partial q}{\partial t}=\frac{1}{r^m}\frac{\partial}{\partial r}\left(r^m\varphi D\frac{\partial p}{\partial r}\right) \tag{7}$$

where D is the diffusion coefficient.

The non-Darcy flows include sorption, diffusion, and slippage. Characterization of these non-Darcy flows in a shale matrix is challenging due to the complex pore structures from nano- to macroscale. For example, the absolute adsorption can be estimated by correcting Gibbs adsorption [36, 118, 122, 145]:

$$V_{\text{abs}}=\frac{V_{\text{Gibbs}}}{1-\rho_{\text{gas}}/\rho_{\text{ads}}} \tag{8}$$

where V_{abs} and V_{Gibbs} are the absolute and Gibbs sorption, respectively, and ρ_{gas} and ρ_{ads} are the gas densities in the gaseous and adsorbed phases respectively.

To date, the multi-mechanistic flow behaviors quantitatively described by apparent permeability have been characterized under unrepresentative field conditions. The impact of true in situ conditions on the apparent permeability and its evolution has not been investigated and the influence of the in situ fluid on pore structures and apparent permeability at elevated pressures remains largely unknown. In addition, gas adsorption to and desorption from shale organic matter causes surface energy variation of the organic matter and results in flow-induced micro-structuring, that is, micro-deformation of the organic matter [85, 87]. Limited effort has been made towards understanding this flow-induced micro-structuring for carbonaceous rocks [86, 156].

5.3 Multiphase Flow Under Microgravity

In space explorations, designing a reliable plant growth system for crop production requires an understanding of pore fluid distribution in unsaturated porous media under reduced gravity and microgravity. Spatial distribution of wetting fluids and discontinuous pore fluid ganglia under microgravity may strongly impact plant growth conditions, such as water transport and root uptake. With gravity, excess water drains along a vertical gradient, and water recovery is easily accomplished. Under microgravity, the distribution of water is less predictable and can lead to flooding as well as anoxia [57]. It is generally regarded that capillarity governs the multiphase flow and distribution in porous media under microgravity. Significant research has been conducted in the past several decades to study multiphase flow and distribution in porous media aboard the International Space Station (e.g., [106, 144]), using the parabolic flight of NASA KC-135 aircraft (e.g., [72, 119]), and through numerical simulations. In addition, due to soil particle rearrangement and pore restructuring that may occur under zero gravity, controlled delivery of water to the plant root zone remains a challenge in the exploration of plant growth under zero gravity, in which soil water retention characteristics are difficult to predict. So far research has focused on terrestrial conditions and zero gravity. The effect of varying gravity on multiphase flow and distribution in porous media is not well understood.

5.4 Erosion in Unsaturated Soil

Particle mobilization (erosion), transport, and immobilization (clogging) phenomena have been studied to understand internal erosion of earthen embankments such as levees and earthen dams and associated filter design. Soil erosion can be generally divided into surface erosion mechanisms such as runoff-induced erosion on slopes and scour in streams and subsurface or internal erosion mechanisms such as piping and suffusion. Briaud et al. [20] pointed out that soil particle dislodging (or mobilization) results from complex interactions of various forces, including electrical forces between particles, forces at contacts between particles, fluid pressure around particles, and shear stress around particles. The contributions of these forces to particle mobilization may vary with degree of saturation. Erodibility depends on soil properties such as water content and unit weight of soil and these soil properties are affected by degree of saturation. Soil erodibility can be represented by critical shear stress, which is the minimum hydraulic shear stress beyond which soil erosion occurs. Chen and Anderson [31] proposed an equation for the critical shear stress for surface erosion for non-cohesive material and showed that critical shear stress increases with the increase of soil's unit weight. Other researchers derived regression equations on critical shear stress for surface erosion, and the critical shear stress increases with the increase of moisture content [148, 161]. These studies suggest that as degree of saturation increases, surface soil erosion is less likely to occur.

Piping progression in a tubular channel is considered a form of subsurface erosion, however, the interaction between the flow and the soil surface of the inner piping wall is mechanistically equivalent to the hydrodynamic process of surface erosion in open channels. Therefore, research methodologies and findings in sediment transport in open channel flow and in surface erosion on slopes can be extrapolated to understand the particle detachment mechanisms in an initial crack inside a soil. Sediment transport has been widely studied in hydraulic engineering on issues such as stream stability, scour of bridge foundations, stable channel design, and riprap design. Many researchers such as Kramer [70], Shields [131], White [160], Tison [149], Simons and Richardson [132], Gessler [52], and Vanoni [153] have studied the problem of initiation of particle motion. The Shields diagram is widely used as a tool to determine the incipient soil erosion at different fluid characteristics. Soil erosion is not only affected by soil properties that can vary with degree saturation, but wetting-drying cycles that naturally occur in soils also affect soils structure and engineering behavior, thus affecting soil's erodibility. Fluctuation of phreatic surfaces in earthen dams and levees due to seasonal water level change and moisture migration in the soil during the year can cause formation of shrinkage cracks and water flowing through such cracks may cause significant erosion. The density and size of shrinkage cracks depend on the initial moisture content and plasticity of the soil. Extreme climates such as drought and flooding that are more frequently seen in modern times exacerbate wetting-drying cycles in soils, further contributing to the problems such as overtopping of levees during hurricanes or floods, river banks erosion, and surface erosion of highway embankments.

6 Closing Remarks

The essential difference between saturated soils and unsaturated soils is inclusion of a variable gas phase in the latter. This completely changes the scenario for considerations of mechanical, hydraulic, biological, chemical, and thermal behavior, as well as coupling among these processes. There is practical motivation to develop seamless links between concepts, theory, and experiments applicable to saturated soils, which form the basis of current geotechnical engineering practice, and those applicable to unsaturated soils, which are ubiquitous in the face of new global challenges.

A framework for quantifying internal stress state in unsaturated soils and its evolution with saturation, pore water potential, and wetting-drying or loading-unloading history is essential to effectively and fully capture mechanical behavior of unsaturated soils. Effectively doing this will require resolving pore water retention by short-ranged hydration mechanisms from water retention by longer-ranged capillary mechanisms. Progress to date has effectively captured how capillary water contributes to unsaturated soil behavior, but capturing the contribution of adsorbed water remains a significant challenge.

Fine-grained soil behavior is dominated by interaction forces occurring at the interface between mineral surfaces and water. A new fundamentals-based paradigm for soil classification that more effectively captures these interactions is needed.

Physical measurements of unsaturated soil behavior remain challenging. Advances in computational experiments are playing an increasingly important role in obtaining better fundamental understanding of unsaturated soil properties and processes, including mineral-water interactions, pore fluid retention, soil fabric, strength, and coupled deformation and fluid flow in multiphase porous media.

Flow in unsaturated porous media is manifest in the forms of unsteady (finger) flow in soils, multiphase transport and transfer in rocks, and seepage-induced particle transport in porous media. Fundamental advances in these areas have multi- and cross-disciplinary applications such as contaminant transport, hydraulic fracturing for oil or natural gas extraction, developing plant growth modules for outer space exploration, and soil erosion in partially saturated earthen structures.

The research advances summarized in this chapter represent only a small taste of activity in the broad area of unsaturated soil mechanics and hopefully will stimulate much needed continuous advances in the future.

References

1. Agus, S.S., Schanz, T., Fredlund, D.G.: Measurements of suction versus water content for bentonite–sand mixtures. Can. Geotech. J. **47**(5), 583–594 (2010)
2. Akin, I.D., Likos, W.J.: Specific surface area of clay using water vapor and EGME sorption methods. Geotech. Test. J. **37**(6), 1–12 (2014). https://doi.org/10.1520/GTJ20140064
3. Akin, I.D., Likos, W.J.: Water vapor sorption of polymer-modified bentonites. Geo-Chicago **2016**, 508–517 (2016)
4. Allen, M.P., Tildesley, D.J.: Computer simulation of liquids. Oxford University Press (1989)
5. Alonso, E.E., Gens, A., Josa, A.: A constitutive model for partially saturated soils. Geotechnique 40(3), 405–430 (1990)
6. Amarasinghe, P.M., Anandarajah, A.: Influence of fabric variable s on clay–water–air capillary meniscus. Can. Geotech. J. **48**(7), 987–995 (2011)
7. Amarasinghe, P.M., Anandarajah, A., Ghosh, P.: Molecular dynamic study of capillary forces on clay particles. Appl. Clay Sci. **88**, 170–177 (2014)
8. Anandarajah, A., Amarasinghe, P.M.: Microstructural investigation of soil suction and hysteresis of fine-grained soils. J. Geotech. Geoenviron. Eng. **138**(1), 38–46 (2011)
9. Anderson, D.M., Tice, A.R.: Predicting unfrozen water contents in frozen soils from surface area measurements. Highway Research Record **393**, (1972)
10. Andrade, J.E., Borja, R.I.: Modeling deformation banding in dense and loose fluid-saturated sands. Finite Elem. Anal. Des. **43**(5), 361–383 (2007)
11. Baker, R., Frydman, S.: Unsaturated soil mechanics: critical review of physical foundations. Eng. Geol. **106**(1), 26–39 (2009)
12. Berendsen, H., Grigera, J., Straatsma, T.: The missing term in effective pair potentials. J. Phys. Chem. **91**(24), 6269–6271 (1987)
13. Berend, et al.: Mechanism of adsorption and desorption of water vapor by homoionic montmorillonites. Clays Clay Miner. **43**(3), 324–336 (1995)
14. Bishop, A.W.: The principle of effective stress. Teknisk ukeblad **106**(39), 859–863 (1959)
15. Borja, R.I.: Bifurcation of elastoplastic solids to shear band mode at finite strain. Comput. Methods Appl. Mech. Eng. **191**(46), 5287–5314 (2002)

16. Borja, R.I.: Cam-clay plasticity. Part V: a mathematical framework for three-phase deformation and strain localization analyses of partially saturated porous media. Comput. Methods Appl. Mech. Eng. **193**(48), 5301–5338 (2004)
17. Borja, R.I., Song, X., Rechenmacher, A.L., Abedi, S., Wu, W.: Shear band in sand with spatially varying density. J. Mech. Phys. Solids **61**(1), 219–234 (2013)
18. Borja, R.I., Song, X., Wu, W.: Critical state plasticity. part vii: triggering a shear band in variably saturated porous media. Comput. Methods Appl. Mech. Eng. **261**, 66–82 (2013)
19. Borja, R., Song, X.: Strain localization in porous materials with spatially varying density and degree of saturation. Comput. Methods Recent Adv. Geomech. p. 13 (2014)
20. Briaud, J.-L., Chen, H.-C., Govindasamy, A., Storesund, R.: Levee erosion by overtopping in New Orleans during the Katrina Hurricane. J. Geotech. Geoenviron. Eng. **134**(5), 618–632 (2008)
21. Brooks, B.R., Bruccoleri, R.E., Olafson, B.D., States, D.J., Swaminathan, S.A., Karplus, M.: CHARMm: a program for macromolecular energy, minimization, and dynamics calculations. J. Comput. Chem. **4**(2), 187–217 (1983)
22. Burns, S.E., Culligan, P.J., Lu, N., Santamarina, J.C., Wayllace, A.: NSF workshop on geotechnical fundamentals. Geo-Strata Geo Inst. ASCE **21**(2), 62–63 (2017)
23. Callari, C., Armero, F., Abati, A.: Strong discontinuities in partially saturated poroplastic solids. Comput. Methods Appl. Mech. Eng. **199**(23), 1513–1535 (2010)
24. Carrier, B., Vandamme, M., Pellenq, R.J.-M., Van Damme, H.: Elastic properties of swelling clay particles at finite temperature upon hydration. J. Phys. Chem. C **118**(17), 8933–8943 (2014)
25. Cases, J., Berend, I., Besson, G., Francois, M., Uriot, J., Thomas, F., Poirier, J.: Mechanism of adsorption and desorption of water vapor by homoionic montmorillonite. 1. The sodium-exchanged form, Langmuir **8**(11), 2730–2739 (1992)
26. Cerato, A.B.: Influence of specific surface area on geotechnical characteristics of fine-grained soils, Unpublished M.Sc. Thesis, Department of Civil and Environmental Engineering, University of Massachusetts (2001)
27. Cerato, A., Lutenegger, A.: Determination of surface area of fine-grained soils by the Ethylene Glycol Monoethyl Ether (EGME) method. Geotech. Test. J. **25**(3) 315–321. https://doi.org/10.1520/GTJ11087J. ISSN: 0149-6115 (2002)
28. Cerato, A.B., Lutenegger, A.J.: Activity, relative activity and specific surface area of fine-grained soils. In: Proceedings of the International Conference on Soil Mechanics and Geotechnical Engineering, vol. 16, Balkema (2005)
29. Chen, F.H.: Foundations on expansive soils, vol. 12. Elsevier (1988)
30. Chen, S., Doolen, G.D.: Lattice Boltzmann method for fluid flows. Annu. Rev. Fluid Mech. **30**(1), 329–364 (1998)
31. Chen, Y.-H., Anderson, A.: Methodology for estimating embankment damage caused by flood overtopping. Transport. Res. Rec. **1151** (1987)
32. Chittoori, B., Puppala, A.J.: Quantitative estimation of clay mineralogy in fine-grained soils. J. Geotech. Geoenviron. Eng. **137**(11), 997–1008 (2011)
33. Chuoke, R., Van Meurs, P., van der Poel, C. et al.: The instability of slow, immiscible, viscous liquid-liquid displacements in permeable media (1959)
34. Churchman, G., Burke, C.: Properties of sub soils in relation to various measures of surface area and water content. Eur. J. Soil Sci. **42**(3), 463–478 (1991)
35. Civan, F., Rai, C.S., Sondergeld, C.H., et al.: Determining shale permeability to gas by simultaneous analysis of various pressure tests. SPE J. **17**(03), 717–726 (2012)
36. Clarkson, C., Bustin, R.: The effect of pore structure and gas pressure upon the transport properties of coal: a laboratory and modeling study. 1. isotherms and pore volume distributions. Fuel **78**(11), 1333–1344 (1999)
37. Collis-George, N.: The hydration and dehydration of Na-montmorillonite (belle fourche). Eur. J. Soil Sci. **6**(1), 99–110 (1955)
38. Cui, X., Bustin, A., Bustin, R.M.: Measurements of gas permeability and diffusivity of tight reservoir rocks: different approaches and their applications. Geofluids **9**(3), 208–223 (2009)

39. Cygan, R.T., Liang, J.-J., Kalinichev, A.G.: Molecular models of hydroxide, oxyhydroxide, and clay phases and the development of a general force field. J. Phys. Chem. B **108**(4), 1255–1266 (2004)
40. Dasog, G., Acton, D., Mermut, A., JONG, E.D.: Shrink-swell potential and cracking in clay soils of Saskatchewan. Can. J. Soil Sci. **68**(2), 251–260 (1988)
41. De Borst, R., Sluys, L., Mühlhaus, H.-B., Pamin, J.: Fundamental issues in finite element analyses of localization of deformation. Eng. Comput. **10**(2), 99–121 (1993)
42. Dong, Y., Lu, N.: Measurement of suction-stress characteristic curve under drying and wetting conditions. Geotech. Test. J. **40**(1), (2017)
43. Dos Santos, M., DeCastro, E.: Soil erosion in roads. In: 6th International Conference on Soil Mechanics and Foundation Engineering **1**, 116–118 (1965)
44. Ebrahimi, D., Pellenq, R.J.-M., Whittle, A.J.: Nanoscale elastic properties of montmorillonite upon water adsorption. Langmuir **28**(49), 16855–16863 (2012)
45. Ehlers, W., Graf, T., Ammann, M.: Deformation and localization analysis of partially saturated soil. Comput. Methods Appl. Mech. Eng. **193**(27), 2885–2910 (2004)
46. Eliassi, M., Glass, R.J.: On the porous-continuum modeling of gravity-driven fingers in unsaturated materials: extension of standard theory with a hold-back-pile-up effect. Water Resour. Res. **38**(11) (2002)
47. Farrar, D., Coleman, J.: The correlation of surface area with other properties of nineteen British clay soils. Eur. J. Soil Sci. **18**(1), 118–124 (1967)
48. Finno, R.J., Harris, W.W., Mooney, M.A., Viggiani, G.: Strain localization and undrained steady state of sand. J. Geotech. Eng. **122**(6), 462–473 (1996)
49. Fredlund, D.G., Morgenstern, N.R.: Stress state variables for unsaturated soils. J. Geotech. Eng. Div. **15**(3), 313–321 (1977)
50. Fredlund, D.G., Rahardjo, H.: Soil mechanics for unsaturated soils. Wiley, New York (1993)
51. Garcia, M.: Sedimentation engineering: processes, measurements, modeling, and practice. American Society of Civil Engineers (2008)
52. Gessler, J.: Beginning and Ceasing of sediment motion, Chap. 7 River Mechanics. In: Shen, H.W. (ed.) Water Resources Publication, Littleton, Co. (1971)
53. Gray, W.G., Miller, C.T.: Introduction to the thermodynamically constrained averaging theory for porous medium systems. Springer (2014)
54. Held, R.J., Illangasekare, T.H.: Fingering of dense nonaqueous phase liquids in porous media: 1. experimental investigation. Water Resour. Res. **31**(5), 1213–1222 (1995)
55. Hill, S., et al.: Channeling in packed columns. Chem. Eng. Sci. **1**(6), 247–253 (1952)
56. Hillel, D.: Environmental soil physics: fundamentals, applications, and environmental considerations. Academic Press, Cambridge, MA (1998)
57. Hoehn, A., Scovazzo, P., Stodieck, L.S., Clawson, J., Kalinowski, W., Rakow, A., Simmons, D., Heyenga, A.G., Kliss, M.H.: Microgravity root zone hydration systems, Technical report, SAE Technical Paper (2000)
58. Holtz, W.G., Gibbs, H.J.: Engineering properties of expansive clays. Trans. Am. Soc. Civ. Eng. **121**(1), 641–663 (1956)
59. Homsy, G.M.: Viscous fingering in porous media. Annu. Rev. Fluid Mech. **19**(1), 271–311 (1987)
60. Iwata, S., Tabuchi, T., Warkentin, B.P., et al.: Soil-water interactions—mechanisms and applications. Marcel Dekker Inc., New York, NY (1988)
61. Jang, J., Santamarina, J.C.: Fines classification based on sensitivity to pore-fluid chemistry. J. Geotech. Geoenviron. Eng. **142**(4), 06015018 (2016)
62. Javadpour, F., Fisher, D., Unsworth, M. et al.: Nanoscale gas flow in shale gas sediments. J. Can. Pet. Technol. **46**(10), (2007)
63. Johnson, L.D.: Evaluation of laboratory suction tests for prediction of heave in foundation soils, Department of Defense, Department of the Army, Corps of Engineers, Waterways Experiment Station, Soils and Pavements Laboratory (1977)
64. Jury, W.A., Wang, Z., Tuli, A.: A conceptual model of unstable flow in unsaturated soil during redistribution. Vadose Zone J. **2**(1), 61–67 (2003)
65. Keren, R., Shainberg, I.: Water vapor isotherms and heat of immersion of Na/Ca-montmorillonite systems: I, homoionic clay. Clays Clay Miner. **23**(3), 193–200 (1975)

66. Khalili, N., Geiser, F., Blight, G.: Effective stress in unsaturated soils: review with new evidence. Int. J. Geomech. **4**(2), 115–126 (2004)
67. Khalili, N., Khabbaz, M.: A unique relationship of chi for the determination of the shear strength of unsaturated soils. Geotechnique **48**(5), 681–687 (1998)
68. Khorshidi, M., Lu, N.: Intrinsic relation between soil water retention and cation exchange capacity. J. Geotech. Geoenviron. Eng. **143**(4), 04016119 (2016)
69. Knight, R., Chapman, A., Knoll, M.: Numerical modeling of microscopic fluid distribution in porous media. J. Appl. Phys. **68**(3), 994–1001 (1990)
70. Kramer, H.: Sand mixtures and sand movement in fluvial models. ASCE Trans. **100** (1935)
71. Laird, D.A.: Influence of layer charge on swelling of smectites. Appl. Clay Sci. **34**(1), 74–87 (2006)
72. Langbein, D., Grossbach, R., Heide, W.: Parabolic flight experiments on fluid surfaces and wetting. Appl. Microgravity Technol. **2**, 198–211 (1990)
73. Lawson, W.D.: A survey of geotechnical practice for expansive soils in Texas. Unsaturated Soils **2006**, 304–314 (2006)
74. Lazari, M., Sanavia, L., Schrefler, B.: Local and non-local elasto-viscoplasticity in strain localization analysis of multiphase geomaterials. Int. J. Numer. Anal. Meth. Geomech. **39**(14), 1570–1592 (2015)
75. Lebeau, M., Konrad, J.-M.: A new capillary and thin film flow model for predicting the hydraulic conductivity of unsaturated porous media. Water Resour. Res. **46**(12) (2010)
76. Likos, W.J.: Measurement of crystalline swelling in expansive clay. Geotech. Test. J. **27**(6), 540–546 (2004)
77. Likos, W.J.: Effective stress in unsaturated soil: accounting for surface tension and interfacial area. Vadose Zone J. **13**(5) (2014)
78. Likos, W.J., Lu, N.: Water vapor sorption behavior of smectite-kaolinite mixtures. Clays Clay Miner. **50**(5), 553–561 (2002)
79. Likos, W.J., Lu, N.: Automated humidity system for measuring total suction characteristics of clay. Geotech. Test. J. **26**(2), 178–189 (2003)
80. Likos, W.J., Lu, N.: Pore-scale analysis of bulk volume change from crystalline interlayer swelling in Na^{+}- and Ca^{2+}-smectite. Clays Clay Miner. **54**(4), 515–528 (2006)
81. Likos, W.J., Lu, N., Wenszel, W.: Performance of a dynamic dew point method for moisture isotherms of clays. Geotech. Test. J. **34**(4), 373–382 (2011)
82. Likos, W.J., Wayllace, A.: Porosity evolution of free and confined bentonites during interlayer hydration. Clays Clay Miner. **58**(3), 399–414 (2010)
83. Lin, B.: A comprehensive investigation on microscale properties and macroscopic behavior of natural expansive soils, Thesis, The University of Oklahoma (2012)
84. Lin, B., Cerato, A.B.: Prediction of expansive soil swelling based on four micro-scale properties. Bull. Eng. Geol. Env. **71**(1), 71–78 (2012)
85. Liu, S., Harpalani, S.: A new theoretical approach to model sorption-induced coal shrinkage or swelling. AAPG Bulletin **97**(7), 1033–1049 (2013)
86. Liu, S., Harpalani, S.: Compressibility of sorptive porous media: Part I—background and theory. AAPG Bulletin **98**(9), 1761–1772 (2014)
87. Liu, S., Harpalani, S.: Compressibility of sorptive porous media: Part II–experimental study on coal. AAPG Bulletin **98**(9), 1773–1788 (2014)
88. Liu, W.K., Karpov, E.G., Park, H.S.: Nano Mechanics and Materials: Theory, Multiscale Methods and Applications. Wiley & Sons (2006)
89. Low, P.F.: The swelling of clay: I. montmorillonites. Soil Sci. Soc. Am. J. **44**(4), 667–676 (1980)
90. Lu, N.: Generalized soil water retention equation for adsorption and capillarity. J. Geotech. Geoenviron. Eng. **142**(10), 04016051 (2016)
91. Lu, N., Dong, Y.: Correlation between soil-shrinkage curve and water-retention characteristics. J. Geotech. Geoenviron. Eng. **143**(9), 04017054 (2017)
92. Lu, N., Dong, Y.: Vapor condensation technique for measuring stress-strain relation of unsaturated soil. J. Geotech. Geoenviron. Eng. **143**(6), 02817002 (2017)

93. Lu, N., Godt, J.W., Wu, D.T.: A closed-form equation for effective stress in unsaturated soil. Water Resour. Res. **46**(5) (2010)
94. Lu, N., Kaya, M.: A drying cake method for measuring suction-stress characteristic curve, soil–water-retention curve, and hydraulic conductivity function. Geotech. Test. J. **36**(1), 1–19 (2013)
95. Lu, N., Kaya, M., Godt, J.W.: Interrelations among the soil-water retention, hydraulic conductivity, and suction-stress characteristic curves. J. Geotech. Geoenviron. Eng. **140**(5), 04014007 (2014)
96. Lu, N., Khorshidi, M.: Mechanisms for soil-water retention and hysteresis at high suction range. J. Geotech. Geoenviron. Eng. **141**(8), 04015032 (2015)
97. Lu, N., Kim, T.-H., Sture, S., Likos, W.J.: Tensile strength of unsaturated sand. J. Eng. Mech. **135**(12), 1410–1419 (2009)
98. Lu, N., Likos, W.J.: Unsaturated Soil Mechanics. Wiley (2004)
99. Lu, N., Likos, W.J.: Suction stress characteristic curve for un-saturated soil. J. Geotech. Geoenviron. Eng. **132**(2), 131–142 (2006)
100. Lu, N., Zeidman, B.D., Lusk, M.T., Willson, C.S., Wu, D.T.: A Monte Carlo paradigm for capillarity in porous media. Geophys. Res. Lett. **37**(23) (2010)
101. McKeen, R.: A model for predicting expansive soil behavior: proceedings of the 7th international conference on expansive soils, Dallas, TX American Society of Civil Engineers Geotechnical Division, pp. 1–6 (1992)
102. McKeen, R.G., Nielsen, J.P.: Characterization of expansive soils for airport pavement design. Technical report, University of New Mexico, Eric H Wang Civil Engineering Research Facility (1978)
103. Merry, S.M., Kavazanjian Jr., E., Fritz, W.U.: Reconnaissance of the July 10, 2000, Payatas Landfill failure. J. Performance Constr. Facil. **19**(2), 100–107 (2005)
104. Mitchell, J.: Fundamentals of Soil Behavior. Wiley and Sons Inc., New York (1993)
105. Mitchell, J.K., Soga, K., et al.: Fundamentals of Soil Behavior, 3rd edn. John Wiley & Sons Inc., New Jersey (2005)
106. Monje, O., Stutte, G., Wang, H., Kelly, C.: Nds water pressures affect growth rate by changing leaf area, not single leaf photosynthesis, Technical report, SAE Technical Paper (2001)
107. Mooney, R., Keenan, A., Wood, L.: Adsorption of water vapor by montmorillonite. II. Effect of exchangeable ions and lattice swelling as measured by x-ray diffraction. J. Am. Chem. Soc. **74**(6) 1371–1374 (1952)
108. Morgenstern, N., Balasubramonian, B.: Effects of pore fluid on the swelling of clay-shale, pp. 190–205. Expansive Soils, ASCE (1980)
109. Muhunthan, B.: Liquid limit and surface area of clays. Chem. Clays Clay Min. **6**, 237–274 (1991)
110. Nelson, J., Miller, D.J.: Expansive soils: problems and practice in foundation and pavement engineering. Wiley & Sons Inc., New Jersey (1997)
111. Newman, A.: The interaction of water with clay mineral surfaces. Chem. Clays Clay Min. **6**, 237–274 (1987)
112. Nieber, J.L., Dautov, R.Z., Egorov, A.G., Sheshukov, A.Y., et al.: Dynamic capillary pressure mechanism for instability in gravity-driven flows; review and extension to very dry conditions. Transp. Porous Media **58**(1–2), 147–172 (2005)
113. Nixon, J.: Discrete ice lens theory for frost heave in soils. Can. Geotech. J. **28**(6), 843–859 (1991)
114. Norrish, K.: The swelling of montmorillonite. Discuss. Faraday Soc. **18**, 120–134 (1954)
115. Or, D., Tuller, M.: Liquid retention and interfacial area in variably saturated porous media: upscaling from single-pore to sample-scale model. Water Resour. Res. **35**(12), 3591–3605 (1999)
116. Peric, D., Zhao, G., Khalili, N.: Strain localization in unsaturated elastic-plastic materials subjected to plane strain compression. J. Eng. Mech. **140**(7), 0401405 (2014)
117. Petersen, L.W., Moldrup, P., Jacobsen, O.H., Rolston, D.: Relations between specific surface area and soil physical and chemical properties. Soil Sci. **161**(1), 9–21 (1996)

118. Pillalamarry, M., Harpalani, S., Liu, S.: Gas diffusion behavior of coal and its impact on production from coalbed methane reservoirs. Int. J. Coal Geol. **86**(4), 342–348 (2011)
119. Reddi, L.N., Xiao, M., Steinberg, S.L.: Discontinuous pore fluid distribution under microgravity-kc-135 flight investigations. Soil Sci. Soc. Am. J. **69**(3), 593–598 (2005)
120. Rethore, J., De Borst, R., Abellan, M.-A.: A two-scale model for fluid flow in an unsaturated porous medium with cohesive cracks. Comput. Mech. **42**(2), 227–238 (2008)
121. Revil, A., Lu, N.: Unified water isotherms for clayey porous materials. Water Resour. Res. **49**(9), 5685–5699 (2013)
122. Rexer, T.F., Benham, M.J., Aplin, A.C., Thomas, K.M.: Methane adsorption on shale under simulated geological temperature and pressure conditions. Energy Fuels **27**(6), 3099–3109 (2013)
123. Rieke, R.D.: The role of specific surface area and related index properties in the frost susceptibility of soils. Thesis, Oregon State University (1982)
124. Romero, E., Simms, P.H.: Microstructure investigation in unsaturated soils: a review with special attention to contribution of mercury intrusion porosimetry and environmental scanning electron microscopy. Geotech. Geol. Eng. **26**(6), 705–727 (2008)
125. Ross, G.: Relationships of specific surface area and clay content to shrink-swell potential of soils having different clay mineralogical compositions. Can. J. Soil Sci. **58**(2), 159–166 (1978)
126. Rudnicki, J.W., Rice, J.: Conditions for the localization of deformation in pressure-sensitive dilatant materials. J. Mech. Phys. Solids **23**(6), 371–394 (1975)
127. Saffman, P.G., Taylor, G.: The penetration of a fluid into a porous medium or hele-shaw cell containing a more viscous liquid. In: Proceedings of the Royal Society of London A: Mathematical, Physical and Engineering Sciences, vol. 245, The Royal Society, pp. 312–329 (1958)
128. Santamarina, J.C., Klein, A., Fam, M.A.: Soils and waves: particulate materials behavior, characterization and process monitoring. J. Soils Sediments **1**(2), 130 (2001)
129. Schiava, R., Etse, G.: Constitutive modeling and discontinuous bifurcation assessment in unsaturated soils. J. Appl. Mech. **73**(6), 1039–1044 (2006)
130. Seed, H.B., Woodward, R.J., Lundgren, R.: Prediction of swelling potential for compacted clays. Trans. Am. Soc. Civ. Eng. **128**(1), 1443–1477 (1962)
131. Shields, A.: Application of similarity principles and turbulence research to bed-load movement. California Institute of Technology, Pasadena, CA (1936). (translated from German)
132. Simons, D.B., Richardson, E.V.: Resistance to flow in alluvial channels. US Government Printing Office (1966)
133. Song, X.: Strain localization in unsaturated porous media, Ph.D. Thesis, Stanford University (2014)
134. Song, X.: Transient bifurcation condition of partially saturated porous media at finite strain. Int. J. Numer. Anal. Meth. Geomech. **41**(1), 135–156 (2017)
135. Song, X.: A physical based multi-scale computational framework for triphasic geomaterials. In: White paper and presentation, NSF Workshop on Geotechnical Fundamentals in The Face of New World Challenges, National Science Foundation (2016)
136. Song, X., Borja, R.I.: Finite deformation and fluid flow in unsaturated soils with random heterogeneity. Vadose Zone J. **13**(5), 1 (2014)
137. Song, X., Borja, R.I.: Mathematical framework for unsaturated flow in the finite deformation range. Int. J. Numer. Meth. Eng. **97**(9), 658–682 (2014)
138. Song, X., Borja, R. I., Wu, W.: Triggering a shear band in variably saturated porous materials. In: Poromechanics V: Proceedings of the Fifth Biot Conference on Poromechanics, pp. 367–370 (2013)
139. Song, X., Idinger, G., Borja, R.I., Wu, W.: Finite element simulation of strain localization in unsaturated soils. Unsaturated Soils: Research and Applications, pp. 189–195 (2012)
140. Song, X., Wang, K., Ye, M.: Localized failure in unsaturated soils under non-isothermal conditions. Acta Geotechnica, pp. 1–13 (2017)
141. Song, X., Ye, M., Wang, K.: Strain localization in a solid-water-air system with random heterogeneity via stabilized mixed finite elements. Int. J. Numer. Methods Eng. **112**, 1926 (2017)

142. Song, X., Zhang, K., Wang, M.: Molecular dynamics modeling of a partially saturated clay-water system at finite temperature. Int. J. Numer. Anal. Methods Geomech., In submission (2017)
143. Sposito, G., et al.: The thermodynamics of soil solutions. Oxford University Press, Oxford (1981)
144. Stutte, G., Monje, O., Anderson, S.: Wheat (triticum aesativum l. cv. usu apogee) growth onboard the international space station (ISS): Germination and early development. Proc. Plant Growth Regul. Soc. Am. **30**, 66–71 (2003)
145. Sudibandriyo, M., Pan, Z., Fitzgerald, J.E., Robinson, R.L., Gasem, K.A.: Adsorption of methane, nitrogen, carbon dioxide, and their binary mixtures on dry activated carbon at 318.2 K and pressures up to 13.6 MPa. Langmuir **19**(13), 5323–5331 (2003)
146. Taylor, G.: The instability of liquid surfaces when accelerated in a direction perpendicular to their planes, I. In: Proceedings of the Royal Society of London A: Mathematical, Physical and Engineering Sciences, vol. 201, The Royal Society, pp. 192–196 (1950)
147. Teich-McGoldrick, S.L., Greathouse, J.A., Cygan, R.T.: Molecular dynamics simulations of structural and mechanical properties of muscovite: Pressure and temperature effects. J. Phys. Chem. C **116**(28), 15099–15107 (2012)
148. Thoman, R.W., Niezgoda, S.L.: Determining erodibility, critical shear stress, and allowable discharge estimates for cohesive channels: case study in the powder river basin of Wyoming. J. Hydraul. Eng. **134**(12), 1677–1687 (2008)
149. Tison, L.: Studies of the critical tractive force of entrainment of bed materials. Proceedings: Minnesota International Hydraulics Conference, Minneapolis, MN (1953)
150. Tuller, M., Or, D., Dudley, L.M.: Adsorption and capillary condensation in porous media: Liquid retention and interfacial configurations in angular pores. Water Resour. Res. **35**(7), 1949–1964 (1999)
151. Van Olphen, H.: Thermodynamics of interlayer adsorption of water in clays. J. Colloid Sci. **20**(8), 822–837 (1965)
152. Van Olphen, H.: Clay colloid chemistry (reprinted edition) (1991)
153. Vanoni, V.A.: Sedimentation engineering, ASCE manuals and reports on engineering practice No. 54, American Society of Civil Engineers, New York, NY (1975)
154. Vardoulakis, I.: Deformation of water-saturated sand: II. Effect of pore water flow and shear banding. Geotechnique **46**(3), 457–472 (1996)
155. Wang, S., Elsworth, D., Liu, J.: A mechanistic model for permeability evolution in fractured sorbing media. J. Geophys. Res. Solid Earth **117**(B6) (2012)
156. Wang, Y., Liu, S.: Estimation of pressure-dependent diffusive permeability of coal using methane diffusion coefficient: laboratory measurements and modeling. Energy Fuels **30**(11), 8968–8976 (2016)
157. Wang, Z., Feyen, J., Elrick, D.E.: Prediction of fingering in porous media. Water Resour. Res. **34**(9), 2183–2190 (1998)
158. Wang, Z., Tuli, A., Jury, W.A.: Unstable flow during redistribution in homogeneous soil. Vadose Zone J. **2**(1), 52–60 (2003)
159. Weinan, E.: Principles of Multiscale Modeling. Cambridge University Press (2011)
160. White, C.: The equilibrium of grains on the bed of a stream. In: Proceedings of the Royal Society of London. Series A, Mathematical and Physical Sciences, pp. 322–338 (1940)
161. Wynn, T.M., Mostaghimi, S., Alphin, E.F. et al.: The effects of vegetation on stream bank erosion. In: 2004 ASAE Annual Meeting, American Society of Agricultural and Biological Engineers, p. 1 (2004)
162. Xiao, M., Reddi, L.N., Syeinberg, S.L.: Variation of water retention characteristics due to particle rearrangement under zero gravity. Int. J. Geomech. https://doi.org/10.1061/(asce)1532-3641. **9**, 4(179) (2009)

163. Yong, R.: Soil suction and soil-water potentials in swelling clays in engineered clay barriers. Eng. Geol. **54**(1), 3–13 (1999)
164. Zeidman, B.D., Lu, N., Wu, D.: Coarse-grained Monte Carlo simulation of the distribution and capillarity of multiple fluids in porous media, Pore Scale Phenomena: Frontiers in Energy and Environment. In: J. Poate, T. Illangasekare, H. Kazemi, and R. Kee (Eds.) (World Scientific, Singapore, 2015) pp. 263–278 (2015)

Research Challenges Involving Coupled Flows in Geotechnical Engineering

Charles D. Shackelford, Ning Lu, Michael A. Malusis and Kristin M. Sample-Lord

Abstract Coupled fluid, chemical, heat, and electrical flows are common phenomena that are relevant to a wide variety of applications in Geotechnical Engineering, including the use of engineered clay barriers for waste containment, electro-osmosis for soil consolidation, highly compacted bentonite buffers for high-level radioactive nuclear waste disposal, and electrokinetics for soil contaminant removal, among others. For all of these applications, a fundamental understanding of coupled flow phenomena is required, including the basis of the various phenomena, the potential effect of the phenomena on fundamental soil behavior, and the applicability of the phenomena in both natural and built environments. This chapter highlights some of the advances over the past approximate three decades, including the effects of osmotic phenomena (chemico-osmosis, electro-osmosis, and thermo-osmosis) on the mechanical behavior of clays, the formulations and measurement of coupled flow phenomena, the distinction between phenomenological and microscopic (physical-based) formalisms, and considerations with respect to both saturated and unsaturated soil conditions. Based on the description of these advances, research challenges pertaining to the study of coupled flow phenomena for Geotechnical Engineering applications are identified.

Keywords Anion exclusion · Chemico-osmosis · Conduction phenomena · Coupled flows · Darcy's law · Diffusion · Electro-osmosis · Fick's law · Fourier's law · Membrane behavior · Ohm's law · Osmosis · Solute restriction · Thermo-osmosis

C. D. Shackelford (✉)
Colorado State University, Fort Collins, CO, USA
e-mail: shackel@engr.colostate.edu

N. Lu
Colorado School of Mines, Golden, CO, USA

M. A. Malusis
Bucknell University, Lewisburg, PA, USA

K. M. Sample-Lord
Villanova University, Villanova, PA, USA

N. Lu and J. K. Mitchell (eds.), *Geotechnical Fundamentals for Addressing New World Challenges*, Springer Series in Geomechanics and Geoengineering,
https://doi.org/10.1007/978-3-030-06249-1_9

1 Introduction

Conduction phenomena refers to the combination of direct and coupled flow phenomena associated with the transfer of liquids, chemicals (solutes), electrical current, and heat through porous media (e.g., soils or rocks) due to hydraulic, chemical, electrical, and thermal gradients, as summarized in Table 1. The direct conduction phenomena represent flows that are linearly related to the corresponding driving force (gradient) as represented by Darcy's, Fick's, Ohm's and Fourier's laws. The indirect or coupled flow phenomena represent flows of one type due to driving forces or gradients of another type. For example, fluid flow can result not only from a hydraulic gradient, but also from chemical, electrical, and thermal gradients with, the latter three processes commonly being referred to as chemico-osmosis, electro-osmosis, and thermo-osmosis, respectively [71].

All coupled flows, i.e., the off-diagonal flows identified in Table 1, are macroscopic manifestations of fundamental physico-chemical processes that occur at the pore scale. The constituents of soil or rock, viz., the solid mineral, pore liquid and dissolved chemicals (solutes) therein, and the gas phase, determine the chemical potential of the pore fluid. The driving force originates from the mineral structure that generates electromagnetic fields within the crystalline structure and near the particle surfaces within the pores. Specific surface area (SSA) and cation exchange capacity (CEC) are indicators of the strength of such forces (see Chapter 4 "Linking Soil Water Adsorption to Geotechnical Engineering Properties"). Together with the dielectric pore constituents of liquid, solutes, and gases, these electromagnetic fields generate forces and hydrodynamic pressure within the pores, which are manifestations of the

Table 1 Direct and indirect (coupled) flow phenomena (modified after [12, 72, 76])

Flow	Driving force or gradient			
	Hydraulic (Pressure)	Chemical (Concentration)	Electrical (Voltage)	Thermal (Temperature)
Fluid	Hydraulic Conduction (Darcy's law)	Chemico-Osmosis	Electro-Osmosis	Thermo-Osmosis
Solute	Streaming Current (Advection), or Ultrafiltration	Diffusion (Fick's law)	Electrophoresis	Thermal Diffusion (Soret Effect)
Current	Streaming Current (Rouss Effect)	Sedimentation Current	Electrical Conduction (Ohm's law)	Thermo-Electricity (Seebeck Effect)
Heat	Thermal Filtration or Isothermal Heat Transfer	Dufour Effect	Peltier Effect	Thermal Conduction (Fourier's law)

surface charge density, surface electrical potential, and the thickness of the electric double layers associated with individual solid particles.

Four types of electromagnetic forces in earthen materials are known to exist (see Chapter 4 "Linking Soil Water Adsorption to Geotechnical Engineering Properties"), viz., (i) the van der Waals force between the solid phase and nearby pore liquid; (ii) the electric double layer force formed by the negative surface potential (charge) associated with the solid surface and the counter-cations in the nearby liquid; (iii) hydrogen bonding between the solid surface and hydrogen of the water molecule (H_2O); and (iv) the cation hydration force resulting from the presence of exchangeable cations associated with the clay minerals. These forces strive to reach energy equilibrium among the constituents of the pore fluid, i.e., ions or electrolytes and solvents, following the laws of thermodynamics. Thus, if one constituent changes (e.g., liquid displacement), another constituent (e.g., dissolved electrolytes) also will displace, resulting in a nonequilibrium condition that leads to the existence of a coupling phenomenon to re-establish equilibrium. As such, all participating constituents strive to reach a new equilibrium, leading to coupled flows. In general, the closer these constituents (e.g., the lower the porosity) and the higher the charge density, the stronger the coupling effects. For example, when the concentrations of solutes within the pore water of a dense clay with high surface charge density are low, the repulsive electrical force generated by the overlap in the electric diffuse double layers (DDLs) of adjacent clay particles results in a net negative potential within the pore that restricts the entrance of anions into the pore (anion exclusion), resulting in the rise of chemico-osmosis. The most widely used theoretical framework to describe coupled flow processes at the macroscopic scale is the so-called theory of "nonequilibrium" or "irreversible" thermodynamics (e.g., [29, 45, 63]).

1.1 Coupled Flow Processes

In some cases, direct and/or indirect flows associated with the aforementioned conduction phenomena occur simultaneously. For example, solute migration through porous media involves both advection in accordance with Darcy's law and diffusion in accordance with Fick's law. Advection tends to dominate solute migration in high permeability porous media (e.g., coarse-grained soils such as aquifers), whereas diffusion tends to dominate solute migration in low permeability porous media (e.g., aquitards and clay barriers for waste containment).

An example of direct and indirect flows occurring simultaneously is electrokinetic remediation, whereby a voltage gradient is applied across electrodes (anode and cathode) inserted into contaminated fine-grained soils for the purpose of removing the contaminants. In this case, three primary processes are known to contribute to electrokinetics, viz. diffusion, electro-osmosis, and ion migration (electromigration), although diffusion generally is negligible relative to electro-osmosis and ion migration [1].

Finally, both direct and indirect conduction phenomena may be coupled with other processes, such as mechanical deformation (e.g., consolidation) of porous media (e.g., [3]), chemical reactions (e.g., ion exchange, precipitation), and biological reactions (e.g., bioclogging, microbial mediated precipitation). Physico-chemical interactions between migrating solutes and the host porous medium also can significantly affect both direct and indirect conduction phenomena, particularly in high activity clays such as sodium bentonites ([105, 106]).

1.2 Relevance of Coupled Flows in Geotechnical Engineering

Mitchell [72] summarized the relevance of the 12 coupled (indirect) flows shown in Table 1 to soil-water systems. Examples of the relevance to Geotechnical Engineering were provided for seven of these 12 coupled flows, viz., thermo-, electro-, and chemico-osmosis, isothermal heat transfer, streaming current both in terms of hydraulically driven electrical current and hydraulic driven ion (solute) migration (i.e., advection), and electrophoresis (e.g., ion migration). Of the remaining five coupled flows, the relevance of three, viz., thermal-electricity (Seebeck effect), sedimentation current, and thermal diffusion of electrolytes (Soret effect), was somewhat uncertain, whereas electrically and chemically driven heat flow (i.e., Peltier and Dufour effects, respectively) were considered to be irrelevant, although these last two flows had not been studied to any significant extent at that time.

Nowadays, direct and coupled flows are particularly relevant to two subdisciplines of Geotechnical Engineering, i.e., Environmental Geotechnics and Energy Geotechnics. For example, advection, diffusion, chemico-osmosis, thermo-osmosis, and thermal diffusion of electrolytes (e.g., dissolved metals and radionuclides) are relevant to the use of engineered clay barriers for chemical containment applications, such as municipal and hazardous solid waste disposal, liquid storage, low-level radioactive waste (LLRW) and high-level radioactive waste (HLRW) disposal, mine waste management, and carbon sequestration (i.e., long-term storage of carbon dioxide or other forms of carbon for the purpose of mitigating anthropogenic climate change). As previously noted, diffusion, electro-osmosis and electromigration (ion migration) are relevant flows for electrokinetic remediation. Finally, thermal conduction (see Chapter 10 "Emerging Thermal Issues in Geotechnical Engineering") is relevant to geothermal piles that serve both as foundations for buildings and as heat exchangers used to store and extract heat from the subsurface, and the production of electrical power via geothermal reservoirs involves consideration of fluid and heat flows through porous media (soils and rocks) coupled with mechanical and chemical processes, commonly referred to as coupled thermal-hydrological-mechanical-chemical (THMC) processes, under unsaturated conditions [120]. These applications of coupled flow processes are critical for addressing the new world challenges described in Chapter 1 "The Role of Geotechnics in Addressing New World Problems".

2 Osmotic Phenomena and Mechanical Behavior of Clays

Coupled flows can have a profound impact on the mechanical behavior of clays. For example, consolidation of clays can be accomplished via both electro-osmosis (e.g., [5, 7, 8, 22, 27, 37, 50, 73, 110, 126]) and chemico-osmosis (e.g., [4, 15, 28, 77]). Since consolidation of clays results in a decrease in the void ratio of the clay, consolidation resulting from coupled flows also can increase the strength of clays.

In general, the impact of coupled flows on the mechanical behavior of clays becomes more significant with an increase in the activity of the clay, which in turn is a function of the mineralogy of the clay. For example, the effects of coupled flows on the mechanical behavior of clays generally are greater for clays comprising predominantly high activity, smectite clay minerals (e.g., montmorillonite), such as bentonites, versus those comprising primarily lower activity clay minerals, such as illite and kaolinite. This difference results from the greater significance of electrostatic interactions between adjacent clay particles associated with higher activity clay minerals versus lower activity clay minerals (e.g., [98]).

Medved and Černy [71] provide a comprehensive review of coupled flows, specifically chemico-osmosis, electro-osmosis, and thermo-osmosis, in "bulky porous media" (i.e., as opposed to "thin membranes"). The focus of their review is primarily on the various theoretical formulations and models describing these osmotic phenomena, although they also summarize some experimental studies associated with the theories. The focus of this section is on the role of these osmotic phenomena in affecting volume change in soils, principally fine-grained soils such as silts and clays.

2.1 Chemico-Osmosis

Chemico-osmosis is the process whereby water (H_2O) flows in response to a difference in solute concentration or in response to a concentration gradient, from a region (zone) of lower solute concentration (higher chemical activity of water) to a region (zone) of higher solute concentration (lower chemical activity of water) (e.g., [58, 61]). For chemico-osmosis to occur, the porous medium must exhibit solute restriction (membrane behavior), which in clay soils has been attributed to the interaction of the negative potentials associated with the surfaces of the individual clay particles at the pore scale [23]. When adjacent clay particles are sufficiently close such that the negative potentials of the particle surfaces overlap, the net electrical potential within the pore space between the particles is negative, resulting in the repulsion of anions (e.g., Cl^-) that try to enter the pore, a process often referred to as "anion exclusion." Because of the requirement for electroneutrality (charge balance) among all ionic chemical species, cations associated with the anions (e.g., Na^+, K^+, Ca^{2+}, Mg^{2+}) are similarly excluded from entering the pore space.

In clay soils that exhibit membrane behavior, the pore sizes generally vary such that not all pores are exclusionary, because not all the clay particles are sufficiently close to result in overlap of the negative surface potentials. Thus, the membrane efficiency of most clay soils exhibiting solute restriction ranges between zero for non-membrane behavior (no solute restriction) and 100% for "perfect" or "ideal" membrane behavior (complete solute restriction). The magnitude of membrane efficiency in a given clay soil is affected by the pore-water chemistry, as this chemistry affects the extent of the negative surface potentials associated with individual clay particles. Also, membrane efficiency is influenced by volume change of the soil, which affects the proximity of adjacent clay particles and the concomitant sizes of the pores [100].

For clay soils exhibiting membrane behavior, volume change can be imposed via traditional mechanical consolidation resulting from applied (external) loading or induced via osmotic phenomena. In either case, the volume change results from a change in the true effective stress, σ^*, of clay soil, or $\Delta\sigma^*$, where σ^* is defined as follows for water saturated porous media [4, 9, 76, 111]:

$$\sigma^* = \sigma - u_w - (R - A) = \sigma' - (R - A) \tag{1}$$

where σ is the total (applied) stress, u_w is the pore-water pressure, σ' $(= \sigma - u_w)$ is the conventional effective stress, R is the interparticle repulsive stress resulting from the electrostatic repulsion between the negatively charged surfaces of adjacent clay particles, and A is the attractive stress between adjacent clay particles typically attributed to van der Waals forces. Thus, the $R - A$ in Eq. 1 represents the net interparticle repulsive-minus-attractive stress, which is a function of the pore-water chemistry in that R generally decreases with increasing concentration and valence (charge) of counterions (cations) in the pore water, and with decreasing dielectric constant and pH of the pore water, while A remains relatively independent of the pore-water chemistry and, therefore, relatively constant [76, 114].

Volume change occurs due to changes in the true effective stress, with expansion (swelling) resulting from a decrease in σ^* (i.e., $\Delta\sigma^* < 0$) and compression (consolidation) resulting from an increase in σ^* (i.e., $\Delta\sigma^* > 0$). Based on Eq. 1, $\Delta\sigma^*$ is defined as follows:

$$\Delta\sigma^* = \Delta\sigma - \Delta u_w - \Delta(R - A) = \Delta\sigma - \Delta u_w - \Delta R + \Delta A \tag{2}$$

As previously noted, A is relatively constant (i.e., $\Delta A \approx 0$), such that Eq. 2 essentially reduces to the following form:

$$\Delta\sigma^* = \Delta\sigma - \Delta u_w - \Delta R \tag{3}$$

For example, in the absence of physico-chemical interactions (i.e., $\Delta R = 0$), conventional consolidation occurs as a result of external loading (i.e., $\Delta\sigma > 0$) such that, by the end of the consolidation process, all of the applied stress has been

converted to a change in conventional and, therefore, true effective stress (i.e., $\Delta u_w = 0$, $\Delta\sigma = \Delta\sigma' = \Delta\sigma^* > 0$).

In the absence of external loading (i.e., $\Delta\sigma = 0$), Eq. 3 reduces to the following form:

$$\Delta\sigma^* = -\Delta u_w - \Delta R \tag{4}$$

Thus, in accordance with Eq. 4, consolidation ($\Delta\sigma^* > 0$) can occur when there is a decrease in the pore-water pressure ($\Delta u_w < 0$) and/or a decrease in the interparticle repulsive stress ($\Delta R < 0$).

In this context, Barbour and Fredlund [4] identified two osmotic consolidation mechanisms based on Eq. 4, viz., osmotically induced consolidation and osmotic consolidation. As illustrated in Fig. 1a, osmotically induced consolidation results when chemico-osmotic flow of pore water occurs from the pores of a clay to a surrounding zone of higher solute concentration, resulting in a decrease in pore-water pressure ($\Delta u_w < 0$) and an increase in the conventional and, therefore, true effective stresses ($\Delta\sigma' > 0$, $\Delta\sigma^* > 0$). Osmotic consolidation occurs simultaneously as solutes diffuse from the zones of higher solute concentration into the pores, resulting in a decrease in the interparticle repulsive stress ($\Delta R < 0$) and an increase in the true effective stress ($\Delta\sigma^* > 0$). Note that the opposite scenario is also possible, whereby a higher solute concentration within the pore water of a clay results in chemico-osmotic flow into the clay ($\Delta u_w > 0$) and diffusion of solutes from the clay ($\Delta R > 0$), resulting in a decrease in effective stress ($\Delta\sigma^* < 0$) and swelling (see Fig. 1b). These processes are relevant both macroscopically, such as in the case where a geologic finer-grained soil layer is bounded by geologic coarser-grained soils, such as a shale layer bounded by sandstones (e.g., [79]), and microscopically, such as in the case of thin bentonite-based barriers comprising granular bentonite, whereby the interlayer regions of the individual bentonite particles are distinguished from the intra-aggregate regions comprising essentially immobile water and intergranular (inter-aggregate) regions comprising mobile pore water (e.g., [39]).

Barbour and Fredlund [4] evaluated experimentally both osmotic consolidation mechanisms for two soils, (1) a mixture of 20% sodium bentonite and 80% Ottawa sand, and (2) Regina Clay, a naturally occurring calcium montmorillonite soil, based on exposure to a 4 M NaCl solution. They concluded that osmotic consolidation ($\Delta R < 0$) was the dominant mechanism of consolidation, with the rate of volume change being controlled by the rate of diffusion of the salt (NaCl) into the specimen. Although chemico-osmotic flow was measured, osmotically induced consolidation ($\Delta u_w < 0$) was determined to be insignificant.

Di Maio [15] evaluated the effect of exposure of specimens of Ponza bentonite to saturated salt solutions containing NaCl, KCl, or $CaCl_2$ on both the volume change and the residual shear strength of the specimens. The results indicated significant decreases in the volume of the specimens and significant increases in the residual strength of the specimens exposed to all three salt solutions. The volume changes were attributed to osmotic consolidation resulting from diffusion of the salts into the

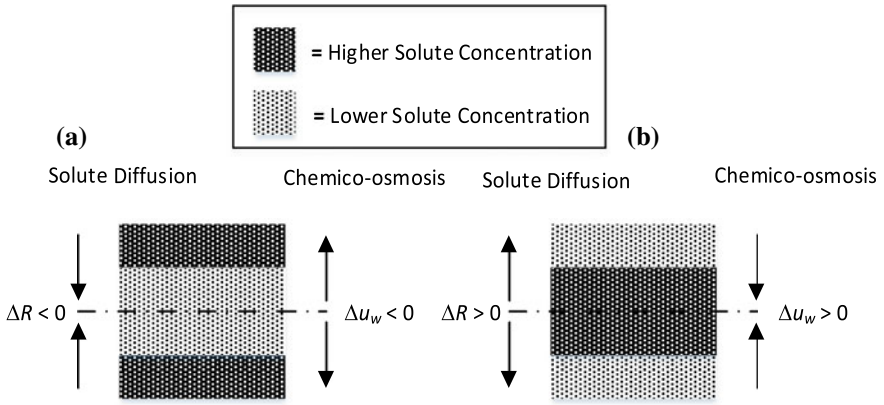

Fig. 1 Directions of chemico-osmotic flow and solute diffusion associated with the osmotic induced and osmotic volume-change mechanisms for a fine-grained soil layer, e.g., clay (middle section): **a** consolidation; **b** swelling (modified after [77]). [Note: R = interparticle repulsive stress; u_w = pore-water pressure]

pore water of the specimens. However, upon re-exposure of the specimens to water, the volume changes associated with the NaCl solution were found to be reversible, whereas those associated with the KCl and $CaCl_2$ solutions were essentially irreversible. This difference in behavior was attributed to whether the principal salt cation was the same as (Na^+) or different than (K^+, Ca^{2+}) the principal counter-ion (Na^+) initially dominating the exchange sites of the clay particles. In the case of KCl or $CaCl_2$, the irreversible volume change was attributed to cation exchange of K^+ or Ca^{2+} for the initially bound Na^+.

Kang and Shackelford [42] describe the use of a flexible-wall cell for measuring the membrane efficiency coefficient of specimens of a geosynthetic clay liner (GCL) comprising sodium bentonite (Na-bentonite) under closed-system boundary conditions at a constant applied effective stress, σ' (Eq. 1), of 241 kPa. The membrane efficiency coefficient, designated herein as ω, is a measure of the relative degree of solute restriction of a semipermeable membrane, with values of ω typically ranging from zero for no solute restriction to unity for complete solute restriction corresponding to ideal or perfect membrane behavior (i.e., $0 \leq \omega \leq 1$), although negative values of ω (<0) also have been measured under special circumstances (e.g., [6, 47, 83]). The measured values of ω for the two GCL specimens are shown in Fig. 2a as a function of the average salt (KCl) concentration, C_{ave}, within the specimens during testing, whereby salt solutions with different source concentrations of KCl, C_o, were circulated across the top boundary of the specimen while de-ionized water (DIW) was circulated simultaneously across the bottom boundary of the specimen (i.e., $C_{ave} = C_o/2$). For comparison, values of ω previously reported by Malusis and Shackelford [58] for the same GCL and salt concentrations measured using a rigid-wall cell also are shown in Fig. 2a. Kang and Shackelford [42] attributed the difference in the trends shown in Fig. 2a (i.e., the semi-log linear trend for the rigid-wall data

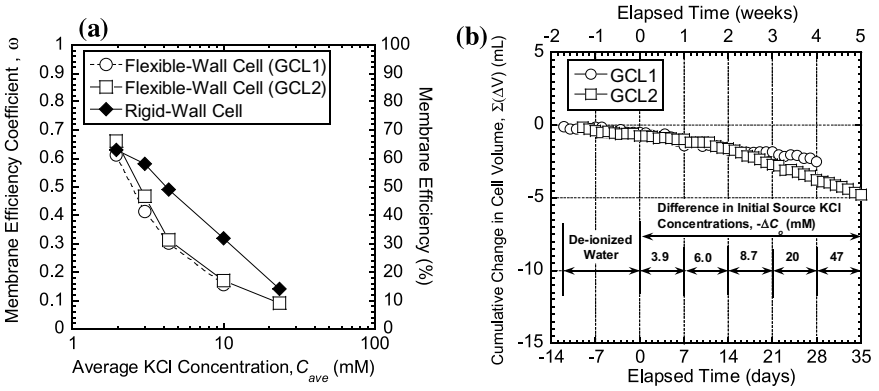

Fig. 2 Membrane behavior of two specimens of a bentonite-based geosynthetic clay liner (GCL) as measured in a flexible-wall cell under closed-system boundary conditions at constant applied effective stress (σ') of 241 kPa: **a** comparison of trends in membrane efficiency coefficient versus salt (KCl) concentration based on flexible-wall versus rigid-wall cells; **b** volume change during flexible-wall testing (Reprinted from Ref. [42], with permission from Elsevier)

and the semi-log nonlinear trend for the flexible-wall data) to drainage and consolidation of the specimens measured in the flexible-wall cell that occurred during the brief periods ($\leq$2 min) in the tests when the system was opened to refill and sample the circulating liquids, resulting in a decrease in volume of the specimen as shown in Fig. 2b. Because σ' was maintained constant during the tests, the drainage and consolidation were attributed to the $R - A$ effect due to the processes illustrated in Fig. 1a resulting in $\Delta\sigma^* > 0$ (Eq. 4).

2.2 *Electro-Osmosis*

Electro-osmosis is the movement of water in response to an applied electrical gradient. As illustrated schematically in Fig. 3, electro-osmosis in clays occurs when electrodes are inserted at a desired spacing, and a voltage difference (ΔV) is applied via a direct current (DC) power supply across the electrodes, thereby inducing electrolysis reactions at the electrodes, such that one electrode loses electrons ($\Delta e^- < 0$) and becomes positively charged (anode) while the other electrode gains electrons ($\Delta e^- > 0$) and becomes negatively charged (cathode). As a result, the excess of cations in DDLs associated with the clay particle surfaces results in the net migration of the hydrated cations in the DDL towards the cathode, which in turn results in viscous drag of mobile water within the pores that exists outside the influence of the negative potential of the clay particle surfaces. Protons (H^+) are generated via electrolysis at the anode, resulting in an acid front (pH < 7) migrating from the anode to the cathode. Simultaneously, electrolysis at the cathode results in generation of

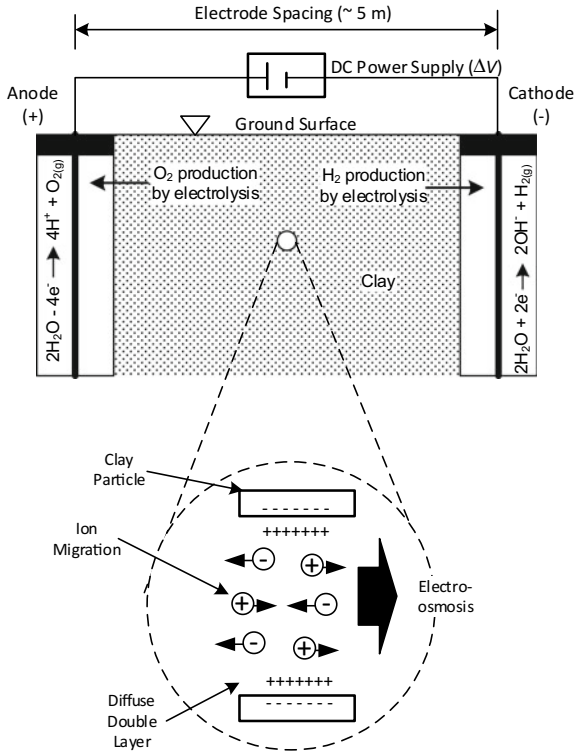

Fig. 3 Schematic profile view illustrating the concept of electro-osmosis in saturated clay (modified after [103])

hydroxide (OH^-), resulting in a basic front (pH > 7) migrating from the cathode to the anode. The net electro-osmotic water flow to the cathode results in the generation of negative pore-water pressures within the clay near the anode, resulting in an increase in effective stress and consolidation that simultaneously reduces the void ratio and compressibility of the clay and, therefore, increases the shear strength of the clay.

In comparison to chemico-osmosis and thermo-osmosis, electro-osmosis has been well studied in Geotechnical Engineering, with much of the earliest work focused on the use of electro-osmosis to reinject salts into the pores of metastable quick clays for the purpose of stabilizing these clays against collapse upon loading (e.g., [5, 7, 8]), and then subsequently for the purpose of stabilizing soft, low permeability clays by inducing consolidation (e.g., [13, 14, 21, 22, 27, 37, 38, 50, 73, 75, 116–118, 126, 127]). Over the past approximately 30 years, electro-osmosis has been studied extensively as one of the mechanisms governing electrokinetic remediation of con-

taminated fine-grained soils (e.g., [1, 40, 115, 122]). More recently, some studies have focused on electrokinetic remediation under unsaturated soil conditions (e.g., [69, 70, 124]), as well as the development of more comprehensive electrokinetic models [53].

2.3 Thermo-Osmosis

Thermo-osmosis is the movement of a fluid (gas and/or liquid) in response to a gradient in temperature, from a region of higher temperature to a region of lower temperature (e.g., [76]). The primary soil property associated with thermo-osmosis is the thermo-osmotic conductivity, k_T, which generally is considered to range from 10^{-14} to 10^{-10} m^2 K^{-1} s^{-1} [125]. In general, the higher the magnitude of k_T, the greater the thermo-osmotic flux.

Compared to other coupled flow phenomena, the study of thermo-osmosis has been largely ignored on the basis that the magnitude of the thermo-osmotic flux is negligible [97]. However, the significance of thermo-osmosis is based not so much on the absolute magnitude of the thermo-osmotic liquid flux, but rather on the magnitude of the thermo-osmotic flux relative to other flux processes, such as hydraulic (Darcian) flux. In addition, the significance of thermo-osmosis increases with decreasing saturation of the soil because the significance of Darcian flux decreases rapidly with decreasing saturation (e.g., [76]). Finally, although the extent of the thermo-osmotic liquid flux may be small in the near term, the extent of thermo-osmosis in certain applications involving long-term considerations, such as containment of LLRW and HLRW where the design lives are on the order of 1000 and 10,000 years, respectively, can be significant.

For example, Horseman and McEwen ([35]) reported that the thermo-osmotic water flux in a saturated compacted kaolinite clay subjected to a temperature gradient of 20 °C m^{-1} could reach a magnitude of 0.5 m y^{-1}, which equates to 500 m in 1000 years or 5000 m in 10,000 years. Although a water flux of 0.5 m y^{-1} may be considered small, Horseman and McEwen [35] indicated that the thermo-osmotic water flux could be as much as 1000 times greater than the hydraulic (Darcian) flux of water, which could be of practical consequence over this time period.

Based on a physical molecular theory for thermo-osmosis, Gonçalvès et al. [26] evaluated the relative contributions of hydraulic flow and thermo-osmosis directed vertically upward through an illitic shale located within a sedimentary basin. Their analysis was based on "standard conditions" including a hydraulic gradient of 0.1 and a thermal gradient of 0.033 K m^{-1} (= 0.033 °C m^{-1}), which was considered to represent the natural geothermal gradient. Their results indicated that thermo-osmosis could be up to 10 times greater than the hydraulic flow. They also noted that the relative contribution of thermo-osmosis to hydraulic flow would be expected to be greater if heat-emitting nuclear wastes were stored in deep shale layers resulting in higher temperature gradients.

Gonçalvès et al. [26] also performed an analysis showing that thermo-osmosis could contribute to the anomalous (non-hydrostatic) pressures that have been measured in shales (e.g., [79]). Their analysis pertained to the Callovo-Oxfordian formation in northeastern France, and indicated that when both thermo- and chemico-osmotic flows are considered, the estimated excess pore-water pressure of 480 kPa was close to the maximum measured value of 530 kPa, suggesting that thermo-osmosis could be another factor contributing to the observed excess pore-water pressures.

Thermo-osmosis also can be a significant factor in dissipating excess pore-water pressures generated by temperature increases at a heat source, depending on the magnitude of k_T [125]. A relatively rapid increase in temperature results in the generation of excess pore-water pressures near the heat source that dissipate with time due to both hydraulic and thermo-osmotic drainage of water from the heat source to a surrounding drainage boundary. The generation of excess pore-water pressures results from the difference between the thermal expansion of the solid and liquid phases. The resulting dissipation of excess pore-water pressures results in a concurrent increase in effective stress and consolidation. Zagorščak et al. [125] performed an analysis showing that the magnitude of the excess pore-water pressures generated at the heat source tends to decrease with increase in k_T, such that failure to account for thermo-osmosis results in an overestimation of the excess pore-water pressures.

3 Recent Advances in Coupled Flow Phenomena

3.1 Coupled Flows Under Saturated Conditions

Theoretical approaches employed to create a mathematical framework for coupled flows in porous media have included both a *phenomenological* approach and a *physical* approach, where the former involves description of coupled phenomena based on macroscopic-scale observations derived from experimentation and the latter involves characterizing the phenomena based on physical and chemical interactions that occur at the microscopic or pore scale (e.g., [18, 91]). Malusis et al. [63] provide a critical review of coupled flow formulations for liquid, electrical current, and solutes through a saturated semipermeable porous medium under an isothermal condition based on the phenomenological approach. The primary outcomes from this review were that differences among the various phenomenological formulations that have appeared in the literature over the past approximately 30 years (e.g., [17, 55, 60, 65, 122, 123]) result primarily from the type and number of solutes (e.g., a single solute, a single salt, or multiple ionic species) and the nature of the solute diffusion process assumed in the formulation (i.e., salt diffusion versus counter diffusion). Formulations based on the physical approach have been introduced more recently (e.g., [18, 68, 91]), and complement the phe-

nomenological approach by providing constitutive expressions for the pore-scale mechanisms controlling the macroscopic soil properties or coupling coefficients utilized in phenomenological formulations (e.g., hydraulic conductivity, effective diffusion coefficient, membrane efficiency coefficient). A brief summary of these considerations and their major differences is provided subsequently.

3.1.1 Phenomenological Formulations

The phenomenological framework for coupled flow formulations is based on the second law of thermodynamics, adapted for nonequilibrium systems in which irreversible processes occur (see [45, 121]). Coupled fluxes (representing the flows per unit cross-sectional area) are derived from the dissipation of free energy (i.e., the dissipation function; see [76]) and are represented as a set of equations in which the fluxes are linearly related to the driving forces. Assuming a one-dimensional, isothermal porous medium, the resulting equations for simultaneous (coupled) fluxes of fluid (water), electrical current, and chemicals can be expressed in general form for an ideal (dilute) chemical solution containing M solute species as follows:

$$q = L_{11}\frac{\partial(-P)}{\partial x} + L_{12}\frac{\partial(-\Psi)}{\partial x} + \sum_{i=1}^{M} L_{1,i+2}\frac{RT}{C_i}\frac{\partial(-C_i)}{\partial x} \tag{5a}$$

$$I = L_{21}\frac{\partial(-P)}{\partial x} + L_{22}\frac{\partial(-\Psi)}{\partial x} + \sum_{i=1}^{M} L_{2,i+2}\frac{RT}{C_i}\frac{\partial(-C_i)}{\partial x} \tag{5b}$$

$$J_j^d = L_{j+2,1}\frac{\partial(-P)}{\partial x} + L_{j+2,2}\frac{\partial(-\Psi)}{\partial x} + \sum_{i=1}^{M} L_{j+2,i+2}\frac{RT}{C_i}\frac{\partial(-C_i)}{\partial x}; \quad j = 1, 2, \ldots, M \tag{5c}$$

where q is the liquid (solution) flux (i.e., the volumetric liquid flow rate per unit total cross-section area of the porous medium), P is the liquid pressure, I is the electrical current flux, Ψ is the electrical potential, J_j^d is the diffusive flux of solute species j, C_i is the concentration of solute species i, R is the universal gas constant, T is absolute temperature, and x is the flux direction. The coefficients L are phenomenological coefficients representing the properties of the porous medium, as follows [63]:

$$L_{11} = \frac{k_h}{\gamma_w} + \frac{k_e^2}{n\sigma_e^*} \tag{6a}$$

$$L_{21} = L_{12} = k_e \tag{6b}$$

$$L_{22} = n\sigma_e^* \tag{6c}$$

$$L_{1,j+2} = L_{j+2,1} = \frac{\omega\, C_j k_h}{\gamma_w} \pm \frac{k_e C_j u_j^*}{\sigma_e^*} \tag{6d}$$

$$L_{2,j+2} = L_{j+2,2} = \pm n C_j u_j^* \tag{6e}$$

$$L_{j+2,i+2} = \delta_{ij}\left(\frac{n D_j^* C_j}{RT} + \frac{\omega^2 C_j C_i k_h}{\gamma_w}\right) \tag{6f}$$

where k_h is hydraulic conductivity, γ_w is the unit weight of water, k_e is electro-osmotic conductivity, n is total soil porosity, σ_e^* is the effective electrical conductivity of the soil, ω is the membrane efficiency coefficient, δ_{ij} is the Kronecker delta function (i.e., $\delta_{ij} = 1$ when $i = j$ and $\delta_{ij} = 0$ when $i \neq j$; see [113]), and u_j^* and D_j^* are the effective ionic mobility and effective self-diffusion coefficient for solute species j, respectively. The "±" operator in Eqs. 6d and 6e is positive if species j is a cation and negative if species j is an anion. The expressions given by Eqs. 6a–6f assume that the chemical solution is dilute and that the diffusion process governing solute migration is mutual (or salt) diffusion, whereby solutes diffuse in the same direction.

A separate expression of Eq. 6c is required for each solute species. Thus, a complete set of coupled flux equations for an isothermal system with M solute species consists of $M + 2$ equations, with the equations each containing $M + 2$ terms and collectively containing $(M + 2)^2$ phenomenological coefficients (L_{ij}) that must be known in order to compute the fluxes. The off-diagonal coefficients are assumed to be equivalent (i.e., $L_{ij} = L_{ji}$) based on Onsager's reciprocal relations (see Eqs. 6b, 6d, and 6e), which reduces the number of unique coefficients to $[(M + 3)(M + 2)]/2$. Nonetheless, the complexity of the formulation increases as the number of solutes increases. As a result, most coupled flux formulations presented in the literature consider systems containing a single solute ($M = 1$) or the cation and anion of a single binary salt ($M = 2$) (e.g., see [28–30, 55, 65, 81, 121, 123]).

For example, the set of coupled flux equations for a system containing a single cation (c) and a single anion (a) may be written as follows ([121, 123]):

$$q = L_{11}\frac{\partial(-P)}{\partial x} + L_{12}\frac{\partial(-\Psi)}{\partial x} + L_{13}\frac{RT}{C_c}\frac{\partial(-C_c)}{\partial x} + L_{14}\frac{RT}{C_a}\frac{\partial(-C_a)}{\partial x} \tag{7a}$$

$$I = L_{21}\frac{\partial(-P)}{\partial x} + L_{22}\frac{\partial(-\Psi)}{\partial x} + L_{23}\frac{RT}{C_c}\frac{\partial(-C_c)}{\partial x} + L_{24}\frac{RT}{C_a}\frac{\partial(-C_a)}{\partial x} \tag{7b}$$

$$J_c^d = L_{31}\frac{\partial(-P)}{\partial x} + L_{32}\frac{\partial(-\Psi)}{\partial x} + L_{33}\frac{RT}{C_c}\frac{\partial(-C_c)}{\partial x} + L_{34}\frac{RT}{C_a}\frac{\partial(-C_a)}{\partial x} \tag{7c}$$

$$J_a^d = L_{41}\frac{\partial(-P)}{\partial x} + L_{42}\frac{\partial(-\Psi)}{\partial x} + L_{43}\frac{RT}{C_c}\frac{\partial(-C_c)}{\partial x} + L_{44}\frac{RT}{C_a}\frac{\partial(-C_a)}{\partial x} \tag{7d}$$

where the phenomenological coefficients given by Eqs. 6a–6f reduce to the following expressions:

$$\begin{bmatrix} L_{11} & L_{12} & L_{13} & L_{14} \\ L_{21} & L_{22} & L_{23} & L_{24} \\ L_{31} & L_{32} & L_{33} & L_{34} \\ L_{41} & L_{42} & L_{43} & L_{44} \end{bmatrix} = \begin{bmatrix} \frac{k_h}{\gamma_w} + \frac{k_e^2}{n\sigma_e^*} & k_e & -\frac{\omega C_c k_h}{\gamma_w} + \frac{k_e C_c u_c^*}{\sigma_e^*} & -\frac{\omega C_a k_h}{\gamma_w} - \frac{k_e C_a u_a^*}{\sigma_e^*} \\ k_e & n\sigma_e^* & nC_c u_c^* & -nC_a u_a^* \\ -\frac{\omega C_c k_h}{\gamma_w} + \frac{k_e C_c u_c^*}{\sigma_e^*} & nC_c u_c^* & \frac{nD_c^* C_c}{RT} + \frac{\omega^2 C_c^2 k_h \upsilon}{\gamma_w \upsilon_c} & 0 \\ -\frac{\omega C_a k_h}{\gamma_w} - \frac{k_e C_a u_a^*}{\sigma_e^*} & -nC_a u_a^* & 0 & \frac{nD_a^* C_a}{RT} + \frac{\omega^2 C_a^2 k_h \upsilon}{\gamma_w \upsilon_a} \end{bmatrix} \quad (8)$$

where ν_c, ν_a, and ν are the numbers of cations, anions, and total ions, respectively, per molecule of the salt. The coefficients in Eq. 8 are similar to those presented by Yeung [121] except that the coefficients in Eq. 8 are defined based on the total cross-sectional area of the soil, whereas the coefficients given by Yeung [121] were defined based on the cross-sectional area of the voids. Also, the definitions for L_{33} and L_{44} given by Yeung [121] do not include the second term in Eq. 8, which arises as a result of the aforementioned assumption of salt diffusion. The formulation of Yeung [121] was based on the assumption of counter diffusion (or inter-diffusion) in which solutes migrate in opposite directions. The salt-diffusion formulation is considered more fundamentally correct, as discussed by Lu et al. [55] and Malusis et al. [63].

An alternative to the single-cation, single-anion formulation given by Eqs. 7a–8 is the single-salt formulation (see [55]) in which the cation and anion are treated as a single solute ($M = 1$), assuming that the salt cation and salt anion must migrate through the soil at the same rate to preserve electroneutrality in solution. For the case in which no electrical current is applied across the soil ($I = 0$), the single-salt formulation is consistent with the formulation for a single uncharged solute given by Manassero and Dominijanni [65]. Regardless of whether or not the cation and anion are tracked separately, both of these formulations are valid only when no ionic species other than the salt cation and the salt anion are migrating through the soil. This condition does not exist when ion exchange of the salt cation and/or the salt anion is occurring, as ion exchange results in the release of other ionic species. Thus, while these simplified formulations are applicable for describing coupled fluxes in the absence of ion exchange processes, a more rigorous formulation is required for describing coupled fluxes under transient conditions in which the migrating salt ions exchange with other ions held electrostatically to the solid phase of the soil ([60, 113]). In addition, electrolyte solutions in the natural environment typically contain multiple cationic or anionic species. For these more complex cases, the more general formulation given by Eqs. 5a and 6a is required.

3.1.2 Total Liquid and Solute Flux Through Semipermeable Clay Membranes

The aforementioned coupled flux formulations have been utilized to develop expressions for liquid flux and total (advective-diffusive) solute flux through engineered soil barriers (e.g., compacted clay liners, geosynthetic clay liners, vertical cutoff walls) that act as semipermeable membranes (i.e., $\omega > 0$), restricting the migration of solutes while allowing relatively unimpeded migration of water. For example, in the case where there is no applied current ($I = 0$), the total liquid flux (q) and total mass or molar flux of a solute (J_j) for one-dimensional flow and transport through a saturated porous membrane can be expressed as follows based on Eqs. 5a and 6a:

$$q = q_h + q_\pi = k_h i_h + \omega\, k_h i_\pi = -k_h \frac{\partial h}{\partial x} + \frac{\omega\, k_h}{\gamma_w} \frac{\partial \pi}{\partial x} \tag{9a}$$

$$J_j = J_{ha,j} + J_{\pi,j} + J_j^d = (1-\omega) q_h C_j + (1-\omega) q_\pi C_j - n D_{sj}^* \frac{\partial C_j}{\partial x} \tag{9b}$$

where q_h is hydraulic liquid flux, q_π is chemico-osmotic liquid flux, h is hydraulic head, π is chemico-osmotic pressure, i_h is the hydraulic gradient, i_π is the chemico-osmotic pressure gradient, $J_{ha,j}$ is the hyperfiltrated advective flux of solute species j, $J_{\pi,j}$ is the chemico-osmotic flux of solute species j, D_{sj}^* is the effective salt-diffusion coefficient of species j, and all other terms are as defined previously. For dilute solutions containing M solutes, $\partial\pi/\partial x$ and D_{sj}^* are influenced by of all the species present in the system, as follows [60]:

$$\frac{\partial \pi}{\partial x} = RT \sum_{i=1}^{M} \frac{\partial C_i}{\partial x} \tag{10}$$

and

$$D_{sj}^* = D_j^* \pm \frac{D_j^* |z_j| C_j \sum_{i=1}^{M} \left[-D_i^* z_i (\partial C_i / \partial x) \right]}{(\partial C_j / \partial x) \sum_{i=1}^{M} \left(D_i^* |z_i| C_i \right)} \tag{11}$$

where z is ion valence and the "±" term in Eq. 11 is positive when species j is a cation and negative when species j is an anion. For the single-cation, single-anion system, Eqs. 10 and 11 reduce to:

$$\frac{\partial \pi}{\partial x} = RT \left(\frac{\partial C_a}{\partial x} + \frac{\partial C_c}{\partial x} \right) \tag{12}$$

and

$$D_{sc}^* = D_{sa}^* = D_s^* = \frac{D_c^* D_a^* (|z_a| + |z_c|)}{D_a^* |z_a| + D_c^* |z_c|} \tag{13}$$

Note that Eq. 13, which represents the effective or porous medium form of the liquid-phase Nernst-Einstein equation [102], yields equivalent effective salt-diffusion coefficients for the cation and anion, since the rate of diffusion of both species must be the same to satisfy electroneutrality. Alternatively, Eq. 13 may be expressed as follows:

$$D_s^* = \tau_a D_{so} = \tau_a \left[\frac{D_{oc} D_{oa} (|z_a| + |z_c|)}{D_{oa}|z_a| + D_{oc}|z_c|} \right] \tag{14}$$

where D_{so} is the salt-diffusion coefficient in free solution, D_{oc} and D_{oa} are the self-diffusion coefficients of the cation and anion in free solution, respectively, and τ_a is an apparent tortuosity factor ($0 < \tau_a < 1$) accounting for the presence of the porous medium [104]. According to Malusis and Shackelford [59], τ_a may be defined further as the product of a matrix tortuosity factor, τ_m, and a restrictive tortuosity factor, τ_r, as follows:

$$\tau_a = \tau_m \tau_r \tag{15}$$

where τ_m represents the tortuosity solely associated with the geometry of the interconnected pores and τ_r represents additional tortuosity associated with factors such as membrane behavior that further restrict diffusion by reducing the conductive fraction of the pore space. In the absence of membrane behavior ($\omega = 0$), $\tau_r = 1$ and, therefore, $\tau_a = \tau_m$, provided that other potential mechanisms for restricting diffusion are insignificant (e.g., [101]).

The directions of the components of q and J_j for typical geoenvironmental containment scenarios are illustrated in Fig. 4. Note that, for the vertical barrier, q_h and J_{ha} are actually two-dimensional, but usually are assumed to be one-dimensional for convenience, on the basis that the head loss across the barrier is small relative to the aquifer thickness. The chemico-osmotic solute flux, J_π, represents the advective drag of solutes by q_π in the direction opposite to the direction of diffusion (and, for the scenarios in Fig. 4, also opposite to the direction of the hydraulically driven advective flux J_{ha}). Hence, J_π has been referred to as counter-advection (see [57, 60, 63]). Analyses presented by Malusis et al. [63] and, more recently, by Malusis et al. [57] indicate that the contribution of J_π to the total solute flux tends to be minor, particularly for diffusion-dominated conditions that are expected to exist in typical geoenvironmental containment scenarios. Nonetheless, inclusion of chemico-osmotic effects represents a more rigorous approach for evaluating liquid and solute transport through clay barriers that behave as semipermeable membranes.

3.1.3 Limitations of the Phenomenological Approach

The efficacy of the phenomenological approach for describing coupled solute transport in clay membranes may be assessed, at least in part, by examining the total solute flux expression given by Eq. 9b for the extreme conditions of (1) a soil exhibiting no

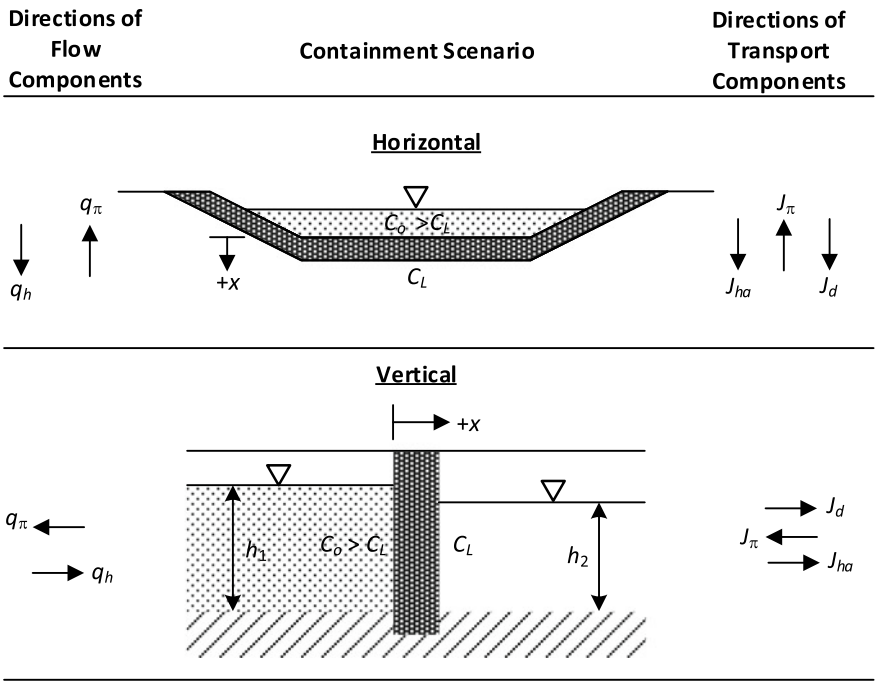

Fig. 4 Directions of the components of liquid flow and solute transport across a porous membrane barrier used for horizontal or vertical chemical containment scenarios [h_1, h_2 = up-gradient and down-gradient hydraulic heads; C_o, C_L = source and exit solute concentrations]. Reprinted from Ref. [62], with permission of ELSEVIER

membrane behavior ($\omega = 0$) and (2) a soil acting as an ideal or perfect membrane ($\omega = 1$). For the case of $\omega = 0$, $q_\pi = 0$ (see Eq. 9a) and, therefore, Eq. 9b reduces to the conventional expression for advective-diffusive solute flux through a porous medium:

$$J_j(\omega = 0) = q_h C_j - nD^*_{sj}\frac{\partial C_j}{\partial x} \tag{16}$$

In contrast, for the case of $\omega = 1$, Eq. 9b reduces to the following expression:

$$J_j(\omega = 1) = -nD^*_{sj}\frac{\partial C_j}{\partial x} \tag{17}$$

In this latter case pertaining to $\omega = 1$, the solute flux should reduce to zero, since an ideal membrane completely restricts solute migration through the membrane pores [55]. Thus, in theory, D^*_s should decrease toward zero as ω increases toward unity, a trend that has been supported by the results of several experimental studies related to semipermeable clay membranes (e.g., [56, 59, 64, 107]). Failure to recognize

this requirement can result in erroneous predictions of solute concentration profiles within ideal semipermeable membranes in that concentration profiles are shown to exist for the case of an ideal semipermeable membrane (e.g., see Fig. 4b in [109]). Similarly, a considerable body of experimental data shows that ω is not constant for a given clay membrane, but rather increases with decreasing solute concentration (e.g., [47, 48, 58]), as previously indicated in Fig. 2. As a result, decreases in D_s^* reported in the aforementioned studies also correlate with decreasing source concentration.

The concentration dependencies of both ω and D_s^* are interrelated, in that decreasing solute concentration results in greater expansion of the DDLs surrounding individual clay particles, leading to higher ω and lower D_s^* due to greater ion exclusion in the pore spaces. Thus, in reality, both ω and D_s^* vary spatially within a membrane (due to spatial variations in solute concentration) and, therefore, values of ω and D_s^* reported in experimental studies on clay membranes are global (macroscopic) values that lie somewhere between the maximum and minimum values that occur on a local (microscopic) basis within the membrane ([16, 68, 77, 79]).

These considerations reveal two limitations of the phenomenological approach. First, the approach explicitly fails to account for the concentration dependence of ω. Second, the approach also fails to account for the interrelationship between ω and D_s^*, which has been referred to as "implicit coupling" [59]. As a result, in the phenomenological approach, both ω and D_s^* typically are treated as constants for the porous medium, such that modeling of coupled solute migration through a semipermeable porous medium based strictly on the phenomenological approach requires appropriate selections of ω and D_s^* for the range of solute concentrations expected in the system being studied.

3.1.4 Insights from the Physical Approach

The physical approach, which involves the development of constitutive relationships for the phenomenological coefficients based on physical and chemical interactions between the solid and liquid phases at the pore (microscopic) scale, has been used to address the aforementioned limitations of the phenomenological approach. For example, Manassero [68] describes a physical model developed for a bentonite (montmorillonite) membrane barrier in contact with an electrolyte solution containing a single, monovalent (1:1) salt ([16, 18, 19, 66, 67, 77]). The model was obtained by upscaling (volume-averaging) the Poisson, Navier-Stokes, and Nernst-Planck equations at the pore scale and using the Donnan equations for electrochemical potential, resulting in the following expressions that can be used to predict the global ω for a bentonite barrier based on the salt concentrations present at the entry boundary (C_o) and exit boundary (C_L):

$$\omega = 1 + \frac{\bar{c}_{sk,0}}{2e_m \Delta C_s}\left[Z_2 - Z_1 - (2t_c - 1) \cdot \ln\left(\frac{Z_2 + 2t_c - 1}{Z_1 + 2t_c - 1}\right)\right] \tag{18}$$

and

$$Z_1 = \sqrt{1 + \left(2C_o e_m / \bar{c}_{sk,0}\right)^2}; Z_2 = \sqrt{1 + \left(2C_L e_m / \bar{c}_{sk,0}\right)^2} \tag{19a}$$

$$t_c = \frac{D_{oc}}{D_{oc} + D_{oa}} \tag{19b}$$

where $\bar{c}_{sk,0}$ is the effective solid charge concentration of the montmorillonite, e_m is the void ratio representing the void space between montmorillonite tactoids, ΔC_s is the difference in salt concentration across the barrier (i.e., $\Delta C_s = C_o - C_L$), t_c is the cation transport number, and D_{oc} and D_{oa} are the free-solution or self-diffusion coefficients of the cation and anion, respectively. Based on Eqs. 18–19a, ω can be predicted for a given salt species and given boundary salt concentrations (i.e., known values of t_c, C_o, and C_L) provided that two material properties of the membrane, $\bar{c}_{sk,0}$ and e_m, are known.

In addition, Dominijanni and Manassero [18] show that D_s^* may be expressed as a linear function of ω based on the physical model, as follows:

$$D_s^* = (1 - \omega) D_{se} = (1 - \omega) \tau_m D_{so} \tag{20}$$

where D_{se} is a modified effective salt-diffusion coefficient that accounts only for the matrix tortuosity (i.e., $D_{se} = \tau_m D_{so}$). Substitution of Eq. 20 into Eq. 9b yields the following revised expression for coupled solute flux:

$$J_j = J_{ha,j} + J_{\pi,j} + J_j^d = (1 - \omega) q_h C_j + (1 - \omega) q_\pi C_j - (1 - \omega) n D_{se,j} \frac{\partial C_j}{\partial x} \tag{21}$$

Thus, incorporation of the physical model into the phenomenological framework resolves the limitation identified by Eq. 17, as the total solute flux given by Eq. 21 reduces to zero for the case of an ideal membrane (ω = 1). Because the physical model assumes that pore-scale variations in pressure, ion concentration, and water velocity within the porous medium are negligible [18], Eq. 20 is an approximation of the true relationship between D_s^* and ω. However, a growing body of experimental evidence indicates that Eq. 20 represents a reasonable approximation for bentonite membranes (e.g., [20, 56, 59, 64]).

The aforementioned recent advances suggest that a combined physical-phenomenological model offers the most promise for future advances in our understanding of coupled flow phenomena in porous media. However, one of the primary challenges associated with employing the physical model within the phenomenological framework is determining the required material properties, viz., $\bar{c}_{sk,0}$, e_m, and τ_m. For bentonite membranes, $\bar{c}_{sk,0}$ and e_m can be estimated by considering an idealized model for the bentonite fabric in which the solid particles (or tactoids) consist solely of layered, parallel lamellae (or platelets) with relatively immobile pore solution within the interlayer spaces between the lamellae. Estimates of $\bar{c}_{sk,0}$ based on this model require estimation of the bentonite specific surface, surface charge, and the fraction of the surface charge compensated by the cations in the Stern layer [68], whereas estimates of e_m further require estimation of the Stern layer thickness,

the distance between tactoids, the number of platelets comprising each tactoid, and the distance between platelets. Also, $\bar{c}_{sk,0}$ can be estimated by non-linear regression of Eq. 18 through experimental data sets of ω plotted as a function of a suitable reference salt concentration ([16, 20, 77]). In this latter approach, since $\bar{c}_{sk,0}$ is a fitting parameter, the extent to which regressed values of $\bar{c}_{sk,0}$ are representative of the actual $\bar{c}_{sk,0}$ or the $\bar{c}_{sk,0}$ predicted based on an idealized fabric must be established. Furthermore, some experimental studies indicate that the linear approximation given by Eq. 20 may not be appropriate in all cases (e.g., [107]). This aspect of the physical approach represents an existing research challenge with respect to coupled flows in porous media for Geotechnical Engineering applications.

3.2 Coupled Flows Under Unsaturated Conditions

In recent years, the existence and magnitude of coupled flows in unsaturated porous materials have been evaluated with respect to applications pertaining to electro-osmosis in shallow geophysical explorations (e.g., [85]) and chemico-osmosis related to both chemical containment barriers (e.g., [96]) and deep geologic sequestration of CO_2 (e.g., [10]). A summary of some of the recent studies is provided in Table 2.

In sandy soil, even though the salt membrane behavior due to chemico-osmosis is essentially negligible, electro-osmosis can be significant. For example, Revil et al. [85] found that the streaming potential or electro-osmosis coefficient increases with increasing temperature and grain size, but decreases with increasing liquid saturation and salinity. In contrast, based on the results of a column experiment on unsaturated sand, Guichet et al. [31] found that the electro-osmosis coefficient decreases with decreasing saturation (100 and 40%). Revil et al. [85] developed an electro-osmosis theory by using the physical-based approach and found that the

Table 2 Recent studies on coupled flows in unsaturated porous materials

References	Hydraulic (Pressure)	Chemical (Concentration)	Electrical (Voltage)
Revil et al. [85]	Sandy soil		Sandy soil
Guichet et al. [31]	Sand		Sand
Linde et al. [52]	Sand		Sand
Revil et al. [91]	Dolomite		Dolomite
Jougnot et al. [41]	Clay rock		Clay rock
Chen and Hicks [10]	Rock	Rock	
Schmid et al. [99]	Rock	Rock	
Revil [86, 87]	Porous media	Porous media	Porous media
Sample-Lord and Shackelford [95, 96]	Clay soil	Clay soil	

streaming potential could either increase or decrease, depending on not only the degree of saturation but also the type of material and the history of the saturation. Linde et al. [52] conducted an electro-osmosis test involving a sand column and concluded that the magnitude of streaming potential depends primarily on the fluid velocity, the excess of electric charge in pore fluid, and the porosity.

In many natural geomaterials, shallow unsaturated subsurface fluid flow can cause significant streaming potential differences both spatially and temporally that can be easily detected and mapped on the soil surface. These self-potential distributions mapped either on the soil surface or in the subsurface via boreholes can be used as boundary values for inversed numerical solutions of groundwater velocity and temperature. Similarly, mapped self-potential changes due to chemico-osmosis can be used to quantify spatial and temporal migration of contaminants in the unsaturated shallow subsurface or vadose zone.

In clayey soil or rocks, particularly those rich in smectite minerals, both electro-osmosis and chemico-osmosis can be significant due to high surface charge and high CEC (i.e., high pore fluid charge density and small pore sizes). For example, Jougnot et al. [41] conducted a series of laboratory, humidity-controlled tests on smectite-rich rock (Callovo-Oxfordian clay) and evaluated the results based on a physical-based electro-osmosis coupling model. They found that the streaming potential coupling coefficient follows a power law with respect to fluid saturation. They also found that the flux of the gas phase with respect to the liquid flux cannot be ignored when the relative humidity is less than 30%. Schmid et al. [99] developed a theory of coupled fluid and chemical flows and demonstrated that the capillary pressure in rocks with micropores can be strongly dependent on pore fluid salinity. Revil [86, 87] developed a theory for coupled fluid, electric, and chemical flows under unsaturated conditions, and demonstrated that the chemico-osmotic membrane coefficient can be functionally related to fundamental pore-scale physical properties, including CEC, porosity, chemical concentration, and liquid saturation.

Smectite-rich clays, such as Na-bentonites used in GCLs for near-surface waste containment and highly densified bentonite buffers for deep geologic waste repositories (i.e., for high-level radioactive wastes), have been studied extensively. For example, Sample-Lord and Shackelford [95, 96] conducted laboratory-scale membrane tests on specimens of a Na-bentonite at constant degrees of saturation ranging from 79 to 100% using salt solutions with different concentrations of KCl. They found that, for a given concentration gradient, the chemico-osmotic membrane coefficient increases as the saturation decreases (Fig. 5). However, for a given saturation, the membrane efficiency coefficient decreased as the solution concentration increased, which is consistent with previous results based on similar specimens evaluated under saturated conditions. For the range of the saturations tested, the effective diffusion coefficient of Na-bentonite remained relatively unchanged. These results represent the first quantitative evidence of chemico-osmotic behavior in clay under unsaturated conditions.

Several research challenges exist for providing a better understanding of chemico-osmotic behavior in unsaturated porous materials. Except for the study of Jougnot et al. [41], all of the experimental studies on unsaturated materials have been con-

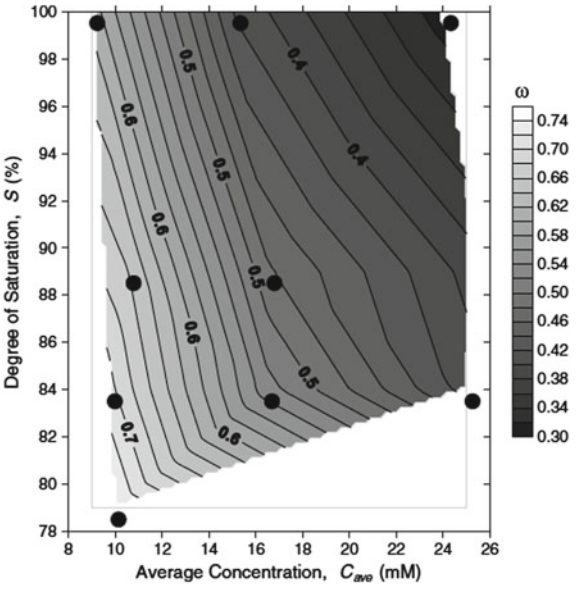

Fig. 5 Contour plot of measured values of membrane coefficient (ω) as a function of average KCl concentration and degree of saturation for Na-bentonite with a porosity of 0.88 (from [96] Reproduced with permission of AMERICAN SOCIETY OF CIVIL ENGINNERS)

ducted at saturations greater than 40%, due to limitations on the ability to achieve lower saturations using the axis translation technique to control suction (e.g., [54]). Other suction control techniques, such as relative humidity control, are promising for lower saturations (e.g., [51]). The effects of solute restriction leading to membrane behavior, chemico-osmosis, and restricted liquid-phase solute diffusion at lower saturations (i.e. <40%) are expected to be more significant than at higher saturations, since much of the pore water at lower saturations would be located near the clay particle surfaces where the ion-restricting electromagnetic fields have greater intensity [96].

Most of the studies conducted to date also have been limited to testing under steady-state conditions resulting in lengthy test durations ranging from several months to more than a year for a given set of conditions. For example, the three tests conducted by Sample-Lord and Shackelford [96] lasted from 232 to 335 days, yielding a combined total testing duration of 1171 days (3.2 years). Shorter test durations may be possible through the development of transient testing methods, which may involve transient forward and inverse modeling for parameter identification (e.g., [119]).

There also is a significant absence in the literature with respect to the development of coupled flow theories under unsaturated conditions. Without these theories, experimental results cannot be properly interpreted. As previously described, some physical-based theories have been developed for chemico-osmosis or electro-osmosis under unsaturated conditions. However, these theories are not useful for interpreting laboratory test results, as further assumptions or simplifications are needed. No theory based on the phenomenological approach for all four coupled flows (i.e., liq-

uid flow, heat transfer, electric current, and chemical transport) under unsaturated conditions has been developed.

3.3 Phenomenologically-Based Material Property Determination

As previously noted, two distinct approaches have been undertaken for understanding coupled flows, viz., the phenomenological approach and the physical-based approach. Although both approaches are based on thermodynamic principles, the scales, physical properties, and theories of these two approaches differ significantly.

The phenomenological approach seeks macroscopic relationships among the fluxes and the corresponding gradients (e.g., Table 1), leading to the material properties defined as the ratios between a specific flux and gradient. For example, the ratio of fluid flux and hydraulic gradient without the involvement of other gradients is the hydraulic conductivity, and the ratio of fluid flux to the chemical concentration gradient is the chemico-osmosis coupling coefficient. Based on this approach, macroscopic laboratory experiments can be conducted to determine the appropriate phenomenological coefficients.

The physical-based approach starts at the pore scale where coupling phenomena occur. By defining the governing physics laws for the coupled phenomena pertaining to fluid flow, heat transfer, electric current, and chemical transport, mass and energy conservation principles can be applied to define boundary value problems within the representative elementary volume (REV) at the pore scale. Solving the boundary value problem by volume-averaging techniques provides upscaling to the macroscopic variables and associated relationships in terms of physical properties at the pore scale, such as pore fluid charge density, porosity, local and reservoir chemical concentrations, etc. The resulting relationships among the fluxes and relevant gradients provide direct linkages between the phenomenological coefficients and fundamental physical properties.

The existing experimental methods for determining the relevant material properties required to describe coupled flows in porous media are summarized in Table 3. The testing principles generally are founded upon basic theories for coupled flows, including flow laws and mass and energy conservation principles. The experimental methods vary in terms of the testing principles, whether the variables are controlled or measured, and the interpretation techniques. Although each experimental method is specifically designed and executed for measuring material properties or coefficients for coupled flows, reference is made only to what is controlled or measured, since deducing material properties from experimental observations relies upon the specific theory employed.

In some cases, the fundamental flow laws given by Darcy's, Fick's, Ohm's, and Fourier's equations are utilized, and the tests are conducted under well-controlled laboratory conditions by controlling gradients or fluxes and measuring the mate-

Table 3 Direct or indirect measurement methods for coupled flow phenomena

References	Controlled (C), Measured (M), Direct (-d), Indirect (-i)			
	Hydraulic (Pressure)	Chemical (Concentration)	Electrical (Voltage)	Thermal (Temperature)
Kemper and Rollins [48]	C-d or M-d	C-d or M-d		
Olsen [81, 82]	C-d or M-d	C-d or M-d	C-d or M-d	
Shackelford [102]	M-d	C-d or M-d		
Yeung and Mitchell [123]	M-d	C-d or M-d	C-d or M-d	
Alshawabkeh and Acar [2]	M-i	M-i	C-i	
Keijzer et al. [46]	M-d	C-d or M-d		
Neuzil[a] [78]	C-i	C-i or M-i		
Sherwood and Craster [108]	M-i	C-i or M-i		
Malusis and Shackelford [58]	C-d or M-d	C-d or M-d		
Rosanne et al. [92]	C-d or M-d-i		C-d or M-d-i	
Heister et al. [33]	C-d or M-d	C-d or M-d	C-d or M-d	
Revil et al. [90]	C-d	C-d or M-i	M-d	
Garavito et al.[a] [24]	C-i	C-i or M-i		
Heister et al. [34]	C-d or M-d	C-d or M-d	C-d or M-d	
Paszkuta et al. [84]	C-d or M-d	C-d or M-d	C-d or M-d	C-d or M-d-i
Rosanne et al. [94]	C-d or M-d-i	C-d or M-d-i	C-d or M-d-i	C-d or M-d-i
Garavito et al.[a] [25]	C-i	C-i or M-i		
Horseman et al. [36]	C-d or M-d	C-d or M-d		
Cruchaudet et al.[a] [11]	M-i	C-i		
Kang and Shackelford [42]	C-d or M-d	C-d or M-d		
Kim and Mench [49]	M-d			C-d or M-d
Oduor et al. [80]	C-d or M-d	C-d or M-d		
Jougnot et al.[b] [41]	C-i		C-i or M-i	
Kang and Shackelford [43]	C-d or M-d	C-d or M-d		
Tremosa et al.[a] [112]		C-i or M-i		C-i
Kang and Shackelford [44]	C-d or M-d	C-d or M-d		
Shackelford et al. [107]	C-d or M-d	C-d or M-d		
Sample-Lord and Shackelford[b] [95]	C-d or M-d	C-d or M-d		

[a]Field-scale measurement conditions; all others laboratory measurement conditions
[b]Unsaturated conditions; all others fully saturated conditions

rial properties after steady-state conditions have been achieved. These methods are referred to as direct methods and are denoted as "–d" in Table 3. The material properties pertinent to direct flows generally can be measured reliably within the resolutions of the experimental measurements. In contrast, indirect methods, denoted as "–i" in Table 3, refer to those methods requiring numerical solution of a set of partial differential equations to estimate material properties from transient experimental data. The material properties obtained by indirect methods are constrained by not only the coupled flow theories utilized, but also the boundary and initial conditions and the measurement resolution. These methods often are applied to field experiments or transient laboratory experiments. Direct methods generally provide for the best control of the boundary conditions and are subject to less uncertainty than the indirect methods. However, material properties obtained by direct methods can be subject to different interpretations, depending on the theory utilized, the underlying assumptions and physical limitations of the method, and the experimental conditions. For example, using the same experimental data set resulting from evaluation of a saturated, bentonite-based GCL, Malusis et al. [63] showed that the effective diffusivity of salt inferred from two different chemico-osmosis theories can differ by as much as 12%. Also, a major drawback for any direct method is the limitation on the experimental time required to reach and establish steady-state conditions. Depending on the material type and specimen dimensions, some of the transport processes like heat, fluid, and chemical transport are slow, such that establishing a steady state condition even for typically small laboratory specimen dimensions may take months or years (e.g., [96]).

Also, for materials such as smectite-based clays (e.g., bentonites) where the coupling among the different flows can be significant, interpretation of the material properties pertinent to the direct flows can be non-unique for the same experimental data set. For example, if a hydraulic gradient is applied to a saturated bentonite specimen, Darcy's law can be used directly to estimate hydraulic conductivity if a steady-state head loss across the specimen is measured. However, constant, imposed fluid flow also has been shown to result in a measurable streaming potential gradient (electro-osmosis) leading to an additional component of fluid flow (e.g., [33, 82, 84]). Failure to account for this latter component would result in conflation of hydraulic conductivity and electro-osmotic conductivity (i.e., k_e in Eq. 8). Alternatively, use of coupled flow theory and an appropriate experimental setup will allow both hydraulic conductivity and electro-osmotic conductivity to be inferred and will yield a different value of hydraulic conductivity than that based solely on Darcy's law.

One potential issue in some of the previous experimental studies is the omission of the measurement of variables that can affect the interpretation of the experimental results. For example, most experimental studies pertaining to chemico-osmosis and semipermeable membrane efficiency have not included measurement of the electrical potential or current, on the basis that the material used to construct the cells containing the specimens is nonconductive (e.g., plastic), such that short-circuiting of the system is prevented and the induced electrical potential or current or both are zero. However, in the case where the cell material is electrically conductive (e.g., steel), short-circuiting of the system is possible such that the induced electrical

potential can be significant and alter the interpretation of the properties pertinent to chemico-osmosis (e.g., [33, 34]).

3.4 Microscopic Physical-Based Material Property Determination

The physical-based approach seeks relationships between physico-chemical parameters at the pore scale and the phenomenological coefficients (e.g., [41, 84, 88, 90, 93]). This approach provides not only the scientific basis but also the quantitative linkages between pore-scale constituent properties and microstructural parameters to macro-scale phenomenological parameters. For example, the membrane efficiency coefficient can be related directly to pore-scale electrical charge density, CEC, pore chemistry, and porosity, among other fundamental material parameters at an atomic scale. This approach is used together with the phenomenologically-based approach to better interpret the experimental results.

The physical-based approach is mathematically complex and typically includes the following steps (e.g., [84, 88, 89]): (1) physically conceptualizing of all the coupled physico-chemical processes within a pore-scale REV, (2) defining the proper laws governing the variables of temperature, pressure, chemical, and electrical potential within the REV, and the governing equations (principles) describing the spatial and temporal variations of these variables within the REV, (3) averaging of these variables over the entire REV by solving the well-defined boundary value problems and employing a specific averaging theorem, and (4) defining the phenomenological parameters by comparing the resulting coupled flow laws with those by the phenomenological flow equations. For example, based on this approach, Gupta et al. [32] show that the electro-osmotic coefficient can be linked to zeta potential (i.e., the electrical potential within the DDL at the interface between the stationary liquid directly adjacent to the charged particle surface and the mobile liquid between adjacent charged particles, also referred to as the slip plane), electrolyte concentrations and other pore-scale parameters.

The most commonly used pore-scale physical conception is the triple layer model (TLM) wherein a pore-scale REV consists of three domains, viz., the clay mineral particle surface, the Stern layer (immobile for ions), and a Gouy-Chapman layer (diffuse double layer of ions). For example, by using the afore mentioned approach, Revil and Leroy [88] established a coupled flow theory for fluid, salt, and electricity, and the relationships between the coupling coefficients for chemico-osmosis, electric-osmosis, and thermo-osmosis, and pore-scale properties of charge density, porosity, CEC, salt concentration, and other fundamental physical properties. A comparison of their theoretical model predictions and measured results from Malusis and Shackelford [58] is shown Fig. 6.

Although the physical-based methodology provides a fundamentally attractive way to understand coupled flows in porous media, there are challenging gaps between

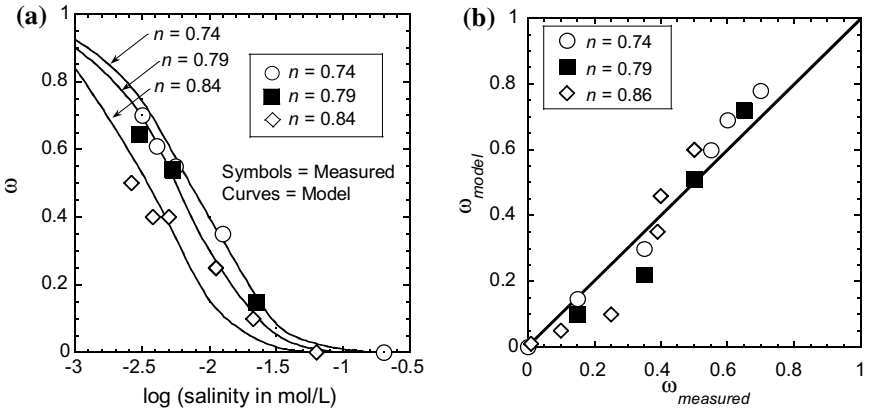

Fig. 6 Comparison of osmotic efficiency (membrane) coefficient (ω) based on theoretical model results versus experimental results from [58] for a saturated geosynthetic clay liner exposed to KCl salt solutions under isothermal conditions: **a** ω as a function of concentration; **b** measured versus modeled ω (data from [88]) (*Note* n = porosity)

the established theories and macroscopically measurable parameters suitable for engineering applications. These challenges include the nature of the specific REV model, the determination of the physical properties at the atomic and/or pore scale, the averaging techniques, and the experimental verification of the developed theory. In terms of the REV model, physical laws have to be simplified to make the volume-averaging mathematically trackable for analytical solutions at the REV level. For example, the TLM is a more realistic conceptualization than the Gouy-Chapman double layer theory. However, the TLM also deviates from reality in that local chemical potentials exist that are more electrical in nature than the chemical potential captured by the TLM, including van der Waals forces between solid particles and the surrounding fluid, cation hydration both near the solid-fluid interface and inside the mineral crystal, and hydration bonding between solid surfaces and the fluid (see Chapter 4 "Linking Soil Water Adsorption to Geotechnical Engineering Properties"). As a result, the corresponding hydrodynamic responses of these chemical potentials could be different than those based on the TLM, resulting in different laws and coupled physical processes within the REV.

Additional challenges with the physical-based approach lie in the requirement to determine the fundamental atomic- and pore-scale physical parameters, such as the zeta potential, CEC, and the ionic mobilities of multiple chemical species. The methodologies for the measurement of these parameters generally are not well established and are fraught with uncertainty. As a result, model predictions based on these measured values also are uncertain, and experimental verification of the theories underpinning the physical-based approach is subject to more uncertainty than that for the phenomenological approach.

4 Challenges for Research on Coupled Flow Phenomena

Based on the aforementioned presentation, several research challenges pertaining to coupled flow phenomena for Geotechnical Engineering applications remain. These challenges can be summarized as follows.

4.1 Experimental Versus Theoretical Research

In the field of physics, theoretical physicists have been decades if not centuries ahead of experimental physicists. A classic example of this observation is Albert Einstein's field equations for the Theory of General Relativity, which were postulated in November of 1915. Although the Theory of General Relativity now forms the basis for our current understanding of the interaction of space, time, and gravity, which is used to explain the expansion of the Universe, the motion of the planets, and the existence of black holes, some postulates of this Theory, such as the existence of gravity waves, remained unproven experimentally until only recently (i.e., 2017).

Similarly, the theories describing coupled flows and coupled processes for applications relevant to Geotechnical Engineering seem, in some cases, to be far ahead of the experimental evidence in support of these theories (e.g., the application of coupled THMC processes for radioactive waste containment). Some of the factors that have contributed to this gap between theory and experimental verification include lengthy testing durations, the need for specialty (customized) testing equipment, limitations in the accuracy of the measurements and the ability to control boundary conditions, and limitations associated with the specimen size and the associated scale effects. Therefore, the challenge is to provide experimental evidence in support of existing theory.

4.2 Fundamental Versus Applied Research

Although all research in Geotechnical Engineering should be related to an application, fundamental research focusing on mechanisms is necessary for accurate, long-term prediction of the performance of engineered systems, e.g., engineered barriers used for LLRW and HLRW containment where the design lives are 1000 and 10,000 years, respectively. Despite the apparent difficulty in comprehending such long time periods, there is relatively recent, tangible evidence that consideration of long time frames is relevant. For example, the current impact of anthropogenic climate change can be traced to the onset of the industrial revolution, which started circa 1760 to ~1820, or about 195–255 years ago. Second, several 1000-year precipitation events were associated with the flooding that occurred along the front range of the Rocky Mountains in Colorado, USA, in September 2013, referred to as the *2013 Colorado*

Front Range Flood. Clearly, our ability to predict system performance over such large time scales will be accurate only if the models being used for this purpose are based on fundamental mechanisms that account for all of the factors impacting long-term performance, including time-dependent changes in material properties.

For example, as previously noted, relatively recent research has shown that bentonite-based containment barriers can exhibit chemico-osmosis, which is derived from the ability of the bentonite to behave as a semipermeable membrane resulting in solute restriction. Such solute restriction or membrane behavior also has been recognized to exist in high–density bentonite buffers (dry (bulk) densities ranging from 1.8 to 2.0 Mg/m^3) used for HLRW containment. However, chemico-osmosis often is ignored in the models used to predict the long-term performance of these buffers, and solute exclusion often is treated in an empirical, rather than fundamental, manner in terms of the migration of radionuclides (e.g. [101]). Thus, the challenge is to conduct fundamental research focused on mechanisms that take into account time-dependent changes in material properties over long time frames.

4.3 Saturated Versus Unsaturated Research

The bulk of experimental studies on coupled flows and processes have been conducted under saturated soil conditions (e.g., see Table 3). Although the assumption of saturated soil conditions may be appropriate in some cases and/or conservative in other cases, the assumption of saturated soil conditions frequently has been made for convenience, i.e., because measurement of the governing parameters under unsaturated soil conditions is more difficult than measurement under saturated soil conditions.

For example, the recent study by Sample-Lord and Shackelford [95, 96] evaluated the effect of the degree of water saturation, S, on the existence and magnitude of semipermeable membrane behavior in sodium homo-ionized bentonite. As hypothesized on the basis of classic diffuse double layer theory, the magnitude of the solute restriction increased with decreasing S. However, due to long test durations (~1 year) and the complexity and limitations of the testing equipment, the lowest S evaluated was limited to 79%. Since many problems faced in Geotechnical Engineering occur under unsaturated soil conditions (e.g., water-balance covers for waste containment, subsurface contaminant migration in the vadose zone, etc.), a challenge is to extend our understanding of the existence, magnitude, and relevance of coupled flows and processes under unsaturated conditions.

4.4 Abiotic Versus Biotic Research

Biological activity can play a major role in affecting coupled flow processes. For example, in the studies by Sample-Lord and Shackelford [95, 96] pertaining to the effect of S on semipermeable membrane behavior, biological activity was shown

to affect the measurement of the chemico-osmotic pressure under unsaturated soil conditions to an extent that the addition of a biocide to the circulating chemical solutions was required in order to eliminate the biological effect. Also, electrokinetics has been proposed as a method to induce biodegradation of contaminants in clays via either bioaugmentation, whereby specific non-indigenous microbes are used to degrade susceptible contaminants, or biostimulation, whereby nutrients are injected to stimulate biodegradation by indigenous microbes (e.g., [103]). However, due to the complexity associated with biological processes, the inclusion of biological activity can significantly complicate research. Therefore, our ability to conduct relevant research related to the effects of biology on coupled flows and processes remains a significant research challenge.

4.5 Laboratory- Versus Field-Scale Research

Fundamental studies typically are conducted under controlled conditions in the laboratory. For example, the vast majority of experimental research pertaining to coupled flow processes has been conducted in the laboratory using relatively small-scale specimens and homogeneous soils, such as processed clays (e.g., kaolin, bentonite) and mixtures of sands with processed clays (e.g., see Table 2). While these studies provide a basis for determining fundamental behavior, the justification for upscaling the results of these studies to the field scale often is problematic, due in part to complexity of the conditions that can occur at larger scales (e.g., variations in boundary and initial conditions, heterogeneities in the materials). This reality suggests the need for long-term, large-scale field laboratories as recommended by Mitchell et al. [74]. Several such field-scale research facilities exist around the world related to deep disposal of HLRW in argillaceous deposits, such as the Hades Underground Research Laboratory (URL) located in the Boom Clay formation in Belgium, the Meuse/Haute Marne URL in France, and the Mont Terri URL located in the Opalinus Clay formation in Switzerland. However, no similar laboratories exist in the USA. Therefore, the challenge is to develop capabilities that allow for an evaluation of performance at more realistic field scales.

5 Concluding Remarks

Coupled flow phenomena will continue to be important in many Geotechnical Engineering and natural science problems. For most engineering problems, the macroscopic phenomenological approach has been shown to be effective for describing fluxes. However, because the phenomenological coefficients often cannot be directly measured, transformations to express the phenomenological coefficients in terms of experimentally determinable material properties become necessary. Such transformations typically involve assumptions, some of which are justifiable and others which

are not, leading to inconsistencies among the various coupled flux formulations presented in the literature and incorrect descriptions of fluxes resulting from failure of the phenomenological approach to explicitly account for inter-dependencies among the material properties and the state variables (e.g., the dependence of chemico-osmotic membrane efficiency on solute concentration).

In recent years, the physical-based approach based on physical processes that occur at the pore scale has been adopted. In this approach, pore-scale physical properties are used to express the phenomenological coefficients and the commonly measured macroscopic material properties. This approach uses the pore-scale physical properties as the common threads for the phenomenological coefficients and the macroscopic material properties, providing a powerful methodology for overcoming some limitations in the phenomenological approach. The challenges in the physical-based approach are the assumptions made in the pore-scale physical processes, which often are driven by both physics and mathematical simplicity to make the problem solutions more analytically trackable, and the difficulty associated with determining microscopic material properties (e.g., surface charge density).

The major challenges in experiments include: (a) complexity, uncertainties, and capability in controlling and measuring boundary conditions of variables, their gradients, and fluxes; (b) limitations in controlling or measuring saturation or pore-water pressures; and (c) long test durations. These experimental challenges restrict our ability to quantify coupled flow phenomena for more realistic systems and a wider range of conditions which, in turn, limits our ability to consider the effects of coupled flows in many Geotechnical Engineering applications.

References

1. Acar, Y.B., Alshawabkeh, A.N.: Principles of electrokinetic remediation. Environ. Sci. Technol. **27**(13), 2638–2647 (1993)
2. Alshawabkeh, A.N., Acar, Y.B.: Electrokinetic remediation. II: Theoretical model. J. Geotech. Eng. 122(3), 186–196 (1996)
3. Bai, M., Elsworth, D.: Coupled processes in subsurface deformation, flow, and transport. ASCE Press, Reston, Virginia (2000)
4. Barbour, S.L., Fredlund, D.G.: Mechanisms of osmotic flow and volume change in clay soils. Can. Geotech. J. **26**(4), 551–562 (1989)
5. Bjerrum, L., Moum, J., Eide, O.: Application of electro-osmosis to a foundation problem in a Norwegian quick clay. Géotechnique **17**(3), 214–235 (1967)
6. Bresler, E.: Anion exclusion and coupling effects in nonsteady transport through unsaturated soils: I. Theory. Soil Sci. Soc. of America, Proc. **37**(5), 663–669 (1973)
7. Casagrande, L.: Electro-osmotic stabilization of soils. Boston Soc. Civil Eng. J. **39**(1), 51–83 (1952)
8. Casagrande, L.: Electro-osmosis in soils. Géotechnique, 1(3), 159-177 (1949)
9. Chatterji, P.K., Morgenstern, N.R.: A modified shear strength formulation for swelling clay soils. In: Hoddinott, K.B., Lamb, R.O. (eds.) Physico-Chemical Aspects of Soil and Related Materials, STP 1095, pp. 118–135. ASTM, West Conshohoken, PA (1990)
10. Chen, X., Hicks, M.A.: Unsaturated hydro-mechanical-chemo coupled constitutive model with consideration of osmotic flow. Comput. Geotech. **54**, 94–103 (2013)

11. Cruchaudet, M., Croisé, J., Lavanchy, J.M.: In situ osmotic experiment in the Callovo-Oxfordian argillaceous formation at the Meuse/Haute-Marne URL (France): Data and analysis. Phys. Chem. Earth, Parts A/B/C **33**, S114–S124 (2008)
12. de Marsily, G.: Quantitative hydrogeology. Academic Press Inc, Orlando, Florida (1986)
13. Deng, A., Zhou, Y.: Modeling electroosmosis and surcharge preloading consolidation. I: Model formulation. J. Geotech. Geoenviron. Eng. **142**(4), 04015093 (2016a)
14. Deng, A., Zhou, Y.: Modeling electroosmosis and surcharge preloading consolidation. II: Validation and simulation results. J. Geotech. Geoenviron. Eng. **142**(4), 04015094 (2016b)
15. Di Maio, C.: Exposure of bentonite to salt solutions: osmotic and mechanical effects. Géotechnique **48**(3), 433–436 (1996)
16. Dominijanni, A., Guarena, N., Manassero, M.: Laboratory assessment of the semipermeable properties of a natural sodium bentonite. Can. Geotech. **55**(11), 1611–1631 (2018)
17. Dominijanni, A., Manassero, M.: Modelling the swelling and osmotic properties of clay soils. Part I: The phenomenological approach. Int. J. Eng. Sci. **51**, 32–50 (2012b)
18. Dominijanni, A., Manassero, M.: Modelling the swelling and osmotic properties of clay soils. Part II: The physical approach. Int. J. Eng. Sci. **51**, 51–73 (2012a)
19. Dominijanni, A., Manassero, M.: Modelling osmosis and solute transport through clay membrane barriers. In: Alshawabkleh, A. et al. (eds.) Waste Containment and Remediation, ASCE Geotechnical Special Publication No. 47, ASCE, Reston, Virginia (2005)
20. Dominijanni, A., Manassero, M., Puma, S.: Coupled chemical-hydraulic-mechanical behaviour of bentonites. Géotechnique **63**(3), 191–205 (2013)
21. Esrig, M.I.: Pore pressures, consolidation, and elctrokinetics. J. Soil Mech. Found. Div. **94**(SM4), 899–921 (1968)
22. Esrig, M.I., Gemeinhardt Jr., J.P.: Electrokinetic stabilization of an illitic clay. J. Soil Mech. Found. Div. **93**(SM3), 109–128 (1967)
23. Fritz, S.J.: Ideality of clay membranes in osmotic processes: a review. Clays Clay Miner. **34**(2), 214–223 (1986)
24. Garavito, A.M., Kooi, H., Neuzil, C.E.: Numerical modeling of a long-term in situ chemical osmosis experiment in the Pierre Shale, South Dakota. Adv. Water Resour. **29**(3), 481–492 (2006)
25. Garavito, A.M., De Cannière, P., Kooi, H.: In situ chemical osmosis experiment in the Boom Clay at the Mol underground research laboratory. Phys. Chem. Earth, Parts A/B/C **32**(1), 421–433 (2007)
26. Gonçalvès, J., de Marsily, G., Tremosa, J.: Importance of thermal osmosis for fluid flow and transport in clay formations hosting a nuclear waste repository. Earth and Planet. Sci. Lett. **339**, 1–10 (2012)
27. Gray, D.H., Mitchell, J.K.: Fundamental aspects of electro-osmosis in soils. J. Soil Mech. Found. Div. **93**(SM6), 209–236 (1967)
28. Greenberg, J.A., Mitchell, J.K., Witherspoon, P.A.: Coupled salt and water flows in a groundwater basin. J. Geophys. Res. **78**(27), 6341–6353 (1973)
29. Groenevelt, P.H., Bolt, G.H.: Non-equilibrium thermodynamics of the soil-water system: review paper. J. Hydrol. **7**(4), 358–388 (1969)
30. Groenevelt, P.H., Elrick, D.E.: Coupling phenomena in saturated homo-ionic montmorillonite: II. Theor. Soil Sci. Soc. America, J. **40**, 820–823 (1976)
31. Guichet, X., Jouniaux, L., Pozzi, J.P.: Streaming potential of a sand column in partial saturation conditions. J. Geophys. Res.: Solid Earth **108**(B3) (2003)
32. Gupta, A., Coelho, D., Adler, P.M.: Universal electro-osmosis formulae for porous media. J. Colloid Interface Sci. **319**, 549–554 (2008)
33. Heister, K., Kleingeld, P.J., Loch, J.G.: Quantifying the effect of membrane potential in chemical osmosis across bentonite membranes by virtual short-circuiting. J. Colloid Interface Sci. **286**(1), 294–302 (2005)
34. Heister, K., Kleingeld, P.J., Loch, J.G.: Induced membrane potentials in chemical osmosis across clay membranes. Geoderma **136**(1), 1–10 (2006)

35. Horseman, S.T., McEwen, T.J.: Thermal constraints on disposal of heat-emitting waste in argillaceous rocks. Eng. Geol. **41**(1), 5–16 (1996)
36. Horseman, S.T., Harrington, J.F., Noy, D.J.: Swelling and osmotic flow in a potential host rock. Phys. Chem. Earth, Parts A/B/C **32**(1), 408–420 (2007)
37. Hu, L., Wu, H.: Mathematical model of electro-osmotic consolidation for soft ground improvement. Géotechnique **64**(2), 155–164 (2014)
38. Jeyakanthan, V., Gnanendran, C.T., Lo, S.-C.R.: Laboratory assessment of electro-osmotic stabilization of soft clay. Can. Geotech. J. **48**(12), 1788–1802 (2011)
39. Jo, H.Y., Benson, C.H., Edil, T.B.: Rate-limited cation exchange in thin bentonitic barrier layers. Can. Geotech. J. **43**(4), 370–391 (2006)
40. Jones, C.J.F.P., Lamont-Black, J., Gendinning, S.: Electrokinetic geosynthetics in hydraulic applications. Geotext. Geomembr. **29**(4), 381–390 (2011)
41. Jougnot, D., Revil, A., Lu, N., Wayllace, A.: Transport properties of the Callovo-Oxfordian clay rock under partially saturated conditions. Water Resour. Res. **46**(8) (2010)
42. Kang, J.B., Shackelford, C.D.: Clay membrane testing using a flexible-wall cell under closed-system boundary conditions. Appl. Clay Sci. **44**(1), 43–58 (2009)
43. Kang, J.B., Shackelford, C.D.: Membrane behavior of compacted clay liners. J. Geotech. Geoenviron. Eng. **136**(10), 1368–1382 (2010)
44. Kang, J.B., Shackelford, C.D.: Consolidation enhanced membrane behavior of a geosyntheic clay liner. Geotext. Geomembr. **29**(6), 544–556 (2011)
45. Katchalsky, A., Curran, P.F.: Nonequilibrium thermodynamics in biophysics. Harvard University Press, Cambridge, Massachusetts (1965)
46. Keijzer, Th.J.S., Kleingeld, P.J., Loch, J.P.G.: Chemical osmosis in compacted clayey material and the prediction of water transport. Eng. Geol. **53**(2), 151–159 (1999)
47. Kemper, W.D., Quirk, J.P.: Ion mobilities and electrical charge of external clay surfaces inferred from potential differences and osmotic flow. Soil Sci. Soc. America, Proc. **36**(3), 426–433 (1972)
48. Kemper, W.D., Rollins, J.B.: Osmotic efficiency coefficients across compacted clays. Soil Science Society of America Proceedings **30**(5), 529–534 (1966)
49. Kim, S., Mench, M.M.: Investigation of temperature-driven water transport in polymer electrolyte fuel cell: thermo-osmosis in membranes. J. Membr. Sci. **328**(1), 113–120 (2009)
50. Lamont-Black, J., Jones, C.J.F.P., Alder, D.: Electrokinetic strengthening of slopes-Case history. Geotext. Geomembr. **44**(3), 319–331 (2016)
51. Likos, W.J., Lu, N.: Automated humidity system for measuring total suction characteristics of clay. Geotech. Test. J. **26**(2), 1–12 (2003)
52. Linde, N., Jougnot, D., Revil, A., Matthai, S.K., Arora, A., Renard, D.: Streaming current generation in two-phase flow conditions. Geophys. Res. Lett., **34**, L03306, (2007) https://doi.org/10.1029/2006gl028878
53. López-Vizcaíno, R., Yustres, Á., Leon, M.J., Sáez, C., Cañizares, P., Rodrigo, M.A., Navarro, V.: Multiphysics implementation of electrokinetic remediation models for natural soils and porewaters. Electrochim. Acta **225**, 93–104 (2017)
54. Lu, N., Likos, W.J.: Unsaturated soil mechanics. Wiley, New York (2004)
55. Lu, N., Olsen, H.W., Likos, W.J.: Appropriate material properties for advective—diffusive solute flux in membrane soil. J. Geotech. Geoenviron. Eng. **130**(12), 1341–1346 (2004)
56. Malusis, M.A., Daniyarov, A.S.: Membrane efficiency and diffusive tortuosity of a dense prehydrated geosynthetic clay liner. Geotext. Geomembr. **44**, 719–730 (2016)
57. Malusis, M.A., Scalia, J., Norris, A.S., Shackelford, C.D.: Quantifying the significance of chemico-osmotic counter-advection on solute transport through semipermeable clay barriers. In: International Symposium on Coupled Phenomena in Environmental Geotechnics (CPEG2), 6–7 September 2017, Leeds, University of Leeds, UK, Paper 51 (2017)
58. Malusis, M.A., Shackelford, C.D.: Chemico-osmotic efficiency of a geosynthetic clay liner. J. Geotech. Geoenviron. Eng. **128**(2), 97–106 (2002)
59. Malusis, M.A., Shackelford, C.D.: Coupling effects during steady-state solute diffusion through a semipermeable clay membrane. Environ. Sci. Technol. **36**(6), 1312–1319 (2002)

60. Malusis, M.A., Shackelford, C.D.: Theory for reactive solute transport through clay membrane barriers. J. Contam. Hydrol. **59**(3–4), 291–316 (2002)
61. Malusis, M.A., Shackelford, C.D., Olsen, H.W.: A laboratory apparatus to measure chemico-osmotic efficiency coefficients for clay soils. Geotech. Test. J. **24**(3), 229–242 (2001)
62. Malusis, M.A., Shackelford, C.D., Olsen, H.W.: Flow and transport through clay membrane barriers. Eng. Geol. **70**(3–4), 235–248 (2003)
63. Malusis, M.A., Shackelford, C.D., Maneval, J.E.: Critical review of coupled flux formulations for clay membranes based on nonequilibrium thermodynamics. J. Contam. Hydrol. **138**, 40–59 (2012)
64. Malusis, M.A., Kang, J.-B., Shackelford, C.D.: Restricted salt diffusion in a geosynthetic clay liner. Environ. Geotech. **2**(2), 68–77 (2015)
65. Manassero, M., Dominijanni, A.: Modelling the osmosis effect on solute migration through porous media. Géotechnique **53**, 481–492 (2003)
66. Manassero M., Dominijanni A., Musso G., Puma S.: Coupled phenomena in contaminant transport. In: Bouazza, A. et al. (eds.) Engineers Australia. Proceedings of the 7th International Congress on Environmental Geotechnics, pp. 144–169, November 10–14, 2014, Melbourne, Australia (2014)
67. Manassero M., Dominijanni A.: Coupled modelling of swelling properties and electrolyte transport through geosynthetic clay liner. In: Datta M. et al. (eds.) Proceedings of the 6th International Congress on Environmental Geotechnics, Vol. 1, pp. 260–271, 8–12 November 2010, New Delhi, India. Tata McGraw Hill, New Delhi (2010)
68. Manassero, M.: On the fabric and state parameters of active clays for contaminant control. In: Lee W., Lee J.-S., Kim, H.-K., Kim, D.-S. (eds.) Second R. Kerry Rowe Lecture, Proceedings of the 19th International Conference on Soil Mechanics and Geotechnical Engineering (ICSMGE), pp. 167–189, 17–22 September 2017, Seoul, Korea. Korean Geotechnical Society, International Society for Soil Mechanics and Geotechnical Engineering, Seoul (2017)
69. Mattson, E.D., Bowman, R.S., Lindgren, E.R.: Electrokinetic ion transport through unsaturated soil: 1. Theory, model development, and testing. J. Contam. Hydrol **54**(1–2), 99–120 (2002a)
70. Mattson, E.D., Bowman, R.S., and Lindgren, E.R.: Electrokinetic ion transport through unsaturated soil: 2. Application to a heterogeneous field site. J. Contam. Hydrol. **54**(1–2), 121–140 (2002b)
71. Medved, I., Černý, R.: Osmosis in porous media: a review of recent studies. Microporous Mesoporous Mater. **170**, 299–317 (2013)
72. Mitchell, J.K.: Conduction phenomena: from theory to geotechnical practice. Géotechnique **41**(3), 299–340 (1991)
73. Mitchell, J.K., Banerjee, S.: In-situ volume-change properties by electro-osmosis. J. Geotech. Eng. Div. **106**(GT4), 367–384 (1980)
74. Mitchell, J.K., Alvarez-Cohen, L., Atekwana, E.S., Burns, S.E., Gilbert, R.B., Kavazanjian, Jr., E., O'Riordan, W.H., Rowe, R.K., Shackelford, C.D., Sharma, H.D., Yesiller, N.: Assessment of the performance of engineered waste containment barriers. The National Academies Press, 500 Fifth Street, N.W., Washington, DC 20001 (2007)
75. Mitchell, J.K., Wan, T.-Y.: Electro-osmotic consolidation-its effect on soft soils. In: Proceedings of the Ninth International Conference on Soil Mechanics and Foundation Engineering, pp 219–224, 10–15 July 1977, Tokyo (1977)
76. Mitchell, J.K., Soga, K.: Fundamentals of soil behavior, 3rd edn. Wiley, New York (2005)
77. Musso, G., Cosentini, R.M., Dominijanni, A., Guarena, N., Manassero, M.: Laboratory characterization of the chemo-hydro-mechanical behavior of chemically sensitive clays. Rivista Italiana Geotecnica **2017**(3), 22–47 (2017). https://doi.org/10.19199/2017.3.0557-1405.022
78. Neuzil, C.E.: Osmotic generation of 'anomalous' fluid pressures in geological environments. Nature **403**, 182–184 (2000)
79. Neuzil, C.E., Provost, A.M.: Recent experimental data may point to a greater role for osmotic pressures in the subsurface. Water Resour. Res. **45**, 1–14 (2009)

80. Oduor, P.G., Santos, X., Forward, K., Sharp, N., Bue, C., Casey, F., Abwawo, J.: Semi-empirically derived petrophysical and thermodynamical coefficients of permselective shales—Implications on ore mineralization. J. Membr. Sci. **343**(1), 171–179 (2009)
81. Olsen, H.W.: Simultaneous fluxes of liquid and charge in saturated kaolinite. Soil Sci. Soc. America, Proc. **33**, 338–344 (1969)
82. Olsen, H.W.: Liquid movement through kaolinite under hydraulic, electric, and osmotic gradients. AAPG Bulletin **56**(10), 2022–2028 (1972)
83. Olsen, H.W., Yearsley, E.N., Nelson, K.R.: Chemico-osmosis versus diffusion-osmosis. Transportation Research Record 1288, Transportation Research Board, Washington, D.C., pp. 15–22 (1990)
84. Paszkuta, M., Rosanne, M., Adler, P.M.: Transport coefficients of saturated compact clays. C.R. Geosci. **338**(12), 908–916 (2006)
85. Revil, A., Schwaeger, H., Cathles, L. M., Manhardt, P. D.: Streaming potential in porous media: 2. Theory and application to geothermal systems. J Geophys. Res: Solid Earth **104**(B9), 20033–20048 (1999)
86. Revil, A.: Transport of water and ions in partially water-saturated porous media. Part 1. Constitutive equations. Adv. Water Resour. **103**, 119–138 (2017a)
87. Revil, A.: Transport of water and ions in partially water-saturated porous media. Part 2. Filtration effects. Adv. Water Resour. **103**, 139–152 (2017b)
88. Revil, A., Leroy, P.: Constitutive equations for ionic transport in porous shales. J. Geophys. Res. **109**, B03208 (2004). https://doi.org/10.1029/2003JB002755
89. Revil, A., Linde, N.: Chemico-electromechanical coupling in microporous media. J. Colloid Interface Sci. **302**, 682–692 (2006)
90. Revil, A., Leroy, P., Titov, K.: Characterization of transport properties of argillaceous sediments: Application to the Callovo-Oxfordian argillite. J. Geophys. Res. **110**, B06202 (2005). https://doi.org/10.1029/2004JB003442
91. Revil, A., Linde, N., Cerepi, A., Jougnot, D., Matthäi, S., Finsterle, S.: Electrokinetic coupling in unsaturated porous media. J. Colloid Interface Sci. **313**(1), 315–327 (2007)
92. Rosanne, M., Paszkuta, M., Thovert, J.F., Adler, P.M.: Electro-osmotic coupling in compact clays. Geophys. Res. Lett. **31**(18), (2004)
93. Rosanne, R., Paszkuta, M., Tevissen, E., Adler, P.M.: Thermodiffusion in compact clays. J. Colloid Interface Sci. **267**(1), 194–203 (2003)
94. Rosanne, M., Paszkuta, M., Adler, P.M.: Thermodiffusional transport of electrolytes in compact clays. J. Colloid Interface Sci. **299**(2), 797–805 (2006)
95. Sample-Lord, K.M., Shackelford, C.D.: Apparatus for measuring coupled membrane and diffusion behavior of unsaturated sodium bentonite. Vadose Zone J. **16**(9), (2017) https://doi.org/10.2136/vzj2016.12.0140
96. Sample-Lord, K.M., Shackelford, C.D.: Membrane behavior of unsaturated sodium bentonite. J. Geotech. Geoenviron. Eng. **144**(1), 04017102 (2018). https://doi.org/10.1061/(ASCE)GT.1943-5606.0001803
97. Sánchez, M., Arson, C., Gens, A., Aponte, F.: Analysis of unsaturated materials hydration incorporating the effect of thermo-osmotic flow. Geomech. Energy and the Environ. **6**, 101–115 (2016)
98. Santamarina, J.C., Klein, K.A., Palomino, A., Guimaraes, M.S.: Micro-scale aspects of chemical-mechanical coupling: Interparticle forces and fabric. In: Di Maio, T. Hueckel, and B. Loret, (eds.) Chemico-Mechanical Coupling of Clays: from Nano-Scale to Engineering Applications, 4C, pp. 7–63. A.A. Balkema Publishers, Lisse, The Netherlands (2002)
99. Schmid, K.S., Gross, J., Helmig, R.: Chemical osmosis in two-phase flow and salinity-dependent capillary pressures in rocks with microporosity. Water Resour. Res. **50**(2), 763–789 (2014)
100. Shackelford, C.D., Malusis, M.A., Olsen, H.W.: Clay membrane behavior for geoenvironmental containment. Soil and Rock America Conference 2003. In: Culligan, P.J., Einstein, H.H., Whittle, A.J. (eds.) Proceedings of the joint 12th Panamerican Conference on Soil Mechanics and Geotechnical Engineering and the 39th U. S. Rock Mechanics Symposium. Verlag Glückauf GMBH, Essen, Germany, Vol. 1, pp. 767–774 (2003)

101. Shackelford, C.D., Moore, S.M.: Fickian diffusion of radionuclides for engineered containment barriers: diffusion coefficients, porosities, and complicating issues. Eng. Geol. **152**(1), 133–147 (2013)
102. Shackelford, C.D.: Diffusion of contaminants through waste containment barriers. Transp. Res. Rec. 1219, Geotechnical Engineering 1989, TRB, NRC, National Academy Press, Washington, DC (1989)
103. Shackelford, C.D.: Environmental issues in geotechnical engineering. In: 16th International Conference on Soil Mechanics and Geotechnical Engineering, Vol. 1, pp. 95–122, Osaka, Japan, 12–16 September 2005. Millpress, Rotterdam, The Netherlands (2005)
104. Shackelford, C.D., Daniel, D.E.: Diffusion in saturated soil: I. Background. J. Geotech. Eng. **117**(3), 467–484 (1991)
105. Shackelford, C.D., Lee, J.-M.: The destructive role of diffusion on clay membrane behavior. Clays Clay Miner. **51**(2), 187–197 (2003)
106. Shackelford, C.D., Benson, C.H., Katsumi, T., Edil, T.B., Lin, L.: Evaluating the hydraulic conductivity of GCLs permeated with non-standard liquids. Geotext. Geomembr. **18**(2–4), 133–161 (2000)
107. Shackelford, C.D., Meier, A.J., Sample-Lord, K.M.: Limiting membrane and diffusion behavior of a geosynthetic clay liner. Geotext. Geomembr. **44**(5), 707–718 (2016)
108. Sherwood, J.D., Craster, B.: Transport of water and ions through a clay membrane. J. Colloid Interface Sci. **230**(2), 349–358 (2000)
109. Soler, J.M.: The effect of coupled transport phenomena in the Opalinus Clay and implications for radionuclide transport. J. Contam. Hydrol. **53**(1–2), 63–84 (2001)
110. Spagnoli, G., Klitzsch, N., Fernandez-Steeger, T., Feinendegen, M., Rey, A.R., Stanjek, H., Azzam, R.: Application of electro-osmosis to reduce the adhesion of clay during mechanical tunnel driving. Environ. Eng. Geosci. **XVII**(4), 417–426 (2011)
111. Sridharan, A., Venkatapp Rao, G.: Mechanisms controlling volume change of saturated clays and the role of the effective stress concept. Géotechnique **23**(2), 359–382 (1973)
112. Trémosa, J., Gonçalvès, J., Matray, J.M., Violette, S.: Estimating thermo-osmotic coefficients in clay-rocks: II. In situ experimental approach. J. Colloid and Interface Sci. **342**(1), 175–184 (2010)
113. Van Impe, P.O., Van Impe, W.F., Mazzieri, F., Constales, D.: Coupled flow model for three-ion advective-dispersive-reactive transport in consolidating clay liners. In; 13th European Conference on Soil Mechanics and Geotechnical Engineering, Balkema, Rotterdam, pp. 227–232 (2003)
114. Van Olphen, H.: An introduction to clay colloid chemistry, 2nd edn. Wiley, New York (1977)
115. Virkutyte, J., Sillampää, M., Latostenmaa, P.: Electrokinetic soil remediation—critical overview. Sci. Total Environment **289**, 97–121 (2002)
116. Wan, T.-Y., Mitchell, J.K.: New apparatus for consolidation by electro-osmosis. J. Geotech. Eng. Div. **101**(GT5), 503–507 (1975)
117. Wan, T.-Y., Mitchell, J.K.: Electro-osmotic consolidation of soils. J. Geotech. Eng. Div. **102**(GT5), 472–491 (1976)
118. Wang, J., Fu, H., Liu, F., Cai, Y., Zhou, J.: Influence of electro-osmosis activation time on vacuum electro-osmosis consolidation of a dredged slurry. Can. Geotech. J. **55**(1), 147–153 (2018)
119. Wayllace, A., Lu, N.: Transient water release and imbibitions method for rapidly measuring wetting and drying soil water retention and hydraulic conductivity functions. Geotech. Test. J. **35**, 1–15 (2012)
120. Xiong, Y., Fakcharoenphol, P., Winterfeld, P., Zhang, R., and Wu, Y.-S.: Coupled geomechanical and reactive geochemical model for fluid and heat flow: application for enhanced geothermal reservoir. Soc. Pet. Eng. paper SPE 165982 (2013)
121. Yeung, A.T.: Coupled flow equations for water, electricity and ionic contaminants through clayey soils under hydraulic, electrical, and chemical gradients. J. Non-Equilib. Thermodyn. **15**, 247–267 (1990)

122. Yeung, A.: Milestone developments, myths, and future directions of electrokinetic remediation. Sep. Purif. Technol. **79**(2), 124–132 (2011)
123. Yeung, A.T., Mitchell, J.K.: Coupled fluid, electrical and chemical flows in soil. Geotechnique **43**(1), 121–134 (1993)
124. Yustres, Á., López-Vizcaíno, R., Sáez, C., Cañizares, P., Rodrigo, M.A., Navarro, V.: Water transport in electrokinetic remediation of unsaturated kaolinite. Experimental and numerical study. Sep. Purif. Technol. **192**, 196–204 (2018)
125. Zagorščak, R., Sedighi, M., Thomas, H.R.: Effects of thermo-osmosis on hydraulic behavior of saturated clays. Int. J. Geomech. **17**(3), 04016068 (2017)
126. Zhou, J., Tao, Y.L., Xu, C.J., Gong, X.N., Hu, P.C.: Electro-osmotic strengthening of silts based on selected electrode materials. Soils Found. **55**(5), 1171–1180 (2015)
127. Zhuang, Y.-F., Wang, Z.: Interface electric resistance of electroosmotic consolidation. J. Geotech. Geoenviron. Eng. **133**(12), 1617–1621 (2007)

Emerging Thermal Issues in Geotechnical Engineering

John S. McCartney, Navid H. Jafari, Tomasz Hueckel, Marcelo Sánchez and Farshid Vahedifard

Abstract Application of changes in temperature to soils and rocks may lead to a wide range of flow processes and physical phenomena. This chapter focuses on the fundamental aspects of coupled heat transfer and water flow in saturated and unsaturated soils and rocks, thermal pressurization of pore fluids, thermal volume change, thermal softening of the preconsolidation stress, thermal hydro-shearing, and desiccation cracking. Established applications are also presented, including energy piles, barriers for radioactive waste repositories, and thermal energy storage. Emerging research areas including the role of thermal processes in climate change and elevated temperature landfills are also discussed.

Keywords Geothermal · Coupled thermo-hydro-mechanical processes · Thermal softening · Thermal pressurization · Thermal volume change · Energy piles · Heat storage · Climate change · Elevated temperature landfills

J. S. McCartney (✉)
University of California San Diego, La Jolla, CA, USA
e-mail: mccartney@ucsd.edu

N. H. Jafari
Louisiana State University, Baton Rouge, LA, USA

T. Hueckel
Duke University, Durham, NC, USA

M. Sánchez
Texas A&M University, College Station, TX, USA

F. Vahedifard
Mississippi State University, Starkville, MS, USA

N. Lu and J. K. Mitchell (eds.), *Geotechnical Fundamentals for Addressing New World Challenges*, Springer Series in Geomechanics and Geoengineering,
https://doi.org/10.1007/978-3-030-06249-1_10

1 Introduction

In the last decade, geotechnical engineering has expanded its domain into the field of energy geotechnics, which is associated with the extraction, transfer, storage, and management of energy, energy waste, or energy infrastructure in the subsurface soil or rock. The development of energy geotechnics has led to the identification of new problem classes that require an understanding of the behavior of soils and rocks under complex and potentially extreme pressure and temperature regimes in both water-saturated and unsaturated (multi-phase) conditions, often involving coupled thermo-hydro-mechanical (THM) processes [163, 215].

A schematic illustration of the basic physics and their mutual interactions anticipated in soils and rocks subjected to simultaneous THM boundary conditions is shown in Fig. 1. Heat transfer in soils due to conduction is closely tied to the amount of water in the soil and the porosity. Temperature affects the properties of the pore fluids, including density and viscosity among others, resulting in water and gas flow in the soil. This flow will lead to additional heat transfer due to convection, which may be enhanced in unsaturated soils and rocks due to water vapor diffusion and latent heat transfer due to water phase change. Further, in the case of unsaturated soils, changes in degree of saturation will lead to changes in thermal conductivity and specific heat, altering the heat transfer process. The changes in temperature and water flow processes will also lead to changes in effective stress and soil volume, which in turn are coupled with the heat transfer and water flow processes as the thermal and hydraulic properties of soils are dependent on the porosity. The thermal volume changes may be recoverable (thermo-elastic) or irrecoverable (thermo-plastic) depending on the type of soil, its degree of overconsolidation, and drainage conditions.

Although the range of problems in energy geotechnics requiring an understanding of THM processes is evolving, it is well known in geotechnical engineering that the processes of heat transfer and water flow are closely linked with the mechanical behavior of soils, with potentially different effects depending on the THM paths followed. There has been a long history of research and interest in nonisothermal problems in soil physics and agronomy going back to the early 1900s, with focus primarily on coupled heat transfer and water flow in nondeformable soils. Interest in nonisothermal problems in geotechnical engineering started in the 1950s and 1960s, involving the effects of temperature on soil sampling, engineering properties, thermal pressurization of saturated soils, and design of roads in permafrost regions (Highway Research Board 1969). In the 1970s and 1980s, the topics of interest to geotechnical engineers expanded to offshore storage of nuclear waste, cold regions soil behavior and permafrost characterization, buried high voltage electrical cables, thermal failure, geothermal heat exchangers, and aquifer thermal energy storage systems. Due to the need to provide a long-term management solution for nuclear waste (an idea started in 1956), significant research focused on the development of advanced THM constitutive models and experimental efforts in the 1980s and 1990s. Renewed interest in geothermal heat exchange in the 2000s and 2010s led to interest in energy piles, desiccation of clays, high temperature thermal remediation of

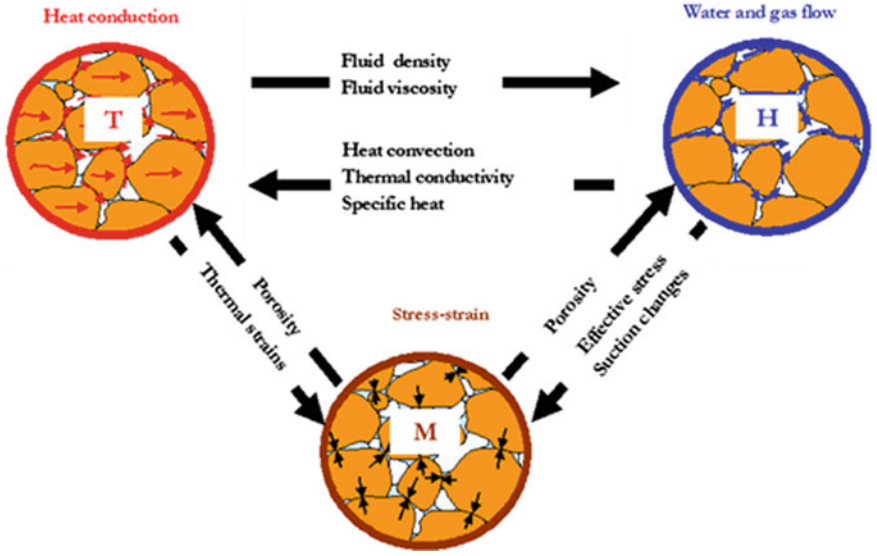

Fig. 1 Inter-relationships between thermal, hydraulic, and mechanical processes in soils ([214] with permission from Elsevier)

contaminated sites, enhanced geothermal systems, and massive hydraulic fracturing. Most recently, energy geotechnics problems have evolved, including borehole thermal energy storage, compressed air energy storage, energy extraction from landfills, methane hydrate behavior, and CO_2 sequestration. Consideration of the effects of climate change on geotechnical infrastructure also requires a deep understanding of the THM behavior of soils. The range of temperatures in these different applications is very broad, ranging from values below 0 °C in cold regions and methane hydrate research, to values between 5 and 80 °C in geothermal heat transfer and storage applications, to values in excess of 100 °C in elevated temperature landfills, thermal remediation applications, and enhanced geothermal systems.

Although a strong body of knowledge has been assembled on the non-isothermal problems, additional efforts are still required before the necessary level of technological maturity is reached to be used in geotechnical engineering practice. Accordingly, the purpose of this chapter is to provide a general overview of the important phenomena and fundamental mechanisms encountered in studying the thermo-hydro-mechanical behavior of soils and rocks, and to point to practical applications and evolving areas of research involving thermal issues. This includes a discussion on the coupling between the effects of temperature on the soil pore fluids (e.g., fluid-solid contact angle, fluid viscosity, surface tension, etc.), the generalized governing equations for heat transfer and water flow in unsaturated soils (in either liquid or vapor forms), as well as coupling between the fundamental properties governing these processes. These properties are in the form of function relationships that describe the changes in the parameters with the degree of water saturation, and include the

soil-water retention curve (SWRC), hydraulic conductivity function (HCF), thermal conductivity function (TCF), and volumetric heat capacity function (VHCF). Interesting challenges can be encountered when coupling flow processes with mechanical effects under nonisothermal conditions. This includes the effects of temperature on the relative expansion and contraction of soil constituents (air, water, solids) and associated volume changes during drained conditions or pore fluid pressurization during undrained conditions. Although temperature does not have a major effect on macroscopic mechanical properties of soils, such as the friction angle and compressibility indices, changes in the yield stress associated with thermal softening may lead to contractile volume changes during heating. Although this has led to the use of elasto-plastic models to simulate thermal volume changes, the actual mechanisms of thermal volume change are not fully understood.

2 Thermo-hydro-mechanical Behavior of Soils

This section is arranged to first focus on the fundamental aspects governing coupled heat transfer and water flow in saturated and unsaturated soils, as this flow mechanism will be present in any thermal application in geotechnical engineering. Next, this section focuses on the mechanical implications of this heat transfer and water flow process, starting with thermal softening of the preconsolidation stress, thermal pressurization during undrained heating, thermal volume change during drained heating, thermal hydro-shearing of brittle soils or rocks, and thermal desiccation cracking. This section concludes with a summary of software available that integrate the fundamental concepts discussed in this section that can be applied in numerical simulations of different energy geotechnics applications.

2.1 Coupled Heat Transfer and Water Flow in Porous Media

Coupled heat transfer and water flow in soils and rocks is critical to the understanding of many thermal geotechnics problems. These topics include radioactive waste disposal (e.g., [96]), ground-source heat pumps [196], energy piles (e.g., [37, 141, 176, 183]), thermally-active embankments [66], heat storage in soils [52, 159], geological CO_2 sequestration (e.g., [81]), and recovery of unconventional hydrocarbon resources (e.g., [105]).

As the properties of water in liquid and gas phases are dependent on temperature, heat transfer may lead to coupled flow of water through soils. Specifically, temperature dependency of the density of liquid water [109] and the viscosity of liquid water [146] may lead to thermally-induced water flow through saturated soils, with a magnitude depending on the hydraulic properties of the soil [52, 216]. Further, the temperature dependency of other properties such as the surface tension of soil water [207], relative humidity at equilibrium [193], saturated vapor concentration in the gas

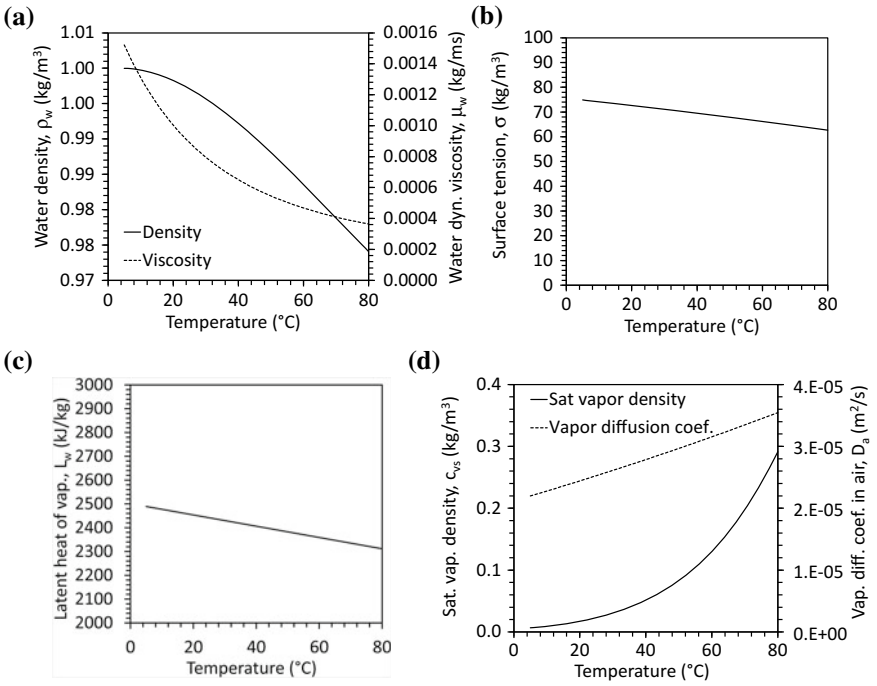

Fig. 2 Effects of temperature on properties of air and water: **a** Water density and viscosity, **b** Air-water surface tension; **c** Latent heat of vaporization of water; **d** Saturated water vapor density in gas phase and water vapor diffusion coefficient in air

phase [47], vapor diffusion coefficient in air [47], and latent heat of vaporization of water [169] may lead to thermally-induced water flow in both liquid and vapor forms through unsaturated soils. Examples of the effects of temperature on the properties of air and water are shown in Fig. 2.

Because of temperature effects on the water-air surface tension σ(T), Grant and Salehzadeh [102] proposed a correction for the capillary pressure, equal to the difference in pore air and pore water pressures ($P_c = u_a - u_w$), as follows:

$$P_c(T) = P_c(T_{ref})\left[\sigma(T)/\sigma(T_{ref})\right] \tag{1}$$

where P_c is the capillary pressure at a given temperature T (K) and T_{ref} is a reference temperature (K). The relative humidity of the pore air at equilibrium R_{he} is related to the capillary pressure and water density through Kelvin's equation, which also incorporates effects of temperature, as follows:

$$R_{he} = exp[P_c M_w/(\rho_w RT)] \tag{2}$$

where R is the universal gas constant and M_w is the molecular weight of water. The product of R_{he} and the saturated vapor density in the gas phase c_{vs} in Fig. 2d is equal to the equilibrium vapor density $\rho_{v,eq}$.

The governing equations for coupled heat transfer and water flow are well-established in the literature for deformable, water-saturated porous media [29, 32, 33, 217, 220]. Although the predictions from these studies match well with observed distributions in pore water pressure and temperature in soils with variable hydraulic conductivities, the mechanisms of thermal volume change in these models is still evolving, as will be discussed in the next section of this chapter. The governing equations for coupled heat transfer and flow of water in liquid and vapor forms have also been investigated for unsaturated porous media in nondeformable conditions [51, 86, 87, 106, 155, 167, 180, 181, 188, 193, 197, 198, 204, 222, 229, 241, 246], deformable conditions [245, 246], and in the presence of pore fluids containing chemicals [62, 103, 104]. There are perhaps more opportunities for advancing the state of the art on the simulation of heat transfer and water flow in unsaturated soils, including: (1) consideration of nonequilibrium water vapor diffusion (i.e., considering water vaporization in unsaturated soils as a time-dependent process), (2) consideration of elasto-plastic volume change mechanisms for unsaturated soils using the single-valued effective stress principle [151, 152, 266] or dual-stress variables. [8, 95], and (3) consideration of coupled, nonisothermal constitutive relationships for deformable and nondeformable soils. Some of these issues have received attention in recent studies (e.g., [23, 63, 170, 171, 229]). Other challenges include consideration of desiccation cracks on the heat transfer and water flow processes in unsaturated soils [192].

Several general observations may be made regarding coupled heat transfer and water flow in unsaturated porous media: (1) heat transfer occurs by a combination of conduction, convection in both liquid and gas phases, and latent heat transfer associated with water phase change; (2) water movement due to a temperature gradient is controlled by both vaporization/condensation processes as well as the development of a suction gradient caused by changes in water properties with temperature (i.e., density, viscosity, solid-liquid contact angle); (3) the magnitude of thermally induced liquid water flow depends on the initial degree of saturation; and (4) the duration required to reach steady-state distributions in degree of saturation and temperature may be different depending on the coupling between the thermal and hydraulic properties of a given soil. Fluid movement in soils due to temperature gradients is caused by buoyancy forces that form due to thermally-induced variations in the fluid density and viscosity. When an unsaturated soil is subjected to thermal gradients, the water in liquid and vapor forms in the pores will decrease in density and viscosity, resulting in flow upward and away from a heat source toward colder regions. In unsaturated soils, thermal gradients also create vapor density gradients that cause the pore water to evaporate from hot regions and flow toward colder regions. When the water vapor eventually condenses, latent heat transfer will occur due to the energy release associated with phase change. Non-uniform distributions in degree of saturation in unsaturated soils will also cause a decrease in the vapor density gradient as well as the development of a matric suction gradient in the direction opposite to the vapor

density gradient. The development of a matric suction gradient causes liquid water to flow from the colder and relatively wetter locations back toward hotter and drier regions.

Philip and de Vries [193] and de Vries [79], derived a widely-used theory for liquid water and water vapor transport building upon the vapor flow theory of Penman [191] under non-isothermal flow conditions as an extension to Richards' equation [200]. In this approach, liquid water and water vapor transport is driven by pressure head and temperature gradients. The model of Philip and de Vries [193] has since become the underlying theory employed in many other studies (e.g., [14, 30, 44, 49, 167, 207, 208, 225, 231, 243, 244]). However, the model of Philip and de Vries [193] includes a number of simplifications and assumptions to reduce complexity that may not represent the mechanisms of heat transfer and water flow on a pore scale [229]. Specifically, the approach of Philip and de Vries [193] proposed two effects occurring at the pore scale that contributed to enhancement of water vapor diffusion through partially saturated soils. First, because of the different thermal conductivities of the soil, air, and water, they hypothesized that a microscopic temperature gradient across air-filled pores would be higher than a macroscopic temperature gradient measured across the soil sample. Second, they hypothesized that water vapor diffusion is enhanced due to condensation and evaporation from liquid islands between the particles, in effect causing an increase in the area available for vapor diffusion. Because vapor flux predictions by Fick's law of diffusion did not match experimental data, Philip and de Vries [193] implemented an enhancement factor to account for the greater diffusion of vapor under nonisothermal conditions. Several studies have measured values of the vapor enhancement factor for different soils (e.g., [49, 50]).

Although the approach of Philip and de Vries [193] has been used in many coupled heat and water flow transfer problems, an issue with their model is that the vapor enhancement factor was explained at the pore scale following the hypotheses mentioned in the previous paragraph, while the vapor diffusion process was formulated macroscopically [229]. Further, their hypotheses of the physical mechanisms leading the enhancement in vapor diffusion have been drawn into question [110, 208, 226]. For example, Ho and Webb [110] used a pore-scale model to estimate the steady state mass flow of water vapor in two different pore-scale transport paths including vapor mass transfer through the liquid islands and around the liquid island. They found that the net water vapor mass transfer through the liquid islands may be only an order of magnitude higher than water vapor transport around the liquid island by Fickian diffusion. More recently, Shokri et al. [226] found that the vapor enhancement factor may not be needed if capillary flow is included, meaning that Fick's law of diffusion may be sufficient. Consideration of capillary flow requires a careful assessment of tortuosity effects for water flow in unsaturated soils [166].

An alternate approach to solving coupled heat transfer and water flow problems is through the theory of irreversible thermodynamics, summarized in detail by Luikov [155] and further investigated by Pandey et al. [188]. A similar approach was used in the model of Taylor and Cary [241] specifically for unsaturated soils. Although Thomas et al. [247] noted that this approach may be more fundamentally correct

than the mechanistic approach of Philip and de Vries [193], it is difficult to calibrate some of the parameters used in the model of Luikov [155].

Another issue is the choice between coupled heat transfer and water flow models that include equilibrium or nonequilibrium phase change. In the case of equilibrium phase change, the pore water is assumed to volatilize instantaneously. This is a common assumption in many coupled heat transfer and water flow models (e.g., [30, 44, 167, 193, 207, 208]). However, experimental studies have identified that time is required for liquid water to volatilize in response to a change in vapor pressure in a pore that may be caused by gas phase vapor diffusion caused by gradients in vapor pressure and/or temperature [12, 26, 27, 54, 59]. To account for this in a model of coupled heat transfer and water flow, a source term for the liquid/gas phase change rate is typically added to the mass balance equations of liquid and vapor. This is the case in the formulations of Bénet and Jouanna [26], Bixler [31], Zhang and Datta [270], Smits et al. [229], Moradi et al. [171], McCartney and Baser [161], and Baser et al. [23]. The phase change rates used in these formulations are based on irreversible thermodynamics, first order reaction kinetics, or the kinetic theory of gases which all contain a phenomenological coefficient that is physics-based or defined as a fitting parameter during modeling efforts. Smits et al. [229] adopted the approach of Bixler [31], who derived a phase change equation from the kinetic theory of gases, making it inherently temperature dependent. In the model of Bixler [31], the vaporization rate is proportional to (a) the difference between local equilibrium vapor pressure and local partial vapor pressure and (b) the difference between local degree of saturation and residual degree of saturation. Smits et al. [229] compared predictions from equilibrium and nonequilibrium models for coupled heat transfer and water flow, and found major differences in the initial stages of evaporation for soils with initially low degrees of saturation.

McCartney and Baser [161] used a form of the model of Smits et al. [229] extended by Moradi et al. [171], but incorporated a new set of coupled thermo-hydraulic constitutive relationships (described in the next section), and presented an experimental approach to define the parameters governing the vapor enhancement factor and the vapor phase change rate. In their model, the governing equation for nonisothermal flow of water in unsaturated soils is given as follows:

$$nS_{rw}\frac{\partial \rho_w}{\partial t} + n\,\rho_w\frac{dS_{rw}}{dP_c}\frac{\partial P_c}{\partial t} + \nabla\cdot\left[\rho_w\left(-\frac{k_{rw}\kappa}{\mu_w}\right)\nabla(P_w + \rho_w g z)\right] = -R_{gw} \quad (3)$$

where n = porosity (m^3/m^3), S_{rw} = degree of water saturation (m^3/m^3), ρ_w = temperature-dependent density of water (kg/m^3) [109], t = time(s), $P_c = P_w - P_g$ = capillary pressure (Pa), P_w = pore water pressure (Pa), P_g = pore gas pressure (Pa), k_{rw} = relative permeability function for water (m/s); κ = intrinsic permeability (m^2); μ_w = temperature-dependent water dynamic viscosity [kg/(ms)] [145], g = acceleration due to gravity (m/s^2) R_{gw} = Phase change rate (kg/m^3s). Similarly, the governing equation for nonisothermal flow of air in unsaturated soils is given as follows:

$$nS_{rg}\frac{\partial \rho_g}{\partial t} + n\,\rho_g \frac{dS_{rg}}{dP_c}\frac{\partial P_c}{\partial t} + \nabla \cdot \left[\rho_g\left(-\frac{k_{rg}\kappa}{\mu_g}\right)\nabla(P_g + \rho_g g z)\right] = R_{gw} \tag{4}$$

where S_{rg} = degree of gas saturation (m^3/m^3), ρ_g = temperature-dependent density of gas (kg/m^3) [229], k_{rg} = relative permeability function for gas (m/s); μ_g = temperature-dependent gas dynamic viscosity [kg/(ms)]. The water vapor mass balance needed to consider the balance of liquid and water vapor is given as follows:

$$n\frac{\partial(\rho_g S_{rg} w_v)}{\partial t} + \nabla \cdot (\rho_g u_g w_v - D_e \rho_g \nabla w_v) = R_{gw} \tag{5}$$

where $D_e = D_v\tau$ = effective diffusion coefficient (m^2/s), D_v = diffusion coefficient of water vapor in air (m^2/s) [47], w_v = mass fraction of water vapor in the gas phase (kg/kg), $\tau = n^{1/3}S_{rg}^{7/3}\eta$ = tortuosity [166]. The enhancement factor for vapor diffusion, η following the approach of Cass et al. [49] is:

$$\eta = a + 3S_{rw} - (a-1)\exp\left\{-\left[\left(1 + \frac{2.6}{\sqrt{f_c}}\right)S_{rw}\right]^3\right\} \tag{6}$$

where a = fitting parameter, f_c = clay fraction. The nonequilibrium gas phase change rate R_{gw} in Eqs. (3), (4), and (5) is given as follows [31, 171]:

$$R_{gw} = \left(\frac{bS_{rw}RT}{M_w}\right)(\rho_{veq} - \rho_v) \tag{7}$$

where b = empirical fitting parameter (s/m^2), R = universal gas constant (J/molK), $\rho_{veq} = R_{he}c_{vs}$ = equilibrium vapor density (kg/m^3) [47], T = Temperature (K), ρ_v = vapor density (kg/m^3), M_w = molecular weight of water (kg/mol). Finally, the heat transfer energy balance that considers both conduction, convection, and phase change is given as follows [171, 267]:

$$(\rho C_p)\frac{\partial T}{\partial t} + \nabla.\left((\rho_w C_{pw})u_w T + (\rho_g C_{pg})u_g T - (\lambda \nabla T)\right) = -L_w R_{gw} + Q \tag{8}$$

where ρ = total density of soil (kg/m^3), C_p = specific heat of soil (J/kgK), C_{pw} = specific heat capacity of water (J/kgK), C_{pg} = specific heat capacity of gas (J/kgK), λ = thermal conductivity (W/mK), L_w = latent heat due to phase change (J/kg), u_w = water velocity (m/s), u_g = gas velocity (m/s), Q = heat source (W/m^3).

A major challenge in applying the coupled set of equations described above is the determination of the material parameters. In particular, the parameters *a* and *b* depend on the soil type [22] and must be determined using physical modeling tests involving inverse analysis of temperature and degree of saturation measurements during heating [161]. The other thermo-hydraulic parameters are more established, but linkages between the individual parameters need to be further explored. In unsaturated soils,

the soil-water retention curve (SWRC) is the fundamental relationship governing the amount of water in the soil and the energy state in the water. A commonly-used SWRC is that of van Genuchten [258], as follows:

$$S_{rw} = S_{rw,res} + (1 - S_{rw,res})\left[\frac{1}{1 + (\alpha_{vG} P_c(T))^{N_{vG}}}\right]^{1-1/N_{vG}} \quad (9)$$

where $S_{rw,res}$ is the residual degree of saturation to water, α_{vG} and N_{vG} are parameters representing the air entry pressure and the pore size distribution, respectively, and $P_c(T)$ is the temperature-corrected capillary pressure according to the model of Grant and Salehzadeh [102]. Although most studies use the van Genuchten [258] SWRC model to fit a smooth function to experimental SWRC data, recent advances indicate that there may be other forms that better capture the mechanisms of water retention. For example, the SWRC of Lu [150] can represent both the capillary regime at low suctions and the adsorbed regime at higher suctions. Another advance is the consideration of volume change on the shape of the SWRC [182, 189, 203, 209, 239, 252, 271] and ways to consider hysteresis [190].

It is well established that the hydraulic conductivity of unsaturated soils depends on the available pathways for water flow through the soil that change with the degree of saturation [174]. The HCF describes the relationship between hydraulic conductivity and degree of saturation (or suction), and can be predicted by incorporating the van Genuchten [258] SWRC, as follows:

$$k_{rw} = \sqrt{\left(\frac{S_{rw} - S_{rw,res}}{1 - S_{rw,res}}\right)}\left[1 - \left(1 - \left(\frac{S_{rw} - S_{rw,res}}{1 - S_{rw,res}}\right)^{1/(1-1/N_{vG})}\right)^{1-1/N_{vG}}\right]^2 \quad (10)$$

where α_{vG} and N_{vG} are the same parameters as in Eq. (9). Although the SWRC is temperature dependent ([101]; She and Sleep [223]; Vahedifard et al. [256], the temperature dependency of the HCF has not been well evaluated. It would be expected that the temperature dependency of the SWRC and the change in viscosity of the pore fluid would both have important effects on the magnitude and shape of the HCF.

As the transfer and storage of heat in unsaturated soils are both dependent on the amount of water in the pores, a logical extension is that the thermal properties are linked to the shape of the SWRC [80]. Several studies have evaluated the effect of degree of saturation on the thermal conductivity [38, 88, 147, 148, 230]. Dong et al. [80] summarized several of the constitutive modeling approaches that have been used to capture the trends in the thermal conductivity with degree of saturation, including multi-phase mixing models that involve series and parallel combinations of solid, air, and water, mathematical models that build upon analogous relationships for other physical properties (electrical conductivity, hydraulic conductivity) and involve volume factions of the different components, and empirical models developed based on curve fitting. Unfortunately, only the empirical models have been shown to have

a good match to the experimental data, so several models have been widely used in practice (e.g., [48, 71, 134, 154]). However, because of the empirical nature of these models, the thermal and hydraulic properties are uncoupled if they are used in coupled heat transfer and water flow models. To address this shortcoming, Lu and Dong [153] developed a new TCF that builds upon the shape of the SWRC, given as follow:

$$\frac{\lambda - \lambda_{\text{dry}}}{\lambda_{\text{sat}} - \lambda_{\text{dry}}} = 1 - \left[1 + \left(\frac{S_e}{S_{\text{f}}}\right)^m\right]^{1/m-1} \tag{11}$$

where λ_{dry} and λ_{sat} are the thermal conductivities of dry and saturated soil specimens, respectively, S_e is the effective saturation, S_f is the effective saturation at which the funicular regime is onset, and m is defined as the pore fluid network connectivity parameter for thermal conductivity. The TCF does not approach λ_{sat} at $S_e = 1$, so this should be considered as an additional fitting parameter. Lu and Dong [153] used a large database of experiments performed in an extended version of the transient-release and imbibition method (TRIM) of Wayllace and Lu [265] to define empirical relationships between the parameters and those of the SWRC. Baser et al. [20] proposed a relationship for the volumetric heat capacity function (VHCF) that uses the same form as the TCF of Lu and Dong [153] that also employs the same parameters, as follows:

$$\frac{C_v - C_{v\,\text{dry}}}{C_{v\,\text{sat}} - C_{v\,\text{dry}}} = 1 - \left[1 + \left(\frac{S_e}{S_{\text{f}}}\right)^m\right]^{1/m-1} \tag{12}$$

where C_{vdry} and C_{vsat} are the volumetric heat capacities of dry and saturated soil, respectively, and are similarly treated as fitting parameters, and S_f and m are the same parameters as in Eq. (11). Examples of the SWRC and HCF of a compacted silt are shown in Fig. 3a, while examples of the TCF and VHCF for the silt are shown in Fig. 3b. The shapes of these coupled thermo-hydraulic relationships are highly nonlinear, with the hydraulic relationships varying over several orders of magnitude and the thermal relationships varying over a single order of magnitude. The VHCF can be calibrated concurrently with the TCF if a dual-thermal needle is used in the nonisothermal TRIM test. However, the VHCF has only been measured for unsaturated silt, so further research is needed to confirm the shape of the VHCF for other soils.

In summary, there are many challenges when evaluating the coupled heat transfer and water flow in soils, especially when the soil is unsaturated. Applications of the governing equations discussed in this section have been presented for surface evaporation from unsaturated soils by Smits et al. [229] and for thermal energy storage systems by Moradi et al. [171] and for geothermal heat exchangers by McCartney and Baser [161]. Future fundamental studies may focus on further linkages between the thermal and hydraulic properties of saturated and unsaturated soils together with the parameters governing phase change and enhanced vapor diffusion. The applica-

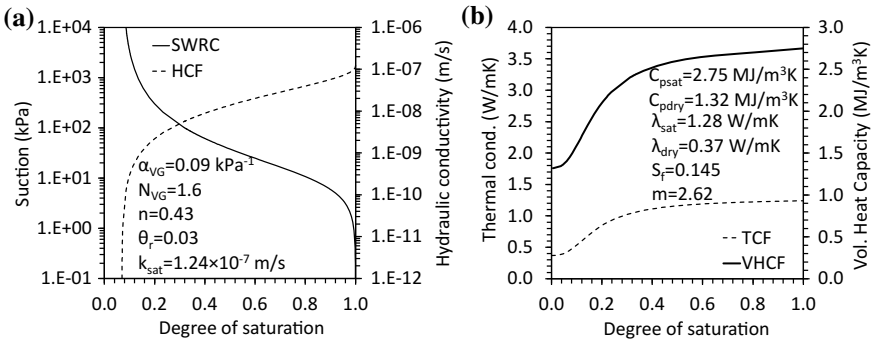

Fig. 3 Coupled properties of unsaturated Bonny silt obtained using the thermal TRIM analysis of Lu and Dong [153]: **a** Hydraulic properties; **b** Thermal properties

bility and validation of the nonequilibrium approach for considering phase change in unsaturated soils could also be further explored for different soil types, such as high plasticity, expansive clays. The role of the liquid island assumption in explaining the concept of enhanced vapor diffusion is another issue that deserves further experimental and pore-scale evaluations, as it has only been investigated for sandy soils that can be approximated as an assembly of bulky particles.

2.2 Thermal Softening of the Preconsolidation Stress

As heat transfer and water flow occur through saturated and unsaturated soils, changes in mechanical behavior are expected. Although most mechanical properties of soils have been found to be temperature independent, like the friction angle [139] and compression indices [46], the preconsolidation stress has been found to be dependent on temperature for saturated soils (e.g., [16, 149]) and unsaturated soils [10, 210, 253]. One source of these changes in mechanical behavior is due to changes in effective stress with changes in suction or degree of saturation [151, 152], but this may not fully explain some of the changes in volume observed in the literature. Instead, the preconsolidation stress, which reflects the stress history in the soil, may have a more significant role. Observations of the role of stress history in the literature encouraged the development of thermo-elasto-plastic models, where temperature is expected to cause changes in the preconsolidation stress [74, 116, 143]. Although these models have been used successfully to capture the observations from element-scale tests, they unfortunately are not related to any underlying micro-scale mechanisms of temperature effects on soils. In particular, two important challenges are: the prediction of the role of temperature variations in changes in the preconsolidation stress of soils and in the volume change of soils. Further, the role of unsaturated conditions in both challenges leads to other concerns including changes in stress state and path depen-

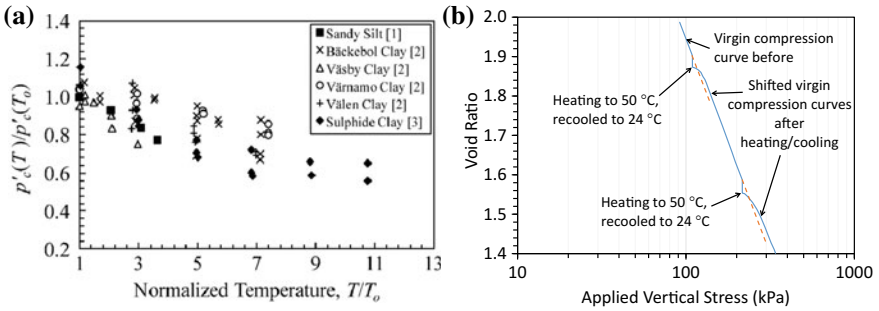

Fig. 4 **a** Change in preconsolidation stress of normally consolidated clays after a change in temperature (data from [83, 210, 242]); **b** Change in compression response of normally consolidated soils after heating and cooling (modified from [194])

dency [10]. An improved understanding of the underlying mechanisms that govern these phenomena along with development of modeling strategies will help better predict the THM behavior of soils. Further study of these topics may help to better understand the impacts of cyclic heating and cooling that have been observed in some studies [42, 120, 260] and on the role of anisotropic stress states [65] which are both particularly relevant to the performance of geothermal heat pumps incorporated into civil engineering infrastructure.

An underlying feature of the thermo-elasto-plastic models mentioned above is the impact of temperature on the preconsolidation stress in soils, which hence is called an apparent preconsolidation stress. A summary of the trends in normalized apparent preconsolidation stress after heating for several saturated soils reported in the literature is shown in Fig. 4a. A trend of decreasing apparent preconsolidation stress with an increase in temperature is observed, indicating thermal softening. Although the slope of the compression curve is not affected by temperature, the trends indicate that plastic strains initiate at an earlier stress. The softening effect on the apparent preconsolidation stress due to heating may not be permanent, and limited sets of data show that drained cooling after a drained heating stage may lead to an increase in preconsolidation stress from before the temperature cycle was applied, as shown in Fig. 4b (see also [15]). Despite these observations, the underlying mechanism behind the change in preconsolidation stress with temperature is not understood.

The interaction between softening mechanisms due to the heating of soils with hardening mechanisms due to increases in suction have been observed to lead to interesting soil behavior, as observed for example in the shear strength results of Alsherif and McCartney [9] shown in Fig. 5a (see also [94, 143]). These results show that the path of heating and suction application can lead to changes in the apparent cohesion. The role of temperature and suction on the effective stress in unsaturated soils is another important issue to consider. The interplay between the effective stress and preconsolidation stress during application of high suction magnitudes for a specimen at room temperature is shown in Fig. 5b. Some soils exhibit different rates

of increase in effective stress and preconsolidation stress with suction, which may lead to metastable structures that are susceptible to collapse [137]. The model of Grant and Salehzadeh [102] indicates that the SWRC will shift downward to reflect lower water retention at higher temperatures due to a decrease in surface tension and soil-particle contact angle, which is expected to affect the effective stress state. Changes in the shape of the SWRC with temperature are expected to lead to changes in the effective stress in unsaturated soils [152]. Further advances may be obtained in effective stress analyses using the new SWRC of Lu [150], which considers the independent roles of capillarity and adsorption in water retention. These two mechanisms of water retention may be affected differently by temperature. Vahedifard et al. [256] accounted for the effects of temperature on capillarity and adsorption and extended commonly-used SWRCs to nonisothermal conditions. The temperature dependency of capillarity was considered through quantifying the impacts of temperature on surface tension, soil-water contact angle, and adsorption by the enthalpy of immersion. The results in Fig. 5c indicate that different path-dependent (i.e., drying first then heating, or heating first then drying) lead to different increases in the preconsolidation stress for unsaturated soils under high suctions and temperatures. Although the underlying mechanism behind the changes in preconsolidation stress and the path effects is not fully understood, empirical models for the preconsolidation stress such as those shown in Fig. 5c are useful to determine trends in the overconsolidation ratio for unsaturated soils. For example, an understanding of the overconsolidation ration permits trends in the thermal volume change of unsaturated silt measured by Alsherif and McCartney [10] to be reconciled with the thermal volume change of saturated silt measured by Vega and McCartney [260], as shown in Fig. 5d. This example highlights the promise of use of the effective stress principle to unify the THM behavior of unsaturated and saturated soils, although further confirmation is needed.

The results in Fig. 5d for the thermal volume change of saturated silt after several cycles of heating and cooling indicate that this may be important to consider. Studies like Burghignoli et al. [42] and Vega and McCartney [260] observed greater cyclic heating and cooling effects in normally consolidated soils, and that cyclic effects diminish after a few cycles. Further research is needed to understand if anisotropic stress states lead to ratcheting effects during heating and cooling similar to those observed during cyclic mechanical loading. Temperature may play an important role in cyclic mechanical loading of soils. Zhou and Ng [272, 273] evaluated the impact of cyclic loading on the modulus from cyclic triaxial tests, and observed that the cyclic threshold strain was insensitive to temperature, but that the accumulation of plastic strains during cyclic loading increases with increasing temperature. Alsherif and McCartney [9] observed that the modulus of soils obtained from triaxial compression tests increase with temperature when heating unsaturated soils at high suction magnitudes, and was proposed to be due to a reduction in the degree of saturation during heating that leads to a hardening effect and an increase in stiffness.

When considering the behavior of unsaturated soils, it is important that constitutive models capture the volume change of soils to consider the role of changes in degree of saturation during changes in void ratio. Mun and McCartney [175]

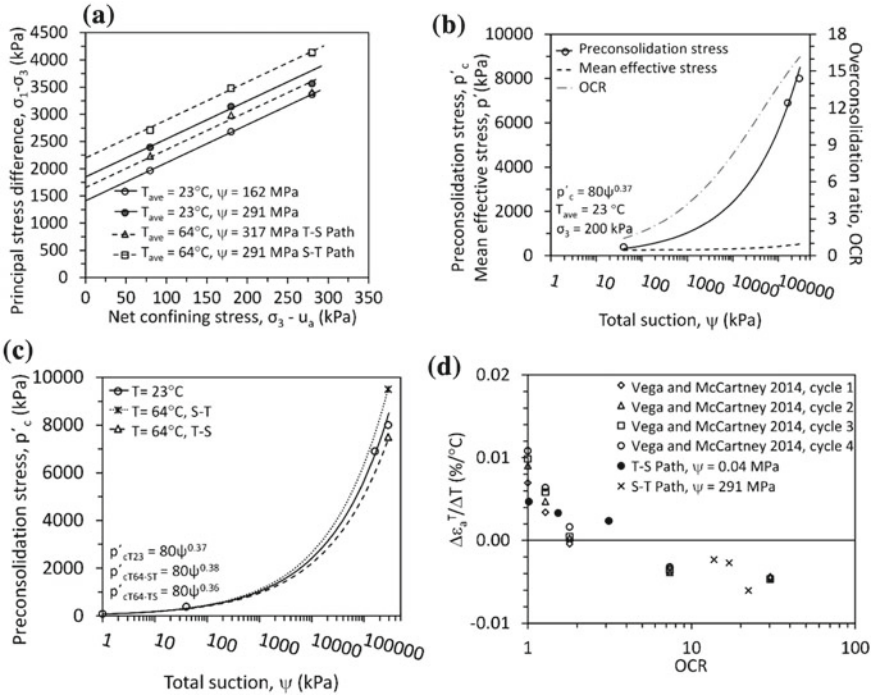

Fig. 5 Thermo-mechanical behavior of compacted silt [10]: **a** Changes in shear strength due to changes in suction and temperature; **b** Changes in preconsolidation stress, effective stress, and OCR with suction; **c** Path dependent changes in preconsolidation stress of unsaturated soils; **d** Thermal volume change trends with OCR

found that the model of Zhou et al. [274] can provide a good means of considering the role of changes in degree of saturation on the compression curve in terms of effective stresses. Models that use bounding surface plasticity concepts to consider nonlinearity in the compression curve may lead to better stress-strain predictions than conventional elasto-plastic models.

2.3 Thermal Pressurization

It is well established that during undrained heating of soils and rocks, positive pore water pressures will be generated [16, 28, 46, 98, 111, 118]. Since the early model of Campanella and Mitchell [46] was developed, several studies have continued the development of thermo-poro-mechanical theories assuming thermo-elasticity to predict thermal pressurization [13, 98, 99, 157, 164, 199] and thermo-elasto-plasticity [16, 261]. In the thermo-elastic models for thermal pressurization, the compatibility of strains during undrained heating is given as follows:

$$\alpha_w V_w \Delta T + \alpha_s V_w \Delta T - (\Delta V_{st})_{\Delta T} = -m_v V_m \Delta u - m_w V_w \Delta u \quad (13)$$

where α_w is the cubical coefficient of thermal expansion of the pore water, α_s is the cubical coefficient of thermal expansion of the mineral solids, V_w is the initial volume of pore water before heating, V_m is the total volume of the soil mass equal to the sum of V_w and V_s, ΔT is the change in temperature of the soil, Δu is the change in pore water pressure, $(\Delta V_{st})_{\Delta T}$ is the volume change of the soil due to the reorientation and relative movement of the soil particles during undrained heating, m_w is the coefficient of volume compressibility of water and m_v is the coefficient of volume compressibility of soil skeleton. This equation can be reorganized to estimate the change in pore water pressure during undrained heating [46]:

$$\Delta u = \frac{n\Delta T(\alpha_s - \alpha_w) + \alpha_{st}\Delta T}{m_v} \quad (14)$$

where α_{st} is the physico-chemical coefficient equal to $(\Delta V_{st})_{\Delta T}/V_m$. As it may be challenging to define the value of m_v, which depends on the effective stress increment, it is possible to incorporate the bi-log-linear compression indices for isotropic loading conditions to define the change in pore water pressure during undrained heating normalized by the initial mean effective stress [98]:

$$\frac{\Delta u}{p'_0} = \frac{[n(\alpha_s - \alpha_w) + \alpha_{st}](1 + e_o)\Delta T}{(1 - \Lambda)\lambda} \quad (15)$$

where p'_0 is the initial mean effective stress, e_0 is the initial void ratio, $\Lambda = \kappa/\lambda$, λ is the slope of the virgin compression in isotropic conditions, κ is the slope of the recompression line in isotropic conditions. The main challenge of applying Eq. (15) is the appropriate definition of material properties governing thermal pressurization [78, 99], in particular the physico-chemical coefficient. Equation (15) was used by Ghaaowd et al. [98] to evaluate the physico-chemical coefficient for different soils in the literature, as shown in Fig. 6a. The correlation for the physico-chemical coefficient shown in Fig. 6a is still approximate but was also used to successfully predict the excess pore water pressure in saturated clays having different overconsolidation ratios (quantified using different initial void ratios and mean effective stresses) in Fig. 6b. Future research is needed to evaluate thermal pressurization in other soil types, especially sands and unsaturated soils. Thermal pressurization may also be encountered in fault shear zones during CO_2 injection [172].

2.4 Thermal Volume Change

Another relevant issue is that volume changes may arise in soils due to coupled heat transfer and water flow, potentially occurring due to changes in effective stress, changes in the apparent preconsolidation stress, or thermally-induced creep. Efforts

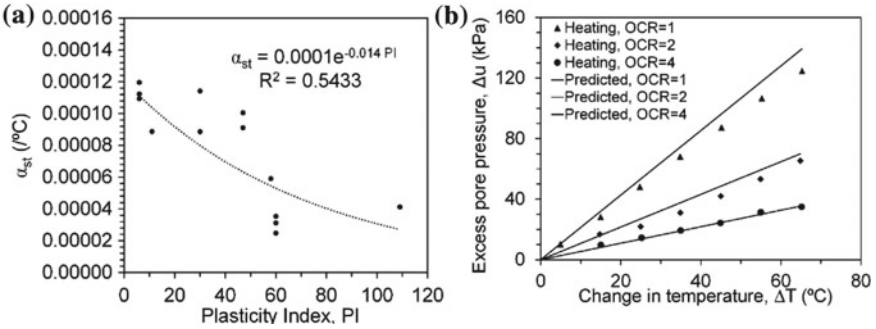

Fig. 6 Thermal pressurization of saturated clays [98]: **a** Physico-chemical coefficient as a function of plasticity index (PI); **b** Impact of temperature change on the change in pore water pressure for Bangkok clay specimens having different OCRs

in the characterization of thermal volume changes have been divided between the development of constitutive models that couple temperature changes with volume change, focusing on equilibrium conditions, and models that consider the impact of volume change on the heat transfer and water flow processes in soils. The motivations of many of these studies have varied, with a few including consideration of temperature effects on soil sampling, thermal stability of buried electrical cables, earthen barriers for radioactive waste disposal, and soil-structure interaction in energy piles.

The conventional explanation of thermal volume change for normally consolidated soils is the dissipation of these excess pore water pressures, which has been incorporated into numerical simulations [40]. However, several sets of data have shown that this explanation may not work in all cases. First, the magnitude of excess pore water pressures during undrained heating has not been linked to a volumetric strain expected after drainage, even though Delage et al. [77] and Cui et al. [75] showed that the process still follows a time dependent process similar to consolidation. Further, Burghighnoli et al. [42] and Towhata et al. [250] found that preparation of overconsolidated specimens by unloading will lead to thermal expansion upon heating, while preparation by reloading to a low OCR leads to contraction. As the thermally-induced excess pore water pressures during undrained heating are expected to be positive in all soils, the dissipation of pore water pressures is not a sufficient explanation. Also, the changes in pore water pressure will lead to a change in effective stress during undrained heating, but the effective stress will not change after cooling, making this explanation difficult to apply.

The possibility for thermal volume changes to be due to thermally-accelerated creep has been proposed in several previous studies [42, 46, 111, 187]. Following these studies, Coccia and McCartney [68, 69] proposed a new model using a testing methodology developed by Coccia and McCartney [70] that assumed the coefficient of secondary compression C_α is sensitive to the temperature and dependent on the change in viscosity of the pore water with temperature. This means that the secondary compression expected under the increment of effective stress applied before

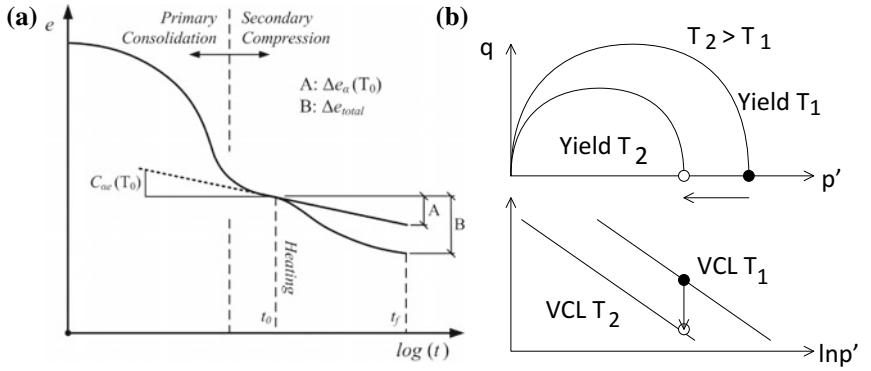

Fig. 7 Alternate mechanisms of thermal volume change: **a** Thermally-accelerated creep ([68] with permission from Elsevier); **b** Thermal collapse during an increase in temperature from T_1 to T_2

a temperature change may be enhanced by an amount equal to $\Delta e_\alpha(T_0)$ defined by Coccia and McCartney [69], as shown in Fig. 7a. This mechanism may reflect the ease of clay particles to rearrange into the direction of shear at elevated temperatures, or potentially a time-dependent change in the diffuse double layer due to temperature changes. Thermally-enhanced creep behavior was also observed in in situ pull-out tests on energy piles in high-plasticity clays [6].

The thermal volume change of unsaturated soils also presents a complex scenario to explain if using the dissipation of thermally-induced excess pore water pressures as the cause of thermal volume changes. Specifically, heating is expected to lead to expansion of the pore water, which should lead to an increase in degree of saturation, decrease in suction, and decrease in effective stress, all of which should lead to thermal expansion. However, in many unsaturated soils a contractive behavior is observed. This permanent contraction has been satisfactorily explained by Coccia and McCartney [69] using the thermal creep mechanism. However, a collapse mechanism related to the decrease in preconsolidation (yield) stress with temperature may be an alternate mechanism, as described schematically in Fig. 7b. Heating of a normally consolidated soil will lead to a decrease in the preconsolidation stress, which will mean that the soil is in an unstable state requiring permanent collapse to a stable preconsolidation stress, causing a downward shift from one virgin compression line (VCL) to another.

Regarding constitutive model development, some efforts focused on poromechanical models to predict thermal pressurization of pore fluids during undrained heating [46, 98] and thermo-elasto-plastic models to predict thermal volume changes of saturated and unsaturated soils [2, 74, 114–116, 140, 143, 144]. Thomas and He [244] and Thomas et al. [246] developed coupled THM models that can consider heat transfer and water flow processes as well as deformations, which have been validated by subsequent experimental studies (e.g., [211, 262]). An issue with this topic is that some of the advances in the constitutive model development have not been incor-

porated into the coupled THM models to better capture the response of some soils (i.e., soft clays, unsaturated compacted soils). Alsherif and McCartney [9] found that the effective stress principle is valid even under elevated temperatures and high suctions in unsaturated soils (where the soil would be expected to behave in a brittle fashion), and Alsherif and McCartney [10] used trends in the preconsolidation stress defined in terms of the effective stress using the approach of Khalili and Khabbaz [136] to unify the thermal volume change behavior of saturated soils tested by Vega and McCartney [260] with unsaturated soils tested by Alsherif and McCartney [9].

As mentioned, changes in volume of saturated soils may occur during heating, typically with elastic expansion observed for overconsolidated soils and elasto-plastic contraction observed for normally consolidated soils [1, 15, 16, 42, 53, 101, 118, 142, 236, 250]. These volume changes will have important effects on the thermal and hydraulic properties of saturated soils, in particular the hydraulic conductivity is expected to decrease with decreasing void ratio and the thermal conductivity is expected to increase with decreasing void ratio. The changes in these two parameters may lead to changes in the heat transfer pattern in saturated soils, especially those with substantial thermally-induced water flow (e.g., [216]).

The main fundamental topics where further developments may be investigated for water-saturated porous media include the consideration of coupling effects associated with large-strain thermal consolidation of very soft clays, the role of fluid pressurization during undrained heating leading to thermal failure, and the underlying mechanisms of thermal volume change. On the last topic, Coccia and McCartney [68, 69] evaluated different mechanisms for thermal volume change including thermo-poro-elastic evaluations (e.g., [46, 98, 238]) and thermo-elasto-plastic models [2, 74, 116, 140, 143], and found that both have shortcomings in predicting thermal volume change of overconsolidated soils prepared by re-loading (instead of unloading) evaluated by Towhata et al. [250] and Burghignoli et al. [42]. The thermo-visco-elastic behavior of soils is another topic that deserves further study [35, 69].

2.5 Thermal Hydro-Shearing

Thermal hydro-shearing is the process of pressurization of fluid in porous media leading to a reduction in effective stress, which in the presence of an initial shear stress may lead to possible shear failure or fracturing. The magnitude of thermal pressurization of pore fluids can be estimated using approaches similar to that described in Sect. 2.3. The problem was first identified in practice during so-called "thermal failure" of clays and shales, arising around heat sources, such as buried cables [39] or nuclear waste canisters [119–121]. Saturated natural clay samples loaded to a total in situ stress, heated slowly, may develop undrained shear failure when the pore pressure grows at a constant principal stress difference and the effective stress path reaches the critical state at about 74 °C. An example of thermal failure of Boom clay are shown in Fig. 8, showing the changes in pore water pressure normalized by the initial effective confining stress during both a room-temperature shearing test

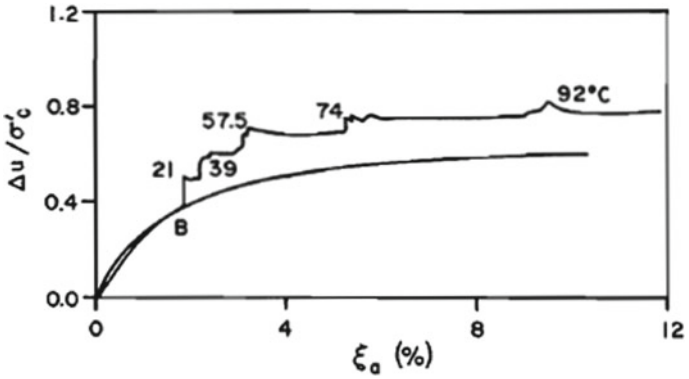

Fig. 8 Normalized pore pressure versus axial strain during undrained heating ([120] with permission from NRC Research Press)

and a test where the specimen was sheared to point B and then the temperature was raised in stages. Similar behavior has also been noted in several other clays and rocks by Hueckel and Pellegrini [119, 120], such as high porosity plastic Boom clay (Belgium), highly fractured stiff Pasquasia shale (Sicily), and Sasamon clayey shale. The strains observed in Fig. 8 cannot be simulated using thermo-elastic models, and must be considered using thermo-elasto-plastic models such as those of Hueckel and Borsetto [116] or Hueckel et al. [121] for clays and Hueckel et al. [123] for rocks.

There are visible differences between the thermal failure and hydro-shearing encountered during hydraulic fracturing processes in energy reservoirs. During hydraulic fracturing, only a part of the pore pressure boost comes from the constrained heating of the cooler injected pore water, while a comparable boost comes from the injection pressure [55]. Further, there is also a difference in heat exchange between rock and water. During hydro-shearing, the rock is cooling as the hydraulic fracturing process proceeds, which means that the rock shrinks and induces further stresses. Hence, the pore water pressure increase is magnified by the collusion of two thermally driven processes: water expansion and rock shrinkage. It is thus clear that the assessment of the amount of pressure boost and activation of the critical shear depends on our understanding of water expansion (highly non-linear with temperature) and thermo-plastic deformation of rock. Rice [199] also observed that there may be another mechanism that could affect the shear strength, referred to as flash heating. In this case, highly-stressed frictional contacts slip during rapid heating. Also, depending upon the shearing rate, dilatant strengthening, which is intrinsic to compacted granular materials, may happen for lower shear rates [218, 219]. In this case there may be a competition between weakening due to thermal pressurization and dilatant strengthening.

In enhanced geothermal systems (EGS), hot water is retrieved through extraction boreholes when it reaches a required temperature, while a corresponding volume of cold water is supplied via an injection well. The cooled rock after the extraction

process undergoes subsequent re-heating by the adjacent rock mass, and a corresponding reduction of pore pressure, while the new cooler water is being mixed with the departing hot water. At this stage, the heated rock is thermally expanding. Notably, cyclic heating/cooling most likely creates dilatancy associated with a progressive damage [118, 120]. This suggests also that the pressure required to inject water at an nth cycle of operation in an EGS system should be considered based on the estimated amount of accumulated damage.

2.6 Thermal Desiccation Cracking

The discussion to this point in the chapter assumes that the soil remains as a continuum during a coupled heat transfer and water flow process. However, near a free surface changes in temperature and water content may lead to desiccation cracking, which may lead to a change in the boundary condition for heat transfer and water flow. Specifically, the thermo-hydraulic surface boundary condition may extend deeper into the soil layer than in the case that the soil layer was intact. Thermal desiccation cracking is a superposition of several parallel and coupled processes: thermal expansion or contraction (depending on the stress history), drying shrinkage or straining, depending on kinematic constraints, air entry connected with water, vapor and air mass transport, heat transport, and the driving phenomenon of evaporation. Cracking is highly undesirable in soil from both the mechanical and hydraulic points of view, usually degrading engineering soil quality including the repeated wetting-drying cycles reducing the soil from peak to fully softened shear strength [228, 234, 268]. Cracking may adversely affect integrity of soil in energy production/storage related projects, such as nuclear waste container barriers, storage/retrieval of heat from energy piles.

Desiccation cracks generally arise in an absence of external forces. Hence, either self-equilibrated stresses resulting from kinematic incompatibilities, or reaction forces at the constraints appear as a cracking cause, when reaching tensile strength [192, 213]. At a meso-scale, tubular drying pores have been modeled near a random imperfection, inducing a stress concentration, in the presence of significant suction [112, 113]. Hu and Hueckel [113] use an effective stress analysis, which away from the stress concentration point yields a criterion paradox: compressive effective stresses are observed in the field, a physically incompatible criterion for formation of a tensile crack. Experiments on clusters of grains suggest that an imperfection of an air entry deep into the medium penetrates over 4–8 radii of a typical pore that yields a tensile effective stress concentration at the air entry finger-tip, sufficient for crack propagation [122].

Subcritical crack propagation resulting from a spontaneous or engineered change in the rock chemical environment is of relevance in several energy technologies, among which are unconventional oil and gas recovery, and enhanced geothermal systems. The enhancement consists of a combination of fluid pressure and injection of acids. Acid chemically softens the material, which occurs relatively quickly,

especially in carbonate rocks. The main question is to correlate the chemical flux to the rate of crack propagation. Hu and Hueckel [113] addressed the effect of mineral mass removal on the material strength, via coupled chemo-plasticity approach. The chemical part of the processes being explicitly rate dependent, requires plasticity to be treated incrementally and iteratively. Simplified calculations with the Extended Johnson approximation (i.e., all fields are axially symmetric round crack tip point) allow following the stress evolution as minerals are dissolved. The effect of coupling of chemicals on elasticity near a crack subject to acidizing under isothermal conditions is another topic of importance. The release of mineral mass into liquid phase affects solute diffusion, while the rate of mass release is dependent on local acidity. Most importantly, when a fraction of mass is removed from a stressed solid, a further strain is induced. This induced strain is assumed to be proportional to the mass removal, with the proportionality (chemical deformation) coefficient, likely dependent on the material damage. In the deviatorically-coupled solution obtained using an adapted Airy function, a dramatic increase in hoop stress is observed in front of the crack tip which can be associated with the shrinkage of the chemically affected zone. Other scenarios and their possible combinations still await suitable solutions, including the impact of cracking on the thermal and hydraulic properties of soils shown in Fig. 2.

2.7 Software to Consider THM Effects in Soils

A theoretical formulation is an appropriate way to integrate the relevant THM phenomena discussed in the previous sections via a consistent and unified framework. In a coupled formulation, the roles of the various physical phenomena and their mutual relationships are clearly expressed with no ambiguity. Once implemented numerically, the mathematical formulation can be used to achieve a better understanding about the interaction between the different physics (e.g., [185, 206]). There are several topics that have received significant attention and are at the point that a good understanding is available for the topics although they could still benefit from further study. These include the development of thermo-hydraulic flow models (TOUGH2, COMSOL), thermo-elasto-plastic models (models from the groups of Hueckel, Laloui, Cui, Gens, etc.), validated research codes (CODE_BRIGHT, COMPASS, LAGAMINE, COMSOL), experimental and theoretical soil-structure interaction analyses for energy piles, development of advanced laboratory tests for THM behavior (thermal triaxial, thermal oedometer, thermal needle, etc.), and field tests (e.g., the thermal response tests on geothermal heat exchangers, FEBEX test on bentonite barriers [96]). Many of these codes are currently only suitable for research purposes, and may need further refinement for use in geotechnical practice.

3 Thermal Energy Applications in Geotechnical Engineering

This section describes three emerging applications of thermal energy in geotechnical engineering that have reached a reasonable stage of maturity but still require varying amounts of research to be fully implemented into engineering practice. The first application involves barrier systems for radioactive waste repositories. Although barriers involving compacted bentonite have been implemented into practice in several situations, the complex behavior of these clays under unsaturated conditions and elevated temperatures is not fully understood. The second application is that of energy piles, which are perhaps the most established energy geotechnics technology that integrates the concept of ground-source heat exchangers into deep foundations. These systems require an understanding of the heat transfer performance of these systems, as well as the thermally-induced stresses and strains in the energy pile. The third application involves storage of thermal energy in the subsurface. Although types of thermal energy storage systems have been evaluated and implemented into practice, an emerging application is the storage of thermal energy in unsaturated soils or rocks, transferred using ground-source heat exchangers. Unsaturated soils and rocks have lower thermal conductivity than when saturated, so they will have lower heat losses. However, the mechanisms of heat transfer in unsaturated soils and rocks are much more complex and must be considered as part of the design of these systems.

3.1 Barrier Systems for Radioactive Waste Repositories

The storage of high level radioactive waste (HLW) is an important topic that involves coupled heat transfer and water flow [195]. Deep geological disposal of HLW is a preferred option for the isolation of high level nuclear waste and requires significant input from geotechnical engineers [93, 94, 96, 117]. Most repositories involve an unsaturated rock deposit that serves as a natural barrier in which tunnels are formed for placing waste canisters, which are encapsulated by a highly densified buffer material (e.g., pure bentonite or a sand-bentonite mixture). The natural and engineered barriers are expected to be subjected to simultaneous thermo-hydro-mechanical-chemo (THMC) phenomena triggered by the heat-emitting nature of the nuclear waste, the swelling character of the unsaturated clay barrier, the highly confined conditions of the isolation system, and the chemical interactions between the barriers material and the pore fluid [211]. Many of the fundamental studies on the THM behavior of saturated and unsaturated soils discussed in Sect. 2 were developed as part of the design of barrier systems for radioactive waste repositories. The FEBEX test on bentonite barriers was a major step forward in providing useful validation data for the different numerical simulations used to design these barrier systems, more recent developments are related to the study of clay structure changes during heating

an hydration (e.g. [212, 248]), the potential of pelletized clayed materials as barrier materials and seals (e.g. [97, 215]). Further efforts will be necessary as different evolutions in modified bentonite materials are developed (e.g., polymer bentonites) and higher temperatures for the storage system are investigated (i.e. above 100 °C).

3.2 Energy Piles

In recent years, reinforced concrete geostructures like piles, walls and slabs have been used as geothermal heat exchangers to access the relatively constant temperature of the ground for efficient heating and cooling of buildings. Full-scale energy piles have been successfully implemented in buildings and experimental tests in Europe [4, 37, 141], Japan [107], the United Kingdom [11, 36], China [91], Australia [34, 263], and the US [7, 160, 176, 237]. The soil-structure interaction response and heat exchange capabilities characterized in these studies have generally indicated that energy piles can serve as sustainable geothermal heat exchangers. The main advantage of energy piles is that they help improve the energy efficiency of building heat without needing additional infrastructure or materials beyond that needed for building support.

Several researchers have evaluated the thermo-mechanical response of energy piles in soils subjected to monotonic or cyclic heating or cooling [11, 100, 176]. Based on findings from previous studies on energy piles in soils, different approaches or guidelines have been developed to analyze the complex interaction between temperature changes and induced thermo-mechanical stresses and deformations in sands and clays, like numerical methods based on the axial load transfer (T-z) approach [57, 138, 235] and finite element or finite difference methods [24, 91, 141, 184, 264]. Of these methods, axial load transfer is most commonly used in the design of piles [168] or to study the behavior of piles under cyclic thermo-mechanical loading [235]. Some design recommendations have been made using finite element analyses via parametric analyses [24]. Future challenges for energy piles involve an assessment of the behavior of energy piles in deformable soils where changes in soil volume may lead to dragdown effects on energy piles [162], as well as the development of design codes that incorporate both structure and geotechnical aspects of energy piles.

3.3 Thermal Energy Storage

An important challenge facing society is the storage of energy collected from renewable sources. One such application is the storage of heat collected from solar thermal panels in the subsurface during summer, so it can be harvested in winter [159, 227]. A practical mode of heat injection into the subsurface involves the circulation of a heated carrier fluid through a closely-spaced array of closed-loop geothermal heat exchangers in boreholes or shallow trenches [18, 56, 60, 61, 73]. Unsaturated soils in the vadose zone are an ideal storage medium for heat because the storage vol-

ume is abundant and lower heat losses can be expected in unsaturated soils due to lower thermal conductivity [18]. However, the mode of heat transfer during injection of heat into the ground in the vadose zone is complex as it may be coupled with thermally-induced water flow in either liquid or vapor forms.

Most models of heat transfer from geothermal heat exchangers employ analytical solutions to the heat equation assuming conduction is the primary mechanism of heat transfer, with constant thermal properties for the soil (e.g., [135]). These include analyses of heat transfer for an infinite line source [25, 124], a finite line source [145], a hollow cylinder source [92, 125], a finite plate source, and one- and two-dimensional solid cylinder sources [240]. Numerical simulations of geothermal heat exchangers have also been performed, although most also consider conduction as the primary mechanism of heat transfer in soils [18, 186]. While these conduction-based numerical simulations may be practical for the design of heat exchangers in dry or saturated low permeability soils, they may not be practical for those in unsaturated soils due to the potential for convective heat transfer associated with thermally-induced liquid water or water vapor flow (e.g., [23, 170, 193, 229]). Further, the thermal properties of unsaturated soils are highly dependent on the degree of saturation even if conduction is assumed to be the primary mode of heat transfer (e.g., [80, 88, 153, 230]). In addition, the analytical solutions for heat transfer from geothermal heat exchangers may not be practical due to convective heat transfer in saturated soils with high permeability due to buoyancy-driven thermally-driven water flow [52].

Most studies on the behavior of geothermal heat storage systems focus on their overall performance during heating and do not consider coupled heat transfer and water transport [61, 84]. However, some recent studies highlighted the importance of considering coupled heat transfer and water flow in unsaturated soils in the vadose zone to better understand heat transfer mechanisms when the soils are subjected to relatively higher temperature gradients as in borehole heat storage systems [17, 19, 21, 52, 171]. Further, the impact of vapor flow during heating and cooling has been investigated by McCartney and Baser [161] and Baser et al. [23], who found that permanent drying during heat injection leads to a longer period of heat storage when the system cools to ambient conditions. Further studies on the impact of this mechanism on the efficiency of heat extraction are still needed.

4 Emerging Thermal Problems in Geotechnical Engineering

Although there are many emerging thermal energy problems in geotechnical engineering (e.g., cold regions problems, temperature effects on expansive soils, landslides, waste containment, increased volatility of weather/climate), this section focuses on some recent developments involving thermal effects in geotechnical engineering associated with climate change and elevated temperature landfills. Climate

change effects have only been simulated due to the large scale of the problem, while the setting of elevated temperature landfills has only been characterized experimentally due to the complex material properties. Both problems are challenging and require application of the fundamental concepts discussed in this chapter.

4.1 Effects of Climate Change on Geotechnical Infrastructure

Historical data as well as projected trends indicate an increase in the frequency and intensity of climatic extreme events related to temperature [126]. Current models indicate temperature increases of 2–4 °C across the United States by the end of the century with prolonged periods of warm spells [58, 165]. Even historical observations indicate substantial increases in warm spells, short-term heatwaves, and concurrent drought and heat waves [76, 158, 224]. Dry and warm spells are coupled and have feedbacks on each other through land-surface processes [221]. Dry spells can potentially trigger or intensify droughts and below average precipitation can increase the likelihood of heatwaves. Recent examples of such droughts, partly attributed to anthropogenic activities, have occurred in Australia, Europe, Texas, Oklahoma, and California [5, 221, 254].

While several large-scale studies have been conducted to evaluate various aspects of climate change, there is a clear gap in the state of our knowledge in terms of assessing the resilience of geotechnical infrastructure (natural and engineered) to extreme events (e.g., drought, extreme precipitation, etc.) under a changing climate [64, 90, 133, 249, 257, 259]. While progress has been made in understanding the unsaturated soil behavior, the impacts of concurrent changes in degree of saturation and temperature, especially for relatively dry soils, remain uncertain. Soil-atmospheric interactions and extreme event patterns in a changing climate may affect both the shear strength and compressibility of near-surface soils through changes in degree of saturation and desiccation, but may also affect the loading on geostructures due to changes in the water table and infiltration [43, 133, 201, 251, 254, 255, 259]. Drought can weaken near-surface soil through desiccation cracking, heat-induced softening, erosion, and subsidence, and soil organic carbon decomposition. Previous cases of drought occurrence have demonstrated that many of the described processes can result in the weakening of earthen structures. The Australian Millennium drought provided examples including slump failure of riverbanks and extensive desiccation cracking [201]. A schematic depiction of potential drought-induced weakening processes in an earthen levee is shown in Fig. 9.

In addition to weakening and cracking, drought conditions may also increase the rate of land subsidence and organic carbon decomposition [201]. For example, California's Delta region has been historically undergoing land subsidence due to microbial oxidation and compaction of organic-rich soils resulting from extreme temperatures and groundwater extraction [41, 173]. The rate of subsidence in the

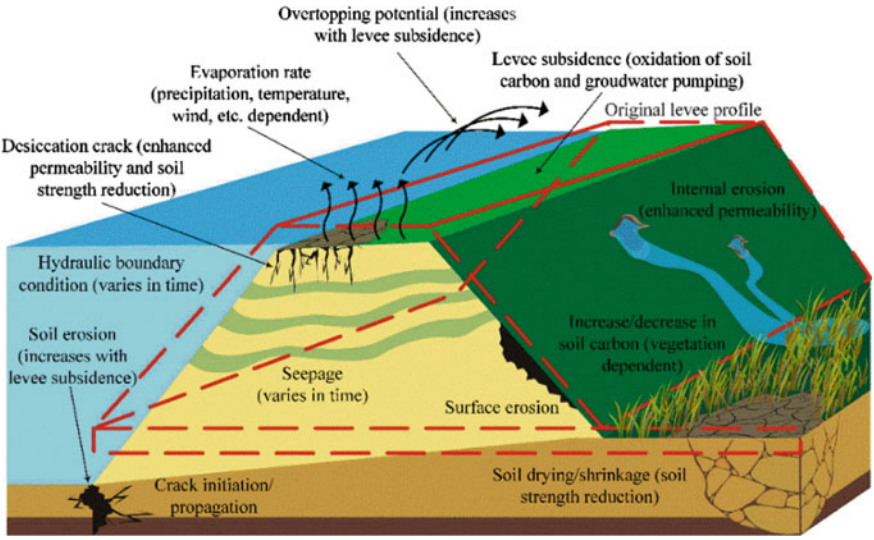

Fig. 9 Potential drought-induced weakening processes in an earthen levee (from [201] with permission from ASCE)

region, however, significantly increased during the recent protracted drought in California, reaching a record-setting rate of around 5 cm per month in some locations during 2014 and 2015 [89]. Land subsidence may occur due to increased ground water consumption and rate of evapotranspiration during drought conditions. Subsidence occurs as previously saturated soils dry out allowing the soil to collapse and fill void space. This behavior is worsened by the decomposition of organic soil that becomes exposed to oxygen under dry conditions [201]. The rate of decomposition is heavily affected by temperature and moisture content with hot dry conditions yielding rapid loss of organic carbon [72]. Drought-accelerated land subsidence can lower the height of levees increasing the risk of overtopping.

Further, it is prudent to consider a multi-hazard scenario when assessing the effects of drought on earthen structures. It is almost inevitable that drought is superimposed or followed by other climatic conditions, such as severe flooding, storm surges, high temperatures, sea level rise, and extreme rainfall events, which can further threaten the structural integrity of earthen structures [254]. One recent example is California, where an extremely wet year in 2017 was superimposed on a record-setting protracted drought, arguably contributing to several damages to earthen structures and slopes [255]. Because of the crack systems developed during a drought, the soil is exposed to rapid infiltration and pore pressure increases, which may cause the soil to reach its limit state [201, 259]. Flow through these cracks can also lead to internal and external erosion [259]. Some types of earthen slopes have also been noted to fail more easily due to the onset of rapid pressure changes and surface erosion due to overland flow

caused by heavy precipitation [202]. The development of piping systems due to high pore pressures due to flooding and sea level rise can also be exacerbated by these crack systems.

4.2 Elevated Temperatures in Landfills

Leachate, gas, and heat are the three most common byproducts of organic waste decomposition in landfills. Landfill monitoring has shown that temperatures in municipal solid waste (MSW) landfills are usually within the mesophilic range of 38 to 54 °C [269]. As a result, most research on landfills, e.g., desiccation of geosynthetic clay liners and cover systems, service life of geomembranes, thermal-chemical-biological modeling, waste mechanics and shear strength, contaminant transport, and in situ monitoring, are focused primarily on temperatures below 65 °C. Recent landfill case studies indicate that extremely high temperatures (above 100 °C) can develop and negatively impact the behavior and performance of waste containment systems. This section provides a summary of current research in elevated temperature landfill engineering and identifies pressing challenges for future research in thermal geotechnics.

Elevated temperatures have been documented in MSW landfills, construction demolition debris landfills, industrial waste fills, and sanitary dumps. Several factors can lead to elevated landfill temperatures (i.e., exceeding 65 °C), including aerobic decomposition, partially extinguished surface fires, exothermic chemical reactions, spontaneous combustion, and smoldering/pyrolysis. For example, the amphoteric reaction of aluminum dross with water produces hydrogen gas and heat [45]. Observed temperatures of MSW landfills undergoing aluminum reactions range from 88 to 110 °C [128, 130, 233]. However, a more common mechanism causing elevated temperatures is the introduction of ambient air into a landfill during gas collection and control operations, thus increasing waste temperatures to 80 °C. The introduction of oxygen in the waste mass and accumulation of heat via aerobic biodegradation or another exothermic process, provides the necessary conditions to initiate and sustain subsurface smoldering of MSW [156]. Smoldering processes have been documented to persist within a solid waste landfill between 100 and 120 °C [85]. In other cases, smoldering temperatures observed in MSW landfills have ranged from 200 to 300 °C and as high as 700 °C [205].

Techniques, such as gas wellhead monitoring, geophysical methods, infrared imagery, and surface elevations, are used to detect elevated temperatures [156]. Jafari et al. [131, 132] shows the initiation and expansion of elevated temperature results in a sequence of indicators that delineates the location, boundary, and movement. These indicators follow the systematic progression: (1) changes in landfill gas composition (decreasing ratio of CH_4 to CO_2 and elevated carbon monoxide and hydrogen levels); (2) increased odors; (3) elevated waste and gas temperatures, e.g., wellhead temperatures greater than 55–90 °C; (4) elevated gas and leachate pressures that cause leachate outbreaks; (5) increased leachate volume and migration; (6) possible slope

movement; and (7) unusual and rapid settlement. Although the global behavior and indicators of elevated temperature events have been defined, fundamental research questions relating to thermal geotechnics remain. The pressing challenges are developing numerical models that can capture the progression of indicators (specifically, landfill slope instability and settlement), evaluating the efficacy of heat extraction for renewable energy and containment of elevated temperatures, and development and performance of novel engineered barriers.

Slope instability and movement have occurred at landfills with elevated temperatures, gas, and leachate pressures [108, 127, 233]. The failure described by Stark et al. [233] resulted in over 6 m of displacement and waste being located outside of the permitted landfill boundary. In general, slope movement is preceded and accompanied by forceful gas and leachate outbreaks. Mechanisms for slope instability usually include elevated gas pressures, perched leachate surfaces, and/or reduced MSW shear strength [232]. For example, the interconnecting plastics and other reinforcing materials that contribute to the high shear strength of fresh MSW are mostly consumed, degraded, burnt, and/or decomposed at elevated temperatures.

The energy balance inside a landfill subjected to elevated temperatures, slope movement, and settlement is shown in Fig. 10. In this schematic, heat is generated by three processes: (1) aerobic decomposition caused by air intrusion into the waste mass from cracks in the soil cover or damaged wellheads; (2) anaerobic decomposition of organic matter by methanogenesis; and (3) exothermic reactions of MSW. Several mechanisms are shown to result in heat loss in the system, but the gas collection and leachate removal systems are likely the most influential. The schematic also shows the possible thermal energy transfer due to elevated temperatures. Heat generated in the exothermic reaction front can induce a thermal gradient inside the landfill. This heat also drives moisture away from MSW (see blue arrows in gas and heating fronts in Fig. 10) and thermally degrades the waste via pyrolysis/smoldering, which produces large quantities of gas (CO_2, H_2, and CO) and results in excessive and rapid settlement beneath the exothermic reaction front and residual material zone. Due to the elevated leachate and gas pressures, the propagation of exothermic processes is leading to slope instability and settlement via heat transfer (conduction, phase change, convection), movement of leachate and gas from hotter regions to cooler areas near the side slopes and surface, and changes in biological and chemical nature of waste.

Some studies, such as Nastev et al. [179] and El-Fadel et al. [82], have developed numerical models to capture generation and transport of gas and heat in landfills. To date, numerical models that capture the heat and gas generation from exothermic reactions, settlement and slope movement, fluid (gas, steam, leachate) flow, and gas-leachate contaminant transport at elevated temperatures has not been investigated, and hence is a pressing challenge for future research. Another challenge is measuring the properties of waste required for input in the numerical models. These inputs include thermal, compressibility and permeability relationships, shear strength, gas production potential, and leachate generation.

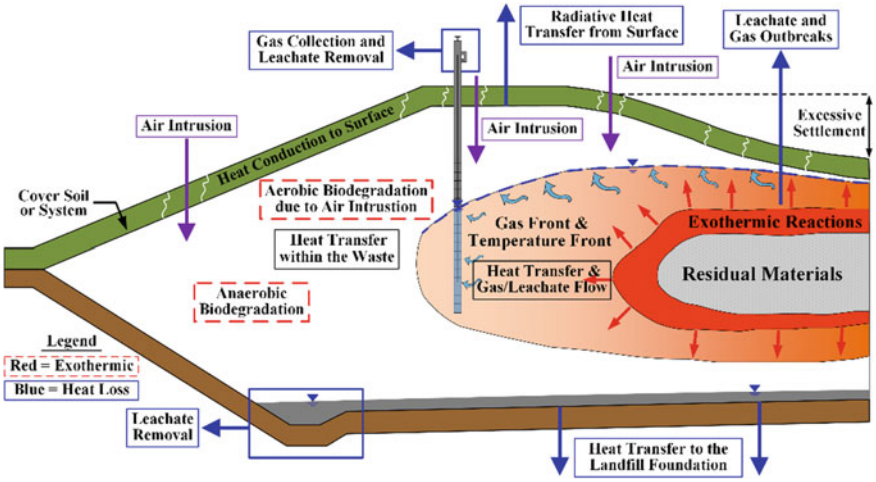

Fig. 10 Schematic of an elevated temperature landfill showing heat transfer mechanisms (from [131] with permission from Elsevier)

Another challenge is isolating and containing elevated temperatures from normal operating areas. In recent cases, landfill owners, design engineers, and environmental regulators have lacked proven containment alternatives, such as vertical barrier walls, ground source heat pumps, and injection of coolants, to isolate and contain heating events. For example, a U-tube heat exchanger system has been installed at a facility to isolate/contain an elevated temperature event. Future research should investigate the design of ground source heat pumps to extract heat from elevated temperature landfills, which otherwise escapes from the gas collection system, for energy applications [67].

Sustained elevated temperatures can degrade and compromise gas extraction, leachate collection, and barrier systems. For example, Jafari et al. [129] evaluate the time-dependent antioxidant depletion and stress cracking to predict high-density polyethylene (HDPE) geomembrane service life. Using time-temperature history of a liner system, they conclude that HDPE geomembrane service life can decrease from several hundred years to less than a decade. As a result, there is a need to develop novel barrier systems for industrial waste leachates, elevated temperatures, and hazardous air pollutants. In particular, future research on novel barriers should investigate the mechanisms of contaminant migration, changes in mechanical properties, bentonite desiccation, polymer chemistry, and degradation.

5 Conclusions

This chapter summarizes the fundamental issues related to the thermal behavior of saturated and unsaturated soils and rocks that may be encountered in geotechnical engineering applications. A major emphasis of this chapter is on the need to consider coupled multi-physical processes that occur in nonisothermal conditions in soils. Heat transfer and water flow processes in soils are closely coupled with changes in degree of saturation and stress state, which may lead to changes in volume which further alter the properties that govern heat transfer and water flow. Changes in the apparent preconsolidation stress and effective stress in saturated and unsaturated soils may have significant effects on the mechanical response of soils, and the interplay between softening mechanisms associated with heating of soils that lead to reductions in preconsolidation stress with other hardening mechanisms associated with unsaturated soil conditions and mechanical loading that lead to increases in apparent preconsolidation stress need to be carefully considered in future studies. Identifying the underlying mechanisms behind changes in apparent preconsolidation stress with temperature and suction may help better explain thermal volume changes, and may help identify if creep or collapse mechanisms should be used to simulate thermal volume change behavior.

There are also other key issues that have not received significant attention and need collaborative research efforts to solve. These include physical modeling or field observation for model validation, evaluation of cyclic heating and cooling or wetting and drying effects, including consideration of creep phenomena and underlying mechanisms of thermal volume change, evaluation of coupled chemical effects with both flow and mechanical processes, understanding of scale effects, including application of pore scale processes to element scale to hydrological scales, study of climate change phenomena that incorporate soil behavior, identification of appropriate hydrogeological siting of energy storage systems and their effects on efficiency, evaluation of soil/rock behavior under low temperatures and freeze/thaw cycles, and thermal remediation of contaminated soils using elevated temperatures of 35–70 °C associated with geothermal heat exchanger operation (e.g., enhanced soil vapor extraction, enhanced bioremediation with bio-augmentation). Future fundamental challenges may be encountered when including biological and chemical effects in the coupling relationships between heat transfer, water flow, and the mechanical response of soils. Big-risk and big-payoff ideas in thermal energy geotechnics include solving key issues with enhanced geothermal systems, such as thermal shock, drilling costs, sampling and field investigations. Others include mega-landfill issues that may be encountered due to the fewer number of large landfills, environmental problems associated with the recovery of gas hydrates, and issues with CO_2 sequestration such as cap rock integrity, cost limited conditions, and induced seismicity.

Acknowledgements JM would like to acknowledge financial support of this work from NSF grants CMMI-0928159 and CMMI-1054190.

References

1. Abuel-Naga, H.M., Bergado, D.T., Bouazza, A.: Thermally induced volume change and excess pore water pressure of soft Bangkok clay. Eng. Geol. **89**, 144–154 (2007)
2. Abuel-Naga, H.M., Bergado, D.T., Bouazza, A., Pender, M.: Thermomechanical model for saturated clays. Géotechnique **59**(3), 273–278 (2009)
3. Acuña, J., Fossa, M., Monzó, P., Palm, B.: Numerically generated g-functions for ground coupled heat pump applications. Proceedings of the COMSOL Conference, Milan, pp. 1–6 (2012)
4. Adam, D., Markiewicz, R.: Energy from earth-coupled structures, foundations, tunnels and sewers. Géotechnique **59**(3), 229–236 (2009)
5. AghaKouchak, A., Feldman, D., Hoerling, M., Huxman, T., Lund, J.: Recognize anthropogenic drought. Nature **524**(7566), 409–4011 (2015)
6. Akrouch, G., Sánchez, M., Briaud, J.-L.: Thermo-mechanical behavior of energy piles in high plasticity clays. Acta Geotech. **9**, 399–412 (2014)
7. Akrouch, G., Sánchez, M., Briaud, J.L.: An analytical and experimental study on the thermal efficiency of energy piles in unsaturated soils. Comput. Geotech. **7**, 207–220 (2014)
8. Alonso, E.E., Gens, A., Josa, A.: A constitutive model for partially saturated soils. Géotechnique **40**(3), 405–430 (1990)
9. Alsherif, N.A., McCartney, J.S.: Nonisothermal behavior of compacted silt at low degrees of saturation. Géotechnique **65**(9), 703–716 (2015)
10. Alsherif, N., McCartney, J.S.: Yielding of silt at high temperature and suction magnitudes. Geotech. Geol. Eng. **34**(2), 501–514 (2016)
11. Amatya, B.L., Soga, K., Bourne-Webb, P.J., Amis, T., Laloui, L.: Thermo-mechanical behaviour of energy piles. Géotechnique **62**(6), 503–519 (2012)
12. Armstrong, J.E., Frind, E.O., McClellan, R.D.: Nonequilibrium mass transfer between the vapor, aqueous, and soil-phases in unsaturated soils during vapor extraction. Water Resour. Res. **30**, 355–368 (1994)
13. Aversa, S., Evangelista, A.: Thermal expansion of Neapolitan yellow tuff. Rock Mech. Rock Eng. **26**(4), 281–306 (1993)
14. Baladi, J.Y., Ayers, D.L., Schoenhals, R.J.: Transient heat and mass transfer in soils. Int. J. Heat Mass Transf. **24**(3), 449–458 (1981)
15. Baldi, G., Hueckel, T., Peano, A., Pellegrini, R.: Developments in modelling of thermo-hydro-geomechanical behavior of boom clay and clay-based buffer materials. Commission of the European Communities, Nuclear Science and Technology, EUR 13365/1 and EUR 13365/2 (1991)
16. Baldi, G., Hueckel, T., Pelegrini, R.: Thermal volume changes of the mineral-water system in low-porosity clay soils. Can. Geotech. J. **25**, 807–825 (1988)
17. Başer, T., Linkowski, D., McCartney, J.S.: Charging and discharging of soil-borehole thermal energy storage systems in the vadose zone. Proceedings of the 7th International Congress on Environmental Geotechnics: ICEG 2014. Bouazza, A., Yuen, S.T.S., Brown, B. eds. Nov. 10–14. Melbourne. Engineers Australia, pp. 362–369 (2014)
18. Başer, T., Lu, N., McCartney, J.S.: Operational response of a soil-borehole thermal energy storage system. J. Geotech. Geoenviron. Eng. https://doi.org/10.1061/(asce)gt.1943-5606.0001432, 04015097 (2016a)
19. Başer, T., Traore, T., McCartney, J.S.: Physical modeling of coupled heat transfer and water flow in soil-borehole thermal energy storage systems in the vadose zone. In: Geothermal Energy: An Emerging Resource. C.B. Dowling, L.J. Florea, and K. Neumann, eds. GSA Books. Boulder, CO. Special Paper 519, pp. 81–93 (2016b)
20. Başer, T., Dong, Y., Lu, N., McCartney, J.S.: Role of considering non-constant soil thermal parameters in the simulation of geothermal heat storage systems in the vadose zone. Proceedings of ISSMGE 8th AYGEC, Astana, Kazakhstan, pp. 1–6 (2016c)
21. Başer, T., Dong, Y., McCartney, J.S.: Heat content in soil-borehole thermal energy systems in the vadose zone. In: Proceedings of the ICEGT 2016, Kiel, Germany, pp. 1–10 (2016d)

22. Baser, T., McCartney, J.S., Dong, Y., Lu, N.: Evaluation of coupled thermal and hydraulic relationships used in simulation of thermally-induced water flow in unsaturated soils. PanAm UNSAT 2017. Dallas, TX. Nov. 12–15. 10 p (2017)
23. Başer, T., Dong, Y., Moradi, A.M., Lu, N., Smits, K., Ge, S., Tartakovsky, D., McCartney, J.S.: Role of water vapor diffusion and nonequilibrium phase change in geothermal energy storage systems in the vadose zone. J. Geotech. Geoenviron. Eng. https://doi.org/10.1061/(asce)gt.1943-5606.0001910 (2018)
24. Batini, N., Rotta Loria, A.F., Conti, P., Laloui, L.: Energy and geotechnical behaviour of energy piles for different design solutions. Appl. Thermal Eng. **86**, 199–213 (2015)
25. Beier, R.A., Acuña, J., Mogensen, P., Palm, B.: Transient heat transfer in a coaxial borehole heat exchanger. Geothermics **51**, 470–482 (2014)
26. Bénet, J.C., Jouanna, P.: Phenomenological relation of phase change of water in a porous-medium-experimental verification and measurement of the phenomenological coefficient. Int. J. Heat Mass Transf. **25**, 1747–1754 (1982)
27. Bénet, J.C., Lozano, A.L., Cherblanc, F., Cousin, B.: Phase change of water in a hygroscopic porous medium: Phenomenological relation and experimental analysis for water in soil. J. Non-Equilib. Thermodyn. **34**, 133–153 (2009)
28. Bergenstahl, L., Gabrielsson, A., Mulabdic, M.: Changes in soft clay caused by increases in temperature, pp. 1637–1640. XIII ICSMFE. New Delhi, India (1994)
29. Biot, M.A.: General theory of three-dimensional consolidation. J. Appl. Phys. **12**, 155–164 (1941)
30. Bittelli, M., Ventura, F., Campbell, G.S., Snyder, R.L., Gallegati, F., Pisa, P.R.: Coupling of heat, water vapor, and liquid water fluxes to compute evaporation in bare soils. J. Hydrol. **362**, 191–205 (2008)
31. Bixler, N.E. NORIA: A Finite Element Computer Program for Analyzing Water, Vapor, Air and Energy Transport in Porous Media. SAND84-2057, Sandia National Laboratories, Albuquerque, NM (1985)
32. Booker, J.R., Savvidou, C.: Consolidation around a spherical heat source. Int. J. Solids Struct. **20**(11/12), 1079–1090 (1984)
33. Booker, J.R., Savvidou, C.: Consolidation around a point heat source. Int. J. Numer. Anal. Meth. Geomech. **9**(2), 173–184 (1985)
34. Bouazza, A., Singh, R.M., Wang, B., Barry-Macaulay, D., Haberfield, C., Chapman, G., Baycan, S., Carden, Y.: Harnessing on site renewable energy through pile foundations. Aust. Geomech. J. **46**(4), 79–90 (2011)
35. Boudali, M., Leroueil, S., Srinivasa Murthy, B.R.: Viscous behavior of natural clays. In: Proceedings of the 13th International Conference on Soil Mechanics and Foundation Engineering, New Delhi, India (1994)
36. Bourne-Webb, P., Amatya, B., Soga, K., Amis, T., Davidson, C., Payne, P.: Energy pile test at Lambeth College, London: Geotechnical and thermodynamic aspects of pile response to heat cycles. Géotechnique **59**(3), 237–248 (2009)
37. Brandl, H.: Energy foundations and other thermo-active ground structures. Géotechnique **56**(2), 81–122 (2006)
38. Brandon, T.L., Mitchell, J.K.: Factors influencing thermal resistivity of sands. J. Geotech. Environ. Eng. **115**(12), 1683–1698 (1989)
39. Brandon, T.L., Mitchell, J.K., Cameron, J.T.: Thermal instability in buried cable backfills. J. Geotech. Eng. **115**(1), 38–55 (1989)
40. Britto, A.M., Savvidou, C., Maddocks, D.V., Gunn, M.J., Booker, J.R.: Numerical and centrifuge modelling of coupled heat flow and consolidation around hot cylinders buried in clay. Géotechnique **39**(1), 13–25 (1989)
41. Brooks, B.A., Bawden, G. Manjunath, D., Werner, C. Knowles, N., Foster, J., Dudas, J., Cayan, D.R.: Contemporaneous subsidence and levee overtopping potential, Sacramento-San Joaquin Delta. San Francisco Estuary Watershed Sci. **10**(1) (2012)
42. Burghignoli, A., Desideri, A., Miliziano, S.: A laboratory study on the thermomechanical behaviour of clayey soils. Can. Geotech. J. **37**, 764–780 (2000)

43. Committee on Adaptation to a Changing Climate (CACC).: Adapting Infrastructure and Civil Engineering Practice to a Changing Climate, ASCE, Reston, VA (2015)
44. Cahill, A.T., Parlange, M.B.: On water vapor transport in field soils. Water Resour. Res. **34**, 731–739 (1998)
45. Calder, G.V., Stark, T.D.: Aluminum reactions and problems in municipal solid waste landfills. J. Hazard. Toxic Radioact. Waste **15**(1), 1–8 (2010)
46. Campanella, R.G., Mitchell, J.K.: Influence of temperature variations on soil behavior. ASCE J. Soil Mech. Found. Div. **94**(SM3), 709–734 (1968)
47. Campbell, G.S.: Soil Physics with BASIC. Elsevier, New York (1985)
48. Campbell, G.S., Jungbauer, J.D., Bidlake, W.R., Hungerford, R.D.: Predicting the effect of temperature on soil thermal conductivity. Soil Sci. **158**, 307–313 (1994)
49. Cass, A., Campbell, G.S., Jones, T.L.: Enhancement of thermal water vapor diffusion in soil. Soil Sci. Soc. Am. **48**(1), 25–32 (1984)
50. Cary, J.W., Taylor, S.A.: Thermally driven liquid and vapor phase transfer of water and energy in soil. Soil Sci. Soc. Am. Proc. **26**, 417–420 (1962)
51. Cary, J.W.: Water flux in moist soil: Thermal versus suction gradients. Soil Sci. **100**(3), 168–175 (1965)
52. Catolico, N., Ge, S., McCartney, J.S.: Numerical modeling of a soil-borehole thermal energy storage system. Vadose Zone Journal. **15**(1), 1–17 (2016). https://doi.org/10.2136/vzj2015.05.0078
53. Cekerevac, C., Laloui, L.: Experimental study of thermal effects on the mechanical behavior of a clay. Int. J. Numer. Anal. Meth. Geomech. **28**, 209–228 (2004)
54. Chammari, A., Naon, B., Cherblanc, F., Cousin, B., Bénet, J.C.: Interpreting the drying kinetics of a soil using a macroscopic thermodynamic nonequilibrium of water between the liquid and vapor phase. Drying Technol. **26**, 836–843 (2008)
55. Chabora, E.R., Benson, S.M.: Brine displacement and leakage detection using pressure measurements in aquifers overlying CO2 storage reservoirs. Energy Procedia **1**, 2405–2412 (2009)
56. Chapuis, S., Bernier, M.: Seasonal storage of solar energy in borehole heat exchangers. In: Proceedings of the IBPSA Conference on Building Simulations, Glasgow, Scotland, pp. 599–606 (2009)
57. Chen, D., McCartney, J.S.: Parameters for load transfer analysis of energy piles in uniform nonplastic soils. ASCE Int. J. Geomech. **17**(7), 04016159 (2017)
58. Cheng, L., Phillips, T.J., AghaKouchak, A.: Non-stationary return levels of CMIP5 multi-model temperature extremes. Clim. Dyn. **44**(11–12), 2947–2963 (2015)
59. Cherblanc, F., Lozano, A.L., Ouedraogo, F., Bénet, J.C.: Non-equilibrium liquid–gas phase change in hygroscopic porous media. In: European Drying Conference, Biarritz, France. 1–2 (2007)
60. Ciriello, V., Bottarelli, M., Di Federico, V., Tartakovsky, D.M.: Temperature fields induced by geothermal devices. Energy **93**(2), 1896–1903 (2015)
61. Claesson, J. and Hellström, G.: Model studies of duct storage systems. In: Millhone, J.P., Willis, E.H. (eds.) New energy conservation technologies and their commercialization. Springer, Berlin, pp. 762–778 (1981)
62. Cleall, P.J., Seetharam, S.C., Thomas, H.R.: Inclusion of some aspects of chemical behavior of unsaturated soil in thermo/hydro/chemical/mechanical models. I: model development. ASCE J. Eng. Mech. **133**(3):338–347 (2007)
63. Cleall, P.J., Singh, R.M., Thomas, H.R.: Non-isothermal moisture movement in unsaturated kaolin: An experimental and theoretical investigation. Geotech. Test. J. **34**(5), 1–11 (2011)
64. Coe, J.A., Godt, J.W.: Review of approaches for assessing the impact of climate change on landslide hazards. In: Proceedings of the 11th International and 2nd North American Symposium on Landslides and Engineered Slopes, Banff, Canada, pp. 371–377 (2012)
65. Coccia, C.J.R., McCartney, J.S.: A thermo-hydro-mechanical true triaxial cell for evaluation of the impact of anisotropy on thermally-induced volume changes in soils. ASTM Geotech. Test. J. **35**(2), 227–237 (2012)

66. Coccia, C.J.R., McCartney, J.S.: Impact of heat exchange on the thermo-hydro-mechanical response of reinforced embankments. Proceedings of Geo Congress 2013. ASCE. San Diego, CA. Mar. 3–5. pp. 343-352 (2013)
67. Coccia, C.J., Gupta, R., Morris, J., McCartney, J.S.: Municipal solid waste landfills as geothermal heat resources. Renew. Sustain. Energy Rev. **19**, 463–474 (2013)
68. Coccia, C.J.R., McCartney, J.S.: Thermal volume change of poorly draining soils I: Critical assessment of volume change mechanisms. Comput. Geotech. **80**(Dec.), 26–40 (2016a)
69. Coccia, C.J.R., McCartney, J.S.: Thermal volume change of poorly draining soils II: Constitutive modelling. Comput. Geotech. **80**(Dec.), 16–25 (2016b)
70. Coccia, C.J.R., McCartney, J.S.: High-pressure thermal triaxial cell for evaluation of the impact of temperature on soil volume change mechanisms. ASTM Geotech. Test. J. 1–18. https://doi.org/10.1520/gtj20150114 (2016c)
71. Côté, J., Konrad, J.-M.: A generalized thermal conductivity model for soils and construction materials. Can. Geotech. J. **42**, 443–458 (2005)
72. Conant, R., Ryan, M., Agren, G., Birge, H., Davidson, E., Eliasson, P., Evans, S., Frey, S., Giardina, C., Hopkins, F., Hyvonen, R., Kirschbaum, M., Lavallee, J., Leifeld, J., Parton, W., Steinweg, M., Wallenstein, M., Martin, W., Bradford, M.: Temperature and soil organic matter decomposition rates—synthesis of current knowledge and a way forward. Global Chang. Biology. **17**, 3392–3404 (2011)
73. Claesson, J., Hellström, G.: Model studies of duct storage systems. In: Millhone, J.P., Willis, E.H. (eds.) New Energy Conservation Technologies and their Commercialization. Springer, Berlin, pp. 763–779 (1982)
74. Cui, Y.J., Sultan, N., Delage, P.: A thermomechanical model for clays. Can. Geotech. J. **37**(3), 607–620 (2000)
75. Cui, Y.-J., Le, T.-T., Tang, A.-M., Delage, P., Li, X.-L.: Investigating the time-dependent behaviour of Boom clay under thermo-mechanical loading. Géotechnique. **59**(4), 319–329 (2009)
76. Damberg, L., AghaKouchak, A.: Global trends and patterns of drought from space. Theoret. Appl. Climatol. **117**(3–4), 441–448 (2014)
77. Delage, P., Sultan, N., Cui, Y.J.: On the thermal consolidation of Boom clay. Can. Geotech. J. **37**, 343–354 (2000)
78. Del Olmo, C., Fioravante, V., Gera, F., Hueckel, T., Mayor, J.C., Pellegrini, R.: Thermomechanical properties of deep argillaceous formations. Eng. Geol. **41**, 87–101 (1996)
79. de Vries, D.A.: Simultaneous transfer of heat and moisture in porous media. Eos Trans. Am. Geophys. Union. **39**, 909–916 (1958)
80. Dong, Y., McCartney, J.S., Lu, N.: Critical review of thermal conductivity models for unsaturated soils. Geotech. Geol. Eng. **33**(2), 207–221 (2015)
81. Ebigbo, A.: Thermal effects of carbon dioxide sequestration in the subsurface. Doctoral dissertation, Institut für Wasserbau, Universität Stuttgart, Germany (2005)
82. El-Fadel, M., Findikakis, A.N., Leckie, J.O.: Numerical modelling of generation and transport of gas and heat in sanitary landfills: II model application. Waste Manage. Res. **14**, 537–551 (1996)
83. Eriksson, L.G.: Temperature effects on consolidation properties of sulphide clays. In: Proceedings of 12th International Conference on Soil Mechanics and Foundation Engineering, Rio de Janeiro, Brazil, 4 p (1989)
84. Eskilson, P. Thermal Analysis of Heat Extraction Boreholes. Dept. of Mathematical Physics, Lund Univ. Lund, Sweden (1987)
85. Ettala, M., Rahkonen, P., Rossi, E., Mangs, J., Keski-Rahkonen, O.: Landfill fires in Finland. Waste Manage. Res. **14**, 377–384 (1996)
86. Ewen, J.: Thermal instability in gently heated unsaturated sand. Int. J. Heat Mass Transf. **31**(8), 1707–1710 (1988)
87. Ewen, J., Thomas, H.R.: Heating unsaturated medium sand. Géotechnique **39**(3), 455–470 (1989)

88. Farouki, O.T.: Thermal Properties of Soils. Cold Reg. Sci. Eng. CRREL, Monogr. **81–1**, 136 (1981)
89. Farr, T. G., Jones, C., Liu, Z. Progress Report: Subsidence in the Central Valley, California, prepared for California Department of Water Resources (DWR), by researchers at NASA's Jet Propulsion Laboratory, Pasadena, California, Aug. 2015 (2015)
90. Gariano, S.L., Guzzetti, F.: Landslides in a changing climate. Earth Sci. Rev. **162**, 227–252 (2016)
91. Gao, J., Zhang, X., Liu, J., Li, K., Yang, J.: Numerical and experimental assessment of thermal performance of vertical energy piles: an application. Appl. Energy **85**(10), 901–910 (2008)
92. Gehlin, S.: Thermal Response Test: Method Development and Evaluation. Ph.D. Thesis. Lulea University of Technology (2002)
93. Gens A.: The role of geotechnical engineering for nuclear energy utilisation. In: Proceedings of the XIII European Conference of Soil Mechanics and Geotechnical Engineering, vol. 3, Prague, pp. 25–67 (2003)
94. Gens, A.: Soil-environment interactions in geotechnical engineering. Géotechnique **60**(1), 3–74 (2010)
95. Gens, A., Sánchez, M., Sheng, D.: On constitutive modelling of unsaturated soils. Acta Geotech. **1**(3), 137–147 (2006)
96. Gens, A., Sánchez, M.Do.N, Guimaraes, O., Alonso, E.E., Lloret, A., Olivella, S., Villar, M.V., Huertas, F.: A full-scale in situ heating test for high-level nuclear waste disposal: Observations, analysis and interpretation. Géotechnique **59**(4), 377–399 (2009)
97. Gens, A., Vallejan, B., Sánchez, M., Imbert, C., Villar, M.V., Van Geet, M.: Hydromechanical behavior of a heterogeneous compacted soil: experimental observations and modeling. Géotechnique **61**(5), 367–386 (2011)
98. Ghaaowd, I., Takai, A., Katsumi, T., McCartney, J.S.: Pore water pressure prediction for undrained heating of soils. Environ. Geotech. **4**(2), 70–78 (2016)
99. Ghabezloo, S., Sulem, J.: Stress dependent thermal pressurization of a fluid-saturated rock. Rock Mech. Rock Eng. J. **42**, 1–24 (2009)
100. Goode, J.C., III, McCartney, J.S.: Centrifuge modeling of boundary restraint effects in energy foundations. J. Geotech. Geoenviron. Eng. **141**(8), 04015034-1–04015034-13. https://doi.org/10.1061/(asce)gt.1943-5606.0001333 (2015)
101. Graham, J., Tanaka, N., Crilly, T., Alfaro, M.: Modified cam-clay modelling of temperature effects in clays. Can. Geotech. J. **38**(3), 608–621 (2001)
102. Grant, S., Salehzadeh, A.: Calculations of temperature effects on wetting coefficients of porous solids and their capillary pressure functions. W. Res. Res. **32**, 261–279 (1996)
103. Guimarães, L., Gens, A., Olivella, S.: Coupled thermo-hydro-mechanical and chemical analysis of expansive clay subjected to heating and hydration. Transp. Porous Media **66**(3), 341–372 (2007)
104. Guimarães, L., Gens, A., Sánchez, M., Olivella, S.: A chemo-mechanical constitutive model accounting for cation exchange in expansive clays. Géotechnique **63**(3), 221–234 (2013)
105. Gupta, S., Helmig, R., Wohlmuth, B.: Non-isothermal, multi-phase, multicomponent flows through deformable methane hydrate reservoirs. Comput. Geosci. http://dx.doi.org/10.1007/s10596-015-9520-9 (2015)
106. Gurr, C.G., Marshall, T.J., Hutton, J.T.: Movement of water in soil due to a temperature gradient. Soil Sci. **74**(5), 335–345 (1952)
107. Hamada, Y., Saitoh, H., Nakamura, M., Kubota, H., Ochifuji, K.: Field performance of an energy pile system for space heating. Energy Build. **39**(5), 517–524 (2007)
108. Hendron, D.M., Fernandez G., Prommer P.J., Giroud J.P., Orozco L.F.: Investigation of the cause of the 27 September 1997 slope failure at the Doña Juana landfill. In: Proceedings of the Sardinia '99—7th International waste management landfill symposium, Cagliari, Italy (1999)
109. Hillel, D.: Fundamental of Soil Physics. Academic, San Diego, CA (1980)
110. Ho, C.K., Webb, S.W.: Review of porous media enhanced vapor-phase diffusion mechanisms, models, and data—Does enhanced vapor-phase diffusion exist? J. Porous Media **1**, 71–92 (1998)

111. Houston, S.L., Houston, W.N., Williams, N.D.: Thermo-mechanical behavior of seafloor sediments. J. Geotech. Eng. ASCE. **111**(12), 1249–1263 (1985)
112. Hu, L.B., Péron, H., Hueckel, T., Laloui, L.: Desiccation shrinkage of non-clayey soils: multiphysics mechanisms and a microstructural model. Int. J. Numer. Anal. Meth. Geomech. **37**, 1761–1781 (2013)
113. Hu, M.M., Hueckel,: Environmentally enhanced crack propagation in a chemically degrading isotropic shale. Geotechnique. **63**(4), 313–321. (2013)
114. Hueckel, T., Borsetto, M., Peano, A.: Thermoelastoplastic-hydraulic response of clays subjected to nuclear waste heat. In: Lewis, R.W., Hinton, E., Bettess, P., Schrefler, B.A. (eds.)Numerical Methods in Transient and Coupled Problems, pp. 213–235 (1987)
115. Hueckel, T., Baldi, M.: Thermoplasticity of saturated clays: experimental constitutive study. J. Geotech. Eng. **116**(12), 1778–1796 (1990)
116. Hueckel, T., Borsetto, M.: Thermoplasticity of saturated soils and shales: constitutive equations. J. Geotech. Eng. **116**(12), 1765–1777 (1990)
117. Hueckel, T., Peano, A.: Some geotechnical aspects of radioactive waste isolation in continental clays. Comput. Geotech. **3**, 157–182 (1987)
118. Hueckel, T., Pellegrini, R., Del Omo, C.: A constitutive study of thermo-elasto-plasticity of deep carbonatic clays. Int. J. Numer. Anal. Meth. Geomech. **22**(7), 549–574 (1998)
119. Hueckel, T., Pellegrini, R.: Thermoplastic modeling of undrained failure of saturated clay due to heating. Soils Found. **31**(3), 1–16 (1991)
120. Hueckel, T., Pellegrini, R.: Effective stress and water pressure in saturated clays during heating-cooling cycles. Can. Geotech. J. **29**(6), 1095–1102 (1992)
121. Hueckel, T., Francois, B., Laloui, L.: Explaining thermal failure in saturated clays. Géotechnique **59**(3), 197–212 (2009)
122. Hueckel, T., EL Mielniczuk, B., Youssoufi, M.S., Hu, L.B., Laloui, L.: A three-scale cracking criterion for drying soils. Acta Geotech. **62**(5), 1049–1059 (2014)
123. Hueckel, T., Peano, A., Pellegrini, R.: A constitutive law for thermo-plastic behavior of rocks: an analogy with clays. Surv. Geophys. **15**(5), 643–671 (1994)
124. Ingersoll, L.R., Plass, H.J.: Theory of the ground pipe heat source for the heat pump. Heating, Piping Air Conditioning. **20**(7), 119–122 (1948)
125. Ingersoll, L.R., Zobel, O.J., Ingersoll, A.C.: Heat Conduction with Engineering, Geological, and Other Applications. University of Wisconsin Press. Rev. Ed., p. 325 (1954)
126. IPCC. *Climate Change 2013: The Physical Science Basis*. Contribution of Working Group I to the Fifth Assessment Report of the Intergovernmental Panel on Climate Change Cambridge University Press, Cambridge, United Kingdom and New York, NY, USA, 1535 (2013)
127. Jafari, N.H., Stark, T.D., Merry, S.M.: The 10 July 2000 Payatas landfill slope failure. Int. J. Geoeng. Case Hist. **2**(3), 208–228 (2013)
128. Jafari, N.H., Stark, T.D., Roper, R.: Classification and reactivity of aluminum production waste. J. Hazard. Toxic Radioact. Waste **18**(4), 1–11 (2014)
129. Jafari, N., Stark, T.D., Rowe, K.: Service life of HDPE geomembranes subjected to elevated temperatures. J. Hazard. Toxic Radioact. Waste **18**(1), 16–26 (2014)
130. Jafari, N.H. Elevated Temperatures in Waste Containment Systems. Ph.D. Dissertation, University of Illinois at Urbana-Champaign (2015)
131. Jafari, N.H., Stark, T.D., Thalhamer, T.: Spatial and temporal characteristics of elevated temperatures in municipal solid waste landfills. Waste Manag. **59**, 286–301 (2017)
132. Jafari, N.H., Stark, T.D., Thalhamer, T.: Progression of elevated temperatures in municipal solid waste landfills. J. Geotech. Geoenviron. Eng. **143**(8). https://doi.org/10.1061/(ASCE)GT.1943-5606.0001683 (2017b)
133. Jasim, F. H., Vahedifard, F., Ragno, E., AghaKouchak, A., Ellithy, G.: Effects of climate change on fragility curves of earthen levees subjected to extreme precipitations. In: Proceedings of the Geo-Risk 2017 Geotechnical Risk Assessment and Management, GSP, vol. 285, pp. 498–507 (2017)
134. Johansen, O.: Thermal Conductivity of Soils. Ph.D. Thesis, University of Trondheim (1975)

135. Kavanaugh, S.P.: A design method for hybrid ground-source heat pumps. ASHRAE Transac. **104**(2), 691–698. (1975) (1998)
136. Khalili, N., Khabbaz, M.H.: A unique relationship for c for the determination of the shear strength of unsaturated soils. Géotechnique **48**(5), 681–687 (1998)
137. Khalili, N., Geiser, F., Blight, G.E.: Effective stress in unsaturated soils, a review with new evidence. Int. J. Geomech. **4**(2), 115–126 (2004)
138. Knellwolf, C., Peron, H., Laloui, L.: Geotechnical analyses of heat exchanger piles. J. Geotech. Geoenviron. Eng. **137**(10), 890–902 (2011)
139. Laloui, L.: Thermo-mechanical behavior of soils. RFGC (French Revue of Civil Engineering). **5**, 809–843 (2001)
140. Laloui, L., Cekerevac, C.: Thermo-plasticity of clays: an isotropic yield mechanism. Comput. Geotech. **30**(8), 649–660 (2003)
141. Laloui, L., Nuth, M., Vulliet, L.: Experimental and numerical investigations of the behavior of a heat exchanger pile. Int. J. Numer. Anal. Meth. Geomech. **30**, 763–781 (2006)
142. Laloui, L., Cekerevac, C.: Non-isothermal plasticity model for cyclic behavior of soils. Int. J. Numer. Anal. Meth. Geomech. **32**, 437–460 (2008)
143. Laloui, L., Francois, B.: ACMEG-T: A soil thermo-plasticity model. J. Eng. Mech. **135**(9), 932–944 (2009)
144. Laloui, L., Moderassi, H.: Non-isothermal plasticity model for cyclic behavior of soils. Int. J. Numer. Anal. Meth. Geomech. **32**(5), 437–460 (1997)
145. Lamarche, L., Beauchamp, B.: A new contribution to the finite line-source model for geothermal boreholes. Energy Build. **39**(2), 188–198 (2007)
146. Lide, D.R.: Handbook of Chemistry and Physics. CRC Press, Boca Raton, FL (2001)
147. Likos, W.J.: Modeling thermal conductivity dryout curves from soil-water characteristic curves". J. Geotech. Geoenviron. Eng. **140**(5), 04013056 (2014a)
148. Likos, W.J.: Pore-scale model for thermal conductivity of unsaturated sand. J. Geotech. Geoenviron. Eng. 1–14 (2014b)
149. Likos, W.J., Lu, N.: Filter paper column for measuring transient suction profiles in expansive clay. Transp. Res. Rec. **1821**, 83–89 (2003)
150. Lu, N. Generalized soil water retention equation for adsorption and capillarity. J. Geotech. Geoenviron. Eng.. 04016051-1-15 (2016)
151. Lu, N., Likos, W.J.: Suction stress characteristic curve for unsaturated soil. J. Geotech. Geoenviron. Eng. **132**(2), 131–142 (2006)
152. Lu, N., Godt, J.W., Wu, D.T.: A closed-form equation for effective stress in unsaturated soil. Water Resour. Res. **46**(5), W05515 (2010)
153. Lu, N., Dong, Y.: A closed form equation for thermal conductivity of unsaturated soils at room temperature. J. Geotech. Geoenviron. Eng. **141**(6), 04015016 (2015)
154. Lu, S., Ren, T., Gong, Y., Horton, R.: An improved model for predicting soil thermal conductivity from water content at room temperature. Soil Sci. Soc. Am. J. **71**(1), 8–14 (2007)
155. Luikov, A.V.: Heat and Mass Transfer in Capillary Porous Bodies, Pergamon Press. Oxford, U.K., 523 p (1966)
156. Martin, J.W., Stark, T.D., Thalhamer, T., Gerbasi-Graf, G.T., Gortner, R.E.: Detection of aluminum waste reactions and associated waste fires. J. Hazard. Toxic Radioact. Waste **17**(3), 164–174 (2013)
157. Mahajerani, M., Delage, P., Sulem, J., Monfared, M., Tang, A.M., Gatmiri, B.: A laboratory investigation of thermally induced pore pressures in the Callovo-Oxfordian Claystone. Int. J. Rock Mech. Min. Sci. **52**, 112–121 (2012). https://doi.org/10.1016/j.ijrmms.2012.02.012
158. Mazdiyasni, O., AghaKouchak, A.: Substantial Increase in Concurrent Droughts and Heatwaves in the United States. Proc. Natl. Acad. Sci. **112**(37), 11484–11489 (2015)
159. McCartney, J.S., Ge, S., Reed, A., Lu, N., Smits, K.: Soil-borehole thermal energy storage systems for district heating. Proceedings of the European Geothermal Congress 2013, European Geothermal Energy Council, Brussels, Belgium, pp. 1–10 (2013)
160. McCartney, J.S., Başer, T., Zhan, N., Lu, N., Ge, S., Smits, K.: Storage of solar thermal energy in borehole thermal energy storage systems. IGSHPA Technical Conference and Expo. Denver, CO. Mar. 14–17, pp. 1–8 (2017)

161. McCartney, J.S., Baser, T.: Role of coupled processes in thermal energy storage in the vadose zone. Second International Symposium on Coupled Phenomena in Environmental Geotechnics (CPEG2). Leeds, UK. Sep. 5–6, pp. 1–6 (2017)
162. McCartney, J.S., Murphy, K.D.: Investigation of potential dragdown/uplift effects on energy piles. Geomech. Energy Environ. **10**(June), 21–28. https://doi.org/10.1016/j.gete.2017.03.001 (2017)
163. McCartney, J.S., Sánchez, M., Tomac, I.: Energy geotechnics: advances in subsurface energy recovery, storage, and exchange. Comput. Geotech. **75**(May), 244–256 (2016). https://doi.org/10.1016/j.compgeo.2016.01.002
164. McTigue, D.F.: Thermoelastic response of fluid-saturated porous rock. J. Geophys. Res. **91**(B9), 9533–9542 (1986)
165. Melillo, J.M., Richmond, T.C., and Yohe, G.W., Eds. Climate Change Impacts in the United States: The Third National Climate Assessment. U.S. Global Change Research Program, p. 841 (2014)
166. Millington, R.J., Quirk, J.M.: Permeability of porous solids. Trans. Faraday Soc. **57**, 1200–1207 (1961)
167. Milly, P.C.D.: Moisture and heat-transport in hysteretic, inhomogeneous porous media: a matric head-based formulation and a numerical model. Water Resour. Res. **18**, 489–498 (1982). https://doi.org/10.1029/WR018i003p00489
168. Mimouni, T., Laloui, L.: Towards a secure basis for the design of geothermal piles. Acta Geotech. **9**(3), 355–366 (2014)
169. Monteith, J.L., Unsworth, M.H.: Principles of Environmental Physics. Routledge Chapman and Hall, New York, NY (1990)
170. Moradi, A.M., Smits, K., Massey, J., Cihan, A., McCartney, J.S.: Impact of coupled heat transfer and water flow on soil borehole thermal energy storage (SBTES) systems: experimental and modeling investigation. Geothermics. **57**(September), 56–72 (2015)
171. Moradi, A.M., Smits, K., Lu, N., McCartney, J.S.: 3-D experimental and numerical investigation of heat transfer in unsaturated soil with an application to soil borehole thermal energy storage (SBTES) systems. Vadose Zone J. 1–17. https://doi.org/10.2136/vzj2016.03.0027 (2016)
172. Mortezaei, K., Vahedifard, F.: Multi-scale simulation of thermal pressurization of fault fluid under CO_2 injection for storage and utilization purposes. Int. J. Rock Mech. Min. Sci. **98**, 111–120 (2017)
173. Mount, J., Twiss, R.: Subsidence, sea level rise, seismicity in the Sacramento-San Joaquin Delta. San Francisco Estuary Watershed Sci. **3**(1). http://repositories.cdlib.org/jmie/sfews/vol3/iss1/art5 (2005)
174. Mualem, Y.: Hysteretical models for prediction of the hydraulic conductivity of unsaturated porous media. Water Resour. Res. **12**(6), 1248–1254 (1976)
175. Mun, W., McCartney, J.S.: Constitutive model for the drained compression of unsaturated clay to high stresses. ASCE J. Geotech. Geoenviron. Eng. 04017014-11-11. https://doi.org/10.1061/(asce)gt.1943-5606.0001662 (2016)
176. Murphy, K.D., McCartney, J.S., Henry, K.S.: Evaluation of thermo-mechanical and thermal behavior of full-scale energy foundations. Acta Geotech. **10**(2), 179–195 (2015)
177. Nassar, I. N., Horton, R.: Water transport in unsaturated non-isothermal salty soil. 1. Experimental results. Soil Sci. Soc. Am. J. **53**, 1323–1329 (1989)
178. Nassar, I.N., Horton, R., Globus, A.M.: Simultaneous transfer of heat, water, and solute in porous-media. II. Experiment and analysis. Soil Sci. Soc. Am. J. **56**, 1357–1365 (1992)
179. Nastev, M., Therrien, R., Lefebvre, R., Gelinas, P.: Gas Production and migration in landfills and geological materials. J. Contam. Hydrol. **52**, 187–211 (2001)
180. Ng, C.W.W., Mu, Q.Y., Zhou, C.: Effects of soil structure on the shear behavior of an unsaturated loess at different suctions and temperatures. Can. Geotech. J. **54**(2), 270–279 (2017)
181. Nordell, B., Hellström, G.: High temperature solar heated seasonal storage system for low temperature heating of buildings. Appl. Energy **69**(6), 511–523 (2000)
182. Nuth, M., Laloui, L.: Advances in modelling hysteretic water retention curve in deformable soils. Comput. Geotech. **35**(6), 835–844 (2008)

183. Olgun, C.G., McCartney, J.S.: Long-term performance of heat exchanger pile groups. Acta Geotech. **10**(5), 553–569 (2014)
184. Olgun, C.G., Ozudogru, T.Y., Abdelaziz, S.L., Senol, A.: Outcomes from the international workshop on thermoactive geotechnical systems for near-surface geothermal energy: from research to practice. J. Deep Found. Inst. **8**(2), 58–72 (2014)
185. Olivella, S., Gens, A., Carrera, J., Alonso, E.E.: Numerical formulation for a simulator (CODE-BRIGHT) for the coupled analysis of saline media. Eng. Comput. **13**(7), 87–112 (1996)
186. Ozudogru, T.Y., Ghasemi-Fare, O., Olgun, C.G., Basu, P.: Numerical modeling of vertical geothermal heat exchangers using finite difference and finite element techniques. Geotech. Geol. Eng. **33**, 291–306 (2015)
187. Paaswell, R.E.: Temperature effects on clay soil consolidation. J. Soil Mech. Found. Eng. Div. **93**(SM3), 9–22 (1967)
188. Pandey, R.N., Srivastava, S.K., Mikhailov, M.D.: Solutions of Luikov equations of heat and mass transfer in capillary porous bodies through matrix calculus: a new approach. Int. J. Heat Mass Transf. **42**(14), 2649–2660 (1999)
189. Pasha, A. Y., Khoshghalb, A., Khalili, N.: Pitfalls in interpretation of gravimetric water content-based soil-water characteristic curve for deformable porous media. Int. J. Geomech. D4015004 (2015)
190. Pasha, A.Y., Khoshghalb, A., Khalili, N.: Hysteretic model for the evolution of water retention curve with void ratio. Eng. Mech. **143**(7), 04017030 (2017)
191. Penman, H.L.: Gas and vapor movement in soil: I. The diffusion of vapors in porous solids. J. Agri. Sci. **30**, 437–462 (1940)
192. Peron, H., Hueckel, T., Laloui, L., Hu, L.B.: Fundamentals of desiccation cracking of fine-grained soils: experimental characterization and mechanism identification. Can. Geotech. J. **46**, 1177–1201 (2009)
193. Philip, J.R., de Vries, D.A.: Moisture movement in porous materials under temperature gradients. Transac. Am. Geophys. Union **38**(2), 222–232 (1957)
194. Plum, R.L., Esrig, M.I.: Some temperature effects on soil compressibility and pore water pressure. Highway Res. Board, Rep. **103**, 231–242 (1969)
195. Pollock, D.W.: Simulation of fluid flow and energy processes associated with radioactive waste disposal in unsaturated alluvium. Water Resour. Res. **22**(5), 765–775 (1986)
196. Preene, M., Powrie, W.: Ground energy system: from analysis to geotechnical design. Géotechnique **59**(3), 261–271 (2009)
197. Prunty, L.: Soil water retention and conductivity when vapor flow is important. J. Irrig. Drainage Eng. **129**, 201–207 (2003)
198. Prunty, L., Horton, R.: Steady-state temperature distribution in nonisothermal unsaturated closed soil cells. Soil Sci. Soc. Am. J. **58**, 1358–1363 (1994)
199. Rice, J.R.: Heating and weakening of faults during earthquake slip. J. Geophys. Res. **111**, B05311 (2006). https://doi.org/10.1029/2005JB004006
200. Richards, L.A.: Capillary conduction of liquids through porous mediums. Physics. **1**(5), 318–333 (1931)
201. Robinson, J.D., Vahedifard, F.: Weakening mechanisms imposed on California's levees under multiyear extreme drought. Clim. Change **137**(1), 1–14 (2016)
202. Robinson, J.D., Vahedifard, F., AghaKouchak, A.: Rainfall-triggered slope instabilities under a changing climate: comparative study using historical and projected precipitation extremes. Can. Geotech. J. **54**(1), 117–127 (2017)
203. Romero, E., Vaunat, J.: Retention curves of deformable clays: Experimental evidence and theoretical approaches in unsaturated soils. In: Proceedings of the International Workshop on Unsaturated Soil, A.A. Balkema, Rotterdam, Netherlands, pp. 91–106 (2000)
204. Rose, C.W.: Water transport in soil with a daily temperature wave I. Theory and experiment. Aust. J. Soil Res. **6**, 31–44 (1968)
205. Ruokojarvi, P., Ruuskanen, J., Ettala, M., Rahkonen, P., Tarhanen, J.: Formation of polyaromatic hydrocarbons and polychlorinated organic compounds in municipal waste landfill fires. Chemosphere **31**(8), 3899–3908 (1995)

206. Rutqvist, J.: Status of the TOUGH-FLAC simulator and recent applications related to coupled fluid flow and crustal deformations. Comput. Geosci. **37**(6), 739–750 (2011)
207. Saito, H., Simunek, J., Mohanty, B.P.: Numerical analysis of coupled water, vapor, and heat transport in the vadose zone. Vadose Zone J. **5**, 784–800 (2006)
208. Sakai, M., Toride, N., Simunek, J.: Water and vapor movement with condensation and evaporation in a sandy column. Soil Sci. Soc. Am. J. **73**, 707–717 (2009)
209. Salager, S., Nuth, M., Ferrari, A., Laloui, L.: Investigation into water retention behaviour of deformable soils. Can. Geotech. J. **50**(2), 200–208 (2013)
210. Salager, S., François, B., El Youssoufi, M.S., Laloui, L., Saix, C.: Experimental investigations of temperature and suction effects on compressibility and pre-consolidation pressure of a sandy silt. Soils Found. **48**(4), 453–466 (2008)
211. Sánchez, M., Gens, A., Guimarães, L.: Thermal-hydraulic-mechanical (THM) behavior of a large-scale in situ heating experiment during cooling and dismantling. Can. Geotech. J. **49**, 1169–1195 (2012)
212. Sánchez, M., Gens., A., Olivella, S.: Thermo-hydro-mechanical analysis of a large scale heating test incorporating material fabric changes. Int. J. Numer. Anal. Meth. Geomech. **36**(4): 391–342 (2012b)
213. Sánchez, M., Manzoli, O., Guimarães, L.: Modeling 3-D desiccation soil crack networks using a mesh fragmentation technique. Comput. Geotech. **62**, 27–39 (2014)
214. Sánchez, M., Arson, C., Gens, A., Aponte, F.: Analysis of unsaturated materials hydration incorporating the effect of thermo-osmotic flow. Geomech. Energy Environ. **6**, 101–115 (2016a)
215. Sánchez, M., Gens, A., Villar, M.V., Olivella, S.: A truly coupled THM formulation for double porosity unsaturated soils. Int. J. Geomech.. ASCE. D4016015-1 (2016b)
216. Savvidou, C.: Centrifuge modelling of heat transfer in soil. Proceedings of Centrifuge 88, Corté, ed., Balkema, Rotterdam, pp. 583–591 (1988)
217. Schiffman, R.L.: A thermoelastic theory of consolidation. Environ. Geophys. Heat Transfer, 78–84 (1971)
218. Segall, P., Rubin, A.M., Bradley, A.M., Rice, J.R.: Dilatant strengthening as a mechanism for slow slip events. J. Geophys. Res. Solid Earth **115**, B12305 (2010). https://doi.org/10.1029/2010JB007449
219. Segall, P., Bradley, A.M.: The role of thermal pressurization and dilatancy in controlling the rate of fault slip. J. Appl. Mech. **79**(3), 031013 (2012)
220. Seneviratne, H.N., Carter, J.P., Booker, J.R.: Analysis of fully coupled thermomechanical behaviour around a rigid cylindrical heat source buried in clay. Int. J. Numer. Anal. Meth. Geomech. **18**, 177–203 (1994)
221. Seneviratne, S.I., Lüthi, D., Litschi, M., Schär, C.: Land-atmosphere coupling and climate change in Europe. Nature **443**(7108), 205 (2006)
222. Shah, D.J., Ramsey, J.W., Wang, M.: An experimental determination of the heat and mass transfer coefficients in moist, unsaturated soils. Int. J. Heat Mass Transf. **27**(7), 1075–1085 (1984)
223. She, H.Y., Sleep, B.E.: The effect of temperature on capillary pressure-saturation relationships for air-water and perchloroethylene-water systems. Water Resour. Res. **34**(10), 2587–2597 (1998)
224. Shukla, S., Safeeq, M., AghaKouchak, A., Guan, K., Funk, C.: Temperature impacts on the water year 2014 drought in California. Geophys. Res. Lett. **42**(11), 4384–4393 (2015)
225. Shepherd, R., Wiltshire, R.J.: An analytical approach to coupled heat and moisture transport in soil. Transp. Porous Media **20**, 281–304 (1995)
226. Shokri, N., Lehmann, P., Or, D.: Critical evaluation of enhancement factors for vapor transport through unsaturated porous media. Water Resour. **45**, W10433 (2009)
227. Sibbitt, B., McClenahan, D., Djebbar, R., Thornton, J., Wong, B., Carriere, J., Kokko, J.: The performance of a high solar fraction seasonal storage district heating system—five years of operation. Energy Procedia. **30**, 856–865 (2012)

228. Skempton, A.W.: Residual strength of clays in landslides, folded strata, and the laboratory. Géotechnique. **35**(1), 3–18 (1985)
229. Smits, K.M., Cihan, A., Sakaki, S., Illangasekare, T.H.: Evaporation from soils under thermal boundary conditions: experimental and modeling investigation to compare equilibrium and nonequilibrium-based approaches. Water Resour. Res. **47**, W05540 (2011). https://doi.org/10.1029/2010WR009533
230. Smits, K.M., Sakaki, T., Howington, S.E., Peters, J.F., Illangasekare, T.H.: Temperature dependence of thermal properties of sands over a wide range of temperatures [30–70 °C]. Vadose Zone J. https://doi.org/10.2136/vzj2012.0033 (2013)
231. Sophocleous, M.: Analysis of water and heat flow in unsaturated-saturated porous media. Water Resour. Res. **15**, 1195–1206 (1979)
232. Stark, T.D., Akhtar, K., Hussain, M.: Stability analyses for landfills experiencing elevated temperatures. Proc. GeoFlorida **2010**, 1–8 (2010)
233. Stark, T.D., Martin, J.W., Gerbasi, G.T., Thalhamer, T.: Aluminum waste reaction indicators in an MSW landfill. J. Geotech. Geoenviron. Eng. **138**(3), 252–261 (2012)
234. Stark, T.D., Choi, H., McCone, S.: Drained shear strength parameters for analysis of landslides. J. Geotech. Geoenviron. Eng. **131**(5), 575–588 (2005)
235. Suryatriyastuti, M.E., Mroueh, H., Burlon, S.: A load transfer approach for studying the cyclic behavior of thermo-active piles. Comput. Geotech. **55**, 378–391 (2014)
236. Sultan, N., Delage, P., Cui, Y.J.: Temperature effects on the volume change behavior of boom clay. Eng. Geol. **64**, 135–145 (2002)
237. Sutman, M., Brettmann, T. Olgun, C.G.: Thermo-mechanical behavior of energy piles: full-scale field test verification. DFI 39th Conference on Deep Found. pp. 1–11 (2014)
238. Takai, A., Ghaaowd, I., Katsumi, T., McCartney, J.S.: mpact of drainage conditions on the thermal volume change of soft clay. GeoChicago 2016: Sustainability, Energy and the Geoenvironment. Chicago. Aug. 14–18. pp. 32-41 (2016)
239. Tarantino, A.: A water retention model for deformable soils. Géotechnique **59**(9), 751–762 (2009)
240. Tarn, J.Q., Wang, Y.M.: End effects of heat conduction in circular cylinders of functionally graded materials and laminated composites. Int. J. Heat Mass Transf. **47**, 5741–5747 (2004)
241. Taylor, S.A., Cary, J.W.: Linear equations for the simultaneous flow of water and energy in a continuous system. Soil Sci. Soc. Am. J. **28**, 167–172 (1964)
242. Tidfors, M., Sällfors, G.: Temperature effect on preconsolidation pressure. Geotech. Test. J. **12**(1), 93–97 (1989)
243. Thomas, H.R., King, S.D.: Coupled temperature capillary potential variations in unsaturated soil. J Eng Mech. ASCE. **117**(11), 2475–2491 (1991)
244. Thomas, H.R., Sansom, M.R.: Fully coupled analysis of heat, moisture and air transfer in unsaturated soil. J. Eng. Mech. **121**(3), 392–405 (1995)
245. Thomas, H.R., He, Y.: A coupled heat-moisture transfer theory for deformable unsaturated soil and its algorithmic implementation. Int. J. Numer. Meth. Eng. **40**, 3421–3441 (1997)
246. Thomas, H.R., He, Y., Sansom, M.R., Li, C.L.W.: On the development of a model of the thermo-mechanical-hydraulic behavior of unsaturated soils. Eng. Geol. **41**, 197–218 (1996)
247. Thomas, H.R., Sansom, M., Rees, S.W.: Non-isothermal flow. In: Environmental Geomechanics. Springer, pp. 131–169 (2001)
248. Thomas, H., Cleall, P., Chandler, N., Dixon, D., Mitchell, H.: Water infiltration into a large-scale in-situ experiment in an underground research laboratory. Géotechnique **53**(2), 207–224 (2003)
249. Toll, D.G., Mendes, J., Hughes, P.N., Glendinning, S., Gallipoli, D.: Climate change and the role of unsaturated soil mechanics. Geotech. Eng. (SEAGS) **43**(1), 76–82 (2012)
250. Towhata, I., Kuntiwattanakul, P., Seko, I., Ohishi, K.: Volume change of clays induced by heating as observed in consolidation tests. Soils Found. **33**(4), 170–183 (1993)
251. Turnbull, K.F.: Transportation Resilience: Adaptation to Climate Change and Extreme Weather Events. Summary of the Fourth EU–US Transportation Research Symposium. In Transportation Research Board Conference Proceedings (No. 53) (2016)

252. Tsiampousi, A., Zdravkovic, L., Potts, D.M.: A three-dimensional soil-water retention curve. Géotechnique **63**(2), 155–164 (2013)
253. Uchaipichat, A., Khalili, N.: Experimental investigation of thermo-hydro-mechanical behavior of an unsaturated silt. Géotechnique **59**(4), 339–353 (2009)
254. Vahedifard, F., Robinson, J.D., AghaKouchak, A.: Can protracted drought undermine the structural integrity of California's earthen levees? J. Geotech. Geoenviron. Eng. **142**(6), 02516001 (2016)
255. Vahedifard, F., AghaKouchak, A., Ragno, E., Shahrokhabadi, S., Mallakpour, I.: Lessons from the Oroville Dam. Science **355**(6330), 1139–1140 (2017)
256. Vahedifard, F., Cao, T.D., Thota, S.K., Ghazanfari, E.: Nonisothermal models for soil water characteristic curve. J. Geotech. Geoenviron. Eng. **144**(9), 04018061 (2018)
257. Vahedifard, F., Williams, J. M., AghaKouchak, A.: Geotechnical Engineering in the Face of Climate Change: Role of Multi-Physics Processes in Partially Saturated Soils. 2018 International Foundations Congress and Equipment Exposition, IFCEE 2018, GSP No. 295. Orlando, Florida, March 15–10, ASCE, Reston, VA, 353-364 (2018b)
258. van Genuchten, M.T.: A closed-form equation for predicting the hydraulic conductivity of unsaturated soils. Soil Sci. Soc. Am. J. **44**(5), 892–898 (1980)
259. Vardon, P.J.: Climatic influence on geotechnical infrastructure: a review. Environ. Geotech. **2**(3), 166–174 (2015)
260. Vega, A., McCartney, J.S.: Cyclic heating effects on thermal volume change of silt. Environ. Geotech. **2**(5), 257–268 (2015)
261. Veveakis, E., Stefanou, I., Sulem, J.: Failure in shear bands for granular materials: Thermo-hydro-chemo-mechanical effects. Géotech. Lett. **3**(2), 31–36 (2013)
262. Villar, M.V., Sánchez, M., Gens, A.: Behaviour of a bentonite barrier in the laboratory: Experimental results up to 8 years and numerical simulation. Phys. Chem. Earth **33**, S476–S485 (2008)
263. Wang, B., Bouazza, A., Singh, R., Haberfield, C., Barry-Macaulay, D., Baycan, S.: Post-temperature effects on shaft capacity of a full-scale geothermal energy pile. J. Geotech. Geoenviron. Eng. https://doi.org/10.1061/(asce)gt.1943-5606.0001266, 04014125 (2014)
264. Wang, W., Regueiro, R., McCartney, J.S.: Coupled axisymmetric thermo-poro-elasto-plastic finite element analysis of energy foundation centrifuge experiments in partially saturated silt. Geotech. Geol. Eng. **33**(2), 373–388 (2015)
265. Wayllace, A., Lu, N.: A transient water release and imbibitions method for rapidly measuring wetting and drying soil water retention and hydraulic conductivity functions. Geotech. Test. J. **35**(1), 103–117 (2012)
266. Wheeler, S.J., Sharma, R.S., Buisson, M.S.R.: Coupling of hysteresis and stress–strain behaviour in unsaturated soil. Géotechnique. **53**(1), 41–54 (2003)
267. Whitaker, S.: Simultaneous heat, mass and momentum transfer in porous media: a theory of drying porous media. Adv. Heat Transfer. **13**, 119–203 (1977)
268. Wright, S.G., Zornberg, J.G., Aguettant, J.E.: The Fully Softened Shear Strength of High Plasticity Clays. FHWA/TX-07/0-5202-3 (2008)
269. Yesiller, N., Hanson, J., Liu, W.: Heat generation in municipal solid waste landfills. J. Geotech. Geoenviron. Eng. **131**(11), 1330–1344 (2005)
270. Zhang, J., Datta, A.K.: Some considerations in modeling of moisture transport in heating of hygroscopic materials. Drying Technol. **22**(8), 1983–2008 (2004)
271. Zhou, C., Ng, C.W.W.: A new and simple stress-dependent water retention model for unsaturated soil. Comput. Geotech. **62**, 216–222 (2014)
272. Zhou, C., Ng, C.W.W.: Simulating the cyclic behavior of unsaturated soil at various temperatures using a bounding surface model. Géotechnique **66**(4), 344–350 (2015)
273. Zhou, C., Ng, C.W.W.: Effects of temperature and suction on plastic deformation of unsaturated silt under cyclic loads. J. Mater. Civ. Eng. **28**(12), 04016170 (2016)
274. Zhou, A.N., Sheng, D., Scott, S.W., Gens, A.: Interpretation of unsaturated soil behavior in the stress–saturation space, I: volume change and water retention behavior. Comput. Geotech. **43**, 178–187 (2012)

The Role of Rock Mechanics in the 21st Century

Antonio Bobet, Chloé F. Arson, Derek Elsworth, Priscilla Nelson, Ingrid Tomac and Anahita Modiriasari

Abstract Rocks and rock masses pose very complex problems that must be addressed by the engineering and scientific communities if the challenges of the 21st century are to be met. New societal demands for improved infrastructure, clean water, sustainable energy, and climate change, all call for an improved understanding of the multi-physics phenomena involving rock and all require a multi-disciplinary approach. The chapter identifies five topics that, among others, limit further developments in the field or are critical to societal demands: (1) Underground construction, geology and geotechnical risks; (2) Microstructure-enriched damage and healing mechanics; (3) Damage detection inside rock; (4) Coupled processes for energy extraction; and (5) Sustainable recovery of subsurface energy resources.

Keywords Rock mechanics · Coupled processes · Efficient mining · Environmental impact · Induced seismicity · Transparent earth · Underground construction

A. Bobet (✉) · A. Modiriasari
Lyles School of Civil Engineering, Purdue University, West Lafayette, IN, USA
e-mail: bobet@purdue.edu

C. F. Arson
School of Civil and Environmental Engineering, Georgia Institute of Technology, Atlanta, Georgia

D. Elsworth
Energy and Mineral Engineering, G3 Center, EMS Energy Institute, Pennsylvania State University, University Park, PA, USA

P. Nelson
Department of Mining Engineering, Colorado School of Mines, Golden, CO, USA

I. Tomac
University of California San Diego, La Jolla, CA, USA

N. Lu and J. K. Mitchell (eds.), *Geotechnical Fundamentals for Addressing New World Challenges*, Springer Series in Geomechanics and Geoengineering,
https://doi.org/10.1007/978-3-030-06249-1_11

1 Introduction

The National Academy of Engineering has identified fourteen Grand Challenges for the 21st Century. Of those, four directly involve rock mechanics and rock engineering: Restore and Improve Urban Infrastructure, Provide Access to Clean Water, Develop Carbon Sequestration Methods, and Engineer the Tools for Scientific Discovery. All call for an improved understanding of the multi-physics phenomena involving rock and all require a multi-disciplinary approach.

Rocks and rock masses are highly heterogeneous, with complex behavior that it is not only stress and time dependent, but also, and this is most important, scale dependent. It can be argued that the behavior at different scales is due to the "defects" that exist in the rock. These defects can be found at the atomic scale, where atom lattices may have irregularities; at the grain scale, where cracks are pervasive at the grain contacts and inside crystals, and up to the regional or continental scale because of different geological formations or due to discontinuities or faults that can range from microns to hundreds of kilometers in size, e.g. the North Anatolian or the San Andreas faults (see Fig. 1).

The complexities that the rock mechanics/geomechanics profession face are many. Rocks are formed from many different minerals, each with different chemo-mechanical properties, and defects (joints) that make the materials highly heterogeneous, anisotropic, and stress, time and scale dependent. The minerals in the rock may weather with time under different environments, joints may propagate due to subcritical crack growth or due to anthropogenic activities, which all change the behavior of the rock mass. Rocks, at great depth, are subject to large temperature and stress gradients and to different fluids such as formation fluids, oil, gas. Fluids in the rock mass originate from either geological processes or anthropogenic interventions such as carbon-dioxide sequestration or leakage from nuclear waste disposal. The stresses in the rock as well as the fluid environment may be engineered, e.g. for oil and gas extraction, for geothermal energy or for energy or waste storage including carbon sequestration.

(a) Micron scale (gypsum crystals) (b) Meter scale (slope in flysch) (c) Kilometer scale (fault in Turkey)

Fig. 1 Rock discontinuities at different scales

The challenges for rock mechanics and rock engineering in the 21st century stem out of society's continuous demand for improved levels of comfort and access to sustainable, safe and renewable resources. Sustainability calls for safe and economic technologies for waste disposal, CO_2 sequestration and new sources of clean energy. The science required to face these problems is inherently interdisciplinary, but not yet available. Finding solutions for these questions is a great challenge but also a great opportunity.

It is not possible to discuss in a single chapter the state of knowledge in rock mechanics/geomechanics, nor the specific research needs for the entire subject. What is done is focus on a few particular aspects that, in the authors' opinions, limit further developments in the field or are critical to societal demands. The topics chosen align with the challenges identified in Chapter 1 "The Role of Geotechnics in Addressing New World Problems", and revolve around the following themes:

- Underground construction, geology and geotechnical risk
- Microstructure-enriched damage and healing rock mechanics
- Damage detection inside rock
- Coupled processes for energy extraction
- Sustainable recovery of subsurface energy resources.

The following sections address the themes and provide insights into fundamental aspects of rock behavior such as damage and healing across the micro-, macro- and time-scales, coupled-processes to e.g., extract geothermal energy, as well as into practical aspects such as the central role that rock mechanics plays on energy resources, waste storage and anthropogenic effects associated to the utilization of the underground space, the pressing need for volumetric imaging of the subsurface, and on the interplay that exists between geology, design, construction and risk associated through all the stages of the infrastructure process, from conception to implementation.

2 Underground Construction, Geology and Geotechnical Risk

The underground construction industry has consistently provided the nation with needed infrastructure, meeting schedule, cost and scope goals. Population growth will continue, and so will the growth of our cities—but not always in predictable ways. In the past, we have lived through urban migration and growth, followed by suburbanization, and now perhaps the concept of the compact city describes how our cities will change in the future. The compact city concept is intimately wedded to increasing and intensive planned use of underground space, but engineers and planners have challenges in preparing our old and new infrastructure for the future.

It is generally appreciated that the nation must invest in the rehabilitation of existing infrastructure, but there continues to be a lack of political and public will to

do so. The value of our underground infrastructure needs to be better communicated to the US population. If our systems become increasingly unreliable, then it is likely that more of the world's leading industries will relocate to countries with more reliable infrastructure.

As we create and use more underground space, particularly in urban environments, we may find ourselves working in ground conditions not experienced before. This means that much of our conventional and current wisdom based on experience in a city may not be applicable. For example, we anticipate increased use of deeper underground space for many purposes. Higher ground stresses and water pressures will likely be encountered, and soil and rock behavior may become more problematic. As new needs for underground space are identified, owners and the public will request larger and more complex 3-D complex geometry for underground space applications. This may require advanced design concepts for long-term performance and stability. And as our coastal cities grow, more of the new infrastructure must be placed into more challenging ground for which risks and costs may be higher. This may require new approaches to ground improvement and displacement control.

The infrastructure can no longer be considered as isolated systems. Our infrastructure networks are developing emergent interdependencies that affect system performance, reliability and expected life. More of our systems are becoming diversified with gridded, distributed and local components not necessarily working together seamlessly, and this threatens to lead to a loss in robustness and resilience of service delivery at a time when the population is growing increasingly risk averse. We must make our systems smarter and able to self-detect problems. We must also commit to developing an IIM (Infrastructure Information Model) for all major cities, analogous to a Building Information Model (BIM) increasingly used for high-rise building design and construction management. The functions of a city must be preserved, and advanced sensing and spatial and temporal registration and tracking of all facilities and functions will elevate our infrastructure to the reliable and resilient systems our society needs [84].

Significant impacts from extreme events, including climate change, earthquakes, tsunamis, floods, storms—are arguably becoming more frequent and costly. Our future global cities must support the population both through disasters and for daily living, perhaps analogous to the human body's resistance and resilience to a high-grade fever and also to manage a low-grade infection. With the growth of population and megacities, our society deserves and demands integrated planning for improved space utilization. The scale and definition of geologic variation are as important as political boundaries. Engineers and planners must realize that:

- Urban growth will extend infrastructure into deeper and more fragile and challenging geologic environments
- Sustainability, terrorism and security drive new constraints for retrofit and new infrastructure system design
- The experienced intensity, impact and frequency of extreme events have been and are expected to continue to increase (data shown in Fig. 2 for weather-related losses).

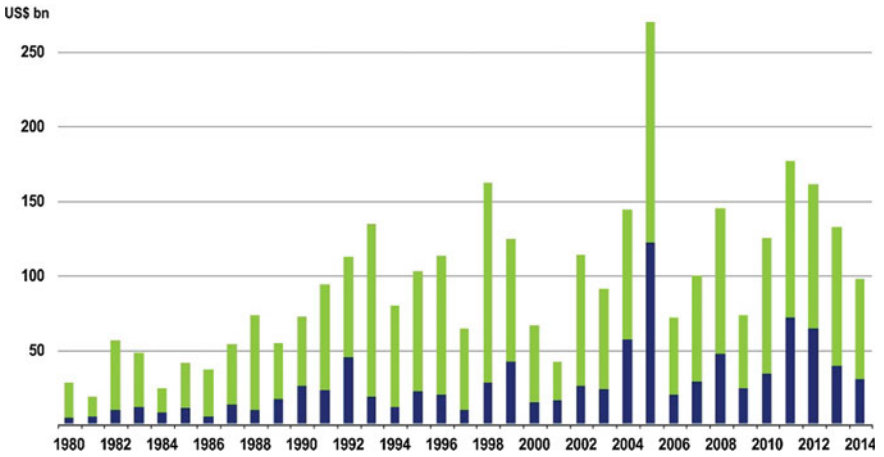

Fig. 2 Weather-related loss events worldwide 1980–2014. (green is overall losses and blue is insured losses, all in 2014 values) [55]

In many cases, the design loads used by engineers at the time of construction of our older infrastructure, may not be the loads we would use now. Our design and professional codes have always incorporated factors of safety against failure by such events, but the impacts of recent events have been more severe and complex with interdependent responses. Engineering professionals, construction contractors, and urban planners and managers must work together to identify new ways to retrofit and bolster our infrastructure against extreme event impacts. Underground engineering can be a part of effective design and solution of problems. Therefore, the underground is an important resource to enhance urban resilience, as is summarized in Table 1.

2.1 Reduction of Costs and Risks

Beyond the need for infrastructure services is the need to manage the budget. It is notable that infrastructure costs for construction and rehabilitation have only increased in recent time. Innovations are needed to reduce costs and support schedule reliability, and best decisions on investments can only be made with increased use of Life Cycle Engineering (LCE) which requires databases that by-and-large do not exist. With increased use of LCE, performance metrics can be established for integrated surface and underground infrastructure planning and design, and to support sustainable multi-hazard design and LCE trade-offs. This need may define a new profession of urban stewards—engineers who design and construct holistically integrating over x, y, z and time.

It is also imperative the physical facilities be made more durable, and the infrastructure performance be made more reliable. Cost increases are often driven by

Table 1 Advantages and disadvantages for underground infrastructure and extreme event impacts

Type of event	Advantages or mitigations	Disadvantages or limitations
Earthquake	Ground motions reduce rapidly below surface	Fault displacements must be accommodated
	Well-built structures move with the geologic material	Instability in weak materials or poor construction
Hurricane, tornado	Wind loadings have minimal impact on fully buried structures	Damage to shallow utilities from toppling of surface structures such as trees and power lines
Flood, tsunami	Ground provides protection from surge and debris flow	Extensive restoration time and cost if entrances are flooded
Fire, blast	Ground provides effective protection, limit damage by compartmentalization	Entrances and exposed surfaces are weaknesses, confined space risk
Radiation, chemical/biological exposure/releases	Ground provides additional protection	Appropriate ventilation system protections required
	Limited exposure with compartmentalization	Confined space may increase personnel risk

increased risks: Risk = Probability x Consequences (or Impact). For consequence evaluation, we need to know the value of underground space. We need an improved ability to quantify risks—including impacts and their probability of occurrence, as well as a framework for evaluation of mitigation strategy and assignment of responsibility. Once we better understand what problems drive risk increases, then we can contemplate where is the will to pay. A majority of the risk associated with underground infrastructure construction and performance is derived from the spatial variability and uncertainty associated with geologic conditions, including soil rock and water. Six areas of focus are discussed below:

- Risk avoidance
- New technologies and methods
- Better subsurface characterization
- Better management of water
- Risk awareness, assessment and management
- Risk communication and willingness to accept and share risk.

Risk Avoidance. Geologic conditions in the subsurface should be primarily managed by invoking the concept of underground zoning which provides spatial thinking and integrated planning to place above- and below-ground facilities in an optimized geologic setting. In New York City and other cities, such a consideration leads to vertical segregation of different infrastructure systems. However, much of the shallow infrastructure represents spatial chaos and project costs are strongly impacted by the need to manage the mayhem of aged near-surface systems.

The Japanese experience is a bit different. The 2001 Deep Underground Utilization Law established that land ownership rights in populated areas (e.g., Tokyo, Osaka) only extend to 40 m below ground, or 10 m below a deep foundation. In the case of public use of the underground space, no compensation to the land owner is required. The first projects using the law have included underground water mains in Kobe, and the Tokyo Gaikan Expressway.

New Technologies and Methods. In many areas of research, the pipeline from fundamental research to application has been thwarted. It is imperative that industry and owners commit to partner with universities to develop new technologies and methods, including new ways to excavate and support underground openings. The underground industry has many methods that can be applied including Tunnel Boring Machines (TBMs) and shields, and the newer slurry, earth pressure balance and hybrid pressure-face equipment, but more developments are needed to decrease costs, and improve safety (e.g., avoid hyperbaric cutter replacements and other interventions). The seemingly inexorable trend is for larger and larger diameters, and this by itself drives up project costs and expands project schedule.

In addition, it is important to incentivize the application of new technologies. For example, ground improvement techniques have come a long way in the past 30 years, and it is important that advances continue, and that techniques of ground improvement be proactively implemented before a project is started to change and remove identified geologic risks, rather than respond to the risks as encountered. Such postures often result in changed condition claims, litigation, increased costs and delays.

Many of our infrastructure projects are designed for low first cost and to comply with right-of-way limitations. Such systems are not necessarily designed for long-term sustainability and maintainability. Engineers must seek new materials and technologies to enhance performance and durability of our infrastructure systems, new and old. In addition, new technologies must not be just implemented—they must be assessed for short and long-term performance. Sober assessment of performance is very often forgotten in the cycle of innovation we seek for the underground industries.

Safety in the underground during construction and operation continues as a concern, and incident rates for heavy construction are considerably higher than for mining projects. Safety innovations continue to be needed, and include personal protective equipment during construction and also fire and explosion incident management, particularly when the public are involved in response.

Spatial and temporal variations in subsurface materials and conditions continue to be a risk, and a new look at integrating geophysical and remote sensing methods is warranted. Engineers should also rethink materials and methods in use. For example, development of new concrete, grout and shotcrete materials for application in the underground are needed, and engineers and contractors should revisit and dramatically improve our “old” or “conventional” technologies such as drill/blast operations.

Better subsurface characterization. Knowledge of the underground conditions has been improving over past decades, but the combination of continuing sore points and

arising new difficulties must be considered in planning. In many urban environments, previous underground works have demonstrated spatial and material property distributions to be expected, so our conventional site investigations should be confirmatory rather than exploratory.

But some geologic issues continue without full resolutions, as a low-grade infection on the industry. Examples include the following:

- Shallow cover, varying depth to rock
- Ground movements, subsidence
- Consolidation settlements
- Weathered rock and rock mass (including karst)
- Rock mass structure and variability
- Time dependency in materials behavior
- Muck abrasiveness and stickiness
- Aggregate reactions and concrete durability.

Geological and Geotechnical Engineers still wrestle with scale effects as well, extrapolating from laboratory behavior to full scale in the field. Many rock mass rating systems have been developed—too many. On a large number of projects, ratings applications have been uninformed and inconsistent, and there have been only limited attempts to validate their inference, or the use of a large number of empirical correlations. This observation also can be applied to the plethora of computational models available for subsurface design. We must make opportunities to validate design assumptions and performance prediction.

More urban infrastructure will necessarily be placed deeper, and the in situ stress state will likely become more important on more projects. Estimation of in situ stress is not easy without a clear geologic framework for interpretation, and most stress assessments are made as point measurements (interpretation of deformation measurements at a point). This can only be addressed by obtaining a better understanding of the spatial variability of rock mass structured which introduces uncertainty. The variety of excavation shapes and dimensions can be expected to vary in the future, with more gallery space rather than plane strain tunnels needed, making the predictions of stress redistribution around an underground opening increasingly important. We need to understand spatial and temporal variations that affect performance of existing facilities for sustainable design and operations.

Geologic material failure and time-dependent response of geologic materials are far more likely to be observed in an underground mine than in a civil works project. Mining engineers develop a strong geologic perspective on risk that would benefit in application to civil construction projects. Such a partnership or collaboration across industries brings an enhanced potential for real spatial understanding of rock mass and water inflow and pressures variability, and for better understanding of time effects, presenting the possibility to develop sustainability performance information. The two industries also have many environmental issues in common, as do they have a mutually beneficial potential for application of automation, robotics, and big data/information systems. This is the era of information: with an expansion in

sensing and measurement capabilities, how should the entire site investigation and construction process be re-thought, not to mention real-time data flows and their importance to effective management for resilience of urban infrastructure systems.

Better management of water. The presence of water in the subsurface changes the behavior of materials and strongly influences the long-term performance of underground facilities. Full consideration of the influence of water includes knowledge and understanding of volume, flow rate, quality, pressure, and changes over time.

Management of water is sometimes a matter of resource conservation, but environmental (bio-geo-chemical) and construction impacts can be profound. During construction, water management includes compressed air, and the use of pressure-faced shields. Microtunneling and trenchless methods are very flexible and work well for smaller diameter emplacements, which potentially can be efficiently and economically reamed to larger diameters.

Water inflows can complicate the construction process, and even compromise the capabilities of installed support. Some of the most active areas of new technology implementation have been the introduction of waterproofing into tunnel linings.

Operational impacts of seepage and inflows are incredibly important since water drives long term deterioration in the underground, and inflows can cause piping and ground loss that affects structures nearby. The long-term performance of waterproofing or drainage management technologies is not well known in most cases. Assessment is needed.

Risk awareness, assessment and management. Many underground construction projects now use the three-legged stool of a Disputes Review Board (DRB), requirement for bid documents to be escrowed, and the development of a Geotechnical Baseline Report (GBR) as a part of the contract documents explicitly developed for geologic risk management.

The GBR is thoughtfully written to present a geologic analysis of "geoproblem event" frequency (temporally and spatially) to be assumed during a project. To be done is the collection of project data to inform statistical probability and consequences of encountering major geotechnically-driven stoppages in underground excavations. The data and information needed include:

- Spatial frequency: km/event
- Typical event sources: excavation and equipment, ground control, water
- Temporal frequency: hours/event
- Response duration distribution
- Quality/performance of contractor.

Not everything about a specific project is "one-off", and the framework of geologic inference and analysis opens the prospect for real predictability of geotechnical event with extreme impact on a project. And for this geologic effort, it is clear that mining and civil industries can share geodata.

An increasing number of projects continue into the project with risk registries which are living documents that characterize risks, assign responsibilities, and record mitigation plans. What is not developed to date is a broad consensus as to the method of risk analysis.

Risk communication and willingness to accept and share risk. The commitment for investment requires far more effective communication of the value of infrastructure and of underground space. The value of the nation's infrastructure may be estimated in several ways, but totals on the order of $70–$100 trillion can be suggested for the US. If this number is divided by the population of the US, the per capita investment in infrastructure is on the order of $300,000, the price of a house in many areas. This $300 K can be interpreted as a birthright for each person born in the US, a pre-investment upon which the economic engine runs, the quality of life is assured, and career potential of each individual is leveraged. Even as families reinvest in a house to retain value, so must the nation reinvest in its infrastructure. This is an example of a metric that can be meaningful to each citizen and politician.

3 Microstructure-Enriched Damage and Healing Rock Mechanics

Plasticity models and failure envelopes have been used in Earth Sciences and Rock Engineering for decades, with little emphasis on the scales and orientations of discontinuities that affect rock macroscopic properties. While thermodynamic equations of crack propagation and rebonding are formulated at the crystal scale, homogenization schemes are based on strong assumptions on microstructure topology. The gap between microscopic and macroscopic rock damage models makes it infeasible to uniquely characterize the pore- and crack- scale mechanisms that control deformation and flow regimes, predict percolation thresholds coupled to changes of rock stiffness, or relate crack rebonding time to stiffness and permeability healing time. A theory that couples rock microstructure descriptors (e.g. pore and crack sizes) and macroscopic thermodynamic variables (e.g. deformation and damage) is presented. Model predictions can be used to recommend the conditions of moisture and temperature necessary to minimize damage and/or enhance healing in rocks and to design safe and sustainable geological storage systems. In addition to preventing subsidence, borehole instabilities and contaminant leakage, the proposed models will be applicable for predicting fault rupture during earthquakes, improving manufacturing methods and designing sustainable materials.

3.1 Continuum Damage and Healing Mechanics

Crack opening. Continuum Damage Mechanics (CDM) provides an efficient framework to predict deformation and stiffness changes (including anisotropy) from purely energetic considerations [65, 68]. However, most damage models proposed for porous rocks were designed for saturated geomaterials and restricted the damage criterion to mechanical tensile loads. Very few studies include an anisotropic dam-

aged permeability model [75]. Almost all models proposed for unsaturated porous media resort to Bishop's effective stress concept, i.e. the extension of Terzaghi's effective stress to unsaturated media, e.g., [14], which partially uncouples damage evolution and poromechanical phenomena. Alternatively, Arson and Gatmiri [3] formulated an orthotropic thermo-hydro-mechanical damage model, using independent strain state variables. Rate-independent CDM models are based on a minimum of two postulates [24]: the expression of the free energy, a damage criterion, plus a dissipation potential if dissipative flow rules are non-associated (Table 2).

Crack Closure. The rotation of the principal base of damage induced by crack closure makes classical CDM frameworks inconsistent [20]. Most models proposed for mechanical crack closure are either isotropic, or restricted to mode I fracture propagation, e.g., [87]. An exception is the model proposed by [49] for cohesive materials, which accounts for the recovery of the shear modulus due to friction. Bargellini et al. [8] proposed an original (but complex) discrete formulation, in which crack displacements are projected on a set of basic tensors of various orders. Crack opening is sometimes assumed to generate irreversible deformation due to geometric incompatibilities at the faces of the cracks that close. It is possible to introduce a damage-induced irreversible component to the deformation tensor, without having to resort to any additional plasticity potential. However, this kind of formulation often falls short when the material response is very different in tension and compression, like in rocks [116]. Moreover, damage and total deformation must be considered as thermodynamically independent, which leads to thermodynamic inconsistencies. As a result, the ambivalent definition of damage used to account for both stiffness degradation and irreversible deformation requires formulating CDM models in terms of general stress variables. Even so, using only one dissipation potential in the formulation makes it challenging to express the lumped damage potential and the corresponding

Table 2 Main postulates needed to formulate a rate-independent CDM model

Postulate	Constitutive relationship
Solid skeleton free energy $\Psi_s(\epsilon, \mathbf{D}, \mathbf{X})$	$\sigma = \frac{\partial \Psi_s(\epsilon,\mathbf{D},\mathbf{X})}{\partial \varepsilon}$, $\mathbf{Y} = \frac{\partial\, \Psi_s(\epsilon,\mathbf{D},\mathbf{X})}{\partial \mathbf{D}}$, $\mathbf{R} = \frac{\partial\, \Psi_s(\epsilon,\mathbf{D},\mathbf{X})}{\partial \mathbf{X}}$
Damage criterion $f_d(\sigma, \mathbf{Y}, \mathbf{X})$	$(**)\dot{\mathbf{D}} = \dot{\lambda}_d \frac{\partial f_d(\sigma,\mathbf{Y},\mathbf{X}(\mathbf{D},\epsilon^{\mathbf{id}}))}{\sigma \mathbf{Y}}$, $\dot{\epsilon}^{id} = \dot{\lambda}_d \frac{\partial f_d(\sigma,\mathbf{Y},\mathbf{X}(\mathbf{D},\epsilon^{\mathbf{id}}))}{\partial \sigma}$
Damage potential $g_d(\sigma, \mathbf{Y}, \mathbf{X})$	$\dot{\mathbf{D}} = \dot{\lambda}_d \frac{\partial g_d(\sigma,\mathbf{Y},\mathbf{X}(\mathbf{D},\epsilon^{\mathbf{id}}))}{\sigma \mathbf{Y}}$, $\dot{\epsilon}^{id} = \dot{\lambda}_d \frac{\partial g_d(\sigma,\mathbf{Y},\mathbf{X}(\mathbf{D},\epsilon^{\mathbf{id}}))}{\partial \sigma}$, $\dot{\mathbf{R}}^{id} = \dot{\lambda}_d \frac{\partial g_d(\sigma,\mathbf{Y},\mathbf{X}(\mathbf{D},\epsilon^{\mathbf{id}}))}{\partial \mathbf{X}}$

ϵ deformation tensor
σ: stress tensor
D: damage tensor
Y: damage-driving force;
X: tensor lumping hardening variables
R: thermodynamic "force", work-conjugate to the hardening tensor **X**
$\epsilon^{\mathbf{id}}$: irreversible deformation induced by damage
Often, (**D**, $\epsilon^{\mathbf{id}}$) are hardening variables
λ_d: damage multiplier
(**) If associate flow rules

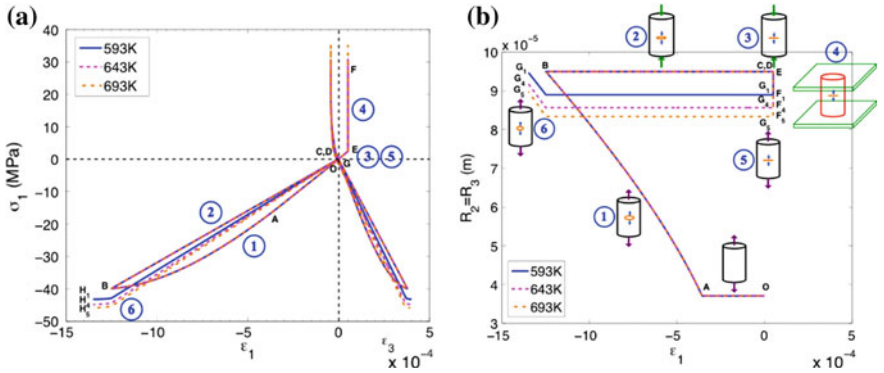

Fig. 3 Simulation of a stress path including a tensile loading (OB), followed by unloading and compression (BE), a heating phase that triggers Diffusive Mass Transfer (DMT) and healing (EF), cooling (FE) and reloading (EH). Stress/strain curves (**a**) and average crack lateral crack radii (**b**) for different heating temperatures. Modified after [119]

damage-driving forces, which become anyway non-physical. It is anticipated that a truly hyper-elastic framework could overcome the shortcomings of CDM models currently available to capture irreversible damage-induced deformation [2].

Crack rebonding. At the scale of a Representative Elementary Volume (REV), measurements of porosity and permeability can be used to assess clogging due to precipitation, but only loading and unloading cycles can provide a measure of potential stiffness recovery by crack rebonding [36]. Recent developments in polymer sciences explain interactions involved in complex chemical chains by modeling molecular movements as crawling mechanisms [115]. The concept of healing by Diffusive Mass Transfer (DMT) was initially introduced to model atomic interactions in cracked glass [114], and refers to crack rebonding by the migration of ions in the lattice forming the solid mass. Numerous studies were conducted at the microscopic scale on halite because this natural geomaterial can heal even in the absence of impurities [98, 102]. Phenomenological healing models proposed for salt rock assume that both crack opening and closure are time-dependent, which makes it possible to represent cracking and healing effects by a viscoplastic dilatant deformation [56]. Some authors combined rate- dependent or rate-independent damage and healing variables [79]. Most damage and healing models are formulated with a "net damage" variable defined as the difference between the CDM damage variable and a healing variable [1]. Figure 3, taken from Zhu and Arson [119], shows an example of salt rock model in which the net damage is alternatively defined as a second-order equivalent crack density tensor, which represents the volume of open cracks, determined by statistical analyses of images taken during a creep test.

The model predicts that in tension, the sample behaves elastically (OA) before horizontal cracks start to open (AB). During the unloading phase, the slope of the stress/strain curve is less steep than during the initial elastic loading phase and the value of damage components remain constant (BC). Unilateral effects are then noted

during the compression phase (DE); internal compressive stress develops due to the restrained thermal expansion of the sample during the creep phase at high temperature (EF), and partial mechanical recovery is achieved after the healing phase (FG_1). Additional damage is produced after recovery (G_1H) when the new damage threshold is reached (larger than the initial threshold but smaller than the threshold obtained after the tension phase). The proposed modeling strategy is ad hoc to model stiffness changes induced by crack opening, closure and healing. However, the expression of the net damage depends on open crack volumes estimated from 2D images. Moreover, simplifying crack shape assumptions were made to distinguish closed and rebonded cracks. Fabric enrichment can circumvent these limitations.

3.2 Homogenization Schemes

Micro-mechanics and microplanes. Micromechanics-based damage models [91] assume that the REV is populated with a distribution of cracks characterized by a specific shape (e.g., penny-shaped), with a tractable density. These geometric hypotheses lead to an explicit expression of the strain concentration tensor and of the free energy of the rock-solid skeleton. For pure mode I cracking, the only damage variable needed to express the energy dissipation associated to the degradation of elastic moduli is the second-order crack density tensor [61], which is a particular form of Oda's fabric tensor, commonly used in structural geology [85]. Mixed crack propagation modes (inducing a non-zero tangential displacement at crack faces) require higher-order damage tensors—of at least order four, e.g., [19]. Increasing the order of the damage tensor improves the compliance of the model to symmetry properties required for the elasticity tensor [72]. In microplane models, e.g., [10], a kinematic constraint is applied to projections of strains on the crack planes. The principle of virtual work is applied on a discrete set of crack plane orientations, which are assigned weights to satisfy macroscopic energy balance equations at the scale of the unit sphere. Bazant's [12] discrete scheme with a 2×21 microplane distribution provides satisfactory accuracy at reasonable computation cost. A detailed discussion about the performance of numerical integration schemes is discussed in Levasseur et al. [69]. In the microplane theory, anisotropy stems from complex microplane orientation distributions and from the use of different evolution criteria for different microplanes orientations.

Homogenization and upscaling. Homogenization schemes were proposed to upscale microscopic gliding mechanisms in granular [6] and polycrystalline [80] media. For instance, in salt polycrystals, plastic and viscous deformation result from several fundamental mechanisms, e.g., dislocation glide, dislocation climb, polygonalization, inter-granular slip, dissolution-precipitation. Under stress and temperature typical of storage conditions, dislocation glide is the predominant mechanism that contributes to macroscopic salt rock deformation [98]. Pouya et al. [89] used the Hill's incremental interaction model to upscale viscous gliding mechanisms formulated at the crystal scale and to predict the viscous behavior of polycrystalline salt.

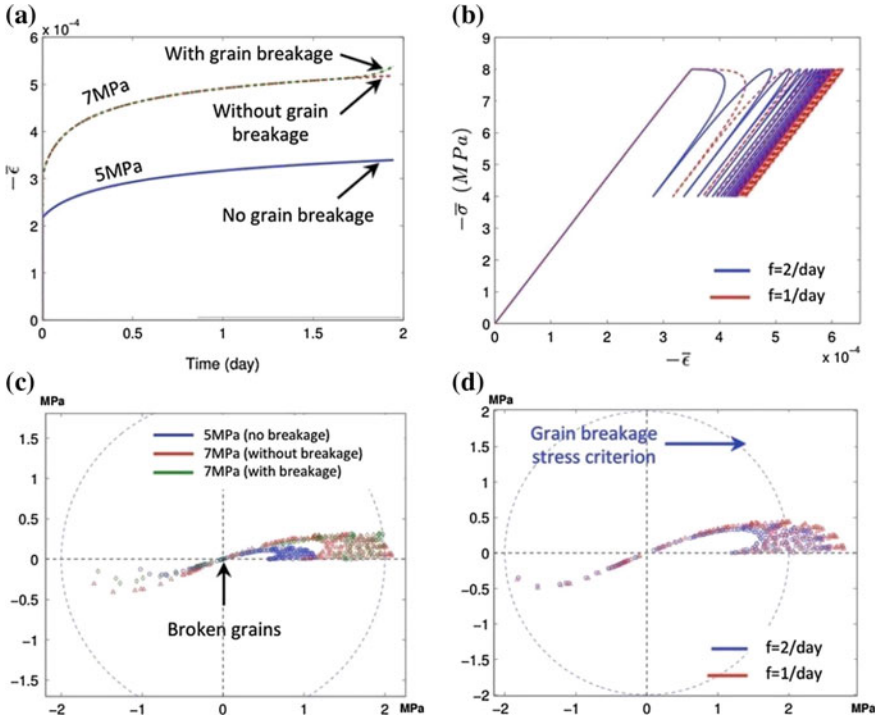

Fig. 4 Macroscopic deformation (**a**, **b**) and major principal micro-stresses (**c**, **d**) during creep tests (**a**, **c**) and a cyclic loading test (**b**, **d**). The micro-stress maps show the stress components in the radial (horizontal axis) and axial (vertical axis) directions. Each of the 200 dots represents the stress in one of the 200 crystals included in the REV. All salt crystals have a different crystallographic orientation, and are thus subject to a different gliding mechanism. Visco-plastic strains that result from glide induce local stress concentrations. When the local major principal stress exceeds salt tensile strength (2 MPa), the crystal is assumed to break and its stress vanishes. Crystal breakage correlates with the initiation of tertiary creep (**a**, **c**). For cyclic loading, the self-consistent approach predicts higher damage at lower frequency, which is consistent with in situ observations. Modified after [89]

Although some simplifying assumptions were made in the micro- macro-approach, the model provides micro-mechanical interpretations to important aspects of salt rock viscoplastic and fatigue behavior, such as strain hardening, creep recovery, as well as damage and accelerated creep due to grain breakage (Fig. 4a, c). Moreover, incremental viscoplastic strains decreased over the cycles, in agreement with the phenomenon of "shakedown" observed in elasto-plastic media; see Fig. 4b, d.

A review of incremental, secant, tangent, affine and variational formulations may be found in [76, 80]. Homogenization schemes allow computing poro-mechanical properties of rock subject to Thermo-Hydro-Chemo-Mechanical (THCM) processes [111]. However, increasing the number of physical processes (e.g., pore-throat suction, DMT) multiplies the number of scales of observation needed. Moreover, crack

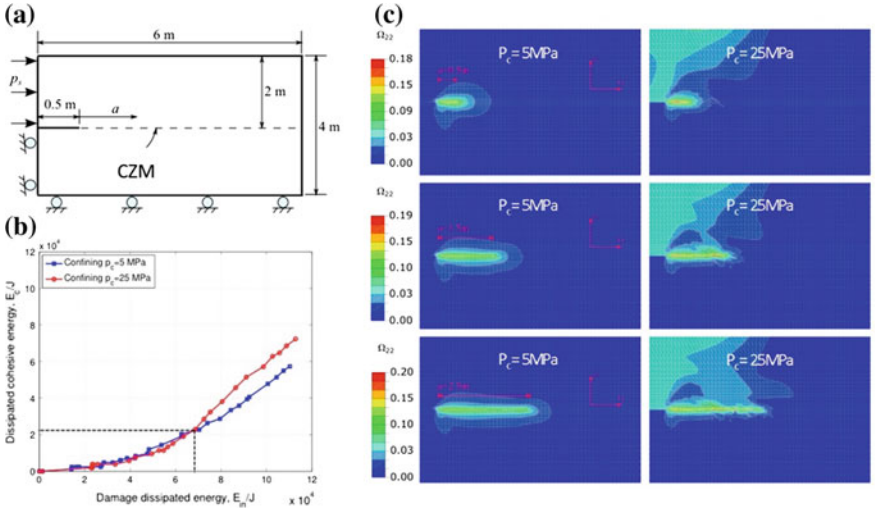

Fig. 5 Propagation of a mode II fracture (CZM) within its damage zone (CDM FEs). **a** Dimensions and boundary conditions. **c** Fracture and damage zone evolution. Ω_{22} is the damage component that refers to horizontal micro-cracks. Under a confining pressure of 5 MPa, the fracture propagates steadily within the damaged zone, while under a confining pressure of 25 MPa, the facture propagates in 'stick-slip' mode. **b** In both cases, more energy is dissipated by micro-crack propagation than by macro-fracture advancement. Modified after [60]

coalescence poses the problem of separation of scale, due to statistical homogeneity requirements. The emergence of macroscopic cracks as a result of the coalescence of micro-cracks can alternatively be predicted by coupling a CDM model to a discrete fracture mechanics model. Figure 5, extracted from Jin et al. [60] shows an example in mode II: when the continuum damage variable exceeds a critical value in a Finite Element (FE), the neighboring Cohesive Zone (CZ) opens, energy in the FE dissipates, and stress relaxes around the CZ. Coupling CDM and Cohesive Zone Models (CZMs) or other discrete fracture models is a very active research area.

3.3 Microstructure Enrichment

Microstructure-based permeability models. Several relationships were established between permeability and microstructure, including: Models based on Kozeny-Carman formulas, initially derived to model fluid flow in a bundle of parallel pipes and modified to account for tortuosity, e.g., [93]; Statistical flow networks models [47] which involve the probability density functions (pdfs) of the dimensions, aspect ratios and orientations of geometric elements of the network (e.g., tubular capillaries, penny-shaped cracks, ellipsoidal pores); Fractal network models [109]; and Mechanical homogenization schemes adapted to fluid flow [31]. Although non-

uniform pore arrangement produces hysteresis in retention curves [92], most models that relate capillary pressure to pore size [110] assume that the pore network is a bundle of pipes of constant cross section, which are entirely filled with either wetting or non-wetting fluid. Several models were proposed to predict emergent porosity modes and consequent permeability changes upon damage propagation [4, 94] and to model fracture propagation in a thermo-poro-elastic rock [28]. However, in continuum mechanics, crack coalescence can only be accounted for if a sufficient number of groups of connected cracks are contained in the REV. In the percolation theory [103], a characteristic flow path length is postulated, and transitions in flow regimes can only be predicted if the probability of fluid saturation is known for each pore or crack.

Non-local damage models. Internal lengths are used to scale the influence of a variable defined at x on a point located at x + dx. In differential formulations, local field variables are developed in Taylor series [27]. In integral formulations [10], space averages are weighted by attenuation functions. Enriched continuum models have additional degrees of freedom for microscopic translations and rotations [40, 41]. Microstructure- and gradient-enriched formulations involve non-physical variables (e.g., third-order tensors), which raises a number of issues for numerical implementation [118]. Non-local models are used to regularize localization problems often encountered in damage and plasticity models with softening [11]. Alternatively, diffusion equations can be used for deformation and dissipation evolution laws: the diffusion coefficient is inversely proportional to the square of an internal length parameter (e.g., percolation distance for DMT). However, the use of a diffusive creep law for brittle-elastic solids can lead to thermodynamic inconsistencies [108].

Fabric tensors. A direct relationship can be established between fabric tensors and rock stiffness tensor [26]. According to Oda [85], the fabric tensor F_{ij} is expressed as:

$$F_{ij} = \int_{\Omega} n_i n_j E(\Omega) d\,\Omega \quad (i, j = 1, 2, 3) \tag{1}$$

where n_1, n_2, n_3 are projections of a unit vector $\boldsymbol{n}$ on the Cartesian reference coordinates; Ω is the whole solid angle corresponding to a unit sphere, and equals 4π; $E(\Omega)$ is a pdf. The key is to choose pdfs with relevant microstructure descriptors to capture damage and healing processes. As shown in Fig. 6, taken from Shen et al., [100], macroscopic deformation and stiffness changes in salt rock correlate to changes of the fabric tensors of grain orientation (G), branch orientation (B), local solid volume fraction (L; the solid volume fraction over a polygon with edges matching grains centroids) and grain solidity (S; the ratio of grain area over the area of the grain's circumscribed circle).

The 'total' fabric tensor H is defined as:

$$H^i = \gamma G^i B^i L^i S^i \tag{2}$$

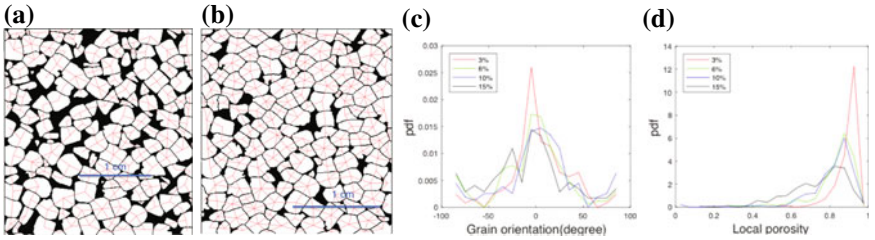

Fig. 6 Dry reagent-grade granular salt samples subjected to a uniaxial compression under 150 °C at 0.034 mm/s. Microstructure images at (**a**) 15% and (**b**) 6% porosity (white area: salt grains, black area: voids, red lines: branches linking the centers of two grains in contact). Evolution of the pdfs of (**c**) grain orientation and (**d**) local porosity for 15, 10, 6 and 3% total macroscopic porosity. Modified after [100]

where γ is a normalizing coefficient. The second-rank fabric tensor H can be written as kI + K. k is a scalar, and K is a traceless second-rank tensor. According to Zysset [121], the expressions of the free energy as functions of k, K and the strain E, are given as:

$$\begin{aligned}\psi(E,k,K) =& a_1 I\otimes I + a_2 I\bar{\underline{\otimes}} I + a_3 K\otimes K + a_4\left(K\bar{\underline{\otimes}} I + I\bar{\underline{\otimes}} K\right)\\ &+ a_5 K^2\otimes K^2 + a_6 K\bar{\underline{\otimes}} K + a_7(I\otimes K + K\otimes I)\\ &+ a_8\left(K\otimes K^2 + K^2\otimes K\right) + a_9\left(I\otimes K^2 + K^2\otimes I\right)\end{aligned} \tag{3}$$

Rock microstructure and mineral composition can be determined in the laboratory and thermodynamic models can be established to explain healing at the mineral scale, e.g., [57]. That is why fabric-enrichment is particularly appealing to model the macroscopic effects of crack propagation and rebonding in rocks.

4 Damage Detection Inside Rock

The mechanical and hydraulic properties of rocks are often controlled by the discontinuities or joints present in the rock mass. The importance of fracturing is attested by the large body of work geared at understanding the problem. Most of the research, understandably, has been concerned with observable damage; that is, at the macroscopic scale. Observations in the laboratory have relied on visual inspection using optical magnification and high-speed cameras. Digital Image Correlation (DIC) is an advanced experimental technique that has been utilized to observe the fracturing process on the surface of specimens by measuring full-field displacements similar to particle tracking in fluids. DIC has been used effectively for kinematic measurements along discontinuities and fractures [70]. While surface imaging techniques have been

instrumental in the understanding of cracking phenomena at the macroscopic scale, what is needed is a local or microscopic characterization of new cracks forming inside brittle materials.

One of the problems that limits advancements in the field of rock mechanics is our inability to scrutinize the interior of the material for the presence of damage and new cracks, and to infer engineering properties of the cracks. Indeed, the state-of-the-art still resides in the work done by Germanovich and his co-workers who observed the initiation of internal cracks in Polymethyl Methacrylate, which is a transparent material [32, 42].

Acoustic Emission (AE) is based on the idea that fracturing and crack propagation produce elastic waves that are somewhat characteristic of the deformation process [104]. AE has been successfully used to provide insights into deformation and damage occurring in intact rocks [46, 74] and along existing discontinuities [95–97] or associated with hydraulic fracturing [17, 50] and mining [113]; however, it is unclear whether AE events are precursors to damage or the results of damage [83]. In addition, it is uncertain whether AE can provide information about the engineering properties or nature of the cracks, as both tensile and shear cracks produce acoustic events [18, 117]. Also, in experimental studies performed on granite samples undergoing frictional sliding, the rate of emission events was nearly constant and did not increase before slip. In other words, AE events may not be precursors to damage, but rather the results of damage [21]. An alternative, or at least complementary technique to the passive AE method, is active seismic monitoring.

Active seismic monitoring, in particular compressional and shear wave propagation, has been used as a successful tool to locate discontinuities, assess the state of the stress along discontinuities and provide information about their engineering properties such as stiffness [23]. The seismic monitoring method includes an array of piezoelectric transducers that transmit elastic waves in the form of ultrasonic pulses through the rock to an array of receivers. Seismically, the fracture behaves as a low pass filter and attenuates the high frequency components of the signal [90]. The seismic monitoring method provides a continuous and non-destructive way to probe the internal structure of the rock and the discontinuity, and has been proven to be successful in detecting slip along pre-existing discontinuities [51], new cracks [81, 82], and impending shear failure of frictional joints [52].

The potential for active seismic monitoring to illuminate the interior of a rock mass was confirmed through Mode I fracture experiments. Three-point bending tests were performed on Berea sandstone, a flat-bedded, light gray, medium- to fine-grained protoquartzite cemented with silica and clay, with uniform grain distribution ranging from 0.1 to 0.8 mm. A prismatic beam with a center notch length of 10 mm was

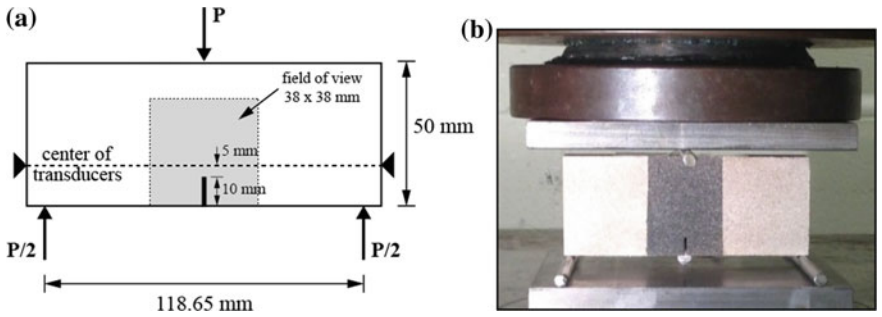

Fig. 7 Three-point bending tests (**a**) specimen geometry and (**b**) testing of sandstone specimen

tested with a span of 118.65 mm, 125 mm long, 50.0 mm tall, and 21.0 mm thick; see Fig. 7a. One surface was selected to place the speckle pattern for image analysis, as shown in Fig. 7b.

An Instron loading machine was used to apply the load to the specimen using a constant displacement rate of 0.03 mm/min. Crack initiation and propagation were identified with the DIC system, which showed that, at the tip of the crack, the horizontal displacement increased linearly at the early stages of loading, consistent with elastic deformation. As additional load was applied, a loss of linearity occurred that indicated damage to the specimen. As the axial load was increased to 86% of the failure load, the process zone grew and large jumps in displacement were observed farther from the tip of the crack. Because crack initiation is unstable in three-point bending tests, the DIC observations can be viewed as indication of the development of the process zone.

Two transducer pairs, one source (on the right side) and one receiver (on the left side), were used to monitor the sample during loading; see Fig. 7a. Two tests were used to determine the best type (P or S) of transducer to detect damage. The transducers were attached to the surface of the specimens using epoxy. After the transducers were placed, the load was increased at a constant displacement rate until the specimen reached failure. Full waveform measurements were taken during loading every 0.2 s. Figure 8 shows some of the waveforms recorded from the tests. The arrival time of the signals (both P-wave and S-wave transducers, irrespective of the polarization of the S-wave transducers) increased and the amplitude decreased with loading.

Graphs of normalized arrival time and amplitude (normalized by their values at the start of the test) as a function of load are shown in Fig. 9a, b, respectively. The arrival time increased monotonically until failure, and thus it did not provide an indication of damage to the specimen. However, the amplitude showed a distinct decrease at the time of formation of the process zone or damage. The amplitude increased with loading up to 1100 N where it reached a maximum, and then decreased until failure. The maximum in amplitude correlated well with the observation of the process zone based on DIC, which is indicated in the plots with a vertical dashed line. The three-

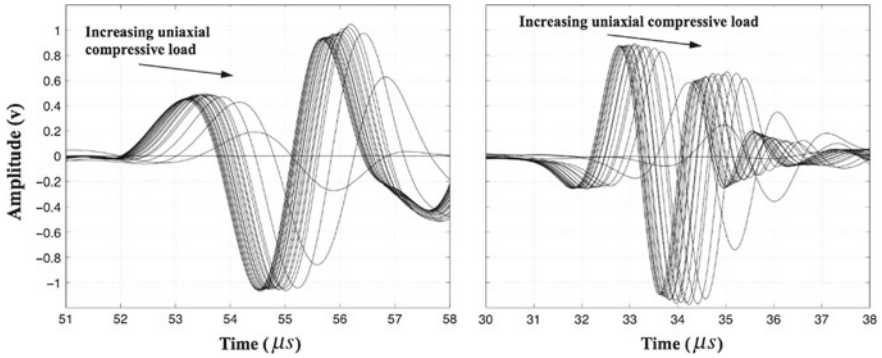

(a) Transmitted 1S-1S (b) Transmitted 1P-1P

Fig. 8 Waveforms from three-point bending tests (**a**) amplitude of shear waves and (**b**) amplitude of compressional waves

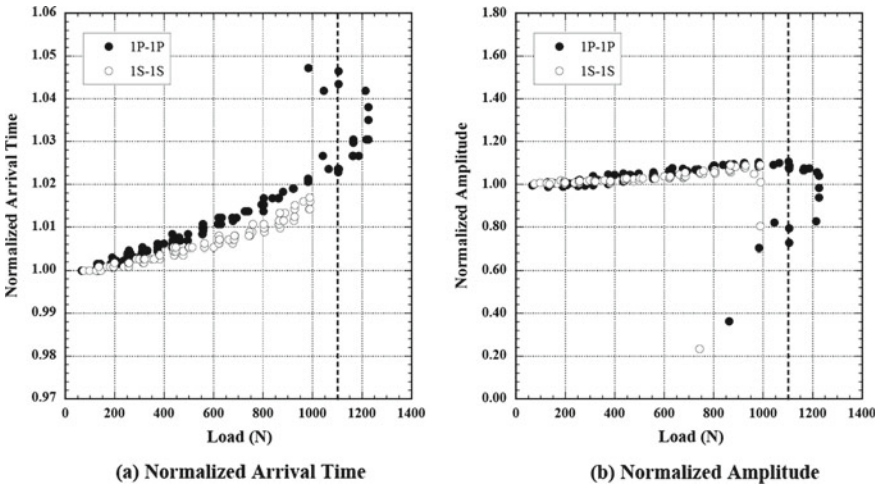

Fig. 9 Changes in arrival time and amplitude with load for P- and S-wave transducers, for three-point bending tests

point bending tests showed that the transducers, when located close to the tip of the notch, reached a maximum in amplitude during loading that was indicative of the formation of the fracture process zone, and thus could be taken as precursors to failure. In fact, the maximum in amplitude was consistently observed at 80% of the failure load.

The ability of detecting the onset of damage in the three-point bending tests by placing the transducers such that the path of the seismic wave intersected the area of impending damage, was tested in uniaxial compression tests on limestone. Figure 10 is a photograph of the experiment setup. Specimens of Indiana limestone with dimen-

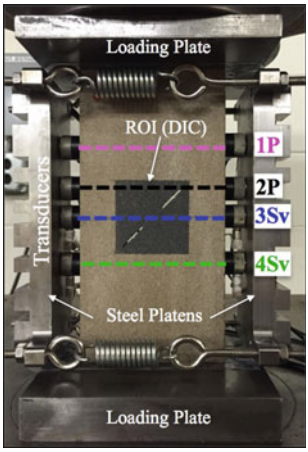

Fig. 10 Experiment setup on Indiana limestone

sions 203.2 mm height, 101.6 mm wide and 38.1 mm thick were loaded in uniaxial compression, at a constant displacement rate of 0.04 mm/min. The specimens had two parallel flaws cut through the thickness of the specimens, each 19.05 mm long. Different flaw arrangements were chosen such that coalescence occurred through a shear crack.

The displacements in the ROI (Fig. 10) were monitored using 2D-DIC imaging. In addition, full waveform compressional, P, and shear, S, waves were recorded, through transducers placed inside steel plates on the sides of the specimen, which were held in place by springs.

Figure 11 plots select results for a specimen with two coplanar flaws inclined at 45° with the horizontal, with a ligament length (distance between the internal tips of the flaws) of 19.05 mm. Figure 11a plots the amplitude of the transmitted waves of transducers 1P, 2P and 3S (polarized in the vertical direction) with load. The amplitude is normalized by the amplitude of each transducer at the start of the test. Transducer pair 1P-1P is located far from the flaws, to monitor the response of the intact rock during the test; transducer pair 2P-2P aligns with the upper tip of the top flaw to monitor crack initiation at this location, and pair 3S-3S goes through the ligament area to monitor crack initiation at the inner tips and crack coalescence. Figure 11b shows the cracks produced at the tips of the flaws and Fig. 11c the cracks at coalescence.

Crack initiation was monitored by both the DIC and the transmitted amplitude through the specimen. The plots of normalized amplitude in Fig. 11a indicate that the tensile crack at the exterior tip of the top flaw was detected by transducers 2P, prior to detection with DIC (see arrows in Fig. 11; T represents a tensile crack, S a shear crack, and "wave" or "DIC" the method of detection). Note that no damage is detected by pair 1P until coalescence, which is followed by unstable cracking, with the tensile crack from the external tip of the upper flaw crossing at this moment the path of the

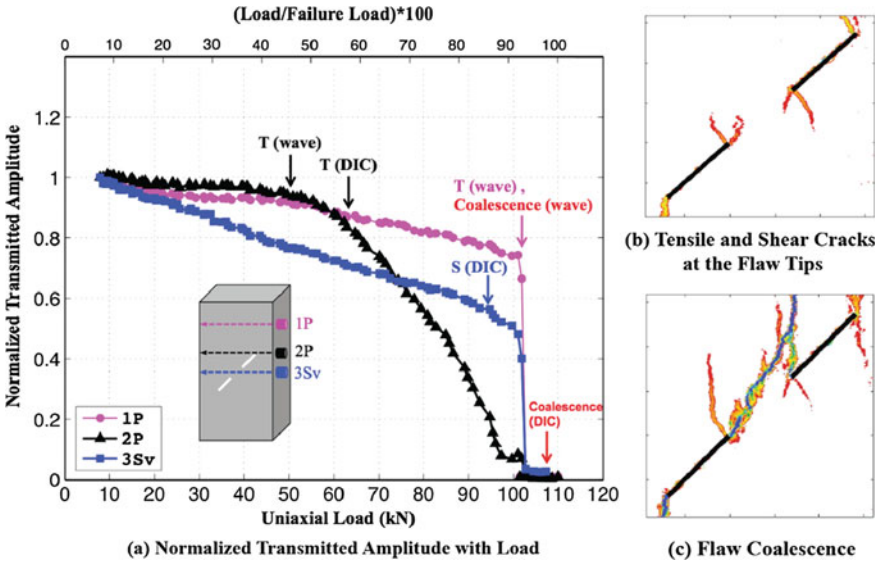

Fig. 11 Crack detection using active seismic monitoring

transducer pair. Coalescence is easily distinguished in the plot of transmitted waves from pair 3S by the abrupt loss of transmission due to the formation of the large, open, shear crack.

Additional tests with different flaw arrangements showed similar results, in that cracking can be detected using active seismic monitoring when the path of the crack intersects the path of the seismic wave, which results in a change of the transmission amplitude of the seismic wave [82].

5 Coupled Processes for Energy Extraction

Global challenges towards increase in sustainable and renewable energy extraction and decrease in carbon dioxide production define new directions in fundamental geotechnics research. Mechanical, hydromechanical, thermal and chemical processes in rock mass are coupled across spatial and temporal scales. Hydraulic fracturing, wellbore drilling, short and long-term fluid circulations, poro-elasticity and injections of carbon-dioxide gas in rock mass and saline aquifers are fundamentally not well understood due to coupled processes. Emergent technologies with relevance for energy sustainability and increase in renewable energy production which involve coupled processes in rocks are Enhanced Geothermal Systems (EGS) and Carbon-dioxide Capture and Sequestration (CCS). Development of renewable and sustainable geothermal energy source utilization, particularly trough location independent EGS,

as well as CCS has a huge potential for addressing climate change challenges and decreasing global warming due to increase in CO_2 in the atmosphere.

Geothermal reservoirs serve for renewable and sustainable energy production, where the hot rock mass turn cold water into steam. Water re-circulation through the fractures of hot rock formation enables running electrical production power plant turbines or is combined with housing heating back on the ground surface. In enhanced geothermal reservoirs (EGS), the basement or sediment reservoir rock permeability enhancement will enable sustainable and long-term stable heat extraction. However, enhancing permeability involves deep well drilling and hydraulic fracturing of highly stressed and hot rock mass, which are still performed with a limited success. An overview of geological, geomechanical and physical characteristics of current pilot EGS sites shows foundation for coupled processes understanding. Most of the experimental EGS sites reside in basement rocks below the sedimentary section, defined as areas of metamorphic or igneous rocks [105].

In the western USA, Tester et al. [105] identified several potential EGS areas with high temperatures (>200 °C) at relatively shallow depths (3–5 km). The Great Basin in USA has extensional stress regime, and highly variable rocks with depths of 4–10 km, where rock is mostly sedimentary with some granite or other basement rock types. At Snake River Plain, details of the geology and stress regime at depths 3–10 km are unknown, but probably volcanic and sediments overlay low permeability granitic basement at 3–5 km deep. In Oregon, the Cascade Range dominates volcanic and intrusive rocks. In Southern Rocky Mountains geothermal areas, which include the northern Rio Grande Rift and the Valles Caldera, big crustal radioactivity and high mantle heat flow were detected. Salton Sea is a young sedimentary basin with very high heat flow, characterized by young metamorphosed sedimentary rock types. Clear Lake Volcanic Field contains low-permeability Franciscan sediments and granite at deeper depths. There are possibilities at the Chena Hot Springs near Fairbanks in Alaska for further development of the existing conventional geothermal power plant. Hawaii is characterized with high temperatures in the basaltic rift, where they use conventional hydrothermal resources, while there is little subsurface information available outside the existing east rift of Kilauea volcano power plant.

Similar favorable conditions for potential development of EGS can be found in other continents, for example Cooper Basin and Paralana in Australia. In Europe, Soultz-sous-Forets in the Upper Rhine Valley area is represented with extensional stress regime [9, 13, 29] at the granitic highly fractured and faulted basement under 1.4 km thick sediment. Several pilot sites exist in Germany, for example granite Falkenberg test site is in northern Bavaria which proved that hydro-fractures can be propagated over significant distances in fractured crystalline rock, Bad Urach and Horstberg in northern Germany near Hannover. The Horstberg geothermal site contains low-permeability sediments which are experimented for geothermal energy extraction. In Basel, Switzerland, a pilot geothermal reservoir is placed in hot granitic basement at depth of 5 km, where the reservoir temperature is 200 °C. The Fjällbacka site in west coast of Sweden is developed as a research facility for studying hydro-mechanical aspects of hot dry rock reservoir development and for addressing geological and hydrogeological questions of Bohus granite.

Other pilot geothermal sites in Europe are Le Mayet de Montagne site in France where granite extends to the surface, Rosemanowes in Cornwall, UK is characterized with continuous granite batholith of early Permian age of more than 200 km in length, where the base of the granite extends bellow 9 km depth. The Hijiori site in Japan is placed on the edge of the caldera of the Pleistocene Gassan volcano with a very complex stress regime, and the reservoir contains several faults and many existing fractures. Ogachi site in Japan has very hot (> 230 °C) Grano-diorite rock. Despite numerous efforts put into EGS research through pilot sites, only few locations reached a commercial scale level for electricity production, for example Soultz-sous-Forets in France [105].

Numerical, theoretical and experimental work has been conducted along with the field work for obtaining a better understanding of various issues of geothermal reservoirs. EGS target hot granite rock mass, sedimentary reservoirs or interface between sediment cover and basement. As a result, the pilot sites yielded different problematic features ranging from in situ stress field to the pre-existing faults and fracture networks [39]. Poorly understood geology is one of the biggest obstacles in development of efficient EGS [58]. The competing tensile or shear failure mechanisms often occur simultaneously in geologically complex reservoir conditions. Non-linearity of key thermal and mechanical rock properties is related to stress state change, pore pressure changes and temperature change, which are accompanied by rock across-scale matrix alterations from micro to macro fracturing and fault shearing mechanisms.

5.1 Coupled Processes in Rock Mass

Coupled hydro-thermo-bio-chemo-mechanical (HTBCM) mechanisms in fractured rock mass are related to a short- and long-term reservoir behavior and energy extraction with respect to fracturing, permeability enhancement, biological microorganism growth and mineral precipitation-dissolution processes at fracture walls in geothermal reservoirs. Hydraulic processes include liquid and gas flow, air dissolution and diffusion in water, phase changes, vapor diffusion and gas generation and transport. Thermal processes are related to conductive and advective heat flow and transport in porous rock mass, but can also be part of thermomechanical gas behavior. Biological processes are considered trough bringing up a variety of ancient or unknown simple organisms from the rock mass. Chemical processes include dissolution and precipitation of minerals into rock pore fluids or fluids which migrate through fractures, and changes in pore fluid chemistry. Finally, mechanical processes are changes in stress, strain, and rock strength, constitutive relationships and laws. Mechanical processes also include poroelastic behavior of rock mass which can be described using Biot's theory.

Although there has been a significant effort to evaluate HTCM processes [15, 38, 43, 44, 54, 64, 77, 106, 107], the long-term HTCM effects have not yet been completely understood in the context of deep fractured geo-reservoirs. First, it was shown that evolution of fluid chemistry is linked to the rock permeability changes under dif-

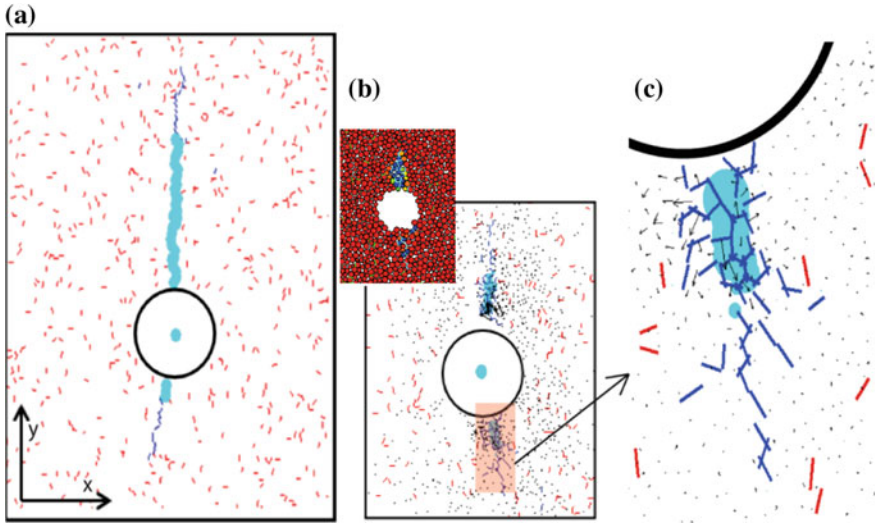

Fig. 12 Effect of hydro-thermo-mechanical coupling on micro-mechanics of hydraulic fracture propagation from a EGS reservoir wellbore in granite [107]

ferent stress states [86]. Second, thermo-mechanical stress changes cause irreversible strain and micro-cracking in granite as a consequence of complex mechanisms [53, 66, 67]. Thermal crack patterns in brittle materials are driven by inhomogeneous shrinkage stress fields, which can be described by fracture mechanics bifurcation analysis [5]. The crack propagation under thermal loading was studied to understand the instability from a straight to a wavy crack propagation [25]. Figure 12 shows results of a Discrete Element Method simulation with the development of a hydraulic fracture and micro-cracks under geothermal reservoir conditions. By comparing a model with and without thermally induced stresses, it can be seen that HTM processes result in a shorter hydraulic fracture, with significant thermal damage and microcracks [107]. As a result, it is still not clear to what extent linear elastic fracture mechanics can be applied to quasi-brittle rocks in geologic reservoirs; also, rock features (micro-structure, grains and existing fractures) effects on fracture propagation have not yet been completely quantified.

5.2 Multi-physics and Across-Scales Problems in Deep Geo-Reservoirs

Besides various process couplings, problems with understanding the rock mass behavior in geothermal reservoirs are due to multi-physics processes which may occur across various temporal and spatial scales. The hydraulic, mechanical, thermal and chemical mass transport and response will propagate throughout the systems at

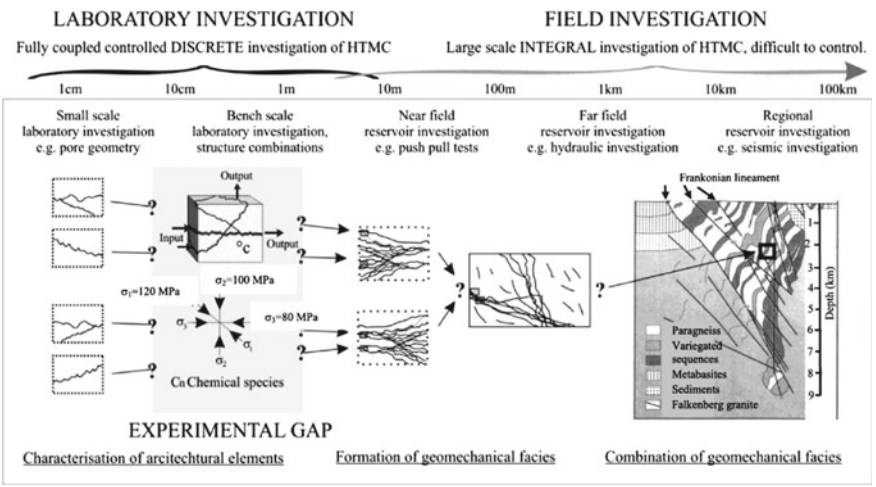

Fig. 13 Across-scale processes in geo-reservoirs, investigation approaches and the experimental gap [78]

rates which are several orders of magnitude different from each other [63]. Fluid flow, energy and mass transport in fractured-porous subsurface formations are characterized by complex interactions between fluid and solid phases, mainly controlled by thermal, hydraulic, mechanical and chemical (THMC) processes. The investigations of complex flow process relationships require both the identification of the relevant fundamental processes and the quantification of process parameters in the laboratory and in the field, as well as development and application of prognostic numerical tools. Linear and non-linear relationships and feedback mechanisms between the processes, the relative importance of processes and process parameters, as well as the influence of the large spectrum of spatial and temporal scales on the long-term performance of a reservoir are a challenge in the investigation and systems quantification. Figure 13 shows complexity of problems related to spatial scale investigation ranging from 1 cm to 100 km scales. Integral large-scale investigation of HTMC is difficult to control [78].

Despite the research efforts conducted in geothermal reservoirs, fundamental multi-physics in fractured subsurface rock simulated in reservoir situ-conditions have not yet been completely understood. Laboratory investigation is usually conducted in high stress and high temperature triaxial tests, but on relatively small rock samples. Larger sample sizes collected form the reservoir wellbores need to be considered, considering existing and new fractures and geological variations within samples. Specifically, further research is needed on: (1) stress-strain behavior in the light of cross-scales rock anisotropy parameters under high stress and increased temperature contrast between rock matrix and fluid in fractures and pores; (2) impact of the in situ stress magnitude, contrast and principal stresses rotation on rock fracture system and fluid flow in fractures; (3) fluid flow field through realistically rough, stressed and

deformable fracture systems; and (4) hydro-thermo-mechanical effects on fracture propagation and induced seismicity in various geological conditions.

Structural heterogeneities of basement rocks are widely present in geo-reservoirs across several spatial magnitude scales. For example, at the Desert Peak geothermal field in Nevada, USA, the basement stratigraphy was found to be complicated by thrust faults and other Mesozoic-aged faults [73]. Decreasing the size of the observed geological rock in geothermal reservoirs from the reservoir scale towards the laboratory scale, numerous petrologic effects on mechanical parameters have been previously identified which cannot be studied on a small lab sample. Some examples include matrix composition, matrix fabric, pre-existing foliation planes, crystal and clast content, ductile grains and clays, vein mineralogy and fracture intensity and primary and secondary porosity [73].

Failure criteria of heterogeneous rocks are complicated due to rock composition. While testing on homogeneous rocks usually results in either elastic-plastic or elastic-brittle stress-strain behavior, highly heterogeneous rocks with a mixture of weak and strong components yield a strain hardening behavior [16]. Fracture propagation upper bound depends on the sample size because of the adjacent crack closure, which occurs before the fracture propagates [30]. Structural heterogeneities are present not only due to rock mineralogy but also at a flow system of fractures in rock mass. Figure 14 shows a current approach for experimenting on fracture-porous rock systems. Even at the laboratory scale, several different scenarios can be identified. Quasi 2-D single fracture flow experiments vary from artificial to natural fracture roughness identification and representation, while in linear core flood experiments flow occurs either through a full flow fracture, a system of porous matrix and isolated fracture or a fracture system. Figure 14f shows a photograph of a fractured rock sample with highlighted flow fractures. Due to a complexity of isolated and interconnected fractures, the flow in the rock mass is still a challenge to understand and relate across scales processes.

Strain hardening and anisotropic rock parameters understanding requires cyclic triaxial testing of rocks. During the cyclic testing, hysteresis loops are observed in stress-strain curves, which correspond to loading-unloading cycles and are associated with fractures and micro-crack development [35]. Particularly, microscopic processes demonstrate initiation, propagation and coalescence of micro cracks or damage, which eventually forms macroscopic features of a brittle failure. The character of the obtained non-linear stress-strain curves depends on the magnitude of the confining pressure in triaxial tests [35]. After initiation by the initial flaw, the fracture can arrest instead of propagating further into the heterogeneous rock, which questions the applicability of the linear elastic fracture mechanics principles for reservoir rocks. Particularly, it was observed how cracks may extend readily through a crystal grain but cannot continue across the grain boundary without a significant increase in driving stress or a reduction in confinement beyond the grain scale [22]. Rotation of principal stresses in rock influences crack propagation, interaction and ultimately coalescence and failure in numerical models [30]. Four patterns of stress changes were identified in rock in the vicinity of fractures; the stress orientation rotates abruptly in the vicinity of fractures; the orientation rotates gradually, breakouts are suppressed at fractures

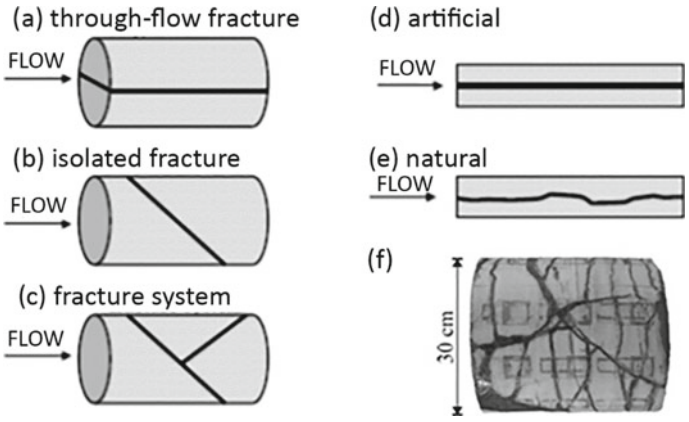

Fig. 14 Types of fracture-porous rock systems used in the experiments. Linear core flood experiments (**a**, **b**, **c**) and quasi-2D single fracture flow experiments (**d**, **e**) [101], with a photography of a fractured rock sample (**f**)

or lithological boundaries; the orientation does not change across fractures [71]. Regions around the wellbore in georeservoirs fail in a manner which is strongly controlled by the magnitude and orientation of the in situ stress field, and they can be also used to identify the in situ stress field [120].

Key Questions: How are chemical, mechanical, thermal and bio processes coupled? Which coupling mechanism is relevant at which temporal or spatial scales? Can some processes be treated as un-coupled in analysis? What is the impact of biological species bringing up to the surface from deep geo-reservoirs? How is mineral dissolution and precipitation affecting long-term performance of geothermal reservoir or carbon dioxide underground storage? How can long-term processes be studied in the laboratory, is there a way to catalyze chemical reactions without negatively affecting the process coupling mechanisms?

6 Sustainable Recovery of Subsurface Energy Resources

Worldwide and US baseload capacity is of the order of 10-15TW and currently relies on large scale industrial processes (~90% thermal combustion of fossil fuels and fission) rather than on distributed generation by truly renewable means (< 10% wind, solar, hydropower). Despite a desired transition to true renewables, the imbalance between energy production by traditional fossil means versus that by renewables is formidable and transitional fuels and bridging energy sources are needed. Feasible transition to a low carbon economy includes the switching from high-carbon coal and oil to lower-carbon natural gas present in gas shales and in potentially augmenting fossil combustion with CO_2 sequestration and in ultimately replacing these methods

with deep geothermal energy and nuclear fission. These transformations require the ability to characterize and control the evolution of the subsurface, in particular the evolution of transport properties that allows the recovery of such fuels and energy and the entombment of undesirable products. This must be completed with minimal environmental impact, including fugitive fluids and induced or triggered seismicity. The following explores the linkage between seismicity and permeability—first where seismicity exists as a hazard and then where it may be applied as a useful tool in characterizing the subsurface.

6.1 Induced Seismicity as a Hazard

Human-induced versus naturally-triggered seismicity differ principally in the magnitude and related duration of the events—human-induced events have historically been smaller but are nonetheless problematic and are not necessarily limited to small events where faults of sufficient size are present [37]. Modern observations in earthquake seismology have identified a rich spectrum of events spanning six decades of duration (e.g. [88] for large "earthquakes" that may evolve either seismically (duration ~10^1 s) or aseismically (duration ~10^7 s) for similar seismic moments (seismic moments of ~10^{20} Nm) (Fig. 15). The energy release in these two prototypical classes of events is identical but the related hazard and prospective damage is much less for the longer duration events because the energy release is dissipated over a period one million times longer.

Slow slip events are also observed in laboratory scale experiments [62] where the length of the fault is necessarily limited to the dimension of the sample (but the stress drop commensurate with that of a plate boundary scale) and in underground research laboratories at the scale of meters [48]. Correspondingly, this richness in the deformation-duration spectrum is inferred at all length scales including those likely for slip in reservoirs. Thus, we seek to understand how this behavior is manifest at the scale of intermediate length fractures and faults in the range of meters to kilometers, rather than tens to hundreds of kilometers, as in the case of earthquake seismology—and infer that laboratory experimentation coupled with mechanistic upscaling provides a viable method to explore this behavior.

Seismic events in reservoirs result where slip occurs typically on pre-existing fractures that are reactivated by a changing stress regime. Depending on the environmental factors, changes in effective stress are induced by fluid pressures, thermal stresses or chemical (dissolution or desorption, [37, 59, 112]) stresses in the reservoir. These effects have been observed in geothermal reservoirs, most notably for the evolution of seismicity at the ill-fated EGS project in Basel, Switzerland [45, 99] and for those at other EGS projects around the world [99]. More prevalent, however is the recent spate of seismicity associated with the reinjection of produced waters from depleting conventional hydrocarbon reservoirs in the mid-western United States, from the reinjection of hydraulic fracturing fluids [33] and triggered from hydraulic fracturing itself [7]. These events can be large ($4 < M < 6$) and are both induced

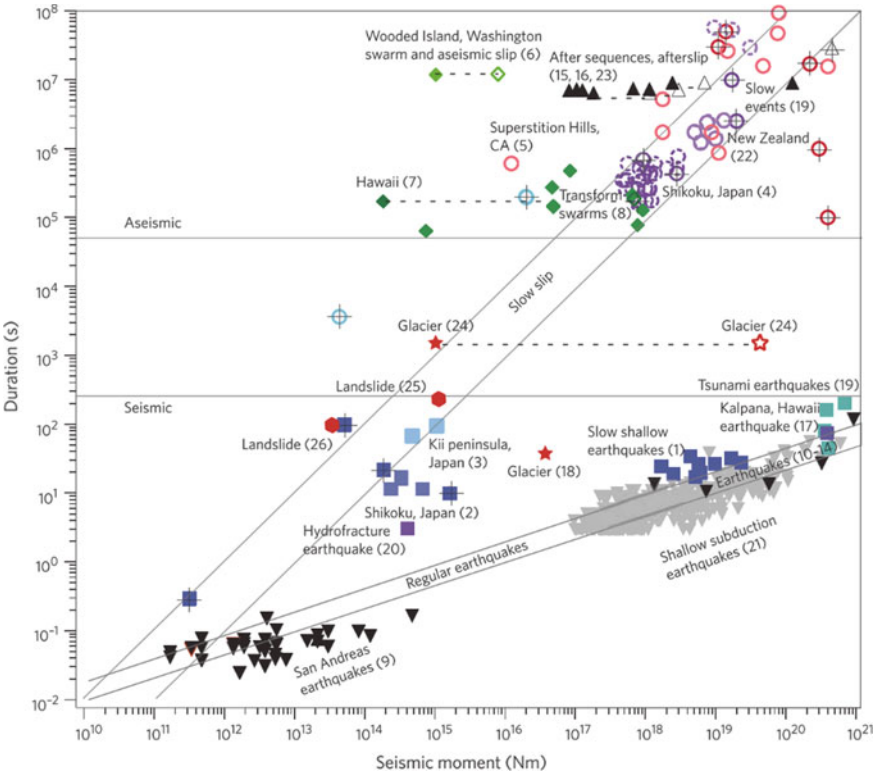

Fig. 15 Classification of slip events with respect to duration and released seismic moment [88]

and triggered. The events result from reducing the clamping stresses on critically oriented faults that may be blind and may be located within the reservoir itself or in underlying basement rocks (Fig. 16).

Key Questions: What is the size of the maximum credible seismic event? What are the controls on this transition in behavior from aseismic to seismic? How do mineralogy, global system stiffness, roles of fluid pressurization and dilatancy affect this transition? How are these individual mechanisms characterized? What are the prospects for control if these features are understood?

6.2 *Induced Seismicity as a Tool*

Evaluating both initial and evolving hydraulic properties of fractured reservoirs is vital for the development of both deep geothermal and shale gas reservoirs and in defining the integrity of caprocks. In this, the presence of passive seismicity as

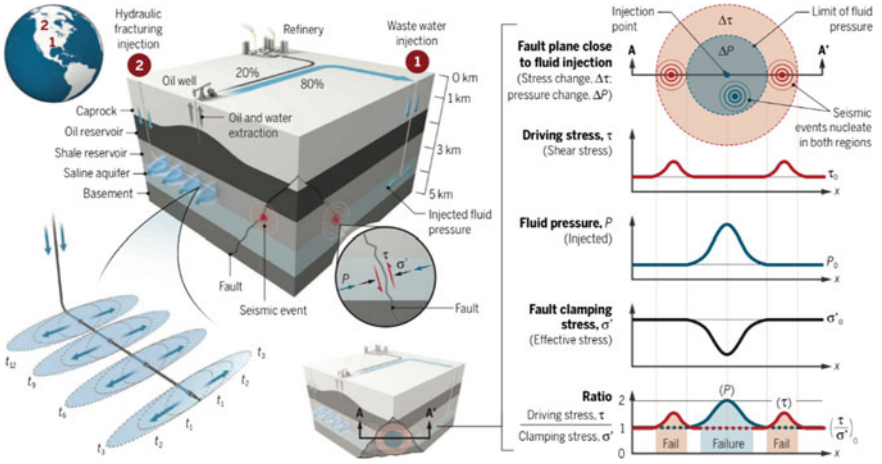

Fig. 16 A vertical well taps a conventional oil reservoir whereas a horizontal well accesses a shale reservoir for gas. Wastewater reinjection into a saline aquifer (shown in 1) and the injection of fracturing fluid (principally water) into the shale reservoir (shown in 2) have the same impact in elevating fluid pressures and driving the stress state on a deeply penetrating fault to failure. In cross section A-A', injection of fluid near the fault causes slip by contrasting mechanisms in both the near-field and the far-field. The net effect of these two mechanisms is to elevate driving stress above the clamping stresses in these two concentric regions, and to potentially induce seismic slip [33]

micro-earthquakes (MEQs) may be used to image the subsurface for the evolution of permeability that is crucial to the recovery of the resource.

During stimulation, the virgin hydraulic diffusivity can be estimated from the spatio-temporal growth rate of abundant in situ microearthquakes (MEQs) (Fig. 17). This method can estimate the permeability at reservoir scale. However, it has limitations in constraining the subsequent evolution of fracture permeability at relatively smaller length scales that are important in defining reservoir response during stimulation and then production.

To constrain regional initial and evolving permeability at relatively smaller length scales, it is possible to provide a linkage between moment magnitudes of observed MEQs and the measured evolution of fracture-network permeability [34]. Thus, the location and moment magnitude of MEQs (Fig. 18) may be used to estimate fracture apertures of individual events that are a function of in situ stresses, fluid pressure, shear displacement and fracture size. Assuming the veracity of the cubic law, results show that the equivalent virgin permeability at reservoir scale may be enhanced by about one order of magnitude while some local fracture permeability can be enhanced by ~2 to ~3 orders of magnitude. This method is of importance as it allows abundant observations of MEQs to constrain the structure and distribution of in situ permeability evolution. Since in situ geomechanical conditions (e.g., fracture stiffness, dilation and friction) also play a crucial role in affecting the accuracy of the permeability estimation, in situ fracture characterization is an important component in constraining these observations.

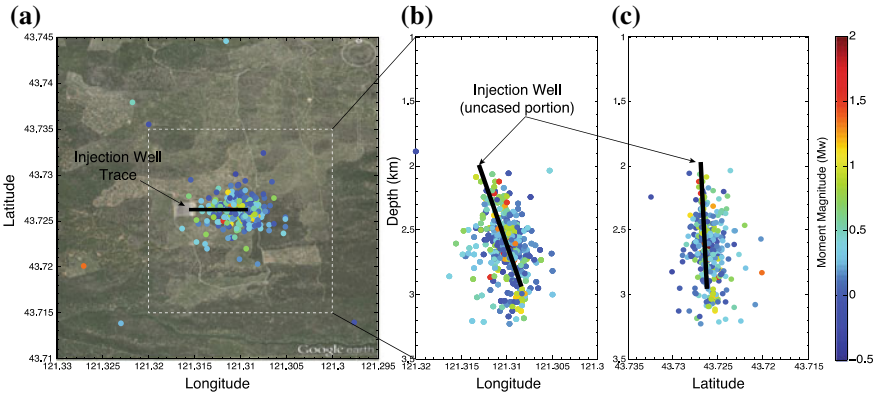

Fig. 17 **a** Map view of distribution of 350 seismic events in Newberry EGS reservoir during 2014 stimulation; **b** Vertical view of MEQ distribution with Longitude; **c** Vertical view of MEQ distribution with Latitude [34]

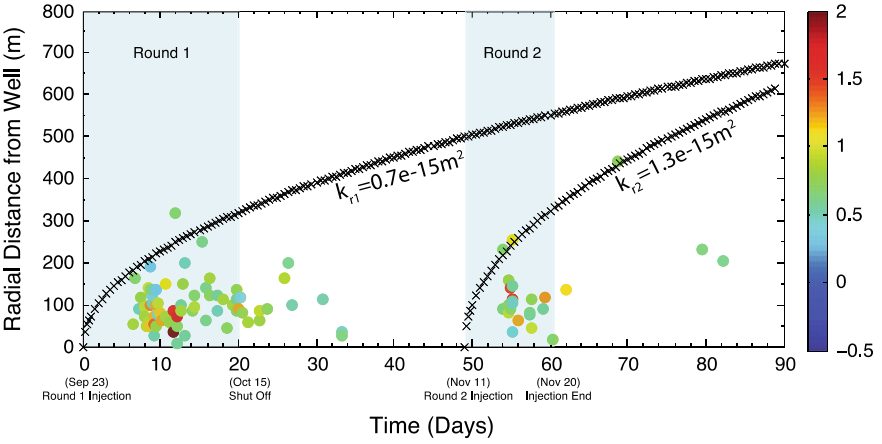

Fig. 18 Spatio-temporal distribution of fluid-injection-induced seismicity during the 2014 Newberry EGS stimulation. Diffusion-length versus time curve labeled for equivalent permeabilities at reservoir scale [34]

Key Questions: What are key mechanisms of permeability evolution in fractured reservoirs? What is the interplay between mechanisms that result in either the creation or destruction of porosity? What are their respective characteristic timescales? How are changes in porosity scaled to the evolution of permeability? How does the seismic energy budget relate to permeability evolution? What are key mechanisms heralding the transition between seismic and aseismic permeability evolution? What is the feasible minimum resolution of detection?

7 Discussion

The material included in this chapter aligns, to a larger extent, with the interest and expertise of the authors. The underlying motivation, and first objective, for putting together all these different views and opinions was to highlight fundamental and key questions that need to be tackled, if the Grand Challenges are to be addressed in ways that will enhance the ability of rock mechanics and rock engineering to aid in solving the problems that our society faces in the 21st century. The second objective was to identify research priorities to address the Grand Challenges. The following topics have been identified, based on the material included in the chapter and on discussions among all the participants of the NSF-sponsored workshop "Geotechnical Fundamentals in the Face of New World Challenges".

Transparent Earth: One of the problems that limits advancements in the field of rock mechanics is the inability to scrutinize the interior of the Earth to assess the current state at every single point and its evolution with time, as well as constitutive behavior. New techniques and approaches are required to characterize the underground at multiple scales.

Complex Coupled Processes across Time and Spatial Scales: Rocks are highly heterogeneous, with complex behavior that is not only stress and time dependent, but also, and this is most important, scale dependent. The interplay that exists between the rock matrix, discontinuities, fluid, temperature and biological processes across scales is not well understood, and such knowledge is critical for many applications such as energy extraction and storage. The theory of damage and healing poromechanics is in its infancy; coupled effects of crack opening, closure and rebonding on stiffness and permeability have not been investigated. Rock permeability models do not account for anisotropic healing processes. Predicting the critical sequences of events that lead to pore connectivity is a challenge. New tools that are robust and accurate are needed.

Fault Reactivation and Induced Seismicity: There is clear evidence that the interaction between anthropogenic activities that change the state of stress in the underground are responsible for both inducing and triggering earthquakes that have the potential to cause severe damage to existing infrastructure. The knowledge required to identify hidden faults as well as assess their potential for slip and to quantify the impact of such slip is insufficient.

Risk removal from underground construction: Significant resources are obtained from the underground, which are then used for critical human activities such as transportation, energy and waste storage, shelter, etc. The risks associated with such activities continue to be much larger than with the aboveground, and impact both human as well as environmental and infrastructure safety. A better holistic approach is needed to reduce the risk to acceptable levels, at least similar to those of the aboveground.

Water, Environmental Impact: Potable water supplies in the subsurface are a critical resource. Any detrimental impact on underground water resources and quality has the potential to have large spatial and temporal consequences that may reach the bio-

sphere. This is a complex coupled problem that requires a comprehensive approach through different scales. New tools to predict flow through the rock mass and coupled bio-chemical-thermal processes between fluid flow and mechanical behavior of the rock are needed.

Selective extraction for more efficient mining: Ore extraction from mining is still based on practices that are rooted on empiricism. The result is a process that is largely inefficient, can rarely be extrapolated to different environments and is associated with high risk, large environmental impact and is not sustainable. Better approaches to benefit resource extraction through mining are required to continue to meet the increasing human needs.

Advances in disciplines such as sensing and remote sensing, numerical methods, theoretical and computational poromechanics, synthetic materials and 3D printing, big data and artificial intelligence, among others, provide opportunities to probe the behavior of the subsurface and obtain new insights, as well as open new avenues for research and education. This cross-disciplinary partnership is required to address the challenges of this century. New approaches and new solutions will be demanded by the public, which will require close collaboration among disciplines. One such challenge will stem out of society's continuous demand for improved levels of comfort and access to sustainable, safe and renewable resources. The science required to face these problems is inherently interdisciplinary, but not yet available. Finding solutions for these questions is a great challenge but also a great opportunity. If the rock mechanics/geomechanics profession wants to participate, it has to do so by outgrowing its traditional niches and embracing other fields.

References

1. Arson, C., Xu, C., Chester, F.M.: On the definition of damage in time-dependent healing models for salt rock. Geotechnique Lett. **2**(2), 67–71 (2012)
2. Arson, C.: Generalized stress variables in continuum damage mechanics. Mech. Res. Commun. **60**, 81–84 (2014)
3. Arson, C., Gatmiri, B.: Thermo-hydro-mechanical modeling of damage in unsaturated porous media: theoretical framework and numerical study of the EDZ. Int. J. Numer. Anal. Meth. Geomech. **36**(3), 272–306 (2012)
4. Arson, C., Pereira, J.M.: Influence of damage on pore size distribution and permeability of rocks. Int. J. Numer. Anal. Meth. Geomech. **37**(8), 810–831 (2013)
5. Bahr, H., Weiss, H., Bahr, U., Hofmann, M., Fischer, G., Lampenscherf, S., Balke, H.: Scaling behavior of thermal shock crack patterns and tunneling cracks driven by cooling or drying. J. Mech. Phys. Solids **58**(9), 1411–1421 (2010)
6. Balendran, B., Nasser, S.M.: Double sliding model for cyclic deformation of granular materials, including dilatancy effects. J. Mech. Phys. Solids **41**(3), 573–612 (1993)
7. Bao, X., Eaton, DW.: Fault activation by hydraulic fracturing in Western Canada. Science, vol. 354 (2016)
8. Bargellini, R., Halm, D., Dragon, A.: Modelling of anisotropic damage by microcracks: towards a discrete approach. Arch. Mech. **58**(2), 93–123 (2006)
9. Baria, R., Baumgartner, J., Gerard, A., Jung, R., Garnish, J.: European HDR research programme at soultz-sous-forets (France) 1987–1996. Geothermics **28**(4–5), 655–669 (1999)

10. Bazant, Z.P., Ozbolt, J.: Nonlocal microplane model for fracture, damage, and size effect in structures. J. Eng. Mech. **116**(11), 2485–2505 (1990)
11. Bazant, Z.P., Jirasek, M.: Nonlocal integral formulations of plasticity and damage: survey of progress. J. Eng. Mech. **128**(11), 1119–1149 (2002)
12. Bazant, Z.P., Oh, B.: Microplane model for progressive fracture of concrete and rock. J. Eng. Mech. **111**(4), 559–582 (1985)
13. Blackwell, D.D., Negraru, P.T., Richards, M.C.: Assessment of the enhanced geothermal system resource base of the United States. Nat. Resour. Res. **15**(4), 283–308 (2006)
14. Bourgeois, F., Burlion, N., Shao, J.: Modelling of elastoplastic damage in concrete due to desiccation shrinkage. Int. J. Numer. Anal. Meth. Geomech. **26**(8), 759–774 (2002)
15. Bower, K.M., Zyvoloski, G.: A numerical model for thermo-hydro-mechanical coupling in fractured rock. Int. J. Rock Mech. Min. Sci. **34**(8), 1201–1211 (1997)
16. Bro, S.: Analysis of multistage triaxial test results for a strain-hardening rock. Int. J. Rock Mech. Mining Sci. **34**(1), 143–145 (1997)
17. Bunger, A.P., Kear, J., Dyskin A.V., Pasternak, E.: Interpreting post-injection acoustic emission in laboratory hydraulic fracturing experiments. In: 48th US Rock Mechanics/Geomechanics Symposium. American Rock Mechanics Association (2014)
18. Carvalho, F., Labuz, J.: Moment tensors of acoustic emissions in shear faulting under plane-strain compression. Tectonophysics **356**(1–3), 199–211 (2002)
19. Cauvin, A., Testa, R.B.: Damage mechanics: basic variables in continuum theories. Int. J. Solids Struct. **36**(5), 747–761 (1999)
20. Chaboche, J.L.: Damage induced anisotropy. on the difficulties associated with the active/passive unilateral condition. Int. J. Damage Mech. **1**(2), 148–171 (1992)
21. Chen, G., Kemeny, J., Harpalani, S.: Fracture propagation and coalescence in marble plates with pre-cut notches under compression. Int. J. Rock Mech. Min. Sci. & Geomech. Abstracts, **30**(5), 279 (1993)
22. Cho, S.H., Ogata, Y.J., Kaneko, K.: Strain-rate dependency of the dynamic tensile strength of rock. Int. J. Rock Mech. Min. Sci. **40**(5), 763–777 (2003)
23. Choi, M., Bobet, A., Nolte, L.P.: The effect of surface roughness and mixed-mode loading on the stiffness ratio x/z for fractures. Geophysics **79**(5), D319–D331 (2014)
24. Collins, I.F., Houlsby, G.T.: Application of thermo mechanical principles to the modelling of geotechnical materials. In: Proceedings of the Royal Society of London a Mathematical, Physical and Engineering Sciences, vol. 453, pp. 1975–2001. The Royal Society (1997)
25. Corson, F., Bedia, M., Henry, H., Katzav, E.: Thermal fracture as a framework for quasi-static crack propagation. Int. J. Fract. **158**(1), 1–14 (2009)
26. Cowin, S.C.: The relationship between the elasticity tensor and the fabric tensor. Mech. Mater. **4**(2), 137–147 (1985)
27. de Borst, R., Pamin, J., Geers, M.D.: On coupled gradient-dependent plasticity and damage theories with a view to localization analysis. Euro. J. Mech.-A/Solids **18**(6), 939–962 (1999)
28. Detournay, E., Garagash, D.: The near-tip region of a fluid-driven fracture propagating in a permeable elastic solid. J. Fluid Mech. **494**, 1–32 (2003)
29. Dezayes, C., Genter, A., Thinon, I., Courrioux, G., Tourliere, B.: Geothermal potential assessment of clastic triassic reservoirs (Upper Rhine Graben, France). In: 32nd Workshop on Geothermal Reservoir Engineering, pp. 28–30 (2008)
30. Diederichs, M.S., Kaiser, P.K., Eberhardt, E.: Damage initiation and propagation in hard rock during tunnelling and the influence of near-face stress rotation. Int. J. Rock Mech. Min. Sci. **41**(5), 785–812 (2004)
31. Dormieux, L., Kondo, D.: Approche micromecanique du couplage permeabilite-endommagement. C.R. Mec. **332**(2), 135–140 (2004)
32. Dyskin, A.V., Germanovich, L.N., Ustinov, K.B.: A 3-D model of wing crack growth and interaction. Eng. Fract. Mech. **63**(1), 81–110 (1999)
33. Elsworth, D., Spiers, C.J., Niemeijer, A.R.: Understanding induced seismicity. Science **354**(6318), 1380–1381 (2016)

34. Fang, Y., Elsworth, D., Cladouhos, T.J.: Reservoir permeability mapping using microearthquake data. Geothermics **72**, 83–100 (2018)
35. Fang, Z., Harrison, J.P.: Application of a local degradation model to the analysis of brittle fracture of laboratory scale rock specimens under triaxial conditions. Int. J. Rock Mech. Min. Sci. **39**(4), 459–476 (2002)
36. Fuenkajorn, K., Phueakphum, D.: Laboratory assessment of healing of fractures in rock salt. Bull. Eng. Geol. Env. **70**(4), 665 (2011)
37. Gan, Q., Elsworth, D.: Analysis of fluid injection-induced fault reactivation and seismic slip in geothermal reservoirs. J. Geophys. Res. Solid Earth **119**(4), 3340–3353 (2014)
38. Gelet, R., Loret, B., Khalili, N.: A thermo-hydro-mechanical coupled model in local thermal non-equilibrium for fractured HDR reservoir with double porosity. J. Geophys. Res. Solid Earth, **117**(B7) (2012)
39. Genter, A., Evans, K., Cuenot, N., Fritsch, D., Sanjuan, B.: Contribution of the exploration of deep crystalline fractured reservoir of soultz to the knowledge of enhanced geothermal systems (EGS). Comptes Rendus Geosci. **342**(7–8), 502–516 (2010)
40. Germain, P.: La methode des puissances virtuelles en mecanique des milieux continus. Première partie: théorie du second gradient. J. Mecanique **12**, 235–274 (1973)
41. Germain, P.: The method of virtual power in continuum mechanics. Part 2: microstructure. SIAM J. Appl. Math. **25**(3), 556–575 (1973)
42. Germanovich, L.N., Carter, B.J., Ingraea, A.R., Dyskin, A.V., Lee, K.K.: Mechanics of 3-D crack growth under compressive loads. In: Rock Mechanics Tools and Techniques. Proceedings of the Second North American Rock Mechanics Symposium: NARMS, vol. 96, pp. 1151–1160 (1996)
43. Ghassemi, A., Tarasovs, S., Cheng, A.H.: Integral equation solution of heat extraction-induced thermal stress in enhanced geothermal reservoirs. Int. J. Numer. Anal. Meth. Geomech. **29**(8), 829–844 (2005)
44. Ghassemi, A., Nygren, A., Cheng, A.: Effects of heat extraction on fracture aperture: a poro-thermoelastic analysis. Geothermics **37**(5), 525–539 (2008)
45. Goertz, B.P., Goertz, A., Wiemer, S.: Stress drop variations of induced earthquakes at the basel geothermal site. Geophys. Res. Lett. **38**(9) (2011)
46. Goodfellow, S.D., Nasseri, M.B.H., Young, R.P.: Source parameters of acoustic emission observed in laboratory and mine environments. In: 48th US Rock Mechanics/Geomechanics Symposium. American Rock Mechanics Association (2014)
47. Gueguen, Y., Dienes, E.: Transport properties of rocks from statistics and percolation. Math. Geol. **21**(1), 1–13 (1989)
48. Guglielmi, Y., Cappa, F., Avouac, J.P., Henry, P., Elsworth, D.: Seismicity triggered by fluid injection-induced aseismic slip. Science **348**(6240), 1224–1226 (2015)
49. Halm, D., Dragon, A.: An anisotropic model of damage and frictional sliding for brittle materials. Euro. J. Mech.-A/Solids **17**(3), 439–460 (1998)
50. Hampton, J.C., Hu, D., Matzar, L., Gutierrez, M.: Cumulative volumetric deformation of a hydraulic fracture using acoustic emission and micro-CT imaging. In: 48th US Rock Mechanics/Geomechanics Symposium. American Rock Mechanics Association (2014)
51. Hedayat, A., Pyrak, L., Bobet, A.: Multi-modal monitoring of slip along frictional discontinuities. Rock Mech. Rock Eng. **47**(5), 1575–1587 (2014)
52. Hedayat, A., Pyrak, L., Bobet, A.: Precursors to the shear failure of rock discontinuities. Geophys. Res. Lett. **41**(15), 5467–5475 (2014)
53. Heuze, F.E.: High-temperature mechanical, physical and thermal properties of granitic rocksa re-view. In International Journal of Rock Mechanics and Mining Sciences and Geomechanics Abstracts, vol. 20, pp. 3–10. Elsevier (1983)
54. Hicks, T.W., Pine, R.J., Willis, J., Xu, S., Jupe, A.J., Rodrigues, N.E.V.: A hydro-thermo-mechanical numerical model for hdr geothermal reservoir evaluation. In: International Journal of Rock Mechanics and Mining Sciences and Geomechanics Abstracts, vol. 33, pp. 499–511. Elsevier (1996)

55. Hoeppe, P.: Trends in weather related disasters—consequences for insurers and society. Weather Clim. Extremes **11**, 70–79 (2016)
56. Hou, Z.: Mechanical and hydraulic behavior of rock salt in the excavation disturbed zone around underground facilities. Int. J. Rock Mech. Min. Sci. **40**(5), 725–738 (2003)
57. Houben, M.E., Hove, A., Peach, C.J., Spiers, C.J.: Crack healing in rocksalt via diffusion in adsorbed aqueous films: microphysical modelling versus experiments. Phys. Chem. Earth Parts A/B/C **64**, 95–104 (2013)
58. Huang, S., Liu, J.: Geothermal energy stuck between a rock and a hot place. Nature **463**(7279), 293 (2010)
59. Izadi, G., Elsworth, D.: The effects of thermal stress and fluid pressure on induced seismicity during stimulation to production within fractured reservoirs. Terra. Nova **25**(5), 374–380 (2013)
60. Jin, W., Xu, H., Arson, C., Busetti, S.: A multi-scale computation tool coupling mode II fracture propagation and damage zone evolution. Inter. J. Numer. Anal. Met. Geomech. **41**, 223–250 (2017)
61. Kachanov, M.: Effective elastic properties of cracked solids: critical review of some basic concepts. Appl. Mech. Rev. **45**(8), 304–335 (1992)
62. Kaproth, B.M., Marone, C.: Slow earthquakes, preseismic velocity changes, and the origin of slow frictional stick-slip. Science **341**(6151), 1229–1232 (2013)
63. Kim, S., Hosseini, S.A.: Hydro-thermo-mechanical analysis during injection of cold fluid into a geologic formation. Int. J. Rock Mech. Min. Sci. **77**, 220–236 (2015)
64. Kohl, T., Evansi, K.F., Hopkirk, R.J., Rybach, L.: Coupled hydraulic, thermal and mechanical considerations for the simulation of hot dry rock reservoirs. Geothermics **24**(3), 345–359 (1995)
65. Krajcinovic, D.: Damage mechanics, vol. 41. Elsevier (1996)
66. Kranz, R.L.: Crack-crack and crack-pore interactions in stressed granite. In International Journal of Rock Mechanics and Mining Sciences and Geomechanics Abstracts, vol. 16, pp. 37–47. Elsevier (1979)
67. Kranz, R.L.: Microcracks in rocks: a review. Tectonophysics **100**(1–3), 449–480 (1983)
68. Lemaitre, J., Desmorat, R.: Engineering damage mechanics: ductile, creep, fatigue and brittle failures. Springer Science and Business Media (2005)
69. Levasseur, S., Collin, F., Charlier, R., Kondo, D.: On micromechanical damage modeling in geomechanics: influence of numerical integration scheme. J. Comput. Appl. Math. **246**, 215–224 (2013)
70. Lin, Q., Yuan, H., Biolzi, L., Labuz, J.K.: Opening and mixed mode fracture processes in a quasi-brittle material via digital imaging. Eng. Fract. Mech. **131**, 176–193 (2014)
71. Lin, W., Yeh, E., Hung, J., Haimson, B., Hirono, T.: Localized rotation of principal stress around faults and fractures determined from borehole breakouts in hole B of the Taiwan Chelungpu-fault drilling project (TCDP). Tectonophysics **482**(1–4), 82–91 (2010)
72. Lubarda, V.A., Krajcinovic, D.: Damage tensors and the crack density distribution. Int. J. Solids Struct. **30**(20), 2859–2877 (1993)
73. Lutz, S.J., Hickman, S., Davatzes, N., Zemach, E., Drakos, P., Robertson, A.: Rock mechanical testing and petrologic analysis in support of well stimulation activities at the desert peak geothermal field, Nevada. In: Proceedings 35th Workshop on Geothermal Reservoir Engineering (2010)
74. Makhnenko, R.Y., Ge, C., Labuz, J.F.: AE from undrained and unjacketed tests on sandstone. In: 46th US Rock Mechanics/Geomechanics Symposium. American Rock Mechanics Association (2012)
75. Maleki, K., Pouya, A.: Numerical simulation of damage-permeability relationship in brittle geomaterials. Comput. Geotech. **37**, 619–628 (2010)
76. Masson, R., Bornert, M., Suquet, P., Zaoui, A.: An affine formulation for the prediction of the effective properties of nonlinear composites and polycrystals. J. Mech. Phys. Solids **48**(6–7), 1203–1227 (2000)

77. McCartney, J.S., Sanchez, M., Tomac, I.: Energy geotechnics: advances in subsurface energy recovery, storage, exchange, and waste management. Comput. Geotech. **75**, 244–256 (2016)
78. McDermott, C.I., Randriamanjatosoa, A.R., Tenzer, H., Kolditz, O.: Simulation of heat extraction from crystalline rocks: the influence of coupled processes on differential reservoir cooling. Geothermics **35**(3), 321–344 (2006)
79. Miao, S., Wang, M., Schreyer, H.L.: Constitutive models for healing of materials with application to compaction of crushed rock salt. J. Eng. Mech. **121**(10), 1122–1129 (1995)
80. Mirkhani, H., Joshi, S.P.: Mechanism-based crystal plasticity modeling of twin boundary migration in nanotwinned face-centered-cubic metals. J. Mech. Phys. Solids **68**, 107–133 (2014)
81. Modiriasari, A., Bobet, A., Pyrak, L.J.: Monitoring of mechanically-induced damage in rock using transmission and reflection of elastic waves. In: 49th US Rock Mechanics/Geomechanics Symposium. American Rock Mechanics Association (2015)
82. Modiriasari, A., Bobet, A., Pyrak-Nolte, L.J.: Active seismic monitoring of crack initiation, propagation, and coalescence in rock. Rock Mech. Rock Eng. **50**(9), 2311–2325 (2017)
83. Moradian, Z., Einstein, H.H.: Monitoring cracking process of gypsum by means of acoustic emission and high-speed camera imaging. In: 48th US Rock Mechanics/Geomechanics Symposium. American Rock Mechanics Association (2014)
84. Nelson, P.P.: A framework for the future of urban underground engineering. Tunneling Underground Space Technol. **55**, 32–39 (2016)
85. Oda, M.: Similarity rule of crack geometry in statistically homogeneous rock masses. Mech. Mater. **3**(2), 119–129 (1984)
86. Ojala, I.O., Ngwenya, B., Main, I.G.: Loading rate dependence of permeability evolution in porous aeolian sandstones. J. Geophys. Res. Solid Earth **109**(B1), 2156–2202 (2004)
87. Ortiz, M.: A constitutive theory for the inelastic behavior of concrete. Mech. Mater. **4**(1), 67–93 (1985)
88. Peng, Z., Gomberg, J.: An integrated perspective of the continuum between earthquakes and slow-slip phenomena. Nat. Geosci. **3**(9), 599–607 (2010)
89. Pouya, A., Zhu, C., Arson, C.: Micro-macro approach of salt viscous fatigue under cyclic loading. Mech. Mater. **93**, 13–31 (2016)
90. Pyrak, N., Myer, L., Cook, N.: Transmission of seismic waves across single natural fractures. J. Geophys. Res. Solid Earth **95**(B6), 8617–8638 (1990)
91. Zhu, Q., Kondo, D., Shao, J.-F.: An homogenization-based nonlocal damage model for brittle materials and applications. ICCS 2007, Part III, LNCS 4489, Springer-Verlag, Shi (eds), **42**, 1130–1137 (2007)
92. Romero E, Gens A, loret A.: Water permeability, water retention and microstructure of unsaturated compacted boom clay. Eng. Geology **54**(1–2):117–127 (1999)
93. Saar, M.O., Manga, M.: Permeability-porosity relationship in vesicular basalts. Geo-phys. Res. Lett. **26**(1), 111–114 (1999)
94. Schubnel, A., Benson, P.M., Thompson, B.D., Hazzard, J.F., Young, Y.P.: Quantifying damage, saturation and anisotropy in cracked rocks by inverting elastic wave velocities. In: Rock Damage and Fluid Transport, Part I, pp. 947–973. Springer (2006)
95. Selvadurai, P.A., Glaser, S.D.: Direct measurement of contact area and seismic stress along a sliding interface. In: 46th US Rock Mechanics/Geomechanics Symposium. American Rock Mechanics Association (2012)
96. Selvadurai, P.A., Glaser, S.D.: Experimental evidence of micromechanical processes that control localization of shear rupture nucleation. In: 47th US Rock Mechanics/Geomechanics Symposium. American Rock Mechanics Association (2013)
97. Selvadurai, P.A., Glaser, S.D.: Insights into dynamic asperity failure in the laboratory. In: 48th US Rock Mechanics/Geomechanics Symposium. American Rock Mechanics Association (2014)
98. Senseny, P.E., Hansen, F.D., Russell JE, Carter NL, Handin JW.: Mechanical behavior of rock salt: phenomenology and micromechanisms. In: International Journal of Rock Mechanics and Mining Sciences and geomechanics abstracts, vol. 29, pp. 363–378. Elsevier (1992)

99. Shapiro, S.A., Dinske, C.: Fluid-induced seismicity: Pressure diffusion and hydraulic fracturing. Geophys. Prospect. **57**(2), 301–310 (2009)
100. Shen, X., Arson, C., Ding, J., Chester, F., Chester, J.: Experimental characterization of microstructure development for calculating fabric and sti ness tensors in salt rock. In: 51st US Rock Mechanics/Geomechanics Symposium. American Rock Mechanics Association (2017)
101. Singurindy, O., Berkowitz, B.: Competition among flow, dissolution, and precipitation in fractured carbonate rocks. Dyn. Fluids Fractured Rock, **81**, 1177–1185 (2004)
102. Spiers, C.J., Schutjens, P.M.T.M., Brzesowsky, R.H., Peach, C.J., Liezenberg, J.L., Zwart, H.J.: Experimental determination of constitutive parameters governing creep of rocksalt by pressure solution. Geological Soc. London, Special Publications **54**(1), 215–227 (1990)
103. Satuffer, D., Aharony, A.: Introduction to percolation theory: revised second edition. CRC press (2014)
104. Stesky, R.M.: Acoustic emission during high-temperature frictional sliding. Pure. appl. Geophys. **113**(1), 31–43 (1975)
105. Tester, J.W., Anderson, B.J., Batchelor, A.S., Blackwell, D.B., DiPippo, R., Drake, E., Garnish, J., Livesay, B., Moore, M.C., Nichols, K.: The future of geothermal energy: impact of enhanced geothermal systems (EGS) on the united states in the 21st century. Massachusetts Inst. Technol. **209** (2006)
106. Tomac, I., Gutierrez, M.: Formulation and implementation of coupled forced heat convection and heat conduction in dem. Acta Geotech. **10**(4), 421–433 (2015)
107. Tomac, I., Gutierrez, M.: Coupled hydro-thermo-mechanical modeling of hydraulic fracturing in quasi-brittle rocks using BPM-DEM. J. Rock Mech. Geotech. Eng. **9**(1), 92–104 (2017)
108. Turcote, D.L., Shcherbakov, R.: Can damage mechanics explain temporal scaling laws in brittle fracture and seismicity? In: Rock Damage and Fluid Transport, Part I, pp. 1031–1045. Springer (2006)
109. Tyler, S.W., Wheatcraft, S.W.: Fractal processes in soil water retention. Water Resour. Res. **26**, 1047–1054 (1990)
110. Van Genuchten, M.T.: A closed-form equation for predicting the hydraulic conductivity of unsaturated soils 1. Soil Sci. Soc. Am. J. **44**(5), 892–898 (1980)
111. Vandamme, M., Brochard, L., Lecampion, B., Coussy, O.: Adsorption and strain: the CO_2-induced swelling of coal. J. Mech. Phys. Solids **58**(10), 1489–1505 (2010)
112. Wang, S., Elsworth, D., Liu, J.: Rapid decompression and desorption induced energetic failure in coal. J. Rock Mech. Geotech. Eng. **7**(3), 345–350 (2015)
113. Westman, E.C., Luxbacher, K.D., Schafrik, S.J., Swanson, P.J., Zhang, H.: Time-lapse passive seismic velocity tomography of longwall coal mines: a comparison of methods. In: 46th US Rock Mechanics/Geomechanics Symposium. American Rock Mechanics Association (2012)
114. Wiederhorn, S.M., Townsend, P.R.: Crack healing in glass. J. Am. Ceram. Soc. **53**(9), 486–489 (1970)
115. Wool, R.P.: Self-healing materials: a review. Soft Matter **4**(3), 400–418 (2008)
116. Xu, H., Arson, C.: Anisotropic damage models for geomaterials: theoretical and numerical challenges. Int. J. Comput. Methods **11**(02), 1342007 (2014)
117. Young, R.P., Thompson, B.D.: Imaging dynamic rock fracture with acoustic emission and x-ray tomography. In: Proceedings of the 11th Congress of International Society for Rock Mechanics (2007)
118. Zhao, J., Sheng, D., Zhou, W.: Shear banding analysis of geomaterials by strain gradient enhanced damage model. Int. J. Solids Struct. **42**(20), 5335–5355 (2005)
119. Zhu, C., Arson, C.: A model of damage and healing coupling halite thermo-mechanical behavior to microstructure evolution. Geotech. Geol. Eng. **33**(2), 389–410 (2015)
120. Zoback, M.D., Moos, D., Mastin, L., Anderson, R.N.: Well bore breakouts and in situ stress. J. Geophys. Res. Solid Earth **90**(B7), 5523–5530 (1985)
121. Zysset, P.K., Curnier, A.: An alternative model for anisotropic elasticity based on fabric tensors. Mech. Mater. **21**(4), 243–250 (1995)